NOVA SCHOOL OF SCIENCE & TECHNOLOGY

DEPARTAMENT OF

EARTH SCIENCES

ALBANERPETONTIDAE (LISSAMPHIBIA) AND OTHER SMALL HERPETOFAUNA (CROCODYLOMORPHA, LEPIDOSAURIA, CHORISTODERA) FROM THE IBERIAN MESOZOIC, WITH FOCUS ON THE UPPER JURASSIC OF PORTUGAL

ALEXANDRE RENAUD DANIEL GUILLAUME

Master in Paleontology

DOCTORATE IN GEOLOGY

NOVA University Lisbon

May, 2024

DEPARTAMENT OF
EARTH SCIENCES

ALBANERPETONTIDAE (LISSAMPHIBIA) AND OTHER SMALL HERPETOFAUNA (CROCODYLOMORPHA, LEPIDOSAURIA, CHORISTODERA) FROM THE IBERIAN MESOZOIC, WITH FOCUS ON THE UPPER JURASSIC OF PORTUGAL

ALEXANDRE RENAUD DANIEL GUILLAUME

Master in Paleontology

Adviser: Miguel Moreno-Azanza
Invited Assistant Professor, NOVA School of Science and Technology, NOVA University Lisbon / Universidade de Zaragoza

Co-adviser: Eduardo Puértolas-Pascual
PhD, Universidade de Zaragoza / NOVA School of Science and Technology, NOVA University Lisbon

Examination Committee:

Chair: José Carlos Kullberg,
Full Professor, NOVA School of Science and Technology, NOVA University Lisbon

Rapporteurs: Susan Elizabeth Evans,
Professor, Department of Cell & Developmental Biology, University College London, United Kingdom

James Gardner,
Curator of Palaeoherpetology, Royal Tyrrell Museum of Palaeontology, Canada

Adviser: Miguel Moreno-Azanza,
Invited Assistant Professor, NOVA School of Science and Technology, NOVA University Lisbon

Members: Hugues-Alexandre Blain,
Researcher, Catalan Institute of Human Paleoecology and Social Evolution (IPHES), Espanha

José Carlos Kullberg,
Full Professor, NOVA School of Science and Technology, NOVA University Lisbon

DOCTORATE IN GEOLOGY

NOVA University Lisbon
May, 2024

Albanerpetontidae (Lissamphibia) and other small herpetofauna (Crocodylomorpha, Lepidosauria, Choristodera) from the Iberian Mesozoic, with focus on the Upper Jurassic of Portugal

Copyright © Alexandre R. D. Guillaume, NOVA School of Science and Technology, NOVA University Lisbon.

The NOVA School of Science and Technology and the NOVA University Lisbon have the right, perpetual and without geographical boundaries, to file and publish this dissertation through printed copies reproduced on paper or on digital form, or by any other means known or that may be invented, and to disseminate through scientific repositories and admit its copying and distribution for non-commercial, educational or research purposes, as long as credit is given to the author and editor. According to Article 8.2 of the ICZN, this work is not issued for purposes of nomenclature and should not be considered published within the meaning of the code. Thus, all nomenclatural acts contained in this thesis dissertation are not valid, and any names that appear here for the first time should not be considered available.

This document was created with Microsoft Word text processor and the NOVAthesis Word template.

Dedicatória lorem ipsum

ACKNOWLEDGMENTS

A PhD. Over four years. One unprecedent, global pandemic. Organizing one international meeting. Tutoring three master students. Portuguese bureaucracy at its (un)finest. Collection visits across the world. A snowstorm (while driving). Some thunderstorms (still driving). And unnumbered crisis events for various reasons.

Without realising it, those are the things that I had to face to accomplish this quest, a dream set since my childhood: becoming a palaeontologist. And even though I knew from my family experience how a PhD looks like; nothing could really prepare me to overcome all the (fewer than I would admit) major and minor obstacles that arose. But I think I have eventually succeeded, and for that, I have many people to thank for.

To begin with, no other than my true and only Céline. Despite the misadventures, the stress, the distance, the waiting, the uncertainties, you remained the pillar on which I could always count to not get loose and become a better version of me. You are not only my spouse, but you are also my best friend, my best supporter, my best guide, and my best help. My best

partner that I would change for nothing in the whole omniverse. You saved me more than once, and never let me down. I am the luckiest man in the world to always have you by my side. I wish our vows to live together forever the life to come will come true. I cannot wait to see what is coming next, because I am sure I can face anything with you.

Second, I would like to thank both my advisors, Miguel and Eduardo, who stood by me in every step and helped me to become not only a better palaeontologist, but a better scientist. I learnt from the best and I feel so lucky to have you both to back me up and oversee me during those years. I knew nothing could go really wrong, which give me the freedom to try and experiment without going off too much out of topic. I am glad you trusted in me for this project, and that you gave me the opportunity to accomplish all this work. Without mentioning the housing in Zaragoza and all the travels to visit all those collections. You have been great mentors and are amazing friends; I only hope that I could be as inspiring as you for future students.

And third, I would like to thank my family for all their support through those tough years. Always here to back me up and support me in that colossal task. It has not been always easy to be far away for this long, especially with all the rough patches that erupted here and there. Most particularly, I want to dedicate this thesis to my grand-mother "Mamy Annie", who always had a thought for me even though she was not understanding everything that was going on; and my grand-parents "Papy

Daniel" and "Mamy Claude", who instilled the curiosity in a very young me and has driven me since then to work in academia.

All this work could not have been executed without the help of many people involved in the research. First and foremost, I credit the people and collaborators that help me through the thesis and the different articles. Hugues-Alexandre Blain, for his advice as the CAT external member and co-author, but also to make me feel welcome at IPHES in Tarragona during my internship, where I learnt a lot about herpetofauna anatomy. Vicente Crespo to have accepted to be the internal CAT member in trouble times. Lope Ezquerro for his help in co-authorship to understand the geology of Lourinhã and start drawing its paleoenvironmental reconstruction. And my co-authors Marc Jones and Roger Benson, for their help to get µCT-scan of our specimens, something that I never thought I would be able to do for my thesis, and all their inputs on the description of the material. I would like to thank all the editors and reviewers that improved my articles/chapters.

A special thanks to Ester Diaz Berenguer from the Museo de Ciencias Naturales de la Universidad de Zaragoza for facilitating the access to the Blasi 2B material and providing space and equipment to work and study these specimens, to Jerome Hidalgo Sanz from the Universidad de Zaragoza for his help acquiring the SEM pictures, and to Manuel Pérez-Pueyo for hosting me meanwhile. Me and my co-authors would like to acknowledge the use of Servicio General de Apoyo a la Investigación-SAI, Universidad de Zaragoza.

I would like to thank Prof. José Carlos Kullberg from the Earth Sciences Department in NOVA School of Science and Technology to have been an extraordinary PhD program coordinator in providing all the help and support needed to navigate around this PhD, as well as Dra Fátima Silva and her endless patience. Similarly, I would like to thank Carla Alexandra Tomás, Carla Abreu, and Micael Martinho from the Museu da Lourinhã, for all the help given in the field work, the lab preparation, the picking, and the cataloguing of the specimens. I would like also to thank them to have accommodated and provided space, facility, and equipment for working in the Museu during those years.

I am infinitely grateful for the Master students from FCT-UNL and all volunteers who participated to the MicroSaurus Citizen Science Project hosted by the DinoPark of Lourinhã and the Museu da Lourinhã, and who helped to pick the thousands and thousands of microfossils I have been studying for the past years. There would not be any thesis at all without their work! I would like also to thank Eng. Jorge Sequeira Museu Geológico de Lisboa, who granted me access to the Guimarota collection through all those years. Reviewing this material is an endless work and it is hard to grasp how massive it is without having to check every single box one by one. I would like to thank Mariana Valente for the help in cataloguing the specimens from Guimarota, allowing to locate the new relevant material. Even if we met (too) late in my work, I am extremely grateful to Prof. Anabela Veiga, from the Escola Superior de Tecnologia e Gestão of the

Politécnico de Leiria, and the Museu de Leiria, to facilitate access to the Guimarota mine and give priceless information regarding the locality.

I would like also to acknowledge Dr. Maxime Lasseron, Prof. Juan Daza, Prof. Susan Evans, Prof. Oliver Rauhut, Prof. Thomas Martin, and Prof. Matthew Carrano for providing their inputs on their works to better understand the anatomy of albanerpetontids and other small lizards, as well as their biology, either being via email or long talks in extraordinary places. All of them were extremely rich and enlightening.

A PhD thesis will not be a PhD thesis without collection visits, and I am happy to have been able to do most of the ones originally planned. I would like to thank Prof. Ronan Allain and Dr. Damien Germain from the Muséum national d'Histoire naturelle in Paris, Dr. Daniel Brinkman and Dr. Vanessa Rhue from the Yale Peabody Museum of Natural History in New Haven, Prof. Matthew Carrano from the Smithsonian National Museum of Natural History, Dr. Mike Day from the National History Museum of London, Dr. Howard Gibbins and Prof. Michael Cadwell from the University of Alberta Laboratory of Vertebrate Palaeontology in Edmonton, Alana Gishlick from the American Museum of Natural History in New York, Dr. Mariella del Re from the Museo di Paleontologia of Napoli, Dr. Mercedes Llandres Serrano from Museo Paleontológico de Castilla-La Mancha, and Dr. William Simpson from the Field Museum of Natural History in Chicago for granting access to comparative material in all these institutions across the world, especially in

a shortly-post-COVID world. None of this work could have been executed without them

I want to show all my gratitude to Carl Mehling from the American Museum of Natural History for his help and support during this PhD thesis, either to get access to material, or to go on amazing fieldworks in Wyoming. But more importantly, you are just the best and cheeriest man there is and that I am so glad to count you as a friend. Similarly, I highly appreciate to have met Prof. James Gardner from the Royal Tyrrell Museum of Palaeontology in Drumheller, for granting access to its collections and providing unique help in understanding albanerpetontid anatomy. But more than that, you are the sweetest and chilliest person I know, and you truly cheered me up at extremely stressful times that were not always easy. For all of that, I am extremely grateful to both of you, and you will always be role models to follow for me.

And obviously, I would like to finish by acknowledging all the people that have been around during those years. André Saleiro and Alexandra Fernandes, who are awesome friends and coworkers, especially when it comes to picking or checking my Portuguese. Probably the ones to thank also to have prevented me to have strangled people in the past years. You are the best best-man/woman I could have dreamt of! Filippo Maria Rotatori, Victor López Rojas, and Arthur Maréchal for all the good laughs and productive collaborations done together. Roberta Martino, João Pratas,

Francisco Costa, Simone Conti, Victor Beccari, Valérian Jésus, Darío Estraviz-Lopez (even if I wanted to dispatch you almost every week), Marc Ricetto, Alexandre Audigane, and Ana Luz, for all the good times around food, drinks, or movies. Huge thanks to Maria Ríos Ibáñez and Cristina Sequero López for their benevolence, kindness, having kept an eye on all of us, and their valuable help at work.

I would like also to thanks all my friends in France that supported me and let me release the pressure time to time: Maxime LeCesne, Thibaut Totis, Charles Rosères, Gwenaël Guery, Elsa Baudot, Audrey Weisseldinger, Amandine "Maddy" Sauvage, and all the HPF community that are too many to be named one by one. Not to mention all Céline's family, who discovered more or less at the same time as me what I was doing but had always been supportive and understanding when I had to spend my days working at Castelnaud during the last summers. And last but not least, the one and only Pippin and his fluffy, endless love.

Thanks everyone!

Funding sources—Fundação para a Ciência e Tecnologia (FCT-MCTES) of Portugal (grant number SFRH/BD/144665/2019 and projects PTDC/CTA-PAL/31656/2017 and PTDC/CTA-PAL/2217/2021), and Research Unit GeoBioTec UIDB/04035/2020. MicroSaurus Citizen Science Project is supported by Microsaurus-superanimais 3 research grant funded by PDL.

“Even if I knew everything, I could not know that I know everything.”

Isaac Asimov, *The Last Answer*

“[…] science is no more than an investigation of a miracle we can never explain, and art is an interpretation of that miracle.”

Ray Bradbury, *The Martian Chronicles*

“Le problème du savoir tient à son irréversibilité.”

Claire Garand, *Paideia*

“No, sir, it doesn’t. Allow me to suggest that you defy the universe with your book.”

James Morrow, *Galápagos Regained*

“The need to interpret the consequences had become greater than the need to understand the cause.”

Christopher Priest, *An American Story*

Abstract

The Upper Jurassic of Portugal has been globally known for its microfossil vertebrate fauna thanks to the Konzentrat-Lagerstätte of the Guimarota mine, which provided thousands of bone fragments, isolated teeth, and even complete specimens. Other vertebrate microfossil assemblages have been studied around the world. Besides Guimarota, only a handful of other Portuguese Jurassic assemblages has been studied, but never extensively.

Hereby, I present my work on microvertebrates from the Lourinhã Formation (Kimmeridgian–Tithonian), with a focus on the small herpetofauna of the Late Jurassic of Portugal. A total of 5,100 vertebrate remains have been identified, belonging to all major vertebrate groups known in other continental and freshwater environments. Stratigraphy and sedimentological analyses of different localities carried in collaboration with Dr. Lope Ezquerro and Dr. Cristina Sequero allowed to draw a first palaeoenvironmental reconstruction, depicting various depositional settings: low sediment supply and long periods of subaerial exposure in Valmitão; area of alternating conditions between wet and dry periods in

Zimbral; and wetter conditions, probably associated with permanent sheet of water and anoxic environments in Porto das Barcas.

Revision of the Guimarota collection allowed to locate misidentified, mislabelled, and unpublished specimens that could be assigned to *Cteniogenys* aff. *C. antiquus*, although different from the material reported in the Middle Jurassic Kirtlington Mammal Beds in the UK; and confirm the presence of a new species of a relic stem-lepidosaur. Overall, the Lourinhã Formation is largely dominated by amphibious vertebrates, more than in other equivalent Mesozoic assemblages around the Jurassic/Cretaceous boundary. Notably, crocodylomorphs shed teeth support a high morphological and ecological diversity of the group; while albanerpetontids remains are quite numerous and diverse in anatomical parts preserved. This allowed to erect the oldest albanerpetontid species from the Iberian Peninsula, and the first of Portugal. Together with another new species, the youngest of the Iberian Peninsula, the new Portuguese material allowed to review the phylogeny of Albanerpetontidae and propose a new hypothesis on their in-group relationship, as well as new insight on their palaeobiogeography at the end of the Cretaceous.

Keywords: Upper Jurassic, Vertebrate microfossil assemblages, Lourinhã Formation, Herpetofauna, Albanerpetontidae

RESUMO

O Jurássico Superior de Portugal é mundialmente conhecido pela sua fauna microfóssil de vertebrados graças ao Konzentrat-Lagerstätte da mina da Guimarota, que forneceu milhares de fragmentos ósseos, dentes isolados e até exemplares completos. Outras aglomerações de microfósseis de vertebrados foram estudadas em todo o mundo. Além da Guimarota, apenas algumas outras aglomerações jurássicas portuguesas foram estudadas, mas nunca extensivamente.

Aqui apresento o meu trabalho sobre microvertebrados da Formação de Lourinhã (Kimeridgiano–Titoniano), com foco na herpetofauna do Jurássico Superior de Portugal. Um total de 5100 restos de vertebrados foram identificados, pertencentes a todos os principais grupos de vertebrados conhecidos noutros ambientes continentais e de água doce. A estratigrafia e análises sedimentológicas de diferentes localidades em colaboração com o Dr. Lope Ezquerro e a Dra. Cristina Sequero permitiram visualizar uma primeira reconstrução paleoambiental, retratando vários cenários deposicionais: baixo importe de sedimentos e longos períodos de exposição subaérea em Valmitão; área de alternância entre períodos chuvosos e secos

em Zimbral; e condições mais húmidas, provavelmente associadas a um lençol de água permanente e ambientes anóxicos em Porto das Barcas.

A revisão da coleção de Guimarota permitiu localizar exemplares incorretamente identificados, incorretamente rotulados e não publicados que poderiam ser atribuídos a *Cteniogenys* aff. *C. antiquus*, embora diferentes do material relatado nas Kirtlington Mammal Beds do Jurássico Médio do Reino Unido; e confirmar a presença de uma nova espécie de um lepidosauro de ramo basal. No geral, a Formação de Lourinhã é primariamente dominada por vertebrados anfíbios, bem mais quando comparada com outras aglomerações mesozóicas equivalentes datada da fronteira Jurássico/Cretáceo. Notavelmente, os dentes isolados de crocodilomorfos são representativos da grande diversidade morfológica e ecológica do grupo; enquanto os restos de albanerpetontídeos são bastante numerosos e diversos no que diz respeito às partes anatómicas preservadas. Isto permitiu a descrever a mais antiga espécie de albanerpetontídeo da Península Ibérica, e a primeira de Portugal. Juntamente com outra nova espécie, a mais jovem da Península Ibérica, o novo material português permitiu rever a filogenia do grupo Albanerpetontidae e propor uma nova hipótese sobre a sua relação intra-grupo, bem como uma nova visão sobre a sua paleobiogeografia durant final do Cretáceo.

Palavras-chave: Jurássico Superior, Aglomeraçoes de microfósseis de vertebrados, Formação da Lourinhã, Herpetofauna, Albanerpetontidae

TABLE OF CONTENTS

ACKNOWLEDGMENTS v

ABSTRACT xv

RESUMO xvii

TABLE OF CONTENTS xix

TABLE OF FIGURES xxvii

TABLE OF TABLES xlvii

ABBREVIATIONS li

Institutional abbreviations li

Anatomical abbreviations lii

Measurements liv

Localities liv

Others lv

1 INTRODUCTION ..... - 1 -

1.1 The vertebrate microfossil assemblage from the Guimarota beds - 1 -

1.1.1 History of the Guimarota excavations ..... - 1 -

1.1.2 Geological setting of the Guimarota microsite ..... - 9 -

1.1.3 Taphonomy and palaeoenvironmental interpretation ..... - 12 -

1.2 Geological settings of the Lourinhã Formation ..... - 15 -

1.2.1 General context of the Upper Jurassic of Portugal ..... - 15 -

1.2.2 The Lusitanian Basin ..... - 19 -

1.2.3 Geology of the Lourinhã Formation ..... - 21 -

1.3 Geological setting of Blasi 2B (Tremp Formation, Upper Maastrichtian, Spain) ..... - 25 -

1.4 Overview of the studied herpetofauna from the Late Jurassic of Portugal ..... - 28 -

1.4.1 The lissamphibians ..... - 28 -

1.4.2 The choristoderes ..... - 33 -

1.4.3 The lepidosauromorphs ..... - 35 -

1.4.4 The crocodylomorphs ..... - 39 -

1.5 Objectives ..... - 41 -

1.6 Material and methods ..... - 43 -

1.6.1 Fieldwork & sieving fossils ..... - 43 -

1.6.2 Repository of the specimens from the Lourinhã Formation - 47 -

1.6.3 The Guimarota collection ..... - 50 -

1.6.4 Collection visits in non-Portuguese institutions ..... - 53 -

1.7 Structure of the thesis ..... - 60 -

2 CHAPTER 1: THE VERTEBRATE MICROFAUNA FROM THE LATE JURASSIC OF PORTUGAL ..... - 65 -

2.1 Sneak peek on the Vertebrate Microfossil Assemblages from the Lourinhã Formation ..... - 65 -

2.1.1 Introduction ..... - 65 -

2.1.2 Material & Methods ..... - 66 -

2.1.3 Palaeoenvironmental reconstruction ..... - 69 -

2.1.4 Palaeoecology of the Lourinhã Formation ..... - 71 -

2.1.5 Conclusion ..... - 76 -

2.2 Chapter 2: Palaeobiodiversity of crocodylomorphs from the Lourinhã Formation based on the tooth record: insights into the palaeoecology of the Late Jurassic of Portugal ..... - 77 -

2.2.1 Introduction ..... - 78 -

2.2.2 Material and Methods ..... - 85 -

2.2.3 Description of tooth morphotypes ..... - 88 -

2.2.4 Review of the *Lusitanisuchus mitracostatus* dentition .... - 116 -

2.2.5 Discussion ..... - 123 -

2.2.6 Conclusion ..... - 143 -

2.3 Chapter 3: The enigmatic duo: revision of *Cteniogenys* (Choristodera) and *Marmoretta* (Lepidosauromorpha) from the Guimarota beds (Upper Jurassic, Portugal) ..... - 145 -

2.3.1 Introduction ..... - 147 -

2.3.2 Material & Methods ..... - 153 -

2.3.3 Systematic Paleontology ..... - 154 -

2.3.4 Discussion ..... - 183 -

2.3.5 Conclusion ..... - 196 -

3 NEW MESOZOIC ALBANERPETONTIDAE FROM THE IBERIAN PENINSULA ... - 199 -

3.1 Chapter 4: Plasticity in the morphology of the fused frontals of Albanerpetontidae (Lissamphibia; Allocaudata) ..... - 199 -

3.1.1 Introduction ..... - 201 -

3.1.2 Geological setting ..... - 206 -

3.1.3 Material and Methods ..... - 210 -

3.1.4 Systematic palaeontology ..... - 221 -

3.1.5 Results ..... - 231 -

3.1.6 Discussion ..... - 243 -

3.1.7 Conclusion ..... - 253 -

3.2 Chapter 5: New albanerpetontid species (Lissamphibia) from the Late Jurassic of Portugal ..... - 255 -

3.2.1 Introduction ..... - 256 -

3.2.2 Geological setting ..... - 258 -

3.2.3 Material and Methods ..... - 261 -

Institutional abbreviations ..... - 267 -

3.2.4 Systematic palaeontology ..... - 268 -

Referred material ..... - 271 -

Stratigraphic and geologic range— ..... - 273 -

Description ..... - 274 -

3.2.5 Discussion ..... - 318 -

3.2.6 Conclusions ..... - 323 -

3.3 Chapter 6: Witnessing the last giants—a new Albanerpetontidae (Lissamphibia) from the latest Maastrichtian of Spain ..... - 325 -

3.3.1 Introduction ..... - 326 -

3.3.2 Geological settings ..... - 333 -

3.3.3 Material & methods ..... - 334 -

3.3.4 Systematic palaeontology ..... - 336 -

3.3.5 Discussion ..... - 363 -

3.3.6 Conclusion ..... - 368 -

3.4 Chapter 7: New phylogeny of Albanerpetontidae and implications on their taxonomy and palaeobiogeography ..... - 371 -

3.4.1 Introduction ..... - 371 -

3.4.2 Material & methods ..... - 372 -

3.4.3 Phylogenetic analysis ..... - 379 -

3.4.4 Discussion ..... - 386 -

3.4.5 Conclusion ..... - 397 -

4 DISCUSSION & FUTURE WORKS ..... - 399 -

5 CONCLUSIONS ..... - 409 -

6 REFERENCES ..... - 413 -

APPENDICES ..... - 477 -

A INTRODUCTION ..... - 479 -

A.1 Specimen list from the Lourinhã Formation ..... - 479 -

A.2 Specimen list from the Guimarota beds ..... - 550 -

B SNEAK PEEK ON THE VERTEBRATE MICROFOSSIL ASSEMBLAGES FROM THE LOURINHÃ FORMATION ..... - 591 -

C PALAEOBIODIVERSITY OF CROCODYLOMORPHS FROM THE LOURINHÃ FORMATION BASED ON THE TOOTH RECORD: INSIGHTS INTO THE PALAEOECOLOGY OF THE LATE JURASSIC OF PORTUGAL ..... - 597 -

D THE ENIGMATIC DUO—REVISION OF *CTENIOGENYS* (CHORISTODERA) AND *MARMORETTA* (LEPIDOSAUROMORPHA) FROM THE GUIMAROTA BEDS (LUSITANIAN BASIN, PORTUGAL) ..... - 599 -

E PLASTICITY IN THE MORPHOLOGY OF THE FUSED FRONTALS OF ALBANERPETONTIDAE (LISSAMPHIBIA; ALLOCAUDATA) ..... - 611 -

E.1 Morphometric analysis - R Markdown script ..... - 611 -

E.1.1 Linear regression ..... - 611 -

E.1.2 Morphometrics analysis; k-means ..... - 617 -

E.2 Frontal morphometric data ..... - 620 -

E.3 Analysis R1, using the hypothesis of two Portuguese species - 625 -

E.4 Analysis R2, using the hypothesis of one Portuguese species - 626 -

E.5 List of characters ..... - 627 -

E.6 Supplementary text ..... - 632 -

E.6.1 Observations on the preservation status ..... - 632 -

E.6.2 Morphometrics analysis ..... - 634 -

E.6.3 Phylogenetic analysis ..... - 635 -

E.7 Bibliography ..... - 638 -

F NEW ALBANERPETONTID SPECIES (LISSAMPHIBIA) FROM THE LATE JURASSIC OF PORTUGAL ..... - 639 -

F.1 Mislabelling of SMNS specimen ..... - 639 -

F.2 Parameters of the µCT-scan. ..... - 641 -

F.3 Extended comparison of New unnamed taxon 2 ..... - 642 -

F.4 Specimens from the Guimarota beds..... - 652 -

F.4.1 Premaxillae..... - 652 -

F.4.2 Maxillae ..... - 654 -

F.4.3 Frontals..... - 655 -

F.4.4 Parietals..... - 656 -

F.4.5 Dentaries..... - 657 -

F.4.6 Articulars ..... - 659 -

F.4.7 Axes..... - 660 -

F.4.8 Humeri ..... - 661 -

F.5 References ..... - 661 -

G NEW PHYLOGENY OF ALBANERPETONTIDAE AND IMPLICATIONS ON THEIR TAXONOMY AND PALAEOBIOGEOGRAPHY ..... - 663 -

G.1 Nexus file for the total phylogenetical analysis ..... - 663 -

G.2 List of characters..... - 664 -

G.2.1 Premaxilla ..... - 665 -

G.2.2 Maxilla..... - 674 -

G.2.3 Frontal..... - 677 -

G.2.4 Lacrimal ..... - 687 -

G.2.5 Parietals..... - 688 -

G.2.6 Dentary ..... - 690 -

G.2.7 Articular-angular ..... - 691 -

G.2.8 Quadrate ..... - 692 -

G.2.9 Atlas ..... - 693 -

G.2.10 Axis ..... - 694 -

G.2.11 Humerus ..... - 694 -

G.2.12 Ilium ..... - 694 -

G.2.13 References ..... - 695 -

TABLE OF FIGURES

Figure 1.1.1: Geographical setting of the Guimarota beds. The entrance of the mine is presented by the red star. **A**, Europe map modified from Erin Dill, scale is 400 km. **B**, geological sketch of the Iberian Peninsula, scale is 200km. **C**, aerial map of Leiria by Google Maps, scale is 1 km. **D**, sketch of the Guimarota mine tunnels based field notes (modified from Gloy, 2000). **E**, overlay of the Guimarota mine outlines on the current neighborhood by Luís Pinela from Leiria municipality. ..... - 3 -

Figure 1.1.2: Pictures of the entrance of Guimarota Mine. **A**, sign indicating the beginning of the Rua das Minas. **B**, end of the Rua das Minas, showing the entrance of the private property leading to the entrance of the mine. **C**, external view of surface above the mine from the adjacent street Rua Rui Hasse Ferreira. **D**, panoramic picture of the remaining building used by the two excavations teams; the entrance is right next to the right wall of the hall on the right. **E** and **F**, picture from within the hall dating from the time of the excavations (Krebs, 2000*a*). **G** and **H**, entrance of the Guimarota Mine nowadays. **I** and **J**, view from top (I) and bottom (J) of the main tunnel that has not been flooded yet. **K**, details on the upper coal steam layer. I, J, and K are kindly shared by Prof. Anabela Veiga from Escola Superior de Tecnologia e Gestão (Politécnico de Leiria). ..... - 5 -

Figure 1.1.3: Picture of a field notebook reporting each finding, the name of the finder, and the price she was rewarded with. Picture kindly shared by Prof. Anabela Veiga from Escola Superior de Tecnologia e Gestão (Politécnico de Leiria). ..... - 8 -

Figure 1.2.1: Global palaeogeographical reconstructions of the Jurassic/Cretaceous transition, illustrating the opening of the North Atlantic Ocean. **A**, Oxfordian (160Mya). **B**, Kimmeridgian (150Mya). **C**,

Berriasian (160Mya). The reddish-purple star points Portugal. Palaeomaps from Colorado Plateau Geosystem. ..... - 17 -

Figure 1.2.2: Palaeogeography of Europe during the Late Jurassic (150Mya). Palaeomaps from Colorado Plateau Geosystem. Scale bar is 400km. ..... - 19 -

Figure 1.2.3: Geology of the Lusitanian Basin. **A**, overview map of Portugal with the location of the Lusitanian Basin indicated; scale is 200km. **B**, simplified geological map of Portugal showing major basin features; scale is 50km. **C**, map showing the distribution of sub-basins in the Western and Central Lusitanian Basin (modified from Martinus & Gowland, 2011; Taylor *et al.*, 2014, Gowland *et al.*, 2017)..... - 21 -

Figure 1.2.4: Lithostratigraphic framework of the Lourinhã Formation in the Consolacão sub-basin, showing simplified depositional elements (modified from Martinus & Gowland, 2011, based on Mateus *et al.*, 2017)..... - 23 -

Figure 1.3.1: Geographic and geological context of Blasi 2B (Arén, Huesca, Spain). **A**. Geological map of the Southern Pyrenees, focused on the Tremp Syncline and its Upper Cretaceous-Palaeogene outcrops (modified from López-Martínez and Vicens, 2012; Pérez-Pueyo, 2023). **B**. Schematic stratigraphic log of the upper Maastrichtian in the Blasi Area; modified from Pereda-Suberbiola *et al.*, 2009. Abbreviations: CH. Chronostratigraphy; DAN., Danian; LIT, Lithostratigraphy; M, Magnetostratigraphy; vl. Vallcebre limestones and equivalents. **C**. Detailed stratigraphic profile of the Tremp Formation in the study area with location of the main vertebrate sites; colours reflect colours of lithology..... - 27 -

Figure 1.4.1: Extant lissamphibians and some relative fossils. **A**, **B**, and **C**, extant lissamphibians, respectively an Anura, an Urodela, and a Gymnophiona (free licences pictures). **D**, MNHN.F.MAE126 holotype of *Triadobatrachus massinoti* (Piveteau, 1936) from the Early Triassic of Madagascar. **E** and **F**, fossil amphibian from Las Hoyas (Berriasian, Spain) in exhibit in MUPA, *Iberobatrachus angelae* Báez, 2013 (**E**) and *Valdotriton gracilis* Evans & Milner, 1996 (**F**). ..... - 29 -

Figure 1.4.2: Relevant albanerpetontid fossils. **A**, M542 holotype of *Celtedens megacephalus* (Costa, 1864); scale is 1cm. **B**, MCCM-LH6020 holotype of *Celtedens ibericus* McGowan & Evans, 1995; scale is 1cm. **C**, GRS-Ref-060829 holotype and JZC Bu154 paratype of *Yaksha perettii* Daza *et al.*, 2020, with images of three-dimensional model of based µCT-scan of the holotype (from Daza *et al.*, 2020). ..... - 31 -

Figure 1.4.3: Extant and fossil relatives of small reptiles found in the Upper Jurassic of Portugal. **A**, **B**, and **C**, extant lepidosaurs, respectively a tuatara, an anguimorph, and a scincid (free licence pictures). **D**, palaeoart reconstruction of *Portugalophis lignites* by Julius Csotonyi. **E**, reconstruction of a Cretaceous choristodere exhibited at the Royal Tyrrell Museum. **F**, Digital skull reconstruction of *Marmoretta oxoniensis*, using information from referred specimens in lateral and dorsal view (from Griffiths *et al.*, 2021). **G**, USNM 6134 holotype of *Cteniogenys antiquus* Gilmore 1928 in medial and lateral views; the scale is 5mm..... - 37 -

Figure 1.6.1: Overview of the sampling and methods used for sieving and storage. **A**, prospecting in Valmitão vertebrate microfossil assemblage. **B**, collecting sediments in Zimbral vertebrate microfossil assemblage. **C**, 50 L buckets used to soak sediment in water. **D–F**, screen-washing facility, pumping water from a well (D) and using garden sprinkler to wash the sediments with three level of meshes (E), while recycling water (F). **G**, picture from a workshop organized at Parque dos Dinossauros de Lourinhã. **H** and **I**, Eppendorf PCR clear polyethylene tubes used for the new repository strategy..... - 45 -

Figure 1.6.2: Taxonomic classification of the new specimen numbers catalogued during this thesis. ..... - 49 -

Figure 1.6.3: Storage of the Guimarota collection at the Museu Geológico in Lisbon. **A**, the storing boxes for the major taxonomic group. **B**, example of different option of storage of squamates specimens, with the MG catalogue. **C**, overview of the amphibian specimens from the Guimarota collection; in frame, albanerpetontid specimen MG28656 illustrating that one specimen number can refer to several individuals, scale is 2mm. ..... - 51 -

Figure 2.1.1: Sample of vertebrate microfossils found in the Lourinhã Formation (Kimmeeridgian–Tithonian, Portugal). **A**, Gnathosaurinae tooth. **B**, *Lusitanisuchus* tooth. **C**, Actinopterygii vertebra. **D**, Choristodere vertebra. **E**, Multituberculata tooth. **F**, Albanerpetontidae right premaxilla. **G**, Caudata atlas. **H**, Plesiosauroidea tooth. **I**, Squamata vertebra. **J**, Anura ilium. **K**, Anura distal humerus. **L**, Neornitischia tooth. **M**, Coelurosauria tooth. Scale is 1 mm. ..... - 67 -

Figure 2.1.2: Rarefaction curves of each sampled locality (dash-lines represent the 95% interval) and general abundance of major vertebrate groups across all localities. ..... - 68 -

Figure 2.1.3: Palaeobiodiversity in the Lourinhã Fm. **A**, correspondence analysis (scaling 1) of microvertebrates sites from the Lourinhã Fm using faunal data. **B**, general taxonomic diversity of major vertebrate groups across all localities. ..... - 73 -

Figure 2.1.4: Palaeoecology of the Lourinhã Formation VMAs compared to others relevant VMAs from the Upper Jurassic and Lower Cretaceous. **A**, habitat relative diversities of microvertebrates site using faunal data (family level). **B**, correspondence analysis (scaling 1) of microvertebrates sites using faunal data (abundance). Data from Carrano & Velez-Juarbe, 2006; Buscalioni *et al.*, 2008; Mazin *et al.*, 2008; Oreska *et al.*, 2013; Carrano *et al.*, 2016; Lasseron *et al.*, 2020; Allain *et al.*, 2022 ..... - 75 -

Figure 2.2.1: Geological and geographical context of the Valmitão vertebrate microfossil assemblage. **A**, geological sketch of the Iberian Peninsula, showing the location of the study area. **B**, map of the onshore part of the Consolação sub-basin south of Peniche (modified from Taylor *et al.*, 2014). **C**, north-south mapping of the main units in the area of study and their corresponding lithostratigraphic framework (modified from Taylor *et al.*, 2014, based on Mateus *et al.*, 2017). **D**, stratigraphic log of the upper part of the Porto Nova/Praia da Amoreira Member at Valmitão Beach. The red star indicates the location of the Valmitão vma. ..... - 83 -

Figure 2.2.2: Morphotype 1 (A) and 2 (B and C) teeth ML2586 (A), ML2497 (B) and ML2498 (C) in labial (1), lateral (2), lingual (3), apical (4) and basal

(5) views. Scale bar is 1 mm. All images are normal-light photomicrographs except for A1–A3 and B4, which are SEM photomicrographs. ..... - 89 -

Figure 2.2.3: Morphotype 3 teeth ML2508 (A), ML2509 (B) and ML2510 (C) in labial (1), lateral (2), lingual (3), apical (4) and basal (5) views. Scale bar is 1 mm. All images are normal-light photomicrographs except for A1, B2 and C3, which are SEM photomicrographs. ..... - 91 -

Figure 2.2.4: Morphotype 4 teeth ML2522 (A), ML2523 (B) and ML2524 (C) in labial (1), lateral (2), lingual (3), apical (4) and basal (5) views. Scale bars are 1 mm. Close-up of the false denticles seen in ML2522 (A6). Scale bar is 200 μm. All images are normal-light photomicrographs except for A3, A6, B2 and C1, which are SEM photomicrographs. ..... - 95 -

Figure 2.2.5: Morphotype 5 teeth ML2532 (A), ML2533 (B), ML2534 (C) and ML2535 (D) in labial (1), lateral (2), lingual (3), apical (4) and basal (5) views. Scale bar is 1 mm. All images are normal-light photomicrographs except for A4, B3, C1 and D2, which are SEM photomicrographs. ..... - 97 -

Figure 2.2.6: Morphotype 6 teeth ML2422 (A), ML2423 (B), ML2424 (C), ML2525 (D) and ML2626 (E) in labial (1), lateral (2), lingual (3), apical (4) and basal (5) views. Scale bar is 1 mm. All images are normal-light photomicrographs except for A1, B4, C3 and D2, which are SEM photomicrographs. ..... - 101 -

Figure 2.2.7: Morphotype 7 teeth ML2455 (A), ML2456 (B), ML2457 (C) and ML2458 (D) in labial (1), lateral (2), lingual (3), apical (4) and basal (5) views. Scale bar is 1 mm. All images are normal-light photomicrographs except for A2, B1, C4, and D3, which are SEM photomicrographs. ... - 105 -

Figure 2.2.8: Morphotype 8 tooth ML2478 in labial (1), lateral (2), lingual (3), basal (4) and apical (5) views. Scale bar is 1 mm. All images are normal-light photomicrographs. ..... - 107 -

Figure 2.2.9: Morphotype 9 teeth ML2479 (A), ML2481 (B), ML2482 (C), ML2483 (D) and ML 2480 (E) in labial (1), lateral (2), lingual (3), basal (4) and apical (5) views. E6 shows ML2480 in lingual view with the root

preserved. The arrows point the lingual groove that can be observed in some specimens. Scale bars are 1 mm. All images are normal-light photomicrographs except for A3, B1, C2, E1–E3 and E5, which are SEM photomicrographs. ..... - 109 -

Figure 2.2.10: Morphotype 10 teeth ML2473 (A), ML2474 (B) and ML2475 (C) in labial (1), lateral (2 and 4), lingual (3), basal (5) and apical (6) views. Scale bar is 1 mm. Close-ups of ML2475 denticles in labial (7, 8), lateral (9) and lingual (10) views. Scale bars are 100 μm. All images are normal-light photomicrographs except for C1–C4 and C6–C10, which are SEM photomicrographs. ..... - 113 -

Figure 2.2.11: *Lusitanisuchus mitracostatus* jaw bones from the Guimarota collection. **A–B**, *Lusitanisuchus mitracostatus* left premaxilla–maxilla MG26103 (IPFUB Gui Croc 8002) in labial (A) and lingual (B) views with enlargements and schematic drawings of one tooth to illustrate tooth morphology. **C**, *Lusitanisuchus mitracostatus* right maxilla (IPFUB Gui Croc 8009) in labial view with enlargement and schematic drawing of one tooth to illustrate tooth morphology. Scale bar for the general views (left) is 1 cm, scale bar for enlargements and drawings (right) is 2 mm for A and B and 1 mm for C. ..... - 117 -

Figure 2.2.12: *Lusitanisuchus mitracostatus* left dentary MG26081 (IPFUB Gui Croc 7505) in labial (A), lingual (B), apicolabial (C) and apicolingual (D) views, with enlargements and schematic drawings of three teeth (from anterior to posterior: a, b, and c) to illustrate tooth morphology. Scale bar for the general views (left) is 1 cm. Scale bar for the enlargements and drawings (right) is 1 mm. ..... - 119 -

Figure 2.2.13: Enlargement of the teeth of the *Lusitanisuchus mitracostatus* dentary MG28911 (IPFUB Gui 75 6.03) (from anterior to posterior: *a* and b) and schematic drawings to illustrate tooth morphology, in labial (A), lingual (B) and apicolingual views (C, D). Scale bar is 1 mm. ..... - 121 -

Figure 2.2.14: Comparison of the maximum height (in mm) of the crocodylomorph teeth recorded from Valmitão (blue) and La Cantalera in Spain (red), and in adult (green) and juvenile specimens (purple). The red

dots for La Cantalera represent the outliers. Data from: Averianov, 2000; Wings *et al.*, 2010; Kuzmin *et al.*, 2013; Puértolas-Pascual *et al.*, 2015a, b; Martin *et al.*, 2016. ..... - 125 -

Figure 2.2.15: Distribution of the teeth according their morphotypes (1–10) and their ecomorphotypes (A–D), and the corresponding taxa to which they are thus attributed. ..... - 129 -

Figure 2.2.16: Palaeogeographic maps of Europe with Upper Jurassic (A) and Lower Cretaceous (B) localities yielding mesoeucrocodylian assemblages with *Goniopholis*, *Theriosuchus* and *Bernissartia*. Blue star indicates the locality of Valmitão, Lourinhã Formation (Ribamar, Portugal). 1. Guimarota Mine, Alcobaça Formation (Leiria, Portugal). 2. Langenberg/Oker, Langenberg Formation (Germany). 3. Andrès, Alcobaça Formation (Pombal, Portugal). 4. Montrouge and La Rochette II, the Formations généreuses (Boulogne-sur-Mer & Wimille, France). 5. Swanage, Purbeck Limestone Group (Dorset, England). 6. Cherves-de-Cognac, gypsum and marlstone units equivalent to Purbeck Limestone Group (France). 7. Arnager, Rabekke Formation (Bornholm, Denmark). 8. Eriksdal, Annero Formation (Skåne, Sweden). 9. Isle of Wight, Wessex Formation (England). 10. Galve, El Castellar Formation and Camarillas Formation (Teruel, Spain). 11. Uña, Uña Formation (Cuenca, Spain). 12. Pio Pajarón, Uña Formation (Cuenca, Spain). 13. Buenache de la Sierra, La Huérguina Limestone Formation (Cuenca, Spain). 14. Vallipón and La Cantalera, Artoles Formation and Blesa Formation (Teruel, Spain). 15. Bernissart, Sainte-Barbe clays (Belgium). Modified from Schwarz-Wings *et al.* (2009); palaeomaps from Colorado Plateau Geosystem. Scale bars are 400 km. ..... - 137 -

Figure 2.2.17: Crocodylomorph tooth distribution from the La Cantalera (Puértolas-Pascual *et al.*, 2015b), the Bornholm & Skåne (Schwarz-Wings *et al.*, 2009) and the Buenache de la Sierra (Buscalioni *et al.*, 2008) assemblages, also with assemblages from the Cloverly Formation (Oreska *et al.*, 2013; Carrano *et al.*, 2016) and the Tremp Formation (Blanco *et al.*, 2020), compared with the Valmitão vma, according to tooth morphotypes (A) and their ecomorphotypes (B). ..... - 139 -

Figure 2.3.1: Geographical and geological context of the vertebrate microfossil assemblages localities from the Alcobaça Formation. **A**, map of Europe, modified from Erin Dill; scale is 400 km. **B**, geological sketch of the Iberian Peninsula, showing the location of the study area (red star); scale is 200 km. **C**, geological sketch of the Leria area, showing the location of the assemblage (modified from Teixeira *et al.* 1966); scale on the map represents 500 m. The entrance of the Guimarota mine, together with the outline of the pit and the approximate location of the fossil beds (blue area) are shown. Note that the fossil locality is located 30 meters below the surface, in the Upper Jurassic formations overlayed by the Cretaceous (see Section 1.1). **D**, stratigraphic position of the Guimarota beds and stratigraphic log of the Guimarota beds. General stratigraphic sketch derived from data in Teixeira et al. 1968. The colours for each stage correspond to the ones used in the map. Detailed stratigraphic log of the Alcobaça Formation from Schudack 2000*a*. ..... - 151 -

Figure 2.3.2: *Cteniogenys* aff. *C. antiquus* jaw material from the Guimarota beds. **A**, left premaxilla MG27600 in labial (A_1), lingual (A_2), and ventral (A_3) views. **B**, right maxilla MG27417 in lateral (B_1) and ventral (B_2) views. **C**, right maxilla MG27419 (Gui L. 234; fig. 4 in Seiffert, 1973) in lingual (C_1) view. **D**, right dentary MG27628 (designated holotype Gui A33 fig. 3 in Seiffert, 1973) in lingual (D_1), dorsal (D_2), and labial (D_3) views. **E**, left dentary MG28514 in lingual (E_1) and labial (E_2) views. **F**, left surangular MG27423 in medial (F_1), lateral (F_2), ventral (F_3) and dorsal (F_4) views. Abbreviations: **ab**, alveolar border; **adf**, adductor facet; **agf**, angular facet; **atf**, lateral articular facets; **dbd**, dorsal border; **dp**, dorsal process; **enf**, external nutrient foramen; **fa**, facet for the articular; **mdp**, medial process; **mkc**, Meckelian canal; **mxf**, maxillary facet; **obp**, orbital process; **paf**, prearticular facet; **ptf**, palatine facet; **sdr**, subdental ridge; **spf**, facet for the splenial; **sym**, symphysis. Scale for A is 1 mm; scales for B and F are 3 mm; scales for C, D, and E are 5 mm. ..... - 159 -

Figure 2.3.3: *Cteniogenys* aff. *C. antiquus* axial and appendicular skeleton. **A**, dorsal vertebra MG28512 in dorsal (A_1), lateral (A_2), ventral (A_3), anterior (A_4), and posterior (A_5) views. **B**, anterior caudal vertebra

MG28514 in dorsal (B_1), lateral (B_2), ventral (B_3), anterior (B_4), and posterior (B_5) views. **C**, dorsal/sacral vertebra MG28552 in dorsal (C_1), lateral (C_2), ventral (C_3), anterior (C_4), and posterior (C_5) views. **D**, mid-caudal vertebra MG28287 in anterior (D_1) and ventral (D_2) views. **E**, left humerus MG28928 in lateral (E_1) and medial (E_2) views. **F**, right ilium MG28289 in medial (F_1) and lateral (F_2) views. Abbreviations: ***a*c**, acetabulum; **ect**, ectotuberosity; **imf**, Iliac medial facet; **is**, iliac shaft; **is*a***, ischial articulation; **mdc**, median crest; **mdf**, mediodorsal facet; **mvf**, Medioventral flanges; **n*a***, neural arch; **p*a***, pubic articulation; **rbf**, rib articular facet; **s*ar***, supraacetabular ridge. Scales for A, B, C, D, and E are 1 mm. Scale for F is 3 mm. ..... - 163 -

Figure 2.3.4: Cranial bones of New unnamed taxon 1. A, right premaxilla MG27588 in ventral (A_1) and dorsal (A_2) views. B, right maxilla MG28841 (putative holotype) in dorsal (B_1), lateral (B_2), ventral (B_3), and medial views (B_4). C, right dentary MG28785 in dorsal (C_1), medial (C_2), and lateral views (C_3); the specimen is broken, but both parts could be put together for the lateral and medial views. Abbreviations: ***a*b**, alveolar border; ***a*np**, anterior process; **cf**, coronoid facet; **dp**, dorsal process; **dr**, dorsal subdental ridge; **enf**, external nutrient foramen; **lcf**, lacrimal facet; **mkc**, Meckelian canal; **mxf**, maxillary facet; **nrp**, narial process; **pde**, *pars dentalis*; **ptf**, palatine facet; **snr**, subnarial ramus; **sym**, symphysis; **vl**, ventral lip. Scale for A is 1 mm. Scales for B and C are 5 mm..... - 175 -

Figure 2.3.5: Frontal bones of New unnamed taxon 1. A, frontal MG28741in ventral (A_1), dorsal (A_2), lateral right (A_3), and lateral left (A_4) views. B, frontal MG28742 MG28741in ventral (B_1), dorsal (B_2), lateral right (B_3), and lateral left (B_4) views. Abbreviations: **cc**, *crista cranii*; **fdp**, frontal paired ventral depressions; **pff**, prefrontal facet; **psf**, postfrontal facet; **vv**, ventral vertex. Scale is 5mm. ..... - 181 -

Figure 3.1.1: Geographical and geological context of the new Albanerpetontidae occurrences from the Lourinhã formation. **A**, Europe map modified from Erin Dill, scale represents 400 km. **B**, geological sketch of the Iberian Peninsula, showing the location of the study area (purple star). **C**, map of the onshore part of the Consolação subbasin south of Peniche

(modified from Taylor *et al.*, 2014). The green star indicates the location of the Valmitão VMA, the pink star indicates the location of Porto Dinheiro VMA, the yellow star indicates the location of Zimbral VMA, the red star indicates the location of Port das Barcas VMA, the brown star indicates the location of Peralta VMA. **D**, north–south mapping of the main units in the area of study and their corresponding lithostratigraphic framework indicated by arrows (modified from Taylor *et al.*, 2014, based on Mateus *et al.*, 2017). Arrow colours correspond to star colours. ..... - 207 -

Figure 3.1.2: Main anatomical features of albanerpetontid frontal bones, based on reconstruction from specimen ML2738, in dorsal, ventral, and lateral views. ***a*p**, anterolateral process; **c*a***, canal; **fo**, foramen; **ip**, internasal process; **lif**, lateroventral internasal facet; **mpf**, middle part of the frontal; **n*a*f**, nasal facet; **om**, orbital margin; **pf**, parietal facet; **pff**, prefrontal facet; **vc**, ventrolateral crest; **vr**, ventral roof; **vs**, ventromedian suture. Scale bar represents 1 mm. ..... - 211 -

Figure 3.1.3: Measurements taken in the frontal bones represented in **Table 3.1.1**. Measurements in blue represent metric measurements; measurements in dark pink represent angle measurements. **CPE**, curvature at the posterior part of the edge (in degrees); **FIW**, frontal inner width between ventrolateral crests, across posterior edges of the frontal ventral roof; **FL**, total length of the frontal; **FML**, frontal length at the midline; **FW**, frontal width across posterior edges; **INL**, internasal length at the midline; **INW**, internasal width at the base; **IVCW**, interventrolateral crests width; **OML**, orbital margin length; **SW**, slot width, between the posterior slots for the prefrontal; **VCAW**, ventrolateral crest anterior width, behind prefrontal facets; **VCC**, ventrolateral crest curvature (in degrees); **VCPW**, ventrolateral crest posterior width, before parietal facets. ..... - 215 -

Figure 3.1.4: Normal-light photomicrograph of aff. Celtedens sp. frontal bones from the Lourinhã Formation in dorsal (left) and ventral (right) views. **A**, ML2738; **B**, ML2739; **C**, ML 2740; **D**, ML2741; **E**, FCT/UNL-CN00016; **F**, FCT/UNL-CN00018. Scale bars represent 1 mm. ..... - 223 -

Figure 3.1.5: Normal-light photomicrograph of aff. Celtedens sp. frontal bones from the Alcobaça Formation in dorsal (left) and ventral view (right). **A**, MG28426; **B**, MG28427; **C**, MG28473; **D**, MG28502; **E**, MG28520; F, MG28521; **G**, MG28532; **H**, MG28539; **I**, MG28541; **J**, MG28543; **K**, MG28562; **L**, MG28570; **M**, MG28572; **N**, MG28692; **O**, MG28694; **P**, MG28733. Scale bars represent 1 mm. ..... - 225 -

Figure 3.1.6: Principal component analysis based on 7 variables in scaling 1 (**A**) and scaling 2 (**B**). Orange dots represent specimens from the Lourinhã Formation, blue dots represent specimens from the Alcobaça Formation. .. - 231 -

Figure 3.1.7: **A**, K-means partitions comparison; each colour represents a different group to which the specimens (x-axis) are attributed. **B**, Simple Structure Index criterion corresponding to each partition (best SSI = 0.59). **C**, Linear discriminant analysis (confusion matrix with Jackknifed resampling = 88.24%). ..... - 233 -

Figure 3.1.8: Linear regression to test the allometry in the ventrolateral crests (**A**), the internasal process (**B**), and slot width, between the posterior slots for the prefrontal (**C**). The blue line represents the model, and the grey area the 95% confidence interval. ..... - 235 -

Figure 3.1.9: Consensus tree of the 10 MPTs recovered under implied weights. Fit= 2.07857; length=73 steps; CI=0.603, RI = 0.724. Black numbers are bootstrap values to the corresponding nodes. Bold number are synapomorphies (italic not related to the frontal bones, blue related to the frontal bones). **Node 1**, Albanerpeton s.l.; **Node 2**, "robust-snouted clade" *sensu* Venczel and Gardner, 2005; **Node 3**, Albanerpeton s.s..... - 237 -

Figure 3.1.10: Consensus tree of the 1 MPT recovered under implied weights. Fit=1.99066; length=72 steps; CI=0.611, RI = 0.714. Black numbers are bootstrap values to the corresponding nodes. Bold number are synapomorphies (italic not related to the frontal bones, blue related to the frontal bones). **Node 1**, Albanerpeton s.l.; **Node 2**, "robust-snouted clade" *sensu* Venczel and Gardner, 2005; **Node 3**, Albanerpeton s.s..... - 239 -

Figure 3.1.11: K-mean partitions comparison and the associated SSI criterion for up to 16 groups. ..... - 244 -

Figure 3.1.12: Evolution of the frontal bone in Albanerpetontidae, based on the consensus tree from the present analysis plotted against time and with geographic occurrences. Frontals are from the literature and associated with their respective species (scale bars represent 1 mm). No frontal has been described yet for Albanerpeton cifellii Gardner 1999c. Synapomorphies related to the frontal bones are indicated by lower-case letters. ..... - 251 -

Figure 3.2.1: Geographical and geological context of the vertebrate microfossil assemblages (VMAs) localities from the Lourinhã Formation. **A**, Europe map modified from Erin Dill, scale represents 400 km. **B**, geological sketch of the Iberian Peninsula, showing the location of the study area (orange sun). **C**, map of the onshore part of the Consolação subbasin south of Peniche (modified from Taylor *et al.* 2014). The green star indicates the location of the Valmitão and red Valmitão VMAs, blue star is Porto Dinheiro VMA, yellow star corresponds to Zimbral VMA, vermillion star is Porto das Barcas VMA, and reddish-purple star indicates the location of Peralta VMA. **D**, north–south mapping of the main units in the area of study, and their corresponding chronostratigraphic framework and location of the sites indicated by stars (modified from Taylor *et al.* 2014, based on Mateus *et al.* 2017). ..... - 259 -

Figure 3.2.2: Count fossil remains referred to Albanerpetontidae collected from the Lourinhã Formation. **A**, count of elements by anatomical region for each five VMAs, with the number total of elements indicated on top of the bars. **B**, count by element, all VMAs combined together: the black dot *indicates* the mean between each VMAs. **C**, correspondence analysis scaling 1 (two first axes explained 76.484% of variation related to association). .. - 263 -

Figure 3.2.3: New unnamed taxon 2 images of three-dimensional models of premaxillary bones. **A**; left premaxilla ML2912 in lateral (a), labial (b), medial (c), lingual (d), dorsal (e), and ventral (f) views. **B**; right premaxilla ML2913 in lateral (a), labial (b), medial (c), lingual (d), dorsal (e), and

ventral (f) views. **C**; right premaxilla ML2914 in lateral (*a*), labial (b), medial (c), lingual (d), dorsal (e), and ventral (f) views. **D**; left premaxilla ML2915 in lateral (*a*), labial (b), medial (c), lingual (d), dorsal (e), and ventral (f) views. Abbreviations: **db**, dorsal boss; **ldn**, laterodorsal notch; **mf**, medial flange; **mxf**, maxillary facet; **mxp**, maxillary process; **pdo**, *pars dorsalis*; **pde**, *pars dentalis*; **plf**, palatal foramen; **pp**, *pars palatinum*; **spp**, suprapalatal pit. Scale bar is 1 mm. ..... - 275 -

Figure 3.2.4: New unnamed taxon 2 images of three-dimensional models of maxillary bones. **A**; right maxilla ML2937 in dorsal (*a*), lingual (b), ventral (c), labial (d), and anterior (e) views. **B**; right maxilla ML2938 in dorsal (*a*), lingual (b), ventral (c), labial (d), and anterior (e) views. Abbreviations: **inm**, internal narial margin; **mxs**, maxillary shelf; **np**, nasal process; **pde**, *pars dentalis*; **pdp**, premaxillary dorsal process; **pfa**, *pars facialis*; **plp**, premaxillary lateral process; **pp**, *pars palatinum*. Scale bar is 1 mm. - 281 -

Figure 3.2.5: New unnamed taxon 2 images of three-dimensional models of fused frontal bones. **A**; frontal ML2741 in dorsal (*a*), ventral (b), anterior (c), and lateral (d) views. **B**; frontal ML2738 in dorsal (*a*), ventral (b), anterior (c), and lateral (d) views. **C**; frontal ML2739 in dorsal (*a*), ventral (b), and lateral (c) views. **D**; frontal ML2743 (putative holotype) in dorsal (*a*), ventral (b), anterior (c), and lateral (d) views. Abbreviations: **ap**, anterolateral process; **ca**, canal; **ip**, internasal process; **naf**, nasal facet; **om**, orbital margin; **pf**, parietal facet; **pff**, prefrontal facet; **vc**, ventrolateral crest; **vr**, ventral roof; **vrd**, ventral ridge of the anterolateral process; **vs**, ventromedian suture. Scale bar is 1 mm. ..... - 285 -

Figure 3.2.6: New unnamed taxon 2 lacrimal bone ML2947 in labial (*a*) and lingual (b) views. Abbreviations: **dp**, dorsal process; **laf**, lacrimal foramen; **llm**, lateral lamina; **naf**, nasal facet; **ob**, orbital border; **vp**, ventral proces. Scale bar is 1 mm. ..... - 287 -

Figure 3.2.7 : New unnamed taxon 2 Parietal bones. **A**, parietal ML2949 in dorsal (*a*, SEM picture) and ventral (b) views. **B**, parietal ML2950 in ventral views (SEM picture). **C**, reconstruction of *a* parietal bone in dorsal (*a*) and ventral (b) views, not to scale. Abbreviations: **faf**, frontoparietal articular

facet; **lm**, lateral margin; **pow**, postorbital wing; **vtc**, ventral transverse crest. Scale bar is 1 mm. ..... - 289 -

Figure 3.2.8: New unnamed taxon 2 images of three-dimensional models of dentary bones, anterior part. **A**; right dentary ML2951 in lingual (*a*), ventral (b), labial (c), dorsal (d), and anterior (e) views. **B**; right dentary ML2952 in lingual (*a*), ventral (b), labial (c), dorsal (d), and anterior (e) views. **C**; right dentary ML2954 in lingual (*a*), ventral (b), labial (c), dorsal (d), and anterior (e) views. Abbreviations: **dlc**, dorsolateral canal; **dpg**, dorsal prong; **dpt**, dental parapet; **enf**, external nutrient foramen; **em**, eminence; **ima**, *intermandibularis* musculature attachment; **mkc**, Meckelian canal; **sds**, subdental shelf; **syf**, symphiseal foramen; **sym**, symphysis; **vpg**, ventral prong. Scale bar is 1 mm. ..... - 293 -

Figure 3.2.9: New unnamed taxon 2 images of three-dimensional models of dentary bones, posterior part. **A**; left dentary ML2953 in lingual (*a*), ventral (b), labial (c), and dorsal (d) views. **B**; right dentary ML2955 in lingual (*a*), ventral (b), labial (c), and dorsal (d) views. **C**, reconstruction of a right dentary in lingual view (not to scale). Abbreviations: **dlc**, dorsolateral canal; **dpg**, dorsal prong; **dpt**, dental parapet; **em**, eminence; **fo**, foramen; **ima**, *intermandibularis* musculature attachment; **mkc**, Meckelian canal; **omk**, opening of the Meckelian canal; **paf**, prearticular facet; **sds**, subdental shelf; **vpg**, ventral prong. Scale bar is 1 mm. ..... - 295 -

Figure 3.2.10 : New unnamed taxon 2 images of three-dimensional models of left articular ML3000 in ventral (*a*), dorsal (b), lateral (c), anterior (d), and medial (e) views. Abbreviations: **df**, dentary facet; **dg**, dorsal groove of the abductor fossa; **gf**, glenoid fossa; **paf**, prearticular facet. Scale bar is 1 mm. ..... - 299 -

Figure 3.2.11: New unnamed taxon 2 left articular ML2999 in medial (*a*, SEM picture) and lateral views (b); and right articular ML3001 in lateral view (SEM picture). Abbreviations: **df**, dentary facet; dg, dorsal groove of the abductor fossa; **gf**, glenoid fossa; **paf**, prearticular facet. Scale bar is 1 mm. ..... - 301 -

Figure 3.2.12: New unnamed taxon 2 quadrate bones. **A**, right quadrate ML3009 in ventral view (SEM picture). **B**, left quadrate ML3010 in ventral (*a*), lateral (b), and dorsal (c, SEM picture) view. Abbreviations: **cd**, condyle; **dp**, dorsal process; **lco**, lateral concavity; **ldm**, laterodorsal margin; **llp**, lateral lip; **lvm**, lateroventral margin; **mb**, medial boss. Scale bar is 1 mm. - 303 -

Figure 3.2.13: New unnamed taxon 2 images of three-dimensional models of cervical vertebral series. **A**, atlas ML3012 in dorsal (*a*), anterior (b), ventral (c), posterior (d), and lateral (e) views; the dash lines delimit the bone. **B**, atlas ML3013 in dorsal (*a*), anterior (b), ventral (c), posterior (d), and lateral (e) views. **C**, axis ML3018 in dorsal (*a*), anterior (b), ventral (c), posterior (d), and lateral (e) views. **D**, axis ML3019 in dorsal (*a*), anterior (b), ventral (c), posterior (d), and lateral (e) views. Abbreviations: **act**, anterior cotyle; **dcd**, dorsal condyle; **op**, odontoid process; **pct**, posterior cotyle; **sf**, spinal foramen; **sg**, spinal groove; **vcd**, ventral condyle. Scale bar is 1 mm. ..... - 307 -

Figure 3.2.14 : New unnamed taxon 2 images of three-dimensional models of dorsal vertebral series. **A**, dorsal vertebra ML3023 in lateral (*a*), ventral (b), lateral (c), dorsal (d), and anteroposterior € views. **B**, dorsal vertebra ML3024 in lateral (*a*), ventral (b), lateral (c), dorsal (d), and anteroposterior (e, f) views. Abbreviations: **naa**, neural arch articulation; **nc**, neural canal; **np**, notochordal pit; **tp**, transverse process. Scale bar is 1 mm. ..... - 309 -

Figure 3.2.15: New unnamed taxon 2 images of three-dimensional models of hindlimbs. **A**, proximal right humerus ML3103 in dorsal (*a*), lateral (b), ventral (c), and medial (d) views. **B**, proximal right humerus ML3108 in dorsal (*a*), lateral (b), ventral (c), and medial (d) views. **C**, distal right humerus ML3109 in dorsal (*a*), lateral (b), ventral (c), and medial (d) views. **D**, distal left humerus ML3110 in dorsal (*a*), lateral (b), ventral (c), and medial (d) views. **E**, distal left humerus ML3111 in dorsal (*a*), lateral (b), ventral (c), and medial (d) views. **F**, proximal right humerus ML3112 in dorsal (*a*), lateral (b), ventral (c), and medial (d) views. Abbreviations: **dpc**, deltopectoral crest; **ec**, ectepicondyle; **en**, entepicondyle; **fcc**, *fossa cubitus*

cristalis; **phc**, proximal humeral condyle; **phf**, proximal humeral fossa; **rcd**, Radial condyle. Scale bar is 1 mm. ..... - 311 -

Figure 3.2.16: New unnamed taxon 2 left ilium ML3128 in lateral (*a*, SEM picture) and medial (b) views. Abbreviations: ***a*c**, acetabulum; **is**, iliac shaft; **is*a***, ischial articulation; **p*a***, pubic articulation. Scale bar is 1 mm. .. - 315 -

Figure 3.2.17 : New unnamed taxon 2 images of three-dimensional models of hindlimb. **A**, proximal left femur ML3131 in proximal (*a*), lateral (b), dorsal (c), medial (d), and ventral (e) views. **B**, distal femur ML3130 in distal (*a*), lateromedial left (b), anterior (c), lateromedial right (d), and posterior € views. Abbreviations: **dep**, distal epiphysis; **lgr**, longitudinal groove; **pep**, proximal epiphysis; **tcg**, trochlear groove; **tch**, trochanter. Scale bar is 1 mm. ..... - 317 -

Figure 3.2.18: Albanerpetontidae skull (lateral view, scale 5mm) and skeleton (dorsal view, scale 10 mm) reconstructions, showing the bones found in the Lourinhã Formation. Dorsal and caudal vertebrae are in blue as their exact position cannot be assessed from isolated fragmented specimens. Skull reconstruction based on *Y. perettii* from Daza *et al*. (2020). Skeleton reconstruction from Schoch (2014), based on *C. ibericus* from McGowan (2002). ..... - 319 -

Figure 3.3.1: New unnamed taxon 3 upper jaw bones. **A**; left premaxilla BLA2-A98 in lingual (*a*), labial (b), medial (c), and ventral (d) views. **B**; left premaxilla MPZ 2023/434 in lingual view. **C**; left maxilla MPZ 2023/433 in ventral view. **D**; right maxilla MPZ 2023/435 in lingual view. A is photostacking photographs, B–D are SEM images. Abbreviations: **ist**, internal strut; **mf**, medial flange; **mxf**, maxillary facet; **pdo**, *pars dorsalis*; **pde**, *pars dentalis*; **plf**, palatal foramen; **pp**, *pars palatinum*; **spp**, suprapalatal pit. Scale bar represents 1 mm. ..... - 339 -

Figure 3.3.2: New unnamed taxon 3 skull roof bones. **A**; fused frontal bones MPZ 2009/219 (putative holotype) in ventral (*a*) and dorsal (b, reconstructed from fragments) views. **B**; frontal MPZ 2023/431 in ventral view. **C**; frontal MPZ 2023/430 in dorsal view. **D**; frontal MPZ 2023/442 in anteroventral (*a*), dorsal (b), anterodorsal (c), and lateral (d) views. **E**;

parietal MPZ 2023/432 in dorsal view. Only the posterior part of MPZ 2009/219 was previously published (fig. 2; Blain *et al.*, 2010), but the anterior section was found with the same label and fits. A is photostacking photographs, B–D are SEM images. Abbreviations: **ap**, anterolateral process; **ip**, internasal process; **lm**, lateral margin; **naf**, nasal facet; **om**, orbital margin; **pf**, parietal facet; **pff**, prefrontal facet; **vc**, ventrolateral crest; **vrd**, ventral ridge of the anterolateral process. Scale bar represents 1 mm. ..... - 343 -

Figure 3.3.3: New unnamed taxon 3 left dentary MPZ 2023/436 in lingual (*a*) and dorsal (b) views (SEM images). Abbrevations: **em**, eminence; **dpg**, dorsal prong; **sym**, symphysis; **vpg**, ventral prong. Scale bar represents 1 mm. ..... - 345 -

Figure 3.3.4: New unnamed taxon 3 articular. **A**; right articular MPZ 2023/437 in medial view. **B**; left articular MPZ 2023/439 in medial view. **C**; left articular MPZ 2023/438 in lateral view. **D**; left articular MPZ 2023/440 in lateral view. **E**; left articular MPZ 2023/443 in dorsal (*a*), posterior (b), dorsolateral (c), and dorsomedial (d) views. All are SEM images. Abbreviations: **atb**, anterior tuberosity; **df**, dentary facet; **dg**, dorsal groove of the abductor fossa; **gf**, glenoid fossa; **paf**, prearticular facet. Scale bar represents 1 mm. ..... - 347 -

Figure 3.3.5: New unnamed taxon 3 left quadrate MPZ 2023/441 in anterior (*a*), ventral (b), dorsal (c), medial (d) and anterolateral (e) views. All are SEM pictures. Abbreviations: **cd**, anterior condyle; **lco**, lateral concavity; **ldm**, laterodorsal margin; **llp**, lateral lip; **lp**, lateral pillar; **lvf**, lateroventral facet; **lvm**, lateroventral margin; **mb**, medial boss. Scale bar is 1 mm.- 349 -

Figure 3.3.6: New unnamed taxon 3 cervical vertebral series. **A**, atlas centrum vertebra BLA2-A43 in anterior (*a*), posterior (b), dorsal (c), ventral (d), and left lateral (e) views. **B**, axis vertebra BLA2-A110 fused with anterior portion of centrum first dorsal vertebra in dorsal (*a*), ventral (b), right lateral (c), and anterior (d) views. A and B are photostacking photographs. Abbreviations: **act**, anterior cotyle; **dcd**, dorsal condyle; **dv**,

1st dorsal vertebra; **op**, odontoid process; **pct**, posterior cotyle; **sf**, spinal foramen; **sg**, spinal groove; **vcd**, ventral condyle. Scale bar represents 1 mm. ..... - 351 -

Figure 3.3.7: New unnamed taxon 3 forelimbs. **A**; proximal end of left humerus MPZ 2023/444 in medial (*a*) and lateral (b). **B**; distal end of left humerus MPZ 2023/445 in dorsal (*a*), lateral (b), and ventral (c) views. **C**; proximal end of left humerus MPZ 2023/428 in medial view. **D**; proximal end of left humerus MPZ 2023/427 in ventral view. **E**; proximal end of left humerus MPZ 2023/429 in lateral view. **F**; distal end of right humerus MPZ 2009/221 in dorsal (*a*), lateral (b), ventral (c), and medial (d) views. A, B, and F are photostacking photographs. C–E are SEM images. A and B are stored under the same label and were broken, but indeed seem to fit together. Abbreviations: **dpc**, Deltopectoral crest; **ec**, ectepicondyle; **en**, entepicondyle; **fcc**, *fossa cubitus centralis*; **pdf**, proximo-distal furrow; **phc**, proximal humeral condyle; **phf**, proximal humeral fossa; **rcd**, Radial condyle. Scale bar is 1 mm..... - 353 -

Figure 3.4.1: Strict consensus tree of the 2 MPTs recovered. Length = 163 steps; CI = 0.472; RI = 0.598. Black numbers above branches are bootstrap values over 50 for the corresponding nodes. Colour numbers are synapomorphies of New unnamed taxon 2 and New unnamed taxon 3 (orange are for frontal characters, reddish purple for parietal characters, yellow for cervical vertebrae characters, vermillion for ilium characters). Alternate branching from the two MPTs (lower left) are provided to illustrate the position of New unnamed taxon 3. **Node 1**, unnamed clade comprising species previously attributed to both *Albanerpeton* s.l. and *Albanerpeton* s.s. (Daza *et al.*, 2020; Carrano *et al.*, 2022); **Node 2**, Albanerpeton; **Node 3**, "robust-snouted clade" *sensu* Venczel & Gardner, 2005. ..... - 379 -

Figure 3.4.2: Palaeogeographic distribution of European albanerpetontid occurrences during the Late Cretaceous (Santonian–Maastrichtian), based on data from **Table 3.3.1**. Shapes refer to the age, colors to the taxonomic affinities. Dark blue occurrences share more affinities with New unnamed taxon 3 than light blue occurrences. Arrows illustrate the putative geographical influences of both European albanerpetontid faunas. Base

map: Late Campanian ~75 Mya, Colorado Plateau Geosystems Inc., Deep Time Maps™. ..... - 395 -

Figure E.1: Character states in *Albanerpeton arthridion* (0), *Wesserpeton evansae* (1), and *Albanerpeton pannonicum* (2) in character 37. ..... - 631 -

Figure E.2: Character states in *Wesserpeton evansae* (0) and *Albanerpeton pannonicum* (1) in character 38. ..... - 632 -

Figure F.1: **A**; MG28568 in labial (right) and lingual view (left). **B**; SMNS 57819/1 in lingual view. **C**; SMNS 57769/3 in lingual view. B and C are from Wiechmann Phd thesis (2003; pl. VII, fig.4-6). Scales are 1 mm. ..... - 640 -

Figure F.2: Premaxillae from Guimarota beds. **A**, MG28600. **B**, MG28611. **C**, MG28612. **D**, MG28624. **E**, MG28630. Specimens are shown from left to right in labial, lateral, lingual, medial, and ventral views. Scale is 1 mm. . - 652 -

Figure F.3: Premaxillae from Guimarota beds. **A**, MG28645. **B**, MG28645. **C**, MG28650. **D**, MG28650. **E**, MG28651. Specimens are shown from left to right in labial, lateral, lingual, medial, and ventral views. B and C and D and E are respectively from the same labelled box, hence the same specimen number. Scale is 1 mm. ..... - 653 -

Figure F.4: Maxillae from Guimarota beds. **A**, MG28432. **B**, MG28487. **C**, MG28675. **D**, MG28683. **E**, MG28724. Specimens are shown from left to right in dorsal, labial, lingual, and ventral views. Scale is 1 mm. ..... - 654 -

Figure F.5: Frontal bones from Guimarota beds in dorsal (left) and ventral view (right). **A**, MG28426. **B**, MG28427. **C**, MG28473. **D**, MG28502. **E**, MG28520. **F**, MG28521. **G**, MG28532. **H**, MG28539. **I**, MG28541. **J**, MG28543. **K**, MG28562. **L**, MG28570. **M**, MG28572. **N**, MG28692. **O**, MG28694. **P**, MG28733. Scale bars represent 1 mm. ..... - 655 -

Figure F.6: Parietals from Guimarota beds. **A**, MG28595. **B**, MG28627. **C**, MG28646. **D**, MG28672. Specimens are shown from left to right in dorsal and ventral views. Scale is 1 mm. ..... - 656 -

Figure F.7: Dentaries from Guimarota beds. **A**, MG28423. **B**, MG28431. **C**, MG28534. **D**, MG28670. **E**, MG28535. **F**, MG28668. **G**, MG28657. Specimens are shown from left to right in dorsal, labial, and lingual views. Scale is 5mm. ..... - 657 -

Figure F.8: Dentaries from Guimarota beds. **A**, MG28677. **B–D**, MG28652. **E–G**, MG28662. Specimens A–D are shown from left to right in dorsal, labial, and lingual views; specimens E–G are shown from left to right in dorsal, labial, lingual, and ventral views. B–D and E–G are respectively from the same labelled box, hence the same specimen number. Scale is 3 mm. - 658 -

Figure F.9: Articulars from Guimarota beds. **A**, MG28208. **B**, MG28677. Specimens are shown from left to right in medial, lateral, and dorsal views. Scale is 1 mm. ..... - 659 -

Figure F.10: Axes from Guimarota beds. **A**, MG28666. **B**, MG28698. **C**, MG28722. **D**, MG28731. Specimens are shown from left to right in anterior, posterior, lateral, dorsal, and ventral views. Scale is 1 mm. ..... - 660 -

Figure F.11: Humeri from Guimarota beds. **A**, MG28506. **B**, MG28690. **C**, MG28720. Specimens are shown from left to right in dorsal, lateral, ventral, and medial views. Scale is 1 mm. ..... - 661 -

TABLE OF TABLES

Table 1.6.1: Chronological list of collection visits in non-Portuguese institutions, with a quick summary of the specimens checked. ..... - 57 -

Table 2.1.1: Faunal composition of the three Vertebrates Microfossil Assemblages (VMA) sampled from the Lourinhã Formation. ..... - 69 -

Table 2.2.1: Tooth counts for the crocodylomorph assemblage from Valmitão. ..... - 87 -

Table 3.1.1: Measurements (in mm) of the best-preserved specimens. **FML**, frontal length at the midline; **FL**, frontal length at the midline; **FW**, frontal width across posterior edges; **FIW**, frontal inner width between ventrolateral crests, across posterior edges of the frontal roof; **INL**, internasal length at the midline; **INW**, internasal width at the base; **SW**, slot width between the posterior slots for the prefrontal; **IVCW**, interventrolateral crests width; **OML**, Orbital margin length; **VCAW**, ventrolateral crest anterior width, behind prefrontal facets; **VCPW**, ventrolateral crest posterior width, before parietal facets; **CPE**, curvature at the posterior part of the edge (in degrees); **VCC**, ventrolateral crest curvature (in degrees). ..... - 213 -

Table 3.1.2: Main indexes calculated for the MPT, and each character considered for the frontal bones. ..... - 241 -

Table 3.3.1: Mesozoic Albanerpetontidae occurrences in Europe and North Africa, ordered from youngest to oldest. Age and correlation of Maastrichtian localities is based on the work of Pérez-Pueyo (2021a); age of the Pietraroja locality based on Bravi and Garassino (1998), Bartiromo (2013), and Graziano *et al*. (2024); and age of the Balve-Beckum locality based on Lanser and Heimhofer (2015). Information adapted and updated

from Gardner and Böhme (2008), Sweetman and Gardner (2013), Szentesi *et al*. (2013), and Venczel *et al*. (2016). ..... - 329 -

Table A.1: List of the new specimens described from the Lourinhã Formation and now housed in Museu da Lourinhã (ML), at the time of the delivery of the thesis (note that some identifications and descriptions may change later). For more information and possible updates, please contact the curator of the museum. Abbreviation: **PB**, Porto das Barcas; **PD**, Porto Dinheiro; **PER**, Peralta; **VAL**, Valmitão; **VALRED**, red layer of Valmitão; **ZIM**, Zimbral. ..... - 479 -

Table A.2: List of specimens from the Guimarota collection that have been checked during this PhD Thesis, with the original information provided by the catalogue of Museu Geológico. Refer to the manuscript for the revision of the relevant material. Please note that several specimen numbers can refer to sample boxes containing dozen or hundreds of fossils. ..... - 550 -

Table B.1: Simplified diversity and abundance data from the Lourinhã Formation. ..... - 591 -

Table B.2: Global counting of microfossil remains in each VMA from the Lourinhã Fm. ..... - 591 -

Table B.3: Raw data of counting from each sample bulk studied in the analysis. ..... - 593 -

Table B.4: Palaeoecological diversity in different Mesozoic VMAs. ... - 594 -

Table B.5: Palaeoecological abundance in different Mesozoic VMAs. - 595 -

Table C.1: List of remains picked from the sediments of the Valmitão VMA in 2019, according to the taxa they have been attributed. ..... - 597 -

Table C.2: Selected measurements (in mm for lengths, in degrees for angles) of the crocodylomorphs teeth morphotypes. **NLgS**, number of lingual striations; **NLbS**, number of labial striations; **DoM**, Denticles on mesial and distal margins. ..... - 598 -

Table D.1: List of the specimens from the Guimarota collection examined to identify *Cteniogenys* and *Marmoretta* specimens. ..... - 599 -

Table E.1: Log-transformed measurements for internasal process linear regression. **FML**, frontal length at the midline; **INL**, internasal length at the midline. ..... - 620 -

Table E.2: Log-transformed measurements for ventrolateral crest linear regression. **FIW**, frontal inner width between ventrolateral crests, across posterior edges of the frontal ventral roof; **VCAW**, ventrolateral crest anterior width, behind prefrontal facets. ..... - 621 -

Table E.3: Log-transformed measurements for slot width linear regression. **FW**, frontal width across posterior edges; **SW**, slot width, between the posterior slots for the prefrontal. ..... - 621 -

Table E.4: PCA scores from the frontal bone measurements. ..... - 622 -

Table E.5: PCA coefficient loadings..... - 623 -

Table E.6: PCA correlation loadings. ..... - 623 -

Table F.1: List of specimens that went under µCT-scan and the parameters associated for each..... - 641 -

ABBREVIATIONS

Institutional abbreviations

AMNH, American Museum of Natural History, New York, USA; **FCT-UNL**, Faculdade de Ciências e Tecnologia – Universidade Nova de Lisboa, Portugal; **FMNH**, Field Museum of Natural History, Chicago, Illinois, USA; **GRS**, Peretti MuseumFoundation and GemResearch Swisslab; **IPFUB**, Institut für Paläontologie, Freie Universität Berlin, Germany; **IPS**, Institut Català de Paleontologia Miquel Crusafont, Sabadell, Barcelona, Spain; **IWCMS**, Isle of Wight County Museums Service, Sandown, UK; **JZC**, James Zigras Collection, housed at the AMNH; **M**, Museo di Paleontologia, Napoli, Italy; **MCCM**, Museo de las Ciencias de Castilla La Mancha, Cuenca, Spain; **MG**, Museu Geológico, Lisbon, Portugal; **ML**, Museu da Lourinhã, Portugal; **MNHN**, Muséum national d'Histoire naturelle, Paris, France; **MPZ**, Museo Paleontológico de Zaragoza (Museo de Ciencias Naturales de la Universidad de Zaragoza), Spain; **NHMUK**, Natural History Museum, London, UK; **NMS**, National Museums of Scotland, Edinburgh, UK; **OMNH**, Oklahoma Museum of Natural History, Norman, Oklahoma, USA; **PDL**, Parque dos Dinossauros de Lourinhã, Portugal; **SGP**, Serviços Geológicos de Portugal, Lisbon; **RTMP**, Royal Tyrrell Museum of Palaeontology, Drumheller, Alberta, Canada;

SMNS, Staatlichen Museum für Naturkunde Stuttgart, Germany; **TMM**, Vertebrate Paleontology Laboratory at the Jackson School Museum of Earth History (University of Texas), Austin, Texas, USA; **UALVP**, University of Alberta Laboratory for Vertebrate Palaeontology, Edmonton, Alberta, Canada; **USNM**, National Museum of Natural History, Smithsonian Institution, Washington, DC, USA; **YPMVP**, Yale Peabody Museum – Vertebrate Paleontology, New Haven, Connecticut, USA.

Anatomical abbreviations

ab, alveolar border; **ac**, acetabulum; **act**, anterior cotyle; **adf**, adductor facet; **agf**, angular facet; **anp**, anterior process; **ap**, anterolateral process; **atf**, lateral articular facet; **ca**, canal; **cc**, *crista cranii*; **cd**, anterior condyle; **cf**, coronoid facet; **db**, dorsal boss; **dbd**, dorsal border; **dcd**, dorsal condyle; **dep**, distal epiphysis; **dg**, dorsal groove of the abductor fossa; **dlc**, dorsolateral canal; **dp**, dorsal process; **dpc**, deltopectoral crest; **dpg**, dorsal prong; **dpt**, dental parapet; **dr**, dorsal subdental ridge; **ec**, ectepicondyle; **ect**, ectotuberosity; **em**, eminence; **en**, entepicondyle; **enf**, external nutrient foramen; **fa**, facet for the articular; **faf**, frontoparietal articular facet; **fcc**, *fossa cubitus cristalis*; **fdp**, frontal paired ventral depressions; **fo**, foramen; **gf**, glenoid fossa; **ima**, *intermandibularis musculature* attachment; **imf**, Iliac medial facet; **inm**, internal narial margin; **ip**, internasal process; **is**, iliac shaft; **isa**, ischial articulation; **ist**, internal strut; **laf**, lacrimal foramen; **lco**, lateral concavity; **lcf**, lacrimal facet; **ldm**, laterodorsal margin; **ldn**,

laterodorsal notch; **lf**, lateral facet; **lgr**, longitudinal groove; **lif**, lateroventral internasal facet; **llm**, lateral lamina; **llp**, lateral lip; **lm**, lateral margin; **lp**, lateral pillar; **lvf**, lateroventral facet; **lvm**, lateroventral margin; **mb**, medial boss; **mdc**, median crest; **mdf**, mediodorsal facet; **mdp**, medial process; **mf**, medial flange; **mkc**, Meckelian canal; **mpf**, middle part of the frontal; **mvf**, medioventral flanges; **mxf**, maxillary facet; **mxp**, maxillary process; **mxs**, maxillary shelf; **na**, neural arch; **naa**, neural arch articulation; **naf**, nasal facet; **nc**, neural canal; **ncp**, notochordal pit; **np**, nasal process; **nrp**, narial process; **ob**, orbital border; **obp**, orbital process; **om**, orbital margin; **omk**, opening of the Meckelian canal; **op**, odontoid process; **pa**, pubic articulation; **paf**, prearticular facet; **pct**, posterior cotyle; **pdf**, proximo-distal furrow; **pde**, *pars dentalis*; **pdo**, *pars dorsalis*; **pdp**, premaxillary dorsal process; **pep**, proximal epiphysis; **pf**, parietal facet; **pfa**, *pars facialis*; **pff**, prefrontal facet; **phc**, proximal humeral condyle; **phf**, proximal humeral fossa; **plf**, palatal foramen; **plp**, premaxillary lateral process; **pow**, postorbital wing; **pp**, *pars palatinum*; **psf**, postfrontal facet; **ptf**, palatine facet; **rbf**, rib articular facet; **rcd**, radial condyle; **sar**, supraacetabular ridge; **sdr**, subdental ridge; **sds**, subdental shelf; **sf**, spinal foramen; **sg**, spinal groove; **snr**, subnarial ramus; **spf**, facet for the splenial; **spp**, suprapalatal pit; **syf**, symphiseal foramen; **sym**, symphysis; **tcg**, trochlear groove; **tch**, trochanter; **tp**, transverse process; **vc**, ventrolateral crest; **vcd**, ventral condyle; **vl**, ventral lip; **vmf**, ventromedial facet; **vp**, ventral process; **vpg**, ventral prong; **vr**, ventral

roof; **vrd**, ventral ridge of the anterolateral process; **vs**, ventromedian suture; **vtc**, ventral transverse crest; **vv**, ventral vertex.

Measurements

CPE, curvature at the posterior part of the edge (in degrees); **DoM**, Denticles on mesial and distal margins; **FIW**, frontal inner width between ventrolateral crests, across posterior edges of the frontal ventral roof; **FL**, total length of the frontal; **FML**, frontal length at the midline; **FW**, frontal width across posterior edges; **INL**, internasal length at the midline; **INW**, internasal width at the base; **IVCW**, interventrolateral crests width; **NLbS**, number of labial striations; **NLgS**, number of lingual striations; **OML**, orbital margin length; **SW**, slot width between the posterior slots for the prefrontal; **VCAW**, ventrolateral crest anterior width, behind prefrontal facets; **VCC**, ventrolateral crest curvature (in degrees); **VCPW**, ventrolateral crest posterior width, before parietal facets.

Localities

PB, Porto das Barcas; **PD**, Porto Dinheiro; **PER**, Peralta; **VAL**, Valmitão; **VALRED**, red layer of Valmitão; **ZIM**, Zimbral.

Others

SEM, scanning electron microscope; **VMA**, vertebrate microfossil assemblages.

1 INTRODUCTION

1.1 The vertebrate microfossil assemblage from the Guimarota beds

The Late Jurassic of Portugal has been proven to be quite productive in vertebrate fossil remains, either being turtles (de Lapparent de Broin, 2001; Pérez-García & Ortega, 2011, 2014, 2022; Pérez-García, 2017), crocodylomorphs (e. g. Krebs & Schwarz, 2000; Schwarz & Fechner, 2004; Puértolas-Pascual & Mateus, 2020; López-Rojas *et al.*, 2024), pterosaurs (Bertozzo *et al.*, 2021; Fernandes *et al.*, 2023), and most famously dinosaurs (e. g. Rauhut, 2003; Malafaia *et al.*, 2010, 2020; Mannion *et al.*, 2012, 2013; Araújo *et al.*, 2013; Hendrickx & Mateus, 2014; Escaso *et al.*, 2014; Mocho *et al.*, 2016, 2019; Costa & Mateus, 2019; Russo & Mateus, 2021; Rotatori *et al.*, 2022, 2024). However, only few localities yielding small herpetofauna remains have been studied (Ortega, 2009; Malafaia *et al.*, 2010); and none has been more productive than the Guimarota beds (Martin & Krebs, 2000).

1.1.1 History of the Guimarota excavations

Guimarota is a locality in Leiria municipality located less than 2km south of the Castle of Leiria (**Figure 1.1.1**). The town of Leiria itself is

approximately located in central Portugal, between Lisbon (146 km north) and Porto (167 km south), near Coimbra. From the 1920s to the late 1950, the Sociedade Mineira do Lena exploited a brown coal mine in Guimarota and extracted lignite to fuel lime kilns installed nearby, as part of their major industrialization plan of the region. At this time, the mine was in the outskirts of Leiria; but the urban expansion of the town eventually absorbed it since then, and Guimarota is now one southern neighbourhood right outside the city centre (**Figure 1.1.1C**).

Although the dead-end street Rua das Minas still allows to find the former entrance at the surface and the hall built nearby to prepare the fossils (which remains on a private property, see **Figure 1.1.2A**, **B**, **D**, **G**, and **H**), most of the area has been constructed to accommodate housings (**Figure 1.1.1E** and **Figure 1.1.2C**). Now flooded and accessible only for the first hundred meters (**Figure 1.1.2I** and **K**), the mine is mostly known to be one of the most famous and richest vertebrate microfossil assemblages in Europe from the Upper Jurassic (Martin, 2000a).

The first prospection was carried in late summer 1959, by Waller Georg Kühne and W. Frey. They heard about the mine, while Kühne was searching for Mesozoic mammals, prompting them to visit and examine the coal (Krebs, 2000a). They found several fragments of shells and osteoderms and eventually unearthed a multituberculate skull. Because of this promising results, more extensive campaigns were conducted in the early

1960s, under the supervision of Kühne and later Siegfried Henkel and the help of locals, notably Luiz Fernandes, the "capataz", or pit foreman (Krebs, 2000a). Henkel, as technical lead, helped to optimize the work proceeded, leading to considerably increase the number of remains recovered.

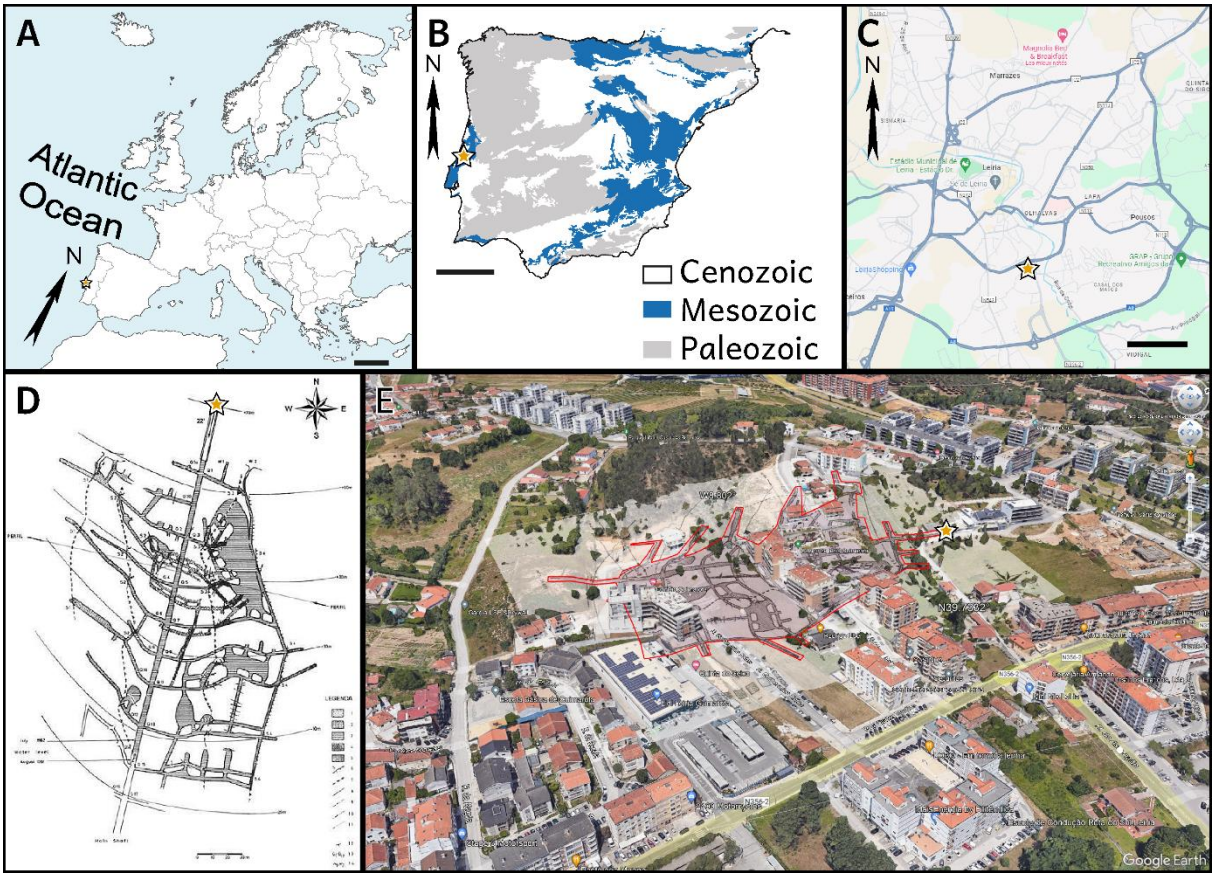

Figure 1.1.1: Geographical setting of the Guimarota beds. The entrance of the mine is presented by the red star. **A**, Europe map modified from Erin Dill, scale is 400 km. **B**, geological sketch of the Iberian Peninsula, scale is 200km. **C**, aerial map of Leiria by Google Maps, scale is 1 km. **D**, sketch of the Guimarota mine tunnels based field notes (modified from Gloy, 2000). **E**, overlay of the Guimarota mine outlines on the current neighborhood by Luís Pinela from Leiria municipality.

One of his main contributions was to develop what is now known as the "Henkel process", a technique of screen-washing with water highly efficient (Henkel, 1966; Krebs, 2000a) and that has been used in numerous

microsites since then. However, the mining stopped as early as 1962, when the company went bankrupt because of economic swift in Leiria. In the rest of this decade, only a handful of bags from the slagheaps were collected and processed. If the property situation certainly play a major role in the interruption of the excavation, Kühne admitted himself he disliked fieldworks spending over decades (Krebs, 2000a).

This first prospection was already successful, with dozens of mammalian jaws, thousands of isolated mammalian teeth, and as many microfossils from fishes, amphibians, and reptiles. Although this discovery was understated at this time, it became the richest mammalian locality for the Late Jurassic (Kühne, 1961, 1968). Not only the mine provided an important diversity of vertebrates, but also revealed to be informative as some taxa were previously known only from dentitions (Krebs, 2000a).

Figure 1.1.2: Pictures of the entrance of Guimarota Mine. **A**, sign indicating the beginning of the Rua das Minas. **B**, end of the Rua das Minas, showing the entrance of the private property leading to the entrance of the mine. **C**, external view of surface above the mine from the adjacent street Rua Rui Hasse Ferreira. **D**, panoramic picture of the remaining building used by the two excavations teams; the entrance is right next to the right wall of the hall on the right. **E** and **F**, picture from within the hall dating from the time of the excavations (Krebs, 2000*a*). **G** and **H**, entrance of the Guimarota Mine nowadays. **I** and **J**, view from top (I) and bottom (J) of the main tunnel that has not been flooded yet. **K**, details on the upper coal steam layer. I, J, and K are kindly shared by Prof. Anabela Veiga from Escola Superior de Tecnologia e Gestão (Politécnico de Leiria).

All the material collected was deposited then at the Freie Universität Berlin, and soon appealed Bernard Krebs, freshly arrived at his new professorship position of palaeontology (Krebs, 2000*a*). After unsuccessfully surveying other localities in Portugal and elsewhere (Spain, Morocco, and Persia) with far less success, Krebs and several colleagues were convinced that Guimarota should be further investigated, despite the opposition of Kühne and the assumption that the site had been sampled entirely (Krebs, 2000*a*). Getting the permission to returning to the mine was a hard and long process with Portuguese authorities, notably Fernando Moitinho de Almeida from the Serviços Geológicos de Portugal, and the landowner of the site (Krebs, 2000*a*).

The SGP agrees on three terms: (1) a local official has to check that the security measures in the mine are correctly followed; (2) the recovered fossils have to be deposited in the museum of the SGP in Lisbon (now known as the Museu Geológico) after the scientific studies are finished; and (3) the results of the scientific work should be published in the publications of the SGP (Krebs, 2000*a*). Krebs and his colleague applied for a regular grant to the Deutsche Forschungsgmeinschaft in 1972, and their project focusing on mammals was granted for one year and renew four times for another year; then they applied for special research project at the Freie Universität Berlin, with a broader scope, which allow five more years of works. In total, this second excavation of the Guimarota mine costed in total 857,550

Deutshmarks (Krebs, 2000*a*), which would represent 1,140,455.45 € for 2020, taking into account the inflation.

Unlike the previous excavation, the second one was not episodic but continuous all around the year, as qualified colliers from previous mining were paid monthly (Krebs, 2000*a*). Once again, Henkel was the technical lead and his contribution allowed to reopen the partially drowned mine, with the help of the former foremen's son, Guilherme Fernandos dos Santos. The previous material were recovered in the lower coal seam, mined through the fifth perpendicular tunnel in the east, which would represent over 260 m to dig, at 80 m below the surface (Krebs, 2000*a*). Therefore, the first couple of years of the mining was dedicated to reach that point.

During the digging, it appeared that the vertebrate, and particularly the mammals (which was the main focus of the Germans), were not evenly distributed through the sediment, with some areas way richer than others (Krebs, 2000*a*). The mining explored these trails, until they finally led to the "Fundflöz", the coal seam yielding the vertebrate microfossil remains. The layer itself is only 50-60 cm thick and could only be mined in the low coal face as a whole. The workers excavated thus around one metric ton of coal every day (Krebs, 2000*a*).

Local Portuguese women examined the split surfaces at the hall of the entrance (**Figure 1.1.2D**, **E**, and **F**), under the supervision of Dona Encarnação, the foreman's wife. They looked for teeth, scales and bones,

and deposited the interesting piece on a tray. Portuguese women were paid individually for each fossil they could find (25.00 Portuguese escudos ($) for basic findings, corresponding to approximately 0.12€; see **Figure 1.1.3**). Every annotated chunk was later investigated by a trained palaeontologist for rough identification and, if considered worthy of interested, was packed and secured (Drescher, 2000; Krebs, 2000a). Senhora Encarnação quickly took more responsibility in the fossil identification, acquiring a remarkable expertise on the Guimarota fauna, while each helper was given a bonus for major discoveries (up to 100$ (≈ 0.50 €) for the best findings).

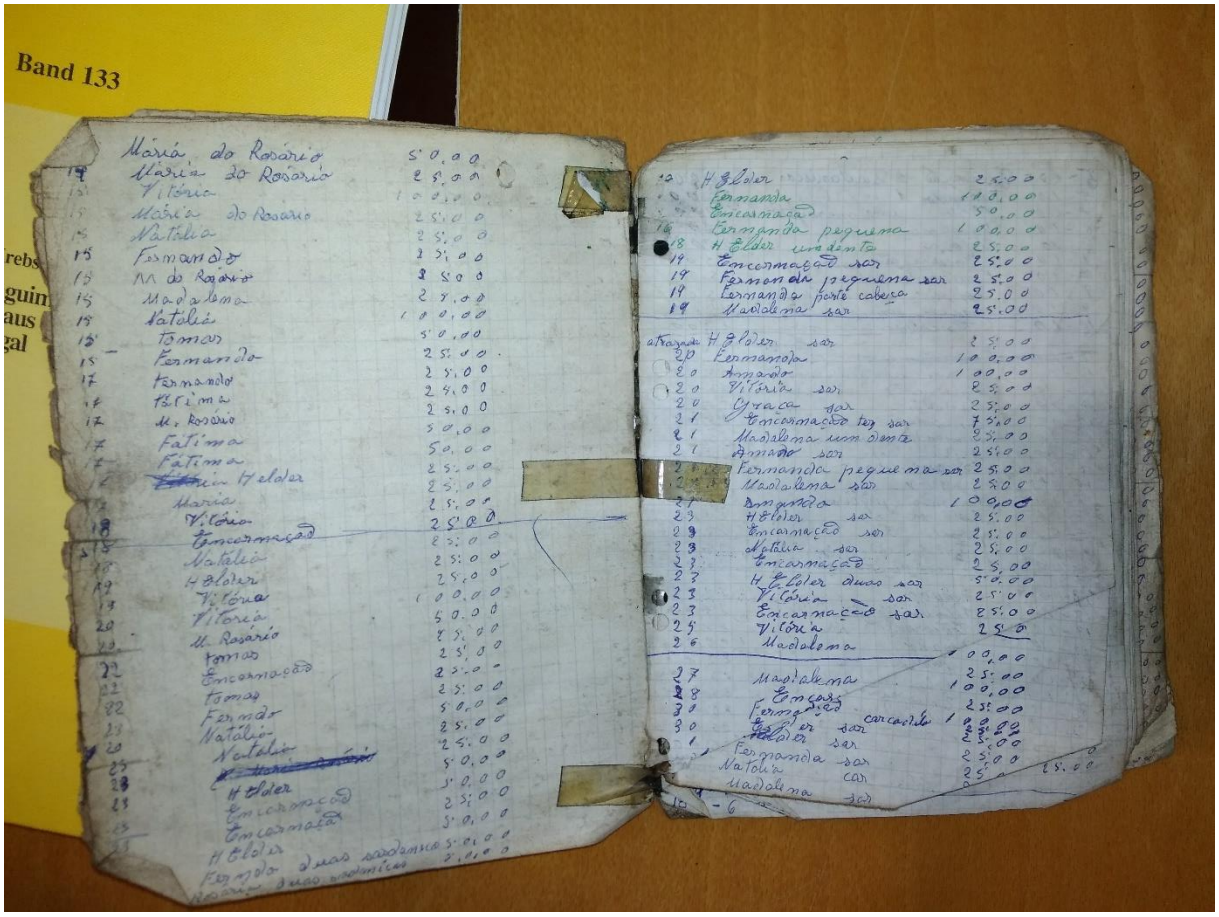

Figure 1.1.3: Picture of a field notebook reporting each finding, the name of the finder, and the price she was rewarded with. Picture kindly shared by Prof. Anabela Veiga from Escola Superior de Tecnologia e Gestão (Politécnico de Leiria).

This technique allowed to recover most of the more complete skeleton, but an substantial part of the coal had also been screen-washed, following the Henkel-process method, to determine the phosphate concentration of the coal, but also keep in check the faunal diversity through the excavation with statistical analyses (Gloy, 2000; Krebs, 2000*a*). The picking was carried out by the foreman's teenager, Guilhermecito, who picked and stored microfossils within over 6,000 little plastic boxes, yielding the rarest elements (Krebs, 2000*a*), as expected for this kind of microsite.

The second excavation followed this routine for ten years, but eventually had to stopped again in 1982. Part because of the temporal limits of the grants, and part because of the mine itself, in which security could not be guaranteed anymore. Worth noticing, the last years did not provide any new taxonomical remain not previously recorded, suggesting that the Upper Jurassic Guimarota fauna was finally sampled (Krebs, 2000*a*). This unvaluable material is still currently under study, more than 40 years after the end of the excavation; and part has been reviewed for this thesis.

1.1.2 Geological setting of the Guimarota microsite

Through the mining, around 20 m of the beds have been exposed (Helmdach, 1971; Schudack, 2000*a*). The outcrop can be summed up as a lower coal seam, named "Fundflöz", and an upper one, names "Ruafolge", both separated by a single layer of limestone, around 5 m thick. Both coal seams exhibits a similar structure, with intercalation of lignitic marls and

marls occasionally rich in bivalve shells (Schudack, 2000a). The nature of the site and the absence of index marine fossils made correlation with surrounding layers difficult and forced palaeontologists to use different sources from the palaeoflora and invertebrates found. Therefore, the exact age of the Guimarota beds had long been a matter of debate up to recently (Schudack, 2000a).

Charophytes were the first used to determine the age of the beds, as they can be abundant in some layers (Helmdach, 1968, 1971). The species *Porochara westerbeckensis* (Mädler, 1952) and *Porochara raskyae* (Mädler, 1952) were identified, suggesting then a Kimmeridgian to upper Tithonian age (Helmdach, 1968; Schudack, 2000a). Later study recovered also the species *Porochara fusca* var. *minor* (Mädler, 1952) and *Mesochara* sp. (Grambast, 1962), which support an upper Oxfordian to Kimmeridgian age (Schudack, 1993). Although charophytes did not allow precise dating, taxa found in both Guimarota and coastal outcrops of Portugal are restricted to Kimmeridgian layers and are absent in older ones (Grambast-Fessard & Ramalho, 1985; Schudack, 1993).

Because of its usually poor preservation, the macroflora of Guimarota could not provide any dating (Schudack, 2000a). However, based on the systematics of the specimens found, it was argue that the beds could not be "older than Kimmeridgian" (Brauckmann, 1978). On the other hand, pollen and spores revealed to be way more useful, and were first thought to

indicate an Oxfordian deposition (Van Erve & Mohr, 1988), before being refuted due to new stratigraphical range of the taxa used (Schudack, 1993).

Ostracods provided further evidence for dating the Guimarota beds, although precision is still lacking. Ten species from seven genera and three superfamilies have been identified so far from the site (Schudack, 2000b). Among them, the Cypridacea indicate a upper Oxfordian to upper Tithonian age (Helmdach, 1971; Schudack, 2000b), but the Cytheracea, more diverse, suggest a more constrain Kimmeridgian age, even if some species stratigraphic range expands in the lower Tithonian or the upper Oxfordian (Helmdach, 1971; Schudack, 2000b).

Since the first attempts to determine their age, the Guimarota beds have been consistently considered as part of the Alcobaça Formation, which has been dated from Kimmeridgian (Ribeiro *et al.*, 1979; Fürsich *et al.*, 2022). It has also been correlated with the marine Abadia unit, which is exposed in outcrops more south to the site and has been originally dated from lower Kimmeridgian, based on ammonites (Ruget-Perrot, 1961) and later reinterpreted from lower to middle Kimmeridgian (Leinfelder & Wilson, 1989). Based on these observations and lithostratigraphic correlations, the Guimarota beds are given a Kimmeridgian age (Ribeiro *et al.*, 1979; Leinfelder & Wilson, 1989; Schudack *et al.*, 1998; Schudack, 2000a), although Helmdach assumed a more constrain age from the transition between lower and upper Kimmeridgian (Schudack, 2000a).

1.1.3 Taphonomy and palaeoenvironmental interpretation

The mining conditions in Guimarota prevented any detailed taphonomic investigation during the excavation, as only a rough location of the area mined instead of an stratigraphic position could be used to locate the fossils (Gloy, 2000; Krebs, 2000*a*). If coal-petrographic and geochemical analyses were considered (Gloy, 2000), the most valuable data is thus provided by the 3D-map drawn from the sketches of the excavation (Gloy, 2000). Although it can be used to determine if isolated bones can belong to a same individual, this map has to be used with caution, since it does not provide any stratigraphic information, neither illustrate fossil location prior to September 10th, 1974 (Gloy, 2000).

With only few exceptions, the Guimarota beds yield only small vertebrates, either juvenile individual from larger taxa, or adult from smaller ones (Krebs, 2000*a*). As in many other vertebrate microfossil assemblages, teeth and scales are by far the most common elements, with also many isolated bones and extremely rare articulated specimens (Gloy, 2000). One may keep also in mind that Guimarota coal is extremely rich in water, because of the drawing period after the closure of the mine. Therefore, dry sediments may crumble and destroy the fossil within. This is why the chunk of coal containing fossils were packed and secured into moist paper, and label with the discovery date, in order to locate its provenance according the horizontal extension of the excavation (Drescher, 2000; Gloy, 2000; Krebs, 2000*a*).

Almost all major vertebrate groups of the Late Jurassic from continental faunas are represented in the Guimarota assemblage: chondrichthyans, including early neoselachians (Kriwet, 2000, 2004); several osteichthyan groups represented by isolated teeth, ganoid scales, and vertebrae, but also jaw remains and articulate skulls (Kriwet, 2000, 2002, 2005); lissamphibians (Evans & Milner, 1994; Wiechmann, 2000, 2003); an important assemblage of mammals extensively studied (Kühne, 1961; Hahn, 1969; Krusat, 1969; Hahn, 1971; Kühne & Krusat, 1972; Hahn, 1977, 1978; Krusat, 1980; Hahn, 1987; Krebs, 1991; Lillegraven & Krusat, 1991; Hahn, 1993; Martin, 1997; Hahn & Hahn, 1998a,b; Krebs, 1998; Hahn & Hahn, 1999a,b; Martin, 1999; Hahn & Hahn, 2000; Krebs, 2000b; Martin, 2000b; Martin & Nowotny, 2000; Martin, 2001, 2002, 2005; Ruf *et al.*, 2009; Luo *et al.*, 2012; Martin, 2013; Jäger *et al.*, 2020; Luo & Martin, 2023); basal lepidosauromorphs (Seiffert, 1973; Evans, 1991b); a diverse assemblage of squamate dominated by scincomorphs and anguimorphs (Seiffert, 1973; Broschinski, 2000), and possibly one of the oldest snake as well (Caldwell *et al.*, 2015); choristoderes (Seiffert, 1973; Evans, 1989); turtles (Gassner, 2000; de Lapparent de Broin, 2001; Pérez-García & Ortega, 2011; Pérez-García, 2017); a diverse assemblage of crocodylomorphs (Krebs, 1968; Krebs & Schwarz, 2000; Schwarz, 2002; Schwarz & Fechner, 2004, 2008; Schwarz & Salisbury, 2005); pterosaurs (Wiechman & Gloy, 2000); and dinosaurs mostly represented by isolated teeth (Thulborn, 1973; Zinke & Rauhut, 1994; Zinke, 1998; Rauhut, 2000, 2001; Mocho *et al.*, 2017), but

also few skeletal remains (Rauhut, 2001, 2003; Rauhut & Fechner, 2005). The flora and the invertebrate fauna recovered were also studied, although it got less coverage (Aberhan *et al.*, 2000; Mohr & Schudack, 2000; Schudack, 2000b).

The amazing high concentration of microfossils remains found, with thousands of specimens, corresponds to the characteristics of a "Konzentrat-Lagerstätte" (Seilacher, 1970). Based on its similarity with other brown coals from Eocene and its geological settings, Guimarota has been regarded as a terrestrial to lagoonal environment similar to modern mangroves, with occasional freshwater influx and salt water flooding (Gloy, 2000; Martin, 2000a). This has been proposed to explain the absence of big dinosaur remains in the assemblage (Gloy, 2000; Rauhut, 2000). The intercalation of limestone below and on top of the coal seam neutralized the acids, preventing the dissolution of organic hard parts (Gloy, 2000).

This specific palaeoenvironment reconstruction underlines its importance for palaeobiogeography and evolution of terrestrial microvertebrates in the Late Jurassic. Indeed, other microvertebrate localities from the coeval Morrison Formation have been reconstructed as swamps, small lakes, and shallow ponds, as well as a permanent water source (Carrano & Velez-Juarbe, 2006; Foster & Heckert, 2011).

1.2 Geological settings of the Lourinhã Formation

1.2.1 General context of the Upper Jurassic of Portugal

The opening of the North Atlantic Ocean, leading to the breakup of Laurasia while Gondwana remained a unique landmass, started in the Late Triassic and gradually occurred all over the Jurassic (Kullberg *et al.*, 2006; Tucholke *et al.*, 2007). However, the breakup accelerated during the Late Jurassic and the Early Cretaceous (**Figure 1.2.1**) throughout major geodynamic events on both regional and global scales, with notably the opening of the Neo-Tethys and the Central Atlantic oceans, which lead to the definitive separation of Gondwana from Laurasia (Gheerbrant and Rage, 2006; Tennant *et al.*, 2017 and reference therein), the former undergoing important fragmentation (Li & Powell, 2001; Stampfli & Borel, 2002; Blakey, 2008). Connecting the proto-Atlantic Ocean to the Pacific Ocean, Tethys was effectively splitting Laurasia from Gondwana, creating a circum-global seaway dotted by islands between northwestern Africa and western Europe (Goodwin *et al.*, 1999; Smith *et al.*, 2004).

Eustatic sea-level curves show a peak in the Kimmeridgian-early Tithonian, before dropping by the Jurassic/Cretaceous boundary (Tennant *et al.*, 2017 and references therein), especially in western Europe (Hallam, 2001; El Albani *et al.*, 2004; Allain *et al.*, 2022). This is correlated with the proportion of evaporitic rocks found in the Late Jurassic, as well as the decline in reef-building organism diversity, fluctuation in global continental

flooding, and terrigenous sedimentation (Tennant *et al.*, 2017 and references therein). Isotopic analyses suggest long-term decrease in the sedimentation rates associated with marine regression, the level of humidity and weathering rates, and the oceanic productivity (Tennant *et al.*, 2017 and references therein).

Associated to the Gondwanan fragmentation, the Jurassic/Cretaceous boundary is also characterized by an increase of the plume-related volcanic activity at regional scales, as well as several meteoritic impacts of various sizes, suggesting potential catastrophic events during that period (Tennant *et al.*, 2017 and references therein). The Late Jurassic was driven by tropical or arid climates, with frequent monsoons at low latitudes, in marine as well as in terrestrial environments: the already warm Oxfordian was followed by an increase in global temperature during the Kimmeridgian, before a cooling and aridity episode at the end of the Tithonian (Tennant *et al.*, 2017 and references therein). The latter may have been characterized by a strong latitudinal climatic gradient (Žák *et al.*, 2011).

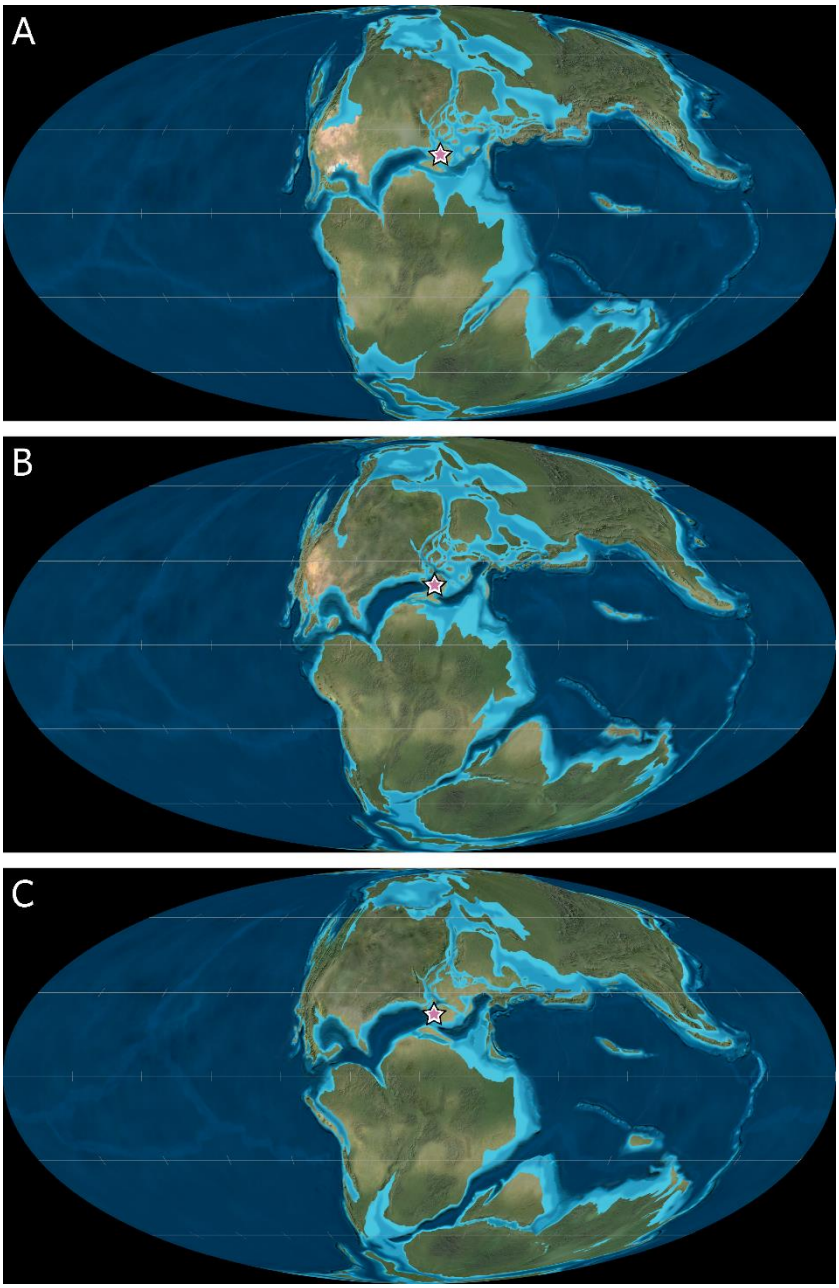

Figure 1.2.1: Global palaeogeographical reconstructions of the Jurassic/Cretaceous transition, illustrating the opening of the North Atlantic Ocean. **A**, Oxfordian (160Mya). **B**, Kimmeridgian (150Mya). **C**, Berriasian (160Mya). The reddish-purple star points Portugal. Palaeomaps from Colorado Plateau Geosystem.

The Iberian Plate was one of the largest islands of the European archipelago system, surrounded by warm, shallow epicontinental sea, with several transgressive/regressive transitions (Moore *et al.*, 1992; Martinius & Gowland, 2011; Myers *et al.*, 2012). During the Late Jurassic, it was

greatly affected by major tectonic events, mainly northward and counterclockwise rotations, that determined its current position (Wilson, 1988; Kullberg *et al.*, 2006). The Iberian Plate was at the crossroad between the Tethys and the proto-Atlantic oceans, while still being connected to the rest of the European archipelago (**Figure 1.2.2**).

Macrofaunal interchanges between North America and Europe through a potential continental bridge have been long consensual, through palaeobiogeographic data (Dercourt *et al.*, 2000; Scotese, 2014; Brikiatis, 2016), but also based on the fossil record (Mateus, 2006; Hendrickx & Mateus, 2014a; Costa & Mateus, 2019; Lasseron *et al.*, 2020; Rotatori *et al.*, 2020; Allain *et al.*, 2022). On the other hand, faunal interchanges between Europe and Africa has been proposed but are less consensual, due to lack of clear established land connection (Vrielynck *et al.*, 1996; Gheerbrant & Rage, 2006; Mannion *et al.*, 2019). However, the Iberian Plate was close to northwestern Africa shore and faunistic evidences suggest that the Tethys was rather a permeable barrier; which allowed dispersal events between Laurasia and Gondwana through ephemeral land connections during the J/K transition (Goodwin *et al.*, 1999; Gheerbrant & Rage, 2006; Haddoumi *et al.*, 2016; Lasseron *et al.*, 2020; Allain *et al.*, 2022).

Figure 1.2.2: Palaeogeography of Europe during the Late Jurassic (150Mya). Palaeomaps from Colorado Plateau Geosystem. Scale bar is 400km.

1.2.2 The Lusitanian Basin

The Lusitanian Basin (**Figure 1.2.3**) is the largest of the six sedimentary basins known in Portugal, developing over the western part of the country and extending offshore over 22,000 km^2 with a maximum sedimentary pile up to 6 km thick (Wilson *et al.*, 1989; Alves *et al.*, 2003). It was formed during the opening of the North Atlantic Ocean and was filled during four rifting episodes and one major sea floor spreading, spanning from the Late Triassic to Early Cretaceous (Martinius & Gowland, 2011; Taylor *et al.*, 2014; Gowland *et al.*, 2017). The third rifting episode, during

the late Oxfordian to earliest Kimmeridgian (Mateus *et al.*, 2017), was the most important. It culminated in the creation of several complex fault-bounded and diapir-bounded sub-basins (Taylor *et al.*, 2014; Gowland *et al.*, 2017), where most of the bounding faults are following a north-east to south-west Hercynian trend (Martinius & Gowland, 2011).

The western part of the Lusitanian Basin is therefore composed by four sub-basins: (1) Arruda; (2) Turcifal; (3) Bombarall-Alcobaça; and (4) Consolação (Martinius & Gowland, 2011; Taylor *et al.*, 2014; Gowland *et al.*, 2017; Mateus *et al.*, 2017). Their filling started with middle-Oxfordian-aged platform carbonates, forming the Montejunto Formation, followed by a mixed clastic and carbonate basin/shelf, forming the Abadia Formation, that shallows into the terrigenous, largely continental deposit of the Lourinhã Formation (Leinfelder & Wilson, 1989; Leinfelder, 1993).

The Consolação sub-basin, in which part of the study area of this thesis is located, is flanked by the Berlengas Horst to the west, the Nazaré Fault to the north, and the north-east trending fault connecting Vimeiro, Bolhos, and Caldas de Rainha diapirs to the east (Martinius & Gowland, 2011; Taylor *et al.*, 2014). During the deposition of the Lourinhã Formation, the Lusitanian Basin was situated around 30-35° northern latitudes (Stampfli & Borel, 2002), and its considered palaeoclimate was warm, with winter-wet and summer-dry seasonality (Martinius & Gowland, 2011).

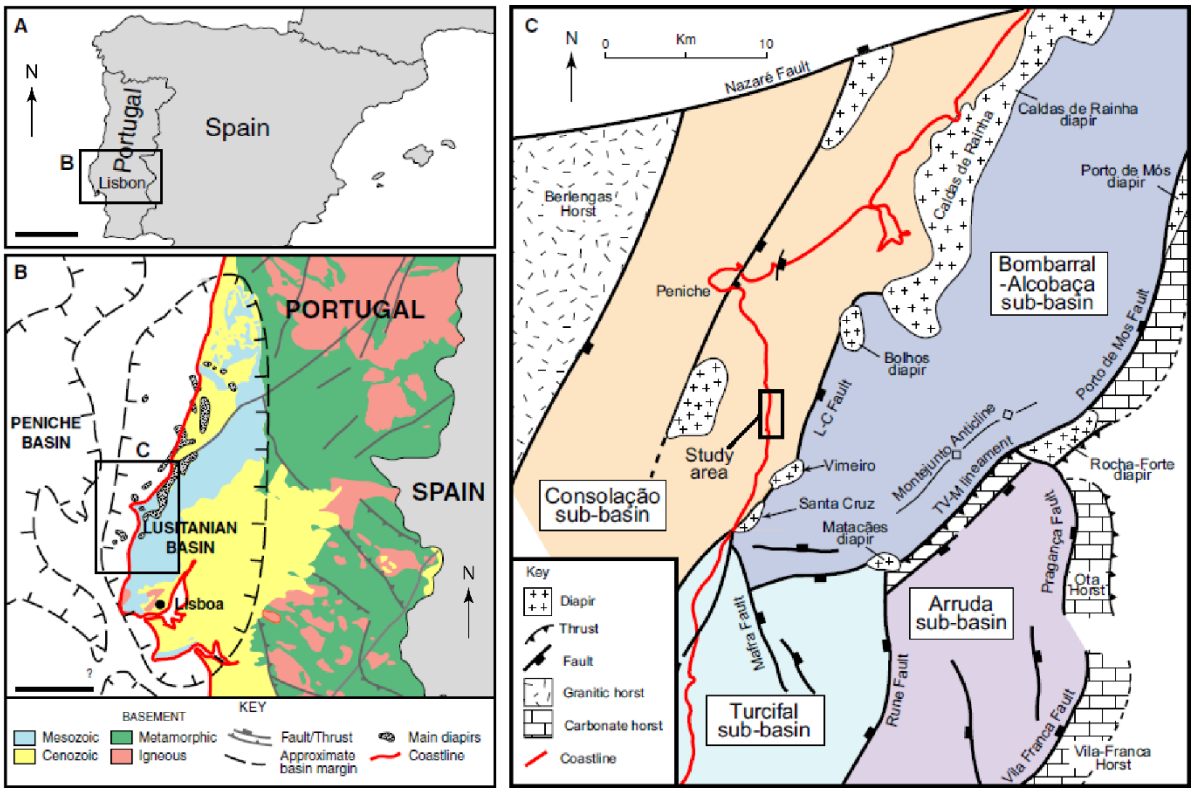

Figure 1.2.3: Geology of the Lusitanian Basin. **A**, overview map of Portugal with the location of the Lusitanian Basin indicated; scale is 200km. **B**, simplified geological map of Portugal showing major basin features; scale is 50km. **C**, map showing the distribution of sub-basins in the Western and Central Lusitanian Basin (modified from Martinus & Gowland, 2011; Taylor *et al.*, 2014, Gowland *et al.*, 2017).

1.2.3 Geology of the Lourinhã Formation

The Lourinhã Formation is named after the local town of Lourinhã, 70 km to North of Lisbon. It is a widely adopted term for the clastic continental succession sediments throughout the Lusitanian Basin, ranging in thickness from 200 m to 1,100 m (Leinfelder & Wilson, 1989; Wilson *et al.*, 1989; Taylor *et al.*, 2014). Most of the variation is due to not full outcrops and the difficulty to identify boundaries. Always considered as Late Jurassic in age, recent studies confirm its age range from Late Kimmeridgian to Late Tithonian: it overlays the Kimmeridgian Consolação unit and its it is overlaid

by the Berriasian Porto da Calada Formation (Hill, 1988, 1989; Taylor *et al.*, 2014). The base of the laterally extensive Lourinhã Fm is traditionally taken as the first significant and sustained development of continental deposits, above either the shallow marine to estuarine sandstones of the Sobral Formation, the oolitic limestone of the Amaral Formation, the shelfal carbonates of the Alcobaça Formation, or the shelf to deepwater clastics of the Abadia Formation (Taylor *et al.*, 2014). Its dominant continental deposits are sandy channel-fills and contemporaneous muddy floodplain deposits (Martinius & Gowland, 2011; Taylor *et al.*, 2014; Gowland *et al.*, 2017).

Some channels exhibit sedimentary structures suggesting tidal modulation, and lacustrine intervals, mouth-bar developments, crevasse channel/splay deposits, and various floodplain palaeosols can also be observed (Hill, 1989; Martinius & Gowland, 2011; Myers *et al.*, 2012). Those facies representing braided to sinuous paralic fluvial systems, with distal alluvial fans and upper delta, punctuated by episodes of estuarine and lagoon sediments, with shallow marine to brackish macrofauna (Mateus *et al.*, 2017). Palaeocurrent data and regional-scale modelling suggest the main fluvial plain were flowing from the igneous Berlengas Horst toward south to southwest deltaic system (Wilson *et al.*, 1989; Mateus *et al.*, 2017).

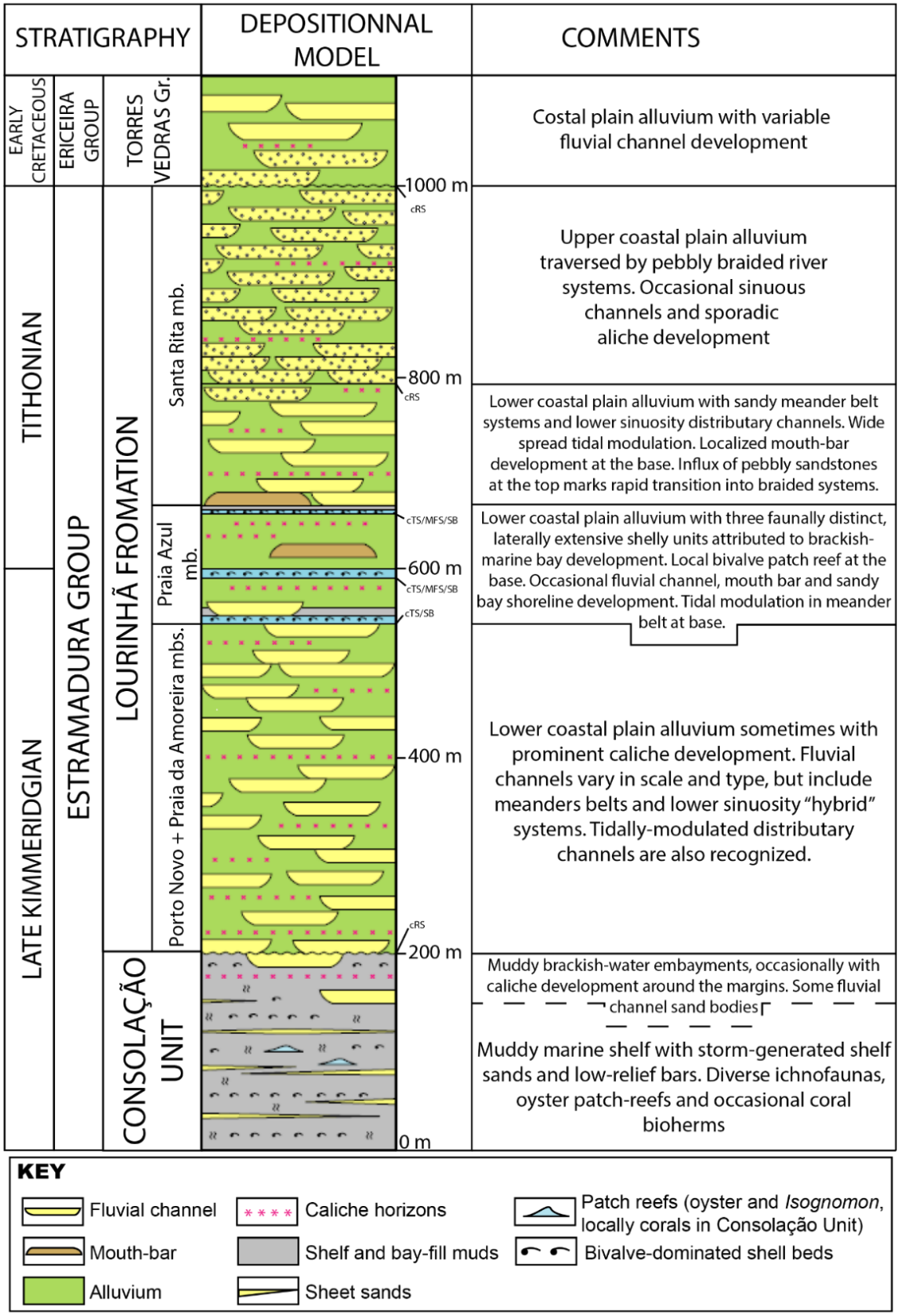

Figure 1.2.4: Lithostratigraphic framework of the Lourinhã Formation in the Consolacão sub-basin, showing simplified depositional elements (modified from Martinus & Gowland, 2011, based on Mateus *et al.*, 2017).

Based on its lithostratigraphic features, the Lourinhã Fm can be subdivided into three to four distinct members (**Figure 1.2.4**): (1) the regressive nature of the base, with the Praia da Amoreira and Porto Novo members; (2) three episodes of marine transgressions, with the Praia Azul member; and (3) a regressive surface above which interpreted fluvial channel morphologies switch from single-channel to braided systems within the Santa Rita member (Hill, 1988, 1989). The latter has been subdivided by some authors into Areia Branca and Ferrel members, with the regressive surface being at the base of the Ferrel member (Martinius & Gowland, 2011; Taylor *et al.*, 2014; Gowland *et al.*, 2017); and it is also referred as the Assenta member toward the Turcifal sub-basin (Hill, 1989; Mateus *et al.*, 2017). Nevertheless, most of the remains of the Lourinhã Fm studied in this thesis come from the Praia da Amoreira/Porto Novo and the Praia Azul members.

With the Alcobaça Formation, it is the Jurassic unit most diverse in vertebrate remains in Portugal, and even in Europe. Studies highlight shared fauna with the Morrison Formation (Mateus, 2006; Escaso *et al.*, 2007; Lockley *et al.*, 2008); but this is most likely an artefact of sampling bias, as both formations have been extremely sampled compared to others of the same period (Foster, 2020). The sedimentology of the Lourinhã Formation suggests a semi-arid climate, with seasonal rainfall lower than 500 mm, wetter conditions than in the Morrison Formation (Myers *et al.*, 2012).

1.3 Geological setting of Blasi 2B (Tremp Formation, Upper Maastrichtian, Spain)

The vertebrate-bearing localities of Arén and Blasi Hill in Ribagorza County (Huesca Province, Aragón Region, northeastern Spain) are exposed along the northwestern flank of the Tremp syncline (or Tremp-Graus Basin) in the South-Pyrenean Basin (*sensu* Seguret, 1972). The Pyrenees, a mountain range between Spain and France, was formed by the collision of the European plate and the Iberian microplate during the Alpine orogeny occurring during the Late Cretaceous to the Miocene (Puigdefàbregas *et al.*, 1986; Muñoz, 1992; Teixell, 1998). This orogeny resulted in a NW-SE oriented belt of folds and thrusts that compartmentalized the South-Pyrenean Basin into several structural heights and associated sub-basins, including the Tremp syncline (Gómez-Gras *et al.*, 2016).

During the Late Cretaceous, due to a global drop in sea levels, the South-Pyrenean Basin gradually accumulated a suite of westward-prograding turbiditic and deltaic sediments (Santonian–Maastrichtian), transitional (Maastrichtian) and continental deposits (Maastrichtian to Paleocene) (Ardèvol *et al.*, 2000; Oms *et al.*, 2016). The unit that includes the K/Pg transition is the Tremp Formation, informally known as the "Garumnian" (Mey *et al.*, 1968). The Tremp Formation is a transitional/coastal to continental diachronous lithostratigraphic unit extending from the Maastrichtian to the Paleocene. From bottom to top, the

Tremp Formation is subdivided into four smaller lithostratigraphic units: "grey unit"; "lower red unit"; "Vallcebre limestones"; and "upper red unit" (Rosell *et al.*, 2001; Oms & Canudo, 2004; Pereda-Suberbiola, 2009).

The Blasi 2B fossils studied here come from the transitional levels of the "grey unit" (or "grey Garumnian unit", see **Figure 1.3.1**). Blasi 2B occurs in a 6.5-m-thick interval of grey marls, directly overlying the top of the deltaic/barrier island deposits of the Arén Formation, and has been interpreted as representing tidal-plain, lagoonal and estuarine environments (López-Martínez *et al.*, 2001; Riera *et al.*, 2009; Moreno-Azanza *et al.*, 2014; Pérez-Pueyo *et al.*, 2021b). Based on biostratigraphy and magnetostratigraphy, Blasi 2B has been dated to the late Maastrichtian based on correlation with the *Abathomphalus mayaroensis* (Bolli, 1951) biozone (López-Martínez *et al.*, 2001) and the polarity chron C30n (Oms and Canudo, 2004; Pereda-Suberbiola *et al.*, 2009). The site is located 210 m below the Danian deposits and has been dated around 66.5 Mya, half a million year before the K/Pg event (Pérez-Pueyo *et al.*, 2021a).

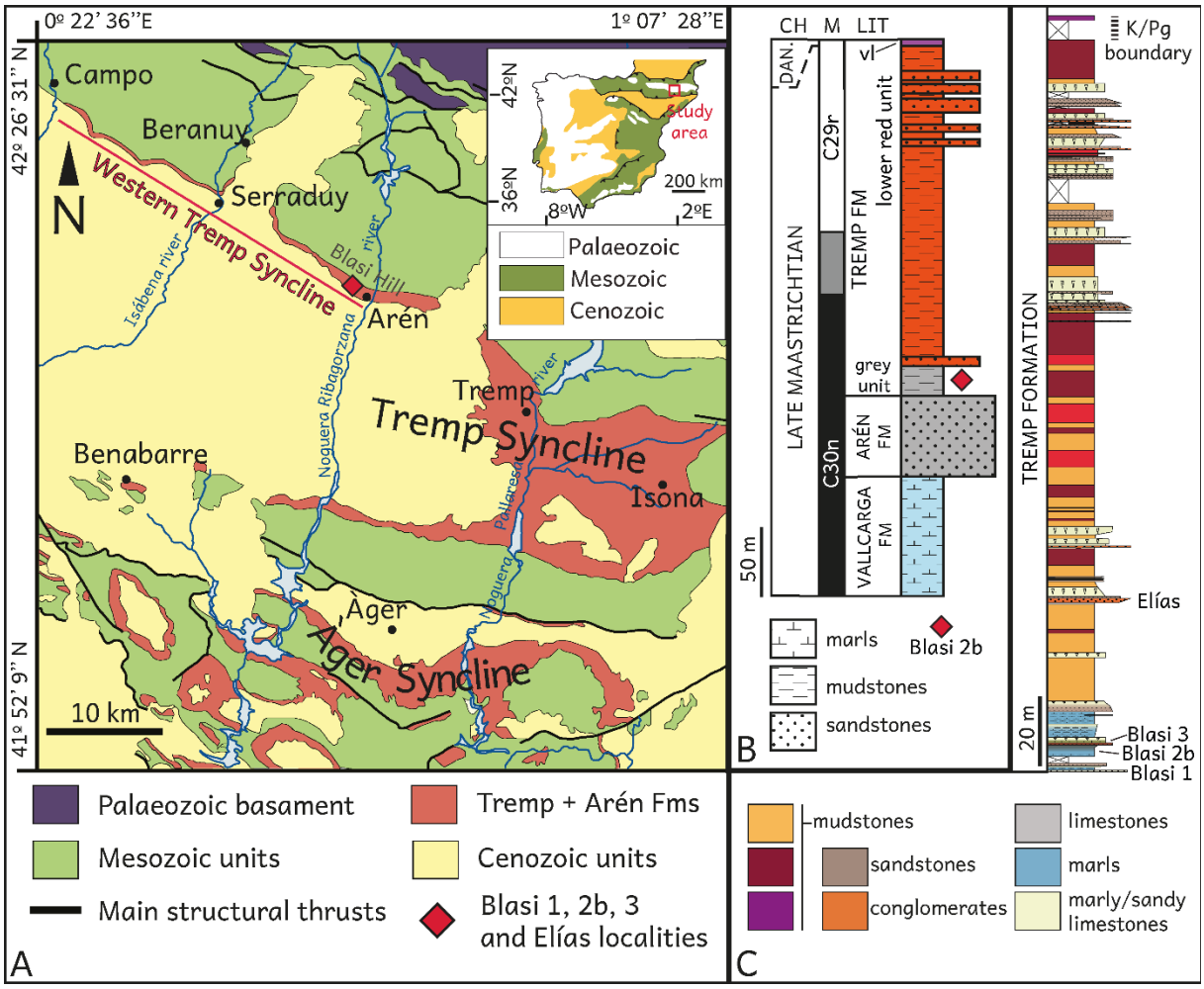

Figure 1.3.1: Geographic and geological context of Blasi 2B (Arén, Huesca, Spain). **A**. Geological map of the Southern Pyrenees, focused on the Tremp Syncline and its Upper Cretaceous-Palaeogene outcrops (modified from López-Martínez and Vicens, 2012; Pérez-Pueyo, 2023). **B**. Schematic stratigraphic log of the upper Maastrichtian in the Blasi Area; modified from Pereda-Suberbiola *et al.*, 2009. Abbreviations: CH. Chronostratigraphy; DAN., Danian; LIT, Lithostratigraphy; M, Magnetostratigraphy; vl. Vallcebre limestones and equivalents. **C**. Detailed stratigraphic profile of the Tremp Formation in the study area with location of the main vertebrate sites; colours reflect colours of lithology.

Nine vertebrate fossil sites have been described in the area within the Arén and Tremp formations. Among the sites with macrovertebrates, Blasi 1 and Blasi 3 are notable for yielding the holotypes of the lambeosaurine dinosaurs *Blasisaurus* (Cruzado-Caballero *et al.*, 2010) and *Arenysaurus*

(Pereda-Suberbiola *et al.*, 2009). Additionally, the holotype of the allodaposuchid crocodylomorph *Arenysuchus* was recovered at the Elías site (Puértolas *et al.*, 2011). Nevertheless, among the sites with microvertebrates, Blasi 2B stands out as the one presenting the richest microvertebrate faunal assemblage. This includes ray-finned fishes, amphibians, squamates, turtles, and isolated dinosaur and crocodylomorph teeth (López-Martínez *et al.*, 2001; Torices Hernández *et al.*, 2004; Murelaga & Canudo, 2005; Pereda-Suberbiola *et al.*, 2009; Blain *et al.*, 2010; Cruzado-Caballero *et al.*, 2013; Torices *et al.*, 2013). The great abundance and variety of eggshells present at the site is also notable. These include the new crocodylomorph ootaxon *Pachykrokolithus* (Moreno-Azanza *et al.*, 2014, 2023; Pérez-Pueyo *et al.*, 2021b).

1.4 Overview of the studied herpetofauna from the Late Jurassic of Portugal

1.4.1 The lissamphibians

Molecular clock analyses estimate the divergence of crown Lissamphibia (**Figure 1.4.1**) in the Carboniferous (Pardo *et al.*, 2017; Kligman *et al.*, 2023); but their fossil record only starts in the Triassic (Rage & Roček, 1989; Evans & Borsuk-Białynicka, 2009; Schoch *et al.*, 2020; Jésus *et al.*, 2022; Kligman *et al.*, 2023) and remains scarce until the Middle Jurassic and the Late Jurassic when the crown-groups diversified

(Marjanović & Laurin, 2014), taking over the stem-groups that became extinct by the Jurassic/Cretaceous boundary (Evans & Milner, 1993; Roček, 2000; Marjanović & Laurin, 2008; Gao *et al.*, 2013; Skutschas, 2013; Jia & Gao, 2016; Li *et al.*, 2023).

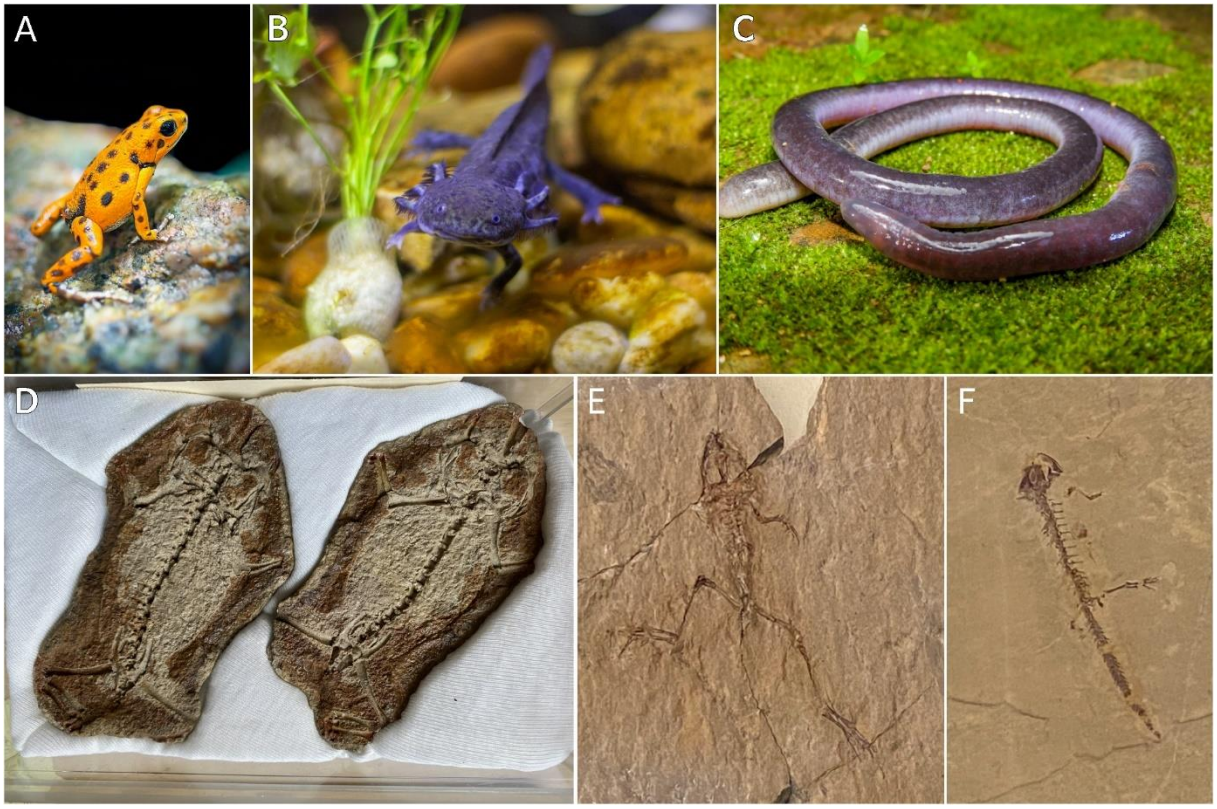

Figure 1.4.1: Extant lissamphibians and some relative fossils. **A**, **B**, and **C**, extant lissamphibians, respectively an Anura, an Urodela, and a Gymnophiona (free licences pictures). **D**, MNHN.F.MAE126 holotype of *Triadobatrachus massinoti* (Piveteau, 1936) from the Early Triassic of Madagascar. **E** and **F**, fossil amphibian from Las Hoyas (Berriasian, Spain) in exhibit in MUPA, *Iberobatrachus angelae* Báez, 2013 (**E**) and *Valdotriton gracilis* Evans & Milner, 1996 (**F**).

Indeed, lissamphibians acquired key innovations during the J/K transition, increasing their ecological diversity and origination of new lineages (Gao & Shubin, 2001; Tennant *et al.*, 2017). Thus, their fossil record suggests amphibians were resilient to the events of the J/K boundary, as

their diversity was not much affected by (Fara, 2004; Tennant *et al.*, 2017) and was linked to palaeotemperature rather than eustatic level changes (Tennant *et al.*, 2016a).

During the Late Jurassic, Anura were already diverse in Euramerica (Evans & Milner, 1993; Roček, 2000; Gardner & DeMar, 2013), while Caudata and Urodela were also well established in Laurasia (Gao & Shubin, 2001, 2003, 2012; Gao *et al.*, 2013; Skutschas, 2013; Jia & Gao, 2016; Li *et al.*, 2023) but less diverse in North America (Gardner & DeMar, 2013). If they have been reported from Portugal (Kühne, 1968; Evans & Milner, 1994, 1996; Wiechmann, 2000), both Anura and Caudata fossil records remain extremely rare and vastly understudied.

Although Albanerpetontidae (**Figure 1.4.2**) were present in Europe and North Africa since the Middle Jurassic and well known in the Berriasian (Seiffert, 1969; Evans & Milner, 1994; Evans & McGowan, 2002; Rees & Evans, 2002; Gardner *et al.*, 2003; Pouech *et al.*, 2006; Haddoumi *et al.*, 2016; Lasseron *et al.*, 2020; Panciroli *et al.*, 2020; Allain *et al.*, 2022), their Late Jurassic fossil record is restricted only to Portugal (Wiechmann 2003). To date, they do not appear in the Late Jurassic fossil record of North America (Gardner & Böhme 2008; Gardner & DeMar 2013; Carrano, pers. comm., 2023), notably in the well-known and exhaustively sampled Quarry 9 site from the Morrison Formation (Carrano, 2006). The earliest North-

American occurrences date only from the Aptian-Albian (Gardner, 1999a,b; Carrano *et al.*, 2022).

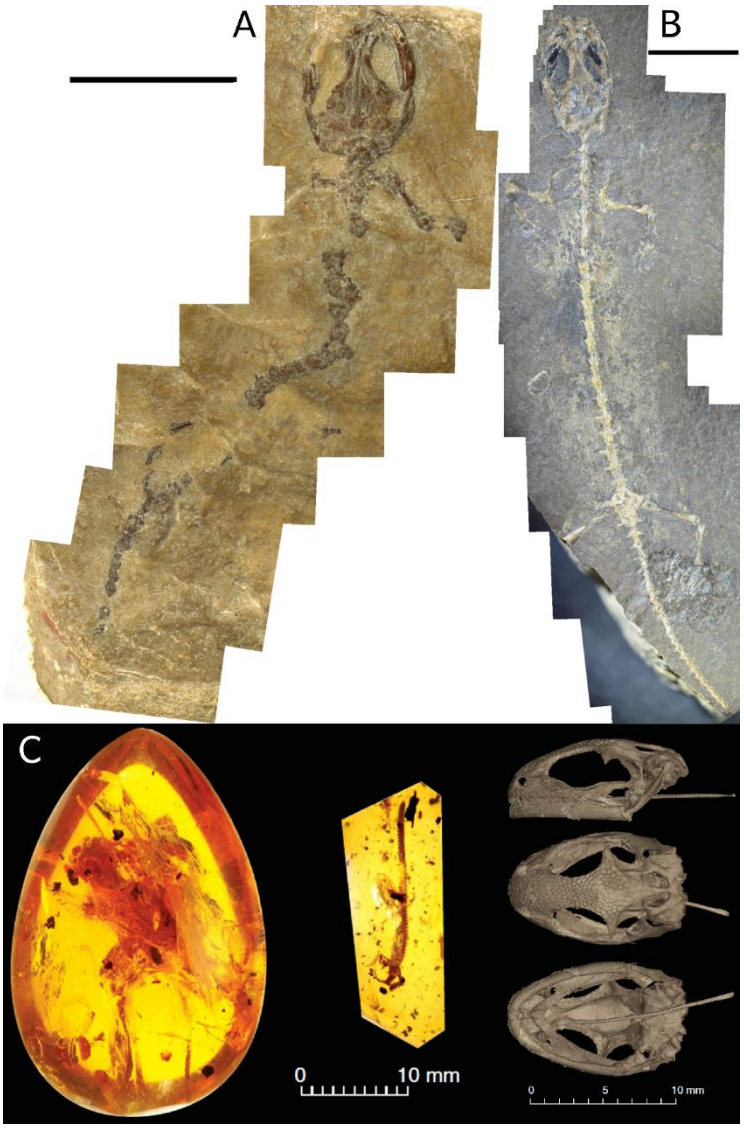

Figure 1.4.2: Relevant albanerpetontid fossils. **A**, M542 holotype of *Celtedens megacephalus* (Costa, 1864); scale is 1cm. **B**, MCCM-LH6020 holotype of *Celtedens ibericus* McGowan & Evans, 1995; scale is 1cm. **C**, GRS-Ref-060829 holotype and JZC Bu154 paratype of *Yaksha perettii* Daza *et al.*, 2020, with images of three-dimensional model of based µCT-scan of the holotype (from Daza *et al.*, 2020).

Amphibians from the Upper Jurassic of Portugal have only been reported from the Guimarota beds and few localities of the coeval Lourinhã Formation, and are only represented by lissamphibians (Wiechmann, 2000,

2003). The Albanerpetontidae constitute by far the most of the material with more than 6,600 dentaries, around 2,350 premaxillae and maxillae, 40 characteristic fused frontals (although most are fragments), six parietals, some distal ends of humeri, and vertebrae (Wiechmann, 2003). As in many other microvertebrates localities, no articulated bones have been recovered, although they lack any sign of prolonged transport (Gloy, 2000; Wiechmann, 2000). The unusual high number of bones could be explained by periodic floods washing the water banks and disarticulating bodies before their burial (Gloy, 2000; Wiechmann, 2000).

Preliminary work on this material suggested all these specimens belongs to a new species of *Celtedens* (Wiechmann, 2000, 2003). However, although Wiechmann's thesis is freely available online, the new species proposal has not yet been published otherwise and, therefore, do not meet International Code of Zoological Nomenclature criteria for a valid nomenclatural published work (Arts. 8 & 9), and the original name and combination remain unavailable (Martín *et al.*, 2012). The material was reviewed in Chapters 3.1 and 3.2.

Beside the unpublished Wiechmann PhD-thesis, almost no works focused on the amphibians from the Late Jurassic of Portugal. Among the specimens recovered in Guimarota, figured a handful frogs remains (ilia and distal humeri), cursorily identified as discoglossid (Evans *et al.*, 1990; Wiechmann, 2000). Few cervical material was putatively attributed to the

cf. *Marmorerpeton* (Evans & Milner, 1994, 1996; Milner, 2000; Wiechmann, 2000; Skutschas, 2014); and some fragmentary long bone bones could be referred as caudate femora. Nevertheless, both statements have never been confirmed so far. Although scarce, this material would require a proper description; unfortunately, the time of this thesis did not allow it. It is worth noticing that while checking the material housed in Museu Geológico, I encountered several specimens wrongly labelled and identified as amphibians (see Chapter 2.3 for more detail).

1.4.2 The choristoderes

The Choristodera (**Figure 1.4.3E**) are an extinct group of enigmatic freshwater amphibious diapsids often ecologically compared to crocodiles because of general features in their cranial and postcranial morphologies (Fox, 1968; Erickson, 1987; Evans & Hecht, 1993; Matsumoto & Evans, 2010; Matsumoto *et al.*, 2022a). They distributed through Laurasia (Matsumoto & Evans, 2010; Matsumoto *et al.*, 2019, 2022b; Dong *et al.*, 2020), with putative occurrences in Gondwana (Haddoumi *et al.*, 2016; Lasseron *et al.*, 2020). Even though they appear in the Bathonian (Evans, 1989; Evans & Waldman, 1996; Averianov *et al.*, 2006; Panciroli *et al.*, 2020), their fossil record remains scarce in the Upper Jurassic (Gilmore, 1928; Evans, 1989; Matsumoto *et al.*, 2019), as they only started to diversify in the Early Cretaceous, especially in Asia and North America (Matsumoto *et al.*, 2013, 2019, 2022b).

Despite being consistently recovered as monophyletic, Choristodera phylogenetic position within Diapsida remains uncertain (Matsumoto & Evans, 2010; Matsumoto *et al.*, 2019). They have been recovered as basal Archosauromorpha (Evans, 1988; Gauthier *et al.*, 1988b), as sister group of Archosauromorpha+ Lepidosauromorpha (Evans, 1988; Dilkes, 1998; Ezcurra *et al.*, 2021), as basal diapsids (Gao & Fox, 1998), within an expanded Lepidosauromorpha clade (Müller, 2004), constrained to the base of either Lepidosauromorpha or Archosauromorpha (Ezcurra, 2016), as basal Neodiapsida (Simoes *et al.*, 2018), or within Archosauromorpha (Simoes *et al.*, 2018; Griffiths *et al.*, 2021).

They displayed various ranges of morphotypes, from brevirostrine to longirostrine, and from short-necked to long necked, with size-range from small lizards to large crocodiles (Matsumoto & Evans, 2010). Notably, they seem to have gone through a major ecological transition during the J/K transition, as their morphology went from smaller, short-necked, lizard-like basal forms in the Bathonian and Kimmeridgian, to larger, long-necked, and longirostrine forms in the Barremian onward (Matsumoto & Evans, 2010; Matsumoto *et al.*, 2019; Wang *et al.*, 2023).

Seiffert reports material he attributed to a new species of *Cteniogenys* from the Guimarota beds, a basal choristodere taxon (Matsumoto *et al.*, 2019), in comparison to the type species *Cteniogenys antiquus* Gilmore 1928 from the Morrison Formation (**Figure 1.4.3G**). However, authors have

challenged that description since then and consider the species being *nomen dubium* (Estes, 1983; Evans, 1989, 1990; Chure & Evans, 1998). This material, as well as unpublished elements mislabeled to amphibian, are reviewed in Chapter 2.3.

1.4.3 The lepidosauromorphs

Based on their fossil record and molecular clock analyses, lepidosauromorph diapsids emerged in the Permian or the Early Triassic (Evans, 1993, 2003; Evans & Jones, 2010; Jones *et al.*, 2013; Simões *et al.*, 2018; Sobral *et al.*, 2020), while true lepidosaurs only diversified into rhynchocephalians (**Figure 1.4.3A**) and squamates later in the Triassic (Evans & Jones, 2010; Herrera-Flores *et al.*, 2022a; Bolet *et al.*, 2022). The latter remained dominant and more abundant in the assemblages through all the Triassic and the Middle Jurassic (Evans, 1998a, 2003; Evans & Jones, 2010; Gauthier *et al.*, 2012). The rhynchocephalian fossil record in the Upper Jurassic is restricted to Euramerica, especially in the Solnhofen limestones and the Morrison Formation (Rauhut *et al.*, 2012; Tennant *et al.*, 2016a; Villa *et al.*, 2021; Herrera-Flores *et al.*, 2022b; DeMar Jr. *et al.*, 2022).

If their fossil record confirms their presence already in the Middle Triassic (Simões *et al.*, 2018), squamates remains are rare until the Middle to Upper Jurassic (Evans, 1993, 2003; Evans & Jones, 2010; Gauthier *et al.*, 2012; Caldwell *et al.*, 2015). Their major modern lineages were already

radiating by that time, before taking over with the decline of rhynchocephalians in the Early Cretaceous (Estes, 1983; Evans, 1993, 1998*a*, 2003; Conrad, 2008; Herrera-Flores *et al.*, 2022*a*; Bolet *et al.*, 2022; Brownstein *et al.*, 2022).

Lizard faunas in the J/K transition and in Middle Jurassic assemblages were similar (Rage, 2013), both being dominated by primitive anguimorphs (**Figure 1.4.3B**), scincomorphs (**Figure 1.4.3C**), and occasional gekkonids (Evans, 1998*a*; Caldwell, 2005). This faunal composition persisted in Europe and North America until the Aptian-Albian, before being eventually replaced by more deeply-nested groups (Nydam, 2013; Tennant *et al.*, 2017). Nevertheless, several genera from the J/K transition do not accommodate within major clades (Evans, 2003).

Squamates geographic range suggests a cosmopolitan distribution already by the Middle Jurassic (Haddoumi *et al.*, 2016). However, Gondwana suffers an important biogeographic gap with a scarce fossil record compared to Laurasia (Evans, 1998*a*; Evans *et al.*, 2002; Evans, 2003; Chatterjee & Scotese, 2007; Simões *et al.*, 2015, 2017; Tennant *et al.*, 2017). Although Early Cretaceous assemblages may yield some archaic forms (Evans, 1998*a*), all stem-lepidosaurs seem to have become extinct in the Triassic (Evans, 2003; Gauthier *et al.*, 2012; Schoch & Sues, 2018; Simões *et al.*, 2018; Sobral *et al.*, 2020; Bolet *et al.*, 2022).

Figure 1.4.3: Extant and fossil relatives of small reptiles found in the Upper Jurassic of Portugal. **A**, **B**, and **C**, extant lepidosaurs, respectively a tuatara, an anguimorph, and a scincid (free licence pictures). **D**, palaeoart reconstruction of *Portugalophis lignites* by Julius Csotonyi. **E**, reconstruction of a Cretaceous choristodere exhibited at the Royal Tyrrell Museum. **F**, Digital skull reconstruction of *Marmoretta oxoniensis*, using information from referred specimens in lateral and dorsal view (from Griffiths *et al.*, 2021). **G**, USNM 6134 holotype of *Cteniogenys antiquus* Gilmore 1928 in medial and lateral views; the scale is 5mm.

While challenging the validity of the *Cteniogenys* described by Seiffert in his work (1973), authors have also noted that some specimens (notably a

premaxilla figured, Gui. 345; Fig. 5) should actually be attributed to *Marmoretta* (**Figure 1.4.3F**), a lepidosauromorph from the Bathonian Kirtlington Mammal Bed from England (Evans, 1991b). Although they did not provide any revision nor description, the author noted that the material from Guimarota was not conspecific with the British species. *Marmoretta* was later also reported in the Bathonian Kilmaluag Formation, from the Isle of Skye in Scotland (Griffiths *et al.*, 2021). The specimens from Guimarota, as well new material mislabeled as amphibians, are reviewed and described in Chapter 2.3.

Few rhynchocephalian cranial material attributed to *Opisthias* have been reported from the ?upper Kimmeridgian-Tithonian Andrés site (Ortega, 2009; Malafaia *et al.*, 2010), but not in the Guimarota beds, making them one of the few groups not represented in that assemblage. However, that material has never been fully described.

The most substantial work on lepidosaurs from the Late Jurassic of Portugal is the monograph of Seiffert, where he extensively described the specimens found during the first excavation in the Guimarota beds (Seiffert, 1970, 1973). Later, a short revision of the material recovered during the second excavation has been published (Broschinski, 2000). The assemblage is dominated by Scincomorpha, with three confirmed genera (*Becklesius*, *Paramaellodus*, and *Saurillodon*) and one indetermined, and early Anguimorpha (*Dorsetisaurus*). The material comprises many jaws and

cranial elements, vertebrae, limb bones, osteoderms, and a handful of associated specimens. It also yields possibly one of the earliest snakes in the fossil record with *Portugalophis lignites* Caldwell *et al.*, 2015 (**Figure 1.4.3D**), known only from jaw elements. As seen previously, this faunal composition, with the absence of Iguania and Gekkota, is congruent with other Late Jurassic assemblages from the Upper Jurassic (Evans, 1998a, 2003; Caldwell, 2005), and as well as with Middle Jurassic of faunas in England (Evans & Milner, 1994; Rage, 2013; Panciroli *et al.*, 2020).

Nevertheless, despite the limited work, the lizard fauna from Guimarota already represents a considerable diversity, both in ecological adaptations and systematics (Broschinski, 2000; Martin, 2000a). For this reason, and because no new relevant material was found in this thesis, lepidosaurs have not been deeply studied in this thesis. However, some specimens that could be referred to either *Cteniogenys* or *Marmoretta* were found while checking the squamate material from Museu Geológico (see Chapter 2.3 for more details).

1.4.4 The crocodylomorphs

Originating in the Late Triassic, Crocodylomorpha are the only pseudosuchian clade to have crossed the Triassic-Jurassic boundary (Nesbitt, 2011; Toljagić & Butler, 2013), with sphenosuchians becoming extinct during the Jurassic (Clark *et al.*, 2004). The remaining crocodylomorphs, the Crocodyliformes became morphologically and

ecologically diverse during the Jurassic and the Cretaceous (e. g. Young & De Andrade 2009; Young *et al.* 2010, 2011, 2016; Pol *et al.* 2013; Parrilla-Bel *et al.* 2013; Bronzati *et al.* 2015; Johnson *et al.* 2022; López-Rojas *et al.* 2024), with the J/K constituting a major landmark in their evolution.

Crocodyliforms went through major pelagic marine radiations in the Jurassic, notably with thalattosuchians which barely crossed the J/K boundary (Young *et al.*, 2011; Tennant *et al.*, 2016b, 2017; Fanti *et al.*, 2016; Johnson *et al.*, 2022), as well as important terrestrial diversifications with Protosuchia in the Jurassic and Notosuchia in the Cretaceous (Carvalho *et al.*, 2010; Wilberg *et al.*, 2019), as well as the more amphibious Neosuchia. The latter was the dominant clade in Europe during the Mesozoic and the Cenozoic. During the Jurassic, it includes predominantly pelagic clades such as pholidosaurids (Fortier *et al.*, 2011), but more commonly amphibious forms such as goniopholids, atoposaurids, and bernissartiids, which dominated terrestrial and transitional ecosystems during the J/K transition. Neosuchia includes Eusuchia, which originated the crown-group Crocodylia, but this clade did not appear until the Early Cretaceous (Clark & Norell, 1992; Brochu, 2003; Tennant *et al.*, 2016b; Mateus *et al.*, 2019; Puértolas-Pascual & Mateus, 2020; Novas *et al.*, 2021; Puértolas-Pascual *et al.*, 2023; and references therein).

The Upper Jurassic of Portugal yield diverse crocodyliform faunas including teleosaurids (Krebs, 1968; Young *et al.*, 2014b), goniopholids

(Schwarz, 2002; Puértolas-Pascual & Mateus, 2020; López-Rojas *et al.*, 2024), atoposaurids (Schwarz & Salisbury, 2005; Schwarz *et al.*, 2017), as well as isolated teeth (Malafaia *et al.*, 2010) and eggshells (Russo *et al.*, 2017). One can cite the dwarf crocodylomorphs *Lisboasaurus estesi* Seiffert, 1973 and *Lusitanisuchus mitracostatus* (Seiffert, 1973). Both were originally attributed to Anguimorpha and first thought to be congeneric (Seiffert, 1970, 1973). Later, *L. estesi* was referred to a small theropod, while "*Lisboasaurus mitracostatus*" *sensu* Seiffert, 1973 was considered as *nomen dubium*, because its remains were too fragmentary to be diagnostic (Milner & Evans, 1991; Buscalioni *et al.*, 1996; Krebs & Schwarz, 2000). Eventually, new material from Spain allowed to distinguish both species and genera, and to assess both to Mesoeucrocodylia (Schwarz & Fechner, 2004, 2008); although their exact position remains unclear.

Isolated teeth from the Lourinhã Formation, with a revision from *Lusitanisuchus mitracostatus* from Guimarota, and their palaeoecological implications are described in Chapter 2.2.

1.5 Objectives

During the Late Jurassic, Portugal seems to have played an essential role in biotic dynamics during that period. Vertebrate microfossil assemblages can provide valuable insights for systematic and paleoecological studies, and the Late Jurassic of Portugal is known to yield several vertebrate microfossil assemblages (VMA) localities of interest.

Thus, this PhD thesis focused on characterizing the herpetofauna (amphibian and small reptiles) from the Late Jurassic of Portugal, with the study of the fossil assemblage of Guimarota and the inputs of new localities from the Lourinhã Formation, as well as new insights from a Late Cretaceous locality in Spain. To reach that goal, the main objectives were:

- Evaluate the biodiversity and richness of the Lourinhã Formation, for illustrating its potential for palaeoecological and palaeoenvironmental analysis; and comparing it with the coeval, well known Guimarota bed palaeoecosystem. This includes three subobjectives:
    - characterize the crocodylomorph diversity and its palaeoecology;
    - explore the amphibian diversity, with focus on the albanerpetontids;
    - and describe other small herpetofauna from the Late Jurassic of Portugal, including choristoderes and lepidosauromorphs.
- Review the taxonomy and phylogeny of Albanerpetontidae, with focus on Iberian specimens. This also has two subobjectives:
    - characterize *Celtedens* in the Late Jurassic of Portugal;

- and describe the material of Blasi from the Late Cretaceous of Spain.

1.6 Material and methods

1.6.1 Fieldwork & sieving fossils

All the fieldwork was carried out under the supervision of the Museu da Lourinhã in the outcrops of the Lourinhã Formation exposed along the Portuguese coastline, between the Forte de Nossa Senhora in Paimogo (Lourinhã municipality, Lisbon district) at the North and Praia das Conchas (Lourinhã municipality, Lisbon district) at the South (**Figure 1.6.1A**). Prospection for microfossils have always been part of the activities of the Museu since the 1990s, but they were mostly restricted to surface sampling. Systemic sampling for microvertebrates was done during the digging seasons between 2016 and 2022 (**Figure 1.6.1B**), apart from 2020 because of the COVID-19 outbreak.

The study of vertebrate microfossil assemblages requires several steps (Eberth *et al.*, 2007b; Buscalioni *et al.*, 2008, 2018; Gasca *et al.*, 2017; Rogers *et al.*, 2017): (1) collecting bulk sediment; (2) letting it dry; (3) soaking them in oxidant solution, chosen according to the aim of the study; (4) screen washing them through sieves of different size according to what is sought; (5) picking the concentrates using a binocular lens. It may sometimes be necessary to conduct at several drying/soaking/screen

washing cycles, according to the quality of the process. For this work, two slightly different methodologies have been used according if the sediments have been prepared in the Museu da Lourinhã, or in the Departmento de Ciências da Terra of NOVA School of Science and Technology (FCT-UNL) facilities.

After being collected, bulk sediments have been stored in ML for periods from one week to four years. It seems that the period of storage does not affect the quality of the material found, but sediments stored for shorter time will require a couple more soaking/screen washing cycles. This is most likely due to the high humidity in the museum storage conditions of Lourinhã, which slowed the drying.

From 2016 to 2019, sediments have been soaked in a bucket full of a solution of 50 L of water and 0.5 L to 1 L of hydrogen peroxide (H_2O_2; original solution at 50%, final solution at 0.5 to 1%), for periods from one day to one week (**Figure 1.6.1C**). Then, sediments have been screen washed using a sieving table in ML facilities. The sieving table was composed of three levels of mesh: 2 mm, 1 mm and 0.5 mm. As foraminifera and pollens were not the main focus of my work, considering the high amount of sediments to process, we did not use smaller meshes to saved them. With this set up, one bulk of 20 kg of sediments would usually require up to eight hours of screen-washing.

Figure 1.6.1: Overview of the sampling and methods used for sieving and storage. **A**, prospecting in Valmitão vertebrate microfossil assemblage. **B**, collecting sediments in Zimbral vertebrate microfossil assemblage. **C**, 50 L buckets used to soak sediment in water. **D–F**, screen-washing facility, pumping water from a well (D) and using garden sprinkler to wash the sediments with three level of meshes (E), while recycling water (F). **G**, picture from a workshop organized at Parque dos Dinossauros de Lourinhã. **H** and **I**, Eppendorf PCR clear polyethylene tubes used for the new repository strategy.

Therefore, because of the massive amount of water wasted in the process, as it could not be recycled, and the highly time-consuming process, a new strategy was established in 2019. It was decided to soak sediment in smaller buckets (10 L) using only water, but for a longer period (one to two weeks). Then, we created a circular system allowing us to pump water into a water source, wash our sediments at a higher rate, and recycle the water from the original source (**Figure 1.6.1D–F**). The potential use of natural

(rivers, the ocean) or private (e. g. well) sources motivated to not resort to use H_2O_2 for soaking. We used the same sieving table, with three levels of mesh (2 mm, 1 mm, 0.5 mm) to screen-wash the sediments. With this set up, one bulk of 20 kg of sediments would usually require three to four hours of screen-washing.

In FCT-UNL facilities, sediments have been soaked in small buckets, with a solution of 3 to 4 L of water and 250 to 300 mL of H_2O_2 (original solution at 30%), for a period of 24 to 48 h. Then, sediments were screen washed using only one 0.5 mm sieve. Because of that, only material bigger than 0.5 mm had been concentrated. With this set up, one bulk of 20 kg of sediments would usually require six hours of screen-washing. The resulting concentrates were then dried in a dryer at 50 °C for 24 h and sieved (dry sieving) with a screening machine (10 min at amplitude 60), using three levels of mesh: 2 mm, 1 mm and 0.5 mm.

Once prepared, all sediments have been picked by using stereoscopic microscopes, Leica MZ6, Olympus SZ51, or XXX. Each fraction was picked separately using a paintbrush, and each new specimen has been stored in plastic box specifying the locality, from which bulk sample and its date of sampling, and in which the fraction it has been picked. The picking itself spanned through 2016 up to 2022, and involved the participation of the volunteers at ML, in the Parque dos Dinossauros de Lourinhã (PDL), as well as the students from the Master in Paleontology program held in FCT-UNL.

During 10 months in 2019, picking was also part of the Citizen Science Project "MicroSaurus", that took place in three facilities (ML, PDL, and FCT-UNL). This project aimed to involve the local and visiting communities of Lourinhã in the care of their natural and palaeontological heritage and familiarize them with the work of palaeontologists, targeting mostly pre-teenagers (10-13 years old). With 45-60 min workshops of 10-20 people (**Figure 1.6.1G**), each participant was given a small amount of sediment to pick microfossils they could identify using an illustrated guide. With the help of one preparator of the Museu da Lourinhã, I checked the sediments picked, adding the fossils that could have been unidentified by the participants. In total, 393 participants from all ages were involved in MicroSaurus, resulting into 11,462 microfossils picked over 202 hours.

Eventually, over two tons of sediments have been sampled from the Lourinhã Formation. Screen-washing, picking, and identification are still on-going processes. So far, near 20,000 microfossils have been picked, among which 5,100 vertebrate remains could be identified. A sneak-peak of the palaeontological context of the microvertebrates from the Lourinhã Formation is provided in Chapter 2.1.

1.6.2 Repository of the specimens from the Lourinhã Formation

All specimens from the Lourinhã Formation are currently housed in the Museu da Lourinhã (ML). Although the Museu has been collecting

microfossils for years, its preparation laboratory had to adopt new strategies for processing, storing, and accessing the thousands of new fossils that would implement its vertebrate micropalaeontological collection. Previous methods were using plastic boxes of different sizes occasionally associated with cotton or polyethylene foam, zip lock plastic bags or gelatine capsule associated with polyethylene foam; but none of these techniques presented satisfactory archivable solutions.

To reach a compromise, the preparator and curator team of the Museu da Lourinhã and I discussed on a new protocol, based on my own experience in microvertebrate collections in other institutions and their own requirements. The constrains were: (1) packaging thousands of fossils in materials that are stable, economical, easy to acquire and manipulate, and compatible with the use of imaging techniques and others analyses; (2) assuring the fossils were stored in safe conditions; (3) optimization of the time spent in conditioning and studying the specimens; (4) optimization of the space occupied in museum storage facilities; (5) sustainability in the choice and use of materials; (6) and minimizing specimen handling. This resulted in selecting polyethylene foams of different densities in 0.5 mL Eppendorf PCR clear polyethylene tubes to store the fossils (**Figure 1.6.1H** and **I**); together with the development of specific tools, such as a puncture kit, to optimize time and material.

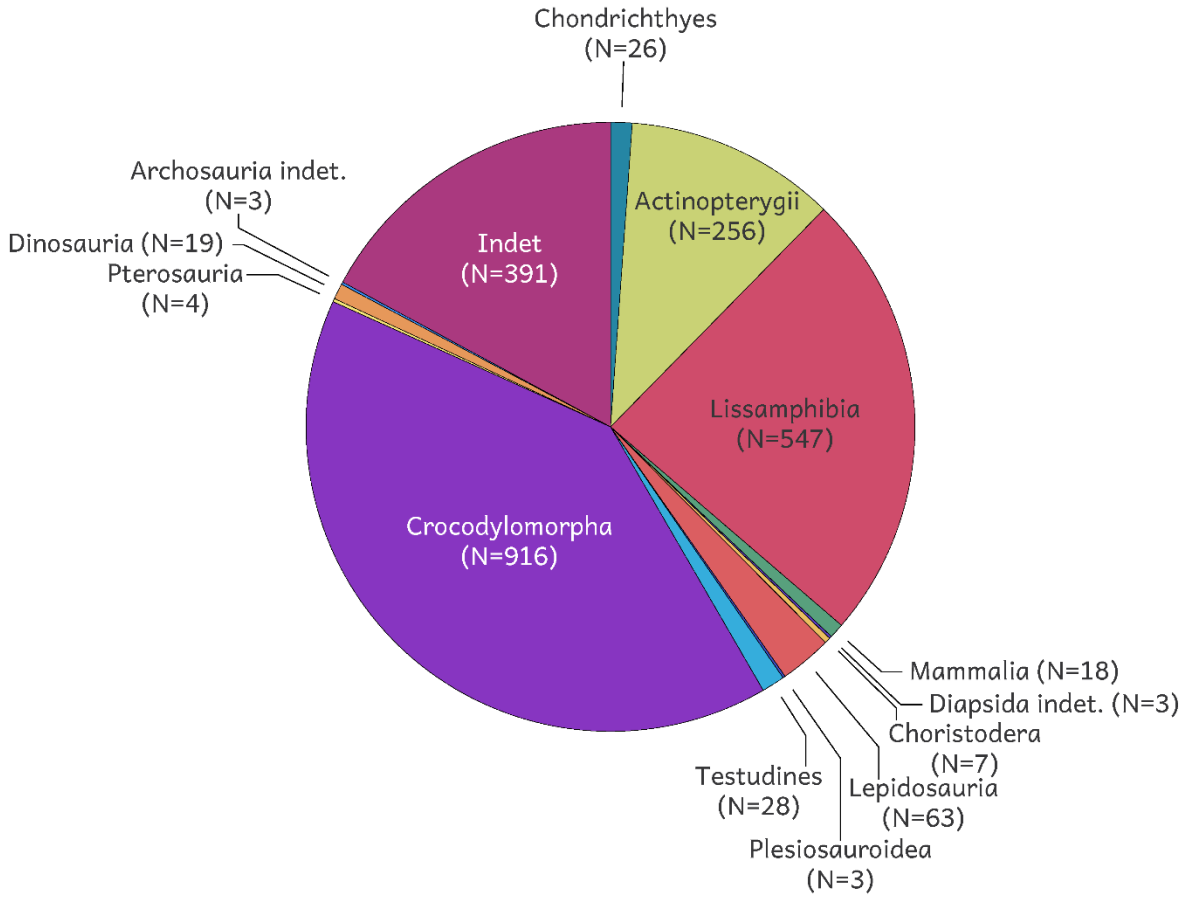

Figure 1.6.2: Taxonomic classification of the new specimen numbers catalogued during this thesis.

Following this new protocol, a total of 2,284 new catalogue numbers have been catalogued (**Figure 1.6.2**), increasing substantially the ML collection (previously around 2,700-2,800 specimens). The full specimen list is available in Appendix A.1. They are highly dominated by crocodylomorph, actinopterygians, lissamphibians, and undetermined vertebrates remains. It is here noted that the number of catalogue numbers (2,284) is lower than the number of remains counted (5,100). This is due to an agreement with the curation team of ML and the decision to not label fish scales and neural arch fragments individually; but instead to group them according the bulk and the fraction they have been picked from, and attribute a single

catalogue number to that batch. Eventually, only the specimens that have been pictured or figured received a dedicated catalogue number.

1.6.3 The Guimarota collection

As explained in section 1.1.1, all specimens recovered by the Germans during the excavations in Guimarota should be returned to the Museu da Geológico (MG) in Lisbon once studied. Since the 2000s, material from Guimarota have been gradually retrieved and catalogued by the people of LNEG. Considering the thousands of specimens it represents, it is impossible to know for sure if all the specimens are back in Portugal. However, Prof. Thomas Martin confirmed in the last repatriation (June 2023) that all the studied and published material should now be in Lisbon.

Nevertheless, cataloguing and curating the Guimarota collection constitute a monumental challenge, as the material represents thousands of fossils from different taxa—so with different biological and taphonomic properties—with different states of preparation. The material was sent back by boxes and labelled sample boxes organized according to the works done by the German, which provided preliminary catalogue lists. Based on these previous works and the labels, the MG organized the specimens by taxa in larger boxes (**Figure 1.6.3A**) and attributed for each sample box a dedicated specimen number, and from there was constitute the current catalogue (**Figure 1.6.3B**).

Figure 1.6.3: Storage of the Guimarota collection at the Museu Geológico in Lisbon. **A**, the storing boxes for the major taxonomic group. **B**, example of different option of storage of squamates specimens, with the MG catalogue. **C**, overview of the amphibian specimens from the Guimarota collection; in frame, albanerpetontid specimen MG28656 illustrating that one specimen number can refer to several individuals, scale is 2mm.

Due to the importance of the Guimarota beds for the Late Jurassic of Portugal, but the few amounts of work focusing on amphibians and small reptiles; checking and reviewing their specimens were a major task planned within the thesis. The first challenge was to locate the specimens previously published and figured, notably potential holotypes. This was complicated by

the fact that the Germans used some accession numbers, but those were not identified neither on the labels of the boxes nor in the MG catalogue lists. Furthermore, some of the taxa identified in the Guimarota beds have seen their taxonomy challenged lately, but the new identification was not implemented in the catalogue list in MG, and the specimen is still stored within the box of its old identification. One good example for this is the crocodylomorph *Lisboasaurus estesi*: most of the specimens are not stored within the rest of the crocodylomorph material, but within the squamate material; and if some referred and figured specimens were located, I failed to find the holotype. Finally, the MG catalogue does not give much information on the content of the box, beside the taxonomic identification and sometimes which bone is in it. However, several boxes can contain mixed elements (cranial and post cranial bones) or even more than one bone. The albanerpetontid collection is a good representative of this tendency, with some boxes filled with hundreds of bones (**Figure 1.6.3C**), which can make identification and descriptions confusing.

If the quantity of the material from the Guimarota beds was anticipated, the challenges faced for its revision were unexpected and, in COVID-2019 pandemic, delayed the work as every single sample box had to be checked to confirm its content and locate key specimens. However, despite the constrains and challenges, I managed to check all the boxes from the lissamphibian material, as well as most of the squamate material. I also helped other students with the mammalian and dinosaurian material. It is

during that work that I stumble upon some misidentified and mislabelled specimen of *Cteniogenys* and *Marmoretta*. In total, 954 sample boxes with unique specimen numbers have been checked (see Appendix A.2) for complete list); however, due to the curation of the collection, the true number of specimens is unknown.

Eventually, mislaying cases like *L. estesi* were more the exception rather than the rule, and it cannot be excluded than the missing specimens have been misidentified, mislabelled, stored elsewhere in the collection, or have not been catalogued yet by MG. The revision of the Guimarota material is a never-ending story, requiring a lot of work and can be overwhelming; but I hope to show in this thesis the value of it for future works.

1.6.4 Collection visits in non-Portuguese institutions

In order to properly describe the new material of the Lourinhã Formation, several collection visits were realized in Europe and North America to study comparative material. Notably, as the albanerpetontid phylogeny required a complete revision, I intended to check as many holotypes, paratypes, and referred material as possible. I included in my work a set of relevant undescribed albanerpetontid specimens that has been reported in previous works.

- The "Paskapoo species" *sensu* Gardner 2002 is an unnamed albanerpetontid species reported from the upper Paleocene Paskapoo

Formation (upper Palaeocene; Alberta, Canada) (Gardner, 1996, 2000a), but never fully described; nevertheless; it has been referred to *Albanerpeton* sp. and have been used in all subsequent phylogenies.

- The "Purbeck species" *sensu* Carrano *et al.*, 2022 referred to material from the Lulworth Fm (Berriasian; England), which has been reported but never fully described (McGowan & Ensom, 1997; Gardner, 2000a; Gardner *et al.*, 2003); it has been referred to *Celtedens* sp. (McGowan & Ensom, 1997; Evans & McGowan, 2002).
- Specimens from the Cedar Mountain Fm (Albian/Cenomanian; Utah, US) has been described as *Albanerpeton* sp., cf. *A. nexuosum* (Gardner, 1999b) and included in some subsequent phylogenies.
- The "Sânpetru species" *sensu* Carrano *et al.*, 2022 referred to material from Pui localities of the Haţeg Basin (Maastrichtian; Romania) which has been referred to *Albanerpeton* sp. but never fully described (Grigorescu *et al.*, 1999; Folie & Codrea, 2005)
- The "Uña species" *sensu* Sweetman & Gardner 2013 referred to material from the Uña locality of the La Huérguina Fm (Berriasian; Spain)

that was described by Wiechmann (2003) has a new *Albanerpeton* species; however, as the work does not meet the criteria for a valid nomenclatural published work (Arts. 8 & 9) of ICZN, the name is now considered unavailable (Martín *et al.*, 2012); the material has since been referred to cf. *Wesserpeton* sp. (Sweetman & Gardner, 2013) and included in subsequent phylogenies.

- The "Csehbánya species" *sensu* Carrano *et al.*, 2022 referred to material from the Csehbánya Fm (Santonian; Hungary) and has been described as Albanerpetontidae indet. (Szentesi *et al.*, 2013).
- Specimens from the Aguja Fm (Lower Campanian; West Texas) have been referred to *Albanerpeton* sp., cf. *A. galaktion* was too fragmentary, *Albanerpeton nexuosum* Estes 1981, or Albanerpetontidae indet. (Wick, 2021).
- Specimens from Guelb el Ahmar locality of the Anoual Syncline (Bathonian; Morocco) have been referred to Albanerpetontidae indet. (Haddoumi *et al.*, 2016).

- Specimens from the Angeac-Charente Lagerstätte (Berriasian; France) have been referred to Albanerpetontidae indet. (Allain *et al.*, 2022).

The selection of the collections to be visited was done based on the following criteria: (1) relevance of the collection (presence of holotypes or paratypes of interest); (2) relevance of the material hosted (faunal composition and age of the assemblages); (3) feasibility of the visit under external constrains (availability of the material, level of COVID-restrictions at the time of the visit, expanses for travel and lodging); and (4) commodity (during field work or international meetings, compromising with other to share the expanses).

Eventually, 13 non-Portuguese institutions were visited (see **Table 1.6.1**), plus a three-months internship at Institut Català de Paleoecologia Humana i Evolució Social, to acquire deep training in lissamphibian and squamate osteology.

Table 1.6.1: Chronological list of collection visits in non-Portuguese institutions, with a quick summary of the specimens checked.

Institutions	City (Country)	Date of the visit	Specimens checked	Remarks
Museo de Ciencias Naturales – Universidad Zaragoza	Zaragoza (Spain)	January 2022 – July 2023	MPZ 2009/179—MPZ 2009/227 (referred material) of *Albanerpeton* aff. *A. nexuosum*; referred material of aff. *Paradiscoglossus* sp.; referred material of Palaeobatrachidae indet.; referred material of Scleroglossa indet.; referred material of Anguidae indet.	The albanerpetontid specimens have been described as a new species in this thesis, with MPZ 2009/219 being the holotype
Museo di Paleontologia	Napoli (Italy)	June 2022	M542 (holotype) of *Celtedens megacephalus*	
Natural History Museum	London (UK)	July 2022	BMNH R.16336 (holotype) and referred material of *Anoualerpeton priscum*; referred material of Albanerpetontidae indet. from Purbeck	The *Wesserpeton evansae* specimens were not available during the visit, as well as some specimens of *Anoualerpeton priscum*, and no further visit could have been scheduled
National Museum of Natural History – Smithsonian Institution	Washington, D.C. (USA)	July 2022	USNM 466050 (Anura from Quarry 9); USNM 466051, USNM 466052, USNM529422, USNM 529413 (Caudata from Quarry 9); USNM 546683 (holotype) and referred material of *Albanerpeton ektopistikon*; USNM 6134 (holotype) and referred material of *Cteniogenys antiquus*	At the time of the visit, *A. ektopistikon* was not described yet but the material could be checked
American Museum of Natural History	New York City (New York, USA)	August 2022	Referred material of *Albanerpeton nexuosum*; AMNH 21500 (Discoglossidae); AMNH 8133 (*Eopelobates*); AMNH 27645, AMNH 2377 (*Paramocellodus*); AMNH 27646, AMNH 27647 (*Dorsetisaurus*); AMNH 2340 (*Cteniogenys*)	
Yale Peabody Museum of Natural History	New Haven (Connecticut, USA)	August 2022	YPM VP 059451, YPM VP 059452, YPM VP 059468 (Albanerpetontidae indet.);	

			YPM VP 001863 (holotype of *Comobatrachus aenigmatis*); YPM VP 001862 (holotype), YPM VP 001394, YPM VP 001568, YPM VP 003919 (paratypes), and referred material of *Eobatrachus agilis*; referred material of *Cteniogenys antiquus* and *Cteniogenys sp.*	
Carnegie Museum of Natural History	Pittsburgh (Pennsylvania, USA)	August 2022	CM6467 (holotype) of *Adelphsiren olivae*; CM6468 (holotype) and referred material of *Opisthotriton kayi*	
Field Museum of Natural History	Chicago (Illinois, USA)	August 2022 & June 2023	FMNH PR 805 (holotype) and referred material of *Albanerpeton arthridion*; FMNH PR 391 (holotype) and referred material of *Prosire, elinorae*; FMNH PR 2078 (holotype) and referred material of *Nezpericus dodsoni*	Part of the specimens were on loan during the first visit, but a second visit could be coordinate after their return
Museo de la Ciencias de Castilla-La Mancha Museu Paleontológica de Castilla-La Mancha	Cuenca (Spain)	January 2023	MCCM-LH6020 (holotype), MCCM-LH030, MCCM-LH17069, and MCCM -LH6001 (paratypes) of *Celtedens ibericum*; MCCM-LH2850, MCCM-LH6021, MCCM-LH26515 (paratypes) of *Valdotriton gracilis*; MCCM-LH21171 (holotype) of *Gracilibatrachus avallei*; MCCM-LH11393 (holotype) of *Iberobatrachus angelae*	The specimens are located in both institutions, according if they are on exhibit or in storage
Muséum national d'Histoire naturelle	Paris (France)	March 2023	MNHN-LGA176 (holotype) and referred material of *Albanerpeton inexpectatum*; MNHN.MCM 187 (holotype) and referred material of *Anoualerpeton unicum*; referred (but unpublished) material from Anoual syncline of Albanerpetontidae indet.; referred material from Angeac-Charentes of Albanerpetontidae indet.;	Part of the *A. inexpectatum* material was on loan with Prof. James Gardner during the visit

			MNHN.F.MAE126 (holotype) of *Triadobatrachus massinoti*	
Royal Tyrrell Museum of Palaeontology	Drumheller (Alberta, Canada)	June 2023	Referred material of *Albanepeton arthridion*; OMNH 25400 (holotype) of *Albanerpeton cifellii*; RTMP 95.181.70 and referred material of *Albanerpeton gracile*; referred material of *A. nexuosum*; referred material to the "Paskapoo species", including UALVP 16243 (putative holotype, J. Gardner, pers. comm., 2023); referred material from type locality of *Albanerpeton inexpectatum*; referred (but unpublished) material from *Albanerpeton pannonicum* (on loan); referred material of *Cteniogenys*	Holotype UCMP 49547 of *A. nexuosum* could not be located and is presumably lost
University of Alberta Laboratory of Vertebrate Palaeontology	Edmonton (Alberta, Canada)	June 2023	UALVP 16203 (holotype) and referred material of *Albanerpeton galaktion*; referred material of *A. nexuosum*; referred material of *Cteniogenys*	

If the global effects of the COVID pandemic were not and could not be anticipated at their levels, most of the institutions that were targeted in amount of the project could eventually be visited and their specimens checked despite the restrictions and time constrains. The major absences being: (1) the Iberian material housed in Berlin and the Hungarian/Romanian albanerpetontid material, due to time constrains; and (2) the albanerpetontid material from Central Asia housed in Saint-Petersburg, due to the current geopolitical crisis.

While checking the comparative material for albanerpetontid from Museo de Ciencias Naturales – Universidad Zaragoza, new specimens previously unpublished and unreported from the same locality were reported. This new observation confirmed that this material could be described as a new species within the scope of the work on albanerpetontid and, because of the new insight the Spanish material could bring, it was decided to include them in the final draft of this thesis.

1.7 Structure of the thesis

This thesis is divided in three sections and seven chapters, comprising the core of this PhD thesis, plus the general introduction and conclusions. Supplementary information is provided in the Appendices at the end of the manuscript.

Section 2 regards a general overview from the Kimmeridgian-Tithonian of Portugal, with a more dedicated focus on small reptiles. Section 2.1 provides a short palaeontological setting from the vertebrate microfossil from the Lourinhã Formation. Section 2.2 is dedicated to described crocodylomorph isolated shed teeth and their palaeoecological implications as well with a short revision of *Lusitanisuchus mitracostatus*. Section 2.3 is dedicated to the revision and description of material attributed to *Cteniogenys* by Seiffert, as well as mislabelled specimens; to confirm the presence of *Marmoretta* in the Guimarota beds.

Section 3 regards description of the albanerpetontids from the Iberian Peninsula and constitutes the biggest chunk of the thesis. Section 3.1 and Section 3.2 are dedicated to the specimens from the Kimmeridgian-Tithonian of Portugal, the former focusing of morphological intraspecific variation in the fused frontal bones, and the latter on describing a new species. Section 3.3 is dedicated to the description of a new species from the Maastrichtian of Spain, which was discovered during a research stay visiting collections abroad for comparative purposes. Section 3.4 proposes a new phylogeny of the group, based on observations from both previous species and others already described in the literature, as well as its implications.

Section 4 provides a general discussion to put all the results in context, as well as drawing future works from this thesis.

The present thesis is a hybrid between thesis manuscript and article-based thesis. At the final stage of the submitted thesis (2nd of April 2024), the latter includes 2 publications, 1 submitted article, and 2 manuscripts in review (with all reviewed a first time by co-authors); in journals with an impact factor ranging from 1.4 to 3.286. The work presented in Section 2.1 has been presented in an international conference meeting and published as a long abstract in an indexed journal with an impact factor of 2.0. It is expected to be submitted in a more extended format after the defence in a Q1/Q2 indexed journal. Sections 3.2 to 3.4 are submitted as two articles, one for each species, and adapting the content according to the scope of each article.

A citation of the published articles, followed by their metrics the year of publication, is given below the title of the corresponding chapter. All papers have been written as a first author, although all have been part of collaborative works to which the student participated and lead.

In order to promote equal access to all levels of education and vocational training for the vulnerable, including persons with disabilities (Goal 4, sections 4.4 of Objectives UN 2030 Agenda for Sustainable Development), the manuscript of this thesis has been written with Andika New Basic, a font specifically designed for dyslexic or visually impaired persons, and formatted (line spacing 1.5, letter spacing 0.5) to facilitate

reading for them; and figures were conceived as much as possible to include colourblind persons.

2 THE VERTEBRATE MICROFAUNA FROM THE LATE JURASSIC OF PORTUGAL

2.1 Chapter 1: Sneak peek on the Vertebrate Microfossil Assemblages from the Lourinhã Formation

Work presented as poster during the 14th Symposium on Mesozoic Terrestrial Ecosystems and Biota, and published as long abstract in a special volume of *The Anatomical Record* (Journal impact factor for 2022: 2.0; CiteScore: 4.3; SJR: 0.554; H-index: 71)

Guillaume ARD, Ezquerro L, Moreno-Azanza M & Mateus O. 2023. Vertebrate microfossil assemblages from the Lourinhã Formation: a sneak peek on the palaeoecology of the Late Jurassic in Portugal. *14th Symposium on Mesozoic Terrestrial Ecosystems and Biota*. *The Anatomical Record (Suppl. 1)* 306:118-121. https://doi.org/10.1002/ar.25219

2.1.1 Introduction

Vertebrates Microfossil Assemblages (VMAs) capture a time averaged, accurate record of their surrounding palaeocommunities, share similar taphonomic history, and provide reliable signals for palaeo-metacommunity analysis (Rogers *et al.*, 2017). They provide a snapshot of the palaeobiodiversity over the period of their formations and allow high-

resolution information and, therefore, constitute a keystone for integrative palaeoecological studies (Eberth *et al.*, 2007c; Gilbert *et al.*, 2018). Despite their proven interests, the task of collecting microfossils is time consuming and in general produces relatively unimpressive fossils, which results in very few, well studied Mesozoic VMAs worldwide.

Portugal represents one of the major data point for the Upper Jurassic, thanks to the Konzentrat-Lagerstätte of the Guimarota beds (Martin & Krebs, 2000). Nevertheless, despite other slightly younger VMAs have been reported from the Alcobaça Formation (Malafaia *et al.*, 2010) and the Lourinhã Formation (Guillaume, 2018), no extensive study has been carried out on them.

2.1.2 Material & Methods

For this study, six samples of bulk rock have been collected in three different localities (Porto das Barcas, Zimbral, and Valmitão), representing a total sampling of over 1,300 kg. From the concentrates retrieved from screen-washing, over 20,000 fossil remains have been collected, among which 3,971 vertebrates fossils could have been identified so far. This sample from three localities represents the first statistically significative approach to the microvertebrate diversity of the Lourinhã Formation and its palaeoecology. Most vertebrates group previously reported from the Upper Jurassic of Portugal were recovered, and all localities yielded a multi-individual, multi-taxic accumulation of fragmented and isolated bones (see

Figure 2.1.1 and **Table 2.1.1**). It is here noted that between the study presented in Section 2.2 and the present overview, more crocodylomorph teeth were recovered, including putative *Machimosaurus* and pholidosaurid teeth, as well as more material that could be attributed to *Lusitanisuchus*.

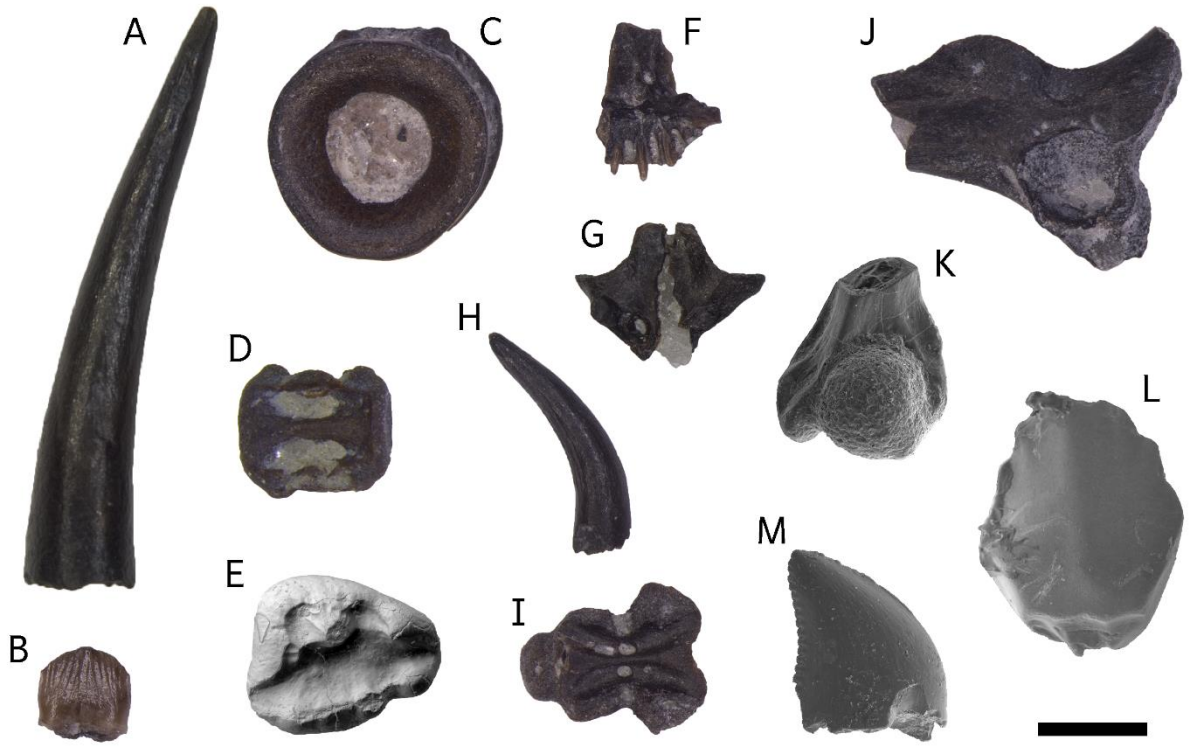

Figure 2.1.1: Sample of vertebrate microfossils found in the Lourinhã Formation (Kimmeeridgian–Tithonian, Portugal). **A**, Gnathosaurinae tooth. **B**, *Lusitanisuchus* tooth. **C**, Actinopterygii vertebra. **D**, Choristodere vertebra. **E**, Multituberculata tooth. **F**, Albanerpetontidae right premaxilla. **G**, Caudata atlas. **H**, Plesiosauroidea tooth. **I**, Squamata vertebra. **J**, Anura ilium. **K**, Anura distal humerus. **L**, Neornitischia tooth. **M**, Coelurosauria tooth. Scale is 1 mm.

As observed in many VMAs (Rogers & Kidwell, 2007; Rogers & Brady, 2010), Osteichthyes and Crocodylomorpha are the most abundant groups (**Figure 2.1.2**), mainly due to ganoine scales and isolated shed teeth, whose histological structure make them harder and easier to fossilized (Brinkman

et al., 2005; Blob & Badgley, 2007; Baszio, 2008; Carrano *et al.*, 2016; Rogers *et al.*, 2017; Simões *et al.*, 2020). Complete counting is provided in Appendix B.

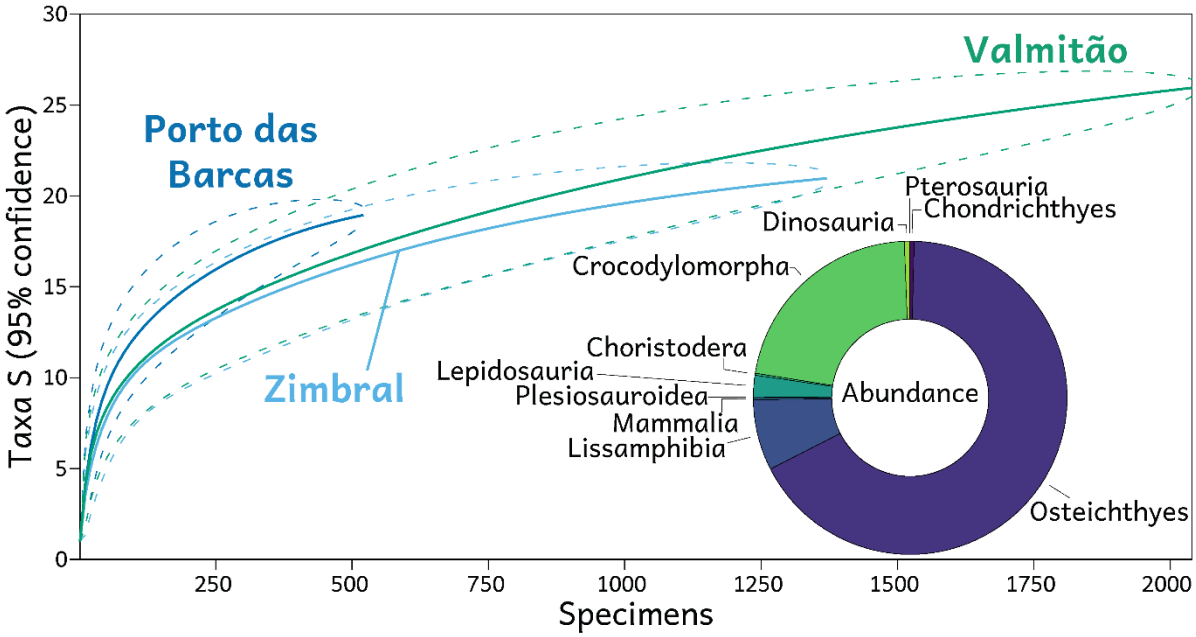

Figure 2.1.2: Rarefaction curves of each sampled locality (dash-lines represent the 95% interval) and general abundance of major vertebrate groups across all localities.

Rarefaction of the sampled localities suggests that Zimbral has been successfully sampled, while Porto das Barcas may require more work. Valmitão, otherwise, present an intriguing profile. Despite having been more sampled than the other two localities, it does not present a plateau yet and instead presents a gradual pace toward the end of the graph. This may due to an overrepresentation of some taxa relatively to rarer new additional clades (Avrahami *et al.*, 2018).

Table 2.1.1: Faunal composition of the three Vertebrates Microfossil Assemblages (VMA) sampled from the Lourinhã Formation.

	Valmitão	*Zimbral*	*Porto das Barcas*
Hybodontidae			x
Batoidea			x
Indet. Actinopterygii			x
Semionotiformes	x	x	x
Pycnodontiformes		x	x
Caturidae	x	x	x
Indet. Amphibia	x	x	
Albanerpetontidae	x	x	x
Anura indet.	x	x	x
Caudata indet.	x		
Dryolestidae	x		x
Multituberculata	x		x
Plesiosauroidae	x	x	
Lepidosauria	x	x	x
Choristodera	x	x	x
Crocodylomorpha indet.	x	x	x
Atoposauridae	x	x	x
Bernissartiidae	x	x	x
Goniopholidae	x	x	x
Pholidosauridae?	x		
Machimosaurus?	x		x
Lusitanisuchus	x	x	x
Thyreophora	x		
Megalosauridae	x	x	
Heterodontosauria	x	x	
Sauropoda	x	x	
Dromaeosauridae	x	x	x
Theropoda	x	x	
Pterosauria	x	x	

2.1.3 Palaeoenvironmental reconstruction

The Lourinhã Fm. is well known for its vertebrate fossils, mainly dinosaurs, including osteological, ichnological and oological remains of great importance (e.g. Antunes & Mateus 2003; Mateus & Milàn 2010;

Fernandes *et al.* 2021). The Upper Jurassic succession represents transitional to continental environments, (Hill, 1988) and was subdivided in five members: Praia de Amoreira Mb., Porto Novo Mb., Praia Azul Mb., Assenta Mb. and Santa Rita Mb. (Hill, 1988). Traditionally, the formation has been characterized as fluvial and deltaic deposits with shallow marine intercalations, being the marine entrances more common in the Praia Azul Mb., in which three major transgressions have been recognized (e.g. Hill, 1988). The three localities described here are close to the Lourinhã city: Valmitão VMA is located in the upper part of the Porto Novo member while Zimbral VMA and Porto das Barcas VMA belong to the Praia Azul member.

Valmitão VMA (5 m-thick) is characterized by a multicoloured succession of greyish and purplish silty marls, violet and orange mudstones, being common interbedded brownish sandstones. Strata are dm in thickness and show a tabular geometry. The fine-grained lithologies show massive texture and frequently carbonate nodules, while in the mudstones rhizoliths, rhizotubules and mottling are also very common. The fine to medium sandstones comprise massive or cross-laminated strata with some rounded extraclats (< 2 cm in diameter). Zimbral VMA (2.8 m-thick) involves greyish marls with occasional silty levels that comprise three tabular massive beds. The deposits coarsen upwards (m in thickness) and show coal or plants debris along the strata. Porto das Barcas VMA (3.75 m-thick) comprises massive tabular beds of dark marls with occasional silts and very coarse sandstones interbedded. They form five, dm in thickness, coarsening

upwards sequences based on an increase in grain size, intraclasts and bioclasts occurrence. The bioturbation or nodulization are practically absent.

The three localities are dominated by fine-grained deposits but show clear differences in colours, terrigenous fraction, and degree of pedogenesis. The variegated colours, lack of grading, coupled with more carbonate nodules and rhizocasts in the Valmitão locality suggest an environment with low sediment supply and long periods of subaerial exposure. The greyish sediments in Zimbral exhibit coal remains and poor development of nodules related to oscillations in the water availability, implying an area of alternating conditions between wet and dry periods. Finally, the very low degree of pedogenesis and the dark-coloured materials of Porto das Barcas site indicate wetter conditions, probably associated with permanent sheet of water and anoxic environments.

2.1.4 Palaeoecology of the Lourinhã Formation

The correspondence analysis (**Figure 2.1.3A**) performed on the sampled localities shows that they shared similar overall diversity, they still yield some distinctive features. Porto das Barcas is strongly associated with Chondrichthyes, while Zimbral is more associated with Osteichthyes and Dinosauria and Valmitão with Crocodylomorpha and Amphibia. Similarly, undetermined Actinopterygii remains (isolated vertebra and fish scales) and Lepidosauria are each equally represented in all localities. Meanwhile,

Crocodylomorpha and Dinosauria are the most diverse (**Figure 2.1.3B**), but their taxonomic identification relies mostly on isolated teeth.

Although obligate aquatic taxon remains are the most abundant in each VMA, these taxa represent the lower diversity. Indeed, the VMAs from the Lourinhã Fm are more dominated by amphibious taxa, when compared to any other localities (**Figure 2.1.4A**), and share similar clade relative frequencies between them (**Figure 2.1.4B**). Albanerpetontids were considered in this thesis as amphibious, following previous statements in similar analyses in other assemblages where they have been reported (Buscalioni *et al.*, 2008; Carrano *et al.*, 2016; Allain *et al.*, 2022); but further palaeoenvironmental works are required to properly assess their ecology. Notably, the VMAs from the Lourinhã Fm also share relative frequencies with the Ksar Metlili Fm from the Tithonian-Berriasian of Morocco (Lasseron *et al.*, 2020). The Lourinhã Fm and the Ksar Metlili Fm appear also to be particularly richer in Pterosauria and Choristodera than other localities. It is worth noticing that the Lourinhã Fm was the only geological units to yield Plesiosauria in the sample selected for the analysis; but isolated plesiosaur teeth from small individuals or juveniles have been reported in non-marine settings from the Upper Jurassic (Gao *et al.*, 2019; Bunker *et al.*, 2022; Weryński & Błażejowski, 2023).

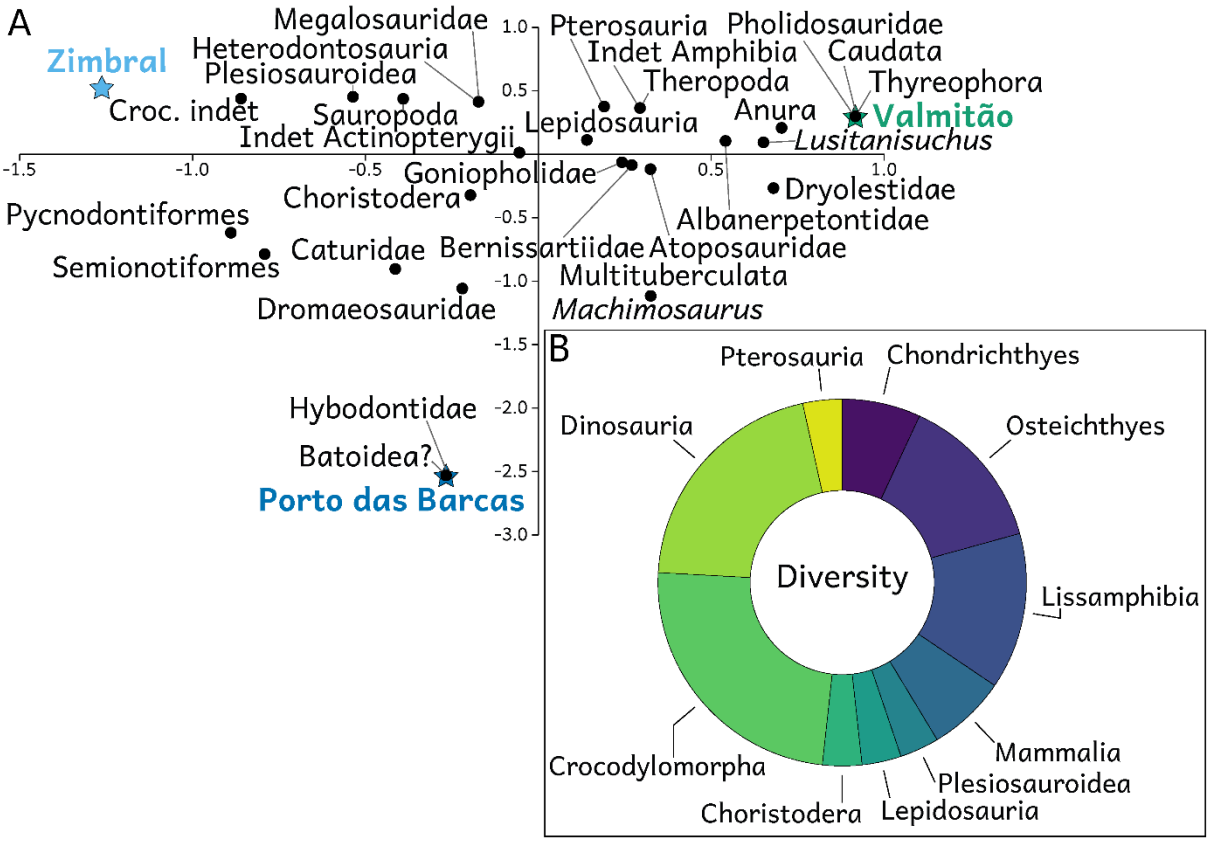

Figure 2.1.3: Palaeobiodiversity in the Lourinhã Fm. **A**, correspondence analysis (scaling 1) of microvertebrates sites from the Lourinhã Fm using faunal data. **B**, general taxonomic diversity of major vertebrate groups across all localities.

On another notice, localities from the Lourinhã Fm differs in their relative frequencies with the Berriasian Angeac-Charente Lagerstätte (southwestern France). The latter is notably richer in dinosaurs and chondrichthyans remains (Allain *et al.*, 2022; Pintore *et al.*, 2023). Furthermore, if lepidosaurian and mammalian remains have been recovered from the three Lourinhanese VMAs, they appear in much less abundance and diversity than expected from this kind of assemblages, especially compared with the Kimmeridgian-Tithonian Quarry 9 from Como Bluff in the US (Carrano & Velez-Juarbe, 2006). This may reflect wetter conditions; but also point towards ecological differences in the palaeobiodiversity between the

Lourinhã Fm and the Morrison Fm, contrary to what has been reported from the macrofauna (Mateus, 2006).

However, slight differences can be spotted from one locality to another (**Figure 2.1.4A**). Compared to the other two, Valmitão VMA is dominated by facultative and amphibious taxa, suggesting it was the most continental of the assemblages, sharing taphonomic similarities the Uña assemblage, from La Huérguina Fm (Buscalioni *et al.*, 2008). Zimbral VMA faunal assemblage is close to the one observed in the Cloverly Fm, being rich in amphibious taxa (Oreska *et al.*, 2013). This would suggest that Zimbral would have been a terrestrial ecosystem, more coastal than Valmitão, which was more upstream. In the contrary, Porto das Barcas VMA seems to have less continental influence compared to the two others VMAs, which is congruent with both the presence of hybodontid sharks and the large number of invertebrate shells recovered in the assemblage. This taphonomic signal is shared with Buenache and Las Hoyas, interpreted as swamp and lacustrine environments (Buscalioni *et al.*, 2008, 2018) but Porto das Barcas is relatively less diverse in obligate taxa, which could be a reflection of a much smaller size.

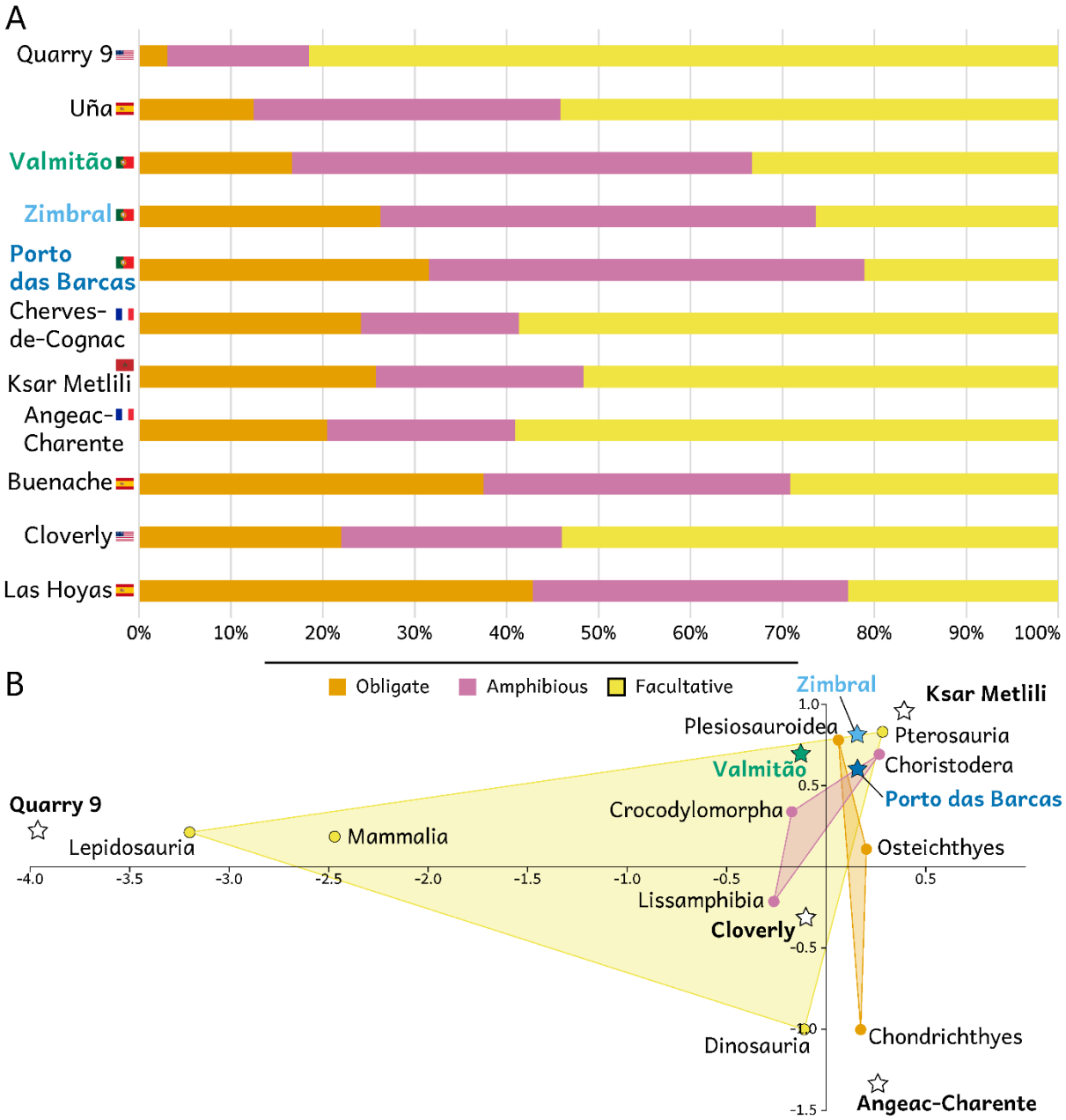

Figure 2.1.4: Palaeoecology of the Lourinhã Formation VMAs compared to others relevant VMAs from the Upper Jurassic and Lower Cretaceous. **A**, habitat relative diversities of microvertebrates site using faunal data (family level). **B**, correspondence analysis (scaling 1) of microvertebrates sites using faunal data (abundance). Data from Carrano & Velez-Juarbe, 2006; Buscalioni *et al.*, 2008; Mazin *et al.*, 2008; Oreska *et al.*, 2013; Carrano *et al.*, 2016; Lasseron *et al.*, 2020; Allain *et al.*, 2022

2.1.5 Conclusion

The analysis of the vertebrate microfossil assemblages, coupled with a detailed sedimentological analysis, shows that the degree of marine influence in the late Jurassic palaeoenvironments recorded by the Lourinhã Formation is much more marked than previously identified. Interestingly, the dominance of obligate aquatic and amphibious faunas in the VMAs of the Praia Azul member points towards a more transitional environment, excluding the three well known transgression levels.

2.2 Chapter 2: Palaeobiodiversity of crocodylomorphs from the Lourinhã Formation based on the tooth record: insights into the palaeoecology of the Late Jurassic of Portugal

Paper published in *Zoological Journal of the Linnean Society* (Journal impact factor for 2020: 3.286; CiteScore: 5.0; SJR: 1.148; H-index: 154)
Alexandre R D Guillaume, Miguel Moreno-Azanza, Eduardo Puértolas-Pascual & Octávio Mateus, Palaeobiodiversity of crocodylomorphs from the Lourinhã Formation based on the tooth record: insights into the palaeoecology of the Late Jurassic of Portugal, Zoological Journal of the Linnean Society, Volume 189, Issue 2, June 2020, Pages 549–583
The article is reproduced with the permission of the editor and is subject to the copyright imposed by the publisher. [] indicate minor modifications from the original article.
Available online: https://doi.org/10.1093/zoolinnean/zlz112

Abstract

Crocodylomorphs were a diverse clade in the Late Jurassic of Portugal, with six taxa reported to date. Here we describe 126 isolated teeth recovered by the screen-washing of sediments from Valmitão (Lourinhã, Portugal, late Kimmeridgian–Tithonian), a vertebrate microfossil assemblage in which at least five distinct crocodylomorph taxa are represented.

Ten morphotypes are described and attributed to five clades (*Lusitanisuchus*, Atoposauridae, Goniopholididae, Bernissartiidae, and an undetermined mesoeucrocodylian). Four different ecomorphotypes are here

proposed according to ecological niches and feeding behaviours: these correspond to a diet based on arthropods and small vertebrates (*Lusitanisuchus* and Atoposauridae), generalist diet (Goniopholididae), a durophagous diet (Bernissartiidae), and [macrocarnivorous diet]. *Lusitanisuchus mitracostatus* material from Guimarota is here redescribed to achieve a better illustration and comparison with the new material.

This assemblage shares similar ecomorphotypes with other Mesozoic west-central European localities, where a diversity of crocodylomorphs lived together avoiding direct ecological competition through niche partitioning. The absence of large marine crocodylomorphs, present in other contemporaneous assemblages, is here interpreted as evidence that the Valmitão assemblage was deposited in a freshwater environment, although sample bias cannot be completely ruled out. These affinities are further supported by the presence of lanceolate and leaf-shaped teeth associated with continental clades.

Key words: Bernissartiidae, Goniopholididae, Atoposauridae, Vertebrate microfossil assemblage, Kimmeridgian-Tithonian.

2.2.1 Introduction

Isolated crocodylomorph teeth are among the most common elements in most Mesozoic vertebrate microfossil assemblages (Thies & Broschinski, 2001; Schwarz-Wings *et al.*, 2009; Lauprasert *et al.*, 2011; Gasca *et al.*, 2012; Ullmann *et al.*, 2012; Kuzmin *et al.*, 2013; Oreska *et al.*, 2013; Vullo

et al., 2014; Puértolas-Pascual *et al.*, 2015b; Carrano *et al.*, 2016; Marmi *et al.*, 2016; Puértolas-Pascual *et al.*, 2016; Blanco *et al.*, 2018, 2020). Although crocodylomorph tooth morphology is strongly correlated with feeding habits and shows a high level of homoplasy, isolated teeth are usually considered elements of low taxonomic and phylogenetic value, being difficult to classify at a generic or specific level (Prasad & de Lapparent de Broin, 2002; Buscalioni *et al.*, 2008; Wings *et al.*, 2010; Puértolas-Pascual *et al.*, 2015b; Young *et al.*, 2016a).

Nevertheless, studies have identified similar crocodylomorph faunal assemblages across Mesozoic European communities, ranging from the Jurassic to the Late Cretaceous. These comprise mainly durophagous feeders, cursorial hunters, insect feeders, and generalist forms, exemplified by taxa such as *Bernissartia*, *Theriosuchus* and *Goniopholis*, in association with other taxa that vary according to the locality (Schwarz-Wings *et al.*, 2009).

The Upper Jurassic of Portugal yields abundant vertebrate remains, notably vertebrate microfossils as illustrated by the Guimarota Mine assemblage (Martin & Krebs, 2000). One of the more diverse clades is the archosaurs, with more than 30 species of dinosaurs described to date (Rauhut, 2000; Antunes & Mateus, 2003; Mateus *et al.*, 2009; Escaso *et al.*, 2014; Hendrickx & Mateus, 2014a; Tschopp *et al.*, 2015; Malafaia *et al.*, 2018; Mocho *et al.*, 2019). Other archosaurs are less well-studied and, to

date, only six crocodylomorph taxa have been described from the Late Jurassic of Portugal, mainly from the Guimarota Mine, located near the town of Leiria (Krebs & Schwarz, 2000).

Krebs (1967, 1968) reported the marine teleosaurid *Machimosaurus hugii* von Meyer, 1837 in Guimarota, and further isolated teeth have been recovered in the Lourinhã Formation (Young *et al.*, 2014a). Buscalioni *et al.* (1996) redescribed *Lisboasaurus estesi* Seiffert, 1973 as a crocodylomorph. Isolated molariform teeth have been attributed to *Bernissartia* sp. (Brinkmann, 1989). Krebs & Schwarz (2000) reported material assigned to goniopholidids, later described as *Goniopholis baryglyphaeus* Schwarz, 2002, as well as material attributed to the atoposaurid *Knoetschkesuchus guimarotae* (Schwarz & Salisbury, 2005) Schwarz *et al.*, 2017, and material attributed to *Lusitanisuchus mitracostatus* (Seiffert, 1973) Schwarz and Fechner, 2004. Despite a lack of detailed study, it is evident that crocodylomorphs were an important component of the Late Jurassic ecosystems of Portugal, occupying specific ecological niches and with different diets, as can be assessed on the basis of differences in their dental morphology (Schwarz *et al.*, 2017).

Here we report a study of a sample of 126 crocodylomorph teeth from the Valmitão vertebrate microfossil assemblage (Valmitão vma). Despite the relatively low productivity of the Lourinhã Fm compared with that of the Guimarota Mine, findings from this formation have provided important

insights into crocodylomorph diversity. For example, the taxonomy of *Lusitanisuchus mitracostatus* and *Lisboasaurus estesi* was for a long time problematic. Both species were originally referred to the same genus, *Lisboasaurus*, and described as anguimorph lacertilians (Seiffert, 1973), later reinterpreted as maniraptoran theropods (Milner & Evans, 1991) and then as mesoeucrocodylian crocodylomorphs (Buscalioni *et al.*, 1996).

New isolated teeth from the Lourinhã Formation, at Porto Dinheiro, allowed the material from the Guimarota Mine referred to *Lisboasaurus mitracostatus* to be attributed to the new genus *Lusitanisuchus* (Schwarz & Fechner, 2004). However, due to the lack of good-quality illustrations in the literature, specimens attributed to *Lusitanisuchus* and housed in the Museu Geológico de Lisboa are here studied, figured and re-described. Material attributed to *Lisboasaurus estesi* was not found in the collection in the Museu Geológico de Lisboa.

2.2.1.1 Geographical and geological settings

The Valmitão vertebrate microfossil assemblage (vma), found at the top of a cliff above Valmitão Beach, near the town of Ribamar in the municipality of Lourinhã, is located within the Lourinhã Formation in the Lusitanian Basin, the largest sedimentary basin in Portugal (Wilson *et al.*, 1989; Alves *et al.*, 2003). The Lusitanian Basin was formed during the opening of the North Atlantic Ocean, and was filled during four rifting episodes and one major seafloor-spreading episode, from the Late Triassic

to the Early Cretaceous (Martinius & Gowland, 2011; Taylor *et al.*, 2014; Gowland *et al.*, 2017; Mateus *et al.*, 2017).

The Lourinhã Formation (**Figure 2.2.1**) consists of a clastic continental succession of sedimentary deposits throughout the Lusitanian Basin, ranging in thickness from 200 m to 1100 m (Leinfelder & Wilson, 1989; Wilson *et al.*, 1989; Taylor *et al.*, 2014). This variation in thickness according the palaeogeographic position can be explained by the transitional/regressive boundaries between the members of the Lourinhã Formation (Mateus *et al.*, 2017). This formation has usually been considered to be Late Jurassic in age, and recent studies confirm an age ranging from late Kimmeridgian to late Tithonian, lying between the Consolação unit and the Porto da Calada Formation (Taylor *et al.*, 2014; Mateus *et al.*, 2017).

The base of the laterally extensive Lourinhã Formation is traditionally considered to represent the first significant and sustained development of continental deposits, above either the shallow marine to estuarine sandstones of the Sobral Formation, the oolitic limestones of the Amaral Formation, the shelfal carbonates of the Consolação unit / Alcobaça Formation, or the shelf to deep-water clastic deposits of the Abadia Fm (Taylor *et al.*, 2014). The dominant continental deposits of the Lourinhã Fm are sandy channel fills and contemporaneous muddy floodplain deposits (Martinius & Gowland, 2011; Taylor *et al.*, 2014; Gowland *et al.*, 2017).

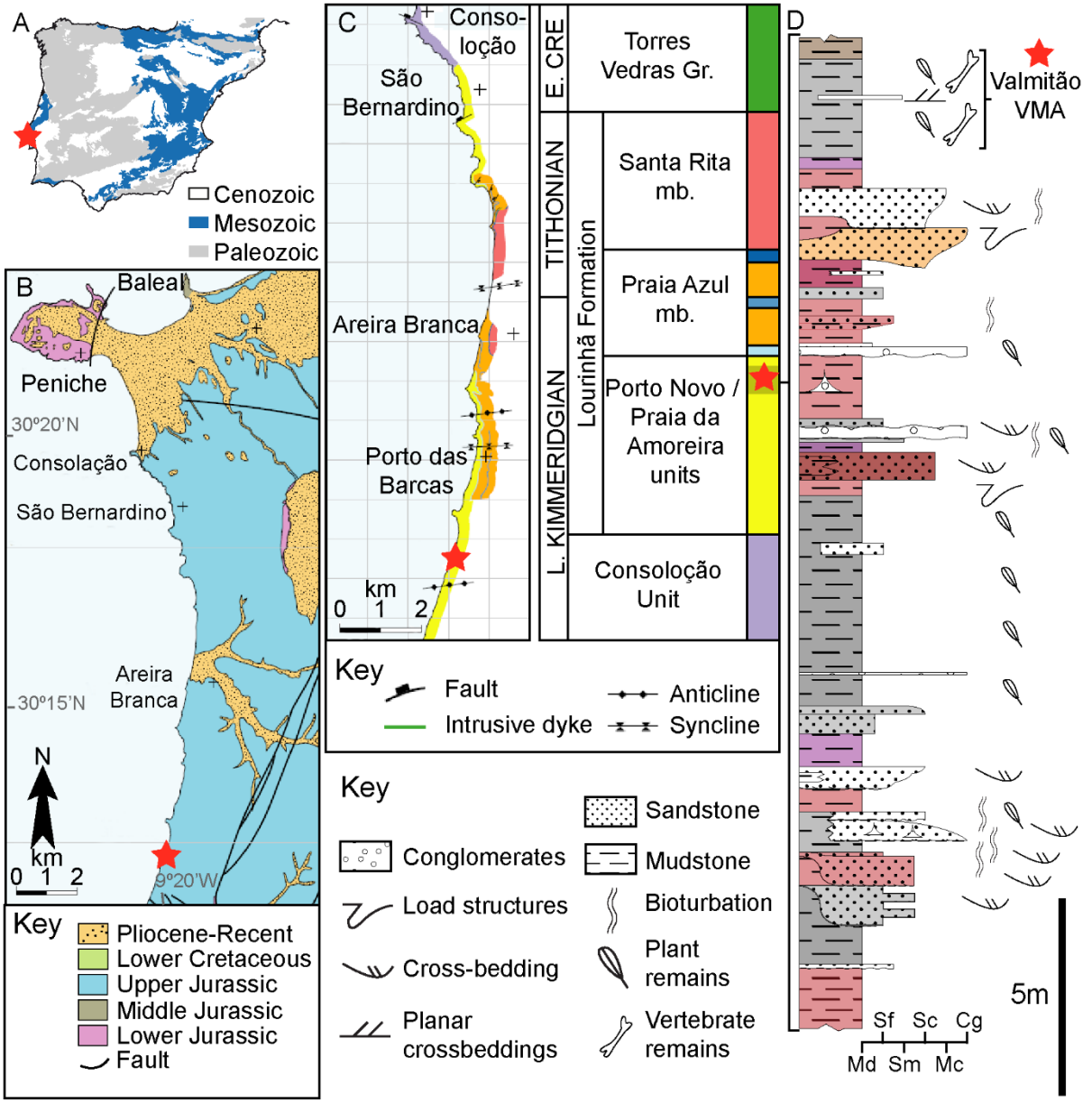

Figure 2.2.1: Geological and geographical context of the Valmitão vertebrate microfossil assemblage. **A**, geological sketch of the Iberian Peninsula, showing the location of the study area. **B**, map of the onshore part of the Consolação sub-basin south of Peniche (modified from Taylor *et al.*, 2014). **C**, north-south mapping of the main units in the area of study and their corresponding lithostratigraphic framework (modified from Taylor *et al.*, 2014, based on Mateus *et al.*, 2017). **D**, stratigraphic log of the upper part of the Porto Nova/Praia da Amoreira Member at Valmitão Beach. The red star indicates the location of the Valmitão vma.

The sedimentology of the Lourinhã Fm suggests a semi-arid climate, with a mean temperature range from 16 °C to 19 °C and seasonal rainfall lower than 500 mm; it is thus more humid than the contemporary Morrison Fm of North America (Mateus *et al.*, 2017).

The Valmitão vma is located in the upper half of the Porto Novo/Praia da Amoreira unit of the Lourinhã Formation, comprising an alternation of metric levels of cross-bedded sandstones and bioturbated mudstones with palaeosols (**Figure 2.2.1D**). These have been interpreted as fluvial channel sands and calcrete-bearing floodplain muds, deposited within a meandering system where crevasse splays are rare (Taylor *et al.*, 2014). The microfossils are distributed within a 3-m thick mudstone layer with occasional intercalations of centimetric sandstones. Darker greyish mudstones rich in organic matter, such as those observed in the Valmitão vma, have been interpreted as lacustrine muds (Gowland *et al.*, 2017) probably deposited in an oxbow lake, with a slow rate of sedimentation.

2.2.1.2 Preliminary overview of the palaeontological assemblage of the Valmitão vma

As part of the larger systematic sampling of the microfauna from the Lourinhã Formation, other vertebrates from the Valmitão vma were collected and studied. In total, 427 vertebrate remains from Valmitão were recovered, among which were 159 teeth from crocodylomorphs, ray-finned fishes, dinosaurs, pterosaurs and undetermined vertebrates, and 210

identified vertebrate remains, including ray-finned fish scales, tetrapod vertebral arches, albanerpetontid vertebrae, dentaries, maxillae and frontal, a putative caudatan vertebra and fragmentary remains from lepidosaurs, an archosaur and an undetermined tetrapod (see Appendix C).

The preliminary palaeoecological analyses suggest that Valmitão was dominated by a terrestrial fauna (Guillaume *et al.*, 2018). As well as the vertebrate remains, gastropods were found in the sample along with fragmented bivalve shells, the latter possibly suggesting a low marine influence in a continental environment.

2.2.2 Material and Methods

This study is based on a 50-kg sample of sediments collected in Valmitão during a field campaign in June 2016. These were dried for three months, then disaggregated in water with hydrogen peroxide (H_2O_2, final solution at 0.5%). The sediments were screen-washed, using a sieving table comprising three levels of mesh (2 mm, 1 mm and 0.5 mm). The study focuses on 126 isolated crocodylomorph teeth (**Table 2.2.1**) recovered from these fractions. These were divided into morphotypes according to their morphologies, on the basis of their overall shape, cross-section shape and the ornamentation of the enamel and the distal and mesial margins.

Since morphological continuity is expected in a heterodont crocodylomorph, because the tooth morphologies are related to their position in the tooth arcade, the tooth count presented in this study

includes a degree of uncertainty concerning morphologically close morphotypes. A subsample of 32 isolated teeth, chosen on the basis of their relatively good preservation and representing the range of morphotype diversity, was used for the measurements and illustration of the different morphologies (see Appendix C). The teeth were photographed with a Leica M165C stereomicroscope equipped with a Leica DFC295 camera and using Leica Application Suite software v.4.10.0, developed by Leica Microsystems CMS GmbH.

The tooth measurements were made using ImageJ (Rasband, 2003). Selected teeth were coated in gold and photographed using a JEOL 6400 scanning electron microscope housed at the Universidad de Zaragoza, Spain. Selected measurements include: height (H), the length of the longitudinal axis from the base of the crown to the apex; width (W), measured at the largest width of the crown, from the mesial to the distal margins; labiolingual width (Lb), the distance between the labial and mesial surfaces at the base of the crown in basal view; mesiodistal width (Mb), the distance between the distal and mesial margins at the base of the crown in basal view. The angle of the apex is the angle formed by the longitudinal axis in mesial/distal view. The angle of the axis is the longitudinal axis angle in lingual view.

A direct examination of the specimens of *Lusitanisuchus* housed at the Museu Geológico de Lisboa was undertaken. Specimens, including teeth,

were photographed using a Dinolite digital microscope and are here figured, described and compared with the material collected in Valmitão. In the present work, we follow the traditional phylogenetic framework that includes *Theriosuchus* and *Knoetschkesuchus* as members of the clade Atoposauridae. This topology has been challenged by Tennant *et al.* (2016b), who removed *Theriosuchus* from Atoposauridae, whereas both genera were included in this clade for their descriptions by Schwarz *et al.* (2017). For the present work, an open and conservative nomenclature is favoured for the taxonomic identification of each morphotype.

Table 2.2.1: Tooth counts for the crocodylomorph assemblage from Valmitão.

Clades	Ecomorphotype	Morphotype	Number of teeth	Percentage	Number of teeth	Percentage
Lusitanisuchus	Ecomorphotype A	Morphotype 1	1	0.79	51	40.48
Atoposauridae		Morphotype 2	14	11.11		
		Morphotype 3	11	8.73		
		Morphotype 4	10	7.94		
		Morphotype 5	15	11.90		
Goniopholididae	Ecomorphotype B	Morphotype 6	33	26.19	51	40.48
		Morphotype 7	18	14.29		
Bernissartiidae	Ecomorphotype C	Morphotype 8	1	0.79	19	15.08
		Morphotype 9	18	14.29		
Mesoeucrocodylia	Ecomorphotype D	Morphotype 10	5	3.97	5	3.97
Total			126	100	126	100

As the Valmitão vma was not part of the stratigraphic study of Gowland *et al.* (2017), a stratigraphic log of the upper layers of this locality

was produced by the authors (**Figure 2.2.1D**) to situate the assemblage geologically and shed light on its palaeoenvironment.

2.2.3 Description of tooth morphotypes

CROCODYLOMORPHA Hay, 1930 (*sensu* Clark, 1986)

MESOEUCROCODYLIA Whetstone & Whybrow, 1983 (*sensu* Benton & Clark, 1988)

Family incertae sedis

Lusitanisuchus mitracostatus (Seiffert, 1970) (**Figure 2.2.2**A)

Referred material—ML2586, one isolated spatulate tooth.

Locality, horizon and age—Valmitão vertebrate microfossil assemblage; Lourinhã Formation, Porto Novo/Praia da Amoreira unit, late Kimmeridgian (Upper Jurassic).

Description

Morphotype 1, spatulate: The tooth is spatulate, with an apiculate (tapering and ending in a short, slender point), sharp apex, similar to a human incisor. The edge of the apex exhibits wears facets and a small denticle pointing outwards from the centre. The crown has a faint constriction at the base. It is 0.73 mm high and 0.83 mm wide, resulting in a height/width (H/W) ratio of 0.88. Its cross-section is labiolingually compressed, with a labiolingual/mesiodistal (Lb/Mb) ratio of 0.5, producing a stadium-shaped

base of the crown. Both labial and lingual surfaces are planar, and both mesial and distal margins bear a carina without denticles.

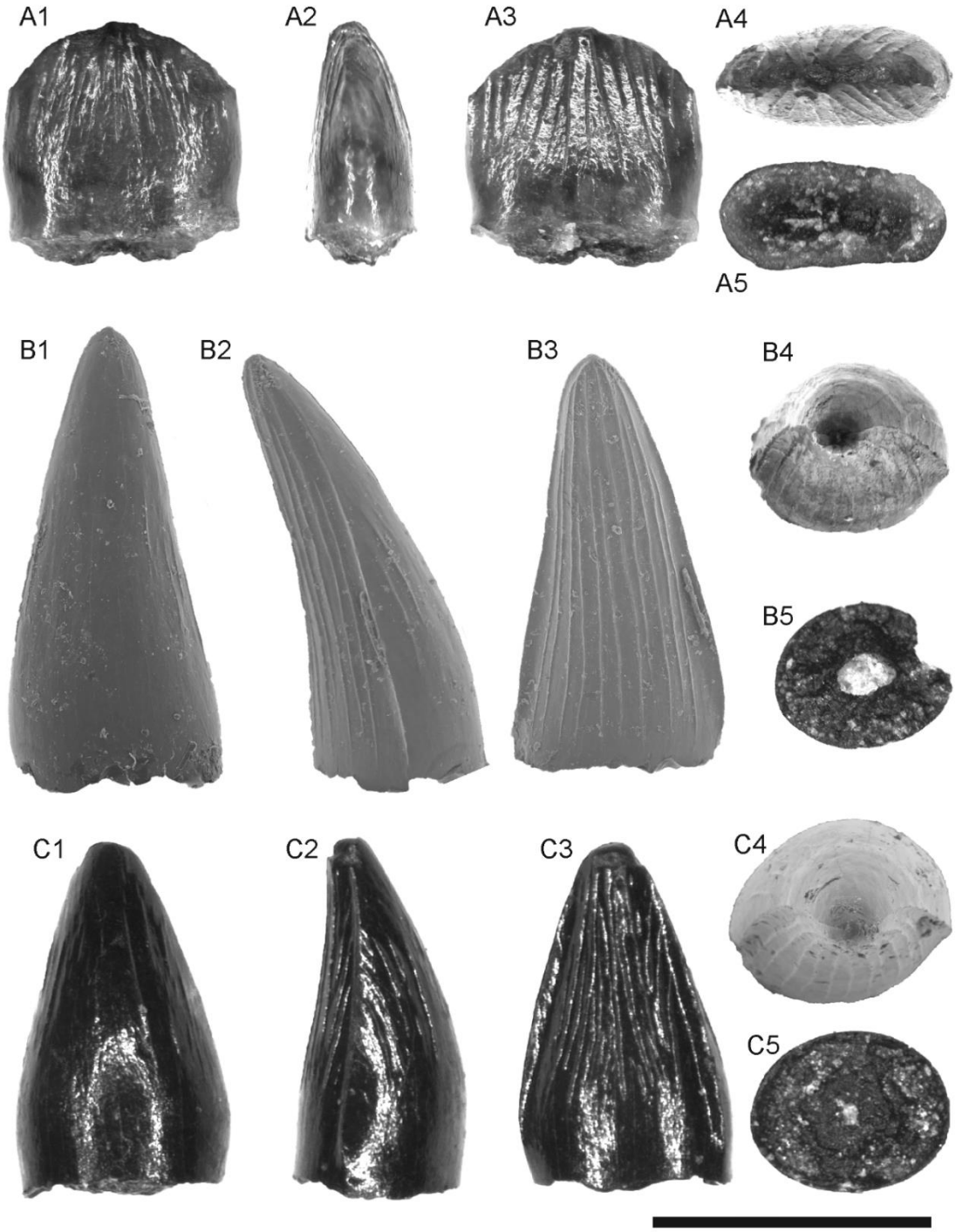

Figure 2.2.2: Morphotype 1 (A) and 2 (B and C) teeth ML2586 (A), ML2497 (B) and ML2498 (C) in labial (1), lateral (2), lingual (3), apical (4) and basal (5) views. Scale bar is 1 mm. All images are normal-light photomicrographs except for A1–A3 and B4, which are SEM photomicrographs.

The enamel on both lingual and labial surfaces is covered by ridges forming basiapical striations, extending toward the apex. There are ten striations on the labial surface, although part of the enamel is not preserved, and 14 on the lingual surface. The central striations converge toward the small denticle of the apex, whereas the lateralmost striations have a flabelliform (fan-shaped) distribution, extending toward the margins and the edge of the apex.

Remarks: This tooth morphology differs from all other morphotypes observed in the sample, which is why, even though it includes only one tooth so far, morphotype 1 can be considered a morphotype in its own. The tooth is not conical, which excludes it from other, conical morphotypes observed in homodont and heterodont taxa. Morphotype 1 differs as well from morphotype 4 and the molariform teeth typical of Bernissartiidae, by having a sharp apex with denticles and different enamel ornamentation (Buffetaut & Ford, 1979; Schwarz & Fechner, 2004). Not being multicuspid, the tooth differs from other spatulate teeth observed in *Simosuchus* and *Uruguaysuchus* (Buckley *et al.*, 2000), and it differs from those observed in *Acynodon* by being less broad and more labiolingually compressed (Buscalioni *et al.*, 1997; Martin, 2007; Delfino *et al.*, 2008; Blanco *et al.*, 2020).

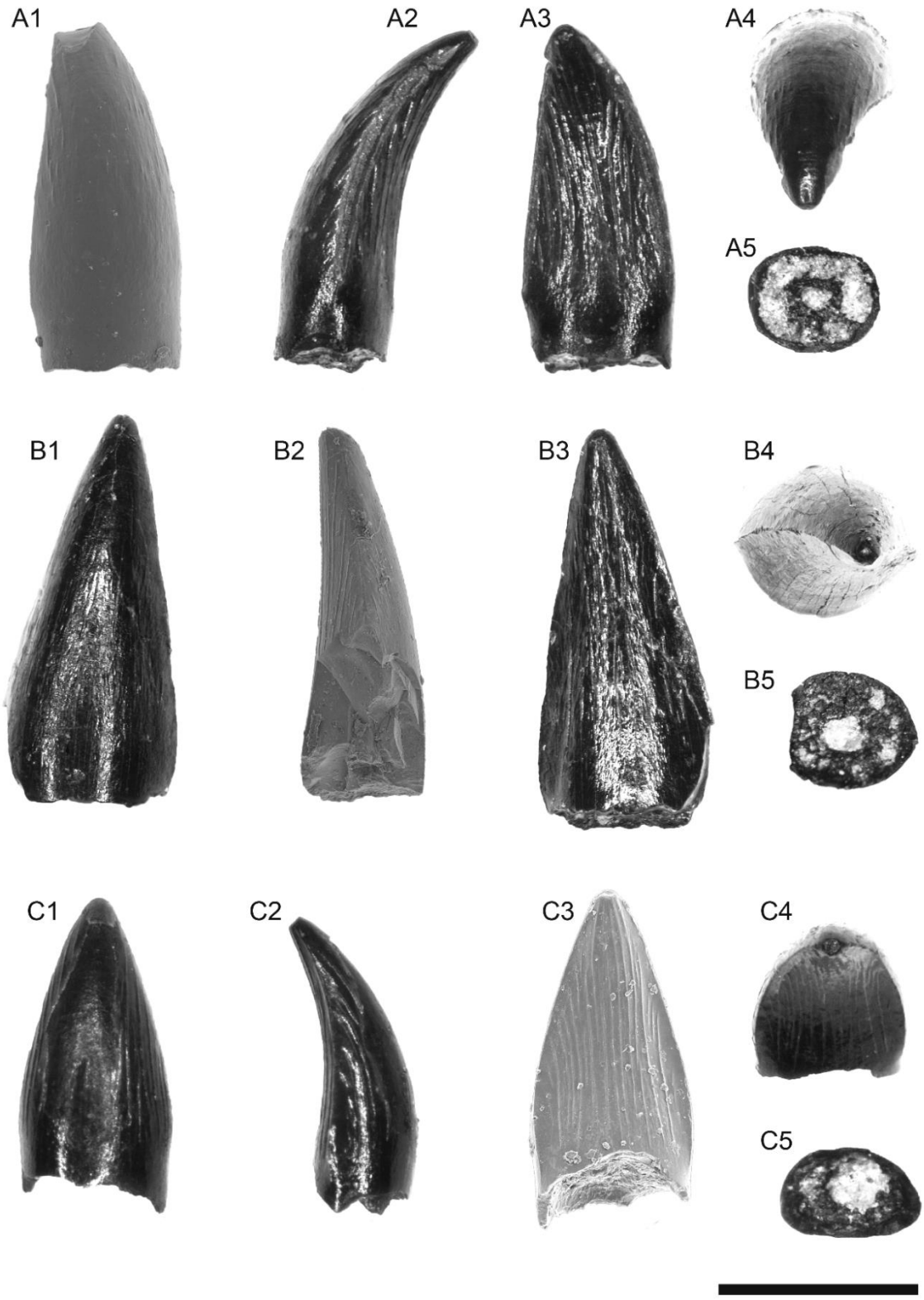

Figure 2.2.3: Morphotype 3 teeth ML2508 (A), ML2509 (B) and ML2510 (C) in labial (1), lateral (2), lingual (3), apical (4) and basal (5) views. Scale bar is 1 mm. All images are normal-light photomicrographs except for A1, B2 and C3, which are SEM photomicrographs.

The tooth shares the flabelliform enamel ornamentation observed in atoposaurids (Brinkmann, 1992; Schwarz-Wings *et al.*, 2009; Salisbury & Naish, 2011; Tennant *et al.*, 2016b; Young *et al.*, 2016a; Schwarz *et al.*, 2017), but differs from these by being spatulate instead of lanceolate to leaf-shaped and by having a truncate, sharp apex with denticles. The tooth has the same spatulate morphology, enamel ornamentation and the typical tip of the apex observed in *Lusitanisuchus mitracostatus* (Seiffert, 1973; Schwarz & Fechner, 2004), particularly in the posterior part of the dentary of the specimens from Guimarota redescribed below, which allows morphotype 1 to be attributed with confidence to this species.

NEOSUCHIA Benton & Clark, 1988

ATOPOSAURIDAE? Gervais, 1871

Atoposauridae indet. (**Figure 2.2.2B, C; Figure 2.2.3—Figure 2.2.5**)

Referred material—ML2511 to ML2521, 11 isolated conical teeth with parallel striations; ML2497 to ML2510, 14 isolated conical teeth with flabelliform striations; ML2522 to ML2546, 10 isolated lanceolate teeth and 15 leaf-shaped teeth.

Description

Morphotype 2, conical with parallel striations (**Figure 2.2.2B**, **C**)*:* The teeth are conical to sublanceolate, with lingually curved, acute apices (16° to 20°). Their height ranges from 1.22 mm to 1.35 mm and their width from 0.67 mm to 0.77 mm, with an H/W ratio that ranges from 1.58 to 2.02. Their cross-

sections are labiolingually compressed with a Lb/Mb ratio of 0.80 to 0.81, resulting in a subcircular base of the crown. Both distal and mesial margins exhibit a carina without denticles. The labial surface is convex in lateral view, the lingual surface less so. In some teeth, the enamel on the labial surface is smooth, whereas it is covered by ten ridges in others, forming parallel basiapical striae. On the lingual surface, the enamel is covered by 11 to 14 parallel basiapical ridges.

Remarks: Conical teeth with parallel basiapical striations on the enamel of the lingual surface, and smooth or ornamented enamel on the labial surface, differ from goniopholidid-like conical teeth, which have basiapical striations on both lingual and labial surfaces, or are smooth on both surfaces. In addition, teeth belonging to Goniopholididae present more conical morphologies and a weak to almost absent constriction at the base of the crown. In contrast, the conical or pseudocaniniform teeth assigned to an atoposaurid-like morphotype are slightly more flattened labiolingually and have a stronger constriction at the base of the crown that gives them a more lanceolate appearance. This morphotype has been described in pseudocaniniform teeth from the premaxilla, and the anteriormost maxilla and dentary, in *Knoetschkesuchus*, *Theriosuchus* and *Sabresuchus* (Schwarz & Salisbury, 2005; Tennant *et al.*, 2016b; Schwarz *et al.*, 2017).

Morphotype 3, conical with flabelliform striations (**Figure 2.2.3**)*:* The teeth are conical to sublanceolate, with a sharp, lingually curved apex (29° to

43°). The smallest teeth are more strongly curved, making them almost hook-shaped (Fig. 3 A2, C2). Their height ranges from 1.49 mm to 1.95 mm and their width from 0.76 mm to 0.95 mm, with an H/W ratio from 1.94 to 2.46. Their cross-sections are labiolingually compressed with a Lb/Mb ratio from 0.41 to 0.82, resulting in a subcircular to elliptical base of the crown. Both distal and mesial margins exhibit a carina lacking denticles. The enamel is smoother on the labial surface, whereas it exhibits twelve to thirteen ridges forming striations on the lingual surface. These striations are flabelliform: the centremost striations are basiapically directed, whereas the lateral striations extend from the base of the crown and diverge to the carinae.

Remarks: Conical teeth with flabelliform basiapical striations on the enamel of the lingual surface and smoother enamel on the labial face, differ from goniopholidid conical teeth, which have parallel basiapical striations on both labial and lingual surfaces. This ornamentation pattern is characteristic of atoposaurids and has been described in teeth from the anterior regions of the dentition in Theriosuchus, Sabresuchus and Knoetschkesuchus (e.g. Brinkmann, 1992; Schwarz-Wings *et al.*, 2009; Salisbury and Naish, 2011; Tennant *et al.*, 2016; Young *et al.*, 2016; Schwarz *et al.*, 2017)

Morphotype 4, lanceolate (**Figure 2.2.4**)*:* These teeth are lanceolate, with a pointed apex and a weak mesiodistal constriction at the base of the crown.

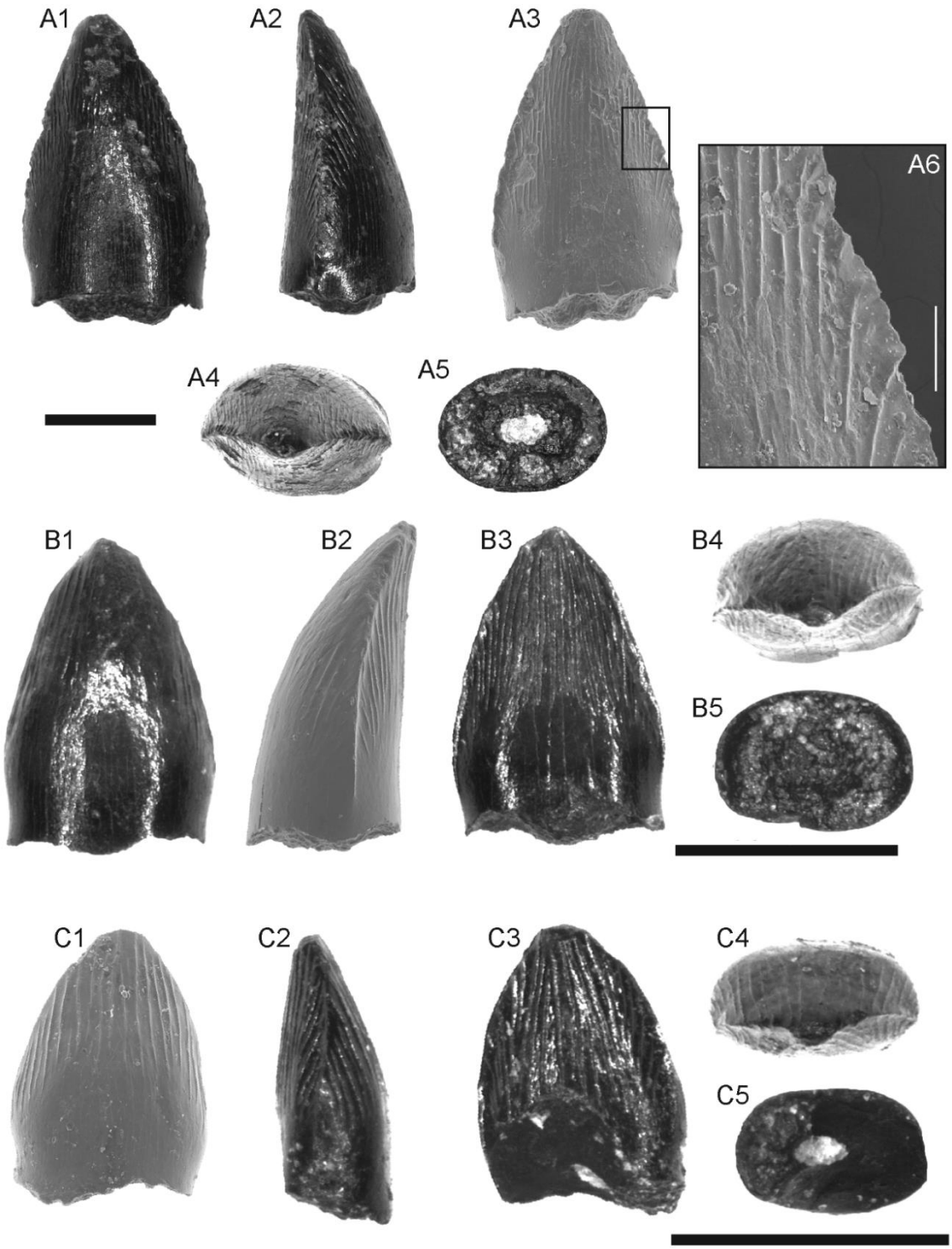

Figure 2.2.4: Morphotype 4 teeth ML2522 (A), ML2523 (B) and ML2524 (C) in labial (1), lateral (2), lingual (3), apical (4) and basal (5) views. Scale bars are 1 mm. Close-up of the false denticles seen in ML2522 (A6). Scale bar is 200 μm. All images are normal-light photomicrographs except for A3, A6, B2 and C1, which are SEM photomicrographs.

Their height ranges from 1.04 mm to 2.58 mm and their width from 0.76 mm to 1.68 mm, with an H/W ratio from 1.36 to 1.53. Their cross-sections are labiolingually compressed, with a Lb/Mb ratio from 0.65 to 0.74, resulting in an elliptical base of the crown. Mesial and distal carinae are present. The labial surface is more convex than the lingual in lateral view. The enamel on the labial surface is smooth at the base and in the centre of the crown, but exhibits parallel, longitudinal ridges, forming basiapical striations extending towards the distal and mesial margins of the carinae apically.

On the lingual surface, the ridges cover almost all the upper part, leaving only the base and a small portion of the centre smooth. The ornamentation consists of striations with a flabelliform distribution. The centremost ridges form striations extending up to the apex, whereas the lateralmost striations extend to the mesial and distal carinae. In some cases, these ridges may give the appearance of denticles on the carinae, which they are not (false-ziphodont dentition; **Figure 2.2.4A6**).

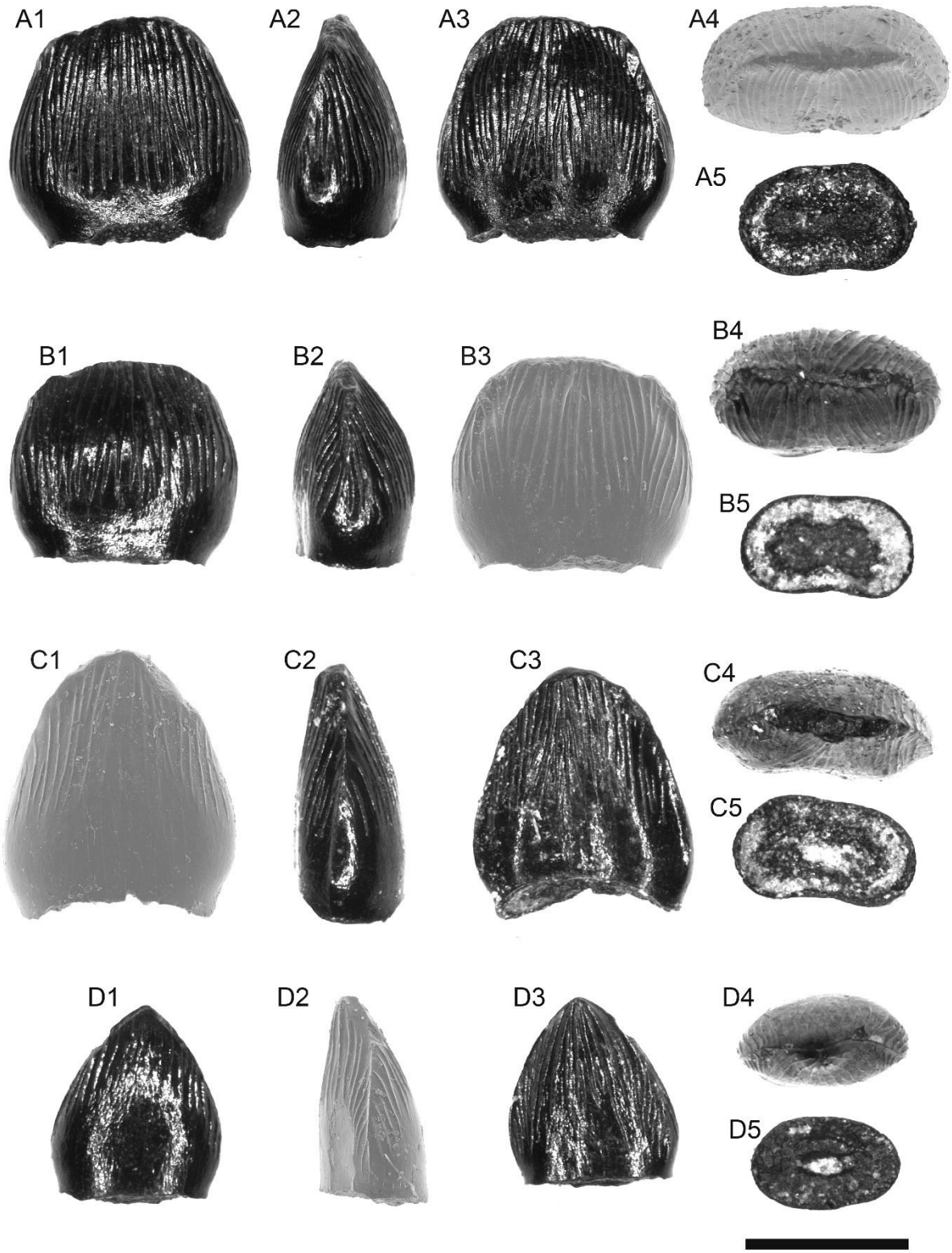

Figure 2.2.5: Morphotype 5 teeth ML2532 (A), ML2533 (B), ML2534 (C) and ML2535 (D) in labial (1), lateral (2), lingual (3), apical (4) and basal (5) views. Scale bar is 1 mm. All images are normal-light photomicrographs except for A4, B3, C1 and D2, which are SEM photomicrographs.

Morphotype 5, leaf-shaped (**Figure 2.2.5**)*:* These teeth are mesiodistally broad and leaf-shaped, with an almost horizontal blunt apex and a weak mesiodistal constriction at the base of the crown. Their height ranges from 1.16 mm to 1.49 mm, with a width from 1.04 mm to 1.47 mm and an H/W ratio from 0.89 to 1.11. Their cross-sections are strongly labiolingually compressed with a Lb/Mb ratio from 0.53 to 0.63, resulting in an elliptical crown base. A faint carina is present on both mesial and distal margins, adjacent to a faint basiapical lingual groove.

The labial surface is strongly convex in the lower part, whereas the lingual surface is less so. The enamel is covered by more than 15 ridges on both labial and lingual surfaces, forming vertical striations extending over the upper two-thirds of the crown. On the labial surface, the striae are basiapical, whereas their distribution on the lingual surface gives the enamel a flabelliform ornamentation. In some cases, the contact of the ridges or striae with the carinae may form false-ziphodont serrations.

Remarks*:* Teeth attributed to atoposaurids show the largest morphological variability observed in the sample, with three clearly different morphologies: conical, lanceolate, and broad leaf-shaped (Schwarz & Salisbury, 2005; Schwarz-Wings *et al.*, 2009; Lauprasert *et al.*, 2011; Puértolas-Pascual *et al.*, 2015b; Schwarz *et al.*, 2017). As has already been noted, this dental variability is related to the position in the dental arcade (Schwarz-Wings *et al.*, 2009; Tennant *et al.*, 2016b).

Among crocodylomorphs, the striation patterns observed in these teeth are typical of atoposaurids such as *Theriosuchus*, *Sabresuchus* and *Knoetschkesuchus*, and allow them to be assigned to Atoposauridae (Schwarz *et al.*, 2017). The degree of development of the striae may be related to ontogeny, as they are more strongly developed in larger teeth than in smaller ones (Schwarz-Wings *et al.*, 2009). In some specimens the ridges may form small, false denticles on the carinae (Schwarz-Wings *et al.*, 2009; Puértolas-Pascual *et al.*, 2015b). Within the above-mentioned genera, the presence of pseudoziphodont teeth is exclusive to *Theriosuchus* and *Sabresuchus* (Lauprasert *et al.*, 2011; Tennant *et al.*, 2016b). In contrast, the carinae of *Knoetschkesuchus* are totally smooth (Schwarz & Salisbury, 2005; Schwarz *et al.*, 2017).

In addition, dentition combining conical, lanceolate and leaf-shaped teeth has previously been attributed to *Sabresuchus* and *Theriosuchus* in other crocodylomorph faunal assemblages (Schwarz-Wings *et al.*, 2009; Lauprasert *et al.*, 2011; Salisbury & Naish, 2011; Gasca *et al.*, 2012; Martin *et al.*, 2014b; Puértolas-Pascual *et al.*, 2015b; Marmi *et al.*, 2016; Tennant *et al.*, 2016b; Young *et al.*, 2016a; Blanco *et al.*, 2018, 2020).

The teeth described in this study can be attributed to one or more of the genera *Theriosuchus*, *Sabresuchus* and *Knoetschkesuchus*. Attribution to the Late Jurassic atoposaurids *Alligatorium* and *Alligatorellus*, which both have smooth-surfaced teeth lacking ridges (Wellnhofer, 1971; Tennant *et*

al., 2016b), can be discounted, because all the Valmitão teeth attributed to atoposaurids have ridges on at least the lingual surface. Moreover, the presence of leaf-shaped teeth and pseudoziphodont teeth precludes attribution of these to *Knoetschkesuchus*, and these morphotypes may represent more than one taxon.

The Valmitão assemblage may thus reflect higher atoposaurid diversity than previously thought, as has been proposed for other fossil assemblages (Tennant & Mannion, 2014; Puértolas-Pascual *et al.*, 2015b; Tennant *et al.*, 2016b; Schwarz *et al.*, 2017). This indicates that in addition to *Knoetschkesuchus guimarotae* there were other atoposaurids in Portugal during the Late Jurassic. The revision of skeletal remains recovered from the Oxfordian Alcobaça Formation, attributed initially to *Theriosuchus* sp. (Malafaia *et al.*, 2010), may cast further light on this hypothesis.

GONIOPHOLIDIDAE? Cope, 1875

Goniopholididae indet. (**Figure 2.2.6**; **Figure 2.2.7**)

Referred material—ML2422 to ML2472; 33 isolated slender conical teeth; 18 broad conical teeth.

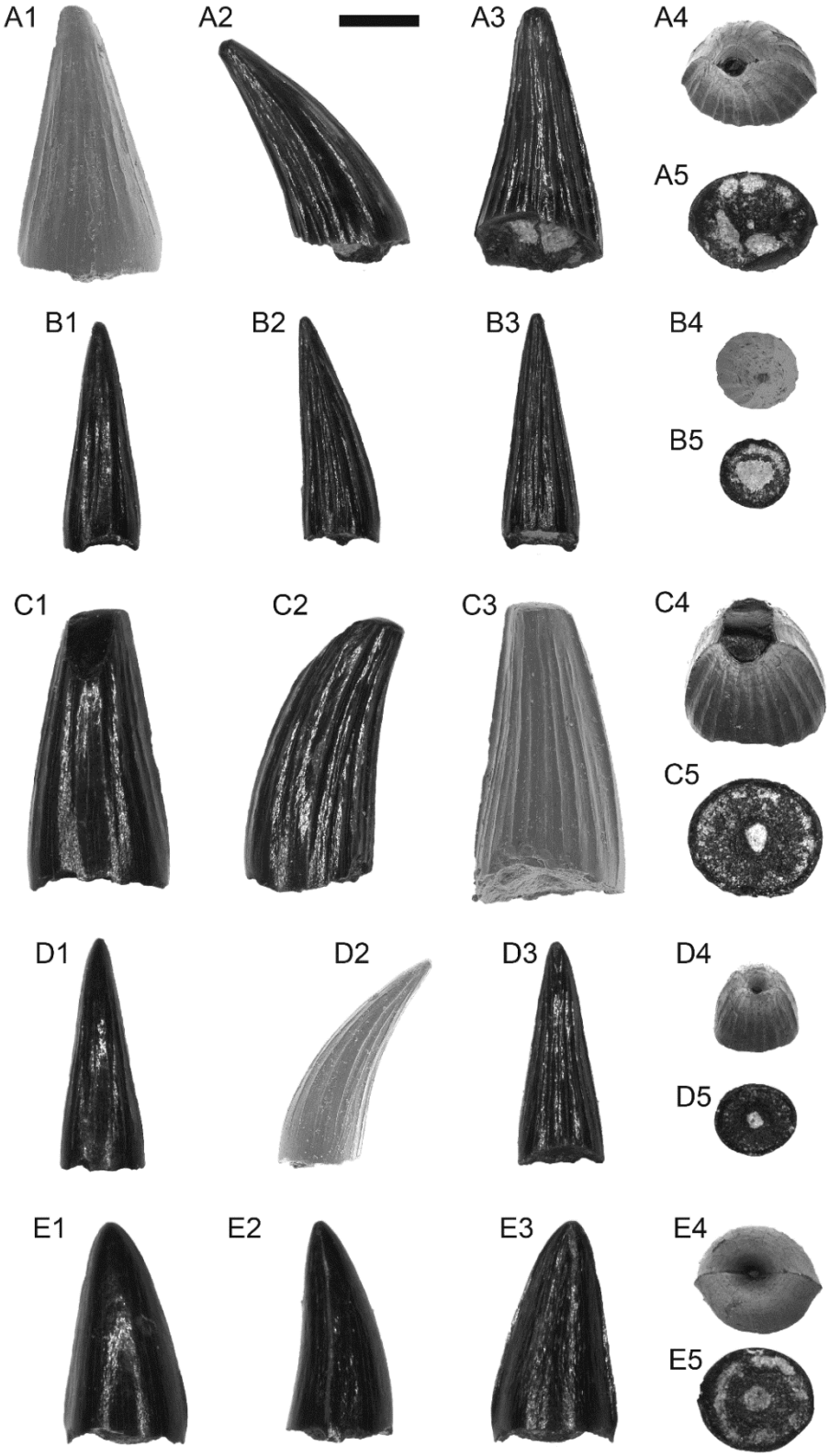

Figure 2.2.6: Morphotype 6 teeth ML2422 (A), ML2423 (B), ML2424 (C), ML2525 (D) and ML2626 (E) in labial (1), lateral (2), lingual (3), apical (4) and basal (5) views. Scale bar is 1 mm. All images are normal-light photomicrographs except for A1, B4, C3 and D2, which are SEM photomicrographs.

Description

Morphotype 6, slender conical (**Figure 2.2.6**)*:* The teeth have a long, slender, conical shape, which can be triangular or more acuminate, with a lingually curved apex (13° to 41°) and a weak mesiodistal constriction at the base of the crown in some teeth. Their height range is between 1.931 mm and 3.337 mm and their width range is between 0.96 mm and 1.18 mm, their H/W ratio ranging from 1.79 to 2.94. Their cross-section is slightly labiolingually compressed with Lb/Mb ratios from 0.72 to 0.99, resulting in a subcircular to ovoid base of the crown. The labial surface is convex toward the base of the crown, whereas the lingual surface is faintly flattened. The lingual and labial surfaces are separated by mesial and distal carinae. These carinae are adjacent to a basiapical groove on the lingual side.

On both surfaces, the enamel is composed of subparallel basiapical ridges: six to ten on the lingual surface, seven to nine on the labial surface. These ridges are more marked on the lingual surface than on the labial surface, which consequently appears smoother. On the lingual face, the ridges extend from the base to the apex of the crown, whereas they only extend over the upper two-thirds of the crown on the labial surface. On both lingual and labial surfaces, the ridges join each other toward the apex, with the lateralmost ones parallel to the mesial and distal margins. In contrast, a few teeth exhibit smooth enamel on both surfaces (**Figure 2.2.6E**).

Morphotype 7, broad conical (**Figure 2.2.7**)*:* The teeth have a broad, conical shape, which is lingually curved in the largest specimens (between 23° to 38°) and blunter in the smallest. Their height range is between 2.09 mm and 4.54 mm, and their width range is between 1.88 mm and 2.47 mm high, with an H/W ratio from 1.11 to 2.10. Their cross-sections are slightly labiolingually compressed with Lb/Mb ratios from 0.75 to 0.96, resulting in a subcircular to ovoid base of the crown. The labial surface is convex toward the base in lateral view, whereas the lingual surface is lingually curved in larger teeth, to straight in smaller teeth. Apart from their broad shape, they are similar to the slender, conical teeth, although they exhibit more striations (nine to ten on the lingual surface, 11 to 12 on the labial). The labial ridges of the biggest teeth are smoother at the base of the crown (bottom one-third of the total height).

Remarks*:* The tooth morphologies described here are characteristic of Goniopholididae (Averianov, 2000; Krebs & Schwarz, 2000; Salisbury, 2002; Schwarz, 2002; Schwarz-Wings *et al.*, 2009; Kuzmin *et al.*, 2013; Puértolas-Pascual *et al.*, 2015b). Nevertheless, these morphologies can be observed in other crocodylomorphs with generalist dentition, and in the anteriorly located teeth of taxa with heterodont dentition (Puértolas-Pascual *et al.*, 2015b). Despite this, all teeth belonging to Goniopholididae are conical in form, with weak, labiolingual compression and an acute, curved apex and more or less developed carinae, according to the size of the crown. The

enamel ridges also vary according to the size of the crown (Schwarz-Wings *et al.*, 2009).

The strongly curved teeth observed in a supposedly juvenile Goniopholis individual (Salisbury, 2002) would suggest that small morphological differences could be related to ontogenetic differences within the genus, or might refer to different species of Goniopholididae (Schwarz-Wings *et al.*, 2009).

Slender to fluted conical teeth with parallel basiapical ridges are also observed in Pholidosauridae (Pouech *et al.*, 2006; Néraudeau *et al.*, 2012; Oreska *et al.*, 2013; Vullo *et al.*, 2014; Martin *et al.*, 2016b; Gônet *et al.*, 2019) and these could, therefore, match some of the teeth attributed to morphotypes 6 and 7. *Sarcosuchus* (Early Cretaceous, Africa and South America) has false-ziphodont dentition and an anastomosing enamel surface (Buffetaut & Taquet, 1977; Sereno *et al.*, 2001), and *Pholidosaurus* (Early Cretaceous, Europe) possesses ornamented teeth with well-marked longitudinal ridges that can hardly be differentiated from the carinae (Martin *et al.*, 2016b).

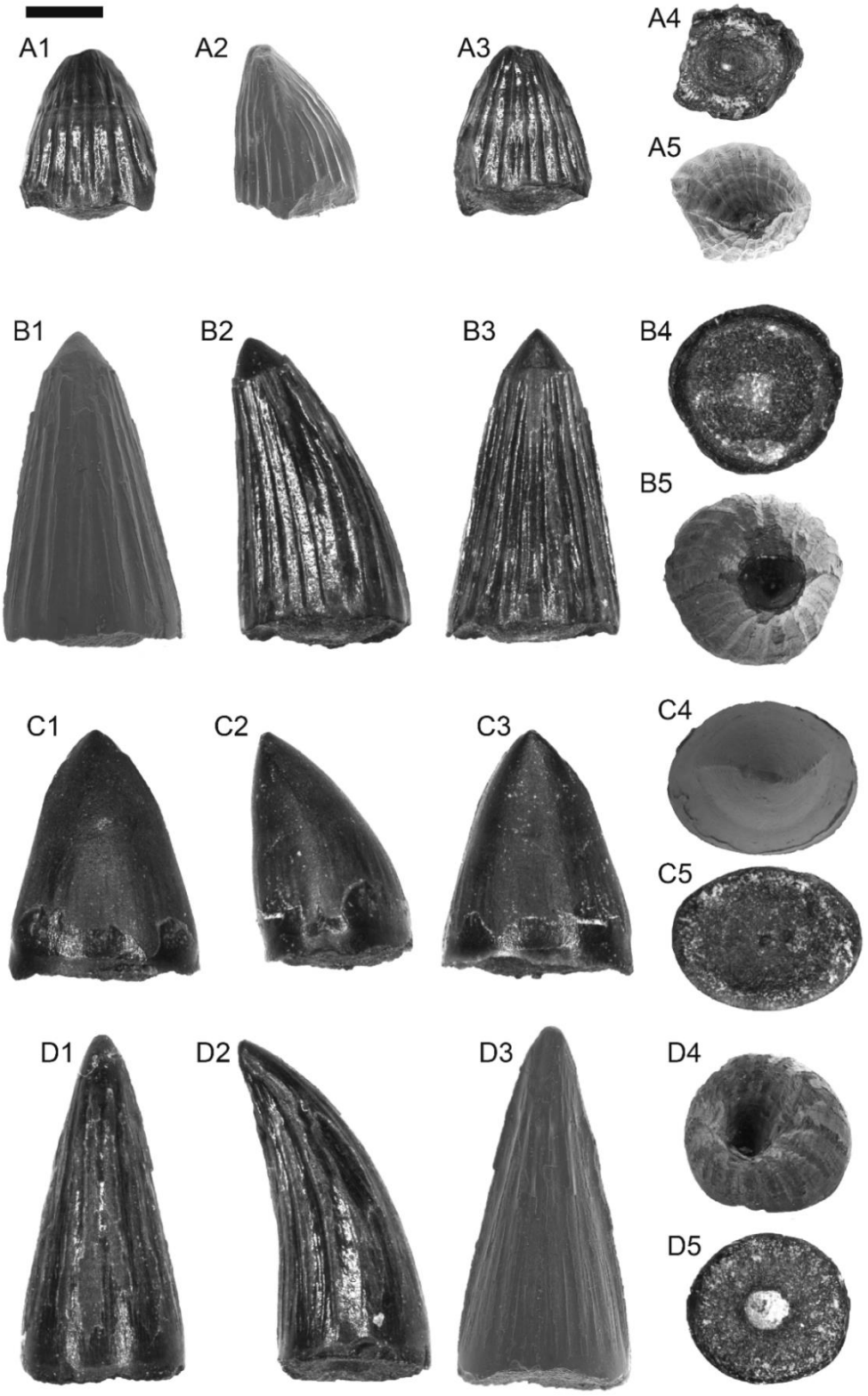

Figure 2.2.7: Morphotype 7 teeth ML2455 (A), ML2456 (B), ML2457 (C) and ML2458 (D) in labial (1), lateral (2), lingual (3), apical (4) and basal (5) views. Scale bar is 1 mm. All images are normal-light photomicrographs except for A2, B1, C4, and D3, which are SEM photomicrographs.

These two taxa can thus be ruled out. In contrast, the dental morphology of other pholidosaurids, such as *Terminonaris* (Late Cretaceous, North America; Wu *et al.*, 2001; Adams *et al.*, 2011), *Oceanosuchus* (Early and Late Cretaceous; Hua *et al.*, 2007), and maybe *Chalawan* (Late Jurassic–Early Cretaceous, Thailand; Martin *et al.*, 2014b), *Elosuchus* (Early Cretaceous, North Africa; de Broin, 2002), and *Meridiosaurus* (Late Jurassic, Uruguay; Fortier *et al.*, 2011), could fall within morphotypes 6 and 7.

However, all these taxa were recovered from more modern deposits and/or different continents than the Valmitão vma. Taking all Pholidosauridae described in the fossil record into account, *Anglosuchus* (Bathonian, England) and *Crocodilaemus* (Kimmeridgian, France) have a closer geographic distribution and are older or contemporary, but their attribution is only putative (Fortier *et al.*, 2011). Given the absence of Pholidosauridae in the fossil record of Portugal to date, Goniopholididae is thus the most parsimonious taxonomic assignment for these morphotypes.

Broad conical teeth have two overall shapes, which could depend on their position in the tooth row. The taller, curved teeth correspond with more anterior positions, probably in the anterior to mid-part of the jaw, whereas the blunter ones represent posterior locations. A conservative approach prevents us from attaining a more rigorous identification of these teeth, despite the fact that all the specimens with this morphology reported

from the Late Jurassic of Portugal until now have belonged to *Goniopholis* (Krebs & Schwarz, 2000; Schwarz-Wings *et al.*, 2009; Malafaia *et al.*, 2010).

BERNISSARTIIDAE Dollo, 1883

Bernissartiidae indet. (**Figure 2.2.8**; **Figure 2.2.9**)

Referred material—ML2478 to ML2496; 1 isolated conical tooth; 18 isolated molariform teeth.

Description

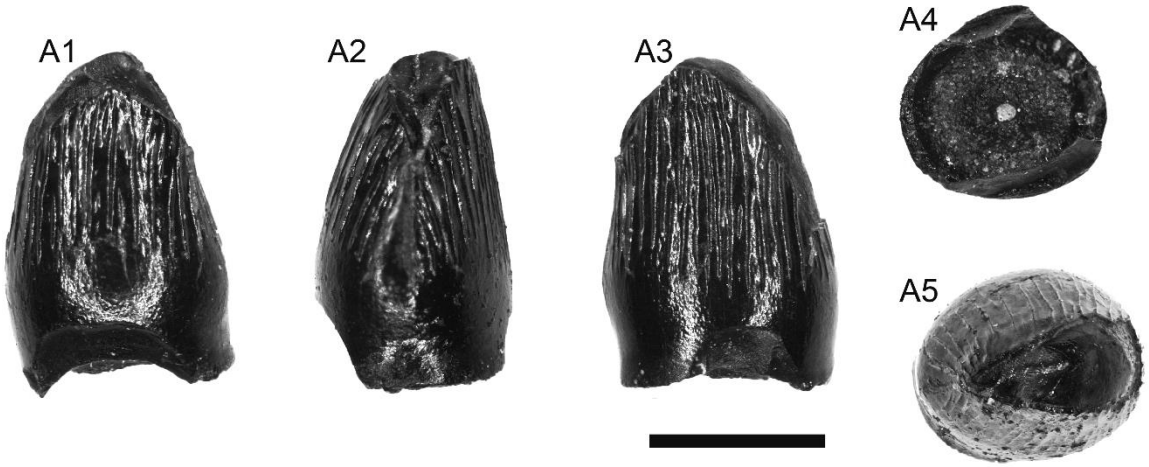

Figure 2.2.8: Morphotype 8 tooth ML2478 in labial (1), lateral (2), lingual (3), basal (4) and apical (5) views. Scale bar is 1 mm. All images are normal-light photomicrographs.

Morphotype 8, conical (**Figure 2.2.8**)*:* Only one tooth of this morphotype was recovered (**Table 2.2.1**). Although the apex is not preserved, the tooth is 1.28 mm wide and seems to be conical and broad in labial and lingual views, with the base of the crown constricted. Its cross-section is labiolingually compressed with a Lb/Mb ratio of 0.89, resulting in a subcircular base of the crown. The lingual surface is convex, whereas the labial surface is

flatter. Both mesial and distal margins are rounded. On both surfaces, it has parallel basiapical striations or ridges, extending two-thirds of the distance to the base of the crown on the labial surface and three-quarters of the distance to the base on the lingual surface. Since the apex is not preserved, the total length of the ridges cannot be determined. The enamel is covered by 14 ridges on the labial surface and 19 ridges on the lingual surface.

Morphotype 9, molariform (**Figure 2.2.9**)*:* The teeth are molariform, with bulky, low, rounded crowns, a blunt apex and a mesiodistal constriction at the base of the crown. Their height ranges from 0.71 mm to 1.48 mm and their width from 0.98 mm to 2.55 mm, with an H/W ratio from 0.58 to 0.80. In basal cross-section, they are labiolingually compressed, with a Lb/Mb ratio from 0.39 to 0.55, resulting in an elliptical to reniform base of the crown. Some teeth exhibit a weak groove on the lingual surface. The labial surface is more convex than the lingual surface. Most of the teeth lack carinae on both mesial and distal margins, but carinae are present in some (**Figure 2.2.9C, E**).

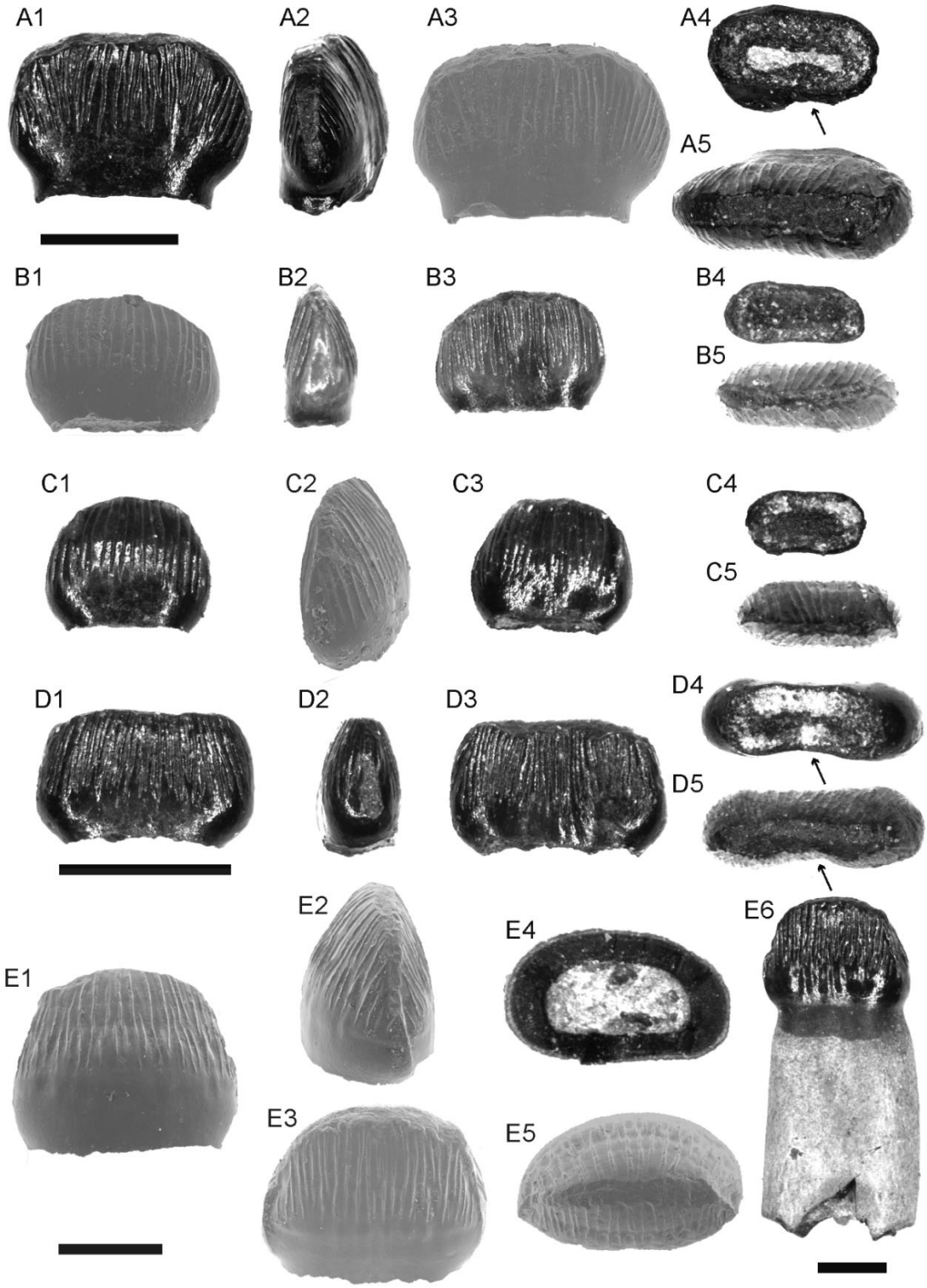

Figure 2.2.9: Morphotype 9 teeth ML2479 (A), ML2481 (B), ML2482 (C), ML2483 (D) and ML 2480 (E) in labial (1), lateral (2), lingual (3), basal (4) and apical (5) views. E6 shows ML2480 in lingual view with the root preserved. The arrows point the lingual groove that can be observed in some specimens. Scale bars are 1 mm. All images are normal-light photomicrographs except for A3, B1, C2, E1–E3 and E5, which are SEM photomicrographs.

The teeth have parallel basiapical striations on both surfaces extending over the upper two-thirds of them, but some teeth exhibit ridges from the base of the crown to the apex. The enamel is covered by 19 to 30 ridges on the labial surface and 17 to 32 ridges on the lingual surface. The apex presents wear facets in all the teeth, even though the wear differs from one tooth to another: the ML2479 (**Figure 2.2.9A**) apex is strongly worn and the wear extends from the apex to almost the base of the crown on the mesial and distal margins, whereas ML2480 and ML2482 (**Figure 2.2.9C, E**) display an apex that is faintly worn in comparison to ML2479 and the wear facet is limited to only the apex margin.

Remarks: Conical teeth with a subcircular cross-section have been considered to come from the anterior part of the dentition in Bernissartiidae, whereas molariform teeth occupy middle and posterior positions (Buffetaut & Ford, 1979; Schwarz-Wings *et al.*, 2009; Puértolas-Pascual *et al.*, 2015b; Sweetman *et al.*, 2015). Although incomplete, the morphotype 8 tooth from Valmitão does not seem to be as pointed and elongated as described for the anteriormost teeth of *Bernissartia* and other bernissartiids (Buffetaut, 1975; Sweetman *et al.*, 2015), but its broad, conical shape makes it similar to the acuminate bulbous teeth observed in the mid-region of the maxilla in *Koumpiodontosuchus* (Sweetman *et al.*, 2015).

Molariform crowns with a reniform or kidney-shaped cross-section are characteristic of Bernissartiidae, as exemplified by the above-cited taxa *Bernissartia* and *Koumpiodontosuchus*, and are associated with a durophagous diet, as suggested by the wear facets observed on the apex of the teeth (Buffetaut & Ford, 1979; Sanz-López *et al.*, 1984; Schwarz-Wings *et al.*, 2009; Ullmann *et al.*, 2012; Puértolas-Pascual *et al.*, 2015b; Sweetman *et al.*, 2015). Bernissartiid molariform teeth can be distinguished from atoposaurid teeth, such as those of *Theriosuchus*, by their blunt, tribodont crowns and the presence of parallel basiapical ridges (Salisbury & Naish, 2011; Sweetman *et al.*, 2015; Tennant *et al.*, 2016b).

Nevertheless, this morphology is also seen in taxa not closely related to Bernissartiidae, such as the hylaeochampsids *Unasuchus* and *Acynodon*, the alligatoroids *Brachychampsa*, *Albertochampsa* and *Allognathosuchus*, and the extant crocodilian *Osteolaemus* (Buffetaut & Ford, 1979; Brinkmann, 1992; Puértolas-Pascual *et al.*, 2015b; Jouve *et al.*, 2019). Some isolated teeth with this morphology and unworn crowns have been attributed to *Bernissartia*, and teeth in the *Bernissartia* holotype were described with a longitudinal carina (Buffetaut & Ford, 1979; Norell & Clark, 1990). This suggests that in less eroded or unworn teeth, such as ML2480 and ML2482, the carina may be preserved, supporting their attribution to this morphotype and to bernissartiids.

Bernissartiid remains are common in many Cretaceous localities: Bornholm in Denmark and Skåne in Sweden (Schwarz-Wings *et al.*, 2009), Swanage and the Isle of Wight in Great Britain (Buffetaut & Ford, 1979; Salisbury, 2002; Sweetman *et al.*, 2015), Cherves-de-Cognac in France (Pouech *et al.*, 2006), Teruel, Uña, Pio Pajarón, Buenache de la Sierra, Vallipón, and La Cantalera in Spain (Sanz-López *et al.*, 1984; Brinkmann, 1989, 1992; Buscalioni *et al.*, 2008; Puértolas-Pascual *et al.*, 2015b), and Bernissart in Belgium (Dollo, 1883; Buffetaut, 1975). Bernissartiid skeletal remains are currently unknown prior to the Cretaceous. However, isolated teeth from the Guimarota vertebrate microfossil assemblage, and from the Purbeck-type bonebeds of Chassiron in France, have been assigned to *Bernissartia* sp. (Brinkmann, 1989; Krebs & Schwarz, 2000; Vullo *et al.*, 2014), providing the only Jurassic records for this clade.

Mesoeucrocodylia indet. (**Figure 2.2.10**)

Referred material—ML2473 to ML2477, 5 isolated teeth.

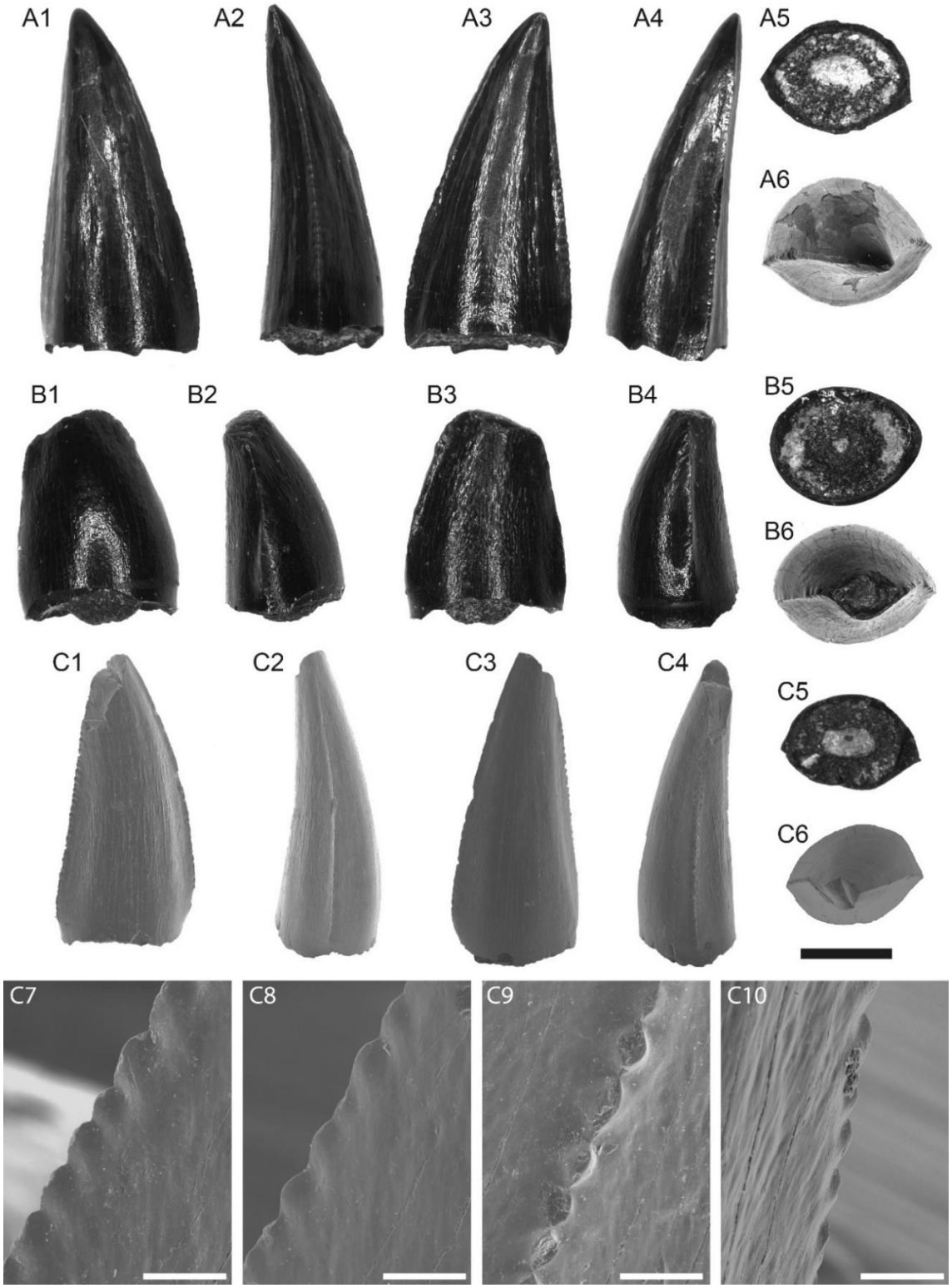

Figure 2.2.10: Morphotype 10 teeth ML2473 (A), ML2474 (B) and ML2475 (C) in labial (1), lateral (2 and 4), lingual (3), basal (5) and apical (6) views. Scale bar is 1 mm. Close-ups of ML2475 denticles in labial (7, 8), lateral (9) and lingual (10) views. Scale bars are 100 μm. All images are normal-light photomicrographs except for C1–C4 and C6–C10, which are SEM photomicrographs.

Description

Morphotype 10, ziphodont: The teeth are conical and lingually curved (14° to 15°), with a sharp apex and slight distal curvature (7° to 13°). Their height ranges from 3.60 mm to 3.65 mm and their width from 1.28 mm to 1.83 mm, with an H/W ratio from 2.00 to 2.35. Their cross-sections are labiolingually compressed, with an occasional labially shifted centre, and with a Lb/Mb ratio of 0.69 to 0.78, resulting in a lenticular base of the crown. The lingual surface is flat to weakly concave labially, whereas the labial surface is convex labially toward the base. The two surfaces are separated by acute and crenulated carinae, where small, true denticles can be observed, especially in the lower half of the carinae. The denticles are irregular in size and shape (**Figure 2.2.10C7–C10**). The enamel on both sides is smooth, but some teeth exhibit shallow ridges on the upper part, forming faint and diffuse striations.

Remarks: Teeth with true denticles on the carinae are termed ziphodont (Prasad & de Lapparent de Broin, 2002; Puértolas-Pascual *et al.*, 2015b), and have been attributed to mesoeucrocodylian taxa without monophyletic relationships. The irregular shape and size of the denticles and the lingual curvature of the tooth crowns differ from the mesiodistal curvature and denticle morphology observed in theropod teeth, confirming their crocodylomorph identity. However, the presence of denticles, which reflects a dentary specialization, cannot be used for taxonomic classification

(Turner, 2006; Andrade & Bertini, 2008; Puértolas-Pascual *et al.*, 2015b), but the presence of serrations, not seen in other elements in the assemblage, distinguishes these teeth from those described above and from other above-mentioned taxa.

Similar ziphodont teeth have been observed in undetermined crocodyliforms from the La Cantalera assemblage in Spain (Puértolas-Pascual *et al.*, 2015b) and the Wessex Formation in Great Britain (Sweetman, 2016). Judging by its shape and the presence of denticles, this morphology also differs from that observed in the material from Guimarota attributed to *Lisboasaurus estesi*, because our specimens lack the median groove on the labial surface, the blunt apex and the conical to triangular shape usually observed in the latter taxon (Schwarz & Fechner, 2008). This morphology also differs from the morphology observed in the dentary and maxillary teeth of one of the other Guimarota taxa, *Lusitanisuchus mitracostatus*, whose maxillary teeth are ornamented and do not exhibit denticles, and whose dentary teeth are spatulate (Schwarz & Fechner, 2004).

The presence of this morphotype, which cannot be assigned to any known taxon from the Late Jurassic of Portugal, further adds to the diversity of the Lourinhã Formation.

2.2.4 Review of the *Lusitanisuchus mitracostatus* dentition

In studying the teeth from the Valmitão vertebrate microfossil assemblage, a striking issue was the apparent absence of teeth from *Lusitanisuchus* and *Lisboasaurus* in the sample, two known taxa from the nearby contemporary site of Guimarota. However, there is a lack of detailed photographs in previous publications (Buscalioni *et al.*, 1996; Schwarz & Fechner, 2004, 2008). Teeth belonging to these taxa might, therefore, be present in the Valmitão vma, but not identifiable. From the figures in these previous works, *Lisboasaurus* teeth, which are characterized by a conical to triangular shape with a blunt apex and a median groove on the labial side, seem to be clearly different from those recovered at Valmitão. However, *Lusitanisuchus* teeth are similar to a morphotype assigned to atoposaurids in this study (morphotype 5).

In order to confirm or rule out the presence of these taxa in the Valmitão vertebrate microfossil assemblage, the material from Guimarota housed in the Geological Museum of Lisbon was studied. Unfortunately, *Lisboasaurus* material is not stored in the collection, so we have not had an opportunity to study it and are, therefore, unable to comment on it here.

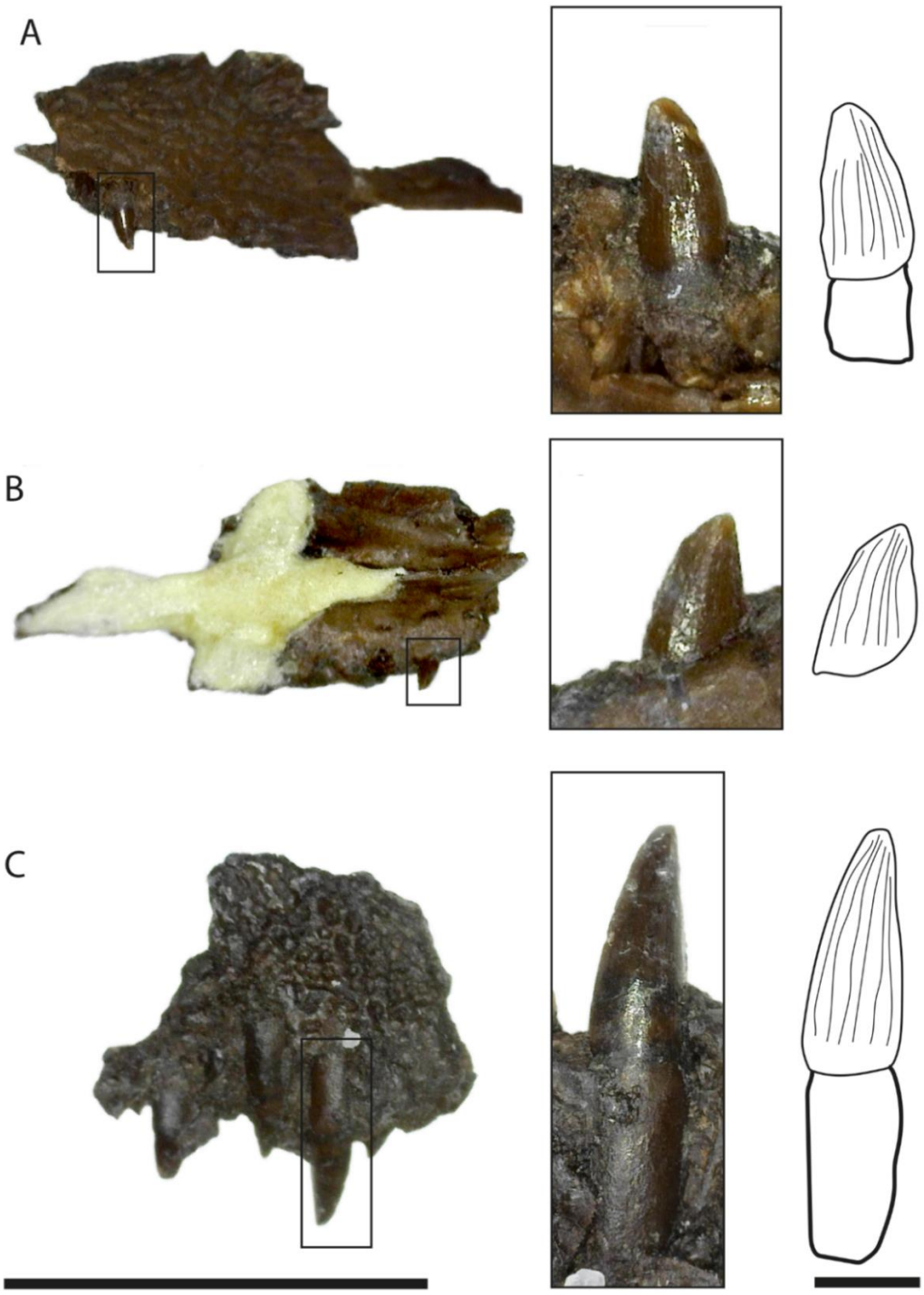

Figure 2.2.11: *Lusitanisuchus mitracostatus* jaw bones from the Guimarota collection. **A–B**, *Lusitanisuchus mitracostatus* left premaxilla–maxilla MG26103 (IPFUB Gui Croc 8002) in labial (A) and lingual (B) views with enlargements and schematic drawings of one tooth to illustrate tooth morphology. **C**, *Lusitanisuchus mitracostatus* right maxilla (IPFUB Gui Croc 8009) in labial view with enlargement and schematic drawing of one tooth to illustrate tooth morphology. Scale bar for the general views (left) is 1 cm, scale bar for enlargements and drawings (right) is 2 mm for A and B and 1 mm for C.

CROCODYLOMORPHA Hay, 1930 (*sensu* Clark, 1986)

MESOEUCROCODYLIA Whetstone & Whybrow, 1983 (*sensu* Benton & Clark, 1988)

Family incertae sedis

Lusitanisuchus mitracostatus (Seiffert, 1970) (**Figure 2.2.11**—**Figure 2.2.13**)

Referred material—MG26081 (IPFUB Gui Croc 7505); MG28911 (IPFUB Gui 75 6.03); (IPFUB Gui Croc 7516); MG26103 (IPFUB Gui Croc 8002); (IPFUB Gui Croc 8009).

Locality, horizon and age—Guimarota Mine (Leiria, Portugal); Alcobaça Fm; Kimmeridgian.

Description

Anterior premaxillary and maxillary teeth (**Figure 2.2.11**)*:* IPFUB Gui Croc 8009 has three teeth preserved, whereas the other specimens have only one preserved. Because they are incomplete, the position in the tooth series cannot be determined. The root is exhibited in MG26103. Their height ranges from 1.014 mm to 2.373 mm and their width from 0.608 mm to 0.882 mm, with an H/W ratio from 1.668 to 2.690. The teeth are conical, with a broad, pointed apex. They do not seem compressed, suggesting a subcircular cross-section, with a faint constriction at the base of the crown. The teeth are weakly posteriorly curved. Both distal and mesial margins seem to exhibit a faint carina with no denticles observed.

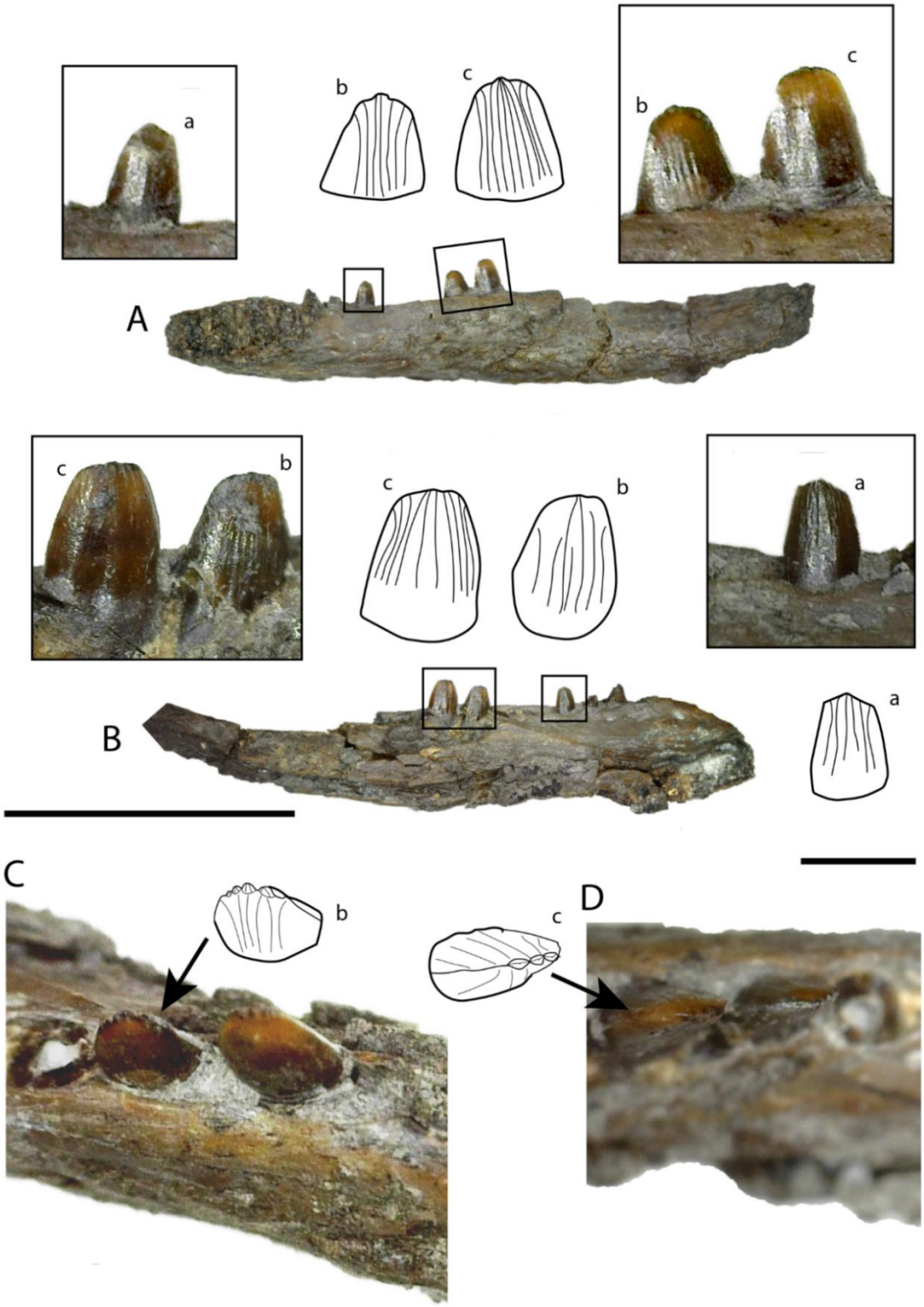

Figure 2.2.12: *Lusitanisuchus mitracostatus* left dentary MG26081 (IPFUB Gui Croc 7505) in labial (A), lingual (B), apicolabial (C) and apicolingual (D) views, with enlargements and schematic drawings of three teeth (from anterior to posterior: a, b, and c) to illustrate tooth morphology. Scale bar for the general views (left) is 1 cm. Scale bar for the enlargements and drawings (right) is 1 mm.

The enamel on both labial and lingual surfaces is covered by subparallel ridges converging toward the apex, forming basiapical striations (Seiffert, 1973; Schwarz and Fechner, 2004; pers. obs.).

Dentary teeth (**Figure 2.2.12Figure 2.2.13**)*:* Three teeth are preserved in MG28911 and three more alveoli without teeth are preserved. However, their position cannot be determined because the dentary is not completely preserved. MG26081 is almost complete, with two teeth preserved in the last positions. The previous two alveoli do not preserve teeth; then two more teeth are preserved, with one broken. The most anterior alveoli are not preserved. The root is exhibited in one tooth in MG28911. The height of the teeth ranges from 0.703 mm to 1.215 mm and their width from 0.54 mm to 0.993 mm, with an H/W ratio from 1.200 to 1.392. The teeth are spatulate, with a sagittate (arrowhead shaped) to truncate (straight and horizontal) apex, similar to a human incisor. They are labiolingually compressed, and there is a faint constriction visible at the base of the crown. Both labial and lingual surfaces are planar, and the edge of the apex is sharp.

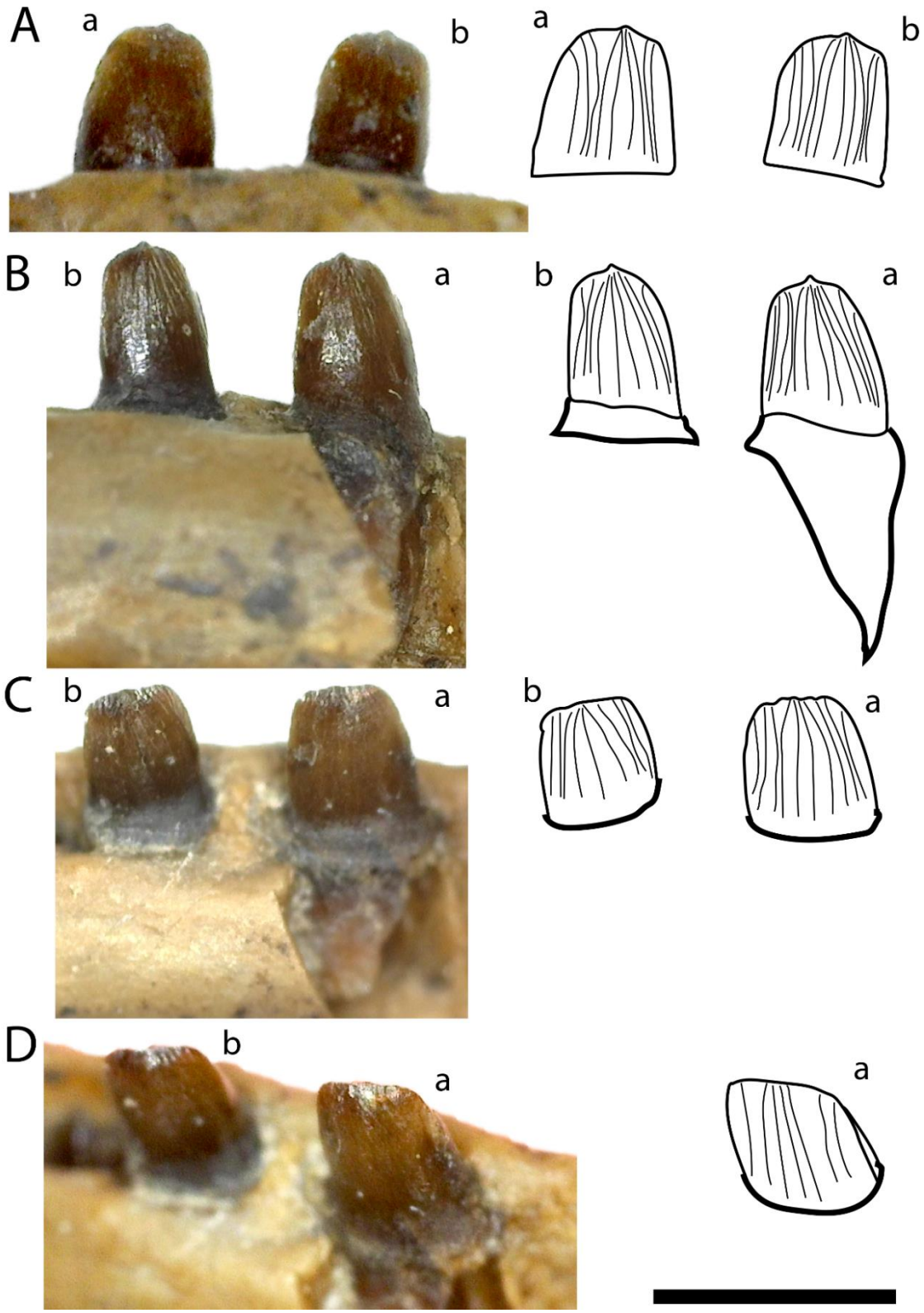

Figure 2.2.13: Enlargement of the teeth of the *Lusitanisuchus mitracostatus* dentary MG28911 (IPFUB Gui 75 6.03) (from anterior to posterior: *a* and b) and schematic drawings to illustrate tooth morphology, in labial (A), lingual (B) and apicolingual views (C, D). Scale bar is 1 mm.

The enamel on both lingual and labial surfaces is covered by ridges forming basiapical striations, extending toward the apex to form vertical false denticles. These denticles are irregular in size; the lateralmost ones are small and barely visible, whereas the centralmost one is pointing outward from the apex, forming a small tip. No denticles are observed on the distal and mesial carinae of the teeth. In the lower part, ridges form parallel basiapical striations, but in the upper part, the central ridges converge toward the small tip of the apex, whereas the lateralmost striations have a flabelliform distribution and extend toward the margins and the edge of the apex, forming small lateral denticles (Seiffert, 1973; Schwarz and Fechner, 2004; pers. obs.).

Remarks: The conical morphotype of the premaxillary and anterior maxillary teeth in *Lusitanisuchus mitracostatus* is commonly observed in Crocodylomorpha. Their overall shape and the ornamentation of the enamel are similar to teeth of morphotype 7, attributed to goniopholidids and usually associated with generalist feeding behaviour (Buffetaut & Ford, 1979; Schwarz & Salisbury, 2005; Lauprasert *et al.*, 2011; Salisbury & Naish, 2011; Puértolas-Pascual *et al.*, 2015b), even though they are smaller and broader, as shown by their H/W ratios. The conical teeth of *L. mitracostatus* can also be compared with teeth of morphotype 2, attributed to atoposaurids, showing a similar shape and proportion, but the labial basiapical ridges in morphotype 2, when present, are more strongly marked

than in *L. mitracostatus*. Material with better exposed teeth will enable us to confirm the difference between these two morphotypes.

The morphology of the dentary teeth differs from that observed in other mesoeucrocodylians (Schwarz & Fechner, 2004), including atoposaurids, despite the similar ornamentation suggesting a particular ecological specialization. This morphology also differs from the molariform teeth characteristic of bernissartiids: the edge of the apex is sharper in *Lusitanisuchus mitracostatus* and comprises small denticles, whereas it is blunt and smooth in bernissartiids, the enamel in bernissartiids is more ornamented and some teeth observed in *L. mitracostatus* have a more pointed apex than is observed in Bernissartiidae. Not being multicuspids, they also differ from the spatulate teeth observed in *Simosuchus* and *Uruguaysuchus* (Buckley *et al.*, 2000) and they differ from those observed in *Acynodon* by being less broad and more labiolingually compressed. Given the preservation of the dentaries, no substantial difference could be observed in the tooth series between anterior and posterior teeth.

2.2.5 Discussion

2.2.5.1 Taphonomy

Most of the crocodylomorph teeth collected from the Valmitão vma sediments are well preserved, showing little or no sign of transport. Most of them have wear facets and sometimes broken apices. This indicates that they were shed teeth – lost during the normal process of tooth replacement

that occurs in crocodylomorphs (Kieser *et al.*, 1993). Some provide evidence of having been digested. This could have originated as a result of predation or from having been swallowed by their owner when they were shed. The predominance of shed teeth suggests that the Valmitão assemblage is located close to the habitat of the crocodylomorphs (Schwarz-Wings *et al.*, 2009).

However, some teeth show traces of abrasion, having partially or completely lost the enamel (**Figure 2.2.7C**) or are broken, and only one tooth has the root preserved (**Figure 2.2.9E**). This suggests that some teeth may have been transported over short distances (Schwarz-Wings *et al.*, 2009). Further, no other crocodylomorph remains but osteoderms were recovered from the sample (see Appendix C), although crocodylomorphs are known from the Lourinhã Formation. This mixture of parautochthonous and allochthonous specimens suggests that accumulation by transport played a role in the formation of the Valmitão vma.

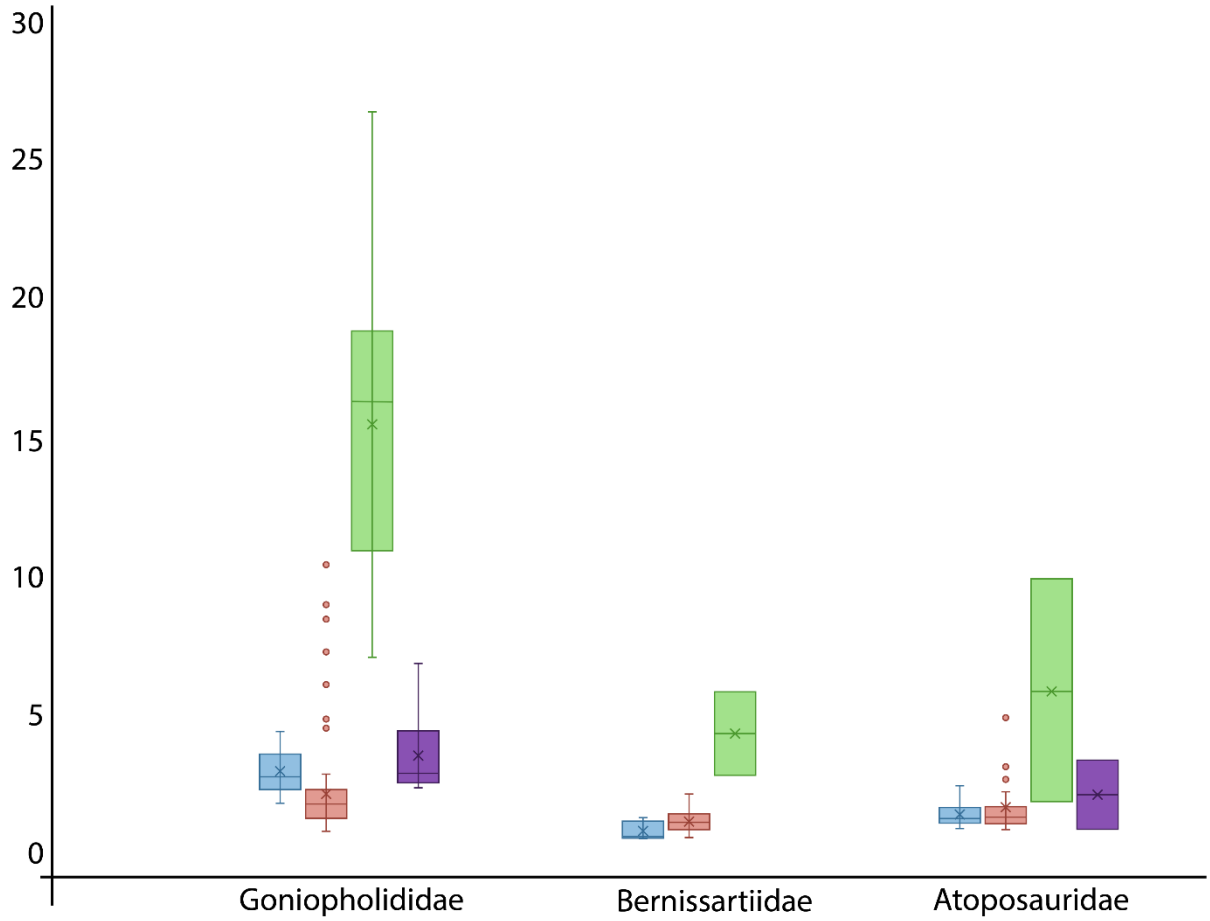

Figure 2.2.14: Comparison of the maximum height (in mm) of the crocodylomorph teeth recorded from Valmitão (blue) and La Cantalera in Spain (red), and in adult (green) and juvenile specimens (purple). The red dots for La Cantalera represent the outliers. Data from: Averianov, 2000; Wings *et al.*, 2010; Kuzmin *et al.*, 2013; Puértolas-Pascual *et al.*, 2015a, b; Martin *et al.*, 2016.

The crocodylomorph teeth from the Valmitão assemblage seem to have belonged to small animals (**Figure 2.2.14**). Indeed, the average size is 2.11 mm in the sample studied, with 3.08 mm for the teeth attributed to goniopholidids, 3.62 mm for the ziphodont teeth, 0.99 mm for the teeth attributed to bernissartiids and 1.52 mm for the teeth attributed to atoposaurids. Atoposaurids and bernissartiids are small crocodylomorphs, reaching a total adult body length of around 500–600 mm (Schwarz-Wings

et al., 2009; Salisbury & Naish, 2011; Puértolas-Pascual *et al.*, 2015b; Schwarz *et al.*, 2017). However, the crown height ranges from 2 mm to 10 mm for atoposaurids and from 3 mm to 6 mm for bernissartiids (Puértolas-Pascual *et al.*, 2015b). This suggests that the Valmitão assemblage is composed of only juvenile bernissartiids and of both juvenile and subadult atoposaurids.

By contrast, goniopholidids are large crocodylomorphs, reaching an adult body length of about 4 m and with centimetric high teeth (Salisbury *et al.*, 1999; Buscalioni *et al.*, 2008; Puértolas-Pascual *et al.*, 2015b) ranging from 7 mm to 26 mm (Averianov, 2000; Wings *et al.*, 2010; Kuzmin *et al.*, 2013; Puértolas-Pascual *et al.*, 2015a; Martin *et al.*, 2016a), which suggests that the specimens found in the Valmitão vma are all juvenile.

The crocodylomorph teeth reported here were mostly recovered from the 1 mm and 0.5 mm residue fractions of the Valmitão sediments, and clasts exceeding 5 mm in length are rare in the assemblage. This suggests a taphonomic bias towards small elements in the formation of the accumulation, possibly reflecting the low energy of the fluxes responsible for the accumulation of the specimens (Schwarz-Wings *et al.*, 2009). However, the small size of the teeth could also be an indication that the Valmitão ecosystem was dominated by small crocodylomorph taxa. Small crocodylomorphs have been previously reported from the Lourinhã Formation (Puértolas-Pascual & Mateus, 2020).

2.2.5.2 Palaeoecology and the feeding habits of the Valmitão vma crocodylomorphs

The teeth described in this analysis can be sorted into nine different morphotypes, from which four ecomorphotypes based on ecological niches can be determined: (1) ecomorphotype A, indicating a diet based on small arthropods (insects, crustaceans, softbodied) and occasional small vertebrates such as mammals and amphibians (Owen, 1879; Buscalioni & Sanz-López, 1988; Puértolas-Pascual *et al.*, 2015b), similar to extant juvenile crocodilians (Brinkmann, 1989; Schwarz & Salisbury, 2005; Schwarz *et al.*, 2017); (2) ecomorphotype B, for generalist feeders, with a diet based on shelly and soft prey items, similar to modern alligators (Schwarz, 2002; Schwarz *et al.*, 2017); (3) ecomorphotype C, for durophagous feeders, with a diet based on animals with shells, such as snails or mollusks, and crushing feeding behaviours (Melstrom & Irmis, 2019); and (4) ecomorphotype D, [for macrocarnivorous—the ecological tendency to capture and kill large preys (Miller *et al.*, 2023)—predators].

The five conical tooth morphotypes (morphotypes 2, 3, 6, 7 and 8) are the most abundant in the studied sample (N = 77, 61.6%; **Figure 2.2.15**). Conical teeth are common in several crocodylomorph clades, being present mainly in generalist taxa, but also forming the anterior dentition of most heterodont taxa (Buffetaut & Ford, 1979; Schwarz & Salisbury, 2005; Lauprasert *et al.*, 2011; Salisbury & Naish, 2011; Puértolas-Pascual *et al.*, 2015b).

However, differences in the shape of the cross-section and the enamel ornamentation pattern were observed, allowing the teeth to be separated into the different morphotypes and the ecomorphotypes with which they are associated. Teeth from morphotypes 2 and 3 (N = 25, 19.84%) are attributed to ecomorphotype A, associated here with Atoposauridae. Teeth from morphotypes 6 and 7 (*N* = 51, 40.48%) are attributed to ecomorphotype B, here assigned to Goniopholididae. The only tooth from morphotype 8 (0.79%) is attributed to ecomorphotype C, consistent with Bernissartiidae.

Morphotypes 4 and 5 are represented by 25 teeth (19.84%; **Figure 2.2.15**). These are associated with the high dietary plasticity (Tennant *et al.*, 2016b) of ecomorphotype A. Other authors have even suggested herbivorous (Brinkmann, 1992), ovivorous (Kirkland *et al.*, 1994) or piscivorous diets (Thies *et al.*, 1997) for these dental morphotypes.

Morphotype 9 is represented by 18 teeth (14.29%; **Figure 2.2.15**). Because of its peculiar shape among crocodylomorphs, it has been suggested this morphotype could be closely linked to a specific ecological diet, rather than resulting from phylogenetic relationships, and it has been associated with ecomorphotype C (Buffetaut & Ford, 1979; Puértolas-Pascual *et al.*, 2015b).

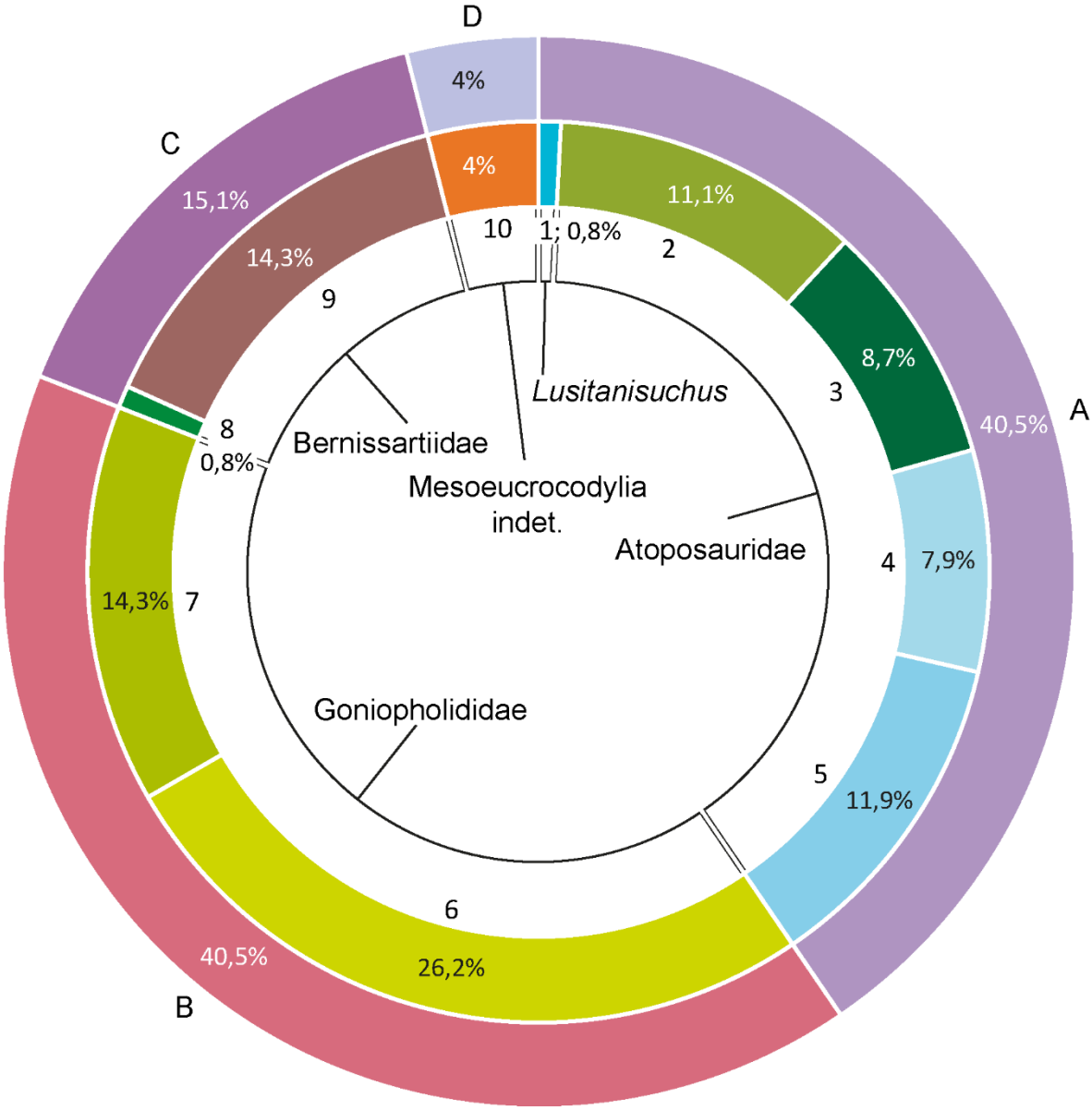

Figure 2.2.15: Distribution of the teeth according their morphotypes (1–10) and their ecomorphotypes (A–D), and the corresponding taxa to which they are thus attributed.

Morphotype 10 is the scarcest, apart from morphotypes 1 and 8, represented by only five teeth (4%; **Figure 2.2.15**). This morphology is found in a broad range of mesoeucrocodylian taxa, such as *Iberosuchus*, *Sebecus*, *Pristichampsus*, *Hamadasuchus*, *Araripesuchus*, and *Ischyrochampsa*, as well as undetermined mesoeucrocodylians. It suggests a highly predatory terrestrial lifestyle (Turner, 2006; Andrade & Bertini, 2008; Puértolas-

Pascual *et al.*, 2015b, 2016; Sweetman, 2016) and can be related with ecomorphotype D.

No feeding behaviours have been proposed for *L. mitracostatus*, which has been described as a small-adult-sized undetermined mesoeucrocodylian (Schwarz & Fechner, 2004) and should, therefore, fit ecological niches for similar-sized taxa. Morphotype 1, and the morphologies of the teeth observed in MG28911 and MG26081, are similar to what is observed in many herbivorous dinosaur clades (Weishampel & Norman, 1989). However, the dental arcade differs from the herbivorous crocodylomorphs *Mariliasuchus amarali* de Souza Carvalho & Bertini, 1999 and *Iharkutosuchus* (Ősi *et al.*, 2007), which exhibit stronger incisiform to conical anterior teeth, and more blunt molariform posterior teeth (Ősi *et al.*, 2007; Andrade & Bertini, 2008; Nobre *et al.*, 2008) than the conical teeth observed in IPFUB Gui 8009 and MG26103. There are no molariform teeth in *L. mitracostatus*. Nor is there extensive tooth wear or a tooth battery that would suggest a herbivorous diet (Barrett, 2000).

Furthermore, the jaw does not seem adapted for a detrivorous diet since the teeth are vertical on the dentary and would not allow the scraping of sediments. Morphotype 1 and the teeth observed in MG28911 and MG26081 share a similar flabelliform ornamentation, false denticles and labiolingual compression with morphotypes 4 and 5, observed in atoposaurids, but the overall shape and the presence of a tip on the

truncate, sharp apex distinguish them. Because of this similarity, and because of the presence of the tip on the apex, it is here proposed that *L. mitracostatus* can be associated with ecomorphotype A. However, more complete cranial material is required in order to gain a better understanding of the feeding behaviour of *L. mitracostatus*.

Of note is the diversity of dental ecomorphotypes observed in the Valmitão vma. Northern South America and South-East Asia currently have the highest crocodylian diversity, with up to six and four living species, respectively, whereas no more than two or three usually occur sympatrically (Scheyer *et al.*, 2013).

In contrast, sympatric crocodylomorph assemblages with higher diversity are known from the Eocene of Messel in Germany (Micklich, 2007), the Mio–Pliocene of Urumaco in Venezuela (Scheyer *et al.*, 2013; Scheyer & Delfino, 2016), and the Maastrichtian of Molí del Baró-1 and L'Espinau in Spain (Marmi *et al.*, 2016; Puértolas-Pascual *et al.*, 2016; Blanco *et al.*, 2020), at each site of which at least seven different species have been recovered. On a bigger scale, the Tremp Formation in Spain yields as many as ten different taxa (Blanco *et al.*, 2020), whereas the Barremian of the Wealden Group of the Isle of Wight records 11 species (Sweetman, 2011a, 2016).

Even so, in some of the richest localities, with most crocodylomorph species living at the same time and in the same area, the three or four tooth

ecomorphotypes for ecological niches and feeding behaviours observed in each case are equal to, or less diverse than, those observed in the Valmitão vma. This implies that the species diversity at the Valmitão site is underestimated. Five taxa are reported here, but there were probably more. Systematic studies of the faunal composition based on the tooth morphotypes are here supported as a good proxy for highlighting the hidden crocodylomorph diversity in assemblages (Marmi *et al.*, 2016; Sweetman, 2016; Blanco *et al.*, 2018, 2020).

Because feeding and access to food are essential parameters in the fitting of organisms to the ecological niche they occupy, the morphological diversity of dentition observed within atoposaurids has been proposed as one of the potential drivers of their evolution in the Middle to Late Jurassic (Young *et al.*, 2016a). The observations made from the Valmitão assemblage are consistent with this proposal and support the biogeographical and taxonomic variation seen in previous studies, suggesting that Atoposauridae were already diverse by the end of the Late Jurassic in Europe (Tennant & Mannion, 2014; Tennant *et al.*, 2016b; Schwarz *et al.*, 2017).

This high trophic diversity, in the context of freshwater crocodylomorphs (Wilberg *et al.*, 2019) that were relatively small in size, represents an adaptation in an ecosystem otherwise dominated by dinosaurs, where predatory niches were already occupied by medium and

large-sized predators, such as the theropods *Lourinhanosaurus*, *Allosaurus* and *Torvosaurus* (Mateus *et al.*, 2006).

2.2.5.3 Palaeoecological differences between the Valmitão vma and the Guimarota Mine assemblage

The apparent absence of *Lisboasaurus* and the scarcity of *Lusitanisuchus* in the Valmitão vma were unexpected given their relative abundance in the similarly aged Guimarota Mine, suggesting that they were relatively uncommon in the Lourinhã Formation. Even though they are slightly different, the conical teeth observed in IPFUB Gui Croc 8009 and MG26103 share similarities with morphotypes 2 and 7. It is thus possible that a certain degree of uncertainty concerning less well-preserved teeth could have led to the misinterpretation of some teeth by the authors.

Lisboasaurus teeth are characterized by their conical to triangular shape, their blunt apex and the median groove on the labial side, and this morphology has not been observed in any of the teeth from the Valmitão vma. *Lisboasaurus* has been a problematic taxon, with fragmentary material (Milner & Evans, 1991; Buscalioni *et al.*, 1996; Schwarz & Fechner, 2008), and the original material from Guimarota could not be accessed and redescribed during this study. More complete material with a complete tooth arcade may thus shed further light on the tooth morphology and the tooth series of *Lisboasaurus*.

Another important difference between the crocodylomorph assemblages of Valmitão and Guimarota is the absence in the former of the large marine thalattosuchian *Machimosaurus hugii*, isolated teeth of which have been reported from different localities of the Lourinhã Formation and in Guimarota, which also provided skeletal remains (Krebs & Schwarz, 2000; Young *et al.*, 2014*a*).

As suggested by the dominance of terrestrial taxa such as dinosaurs and squamates, together with freshwater amphibians in the assemblage, and considering that all the crocodylomorphs reported here are freshwater taxa (Wilberg *et al.*, 2019), the Valmitão vma can be assumed to have been deposited in a freshwater environment, probably with oxbow lakes as previously interpreted (Gowland *et al.*, 2017), where marine inputs, as evidenced by the presence of bivalves, were limited. However, we should take into account that *Machimosaurus hugii* teeth are usually centimetric in size (Young *et al.*, 2014*a*), i.e. well over the dominant bioclast size found in the Valmitão vma, so a taphonomic bias cannot be ruled out.

2.2.5.4 Comparison of the crocodylomorph fauna from Valmitão vma with other Mesozoic vmas

Compared to other Mesozoic assemblages in Europe (**Figure 2.2.16**), the Valmitão crocodylomorph fauna is similar in composition, in that it comprises the four ecomorphotypes described above, even though these ecomorphotypes are not always all represented in the same site in other

localities (Schwarz-Wings *et al.*, 2009). Also, conical teeth are often the most highly represented morphology due to their omnipresence among different taxa and ecomorphotypes. However, significant differences in the relative abundance of each ecomorphotype can be seen between localities (**Figure 2.2.17**).

In the Valmitão vma, ecomorphotypes A and B are equally represented (40.48%), followed by ecomorphotype C (15.08%) and ecomorphotype D (3.97%). This supports the interpretation of Valmitão as a continental environment, as atoposaurids have been proposed to be terrestrial and semi-aquatic crocodylomorphs (Thies *et al.*, 1997; Tennant *et al.*, 2016b; Young *et al.*, 2016a), suggesting an ecological partitioning with goniopholidids (Tennant & Mannion, 2014).

Quarry 9 in the Morrison Formation (United States, Kimmeridgian–Tithonian in age) is famous for providing an important vertebrate microfossil assemblage that displays significant mammal diversity (Marsh, 1880, 1887). Over 1000 crocodylomorph teeth have been recorded and attributed to both *Goniopholis* sp. and *Macelognathus vagans* (Carrano & Velez-Juarbe, 2006), suggesting that ecomorphotype B was the only one represented in this ecosystem, although it has been interpreted as a fully continental, lacustrine palaeoenvironment (Carrano & Velez-Juarbe, 2006).

The Purbeck-type bonebeds of Chassiron (France, Tithonian in age) yield a rich and diverse vertebrate microfossil assemblage, which includes

at least six crocodylomorph taxa (Vullo *et al.*, 2014). From these bonebeds, isolated teeth have been recorded from which the presence of ecomorphotypes A, B, and C can be inferred in equal abundance, as well as a piscivorous ecomorphotype, here associated with the thalattosuchian *Steneosaurus* (Vullo *et al.*, 2014). This assemblage was deposited in a continental lacustrine environment subject to salinity fluctuations (Vullo *et al.*, 2014).

The vertebrate microfossil assemblage from Cherves-de-Cognac (France, Berriasian in age) exhibits an impressive diversity, with 24 vertebrate families represented, including four crocodylomorph ones (Pouech *et al.*, 2006). Although no quantitative data have been provided on the morphotypes observed and the number of teeth recorded for each one, the presence of the three ecomorphotypes A, B and C can be inferred. The Cherves-de-Cognac assemblage was deposited in a lagoon environment that developed under hypersaline to freshwater conditions (El Albani *et al.*, 2004; Mazin *et al.*, 2006).

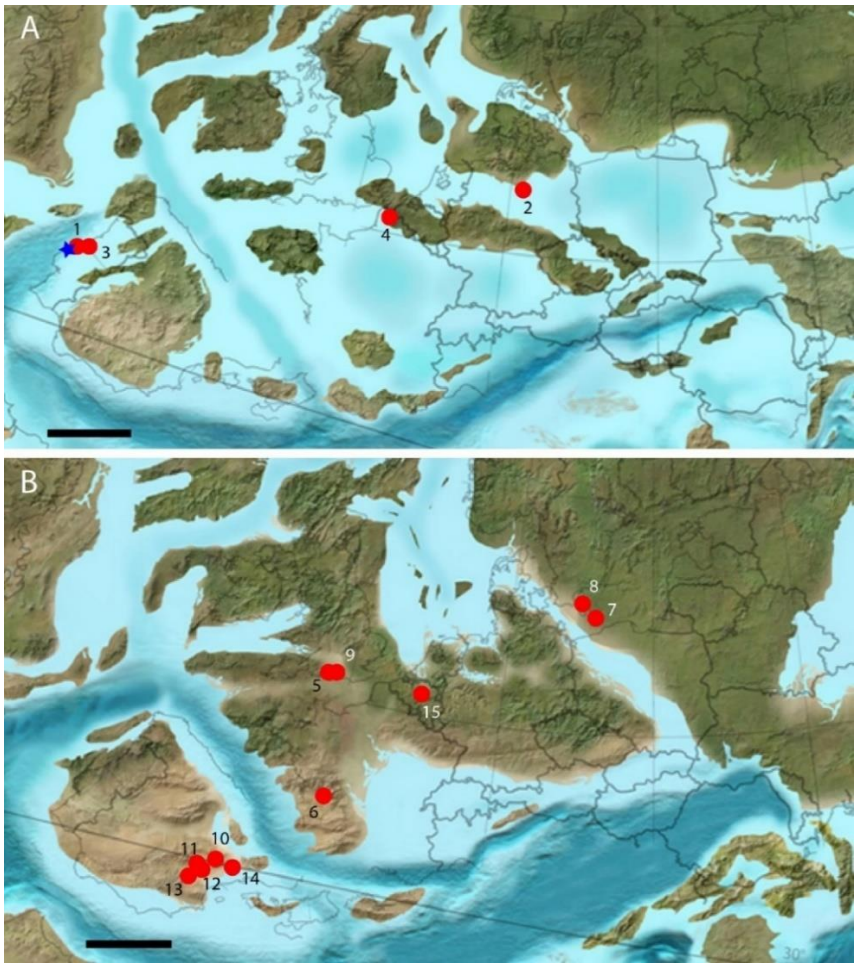

Figure 2.2.16: Palaeogeographic maps of Europe with Upper Jurassic (A) and Lower Cretaceous (B) localities yielding mesoeucrocodylian assemblages with *Goniopholis*, *Theriosuchus* and *Bernissartia*. Blue star indicates the locality of Valmitão, Lourinhã Formation (Ribamar, Portugal). 1. Guimarota Mine, Alcobaça Formation (Leiria, Portugal). 2. Langenberg/Oker, Langenberg Formation (Germany). 3. Andrès, Alcobaça Formation (Pombal, Portugal). 4. Montrouge and La Rochette II, the Formations généreuses (Boulogne-sur-Mer & Wimille, France). 5. Swanage, Purbeck Limestone Group (Dorset, England). 6. Cherves-de-Cognac, gypsum and marlstone units equivalent to Purbeck Limestone Group (France). 7. Arnager, Rabekke Formation (Bornholm, Denmark). 8. Eriksdal, Annero Formation (Skåne, Sweden). 9. Isle of Wight, Wessex Formation (England). 10. Galve, El Castellar Formation and Camarillas Formation (Teruel, Spain). 11. Uña, Uña Formation (Cuenca, Spain). 12. Pio Pajarón, Uña Formation (Cuenca, Spain). 13. Buenache de la Sierra, La Huérguina Limestone Formation (Cuenca, Spain). 14. Vallipón and La Cantalera, Artoles Formation and Blesa Formation (Teruel, Spain). 15. Bernissart, Sainte-Barbe clays (Belgium). Modified from Schwarz-Wings *et al.* (2009); palaeomaps from Colorado Plateau Geosystem. Scale bars are 400 km.

Even though conical teeth of undetermined ecomorphotype and without taxonomic attribution (**Figure 2.2.17A**) are fairly well represented (38.56%) in the Scandinavian assemblages of Bornholm and Skåne (Berriasian–Valanginian in age), there is a considerable predominance of ecomorphotype A (58.56%; **Figure 2.2.17B**). Teeth from ecomorphotype C are extremely rare (2.89%) and ecomorphotype D is not recorded (Schwarz-Wings *et al.*, 2009). This would suggest that Scandinavia was a mainly continental environment in the Early Cretaceous, although the predominance of ecomorphotype A may be biased by misidentification on the part of the authors, and the absence of ecomorphotype B cannot be ruled out, even though it is not supported here.

The Angeac assemblage (France, Hauterivian–Barremian in age) is another microvertebrate site that yields more than 1000 teeth, mainly attributed to Goniopholididae and Pholidosauridae (Néraudeau *et al.*, 2012; Gônet *et al.*, 2019), this ecosystem thus being dominated by ecomorphotype B. The Angeac assemblage has been interpreted as a floodplain deposit with a continental palaeoenvironment and scarce marine influence (Néraudeau *et al.*, 2012), which is congruent with the relative abundances of crocodylomorph tooth ecomorphotypes.

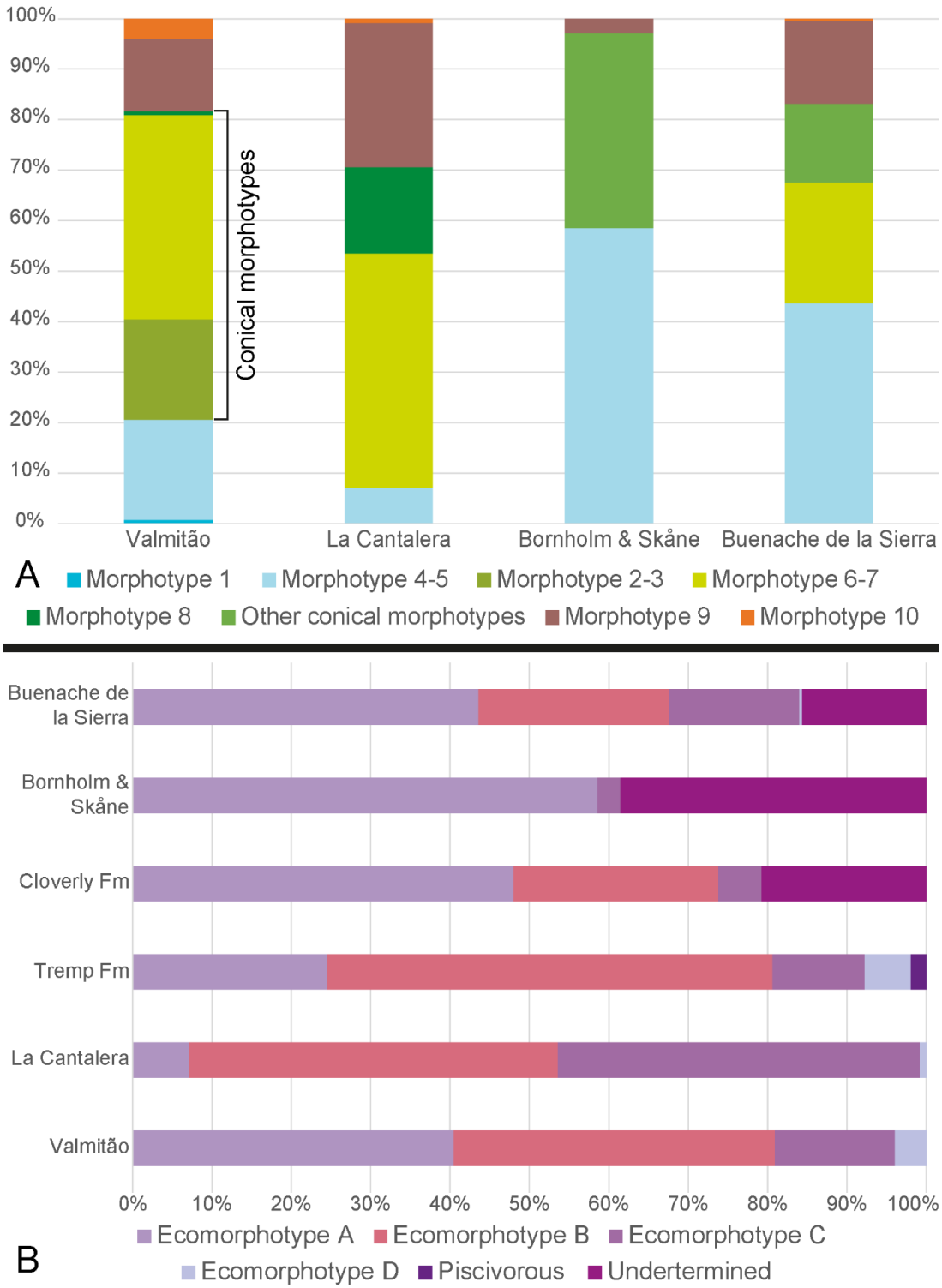

Figure 2.2.17: Crocodylomorph tooth distribution from the La Cantalera (Puértolas-Pascual *et al.*, 2015b), the Bornholm & Skåne (Schwarz-Wings *et al.*, 2009) and the Buenache de la Sierra (Buscalioni *et al.*, 2008) assemblages, also with assemblages from the Cloverly Formation (Oreska *et al.*, 2013; Carrano *et al.*, 2016) and the Tremp Formation (Blanco *et al.*, 2020), compared with the Valmitão vma, according to tooth morphotypes (A) and their ecomorphotypes (B).

Ecomorphotypes B and C are similar in abundance (46.43% and 45.6%, respectively; **Figure 2.2.17B**) in the La Cantalera assemblage (Spain, Lower Barremian in age), whereas teeth attributed to ecomorphotype A are underrepresented (7.14%) and ecomorphotype D (0.82%) is the scarcest (Puértolas-Pascual *et al.*, 2015b). This distribution of ecomorphotypes supports the interpretation of the La Cantalera assemblage as a floodplain deposit in a lentic ecosystem with short lacustrine episodes of swamp vegetation (Aurell *et al.*, 2004; Canudo *et al.*, 2010), dominated by terrestrial taxa, suggesting that the site could have been a feeding area for herbivorous dinosaurs (Puértolas-Pascual *et al.*, 2015b).

In contrast to La Cantalera and similar to the Scandinavian sites, the Buenache de la Sierra assemblage (Spain, Upper Barremian in age) is dominated by teeth of ecomorphotype A (43.6%; **Figure 2.2.17B**) (Buscalioni *et al.*, 2008). Unlike other localities with a predominance of ecomorphotype A, the dominance of ecomorphotype B (24%) towards the ecomorphotype C (16.4%) is not as marked, although a significant number of conical teeth (15.6%) could not be attributed to any ecomorphotype (Buscalioni *et al.*, 2008). The Buenache de la Sierra assemblage is dominated by both obligate and amphibious taxa and has been interpreted as a swamp environment (Buscalioni *et al.*, 2018), supposedly wetter than La Cantalera (Puértolas-Pascual *et al.*, 2015b).

Although atoposaurids are semi-aquatic, the interpretation of the ecomorphotypes does not strongly support the palaeoenvironmental interpretation. This may be due either to a taphonomic or a sampling bias. Alternatively, teeth of ecomorphotype A were misinterpreted by the authors as teeth of ecomorphotype C in La Cantalera, or vice versa in Buenache de la Sierra. It is notable that the authors did not observe any teeth from morphotypes 2 or 3 in La Cantalera, or from morphotype 8 in Buenache de la Sierra (**Figure 2.2.17A**).

The Wealden Group of the Isle of Wight (England, Barremian in age) yields a vertebrate microfossil assemblage (Sweetman, 2011a) with 11 crocodylomorph species recorded to date (Salisbury & Naish, 2011; Sweetman, 2016). Quantitative data are not provided regarding the different morphotypes observed among the isolated teeth, or their abundance in the assemblages. However, it can be inferred that the four ecomorphotypes A, B, C and D are represented, and possibly more could be present (Sweetman, 2016). The group was deposited in a floodplain setting (Stewart, 1981, 1983; Sweetman, 2016) and has been interpreted as a continental lacustrine palaeoenvironment (Sweetman, 2011b).

The Cloverly Formation (United States, Aptian in age) yields a large number of vertebrate microfossil assemblages in which crocodylomorph teeth have been recorded (Oreska *et al.*, 2013; Carrano *et al.*, 2016). Ecomorphotype A is the most frequent (48.02%; **Figure 2.2.17B**), whereas

ecomorphotype B (25.82%) and ecomorphotype C (5.43%) are underrepresented and ecomorphotype D is absent (Oreska *et al.*, 2013; Carrano *et al.*, 2016). However, a significant number of teeth (20.72%) were not attributed to any ecomorphotypes and only taxonomically attributed to crocodyliforms. The Cloverly Formation assemblages are dominated by terrestrial taxa, and semi-aquatic taxa are not diverse there (Carrano *et al.*, 2016). The relative abundance of crocodylomorph tooth ecomorphotypes recorded in the Cloverly Formation assemblages is congruent with the interpretation of a continental lacustrine palaeoenvironment, with a setting near a coastal margin (Oreska *et al.*, 2013; Carrano *et al.*, 2016).

The Tremp Formation (Spain, Maastrichtian in age) also yields relevant vertebrate microfossil assemblages (Marmi *et al.*, 2016), in which up to ten crocodylomorph taxa have been identified (Blanco *et al.*, 2018, 2020). Although different morphotypes from those of Valmitão were observed, mostly due to the temporal and spatial gap, the four ecomorphotypes A, B, C and D were represented (**Figure 2.2.17B**), together with a piscivorous ecomorphotype (Blanco *et al.*, 2020). Ecomorphotype B (56.13%) is by far the most abundant, whereas ecomorphotypes C (11.61%) and A (24.52%) are underrepresented and ecomorphotype D (5.81%) and the piscivorous ecomorphotype (1.94%) are scarce (Blanco *et al.*, 2020), suggesting a floodplain deposit in a continental lacustrine palaeoenvironment. Using different vmas, the authors inferred

environmental preferences for each taxon according to the depositional environment (Blanco *et al.*, 2020).

Further studies are needed to confirm whether these dietary signals correlate with differences in the proportions of arthropods and small vertebrates in the corresponding ecosystems. Including the crocodylomorph teeth, the Valmitão vma yielded 427 vertebrate remains, of which 283 could be identified and attributed to a low taxonomic rank, resulting in four obligate taxa, six amphibious taxa and nine facultative taxa. The preliminary list of the elements picked can be found in Appendix C.

2.2.6 Conclusion

As part of a systematic sampling of the vertebrate microfauna of the Lourinhã Formation, sediments from the locality of Valmitão were sampled and sieve residues picked. A new collection of 126 crocodylomorph teeth is here described. These were identified in order of abundance as belonging to Goniopholididae, Atoposauridae, Bernissartiidae, an undetermined mesoeucrocodylian taxon, and *Lusitanisuchus mitracostatus*.

Compared to the contemporary Portuguese locality of Guimarota Mine, the absence of big marine crocodylomorphs, such as *Machimosaurus hugii*, in conjunction with the palaeofaunal composition of the assemblage, suggests a more continental environment for Valmitão vma, dominated by terrestrial and amphibious taxa. The apparent scarcity of *Lusitanisuchus mitracostatus* and the absence of *Lisboasaurus estesi* suggest that these animals were rare

components in Valmitão, although a certain degree of uncertainty concerning less well-preserved teeth could have led to the misinterpretation of some conical teeth by the authors.

The teeth were classified according to four different ecomorphotypes, associated with four different feeding habits: (A) spatulate, broad-leafshaped, lanceolate to conical teeth associated with arthropods and small-vertebrate feeders, (B) conical teeth associated with generalist taxa, (C) molariform to conical teeth associated with durophagous taxa and (D) subconical ziphodont teeth associated [with macrocarnivorous predators]. The Valmitão crocodylomorph assemblage is consistent with assemblages observed in other European Late Jurassic–Early Cretaceous localities as regards the presence of the four ecomorphotypes described. Compared with other Mesozoic vmas, the Valmitão vma is co-dominated by ecomorphotypes A and B, whereas ecomorphotype C is underrepresented and ecomorphotype D scarce.

Using crocodylomorph teeth, vertebrate microfossil assemblages bring to light the hidden diversity of this group. Other assemblages with similar ecomorphotype diversity but higher taxonomic diversity suggests that the species diversity at the Valmitão site is underestimated.

2.3 Chapter 3: The enigmatic duo: revision of *Cteniogenys* (Choristodera) and *Marmoretta* (Lepidosauromorpha) from the Guimarota beds (Upper Jurassic, Portugal)

Paper in revision in *Acta Palaeontologica Polonica* (Journal impact factor for 2022: 1.8; CiteScore: 3.5; SJR: 0.694; H-index: 59)
Alexandre R D Guillaume, Eduardo Puértolas-Pascual & Miguel Moreno-Azanza. The enigmatic duo: revision of *Cteniogenys* (Choristodera) and *Marmoretta* (Lepidosauromorpha) from the Guimarota beds (Upper Jurassic, Portugal)

Abstract

The Guimarota beds (Kimmeridgian, Portugal) constitute one of the richest microvertebrate assemblages for the Late Jurassic, which include a diverse fauna of small reptiles. Among others, was described a new species of a small choristodere, "*Cteniogenys reedi*". The genus—also known from the Morrison Formation (Late Jurassic, USA), the Kirtlington mammal Beds (Middle Jurassic, England), and the Kilmaluag Fm (Middle Jurassic, Scotland)—constitutes one of the oldest and most basal forms of this aquatic reptile lineage considered to be ecologically similar to crocodylomorphs. However, later works considered this species to be a junior synonym; and challenged the assignment of some of this material, ascribing them to the aquatic stem-lepidosaur *Marmoretta*. Here, we

provided a revision of the published material from the Guimarota beds that was assigned to *Cteniogenys*, together with unreported and mislabeled specimens. We confirmed that the Portuguese specimens are probably non-conspecific with the taxa described in the Upper Jurassic of North America and in the Middle Jurassic of England. Unfortunately, the lack of diagnostic features from the only valid species prevented to confirm the original description as a distinct new species. Therefore, we only referred it to *Cteniogenys* aff. *C. antiquus*. We further supported the presence of *Marmoretta* in the Late Jurassic of Portugal, and that these specimens belong to a new species, New unnamed taxon 1. Those occurrences support original paleoenvironmental interpretations of the Guimarota beds as a wetland, probably close to mangrove-like, with important freshwater inputs. The presence of *Cteniogenys* in Portugal further supports faunal interchanges between North America, Europe, and potentially Northwestern Africa during the Jurassic/Cretaceous transition, if later occurrences are to be confirmed. The presence of *Marmoretta* also extend the temporal range of this relict reptile lineage at a time where squamates were radiating. However, its absence in other contemporary Jurassic localities, notably in the Lourinhã and Morrison formations, could hint towards ecological differences between those assemblages.

Keywords: Lusitanian Basin, Diapsida, Reptilia, paleobiogeography, systematics

2.3.1 Introduction

The Guimarota beds are one of the richest vertebrate microfossil assemblages for the Late Jurassic, yielding thousands remains from various groups of vertebrates (Martin & Krebs, 2000), including a vast diversity of "lizards", despite only few works focusing on them (Seiffert, 1973; Broschinski, 2000). Among them, a choristodere have been described and a putative stem-lepidosaur have been reported (Seiffert, 1973; Evans, 1989, 1991b).

The Choristodera Cope, 1884 are an extinct group of enigmatic freshwater amphibious diapsids, distributed through Laurasia (Matsumoto & Evans, 2010; Matsumoto *et al.*, 2019, 2022b; Dong *et al.*, 2020), with putative occurrences in Gondwana (Haddoumi *et al.*, 2016; Lasseron *et al.*, 2020). They range from the Middle Jurassic of UK and Kyrgyzstan to the Miocene of Europe (Evans, 1990; Evans & Klembara, 2005; Averianov *et al.*, 2006; Matsumoto *et al.*, 2013; Panciroli *et al.*, 2020). They displayed various ranges of morphotypes, from brevirostrine to longirostrine, and from short-necked to long necked, with size-range from small lizards to large crocodiles (Matsumoto & Evans, 2010). They can be distinguished between Neochoristodera, the informal "allochoristoderes", and more primitive forms such as *Cteniogenys* (Matsumoto *et al.*, 2019; Dong *et al.*, 2020; Dudgeon *et al.*, 2023).

Despite being consistently recovered as monophyletic, Choristodera phylogenetic position within Diapsida remains uncertain (Matsumoto & Evans, 2010; Matsumoto *et al.*, 2019). They have been recovered as basal Archosauromorpha (Evans, 1988; Gauthier *et al.*, 1988b), as sister group of Archosauromorpha+ Lepidosauromorpha (Evans, 1988; Dilkes, 1998; Ezcurra *et al.*, 2021), as basal diapsids (Gao & Fox, 1998), within an expanded Lepidosauromorpha clade (Müller, 2004), constrained to the base of either Lepidosauromorpha or Archosauromorpha (Ezcurra, 2016), as basal Neodiapsida (Simoes *et al.*, 2018), or within Archosauromorpha (Simoes *et al.*, 2018; Griffiths *et al.*, 2021).

Cteniogenys was first recognize as an undetermined reptile (Gilmore, 1928), later associated to "eolacertilians" based on the tooth implantation (Seiffert, 1973; Estes, 1983), before being recognized as a Choristodera based on new material from the Bathonian of England (Evans, 1989). Since then, it has been consistently described as the most basal taxon (Gao & Fox, 1998; Matsumoto & Evans, 2010; Matsumoto *et al.*, 2013, 2019; Dong *et al.*, 2020; Dudgeon *et al.*, 2023) and one of the oldest occurrences of the group (Evans, 1989, 1990; Averianov *et al.*, 2006). *Cteniogenys antiquus* Gilmore 1928 is currently the only valid species, and has been described only by dentaries from North America.

Dentaries have been found in Europe, but could only be referred to *Cteniogenys* sp., due to the lack of diagnostic features differing from the *C.*

antiquus (Estes, 1983; Evans, 1989; Chure & Evans, 1998). The Bathonian Kirtlington Mammal Bed (UK) yield a more prominent cranial and post-cranial material, allowing a better characterization of *Cteniogenys* (Evans, 1990, 1991a). More jaw and vertebral elements assigned to *Cteniogenys* sp. or referred to cf. *Cteniogenys* have been since reported in the Kimmeridgian–Tithonian of North America and from the Tithonian to the Berriasian of western Europe (Chure & Evans, 1998; Foster & Trujillo, 2000; Foster, 2001; Vullo *et al.*, 2014; Allain *et al.*, 2022), as well as allegedly in the Bathonian and Berriasian of Morocco (Haddoumi *et al.*, 2016; Lasseron *et al.*, 2020) and the Bathonian of Scotland (Panciroli *et al.*, 2020). More recently, scarce choristodere material was reported from the Lourinhã Formation (Guillaume *et al.*, 2023a), but it is pending further description.

A new species, "*Cteniogenys reedi*", was described from the Guimarota beds (Seiffert, 1973), but it was later considered as a junior synonym of the type species (Estes, 1983), as the characters originally used could be included within the range of intraspecific variation observed in the American material (Estes, 1983; Evans, 1989; Chure & Evans, 1998). Furthermore, some specimens identification has been considered questionable (Evans, 1989); while others have been since then reattributed to the stem-lepidosaur *Marmoretta* (Evans, 1991b).

Occurrences of *Marmoretta oxoniensis* Evans, 1991b, the only described species, are restricted to the Middle Jurassic of England (Evans,

1991b, 1992, 1998b; Evans & Milner, 1994; Panciroli *et al.*, 2020; Griffiths *et al.*, 2021). Additional associated cranial and postcranial material are known in the Middle Jurassic of Scotland (Waldman & Evans, 1994; Griffiths *et al.*, 2021). It has been originally described as a non-lepidosaurian lepidosauromorph, outside the crown-group of Lepidosauria (Evans, 1991b; Conrad, 2008), and subsequent material and analyses confirmed this original hypothesis (Waldman & Evans, 1994; Evans, 2009; Evans & Borsuk-Białynicka, 2009; Evans & Jones, 2010; Jones *et al.*, 2013). Latest phylogenies also recovered *Marmoretta* as a stem-lepidosaur (Bolet *et al.*, 2022), and as sister-taxon of *Fraxinisaura* from the Ladinian of Germany (Schoch & Sues, 2018; Griffiths *et al.*, 2021), despite being significantly younger than its counterpart. Other studies recovered it as a stem-squamate within Lepidosauria, along with either *Megachirella* or *Huehuecuetzpalli* (Simoes *et al.*, 2018; Sobral *et al.*, 2020). Although not described, the Portuguese material has been considered to not be conspecific with the British specimens (Evans, 1991b; Evans & Milner, 1994).

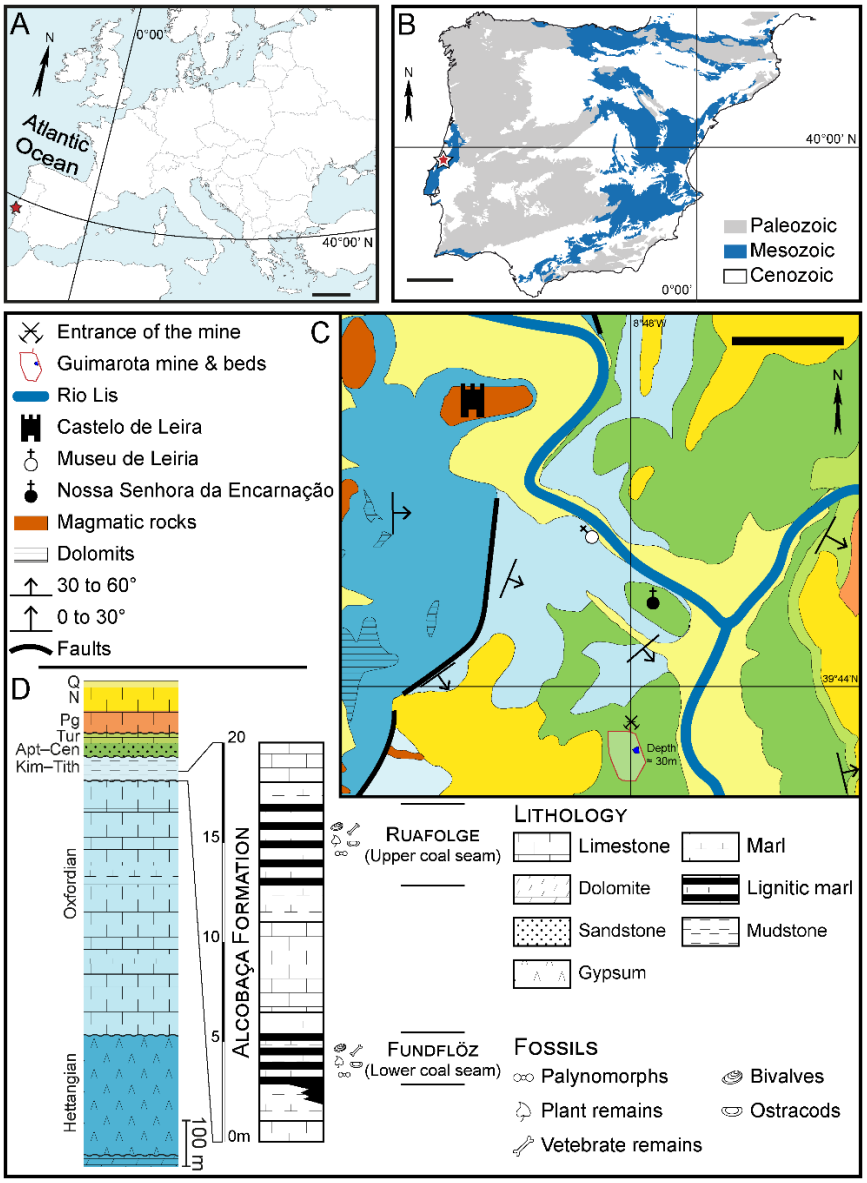

Figure 2.3.1: Geographical and geological context of the vertebrate microfossil assemblages localities from the Alcobaça Formation. **A**, map of Europe, modified from Erin Dill; scale is 400 km. **B**, geological sketch of the Iberian Peninsula, showing the location of the study area (red star); scale is 200 km. **C**, geological sketch of the Leria area, showing the location of the assemblage (modified from Teixeira *et al.* 1966); scale on the map represents 500 m. The entrance of the Guimarota mine, together with the outline of the pit and the approximate location of the fossil beds (blue area) are shown. Note that the fossil locality is located 30 meters below the surface, in the Upper Jurassic formations overlayed by the Cretaceous (see Section 1.1). **D**, stratigraphic position of the Guimarota beds and stratigraphic log of the Guimarota beds. General stratigraphic sketch derived from data in Teixeira et al. 1968. The colours for each stage correspond to the ones used in the map. Detailed stratigraphic log of the Alcobaça Formation from Schudack 2000*a*.

Here, we review the material from the Guimarota beds originally attributed to *Cteniogenys*. We provide new descriptions as well as material previously unpublished or unreported. However, the material available does not allow to confirm the validity of the species described by Seiffert. Part of this material also confirms the presence of *Marmoretta* in the Guimarota beds, with new fossils previously misidentified, unpublished, or unreported, and provide support for a new lepidosauromorph species in the Upper Jurassic of Portugal.

2.3.1.1 Geological setting

The Guimarota beds were prospected in the 1960s and 1970s by the Institut für Paläontologie, Freie Universität Berlin (IPFUB), in which thousands of microfossil remains have been recovered (Martin & Krebs, 2000). They are located in Guimarota, a neighbourhood of Leiria over 100km north-east of Lisbon (**Figure 2.3.1**).

Since the first attempts to determine their age, the Guimarota beds have been consistently considered as part of the Alcobaça Formation (Ribeiro *et al.*, 1979; Mateus *et al.*, 2017; Fürsich *et al.*, 2022), and have been given a Kimmeridgian age based on ammonites, charophytes, ostracods, pollens, lithostratigraphic correlation, and isotopic analyses (Ribeiro *et al.*, 1979; Leinfelder & Wilson, 1989; Schudack *et al.*, 1998; Schudack, 2000a; Fürsich *et al.*, 2022). The fossiliferous series consists into two coal seams (**Figure 2.3.1C**), with intercalation of lignitic marls

occasionally rich in bivalve shells, separated by a single 5 m-thick layer of limestone, around 5 m thick (Schudack, 2000b).

Due to the mining conditions in Guimarota, the exact stratigraphic position of the specimens is unknown (Gloy, 2000; Krebs, 2000a). However, it is our understanding that material here reviewed comes from specimens collected during both expeditions, and therefore from the Alcobaça Fm (Kimmeridgian). Based on its similarity with other brown coals from Eocene and its geological settings, Guimarota has been regarded as a terrestrial to lagoonal environment similar to modern mangroves, with occasional freshwater influx and salt water flooding (Gloy, 2000; Martin, 2000a).

2.3.1.2 Institutional abbreviation

IPFUB, Institut für Paläontologie, Freie Universität Berlin; **MG**, Museu Geológico, Lisbon; **NMS**, National Museums of Scotland, Edinburgh.

2.3.2 Material & Methods

All specimens revised come from the excavations of the Guimarota beds by the IPFUB. The specimen numbers attributed by IPFUB during the excavations have been changed when the specimens were returned to the Museu Geológico of Lisbon, where they are now housed, following the agreements signed at the time of the excavations. Therefore, they are here published with their final specimen numbers from the Museu Geológico. However, it must be noted that specimen numbers are given to sample boxes

or specimen holders, and that some boxes may yield more than one element, sometimes dozens of fragments.

Because of the quantity of the material that represent the fossils from Guimarota, we focus our effort on specimens that were stored with the material described by Seiffert (1973) or mentioned in later works (Evans, 1989, 1991b). Only the specimens that could be safely attributed either to *Cteniogenys* (77 specimen numbers) or *Marmoretta* (73 specimen numbers) are here described (see Appendix D). Most relevant specimens were photographed using a DinoLite AM7013MZT, using DinoCapture 2.0 software.

2.3.3 Systematic Paleontology

Reptilia Linnaeus, 1758

Diapsida Osborn, 1903

Choristodera Cope, 1884

Cteniogenys Gilmore, 1928

Type species—*Cteniogenys antiquus* Gilmore, 1928

Type locality and horizon—Quarry 9, Como Bluff (Wyoming, USA); Morrisson Formation, Kimmeridgian-Tithonian

Stratigraphic and geographic range—Kilmaluag Fm from the Isle of Skye (Bathonian), Middle Jurassic of Scotland (Panciroli *et al.*, 2020); Kirtlington Mammal Bed (Bathonian), Middle Jurassic of England (Evans, 1990);

Guimarota lignite beds (Kimmeridgian) and Lourinhã Formation (Kimmeridgian–Tithonian), Upper Jurassic of Portugal (Seiffert, 1973; Evans, 1990; Guillaume *et al.*, 2023a); Como Bluff and others localities from Wyoming (Gilmore, 1928; Foster & Trujillo, 2000), Dinosaur National Monument in Utah (Chure & Evans, 1998), and Wonderland Quarry in South Dakota (Foster & Trujillo, 2000), Morrison Formation (Kimmeridgian–Tithonian), Upper Jurassic of USA; Charisson boned beds (Tithonian), Upper Jurassic of France (Vullo *et al.*, 2014); Angeac-Charente Lagerstätte (Berriasian), Lower Cretaceous of France (Allain *et al.*, 2022); and Oldman and Dinosaur Park formations (mid-Campanian), Upper Cretaceous of Alberta, Canada (Gao & Fox, 1998).

Diagnosis

Small choristoderes that differ from other members of the order by the following character states: contact between premaxillae and nasals absent; orbits significantly narrow and elongate relative to skull dimensions; frontals subrectangular, anterior border of which retracted slightly posterior to anterior level of orbits; dorsal process of maxilla prominent, confined to anterior part of maxilla, and slightly inrolled dorsally; prefrontal short, wide, having elongate palatal process. The genus is further distinguished from more derived neochoristoderes in having separate postorbital and postfrontal, both entering orbital rim; quadrate with weakly developed quadratojugal process; marginal teeth short, with striated

crowns; tooth bases having large replacement pits, but lacking basal plicidentine infolding (modified Gao & Fox, 1998).

***Cteniogenys* aff. *Cteniogenys antiquus* (Figure 2.3.2 and Figure 2.3.3)**

Synonymy

1973 *Cteniogenys reedi* Seiffert, 1973

1983 *Cteniogenys reedi* Seiffert, 1973 *nomen dubium*; (Estes, 1983)

Referred material—premaxilla (n=1), MG27600; maxillae (n=2), MG27417, MG27419, and eight highly fragmented specimens; dentaries (n=18), MG27605, MG27609, MG27627, MG27628, MG27638, MG27646, MG27652, MG27653, MG27662, MG27664, MG27666, MG28761, MG28826, MG28831, MG28843, MG28882, MG28901, MG28914, and 33 specimen holders with highly fragmented specimens; surangular (n=2), MG28420, MG28423; vertebra (n=5), MG28284, MG28287, MG28512, MG28514, MG28552; humeri (n=2), MG28890, MG28928; ilia (n=5), MG28282, MG28288, MG28289, MG28290, MG28291; and MG28792, bloc of associated bones, vertebra, frontal, and putative jugal and postorbitofrontal (Evans, 1991*a*).

Stratigraphic and geographic range—Guimarota lignite beds (District of Leiria); Alcobaça Formation (Kimmeridgian), Upper Jurassic of Portugal (Seiffert, 1973; Evans, 1990)

Description

Premaxilla (**Figure 2.3.2A**)—Only one specimen, a left premaxilla, was identified, but the very short anteromedial sutured border suggests it was

paired in the live animal. The border surface is rather smooth, with two small pits (**Figure 2.3.2A$_2$**). The dorsal process indents the anterodorsal margin of the external nares (**Figure 2.3.2A$_1$** and **A$_2$**). It is anteroposteriorly elongated, projecting strongly with an acute posterior apex. Although posteriorly broken, it extends up to 2.5 tooth loci (**Figure 2.3.2A$_3$**). Its smooth dorsal margin is beveled and diverges medially from the anterior midline of the bone.

The alveolar border displays three tooth loci (**Figure 2.3.2A$_3$**). Locus 1 and 3 preserved the root and part of the crown. The teeth are subcircular, thecodont with the labial wall higher than the lingual wall. Locus 2 is empty and seems larger than the other ones. Although only three tooth loci are preserved, but it seems to be almost complete. Indeed, the premaxilla displays a strong posterior suture to articulate with the maxilla, as well as a deep, short lateral facet (**Figure 2.3.2A$_1$**). The palatal shelf is not preserved. In lateral view, the premaxilla is relatively low, without anterior extension. Instead, it is subvertical, facing anteroventrally (**Figure 2.3.2A$_1$**). Two anterior sensory foramina are preserved, one dorsal and one ventral, followed posteriorly by fainter foramina organized in line.

Maxilla (**Figure 2.3.2B** and **C**)—Maxillary elements are mostly fragments from the posterior ramus. The maxilla is a long, slender bone with at least 21 teeth based on MG27419 (**Figure 2.3.2C**). The dorsal process is flabellate, like a crest, with a dorsomedial facet ornamented by striae

(**Figure 2.3.2C$_1$**). The labial surface displays heavy ornamentations similar to the dentary (**Figure 2.3.2B$_1$**): nutritive foramina extending into short anteroposterior striae. The anterior process is not preserved in MG27419, despite what was previously illustrated (Seiffert, 1973), and could not be identified among other fragments. The bone tapers posteriorly into a long, low orbital process, forming a dorsoventrally compressed ramus, as a plate (**Figure 2.3.2C$_1$**). It displays a very shallow posterodorsal facet, which extend on all its width. The alveolar border exhibits a broad, elongated medial facet for the vomer (**Figure 2.3.2C$_1$**), with a large gap between vomerine and palatine facets to form the internal nares. It is associated with a large foramen connected to a deep anteroposterior groove, posterior to the dorsal process, for the opening of the superior alveolar canal.

Dentary (**Figure 2.3.2D** and **E**)—Dentaries are by far the most common bone, although most of the specimens consists in highly fragmented small elements of which any assessment cannot be safely confirmed. The dentary is a long, slender, mostly straight bone. Due to the preservation of the specimens, the tooth row displays between 24 and 33 teeth. The symphyseal surface is posteriorly elongated, dorsally and ventrally encapsulating the Meckelian canal (**Figure 2.3.2D$_1$** and **E$_1$**). Its surface is rugose, but not ornamented.

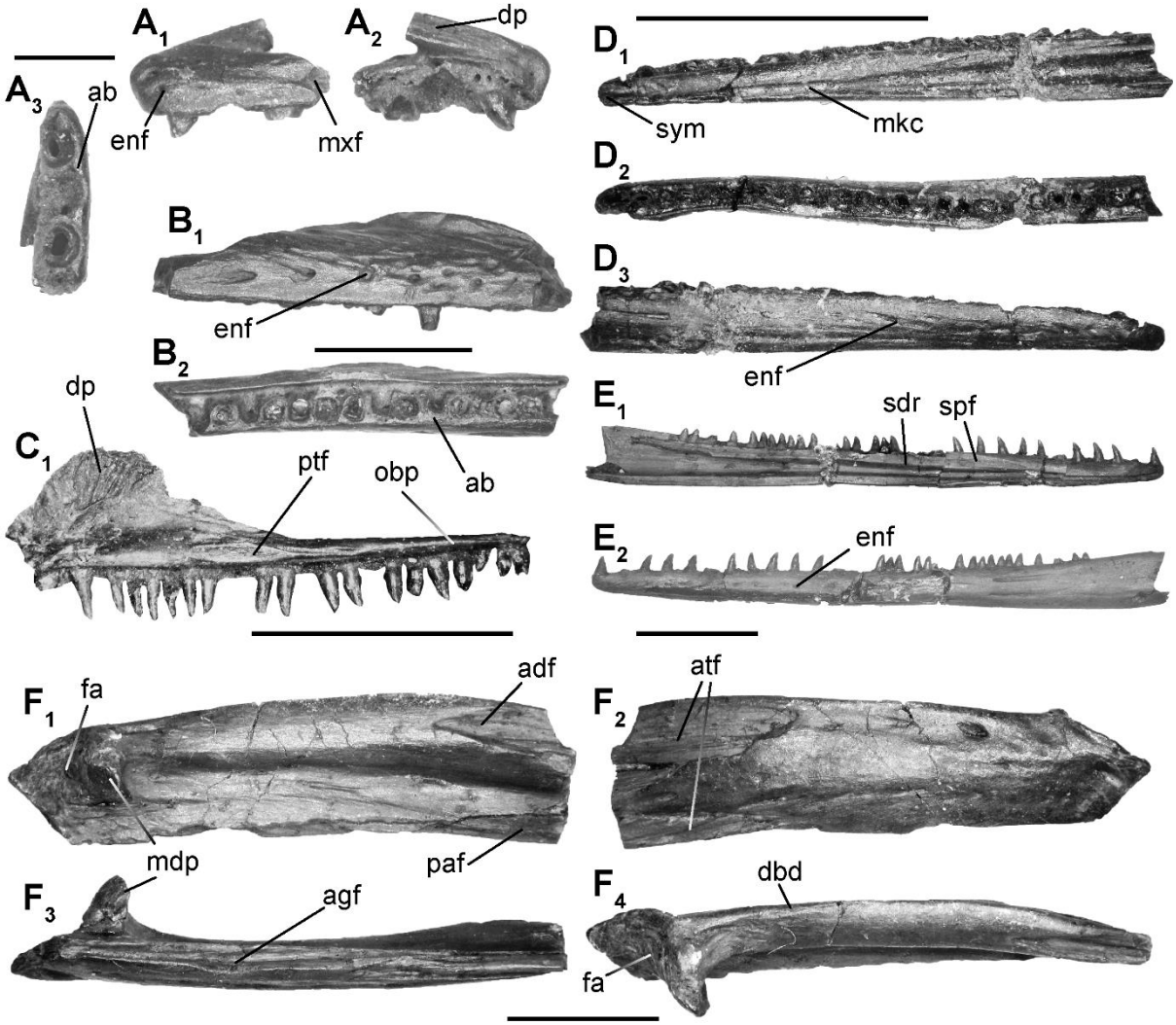

Figure 2.3.2: *Cteniogenys* aff. *C. antiquus* jaw material from the Guimarota beds. **A**, left premaxilla MG27600 in labial (A_1), lingual (A_2), and ventral (A_3) views. **B**, right maxilla MG27417 in lateral (B_1) and ventral (B_2) views. **C**, right maxilla MG27419 (Gui L. 234; fig. 4 in Seiffert, 1973) in lingual (C_1) view. **D**, right dentary MG27628 (designated holotype Gui A33 fig. 3 in Seiffert, 1973) in lingual (D_1), dorsal (D_2), and labial (D_3) views. **E**, left dentary MG28514 in lingual (E_1) and labial (E_2) views. **F**, left surangular MG27423 in medial (F_1), lateral (F_2), ventral (F_3) and dorsal (F_4) views. Abbreviations: **ab**, alveolar border; **adf**, adductor facet; **agf**, angular facet; **atf**, lateral articular facets; **dbd**, dorsal border; **dp**, dorsal process; **enf**, external nutrient foramen; **fa**, facet for the articular; **mdp**, medial process; **mkc**, Meckelian canal; **mxf**, maxillary facet; **obp**, orbital process; **paf**, prearticular facet; **ptf**, palatine facet; **sdr**, subdental ridge; **spf**, facet for the splenial; **sym**, symphysis. Scale for A is 1 mm; scales for B and F are 3 mm; scales for C, D, and E are 5 mm.

The facet for the splenial is visible, posteriorly to the symphysis (**Figure 2.3.2E$_1$**). Its anterior apex is acute. It participates ventrally, then medially, to the subdental shelf, with a beveled rim. The facet keeps the Meckelian canal open dorsally and extends to the end of the tooth row based on MG28914 (**Figure 2.3.2E$_1$**). The subdental ridge is strong and robust, more marked than the ventral part of the dentary. Its mediolateral surface is blunt anteriorly but becomes posteriorly a horizontal shelf which separates the coronoid facet to the ventral prearticular facet.

The Meckelian canal is open all along the dentary, although the opening becomes wider towards the posterior end of the tooth row (**Figure 2.3.2D$_1$** and **E$_1$**). MG28914 does not display an angular facet, but a posterior alveolar opening on the ventral wall. The labial surface is highly ornamented with anteroposterior short striae extending nutritive foramina in a double line (**Figure 2.3.2D$_3$** and **E$_2$**). The teeth are conical, with an acute apex, and subthecodont. They are striated mostly on their lingual surface, although this is restricted to the top of the crown. The striations are absent in MG28901, of which teeth are more triangular with a blunt apex, but they are well pronounced in MG28914. The teeth have a cylindric base, with a slight anteroposterior compression. The anterior-most teeth are slightly curved distally.

Surangular (**Figure 2.3.2F**)—Two elements could be identified as surangular, with MG27420 being still articulated with the posterior part of

a dentary. It is a robust, elongated, subrectangular bone. The lateral surface is broad, with few foramina extending into short grooves in its anterior section. In MG27423, the large articular facets have an acute posterior apex (**Figure 2.3.2F$_2$**). The dorsal facet is obscured in MG27420 because of the dentary, and the ventral one could not be confirmed. The ventral margin displays a deep anteroposterior groove, the angular facet (**Figure 2.3.2F$_3$**). Its medial flange is shorter and can be seen in medial view. The posterior edge is acute to blunt, displaying a small process (**Figure 2.3.2F$_1$**).

The surangular exhibits a medially extended process, which is anteroposteriorly compressed to form a prominent prong. This process delimits a posterior, more rugose fossa for the articular (**Figure 2.3.2F$_1$**). Dorsally, it is connected to a strong wide ridge forming the dorsal border of the bone (**Figure 2.3.2F$_4$**). It participates to the thick, round adductor region and opens anteriorly into a deep slot with an acute posterior apex (**Figure 2.3.2F$_1$**). Ventrally, the process extends into a shallow ridge participating to the ventral border of the surangular with the angular facet (**Figure 2.3.2F$_1$**). It displays anteriorly a triangular facet for the prearticular, which is less marked than the dorsal slot.

Dorsal/sacral vertebra (**Figure 2.3.3A** and **C**)—MG28512 and MG28552 share a short amphicoelous to platycoelous centrum, with subcircular anterior and posterior articular surfaces. The notochordal canal can be seen

in MG28552 (**Figure 2.3.3C$_4$** and **C$_5$**), suggesting it is an immature. Relatively square-shaped in dorsoventral view, the centrum wider than long. Its dorsal surface is excavated on either side of strong median crest (**Figure 2.3.3A$_1$** and **C$_1$**). Although the excavation is clogged by coal in MG28512, the dorsal ridge of the median crest, as well as the margin of the excavation, can be clearly seen.

Both vertebrae display large, raised lateral articular facets. These facets are roughly triangular, with the apex projecting laterally. In MG28512, it can be dipping lateroventrally, with the apex more ventral than the base (**Figure 2.3.3A$_2$**). The facets are immediately posterior to the anterior margin of the centrum, being separated by a shallow groove. Neither ventral surface exhibits a sharp, midventral keel, as they are rather convex. However, MG28512 is smooth and broad, which would suggest it might be more dorsal than sacral (**Figure 2.3.3A$_3$**); while MG28552 is smooth, but narrower, almost constricted (**Figure 2.3.3C$_3$**), suggesting it might be sacral or transitional. However, the lack of material to compare with, and the fact that MG28552 seems to be more immature, prevent us to confirm the exact identification.

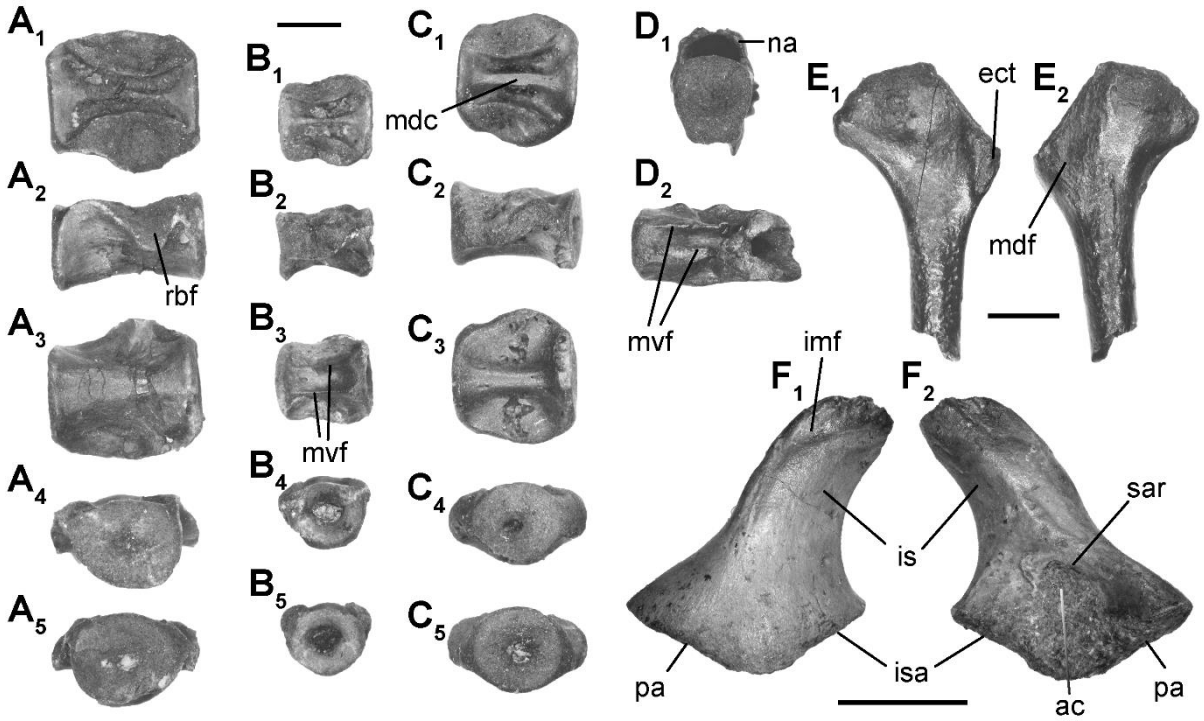

Figure 2.3.3: *Cteniogenys* aff. *C. antiquus* axial and appendicular skeleton. **A**, dorsal vertebra MG28512 in dorsal (A_1), lateral (A_2), ventral (A_3), anterior (A_4), and posterior (A_5) views. **B**, anterior caudal vertebra MG28514 in dorsal (B_1), lateral (B_2), ventral (B_3), anterior (B_4), and posterior (B_5) views. **C**, dorsal/sacral vertebra MG28552 in dorsal (C_1), lateral (C_2), ventral (C_3), anterior (C_4), and posterior (C_5) views. **D**, mid-caudal vertebra MG28287 in anterior (D_1) and ventral (D_2) views. **E**, left humerus MG28928 in lateral (E_1) and medial (E_2) views. **F**, right ilium MG28289 in medial (F_1) and lateral (F_2) views. Abbreviations: **ac**, acetabulum; **ect**, ectotuberosity; **imf**, Iliac medial facet; **is**, iliac shaft; **isa**, ischial articulation; **mdc**, median crest; **mdf**, mediodorsal facet; **mvf**, Medioventral flanges; **na**, neural arch; **pa**, pubic articulation; **rbf**, rib articular facet; **sar**, supraacetabular ridge. Scales for A, B, C, D, and E are 1 mm. Scale for F is 3 mm.

Caudal Vertebra (**Figure 2.3.3B** and **D**)—Only three caudal vertebrae could be safely identified. The morphology of MG28514 (**Figure 2.3.3B**) suggests it is an anterior caudal vertebra. It displays an amphicoelous to platycoelous short centrum, relative square-shaped in dorsal and ventral views (**Figure 2.3.3B$_1$** and **B$_3$**). The opening of the notochordal canal is visible (**Figure 2.3.3B$_4$** and **B$_5$**), suggesting it is an immature specimen. The

anterior and posterior articular surfaces are subcircular. The dorsal surface of the centrum is excavated on either side of strong median crest (**Figure 2.3.3B$_1$**); while the ventral surface displays a large, deep midventral groove with paired ventral flanges (**Figure 2.3.3B$_3$**). The morphology of MG28284 and MG28287 suggests they were caudal and more posterior than MG28514, maybe mid-caudal. They share an amphicoelous to platycoelous subcircular centrum, slightly compressed laterally (**Figure 2.3.3D$_2$**). They display a deep ventral groove flanked by two lateral flanges extending anteroposteriorly (**Figure 2.3.3D$_2$**). They are preserved with the neural arch (**Figure 2.3.3D$_1$**), but the dorsal surface is obscured by sediments. The neural arch exhibits a basal longitudinal thin crest. The neural spine and the zygapophyses are not preserved.

Humerus (**Figure 2.3.3E**)—Two left humeri could be identified, although they are not complete. Based on overlapping material, the humerus displayed a broad proximal and distal head for a slender shaft that looks dense in cross-section and rotates around 90°. The proximal head is anteroposteriorly flattened. It extends on the proximal ridge as a convex bar, with a faint condyle in the middle. The ectotuberosity is well marked on the radial border (**Figure 2.3.3E$_1$**). It is separated from the head by a long proximodistal crest. The mediodorsal border displays a small peg, as well as a long groove on the dorsal surface where it joins the shaft in MG28928. The fossa is well marked. In medial view, along the radial border and distal

to a shallow surface, a dorsoradial small rough area can be observed (**Figure 2.3.3E₂**).

The distal head is mediolaterally flattened and flares dorsoventrally, although the epicondyle is poorly developed as no clear differentiation of articular facet can be observed. The distal head also exhibits a deep but narrow ectepicondylar groove in dorsal view. The lateral supinator region barely extends, almost not separated from the rest of the bone. There is no sign of entepicondylar groove. Both ventral and dorsal surfaces are smooth. The latter displays a shallow fossa, while the former displays a fossa which has a strong anterior rim and becomes fainter posteriorly.

Ilium (**Figure 2.3.3F**)—Only the ventral-most part of the ilia has been preserved. The acetabular region, fully preserved only in MG28289, is mediolaterally flattened. The anterior and posterior margins flare out, making a triangular general outline. The ventral border is wide V-shaped, highly flattened and obtuse, with a bulbous apex. Both ischial and pubic articular facets are preserved, the former being hooked in MG28289 (seemingly more mature than other specimens). The acetabulum is subovoid to triangular, rather shallow—no matter the size of the specimens—, but with a strong rim in MG28289 (**Figure 2.3.3F₂**).

The supraacetabular ridge thickens in the middle, creating a distinct boss which merges with the ridge running along the iliac shaft; and is ventrally bordered in MG2882 by a round cavity that may yield a small

foramen. The ilium narrows dorsally into a posteriorly curved blade, with a lateral shallow ridge running along. There is no sign of dorsal tuberosity. The iliac shaft is mediolaterally flattened with a sharp posterior edge and a blunter anterior edge. Its width remains similar in all the section, but the dorsal-most part is not preserved. It bears a medial facet (**Figure 2.3.3E$_1$**). However, its ventral margin can be either convex, making it like a strip, or concave, making it circular.

Remarks

The dentaries here described display the typical morphology and ornamentation previously observed in the *Cteniogenys* sp. material from Kirtlington in UK (Evans, 1989, 1990), as well as in the material found in the Morrison Formation (Chure & Evans, 1998; Foster & Trujillo, 2000) and to the type species *Cteniogenys antiquus* (Gilmore, 1928; Evans, 1989), based on holotype and referred material currently housed in the Smithsonian National Museum of Natural History and the Yale Peabody Museum (USA; ARDG, pers. obs, 2022). They display the characteristic double row of nutritive foramina extended in striae on the labial surface, visible splenial facets tapered anteriorly, the medially directed symphysis, the broad conical teeth with subthecodont implantation—the base of each tooth is sitting in a shallow, rounded socket, but there is not root—, and striae restricted to the apical part of the tooth crown (Seiffert, 1973; Evans, 1989, 1990).

In his original work, Seiffert used the depth of the subdental ridge and the compression of the tooth crowns to distinguish the Guimarota taxon to *C. antiquus* (Seiffert, 1973). However, it was later argued that the designated holotype MG27628 (Gui A. 33 in the original publication, see **Figure 2.3.2D**) does not exhibit any significant difference in depth, neither does it preserve any tooth crown (Estes, 1983); and being relatively small, it could belong to a juvenile (Evans, 1989). Our examination of the Portuguese material, as well as holotype and referred material of *C. antiquus*, confirmed the limitation of the dentary to distinguish the species.

Nevertheless, previous works on the material from Guimarota and Kirtlington (Seiffert, 1973; Evans, 1989, 1990, 1991a) allows to find more elements with affinity between both localities, suggesting they were indeed sharing this faunal component. Notably, Seiffert could identify premaxillae and maxillae aside from the dentaries (1973), although some of the premaxillae were later referred to the lepidosauromorph *Marmoretta* (Evans, 1991b; Griffiths *et al.*, 2021). Although the attribution of the maxilla MG27419 to *Cteniogenys* (Gui L. 234 in the original publication, see **Figure 2.3.2C**) was questioned (Evans, 1989), the other maxillae (MG27417, and other fragmentary specimens) described in this work could confirm the original assessment of Seiffert regarding MG27419: the maxilla displays the characteristic prominent dorsal process, confined to the anterior part of the maxilla, and slightly inrolled dorsally (Evans, 1989, 1990; Gao & Fox, 1998).

No complete maxillae were found associated with *Cteniogenys antiquus* material in North America, and fragments were only referred to *Cteniogenys* sp. (ARDG, pers. obs., 2022). None seem to have preserved the flabellate dorsal process, but the material would require a deeper revision to confirm this statement as the isolated specimens are still embedded in their matrix. Nevertheless, their robustness, their ornamentation, and their tooth implantation match the European material.

Only one premaxilla (MG27600) assignment to *Cteniogenys* could be safely confirmed, based on its differences with other premaxillae attributed to *Marmoretta* and the presence of the dorsal process observed in the *Cteniogenys* sp. from Kirtlington (Evans, 1990, 1991b). However, the Portuguese material slightly differs from the English material: the dorsal process is more acute, projecting not only further posteriorly (2.5 tooth loci instead of 1.5) but also more posteriorly rather than dorsally. The alveolar border from the Guimarota specimen is similar to the one observed in Kirtlington (fig. 5A; Evans 1990), although it preserves only three tooth loci instead of four and seems rather complete, suggesting it was bearing less teeth than the Kirtlington specimen. Finally, the Kirtlington premaxillae display a small anterior extension extending the dorsal process, that can form a small ventral sickle (fig. 5C and fig. 5D; Evans 1990); but that feature is not observed in Guimarota. The well-preserved anterior section of the bone is instead subvertical, facing anteroventrally.

On top of these bones, here are reported for the first time the presence of surangular, isolated vertebrae, humeri, and ilia. All of them display strong affinities with the material from Kirtlington. Surangulars were never reported previously, and they were actually labelled as Albanerpetontidae in the Guimarota collection. Albanerpetontids are an enigmatic group of extinct lissamphibians (Fox & Naylor, 1982), but the surangulars from Guimarota do not resemble to any bone elements known in this group (see Section 3), while their morphology is strikingly similar to the surangulars from Kirtlington (Evans, 1990).

The vertebra MG28512 and MG28514 were also labelled as Albanerpetontidae. However, they display the dorsal excavations in either side of the median crest that is absent in albanerpetontids, and albanerpetontid vertebrae are hourglass shaped (see Section 3.2). On the contrary, the square overall morphology, the dorsal excavations in either side of the median crest, the morphology of the articular facet, and the presence of facet to articulate with the rib match what has been described in dorsal and sacral vertebrae from Kirtlington (Evans, 1991a). MG28552 was only labelled as Amphibia, but the square overall morphology, the dorsal excavations in either side of the median crest, the morphology of the articular facet, and ventral groove flanked by paired flanges also fit the description of caudal vertebrae from Kirtlington (Evans, 1991a). The vertebra MG28287 was labelled as 'Anura? or *Cteniogenys*?', but was not reported in Seiffert's work, but it is closely resembles the vertebra

MG28284, neither referred even though labeled *Cteniogenys* sp, and other mid-caudal vertebrae from Kirtlington (Evans, 1991a), seemingly more elongated than MG28514.

The humerus MG28890 is labelled as *Cteniogenys* sp. but not mentioned in Seiffert's work; while the humerus MG28928 was labelled as Squamata and neither referred. Regarding the ilia, only MG28289 and 28290 were labelled as *Cteniogenys* sp., while MG28291 was labelled as Anura, and MG28282 and MG28288 as 'Anura? or *Cteniogenys*?'; but none was mentioned nor reported previously. However, none of the five ilia displays the dorsal tuberosity characteristic of anurans. Rather, their morphology shares strong similarities with other choristoderes, especially *Cteniogenys* (Evans, 1991a; Matsumoto *et al.*, 2009). Furthermore, even if the ilia from the Guimarota beds exhibit different stage of preservation, they can be assigned of the same taxon.

However, some differences can be noted between the Portuguese and the English material, which would suggest there were several *Cteniogenys* species. The surangular from the Guimarota beds display a small process on the posterior edge of the ventral margin which was not reported in Kirtlington (Evans, 1990). Also, the bones from Guimarota seem longer than the ones from Kirtlington, although this could be due to a preservation bias in the English material. The ectotuberosity in the proximal head of the humerus but appears relatively lower than the one observed in Kirtlington

specimens. Furthermore, the ectotuberosity in Kirtlington is separated from the humeral head by a groove (Evans, 1991a), not a crest as observed in Guimarota. The humeri from Kirtlington also display a proximal roughened region (Evans, 1991a), but this one is absent in Guimarota. Finally, the ectepicondylar grove is less marked in the Portuguese specimens than in the English ones (Evans, 1991a).

Previous statements regarding the validity of the Guimarota species were right (Estes, 1983; Evans, 1989; Chure & Evans, 1998), as the dentaries alone do not allow to differentiate species from North America and Europe. A deeper revision of the material from the type locality of *C. antiquus* (Quarry 9, Como Bluff, Wyoming), as well as more complete redescription of the type species with associated material, is needed to confirm, thus preventing us to erect a new species or to support previous taxonomic claims of its condition as a new species (Seiffert, 1973). Nevertheless, our study confirms that although they are similar, Portuguese and English species are different, hinting toward a higher diversity of early choristodere in the Jurassic.

Lepidosauromorpha Gauthier *et al.*, 1988a

Marmoretta Evans, 1991b

Type species—*Marmoretta oxoniensis* Evans, 1991b

Type locality and horizon—Old Cement Works Quarry, Kirtlington Mammal Bed (Oxfordshire, England); late Bathonian.

Stratigraphic and geographic range—Kilmaluag Fm from the Isle of Skye (Bathonian), Middle Jurassic of Scotland (Panciroli *et al.*, 2020; Griffiths *et al.*, 2021); Kirtlington Old Cement Works and Leigh Delamere (all Bathonian), Middle Jurassic of England (Evans, 1991b, 1998b; Evans & Milner, 1994); and Guimarota lignite beds (Kimmeridgian), Upper Jurassic of Portugal (Evans, 1991b).

Diagnosis

Small lepidosauromorph; large upper and lower temporal fenestrae; premaxillae paired, each with deep posterolateral maxillary facet; specialized maxillary/premaxillary overlap; small posteroventral process of the jugal; narrow fused frontals; fused parietal forming a broad parietal table, parietal foramen absent, large midline sagittal crest; dorsoventrally wide posterior (squamosal) process of the postorbital that overlaps on to a broad shallow facet on the squamosal; palatine with small teeth that decrease in size medially from a larger row along the medial choana margin to smaller scattered teeth on the ventral surface; pterygoids bear three rows of teeth which radiate anteriorly; long and slender dentary with subpleurodont teeth; coronoid with prominent coronoid process having a smooth concave posterior surface that emerges through the lower temporal fenestra (Griffiths *et al.*, 2021).

***Marmoretta* sp. nov. New unnamed taxon 1(Figure 2.3.4** and **Figure 2.3.5)**

Referred material—MG28841, right maxilla (putative holotype; **Figure 2.3.4B**); premaxillae (n=3), MG27588, MG27593, MG27644; maxillae (n=12), MG28751, MG28757, MG28771, MG28798, MG28815, MG28816, MG28842, MG2887, MG28888, MG28907, MG28908, MG28925; dentaries (n=53), MG27626, MG27633, MG27641, MG27643, MG27659, MG27665, MG27667, MG28763, MG28778, MG28779, MG28784, MG28785, MG28791, MG28794, MG28797, MG28803, MG28828, MG28833, MG28857, MG28874, MG28905, MG28910, MG28942, and 30 specimen holders and sample boxes with highly fragmented specimens; frontals (n=4), MG28740-28743.

Stratigraphic and geographic range— Guimarota lignite beds (District of Leiria); Alcobaça Formation (Kimmeridgian), Upper Jurassic of Portugal.

Putative diagnosis

Small lepidosauromorph differing from *Marmoretta oxoniensis* by having a highly constricted margins of the maxillary facet in the paired premaxillae; an anterior rim of the dorsal process in the maxilla more curved, making it rise more sharply; a lacrimal facet not extending dorsally on the dorsal process of the maxilla; maxillary teeth without apicolingual curvature; postfrontal facets not meeting posterodorsally in the fused frontals.

Description

Premaxilla (**Figure 2.3.4A**)—None of the three premaxillae are complete, as the specimens from the Guimarota beds only preserved the anterior part. The alveolar tooth bearing plate is curved and formed by the alveolar border and crest. The premaxilla was not bearing more than five teeth. Although none is preserved, the alveolar border suggests they were pleurodont, being attached via the labial wall only by the rot, and were subcircular, being mesiodistally constricted (**Figure 2.3.4A$_1$**). MG27644 does not preserved the maxillary facet. In other specimens, the facet is located in the posterolateral region of the premaxilla and is anteroposteriorly elongated, with an acute anterior apex (**Figure 2.3.4A$_2$**). It is ventrally deep and V-shaped, with margins highly constricted, making look like a groove or a slot. In MG27588 (**Figure 2.3.4A**), the facet exhibits a shallow, small anterodorsal emargination which is not present in other specimens. The narial process extends posteriorly from the anteromedial part of the bone and participate to the alveolar tooth bearing plate, but it is poorly preserved (**Figure 2.3.4A**). None of the specimens preserved the anterodorsal process (or nasal process *sensu* Evans, 1991b).

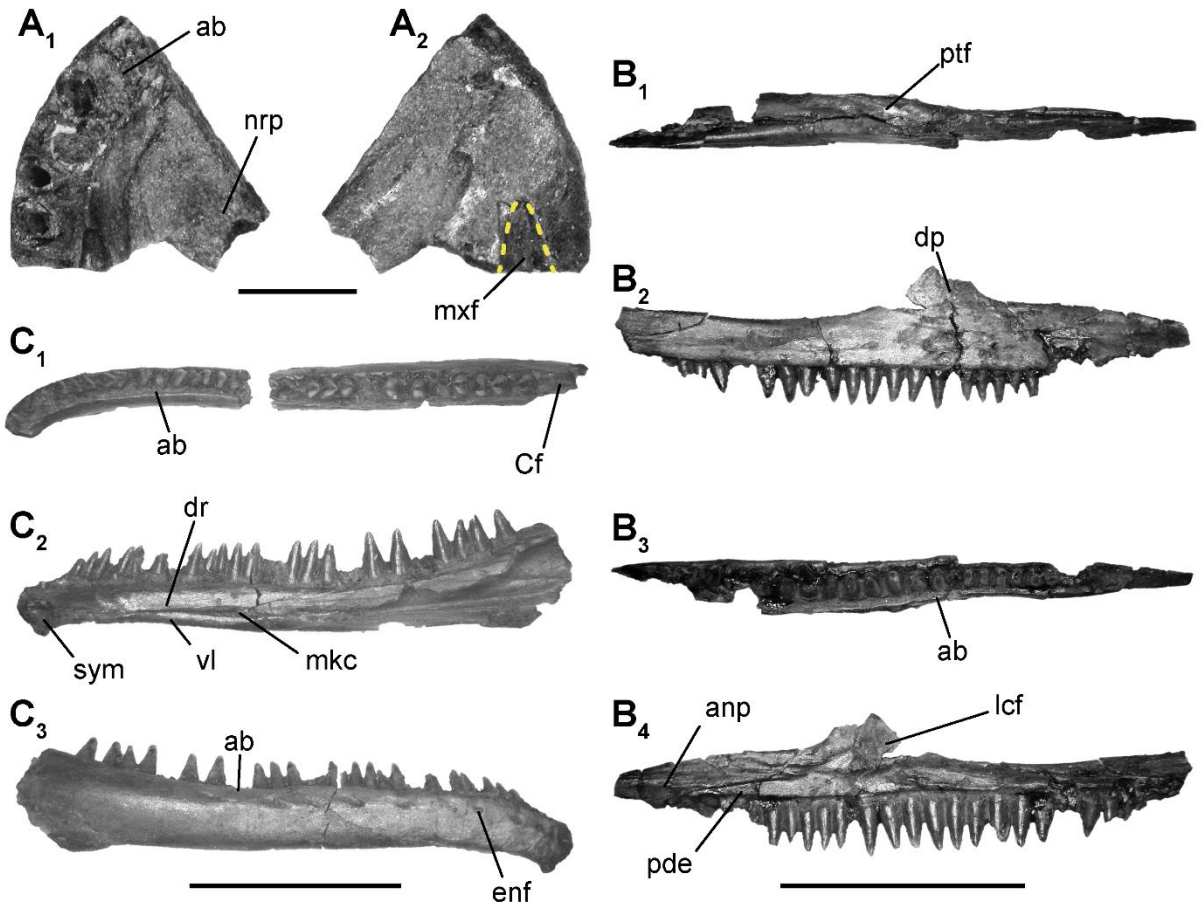

Figure 2.3.4: Cranial bones of New unnamed taxon 1. A, right premaxilla MG27588 in ventral (A_1) and dorsal (A_2) views. B, right maxilla MG28841 (putative holotype) in dorsal (B_1), lateral (B_2), ventral (B_3), and medial views (B_4). C, right dentary MG28785 in dorsal (C_1), medial (C_2), and lateral views (C_3); the specimen is broken, but both parts could be put together for the lateral and medial views. Abbreviations: **ab**, alveolar border; **anp**, anterior process; **cf**, coronoid facet; **dp**, dorsal process; **dr**, dorsal subdental ridge; **enf**, external nutrient foramen; **lcf**, lacrimal facet; **mkc**, Meckelian canal; **mxf**, maxillary facet; **nrp**, narial process; **pde**, *pars dentalis*; **ptf**, palatine facet; **snr**, subnarial ramus; **sym**, symphysis; **vl**, ventral lip. Scale for A is 1 mm. Scales for B and C are 5 mm.

Maxilla (**Figure 2.3.4B**)—The maxilla is a long, slender bone, tapered posteriorly. It is overall quite gracile, but its anterior section appears more robust. It is mediolaterally constricted, forming a long crest in dorsal view. The long, bulked anterior process is anteriorly acute with a round apex (**Figure 2.3.4B$_2$** and **B$_4$**). It is best preserved in MG28841 and MG28908,

and partially in MG28771, MG28816, MG28907, and MG28925; although, based on the shape of the maxillary facets observed in the premaxillae, it seems that no specimens fully preserved the anterior tip. The pars dentalis anteriorly extend up to 1/3 of the process (**Figure 2.3.4B$_4$**). MG28841 and MG28908 do not display a clear premaxillary facet, but MG28925 displays a narrow slot, although its medial surface is convex. The dorsal surface of the anterior process is rather smooth, with faint anteroposterior ridges extending to the dorsal process. The dorsal margin itself is a thin crest (**Figure 2.3.4B$_1$**).

The tip of the dorsal process (or facial process *sensu* Evans, 1991b) is preserved in none of the Portuguese specimens, as it is always dorsally broken (**Figure 2.3.4B$_2$** and **B$_4$**). Therefore, the development of the apex is unknown. Only the ventral section has been preserved in some specimens, allowing some overlapping material for that part. The base is rather large and its unparallel anterior and posterior edges suggest the dorsal process was either triangular or trapezoidal, but not much developed. Also, it does not seem to be medially inclined (**Figure 2.3.4B$_1$**). The anterior rim is thicker than the posterior rim, which looks more like a crest. The anterior rim outline is concave, being extremely marked in MG28816, MG28841, and MG28842. Medially, there is a small foramen at the base of the dorsal process. The lacrimal facet is not clearly marked: there is a deep medial depression posterior to the dorsal process, but it is ventrally restricted and do not extend dorsally.

The long posterodorsal jugal facet exhibits an acute anterior apex on the medial surface. The margin is well marked. It is located in the groove formed by the rim and the alveolar shelf. The palatine facet is well preserved only in the medial surface MG28908. It displays an anterodorsal-posteroventral shallow groove with two facets on the alveolar shelf: the dorsal facet is rather short while the ventral one is longer. It is ventral to the posterior rim of the dorsal process and is pierced by two foramina in its dorsal facet. The lateral surface of the bone is rather smooth. MG28842 and MG28908 display occasional nutritive foramina. Posteriorly, the midline of the surface can be marked by a deep anteroposterior grove.

MG28841 exhibits a tooth row with 17 teeth but is not complete and is missing its anterior section. Teeth are tubular to conical, with an acute apex. They are pleurodont, being attached only via the labial wall only by the root. No apicolingual curvature could be observed. The enamel covers the entire crown and can be slightly apically striated on the lingual side.

Dentary (**Figure 2.3.4C**)—Most of the specimens are broken, although several preserved all the parts, making MG28794 and MG28910 the only ones seemingly complete and not broken. However, the former is embedded in coal matrix, and part of the anterior section of the later is obscured. The dentary is a long, slender bone, relatively gracile. It deepens dorsoventrally in its posterior section. The labial surface is relatively smooth, although it can be covered by small nutritive foramina (**Figure 2.3.4C$_3$**). They are

usually aligned, restricted to the anterodorsal part of the dental parapet. The anterior symphysis is small and short, forming a subvertical wall (**Figure 2.3.4C$_2$**). Lingually, the symphysis is divided in an upper and a lower rim by the Meckelian canal. The symphyseal surface is mostly flat, either is right or left specimens—although more rugose than the rest of the bone—, and is U to V-shaped, the apex being more or less round. Also, the dentary is medially curved in that part (**Figure 2.3.4C$_1$**).

The lingual surface of the dentary is divided in two parts by the Meckelian canal: the dorsal subdental ridge and the ventral lip (**Figure 2.3.4C$_2$**). This canal is anteriorly widely opened at the symphysis and immediately posteriorly. Then, around the 4th and 5th teeth loci, the canal narrows drastically, to the point to form a thin groove or even contacting both the subdental ridges and the ventral lips, making a fold. However, some specimens can be dorsoventrally crushed, making one part looks like it overlaps the other. Posteriorly, the canal reopens broadly, with an acuminate apex. It broadens posteriorly up to the full height of the bone. Due to various preservations and intraspecific variation from one specimen to another, it is difficult to safely determine where this posterior opening starts, but it seems to be around seven or eight teeth loci before the end of the tooth row.

The tooth row is supported by the alveolar border. Posteriorly, where the Meckelian canal fully opens, it becomes a shelf. By the posterior end of

the tooth row, it becomes weaker and bears shallow facet for the coronoid (**Figure 2.3.4C$_1$** and **C$_2$**). Teeth are tubular to conical, sharply pointer, and more apically elongated than in the maxilla. They are pleurodont, being attached via the taller labial wall only by the root; although, the implantation seems weak. The enamel covers most of the crown, with the apex being striated on the lingual surface. Based on specimens with tooth row the most complete, there were at least 19 teeth and up to 26.

Frontal (**Figure 2.3.5**)—All frontal bones are fused, suggesting they are all from mature individuals (Evans, 1991b). MG28740 is broken midway in two pieces, and MG28743 did not preserved the anterior part. In dorsoventral view, their general outline is trapezoidal to subrectangular, with the posterior border being wider than the anterior border, especially in MG28742 (**Figure 2.3.5B**). The lateral margins are embayed for the orbits.

Despite having similar length, MG28741 is broader than MG28742, probably due to intraspecific variation. Only MG28740 exhibits an ornamented dorsal surface, being sculptured by fine furrow and drumlin-shaped knobs. The fused frontals are anteroposteriorly convex in lateral views, being more marked in MG28742 but with upturned lateral edges (medial orbital margin) stronger in MG28741 (**Figure 2.3.5A$_3$**, **A$_4$**, **B$_3$**, and **B$_4$**). Unfortunately, the anterior border is not well preserved in any specimen. MG28742 retains a short process that could be the median process (**Figure 2.3.5B$_1$** and **B$_2$**), but no anterolateral process can be seen.

In dorsal view, the anterior section of the dorsal surface is rather flat and shallow, while the posterior section appears more bulbous in its center. The postfrontal facets are at the posterolateral corners of the bone (**Figure 2.3.5A$_3$**, **A$_4$**, **B$_3$**, and **B$_4$**). They are restricted to the lateral border, with a lenticular to triangular outline, and face lateroventrally. The blunt ventral vertex, where the anterior ridge of the facet meets the ventral surface of the bone, can be located at the midpoint of the facet to slightly posteriorly (MG28741, **Figure 2.3.5A$_3$**, and **A$_4$**), or more anteriorly (MG28742, **Figure 2.3.5B$_3$**, and **B$_4$**; and MG28743, not figured).

The ventral margin is more marked than the dorsal. The posterior margin of the fused frontals is not well preserved, but the postfrontal facets do not seem to meet posterodorsally (**Figure 2.3.5A$_1$**, **A$_2$**, **B$_1$**, and **B$_2$**). The anterolateral prefrontal facets participate to the anterior section of the fused frontal lateral edges (**Figure 2.3.5A$_3$**, **A$_4$**, **B$_3$**, and **B$_4$**). They are quite deep and wide, forming a posteroventral right angle, with posterior and ventral margins strongly marked. The ventral surface of the fused frontals bears distinct paired anteroposterior *crista cranii* (**Figure 2.3.5A$_1$** and **B$_1$**), ventral extensions of the bone that act as dorsolateral walls for the olfactory tract. They lengthen the surface of the fused frontals lateral edges and participate to the orbits. They extend anteriorly after the lateral edges, and border ventrally the prefrontal facets. Both *crista cranii* form an hourglass outline, being lateromedially restricted at the center of the bone. Their width is similar between all specimens.

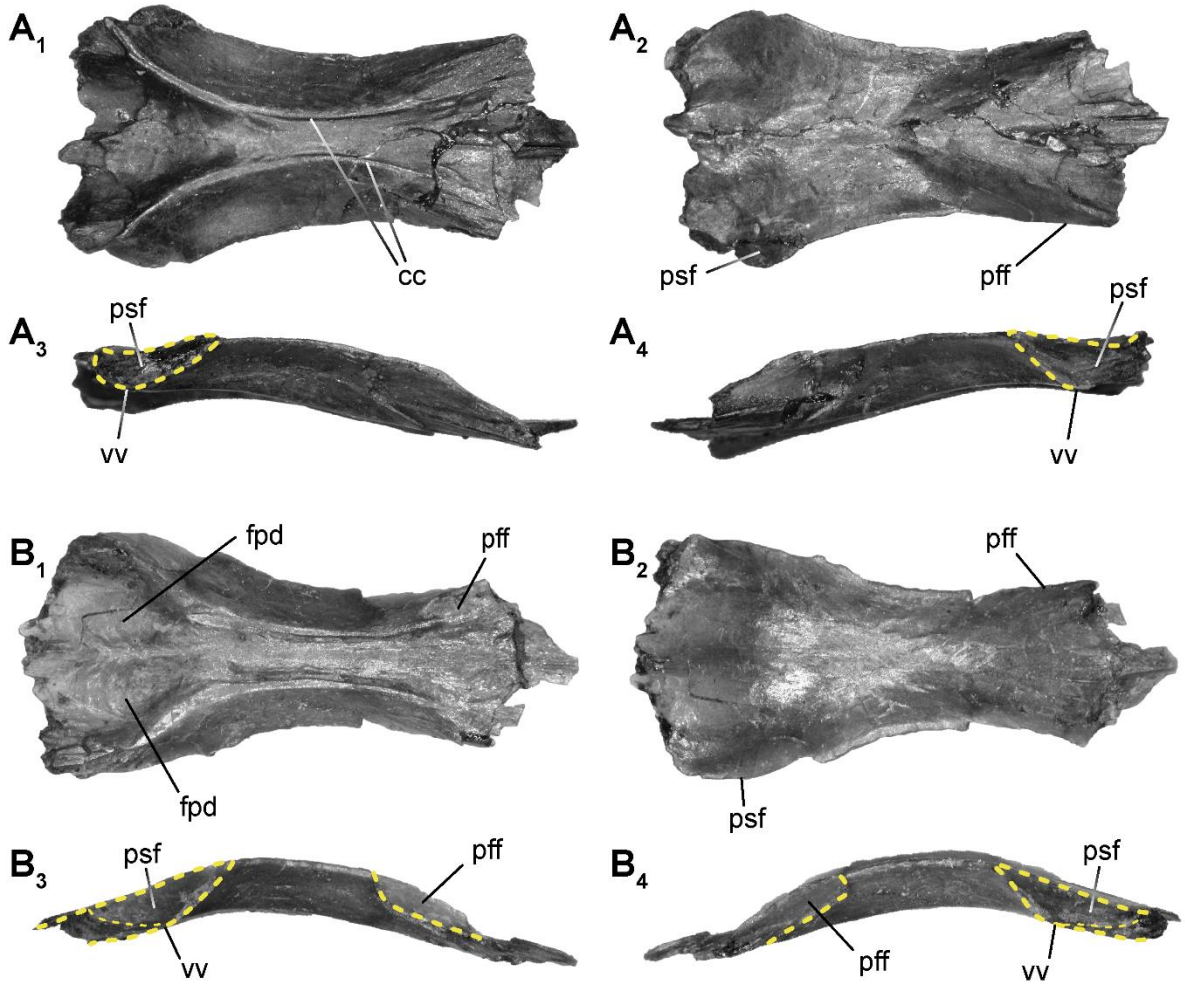

Figure 2.3.5: Frontal bones of New unnamed taxon 1. A, frontal MG28741in ventral (A_1), dorsal (A_2), lateral right (A_3), and lateral left (A_4) views. B, frontal MG28742 MG28741in ventral (B_1), dorsal (B_2), lateral right (B_3), and lateral left (B_4) views. Abbreviations: **cc**, *crista cranii*; **fdp**, frontal paired ventral depressions; **pff**, prefrontal facet; **psf**, postfrontal facet; **vv**, ventral vertex. Scale is 5mm.

The ventral surface of the fused frontals displays a paired depression, separated by a ridge (**Figure 2.3.5A$_1$** and **B$_1$**). The ridge can be marked, as in MG28742, or fainter, as in MG28741 and MG28743, in which the *crista cranii* are posteriorly stronger. These paired depressions might house the dorsal region of the brain and would indicate that both cerebral

hemispheres would be well differentiated by a sagittal sulcus (interhemispheric fissure *sensu* Barrios *et al.*, 2023).

Remarks

Thanks to the previous works on *Marmoretta* from the Middle Jurassic of the British Isles (Evans, 1991b; Waldman & Evans, 1994; Panciroli *et al.*, 2020; Griffiths *et al.*, 2021), more substantial material could be identify from the Guimarota beds and confirm the presence of the genus in the Upper Jurassic of Portugal. Indeed, all bones identified shares similarities with *Marmoretta oxoniensis* material from Kirtlington and the Isle of Skye. The premaxillae are paired and exhibited a deep posterolateral maxillary facet, the maxilla displayed the characteristic anterior process to articulate with the premaxilla, the frontal bones are fused and narrow with shallow hourglass *crista cranii*, and the dentaries are long and slender with subpleurodont teeth.

However, some differences suggest the material from the Guimarota beds belongs to another species, as previously suggested (Evans, 1991b; Evans & Milner, 1994). Notably, the anterior rim of the dorsal process in the maxilla curvature in New unnamed taxon 1 is more marked than in *M. oxoniensis*, where the rim rise smoothly instead (Evans, 1991b; Griffiths *et al.*, 2021). New unnamed taxon 1 does not exhibit a dorsally extended lacrimal facet in the maxilla as represented in the reconstruction based on the specimens from Kirtlington (fig. 2D; Evans, 1991b); and the maxillary

teeth do not display apicolingual curvature as observed in the specimen from the Isle of Skye (Griffiths *et al.*, 2021).

Furthermore, the dorsal process itself is not as medially inclined as observed in the Isle of Skye specimen NMS G1992.47.1a, although this has been suggested to be a postmortem deformation (Griffiths *et al.*, 2021). In the premaxilla, the characteristic maxillary facet exhibits margins more constricted than in *M. oxoniensis*, making the V-shaped facet narrower and acuter. Finally, the postfrontal facets do not meet posterodorsally as observed in the fused frontals from Kirtlington (Evans, 1991b). When the anterior ridge of the postfrontal facets meets the ventral surface of the bone, they form a blunt ventral vertex. This vertex can be located at the midpoint of the facet, as observed in the specimen from the Isle of Skye (Griffiths *et al.*, 2021) or in MG28741; but can also appear more anterior as in MG28742 and MG28743. Unfortunately, the position of the vertex could not be confirmed in frontals from Kirtlington based on figured specimen, but it seems to be also located at the midpoint (Evans, 1991b). It remains unclear if these different positions of the ventral vertex represent some intra specific variation or is due to a preservational bias.

2.3.4 Discussion

Although the Guimarota beds is known for its incredible diversity (Martin & Krebs, 2000), and to have yield extraordinary well-preserved specimens (Jäger *et al.*, 2020), the material used in this study relies mostly

on isolated, fragmented bones. On top of this, very few are complete, and even among those specimens, all are broken and were later glued back during their preparation at IPFUB in Berlin. Eventually, most of the specimens checked consisted of barely identifiable jaw fragments that could not even be distinguished between *Cteniogenys* and *Marmoretta*. For this reason, those were not included in this analysis and remain undetermined.

Cteniogenys from the Morrison Fm (Kimmeridgian–Tithonian, US) was originally referred as a potential lizard but with uncertainty (Gilmore, 1928), and later included within the informal squamate group "Eolacertilla" (Seiffert, 1973). However, new and more complete material from the Kirtlington Mammal beds (Bathonian, UK) allowed a better skull reconstruction, which highlighted a set of characters specific neither to squamates nor other basal lepidosauromorphs, but choristoderes instead despite being an early-branching form: (1) external nares confluent; (2) prefrontals elongated and meeting in the midline; (3) pineal foramen absent; (4) coarse striated dermal bones and complex skull sutures; preorbital skull elongated; (5) skull dorsoventrally flattened with inrolled maxilla; (6) skull akinetic, braincase and quadrate firmly attached to the dermatocranium; (7) diapsid, upper and lower temporal bars complete; (8) lacrimal small, meets both maxilla and palatine; (9) postorbital large, meets jugal and ectopterygoid ventrally; (10) vomer meets maxilla late rally, displacing the choana posteriorly; (11) vomer, palatine and pterygoid separated by a small palatal foramen; (12) pterygoid with broad tooth battery in adult and teeth

on the pterygoid flange; (13) ectopterygoid broadly overlaps pterygoid; (14) basipterygoid processes reduced, sphenoid sutured to pterygoid; (15) hemispherical occipital condyle; (16) paroccipital process of opisthotic sutured to pterygoid flange of quadrate; (17) pterygoid and opisthotic facets separated by a third facet, probably for a neomorph; (18) dentary elongate with double row of lateral foramina; (19) dentary symphysis medial and elongated in mature specimens; (20) implantation subthecodont; and (21) coronoid long and low (Evans, 1989). If the position of Choristedera within Diapsida remains uncertain, more recent findings confirmed the position of *Cteniogenys* as a basal member of this group (Matsumoto *et al.*, 2019; Dong *et al.*, 2020; Dudgeon *et al.*, 2023). Furthermore, the Guimarota material shared clear affinity with the one from the Middle Jurassic of England and the Late Jurassic of US, more than any other reptiles known from the Late Jurassic of Portugal and the Guimarota beds. No evidence found could challenge the original assignment of the specimens to *Cteniogenys*, neither that the genus could not be a choristodere.

As for *Marmoretta*, most of the material here described was previously mislabeled or misidentified. Evans was the first to report that some of the specimens (see below) described by Seiffert as *Cteniogenys* should actually be referred as *Marmoretta* (Evans, 1991b), but no further work on these specimens have been provided. Apart from Guimarota, *Marmoretta* is only known from the Middle Jurassic of UK and was originally identified as a stem-lepidosaur (Evans, 1991b; Griffiths *et al.*, 2021).

Notably, *Marmoretta* lacks some characters found in the crown-group lepidosaurs (notably, the presences of subolfactory processes of the frontals and the lateral conch of the quadrate), while displaying features absent in crown-group lepidosaurs (e. g. quadratojugal present; absence of a notch for the squamosal on the cephalic head of the quadrate; ventral exposure of the entry foramen for the internal carotid artery in the basisphenoid; absence of frontal tabs on the parietal; presence of a splenial; absence of a notochordal canal in adults) (Griffiths *et al.*, 2021). However, this has been challenged more recently (Simoes *et al.*, 2018; Sobral *et al.*, 2020) and no consensus on the position of *Marmoretta* within Lepidosauromorpha has been reached yet. Unfortunately, the specimens here described is too fragmentary and isolated to help in solving this controversy. Nevertheless, they clearly differ from all other reptile material known in the Guimarota beds, while presenting several affinities with the material from the Middle Jurassic of England. Therefore, we have found no evidence contradicting the original claim of Evans to refer these specimens to *Marmoretta* and as a stem-lepidosaur reptile.

2.3.4.1 Reassigning specimens to *Marmoretta*

Previous to this work, the only mention to *Marmoretta* from the Guimarota beds referred specimen MG27644, originally described as "*Cteniogenys reedi*" *sensu* Seiffert, 1973 (Gui. 345, fig. 5; Seiffert, 1973), as a misidentified premaxilla (Evans, 1991b). The revision of the material

nowadays stored in the Museu Geológico of Lisbon allowed us to identify at least 73 specimens and describe them as a new species.

On the 73 specimens here described (see Appendix D), only 27 were formerly identified as *Cteniogenys*, and two more to Choristodera (MG28764 and MG28785) in previous identifications in the MG catalogue; although *Cteniogenys* was the only choristodere species reported in the Guimarota beds. This concerns the three premaxillae, three maxillae, and 23 dentaries. As previously stated, the premaxillae of *Marmoretta* can be differentiated from *Cteniogenys* by the presence of the posterolateral maxillary facet and the absence of the small dorsal process indenting the anterior margin (Evans, 1990, 1991b).

Dentary fragments can be hard to differentiate due to the similarities between both taxa, explaining the original misidentification by Seiffert. However, the tooth implantation is subtly different between them: *Marmoretta* has a slightly weaker subpleurodont implantation (Evans, 1991b; Griffiths *et al.*, 2021), while it is rather subthecodont in *Cteniogenys* (Evans, 1989, 1990). The enamel covers all the teeth in *Marmoretta*, while only the tip of the crown in *Cteniogenys*, and is strongly apically striated in the later, while the striae are smoother in the former (Evans, 1990, 1991b; Griffiths *et al.*, 2021). If both dentaries display an opened Meckelian canal, in *Marmoretta* is less opened in the anterior section, and less regular (Evans, 1991b; Griffiths *et al.*, 2021). Another difference in the dentaries

concerns the labial ornamentation, that is much more marked among *Cteniogenys* specimens (Evans, 1990). Finally, when complete in mature specimens, the dentaries in New unnamed taxon 1 are much shorter and less robust than the dentaries observed in *Cteniogenys* aff. *C. antiquus* from the Guimarota beds.

Similarly, maxillary fragments can be hard to differentiate between both taxa due to their similarities. Nevertheless, the tooth implantation and enamel also differ in the maxillae (Evans, 1990, 1991b). The deep posterior groove observed in *Marmoretta* could not be confirmed in *Cteniogenys* aff. *C. antiquus* from the Guimarota beds. They also differ by the labial surface texture, the maxillae in *Cteniogenys* displaying similar ornamentation than the dentary, while they are rather smooth in *Marmoretta* (Evans, 1990, 1991b; Griffiths *et al.*, 2021). The main difference in complete specimens regards the big anterior process, absent in *Cteniogenys*, and the flabellate dorsal process, which is rather triangular or trapezoidal in *Marmoretta* (Evans, 1990, 1991b).

It is worth noticing that the four fused frontals were all identified as 'Anura' but labelled as albanerpetontid frontals, while they clearly do not display the characteristic bell-shaped outline and the flabellate, bulbous internasal process observed and described in the other albanerpetontid material from Guimarota (Wiechmann, 2003; Guillaume *et al.*, 2023b). Furthermore, these frontals differ in any frontal morphology currently

known in albanerpetontids (Gardner, 2002; Carrano *et al.*, 2022; Guillaume *et al.*, 2023b), or usually observed in frogs. Instead, by being fused with lateral margins embayed for the orbits, anteroposteriorly convex, and exhibiting two marked ventral *crista cranii*, they strongly resemble the ones described in *M. oxoniensisi* (Evans, 1991b; Griffiths *et al.*, 2021). Two more maxillae (MG28751 and MG28757) were also identified as albanerpetontid; but, here again, they are completely different to equivalent material known and described from the Guimarota beds (see Section 3.2).

Three dentaries (MG28811, MG28812, and MG28861) were previously assigned to undetermined Reptilia, but they share the characteristics described above. One dentary was referred to "thecodont" (MG28854), but its anatomy closer matches the one observed in the other New unnamed taxon 1 dentaries, rather than other potential thecodont jaw-bearer known from the Guimarota assemblage (crocodylomorphs, dinosaurs, mammals). The remaining 34 specimens (eight maxillae and 26 dentaries) were assigned to Squamata, but their morphology fits better the one described for New unnamed taxon 1 than in any other squamate species described from the diverse Guimarota assemblage (Seiffert, 1973; Broschinski, 2000). We acknowledge Seiffert and subsequent researchers possibly identify these bones as different from other reptiles in the Guimarota assemblage but were not able to properly identify them.

Nevertheless, this work mostly focused on some cranial bones from *Marmoretta* and *Cteniogenys*, while the Guimarota yields thousands of small diapsid fossils (Martin & Krebs, 2000). Previous works already highlighted one of the main Jurassic diversity for this group (Seiffert, 1973; Broschinski, 2000; Caldwell *et al.*, 2015), but most of the remains are still unidentified or assigned only to higher taxonomic ranks. As exemplified by this work, it would not be surprising that more elements could be assigned to either *Cteniogenys* aff. *C. antiquus*, New unnamed taxon 1, or another diapsid taxon with a deeper revision of the material.

2.3.4.2 Paleobiogeographical implications

During the Late Jurassic, the Iberian Plate was one of the largest islands of the European archipelago system, surrounded by warm, shallow epicontinental seas, with several transgressive/regressive transitions (Moore *et al.*, 1992; Martinius & Gowland, 2011; Myers *et al.*, 2012). At the cross-road between the Tethys and the proto-Atlantic oceans, the Iberian Plate was both connected to North America (Dercourt *et al.*, 2000; Scotese, 2014; Brikiatis, 2016) and close to northwestern African shore (Gheerbrant & Rage, 2006; Haddoumi *et al.*, 2016). Potential continental bridges in the Late Jurassic could allow faunal interchanges with North America (Evans, 1998a, 2003; Mateus, 2006; Tennant *et al.*, 2017; Lasseron *et al.*, 2020; Allain *et al.*, 2022). Meanwhile, the Tethys was rather a permeable barrier (Goodwin *et al.*, 1999), and therefore could allow dispersal events between Laurasia and Gondwana through ephemeral land connections during the

Jurassic/Cretaceous transition (Haddoumi *et al.*, 2016; Lasseron *et al.*, 2020; Allain *et al.*, 2022).

As a primitive choristodere, *Cteniogenys* ranges from the Bathonian of UK (Evans, 1989, 1990, 1991a; Panciroli *et al.*, 2020) to the Berriasian of France (Allain *et al.*, 2022), with occurrences in the Upper Jurassic Morrisson Formation in North America (Gilmore, 1928; Chure & Evans, 1998; Foster & Trujillo, 2000; Carrano & Velez-Juarbe, 2006), the Upper Jurassic Alcobaça and Lourinhã formations (Seiffert, 1973; Guillaume *et al.*, 2023a), both dated from the Kimmeridgian-Tithonian, and the Tithonian of France (Vullo *et al.*, 2014). More material has been attributed to the genus in the Upper Cretaceous of Alberta (Gao & Fox, 1998), despite the important chronological gap with Jurassic species. Notably, the bones used for this identification are extremely fragmented (ARDG, pers. obs., 2023), and have since been regarded as not sufficiently diagnostic to reach this identification and might represent another genus (Gao & Brinkman, 2005; Matsumoto *et al.*, 2009; Matsumoto & Evans, 2010). The material is now considered as an undetermined choristodere (Matsumoto *et al.*, 2009).

The fossil record of *Cteniogenys* further supports faunal interchanges between Europe and North America during the final stages of the Late Jurassic, where the Iberian Plate could have played a connecting role between both realms. Furthermore, fragmentated material from the Bathonian and the Berriasian of Morrocco was attributed to Choristodera,

but the authors highlighted similarities with *Cteniogenys* (Haddoumi *et al.*, 2016; Lasseron *et al.*, 2020). If this identification is confirmed, not only it would extend the geographic range of the genus, but also give more support for faunal interchanges between northwestern Africa, North America, and Europe via the Iberian Plate during the J/K transition.

While choristoderes were emerging and dispersing in the Late Jurassic, "lizards" were going to major changes. Based on their fossil record and molecular clock analyses, lepidosauromorph diapsids emerged in the Permian or the Early Triassic (Evans, 1993, 2003; Evans & Jones, 2010; Jones *et al.*, 2013; Simões *et al.*, 2018; Sobral *et al.*, 2020), before that lepidosaurs diversifies into squamates and rhynchocephalians during the Triassic (Evans & Jones, 2010; Herrera-Flores *et al.*, 2022a; Bolet *et al.*, 2022). The later remained dominant and more abundant in the fossil assemblages through all the Triassic and the Middle Jurassic before declining in the Lower Cretaceous, while the former started radiating in the Middle to Upper Jurassic (Estes, 1983; Evans, 1993, 1998a, 2003; Conrad, 2008; Evans & Jones, 2010; Gauthier *et al.*, 2012; Caldwell *et al.*, 2015; Simões *et al.*, 2018; Herrera-Flores *et al.*, 2022a; Bolet *et al.*, 2022; Brownstein *et al.*, 2022).

Although Early Cretaceous assemblages may yield some archaic forms (Evans, 1998a), all stem-lepidosaur seem to have become extinct in the Triassic (Evans, 2003; Gauthier *et al.*, 2012; Schoch & Sues, 2018; Simões

et al., 2018; Sobral *et al.*, 2020; Bolet *et al.*, 2022). If recent analyses placing *M. oxoniensis* as a stem-lepidosaur are confirmed (Griffiths *et al.*, 2021; Bolet *et al.*, 2022), the new material would extend the temporal range of this relict lineage up to the Kimmeridgian. Nevertheless, its absence from the coeval Lourinhã Formation (Guillaume *et al.*, 2023a), but also from other vertebrate assemblages in North America or Africa (Aberhan *et al.*, 2002; Carrano & Velez-Juarbe, 2006; Lasseron *et al.*, 2020), would support an European endemism of stem-lepidosaurs by the end of the Late Jurassic during in their final decline.

2.3.4.3 Paleoecology of *Cteniogenys* and *Marmoretta*

The structure of the skull in *Cteniogenys* and its postcranial skeleton display anatomical features usually associated with aquatic reptiles (Evans, 1991a), and younger choristoderes could be associated to an aquatic to subaquatic lifestyle in freshwater environments (Matsumoto & Evans, 2010; Matsumoto *et al.*, 2022a; Wang *et al.*, 2023). Although no postcranial material is yet known for *Marmoretta*, its skull morphology reflects as well adaptions for an aquatic to amphibious lifestyle, or a burrowing one, to avoid competition with more terrestrial "lizards" that were rising in the Middle Jurassic (Evans, 1991b; Evans & Milner, 1994). The weaker tooth implantation compared to *Cteniogenys* would suggest a different diet (Evans, 1991b), although *Marmoretta* skull suggests that it could display comparatively strong bit-force for a small diapsid (Evans, 1991b; King, 1996; Pritchard *et al.*, 2018; Griffiths *et al.*, 2021).

Quarry 9, from where *C. antiquus* has been first described, has been interpreted as a low-energy depositional environment, such as a pond or oxbow lake (Carrano & Velez-Juarbe, 2006), which fits the paleoenvironmental of one locality of the Lourinhã Formation where new putative material has been reported (Guillaume *et al.*, 2023a). Meanwhile, the Kirtlington Mammal Bed has been interpreted as a shallow swampy coastal region with lagoons and freshwater lakes, similar to moder-days Everglades in Florida, dominated by aquatic and amphibious taxa (McKerrow *et al.*, 1969; Freeman, 1976, 1979; Sellwood, 1978; Palmer, 1979; Evans, 1991a,b), which fits the interpretations for other localities in the Lourinhã Formation (Guillaume *et al.*, 2023a), but also with a mangrove-like environment in which the Guimarota assemblage is thought to have deposited (Gloy, 2000; Martin, 2000a).

The presence of *Cteniogenys* and *Marmoretta* material in the Guimarota beds and Kirtlington Mammal Bed support an important freshwater component in both ecosystems. However, the absence of *Marmoretta* remains in other Portuguese and North American localities where *Cteniogenys* remains has been reported (Carrano & Velez-Juarbe, 2006; Guillaume *et al.*, 2023a) could hint true ecological differences between Guimarota/Kirtlington Mammal beds and localities from the coeval Morrison and Lourinhã Formation.

Furthermore, choristoderes seem to be less diverse and rarer in environments where crocodiles thrive (Matsumoto & Evans, 2010), to which they are often considered as eco-analogues (Fox, 1968; Erickson, 1987; Evans & Hecht, 1993; Matsumoto & Evans, 2010; Matsumoto *et al.*, 2022a). Such partitioning could be explained by climatic, depositional, and other abiotic factors; but it has also been suggested it could be the result of some preferences or competition for ecological niches between choristoderes and aquatic crocodiles and other freshwater animals of similar size (Matsumoto & Evans, 2010).

This pattern is congruent with the faunal composition of the Guimarota assemblage, in which crocodylomorphs are extremely diverse and common (Schwarz, 2002; Schwarz & Fechner, 2004, 2008; Schwarz & Salisbury, 2005; Schwarz *et al.*, 2017; Guillaume *et al.*, 2020), whereas choristodere material is much rarer. Indeed, because of its small size—reconstructions suggest a total length of 30cm (Evans, 1991a)—, *Cteniogenys* was unlikely competing with the giant marine predator *Machimosaurus*; nor with generalist feeders, such as goniopholids, and other macrocarnivorous terrestrial crocodylomorphs known from the Guimarota beds and the Lourinhã Fm (Schwarz, 2002; Guillaume *et al.*, 2020; Puértolas-Pascual & Mateus, 2020; López-Rojas *et al.*, 2024).

On the other hand, *Cteniogenys* was from a similar size-range than bernissartiids (Sweetman, 2016; Martin *et al.*, 2020), atoposaurids

(Schwarz & Salisbury, 2005; Schwarz *et al.*, 2017) and other small crocodylomorphs *Lusitanisuchus* and *Lisboasaurus* (Schwarz & Fechner, 2004, 2008) reported in the Late Jurassic of Portugal (Guillaume *et al.*, 2020). The conical teeth observed in *Cteniogenys* suggest it was most not sharing with bernissartiids the durophagous diet implied by their molariform teeth (Guillaume *et al.*, 2020). However, *Cteniogenys* could have competed with atoposaurids and other small crocodylomorphs, whose diet was based on small arthropods (insects, crustaceans, soft-bodied) and occasional small vertebrates such as mammals and amphibians (Guillaume *et al.*, 2020).

2.3.5 Conclusion

Revision of material from the well-known Late Jurassic Guimarota beds from Portugal provided support for a *Cteniogenys* taxon non-conspecific with the ones described from the Morrisson Formation and the Kirtlington Mammal Bed, although the clade would require a revision to properly describe its species. It further supports faunal interchanges between North America, Northwestern Africa, and Europe through the Iberian Plate during the Jurassic/Cretaceous transition. Furthermore, specimens from Guimarota formerly attributed to *Cteniogenys* and other herpetofaunal clades were redescribed and gave support for a new stem-lepidosaur species. This new species further extends the temporal range of this relict lineage to the very end of the Jurassic period, at a time where other lizards were going through a major faunal shift. It also highlights either a vestigial

European endemism for stem-lepidosaurs, or hints toward true ecological differences with other localities in Europe and North America.

3 NEW MESOZOIC ALBANERPETONTIDAE FROM THE IBERIAN PENINSULA

3.1 Chapter 4: Plasticity in the morphology of the fused frontals of Albanerpetontidae (Lissamphibia; Allocaudata)

Note: The following work is referring the albanerpetontid material from the Late Jurassic of Portugal (Lourinhã Formation and Guimarota beds) to aff. *Celtedens* sp. However, subsequent works presented later in this thesis has resulted in the erection of a new taxon for this material.

Paper published in *Historical Biology* (Journal impact factor for 2022: 1.4; CiteScore: 3.5; SJR: 0.551; H-index: 40)
Alexandre R. D. Guillaume, Carlos Natário, Octávio Mateus & Miguel Moreno-Azanza (2023) Plasticity in the morphology of the fused frontals of Albanerpetontidae (Lissamphibia; Allocaudata), Historical Biology, 35:4, 537-554
The article is reproduced with the permission of the editor and is subject to the copyright imposed by the publisher. Available online:
https://doi.org/10.1080/08912963.2022.2054712

Abstract

Albanerpetontidae form an enigmatic extinct group of lissamphibians, ranging from the early Bathonian to the early Pleistocene. The Upper

3.1 CHAPTER 4: PLASTICITY OF ALBANERPETONTID FRONTALS

Jurassic outcrops of Portugal yield a large collection of material, suitable for addressing the intraspecific variation in and diagnostic potential of the characteristic fused frontals. We revise 58 specimens from the Guimarota beds of the Kimmeridgian Alcobaça Formation and describe 62 new frontal bones from the Kimmeridgian – Tithonian Lourinhã Formation. Smaller specimens exhibit a vermicular dorsal ornamentation, while it is polygonal in larger specimens and other albanerpetontids. Compared to small specimens, larger specimens display: (1) larger ventrolateral crests extending posteriorly after the parietal margin; (2) a relatively shorter internasal process; (3) a frontal width across posterior edges relatively smaller; and (4) a ventromedian crest less pronounced. Morphometric analyses suggest a single species with different ontogenetic stages. Specimens are attributed to aff. *Celtedens* sp., based on a bell-shaped outline with a curved orbital margin (although variable in Portuguese specimens), and a flabellate, bulbous-shaped internasal process. The species is more similar to *C. megacephalus* than *C. ibericus*, but its phylogenetic position comprises an unresolved trichotomy. Our results show that intraspecific variation and homoplasy render the fused frontal non-diagnostic below the generic level.

Key words: *Celtedens*, Guimarota beds, intraspecific variation, Lourinhã Formation, morphometry, phylogeny.

3.1 CHAPTER 4: PLASTICITY OF ALBANERPETONTID FRONTALS

3.1.1 Introduction

The Albanerpetontidae Fox and Naylor, 1982 form an extinct group of highly derived small amphibians characterized by: (1) fused frontals with polygonal dorsal ornamentation; (2) a 'mortise and tenon' interdentary joint; (3) distinctive non-pedicellate teeth with chisel-shaped, tricuspid crowns; and (4) two modified cervical vertebrae forming a tripartite facet similar to the atlas-axis complex in mammals (Gardner, 2001; Gardner & Böhme, 2008; Sweetman & Gardner, 2013; Matsumoto & Evans, 2018; Daza *et al.*, 2020).

Although they are considered as a distinct lineage (Fox & Naylor, 1982; Gardner, 2001), their position within crown Lissamphibia is still debated (Anderson, 2008; Maddin *et al.*, 2013; Matsumoto & Evans, 2018; Marjanović & Laurin, 2019; Daza *et al.*, 2020). The albanerpetontid fossil record extends from the early Bathonian of France (Seiffert, 1969), England (Evans & Milner, 1994), and Morocco (Haddoumi *et al.*, 2016), to the early Pleistocene of Italy (Villa *et al.*, 2018).

They were predominant in Laurasia (Gardner & Böhme, 2008), although the material is scarce in Asia (Skutschas, 2007; Matsumoto & Evans, 2018; Daza *et al.*, 2020), and specimens from Morocco are the only Gondwanian occurrences (Gardner *et al.*, 2003; Haddoumi *et al.*, 2016; Lasseron *et al.*, 2020).

3.1 CHAPTER 4: PLASTICITY OF ALBANERPETONTID FRONTALS

The family Albanerpetontidae currently comprises six genera: the type genus *Albanerpeton* Estes and Hoffstetter, 1976 (Early Cretaceous–Pleistocene; Central Asia, Europe and North America); *Anoualerpeton* Gardner *et al.*, 2003 (Bathonian–Berriasian; England and Morocco); *Celtedens* McGowan & Evans, 1995 (Kimmeridgian–Albian; Europe); *Shirerpeton* Matsumoto and Evans, 2018 (Barremian; Japan); *Wesserpeton* Sweetman and Gardner, 2013 (Barremian; England); and *Yaksha* Daza *et al.*, 2020 (Cenomanian, Myanmar).

However, the genus *Albanerpeton* as currently defined has been shown to be paraphyletic, although the authors did not review its taxonomy accordingly (Matsumoto & Evans, 2018; Daza *et al.*, 2020). Nevertheless, only Cenozoic species are now regarded as *Albanerpeton sensu stricto* (Daza *et al.*, 2020).

The albanerpetontids are small animals and their fossil record is fragmentary and scarce, most are generally recovered as isolated bones by sieving sediments, with few exceptions. Articulated specimens with soft tissues preserved have been recovered from the Barremian Lagerstätte of Las Hoyas, in Spain (McGowan & Evans, 1995; McGowan, 2002; Evans, 2016), the Albian Pietraroia bone bed in Italy (McGowan, 2002), and from the early Cenomanian amber deposits of Myanmar, in which a complete articulated skull, a partial articulated post-cranial skeleton, and one juvenile specimen have been recorded (Daza *et al.*, 2020). A handful of

three-dimensional skulls in association have also been reported, from the Barremian of Japan (Matsumoto & Evans, 2018) and the Pliocene of Hungary (Maddin *et al.*, 2013).

Therefore, albanerpetontid taxonomy is mostly based on isolated but highly diagnostic bones (Gardner, 2000a, 2001; Gardner *et al.*, 2003; Gardner & Böhme, 2008; Sweetman & Gardner, 2013), among which fused frontals yield a relatively large set of diagnostic characters. The frontal bones have been thus considered to be key to both identifying and diagnosing taxa at the generic and specific level (McGowan, 1998a; Gardner, 2000a). Most of the characters currently considered to be diagnostic for Albanerpetontidae are confined to the skull, and the post-cranial skeleton is still poorly documented (Maddin *et al.*, 2013).

Previous phylogenetic analyses used seven characters relating to the frontal bones, of which: (1) an approximately triangular dorsal or ventral outline of the fused frontal has been considered as a synapomorphy of the clade (*Wesserpeton* + *Yaksha* + *Shirerpeton* + *Albanerpeton* s.l.); (2) a moderate ratio of midline length of fused frontals vs. width across posterior edge of bone, between lateral edges of ventrolateral crests, in large specimens has been considered as a synapomorphy of the clade *Albanerpeton* s.s.; (3) a bulbous dorsal or ventral outline of internasal process on frontals has been considered as a synapomorphy of *Celtedens*; (4) a long internasal process on fused frontals has been considered as a

synapomorphy of the 'robust-snouted' clade (*Albanerpeton nexuosum* Estes, 1981 + *Albanerpeton* s.s.), but is also recovered as an autapomorphy in *Anoualerpeton priscum* Gardner *et al.*, 2003; (5) narrow and triangular ventrolateral crests on large, fused frontals in transverse view, with ventral face flat to shallowly concave was independently acquired in *An. priscum*, *Albanerpeton galaktion* Fox and Naylor, 1982, and *A. nexuosum*; (6) wide and triangular ventrolateral crests on large, fused frontals in transverse view, with ventral face deeply concave has been independently acquired in *Albanerpeton inexpectatum* Estes and Hoffstetter, 1976, and *Albanerpeton pannonicum* Venczel and Gardner, 2005; and (7) the presence of a flattened ventromedial keel extending along posterior two-thirds of fused frontals has been independently acquired in *A. pannonicum* and *Shirerpeton isajii* Matsumoto and Evans, 2018 (Gardner, 2002; Gardner *et al.*, 2003; Venczel & Gardner, 2005; Sweetman & Gardner, 2013; Matsumoto & Evans, 2018; Daza *et al.*, 2020).

The Portuguese albanerpetontid record in the Upper Jurassic is mainly known and represented by the Guimarota beds assemblage, from the Kimmeridgian Alcobaça Formation (Schudack, 2000a). Thousands of specimens were recovered, making albanerpetontids as one of the commonest elements of the assemblage. Among these, more than 40 frontals were counted and attributed to a single new species of the genus *Celtedens* (Wiechmann, 2000, 2003).

Furthermore, the Lourinhã Formation, of late Kimmeridgian-Tithonian age (Mateus *et al.*, 2017), also yields two localities: Porto Dinheiro (often misspelled Porto Pinheiro or Portinheiro), where hundreds of specimens were reported, including 16 frontals attributed to the same Alcobaça Fm *Celtedens* species (Wiechmann, 2003); and Porto das Barcas, where scarce material was referred to an undetermined albanerpetontid taxon, the lack of frontals and premaxillae precluding determination of its conspecificity or otherwise with other Portuguese material (Wiechmann, 2003).

The Guimarota beds and the Lourinhã Fm have important similarities concerning their faunal associations (Martin, 2001; Hahn & Hahn, 2001b; Guillaume *et al.*, 2020). Nevertheless, there is both a geographical (70 km) and, more importantly, a temporal gap (up to 5 million years) between both ecosystems. Furthermore, palaeoenvironmental reconstructions of the Guimarota beds suggest a mangrove-like environment (Gloy, 2000; Martin, 2000a), whereas the Lourinhã Fm has been interpreted as a fluvial environment with marked seasonality (Martinius & Gowland, 2011; Taylor *et al.*, 2014; Gowland *et al.*, 2017; Mateus *et al.*, 2017).

Thus, the presence of two different species, either successive species of a single lineage, or two contemporary species but niche-segregated, needs to be considered; especially when different but coeval species of albanerpetontids have been collected in different ages from the same localities (Gardner, 2000b) or, in contrast, a single species occurred

through a long period of time (Gardner *et al.*, 2021). Being *a priori* diagnostic and one of the most abundant identifiable cranial elements found in Lourinhã and Guimarota collections, fused frontal bones are the potentially optimal specimens to test for the presence or absence of multiple taxa.

We here provide the description of new frontal material, although no specimen is complete. Intraspecific variation was examined to characterize the plasticity in the frontal bones, using linear morphometric analysis together with anatomical comparison. We are proposing an extended list of characters coded for all species and relevant specimens published.

3.1.2 Geological setting

The vertebrate microfossil assemblage (later referred as VMA) localities were sampled at outcrops at the top of cliffs in the municipality of Lourinhã, namely from South to North: Valmitão VMA, Zimbral VMA, and Porto das Barcas VMA (**Figure 3.1.1**). They occur within the Lourinhã Formation in the Lusitanian Basin, the largest sedimentary basin in Portugal (Wilson *et al.*, 1989; Alves *et al.*, 2003). The Lourinhã Fm ranges from late Kimmeridgian to late Tithonian in age and lies between the Consolação unit and the Porto da Calada Formation (Taylor *et al.*, 2014; Mateus *et al.*, 2017).

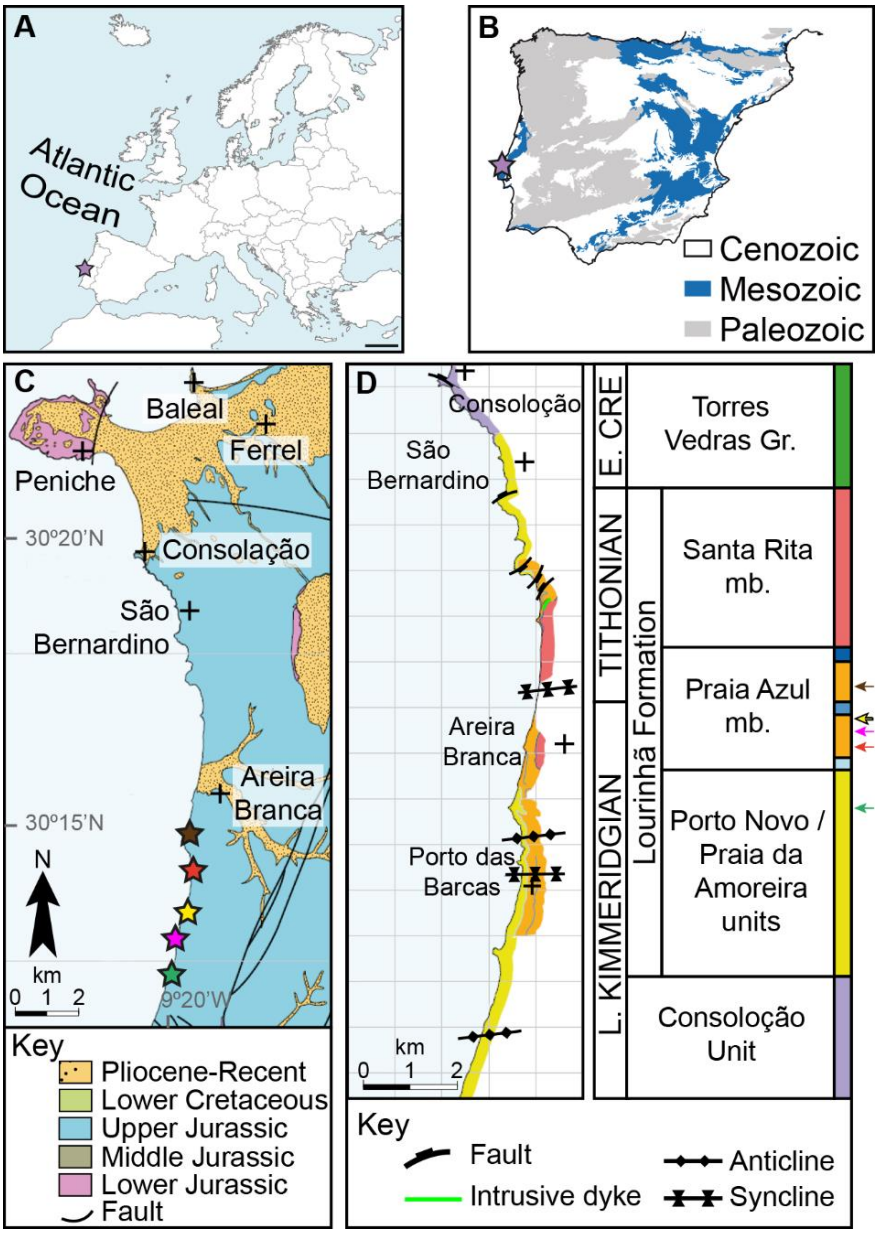

Figure 3.1.1: Geographical and geological context of the new Albanerpetontidae occurrences from the Lourinhã formation. **A**, Europe map modified from Erin Dill, scale represents 400 km. **B**, geological sketch of the Iberian Peninsula, showing the location of the study area (purple star). **C**, map of the onshore part of the Consolação subbasin south of Peniche (modified from Taylor *et al.*, 2014). The green star indicates the location of the Valmitão VMA, the pink star indicates the location of Porto Dinheiro VMA, the yellow star indicates the location of Zimbral VMA, the red star indicates the location of Port das Barcas VMA, the brown star indicates the location of Peralta VMA. **D**, north–south mapping of the main units in the area of study and their corresponding lithostratigraphic framework indicated by arrows (modified from Taylor *et al.*, 2014, based on Mateus *et al.*, 2017). Arrow colours correspond to star colours.

Its dominant continental deposits consist of sandy channel-fills and muddy floodplain deposits (Martinius & Gowland, 2011; Taylor *et al.*, 2014; Gowland *et al.*, 2017), and it is comprised of three members: (1) the Kimmeridgian Porto Novo/Praia da Amoreira unit; (2) the late Kimmeridgian to early Tithonian Praia Azul member; and (3) the early Tithonian Santa Rita member (Taylor *et al.*, 2014; Mateus *et al.*, 2017).

The Valmitão VMA is located in the upper half of the Porto Novo/Praia da Amoreira unit and is distributed within a three-meter-thick mudstone layer with occasional intercalations of sandstones. Porto das Barcas, Porto Dinheiro, and Zimbral VMAs all belong to the Praia Azul member, the latter being younger and located on top of the Porto Dinheiro sequence previously sampled by the expedition of Institute of Geological Sciences, Freie Universität Berlin (IPFUB) in the 1970s. The outcrops are, respectively, distributed within a metric greyish mudstone layer, between the first and second sandy bioclastic limestones characterizing the member.

Although IPFUB sampled a locality also named 'Porto das Barcas', which provided some vertebrate microfossils (Hahn & Hahn, 2001b; Wiechmann, 2003), no data nor coordinates could be found to help to locate it (T. Martin, pers. comm., 2021). Considering the extent of the Praia de Porto das Barcas (almost 2 km), and the extent of Jurassic exposures in the area, we cannot confirm we have sampled the same locality as the previous team. Therefore, we consider that the locality sampled by our team and

referred as Porto das Barcas is not the same as the one sampled by IPFUB. Peralta VMA is located in the Praia Azul member, between the second and the third sandy bioclastic limestones, and so is younger than Zimbral and Porto das Barcas.

The exact age of the Guimarota beds had long been a matter of debate (Schudack, 2000a), although they have consistently been considered as part of the Alcobaça Formation, which has been dated to the middle Kimmeridgian (Ribeiro *et al.*, 1979; Mateus *et al.*, 2017). Based on ammonites, charophytes, ostracods, pollens, and lithostratigraphic correlation, the age of the Guimarota beds is now restricted to the Kimmeridgian (Ribeiro *et al.*, 1979; Leinfelder & Wilson, 1989; Schudack *et al.*, 1998; Schudack, 2000a). Throughout the mining, around 20 m of the beds have been exposed (Helmdach, 1971; Schudack, 2000b). The outcrop consists of two coal seams of similar structure, with intercalation of lignitic marls occasionally rich in bivalve shells, separated by a single layer of limestone, around 5 m thick (Schudack, 2000b).

Due to the mining conditions in Guimarota, the stratigraphic position of the specimens is uncertain, limiting the precise identification of the sedimentary environment where fossils were found (Gloy, 2000; Krebs, 2000b). Based on its similarity to other brown coal deposits and its geological setting, Guimarota has been regarded as a terrestrial to lagoonal

environment similar to modern mangroves, with occasional freshwater influx and saltwater flooding (Gloy, 2000; Martin, 2000a).

3.1.3 Material and Methods

This study is based on a 700 kg sample of matrix collected from Valmitão, Zimbral, and Porto das Barcas (Lourinhã municipality, Portugal) during field campaigns between 2016 and 2019. One of us (CN) independently collected matrix on a regular basis over a period of several years, using bags of 5 kg each to an estimated total of between 100 and 150 kg, from two other localities: Porto Dinheiro and Peralta. The matrix was dried, then disaggregated in water with hydrogen peroxide (H_2O_2, final solution at 0.5%). The samples were screen-washed through a sieving table comprised of three levels of mesh (2 mm, 1 mm and 0.5 mm). The residues were then picked under stereomicroscopes. No significant differences in the degree of fracturing and preservation were observed between both samplings.

In total, around 20,000 microfossils from the three VMAs were recovered. Most of them consist of invertebrate remains, such as ostracods, gastropods, bivalve shells fragments, and charophyte thali. However, the vertebrate microfossils include ray-finned fish scales and teeth, chondrichthyan teeth, fragmentary material from lepidosaurs, amphibians and unidentified archosauriforms, crocodylomorph teeth and osteoderms, dinosaur and pterosaur teeth, tetrapod vertebral arches and long bone

fragments, and eggshell fragments. Two hundred and eighty-five fossils are attributed to Albanerpetontidae, although cataloguing is still ongoing.

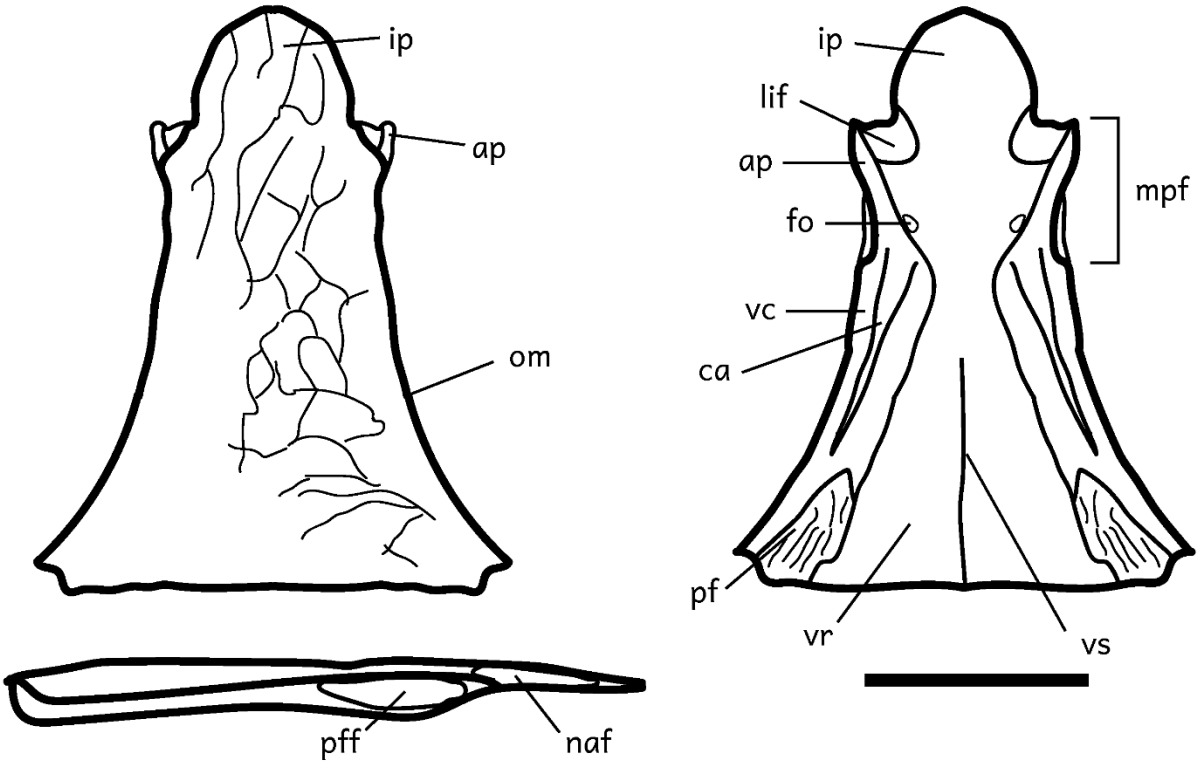

Figure 3.1.2: Main anatomical features of albanerpetontid frontal bones, based on reconstruction from specimen ML2738, in dorsal, ventral, and lateral views. **ap**, anterolateral process; **ca**, canal; **fo**, foramen; **ip**, internasal process; **lif**, lateroventral internasal facet; **mpf**, middle part of the frontal; **naf**, nasal facet; **om**, orbital margin; **pf**, parietal facet; **pff**, prefrontal facet; **vc**, ventrolateral crest; **vr**, ventral roof; **vs**, ventromedian suture. Scale bar represents 1 mm.

The present study focuses on 34 frontals, none of which is complete, recovered from the 1 mm and 0.5 mm residue fractions (see **Figure 3.1.2** for a composite reconstruction of the frontals based on ML2738). The specimens are housed in the Museu da Lourinhã (ML2738 to ML2749 and ML2751 to ML2772). Twenty-eight additional frontals (among 419 albanerpetontid fossil remains) from the private collection of one of us (CN)

are now accessioned at the NOVA School of Science and Technology (FCT/UNL-CN00016 to FCT/UNL-CN00029, FCT/UNL-CN00100 to FCT/UNL-CN00108, and FCT/UNL-CN00398 to FCT/UNL-CN00402).

Fifty-eight additional specimens from the Alcobaça Fm have been included. They all come from the excavations of the Guimarota beds by IPFUB. They were previously studied and presented (Wiechmann, 2000), and resulted in an unpublished PhD thesis where they were informally assigned to a new species, '*Celtedens guimarotae*' (Wiechmann, 2003). However, these specimens are here formally published for the first time. The specimen numbers attributed by IPFUB during the excavations were changed when the specimens were returned to the Museu Geológico of Lisbon, where they are now housed, following the agreements signed at the time of the excavations. Therefore, they are here published with their final accession numbers.

Some of these specimens were already coated in gold (MG28502, MG28532, and MG28694) and MG28520 had fragments glued with Bostik Blu Tack™ by the previous authors. In some cases, the specimen numbers from MG may refer to several fragments, hence a total number of 58 frontals. Two specimens, MG28426 and MG28427, were assembled from multiple fragments of the same individual for imaging and measurements.

Table 3.1.1: Measurements (in mm) of the best-preserved specimens. **FML**, frontal length at the midline; **FL**, frontal length at the midline; **FW**, frontal width across posterior edges; **FIW**, frontal inner width between ventrolateral crests, across posterior edges of the frontal roof; **INL**, internasal length at the midline; **INW**, internasal width at the base; **SW**, slot width between the posterior slots for the prefrontal; **IVCW**, interventrolateral crests width; **OML**, Orbital margin length; **VCAW**, ventrolateral crest anterior width, behind prefrontal facets; **VCPW**, ventrolateral crest posterior width, before parietal facets; **CPE**, curvature at the posterior part of the edge (in degrees); **VCC**, ventrolateral crest curvature (in degrees).

Specimen	Locality	FML	FL	FW	FIW	INL	INW	SW	OML	IVCW	VCAW	VCPW	CPE	VCC
ML2738	Lourinhã	2.6	2.56	2.01	1.37	0.47	0.65	0.79	1.31	0.31	0.34	0.26	23	129.5
ML2739	Lourinhã			2.64	1.93			1.32	2.16	0.43	0.64	0.36	11.8	125.2
ML2741	Lourinhã					0.89	0.97	1.12		0.26	0.46			139.5
FCT/UNL-CN00016	Lourinhã					0.57	0.48	0.76		0.23	0.33			134.1
FCT/UNL-CN00018	Lourinhã					0.64	0.55	0.83		0.25	0.37			136
MG28426	Guimarota	5.85	6.35	4.35	1.52	0.76	1.42	2.16	3.52	0.31	0.89	0.84	18.6	130.6
MG28427	Guimarota		5.83	4.81	2.34	0.94	1.68	2.33	3.41	0.28	1.25	0.85	17	133.5
MG28473	Guimarota	3.99	4.07	2.31	1.24		0.71	1.24	2.02	0.31	0.6	0.41	11.7	142.1
MG28502	Guimarota	5.69	6.03	3.71	1.38	1.24	1.17	1.92	2.67		1.02	0.84	17.8	138.8
MG28520	Guimarota	4.76	4.9	3.48	1.37	1.19	1.68	1.34	2.61		0.8	0.66	14.9	
MG28521	Guimarota	5.76				0.85	1.5	1.94		0.48	0.76	0.61		149.4
MG28532	Guimarota	3.88				0.86	1.04	1.28		0.25	0.47	0.34	13.4	151
MG28543	Guimarota	3.27		2.02	1.25	0.65	0.74	1.23			0.53	0.26		
MG28694	Guimarota					1.05	1.27	1.89			0.91			
MG28733	Guimarota			1.6	1.1			1.05	1.3	0.27	0.44	0.26	12.7	135
MG28539	Guimarota			2.17	1.03			1.07	1.77	0.28	0.41	0.32	17.9	148.1
MG28692	Guimarota			2.46	1.52				1.65		0.56	0.33	21.9	

Specimens from the Lourinhã Fm were photographed using a Canon Model RP reflex camera with a Canon 75-300 mm objective. The objective was coupled with a Nikon Microscope objective APOx10, mounted with an adapter ring. The specimens were laid on a vertical mounting setup with a MJKZZ stacking rail. The set up was remotely controlled with Stackrail 1.7, which allows automated capture for stacking (at least 70 steps for each specimen, 40µm/slice). The RAW image files were converted to TIFF and homogenized using Digital Photo Professional 4. The stacking process was performed with Zerene Stacker 1.4. The resulting images were then fine-tuned, cleaned, and processed for final rendering. The specimens from the Alcobaça Fm were photographed using a DinoLite AM7013MZT, using Dino software. The best-preserved specimens were measured with ImageJ (Rasband, 2003) (see **Table 3.1.1** and **Figure 3.1.3**).

3.1.3.1 Morphometric analysis

Measurements from 17 specimens (5 from the Lourinhã Fm, 12 from the Alcobaça Fm) presented in **Table 3.1.1** were used to perform linear morphometrics, with association of principal component analysis (PCA) and linear discriminant analysis (LDA). A first PCA was performed with all variables. However, this model appeared slightly underfitted, based on the broken stick model (Jackson, 1993), as the second axis explains less variation than expected.

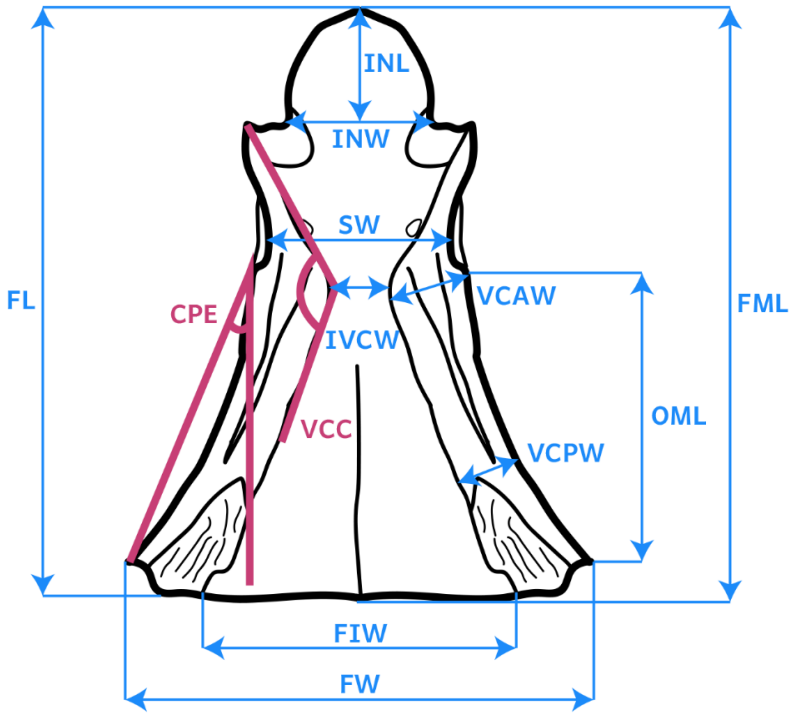

Figure 3.1.3: Measurements taken in the frontal bones represented in **Table 3.1.1**. Measurements in blue represent metric measurements; measurements in dark pink represent angle measurements. **CPE**, curvature at the posterior part of the edge (in degrees); **FIW**, frontal inner width between ventrolateral crests, across posterior edges of the frontal ventral roof; **FL**, total length of the frontal; **FML**, frontal length at the midline; **FW**, frontal width across posterior edges; **INL**, internasal length at the midline; **INW**, internasal width at the base; **IVCW**, interventrolateral crests width; **OML**, orbital margin length; **SW**, slot width, between the posterior slots for the prefrontal; **VCAW**, ventrolateral crest anterior width, behind prefrontal facets; **VCC**, ventrolateral crest curvature (in degrees); **VCPW**, ventrolateral crest posterior width, before parietal facets.

This may represent a sampling bias: not only may there be too few specimens (17) relative to the number of variables (13) but may also be due to the fact that several specimens are highly fragmented. Indeed, only six specimens could provide measurements for at least 70% of the variables; and only seven variables could be measured in at least 70% of the specimens. Therefore, a second PCA was performed using only the seven variables in which at least 70% of the specimens could be measured: INL, INW, SW,

IVCW, VCAW, VCPW, and VCC (see Figure 3 for the measurement abbreviations and definitions). This model appears more robust, as the second axis eigenvalue is above the broken stick model, and is the one described and discussed below.

Both the LDA and PCA were run using Past 4.03 (Hammer *et al.*, 2001). All specimens were used and grouped according to their provenance (Lourinhã or Guimarota beds). As the measures used different units and can have different scales, the analyses were performed using a correlation matrix. Missing values were treated with the iterative imputation option, as recommended by the authors (Hammer *et al.*, 2001). The PC (principal components) scores from the second PCA were used to perform the LDA, to determine if the specimens could be distinguished in different groups.

In order to determine the best optimal partitioning, K-means partition comparison was performed using R4.0.3, with the vegan 2.5-7 package (Oksanen *et al.*, 2020). Firstly, K-means partitions comparison was performed to find the most optimal grouping of our specimens. Based on the Simple Structure Index (SSI), three groups appear to be the most optimal partitioning (SSI = 0.59), which was applied for the LDA. The highest SSI value is regarded as a good indicator of the best partition, as it multiplicatively combines several elements that influence the interpretability of a partitioning solution (Borcard *et al.*, 2018; Oksanen *et al.*, 2020). The comparison was set with number of groups of the cascade

between 2 and 5, considering the sample size. However, as recommended by the author of the package, higher numbers of groups were explored, up to 10.

The confusion matrix of the LDA was corrected using Jackknifed resampling (leave-one-out cross-validation procedure; Hammer *et al.* 2001). Multivariate analysis of variance (MANOVA) was performed on the PCA scores using Pillai trace test to determine if there was a significant difference between the groups, coupled with a Pairwise post-hoc test using Bonferroni-corrected p values to determine which groups were significantly different to the others (Hammer *et al.*, 2001).

The relationships between (1) the frontal inner width between ventrolateral crests, across posterior edges of the frontal ventral roof (FIW) and ventrolateral crest anterior width, behind prefrontal facets (VCAW); (2) the frontal length at the midline (FML) and the internasal length at the midline (INL); and (3) the slot width, between the posterior slots for the prefrontal (SW), and the frontal width across posterior edges (FW) were analysed with linear regressions for sign of allometry, with, respectively, 11, 7, and 11 specimens due to the overall preservation in the sample. Measurements were log-transformed using the log function from PAST 4.03 before using them to run the linear model with R4.0.3, using the implemented R stats package and the package ggplot2 for visualization and

validating the model (Wickham *et al.*, 2021). See Appendices E.1 and E.2 for R script and additional morphometric data used.

3.1.3.2 Phylogenetic analysis

Phylogenetic analyses were performed using TNT 1.5 (Goloboff & Catalano, 2016). Both NEXUS files for the matrix were created with Mesquite 3.61 (Maddison & Maddison, 2019) and exported as a .tnt file that was modified in a text editor to add the necessary settings and commands (see Appendices E.3 and E.4 for the TNT files).

The dataset used is based on the latest iteration of the Gardner (2002) dataset, published by Daza *et al.* (2020). Two additional characters were added based on new observations concerning the frontal bones of the different species (see Appendix E.5 for the character list). The most recent iteration from Carrano *et al.* (2022) was not used as it was published late during the review process. The still uncertain position of Albanerpetontidae within Lissamphibia reflects the lack of a satisfactory outgroup. Previous studies have relied on a hypothetical –all 0– outgroup, assuming 0 was the ancestral condition for each character without further phylogenetic evidence. We followed Matsumoto & Evans (2018) and Daza *et al.* (2020) in choosing *Anoualerpeton priscum* as our outgroup, because the genus *Anoualerpeton* has been consistently recovered as the basal-most Albanerpetontidae (Gardner *et al.*, 2003; Venczel & Gardner, 2005; Sweetman & Gardner, 2013; Matsumoto & Evans, 2018; Daza *et al.*, 2020).

3.1 CHAPTER 4: PLASTICITY OF ALBANERPETONTID FRONTALS

Most of the previous iterations of the dataset employed *Celtedens* only at a generic level, based mainly on the description of *Celtedens ibericus* McGowan & Evans, 1995, because specimen LH 6020 from Las Hoyas is one of the few complete, articulated albanerpetontid fossils known. In the present analysis, as in the one of Carrano *et al.* (2022), *Celtedens* was incorporated as the two described species, *C. ibericus* and *Celtedens megacephalus* (Costa, 1864).

The Portuguese specimens were coded as two terminal taxa, according to their geographic provenance (Guimarota or Lourinhã). All elements in both collections were scored for the purpose of the analyses, although this study focuses only on the frontals. Scoring for Lourinhã Fm elements is based on the microfossils from our picking. Scoring for Alcobaça Fm elements is based on previous work by Wiechmann (2003) and observations during the revision of the material. Scoring for other *Celtedens* taxa is based on the coding provided in the unpublished PhD thesis of Wiechmann (2003), complemented by descriptions and images available in the literature (McGowan, 2002; Maddin *et al.*, 2013).

Two analyses were performed: one considering specimens from the Alcobaça Fm and the Lourinhã Fm as two different species; and the second considering only one species, with polymorphic characters when required. In the final dataset, 22 terminal taxa were selected for the first analysis, and 21 for the second coded for 38 unordered characters. For the same

reason that the data set was not used, the new species described by Carrano *et al.* (2022) was not included. We used the species name following the emendation proposed by Marjanović and Laurin (2008).

TNT requires the definition of a single outgroup, which would result in an artificial placement of *Anoualerpeton unicum* Gardner *et al.*, 2003 as more related to all other Albanerpetontidae than to *Anoualerpeton priscum* contrary to all previous analyses. To work around this problem, a taxonomic outgroup was defined for the genus *Anoualerpeton,* and all MPTs recovered in the different analysis were re-rooted to the taxonomic outgroup after the searchers.

Two analyses were run in TNT, a first analysis using all equally weighted characters, and a second analysis using implied weights, to reduce the effect of homoplasy. Different K values were tested–with lower values causing more drastic downweighing of the homoplasy than higher values (Goloboff *et al.*, 2008), but the results where the same for every K larger than 5. All results shown are using K=12. The analyses were performed with a traditional search using 1000 replications of Wagner trees followed by tree bisection reconnection (TBR) saving 10 trees saved by replication); and an additional round of TBR was performed on the resulting most parsimonious trees (MPT) to further explore the tree space.

A strict consensus tree was generated from all the MPTs recovered by each analysis. Branch support was calculated using bootstrap standard

resampling with 1000 replicates. Consistency and retention indexes were calculated for each MPT and each individual character using the script allstats.run by Peterson Lopes (Universidade do Sau Paulo, Brasil).

3.1.4 Systematic palaeontology

Amphibia Linnaeus 1758

Lissamphibia Haeckel, 1866

Albanerpetontidae Fox & Naylor, 1982

Genus *Celtedens* McGowan & Evans, 1995

aff. *Celtedens* sp. (**Figure 3.1.4** and **Figure 3.1.5**)

Referred material

Sixty-two frontals from the Lourinhã Formation: ML2738 to ML2749; ML2751 to ML2772; FCT/UNL-CN00016 to FCT/UNL-CN00029; FCT/UNL-CN00100 to FCT/UNL-CN00108; and FCT/UNL-CN00398 to FCT/UNL-CN00402.

Fifty-eight frontals from the Alcobaça Formation: MG28426; MG28427; MG28444; MG28451 (two fragments); MG28459; MG28473; MG28488 (three fragments); MG28491; MG28500; MG28502; MG28516; MG28520; MG28521; MG28524; MG28527 (two fragments); MG28531; MG28532; MG28533; MG28536 (three fragments); MG28539; MG28541; MG28542; MG28543; MG28559; MG28562; MG28564 (four fragments); MG28569; MG28570; MG28571; MG28572; MG28639; MG28648; MG28667; MG25672;

MG28673; MG28691; MG28692; MG28694; MG28707; MG28710; MG28713 (three fragments); MG28714; MG28717; MG28721; MG28732; MG28733.

Localities and age of the specimens

All 120 specimens studied come from the Upper Jurassic outcrops of the Lusitanian basin, in Portugal, distributed between 6 different localities: 24 specimens from late Kimmeridgian Valmitão VMA (Lourinhã Municipality, Portugal) in the Porto Novo/Praia da Amoreira Member of the Lourinhã Formation; 1 specimen from late Kimmeridgian Porto das Barcas VMA (Lourinhã Municipality, Portugal), in the Praia Azul member of the Lourinhã Formation; 6 specimens from late Kimmeridgian Porto Dinheiro VMA (Lourinhã Municipality, Portugal), in the Praia Azul member of the Lourinhã Formation; 25 specimens from late Kimmeridgian Zimbral VMA (Lourinhã Municipality, Portugal) in the Praia Azul Member of the Lourinhã Formation; 6 specimens from early Tithonian Peralta VMA (Lourinhã Municipality, Portugal) in the Praia Azul Member of the Lourinhã Formation; and 58 specimens from the Guimarota beds (Leiria Municipality, Portugal) in the Kimmeridgian Alcobaça Formation.

Description

None of the Lourinhã Fm specimens is complete, most of them preserve only a fragmented ventrolateral crest or the anterior part of the middle part of the frontal (see **Figure 3.1.2** for a composite reconstruction based on specimen ML2738, and for anatomical terminologies). Specimens from the

Alcobaça Fm display various states of preservation (see **Figure 3.1.5**), from ventrolateral crest fragments to almost complete specimens. Measurements and the abbreviations applying them throughout the descriptions that follow can be found in **Figure 3.1.3** and **Table 3.1.1**. See Appendix E.6.1 for more details on the preservation of specimens.

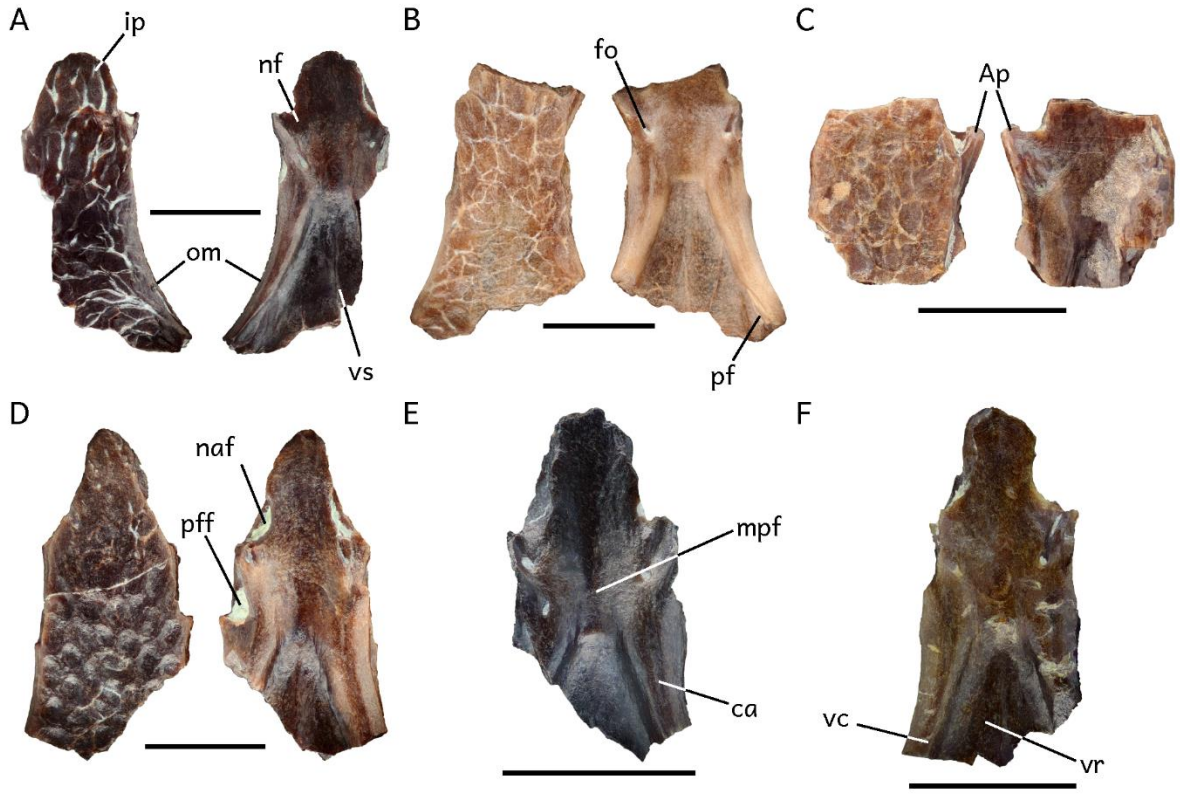

Figure 3.1.4: Normal-light photomicrograph of aff. Celtedens sp. frontal bones from the Lourinhã Formation in dorsal (left) and ventral (right) views. **A**, ML2738; **B**, ML2739; **C**, ML 2740; **D**, ML2741; **E**, FCT/UNL-CN00016; **F**, FCT/UNL-CN00018. Scale bars represent 1 mm.

The frontals exhibit bell-shaped ventral and dorsal outlines: after the anterolateral process, the edge expands posteriorly, parallel to the midline. However posteriorly, it is arched laterally. The FL/FW proportion (see **Figure 3.1.3**) is 1.27 in ML2738, the only specimen in which it could be

measured in Lourinhã Fm, but varies from 1.21 to 1.76 in Alcobaça Fm specimens (see **Figure 3.1.3** and **Table 3.1.1**). The orbital margin curvature at the posterior part of the edge (see **Figure 3.1.3**) is more marked in some specimens (ML2738, MG28692, MG28426) than others (ML2739, MG28473, MG28733), varying from 11.8° to 23° in the Lourinhã Fm specimens, and from 11.7° to 21.9° in the Alcobaça Fm specimens (see **Table 3.1.1**).

The Lourinhã Fm specimens display different degrees of dorsal surface ornamentation. Some, e.g. ML2738, exhibit sculptured tiny grooves expressed as wiggly lines randomly arranged (now referred to as vermicular ornamentation, **Figure 3.1.4A**). In other specimens, e.g. ML2739, ML2740, or ML2742 (not figured), the ornamentation may still present a vermicular pattern, but may also start to display polygonal pits typical of many albanerpetontids (**Figure 3.1.4B** and **C**). A third stage of ornamentation, as illustrated by ML2741, FCT/UNL-CN00016, and FCT/UNL-CN00018, is characterized by deep, polygonal pits with irregular honeycomb ornamentation (**Figure 3.1.4D**). None of the Alcobaça Fm specimens display vermicular dorsal ornamentation. When preserved and not eroded, their dorsal surfaces exhibit one of the two other degrees of ornamentation, with polygonal concave pits of various shapes (irregular polygonal to honeycomb).

Figure 3.1.5: Normal-light photomicrograph of aff. Celtedens sp. frontal bones from the Alcobaça Formation in dorsal (left) and ventral view (right). **A**, MG28426; **B**, MG28427; **C**, MG28473; **D**, MG28502; **E**, MG28520; F, MG28521; **G**, MG28532; **H**, MG28539; **I**, MG28541; **J**, MG28543; **K**, MG28562; **L**, MG28570; **M**, MG28572; **N**, MG28692; **O**, MG28694; **P**, MG28733. Scale bars represent 1 mm.

The internasal process is spatulate to flabellate, with a bulbous broad shape more or less pronounced from one specimen to another, in ventral and dorsal views (**Figure 3.1.4A**, **D**, **E**, and **F**; and **Figure 3.1.5B**, **D**, **F**, **G**, and **O**), with a INW/INL proportion of 0.84 to 1.38 in Lourinhã specimens, and

of 0.94 to 1.87 in the Alcobaça Fm specimens (see **Figure 3.1.3** and **Table 3.1.1**). Each edge bears a deep, longitudinal anterior slot for the nasal facet (**Figure 3.1.4A** and **D**).

When preserved, the anterolateral processes are distinct from the middle part of the frontal and can be seen in dorsal view (**Figure 3.1.4A**, **C**, and E**;** and **Figure 3.1.5C**, **D**, **F**, **M**, and **O**). The process displays an acuminate apex and extends anterolaterally, and yields a deep, lateral slot-facet expanding posteriorly towards the orbital margin comprising the prefrontal facet (**Figure 3.1.2** and **Figure 3.1.4D**). When preserved, the process is short in most specimens, although its expansion varies from one specimen to another, and it can be distinct from the middle part of the frontal, e.g. ML2740 (**Figure 3.1.4C**), MG28444, MG28491, and MG28639 (not figured).

The ventral surface of the nasal facet does not broaden laterally, and the facet cannot be seen in dorsal view, except in ML2741, although this could represent an artifact of preservation. The ventral surface of the internasal process and the middle part of the frontal is flat to weakly concave in the longitudinal axis. Medial to the anterior-most part of the anterolateral processes, the ventral surface of the internasal process bears a faint, triangular facet (**Figure 3.1.4A** and **C**), which would articulate with the nasal and/or the lacrimal.

Ventrally, the anterolateral process expands posteriorly and medially into a thin ridge following the edge where it meets the ventrolateral crest. A foramen, connected to the canals of the ventrolateral crests, is present at the anterior-most part of the ventrolateral crests, where the anterolateral process ridges and the lateroventral internasal facets end **Figure 3.1.4A**, **B**, and **E**; and **Figure 3.1.5F**, **K**, and **P**).

The slot width between the posterior slots for the prefrontal is smaller than the frontal width across the posterior edges (see **Figure 3.1.3**), with a SW/FW proportion between 0.39 and 0.5 in the Lourinhã Fm specimens, and between 0.39 and 0.66 in the Alcobaça Fm specimens (see **Table 3.1.1**).

The ventrolateral crests are broadest anteriorly, with a VCAW/VCPW proportion from 1.31 to 1.78 in Lourinhã specimens, and from 1.06 to 2.04 in the Alcobaça Fm specimens (see **Table 3.1.1**). However, they do not meet medially in any specimen in which both sides are preserved (**Figure 3.1.4A**, **B**, **D**, **E**, and **F**; and **Figure 3.1.5A**, **B**, **F**, **G**, **H**, **I**, **K**, **L**, **M**, **P**). The ventrolateral crests are convex ventrally and are ridge-like in transverse profile. The more lateral part along the orbital margin is beveled and faces ventrolaterally.

The ventrolateral crests exhibit a shallow groove, forming a canal that extends anteroposteriorly from the prefrontal facet to the parietal facet (**Figure 3.1.4A**, **B**, and **D**), or fades into a rugose surface at the middle of the crest in ML2738 and ML2741. In the Alcobaça Fm specimens, this groove

can be eroded or not visible, but extends as far as the parietal facet in MG28473 (**Figure 3.1.5C**). When the frontal ventral roof is preserved, a weak ventromedian suture extends anteriorly towards the middle part of the frontals (**Figure 3.1.4A**, **B**, **D**, and **F**).

Remarks

Frontal bones from the Lourinhã Fm and the Alcobaça Fm are generally similar. They share: (1) the same general bell-shaped outline; (2) a flabellate, bulbous-shaped internasal process; (3) small acute anterolateral processes; (4) ventrolateral crests convex ventrally and ridge-like in transverse profile, with the orbital margin bevelled and facing ventrolaterally; and (5) a weak ventromedian suture extending anteriorly towards the middle part of the frontals.

Differences can be noted between the Portuguese specimens, especially in the curvature of the orbital margin, the extension of the ventrolateral crest canal, and the dorsal ornamentation. However, these differences occur not only between the Lourinhã Fm and the Alcobaça Fm specimens, but also among specimens from same geographic origin. These differences may result from ontogenetic or environmental factors leading to ecophenotypic and intraspecific variations (McGowan, 1998a; Wiechmann, 2003). See intraspecific and ontogenetic variation in the discussion that follows for more details on this aspect. Thus, based on their frontal bones, all Portuguese albanerpetontid specimens are conservatively attributed to

aff. *Celtedens* sp. However, more research on other skeletal elements is required to determine with certainty if specimens from the Lourinhã Fm and the Alcobaça Fm are congeneric and conspecific.

Aff. *Celtedens* sp. differs from *Albanerpeton sensu lato* (*Albanerpeton* s.l.), *Shirerpeton*, *Wesserpeton*, the Uña specimen, and *Yaksha* by having a bell-shaped outline and a bulbous flabellate internasal process (Sweetman & Gardner, 2013; Matsumoto & Evans, 2018; Daza *et al.*, 2020). It differs from *Shirerpeton*, *Yaksha*, and the specimen from Uña by lacking an anterior contact between the ventrolateral crests; from *Albanerpeton* s.l. and *Shirerpeton* by having short anterolateral processes rather than long (Matsumoto & Evans, 2018); from *Albanerpeton* s.l. and *Yaksha* by being rather more elongated than wide (Daza *et al.*, 2020). It resembles *Wesserpeton* in displaying short anterolateral processes (Sweetman & Gardner, 2013).

The bell-shaped outline, the flat ventral surface of the internasal process and short acute anterolateral process constitute features found in *Anoualerpeton*. However, aff. *Celtedens* sp. contrasts with this genus by having a flabellate internasal process with bulbous and broad shape (Gardner *et al.*, 2003).

Aff. *Celtedens* sp. shares the morphology of the frontal recognized in *Celtedens*, especially the general outline (bell-shaped to hourglass in *Celtedens*) and the flabellate, bulbous-shaped internasal process. The

orbital margin appears laterally curved in aff. *Celtedens* sp. of Portugal, as it is observed in *C. megacephalus* (Estes, 1981; McGowan, 1998a, 2002). Although the orbital margin curvature is posteriorly less pronounced in some specimens (ML2739, MG28473, MG28733) or appears less pronounced as an artifact of preservation (ML2741, FCT/UNL-CN00016, FCT/UNL-CN00018, MG28521, MG28543, MG28594), it does not exhibit the hourglass shape observed in *C. ibericus* (McGowan & Evans, 1995; McGowan, 2002) either.

Also, based on what could be observed in published figures of *C. megacephalus* and *C. ibericus*, aff. *Celtedens* sp. shares with *C. megacephalus* a narrower anterior inter-lacrimal width to posterior parietal margin width (**Figure 3.1.3**) than *C. ibericus*, with a proportion ranging between 0.39 and 0.66 in both localities (**Table 3.1.1**). Unfortunately, the anterior part of *C. megacephalus* frontal from Pietraroia remains unknown (McGowan, 2002), and therefore cannot be compared with Spanish specimens from Uña attributed to that species (Wiechmann, 2003) or with Portuguese specimens, although ML2738 might be similar. Moreover, Pietraroia is dated from the early Aptian of Benevento Province in Italy, and the Uña referred but unconfirmed specimen is from the late Barremian.

Thus, based on the anatomy of their frontal bones and their geographical and geological time separation, it can be concluded than even though they

share affinities, Portuguese specimens of aff. *Celtedens* sp. are not conspecific with either *C. megacephalus* or *C. ibericus*.

3.1.5 Results

3.1.5.1 Morphometric analysis

3.1.5.1.1 Linear morphometric analysis

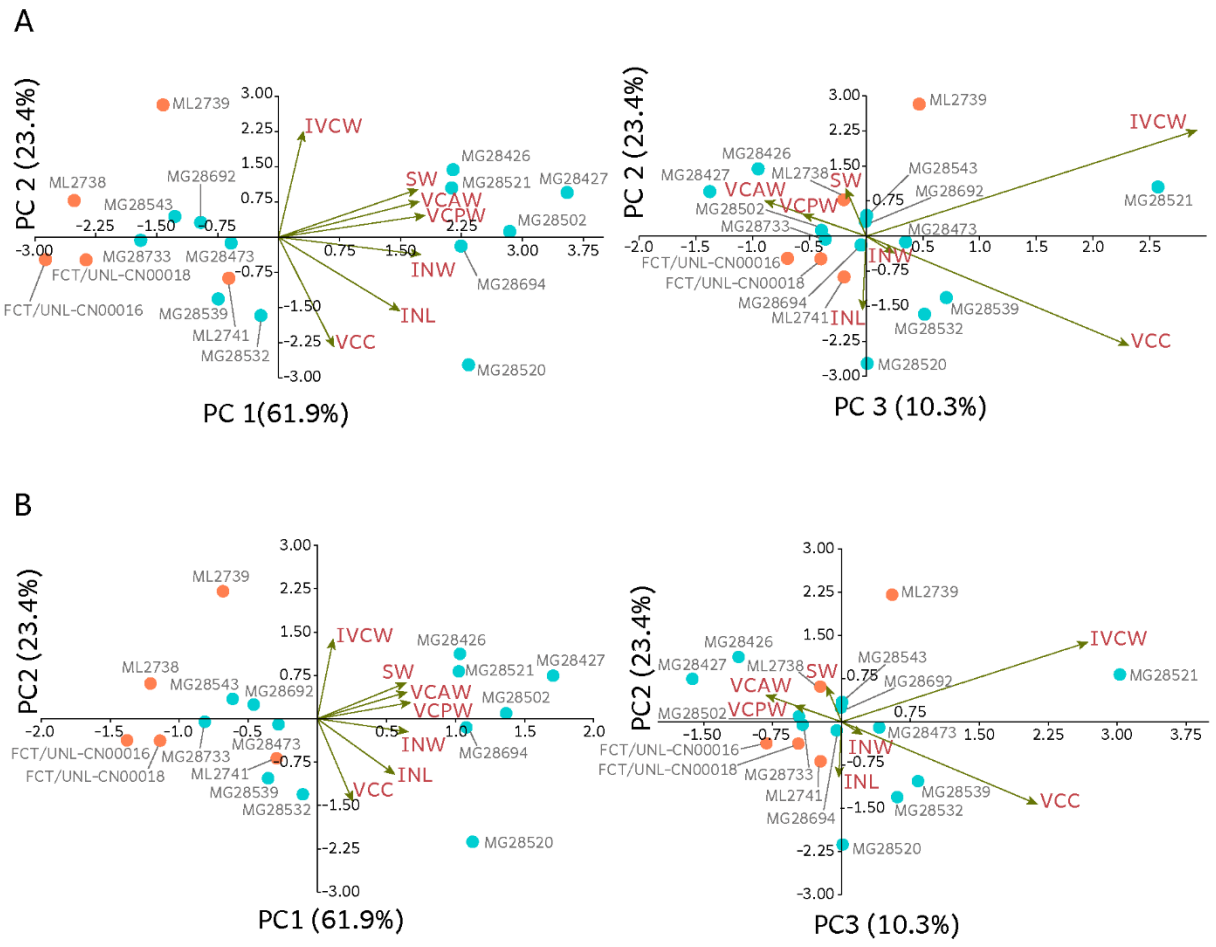

Figure 3.1.6: Principal component analysis based on 7 variables in scaling 1 (**A**) and scaling 2 (**B**). Orange dots represent specimens from the Lourinhã Formation, blue dots represent specimens from the Alcobaça Formation.

The three first axes of the PCA account for 95.6% of the variation. For the PC1-PC2 graph in scaling 1 (**Figure 3.1.6**; **A**), the larger specimens are

grouped together in positive values in PC1 and PC2, except MG28520 that has a negative value in PC2; while the others are grouped together in the negative values in PC1 and spread in positive and negative values in PC2. However, ML2739 presents a higher value in PC2 than the others. For the PC3-PC2 graph in scaling 1, most of the specimens are grouped together toward the centre of the graph, with a negative value for PC3, to a lesser extent for ML2739 and the duo MG28539-MG28532. However, MG28521 presents high positive values in PC3 and is associated with higher values of IVCW and VCC. All PCA scores are presented in Appendix E.2.

For the PC1-PC2 graph in scaling 2 (**Figure 3.1.6**; **B**), all variables are positively correlated to PC1. Meanwhile, VCPW, VCAW, SW, and IVCW are positively correlated to PC2; and INW, INL, and VCC are negatively correlated to PC2. For the PC3-PC2 graph in scaling 2, SW, VCAW, and VCPW are negatively correlated to PC3. INL is almost not correlated to PC3. INW is weakly positively correlated to PC3, while IVCW and VCC are both highly positively correlated to PC3. All PCA loadings (coefficient and correlation) are presented in Appendix E.2. Additional description of the results from the PCA are presented in Appendix E.6.2.

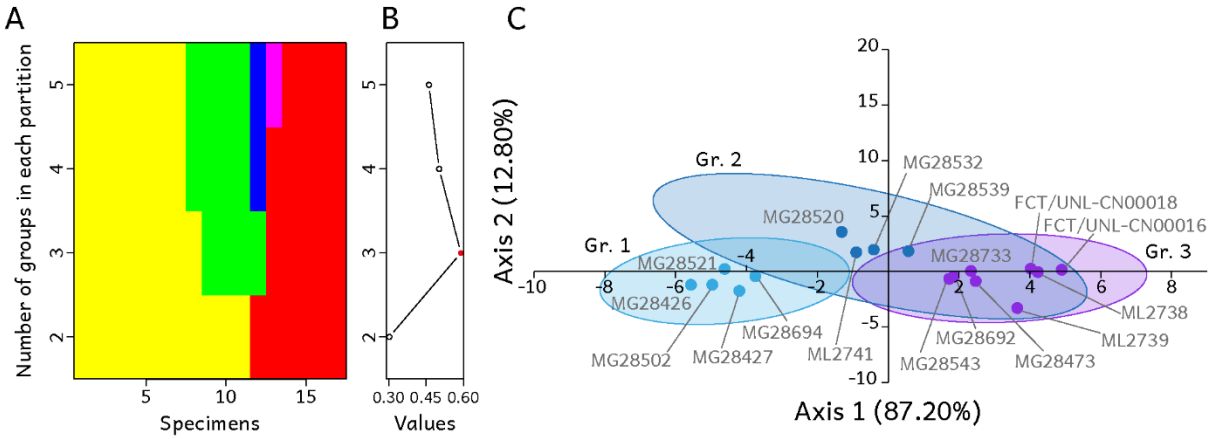

Figure 3.1.7: **A**, K-means partitions comparison; each colour represents a different group to which the specimens (x-axis) are attributed. **B**, Simple Structure Index criterion corresponding to each partition (best SSI = 0.59). **C**, Linear discriminant analysis (confusion matrix with Jackknifed resampling = 88.24%).

All the variation is explained by the two main axis of the LDA (see **Figure 3.1.7**). Group 1 is composed of only five specimens from the Alcobaça Fm; group 2 is composed of only four specimens, including one from the Lourinhã Fm; group 3 is composed of eight specimens, including four from the Lourinhã Fm The confusion matrix corrected by Jackknifed resampling correctly classified 88.24% of the specimens. The MANOVA performed on the scores from the PCA confirms there is a significant difference between the groups (Pillai trace test; F=5.025; df1=14 and df2=18; p-value = 0,0009048), and the post-hoc test that group 1 and group 3 are significantly different (p-value = 0,021737), but group 2 is not significantly different with either group 1 or group 3.

3.1.5.1.2 Linear regression

The first linear regression is set to compare the relationship between ventrolateral crest anterior width, behind the prefrontal facets, and the

frontal inner width between the ventrolateral crests (**Figure 3.1.8**; **A**). Considering those parts of the bone are among the most commonly preserved, 11 specimens could be used. The slope equation (1) is higher than 1. The adjusted R^2 is 0.3617, the p-value lower than 0.05 supports the conclusion that the results are significant, and the residuals behave normally and respect the homoscedasticity (homogeneity of the variance between all values of the residuals; see Appendix E.1.1).

$$Log_{VCAW} = 1.10968 \times Log_{FIW} - 0.36888 \qquad (1)$$

The second linear regression is set to compare the relationship between the internasal process length and the frontal medial length (**Figure 3.1.8**; **B**). Only 7 specimens could be used. The slope equation (2) is lower than 1. The adjusted R^2 is 0.4665, but the p-value is 0.05453, and therefore the results are non-significant. The normality and the homoscedasticity of the residuals could not be certified, but they seem to respect those hypotheses (see Appendix E.1.1).

$$Log_{INL} = 0.7910 \times Log_{FML} - 0.5920 \qquad (2)$$

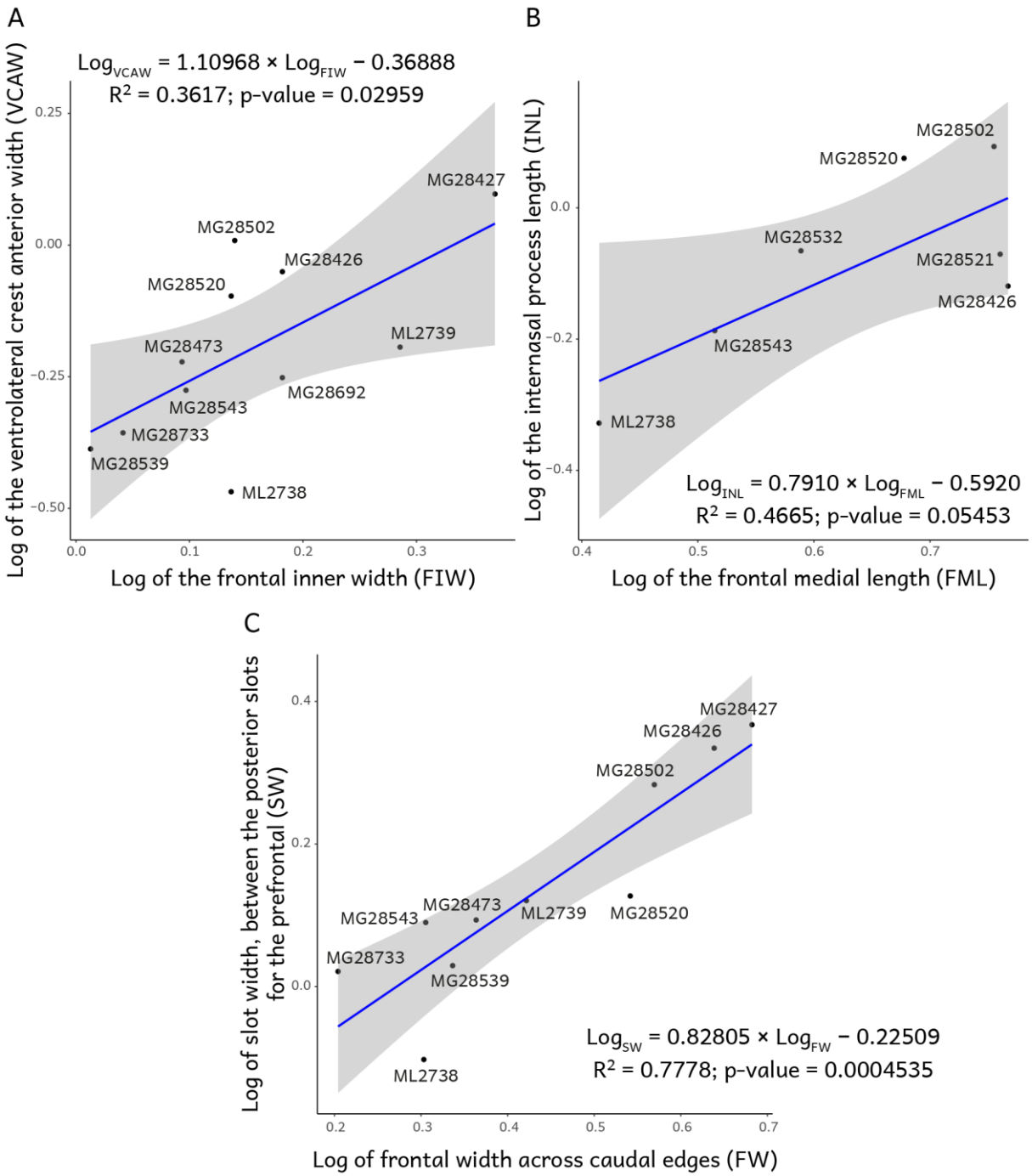

Figure 3.1.8: Linear regression to test the allometry in the ventrolateral crests (**A**), the internasal process (**B**), and slot width, between the posterior slots for the prefrontal (**C**). The blue line represents the model, and the grey area the 95% confidence interval.

The third linear regression is set to compare the relationship between the slot width, between the posterior slots for the prefrontals, and the frontal width across posterior edges (**Figure 3.1.8**; **C**). For this one, 11

specimens could be used. The slope equation (3) is lower than 1. The adjusted R^2 is 0.7778, and the p-value lower than 0.05 supports the conclusion that the results are significant. The residuals behave normally and respect the homoscedasticity (see Appendix E.1.1).

$$Log_{SW} = 0.82805 \times Log_{FW} - 0.22509 \qquad (3)$$

3.1.5.2 Phylogenetic analysis

In the first analysis considering two different Portuguese species, 10 MPTs were recovered during the analysis, with a fit of 2.07857 and 73 steps (see **Figure 3.1.9**). The consistency index (CI) is 0.603 and the retention index (RI) is 0.724. The inclusion of *Celtedens* specimens collapsed the genus and produced a basal polytomy with a clade comprised of all other albanerpetontids.

This latter clade includes a basal trichotomy, between *Wesserpeton evansae* Sweetman and Gardner, 2013, the Uña specimen – which has been described as *Wesserpeton* sp. (Sweetman & Gardner, 2013) – and another monophyletic clade comprised of all other albanerpetontids, previously described as *Albanerpeton* s.l. (Daza *et al.*, 2020).

As already pointed out in most recent studies, the genus *Albanerpeton* is recovered as a paraphyletic taxon (Matsumoto & Evans, 2018; Daza *et al.*, 2020), with the two most recently described albanerpetontid species, *Yaksha perettii* Daza *et al.*, 2020 and *Shirerpeton isajii*, nesting within *Albanerpeton* s.l., and forming a clade sister to the informally named

"robust-snouted clade" *sensu* Venczel and Gardner, 2005 (Gardner & Böhme, 2008). A trichotomy is also recovered between *Albanerpeton galaktion*, *Albanerpeton gracile* Gardner, 2000b, and the clade comprised of more nested Albanerpetontidae.

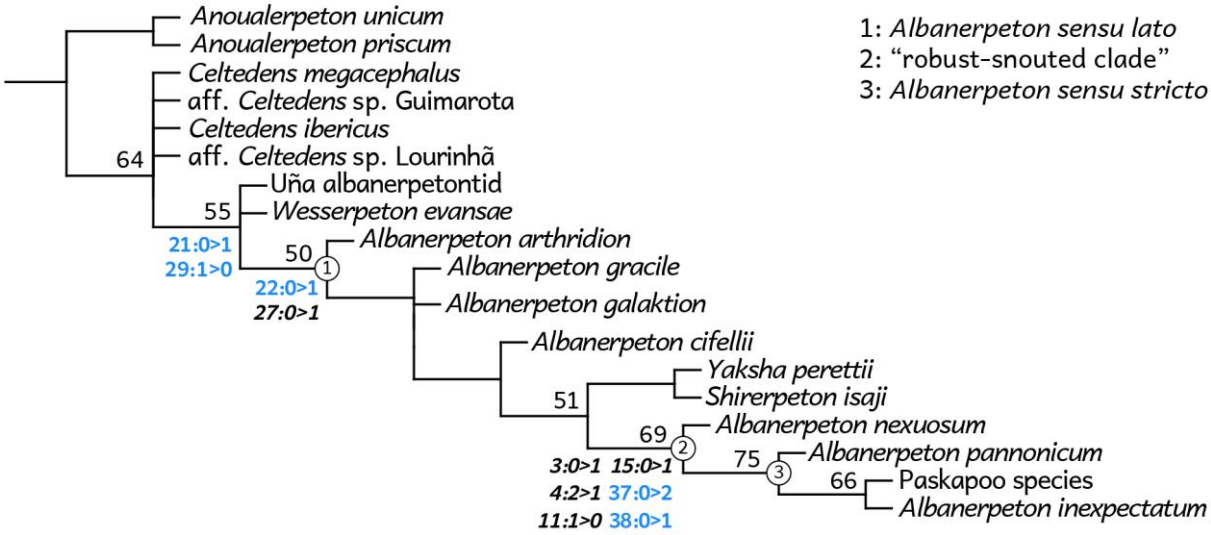

Figure 3.1.9: Consensus tree of the 10 MPTs recovered under implied weights. Fit= 2.07857; length=73 steps; CI=0.603, RI = 0.724. Black numbers are bootstrap values to the corresponding nodes. Bold number are synapomorphies (italic not related to the frontal bones, blue related to the frontal bones). **Node 1**, Albanerpeton s.l.; **Node 2**, "robust-snouted clade" *sensu* Venczel and Gardner, 2005; **Node 3**, Albanerpeton s.s.

In this topology, the Cenozoic species still form the most derived clade, referred to *Albanerpeton* s. s. Note the general low support of these clades, with few values over 50, and only the clade *Albanerpeton* s.s. and clades within show a bootstrap value over 65.

However, the results from the linear morphometric analyses were inconclusive concerning the question of whether specimens from the Alcobaça Fm and the Lourinhã Fm form two distinct species, or if they are

conspecific. Therefore, a second analysis was performed, using only one species with two polymorphic characters (char. 6 and char. 26) to represent all its variability. Only one MPT was recovered in this analysis (**Figure 3.1.10**), with a fit 1.99066, and 72 steps (one step shorter than the first tree). The CI is 0.611 and the RI is 0.714, which are also similar to the first analysis.

The global topology is similar to the previous analysis, with similarly low branch support, but this analysis resolves the basal polytomy, recovering *Celtedens* as a monophyletic genus sister to all other non-*Anoualerpeton* Albanerpetontidae. *W. evansae* is here recovered basal to the Uña specimen. Within *Albanerpeton* s.l., the only difference with the previous analysis is the resolution of the trichotomy within this clade, with *Albanerpeton arthridion* Fox and Naylor, 1982, *A. galaktion* and *A. gracile* being recovered as successive sister clades of all other *Albanerpeton* s.l. In view of the taxonomic uncertainty regarding the Portuguese specimens, this analysis will be used for discussion.

Based on the character set used herein, *Albanerpeton* s.l. is characterized by two unambiguous synapomorphies: 'moderate' ratio of midline length of fused frontals versus width across posterior edge of bone (char. 22: 1); and anterior end of orbital margin in line with or behind the anteroposterior midpoint of frontals (char. 28: 1). The "robust-snouted clade" *sensu* Venczel and Gardner, 2005 is characterized by six

unambiguous synapomorphies: inter-premaxillary contact fused medially (char. 3: 1), premaxillary pars dorsalis minimally overlaps and strongly sutured with anterior end of nasal (char. 4: 1), outline of suprapalatal pit oval (char. 11: 0), short premaxillary lateral process on maxilla relative to height of process at base (char. 15: 1), medial emargination of the prefrontal facet, making a notch visible dorsally and ventrally (the lacrimal sits lateral to the frontal) (char. 37: 2), and edge of ventrolateral crests medial to the orbital margin creating a ventral step, or parapet (char. 38: 1).

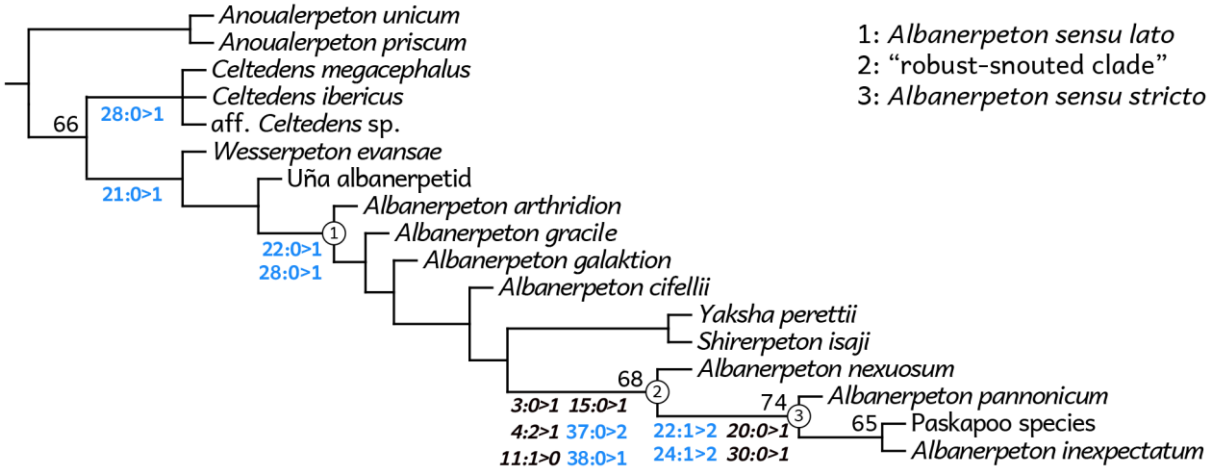

Figure 3.1.10: Consensus tree of the 1 MPT recovered under implied weights. Fit=1.99066; length=72 steps; CI=0.611, RI = 0.714. Black numbers are bootstrap values to the corresponding nodes. Bold number are synapomorphies (italic not related to the frontal bones, blue related to the frontal bones). **Node 1**, Albanerpeton s.l.; **Node 2**, "robust-snouted clade" *sensu* Venczel and Gardner, 2005; **Node 3**, Albanerpeton s.s.

Albanerpeton s.s. is characterized by four unambiguous synapomorphies: anterior end of maxillary tooth row approximately in line with the point of maximum indentation along leading edge of nasal process (char. 20: 1); 'short' (equal to or less than about 1.0) ratio of midline length

of fused frontals versus width across posterior edge of bone, between lateral edges of ventrolateral crests, in large specimens (char. 22: 2); wide and triangular ventrolateral crest on large, fused frontals in transverse view, with ventral face deeply concave (char. 24: 2); and suprapalatal pit divided in about one-third or more of specimens (char. 30: 1).

Celtedens is recovered as a monophyletic group characterized by a single unambiguous synapomorphy: bulbous dorsal or ventral outline of internasal process on frontals (char. 29: 1). *C. megacephalus* is coded for 9 characters, and all are shared with both *C. ibericus* and aff. *Celtedens* sp. The only differences relate to an ambiguity in *C. megacephalus* (coded '?'). Of these 9 characters, only one does not relate to the frontal bones (labial or lingual of occlusal margin of maxilla and dentary essentially straight, char. 18: 0).

Likewise, aff. *Celtedens* sp. and *C. ibericus* share 23 characters in total, but none of them are exclusive as they are either ambiguous or also shared in *C. megacephalus*. Aff. *Celtedens* sp. from Portugal differs from *C. ibericus* in two characters: low ratio (less than about 1.55) of height of premaxillary pars dorsalis versus width across suprapalatal pit (char. 2: 1), and presence of flattened ventromedian keel extending along posterior two-thirds of fused frontals (char. 30: 1). However, both are also ambiguous in *C. megacephalus*.

Table 3.1.2: Main indexes calculated for the MPT, and each character considered for the frontal bones.

		# Character states	Minimum possible changes	Total changes	Consistency index CI	Retention Index RI	Times recovered as synapomorphy
MPT	-	82	44	72	0.611	0.714	49
Ch. 21	*Dorsal or ventral outline of fused frontals*	2	1	1	1	1	1
Ch. 22	*Ratio of midline length of fused frontals versus width across posterior edge of bone,*	3	2	2[1]	1	1	2
Ch. 23	*Proportions of internasal process on fused frontals*	2	1	5	*0.333*	*0.6*	2
Ch. 24	*Form of ventrolateral crest on large, fused frontals*	3	2	5	*0.4*	*0.25*	5
Ch. 28	*Position in frontals of anterior end of orbital margin relative to anteroposterior midpoint of frontals*	2	1	1	1	1	1
Ch. 29	*Dorsal or ventral outline of internasal process on frontals*	2	1	1	1	1	1
Ch. 31	*Flattened ventromedian keel extending along posterior two thirds of fused frontals*	2	1	6	*0.25*	*0,4*	4
Ch. 37	*Frontal-lacrimal contact*	3	2	3	0.667	*0.667*	2
Ch. 38	*Edge of ventrolateral crests, position along the orbital margin*	2	1	2	*0.5*	*0.5*	2

[1] The number of character changes can be up to 4, due to the ambiguous codification of this character for *Yaksha* and *Shirerpeton* (either 0 or 1, but never 2). Nevertheless, the optimization criteria used by TNT always prefers the shortest option, thus reducing the score of this character to 2.

Eight more characters were recovered in aff. *Celtedens* sp. but are ambiguous in both *C. ibericus* and *C. megacephalus*. Likewise, three characters were recovered in *C. ibericus* but are ambiguous in both *C. megacephalus* and aff. *Celtedens* sp. from Portugal. Finally, two characters were ambiguous in all *Celtedens* species (char. 7: distribution of labial ornament on large premaxillae; char. 27: path followed by canal through pars palatinum in premaxilla, between dorsal and ventral openings of palatal foramen).

Due to the high number of character state transformations observed in the characters relating to the fused frontal bones, we calculated individual consistency, and retention indices for each character (**Table 3.1.2**). Five characters (21, 22, 28, 29, and 37) show consistency indexes over the global consistency index of the matrix, whereas 4 of them (23, 24, 32 and 38) show a lower consistency index, implying these characters have more homoplasy than the average for the most parsimonious tree. In addition, these four characters, together with character 37, show a lower retention index than the MPT, implying they have less homology than the average.

3.1.6 Discussion

3.1.6.1 Intraspecific and ontogenetic variation

3.1.6.1.1 Morphometrics

As expected, PC1 suggests a strong component linked to size, as shown by the positive correlation of all variables and the dispersion pattern of the specimens, with smaller ones toward the left and larger ones toward the right (**Figure 3.1.6**). However, the variation explained by PC2 and PC3 does not seem to have a specific dispersion pattern, preventing any clear biological variable being drawn from them. Only MG28521 (**Figure 3.1.5F**) appears distinct from the others, although this could be due to a preservational bias.

The LDA succeeded in correctly classifying all specimens in a most-optimal grouping of 3. Group 1 and Group 3 are significantly different, but not from Group 2, which could indicate a continuity in the sample, with specimens from different ontogenetic stages. Indeed, all large specimens from the Alcobaça Fm that were already near each other in the PCA are present in Group 1, except for MG28520 (**Figure 3.1.5E**), classified in Group 2. The same can be said with Group 3 which contains, among others, the smallest specimens. The high confidence interval observed for Group 2 could be due to the low number of specimens classified in it.

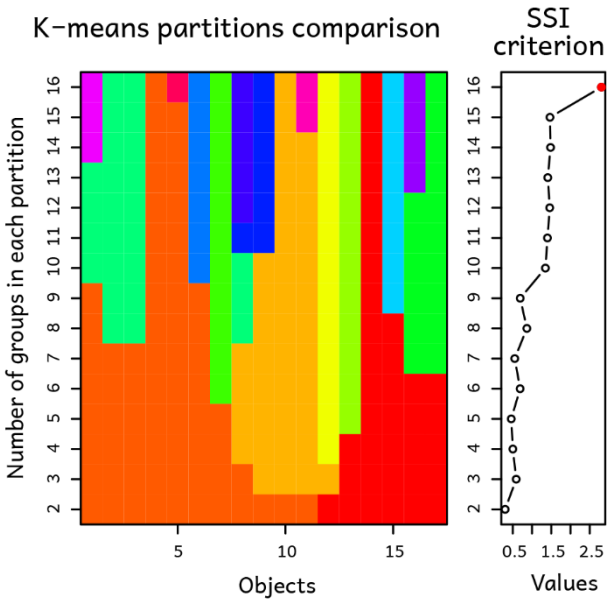

Figure 3.1.11: K-mean partitions comparison and the associated SSI criterion for up to 16 groups.

Furthermore, the pattern of the SSI criterion for inferring the most optimal group partitioning suggests a continuity in the sample. Partitions of 3 to 9 groups tend to have SSI values oscillating irregularly between 0.46 and 0.87 (see **Figure 3.1.11**). However, the values of SSI increase drastically with between 10 and 15 different groups, before forming a plateau between 1.35 and 1.48. Another increase occurs with 16 groups (SSI = 2.80), which is the maximum possible considering the sample size. That would indicate specimens are more optimally partitioned when they are alone than when grouped with other specimens, which is against the aim of grouping specimens together to find a pattern. This is interpreted as a sign of the continuity of the sample, rather than a true categorization.

3.1.6.1.2 Anatomical features

Intraspecific anatomical variations in the frontals of Albanerpetontidae have previously been reported and some attributed to ontogeny. One of the most common is variation in dorsal ornamentation: while the adults present the characteristic deep, polygonal ornamentation, with irregular to honeycomb pits; the juveniles present a shallow polygonal ornamentation (Gardner, 1999a,c, 2000a,b; Gardner *et al.*, 2003; Wiechmann, 2003). This variation can be seen in the Portuguese specimens, but here a third stage is also observed. Some specimens (e. g. ML2738, **Figure 3.1.4A**) exhibit a vermicular ornamentation where the characteristic pattern is absent.

The ventrolateral crest is also wider and extends posteriorly after the parietal margin in specimens representing adults. This is well illustrated by the difference between ML2738, where the unbroken ventrolateral crests end right before the parietal margin, while in MG28502 (**Figure 3.1.5D**) they appear relatively larger and extend beyond it. It has also been proposed that the ventromedian suture could be a sign of ontogeny, as it is less marked in adults (Gardner, 1999c; Gardner *et al.*, 2003; Wiechmann, 2003; Venczel & Gardner, 2005). The Portuguese specimens seem to present the same pattern, although for those from the Alcobaça Fm it is difficult to assess whether this represents a taphonomic artefact or relate to the gold coating.

The proportion between ventrolateral crest anterior width, behind the prefrontal facets, and the frontal inner width between the ventrolateral crests (VCAW/FIW) may also relate to ontogeny (Gardner, 1999c, 2000b; Gardner *et al.*, 2003; Wiechmann, 2003; Venczel & Gardner, 2005). In Portuguese specimens preserving both measurements, a significant linear response can be observed between their log-transformed values, even though the low adjusted R^2 could explain the large 95% confidence interval. Larger specimens tend to have wider ventrolateral crests, which is confirmed by the positive allometry, suggesting that the ventrolateral crest anterior width grows relatively faster than the frontal inner width in adult specimens from Portugal.

However, our observations of the Alcobaça Fm specimens contradict those of a previous study concerning these specimens (Wiechmann, 2003), both in the range of variation of the VCAW/FIW proportion and its interpretation. Indeed, an interval of between 0.3 and 0.37 was reported, with a decline observed in larger individuals (Wiechmann, 2003), while among the 11 specimens studied here, the VCAW/FIW proportion ranges from 0.25 to 0.74 (0.37 to 0.73 among the 9 specimens from the Alcobaça Fm), with an increase in larger specimens.

It is still uncertain why such a dramatic contradiction is reported between the measurements of the same specimens, as they were taken following the same methodology. The VCAW/FIW proportion has also been

used as diagnostic for *A. inexpectatum*, where it can reach higher values than 0.6, while fluctuating between 0.25 and 0.40 in other published species (Gardner, 1999c; Wiechmann, 2003). However, data from the Portuguese specimens suggests this character needs to be reviewed in other species to clarify its taxonomic relevance.

It was also proposed that the internasal process is relatively shorter in adults (Gardner, 1999c; Gardner *et al.*, 2003; Sweetman & Gardner, 2013). Portuguese specimens present a linear response between the log-transformed values of the internasal process length and the frontal medial length. The slope suggests a negative allometry, confirming that the internasal process is relatively shorter in adults. However, the results are not significant and residual behaviours could not be properly interpreted. Both could be due to the low number of specimens (7) that preserved both measurements. Therefore, we cannot draw definitive conclusions on this anatomical feature and more and better-preserved specimens are required.

Additionally, the relation of the slot width, between the posterior slots for the prefrontal (SW), to the frontal width across posterior edges (FW) was also analysed, in this study. Indeed, it has not been proposed to be subject to intraspecific variation, but it is part of the diagnosis of *C. ibericus*, whose SW/FW proportion is equal (or near to) 1, and *C. megacephalus*, whose SW/FW proportion is characterized as lower than 0.5 (McGowan & Evans, 1995; McGowan, 1998a). In Portuguese specimens, the

proportion ranges from 0.39 to 0.66. The negative slope from the linear response suggests a negative allometry, meaning that frontal width across posterior edges is relatively smaller than the slot width in adults.

Above mentioned intraspecific variations that can be linked to ontogeny suggest that the Lourinhã Fm and the Alcobaça Fm share one species, with intraspecific variation, despite being derived from different ecosystems and from different ages (late Kimmeridgian to early Tithonian for the former; Kimmeridgian for the latter). Based on its features, it is here proposed that, at the very least, ML2738 (**Figure 3.1.4A**) could represent a juvenile.

However, frontal bones in albanerpetontids appear to be plastic enough, at least at the specific level to be less diagnostic than previously thought. This may be significant in the case of the genus *Celtedens*, as its diagnosis is based entirely on characters of the frontals (McGowan, 1998a; Gardner, 2000a). Similar plasticity had also been reported in other diagnostic bones of albanerpetontids (Sweetman & Gardner, 2013), which reinforces the need to consider this variation, to determine whether or not it reflects true intraspecific or interspecific variation. However, such distinction may prove problematic in the case of the fragmentary and isolated the material.

3.1.6.2 Phylogenetic position and systematic implications of the new material

The phylogeny presented in this study confirms the paraphyly observed in the genus *Albanerpeton* (Matsumoto & Evans, 2018; Daza *et al.*, 2020), which appears now to be invalid for a number of species as it is currently defined. However, due to the instability of the current phylogeny, revising the monophyly of *Albanerpeton* is beyond the scope of this paper and will be part of a further dedicated study of Albanerpetontidae. In summary, this preliminary analysis heightens the need for a complete revision for the phylogeny of the group: attribution of the Uña specimen to *Wesserpeton* is not supported, contradicting previous assessment (Sweetman & Gardner, 2013) and suggesting the specimen needs a detailed description; and the genus *Celtedens* collapsed into a basal polytomy of the group when characters relating to both species were included in the analysis.

The 9 characters relating to the frontal bones in our matrix were recovered in 20 characters changes through the phylogeny (**Figure 3.1.12**, Appendix E.6.3). The high degree of homoplasy and low homology observed in four of the frontal bone related characters (23, 24, 32 and 38), coupled with the general low support of the recovered tree, suggests that the synapomorphic condition of these character state transformations should be considered with caution. Our results support the use of frontal bones to

differentiate genera of Albanerpetontidae but suggest they are not diagnostic at species level.

Portuguese specimens do indeed share the diagnostic characters of *Celtedens*: fused frontals bearing bulbous-shaped internasal process and retaining a bell-shaped outline; proportion of midline length to width across posterior edge between lateral edges of ventrolateral crests greater than 1.2; internasal process ventrolaterally has a facet for dorsally overlapping medial edge of nasal; dorsal and ventral edges of slot for receipt of prefrontal not excavated medially; anterior end of orbital margin located anterior to anteroposterior midpoint of frontals; and orbital margin deeply concave in dorsal or ventral outline, occasionally deflected posterolaterallly near posterior end (McGowan, 1998a; Gardner, 2000a). However, the frontals do exhibit differentiated anterolateral processes.

It could not be determined if the lacrimal facets are indented; hence their assignment to aff. *Celtedens* sp. They share 9 characters with *C. ibericus* and *C. megacephalus*, of which 8 are characters of the frontal, *Celtedens* being diagnosed on characters of the frontals alone (McGowan, 1998a; Gardner, 2000a). Among those characters, aff. *Celtedens* sp. shares the diagnostic bulbous internasal process (char 29; 1). In the present analysis, this character is the only synapomorphy characterizing *Celtedens*. Furthermore, *C. ibericus* and aff. *Celtedens* sp. share 14 additional characters and differ in two more.

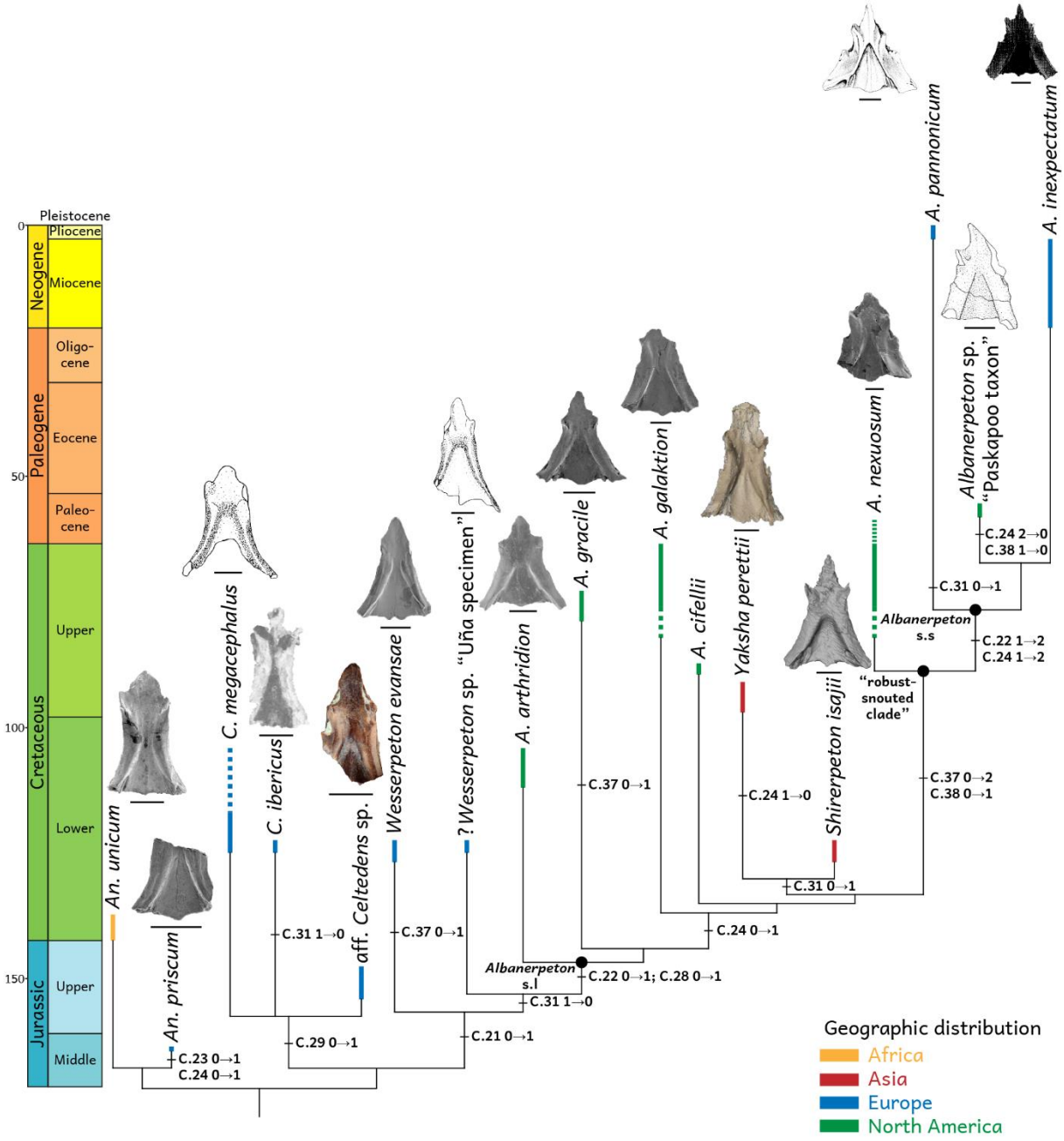

Figure 3.1.12: Evolution of the frontal bone in Albanerpetontidae, based on the consensus tree from the present analysis plotted against time and with geographic occurrences. Frontals are from the literature and associated with their respective species (scale bars represent 1 mm). No frontal has been described yet for Albanerpeton cifellii Gardner 1999c. Synapomorphies related to the frontal bones are indicated by lower-case letters.

However, these 16 characters, unrelated to the frontals, are inconclusive, as they are not coded in *C. megacephalus*, despite being related to other bones that could provide insights concerning relationships

among *Celtedens* species. The specimen from Pietraroia is poorly documented and preserved (Gardner, 2000a; McGowan, 2002; Maddin *et al.*, 2013) with only 9 characters coded in this matrix (23.7%), among which 8 are related to the frontal bones. All these characters are those shared with the other *Celtedens* species. A complete revision of the Italian specimen, together with specimens from Las Hoyas, using modern digital techniques may yield a new and better diagnosis of the genus, as illustrated in recent works for Asian specimens (Matsumoto & Evans, 2018; Daza *et al.*, 2020).

Indeed, diagnoses of *C. megacephalus* and *C. ibericus* are only based on putative autapomorphies of the frontal bones (McGowan, 1998a): the curvature of the orbital margin and the relative proportion of the anterior inter-lacrimal width (slot width, between the posterior slots for the prefrontal SW in our measurements, **Figure 3.1.3**) to the posterior parietal margin width (frontal width across posterior edges FW in our measurements, **Figure 3.1.3**). In both characters, aff *Celtedens* sp. is more similar to *C. megacephalus* than it is to *C. ibericus*. However, as seen in the morphometric analysis, both characters also present disparity in the Portuguese specimens and may be affected by ontogeny, which would question the validity of this character for the respective diagnoses. However, accurate measurements on specimens of both published species would be required to characterize this ratio, as it appears to be quite variable in our sample.

3.1.7 Conclusion

Sixty-two new frontals from the Lourinhã Formation are described, together with 58 revised specimens from the Guimarota beds, and are attributed to aff. *Celtedens* sp., based on their frontal bone morphology: a bell-shaped outline; and a flabellate, bulbous internasal process. This material confirms the plastic nature of the frontal bone, a key element in the characterization of Albanerpetontidae. While frontal morphology can be used in isolation to discriminate some genera, it should not be used in isolation to diagnose species.

Linear morphometric analysis paired with anatomical description highlights several features (notably the dorsal ornamentation, the shape and extent of the ventrolateral crests, the curvature of orbital margins, the size of the internasal process relative to the midline length of the frontals, the size of the slot width relative to the frontal width across posterior edges, and the presence of a ventromedian crest), that vary greatly from one specimen to another and, therefore, could affect taxonomic assessment, especially as some features are considered diagnostic in *Celtedens*.

Preliminary phylogenetic analysis confirms the paraphyly of *Albanerpeton* s.l., and thus the need for nomenclatural revision of most its species, as previously reported. Furthermore, our results confirm the validity of *Celtedens*, but suggest the need for a complete revision of the specimens referred to this genus. Finally, frontal bones show a high degree

of homoplasy in details of their morphology, so characters based on this skeletal element should be carefully analysed before being regarded as diagnostic for a taxon.

3.2 Chapter 5: New albanerpetontid species (Lissamphibia) from the Late Jurassic of Portugal

Paper to in revision in *Journal of Systematic Palaeontology* (Journal impact factor for 2022: 2.2; CiteScore: 5.3; SJR: 0.836; H-index: 56)
Alexandre R. D. Guillaume, Marc E. H. Jones, Eduardo Puértolas-Pascual & Miguel Moreno-Azanza. New albanerpetontid species (Lissamphibia) from the Late Jurassic of Portugal

Abstract

The Albanerpetontidae are a group of small extinct lissamphibians ranging from the Bathonian to the early Pleistocene. The Upper Jurassic of Portugal is known to yield a large collection of albanerpetontid remains, attributed to the genus *Celtedens*. However, recent works showed the frontal bones used to diagnose the species display important intraspecific variation. Here, we describe 468 bones from the Kimmeridgian-Tithonian Lourinhã Formation, together with remains from the Guimarota beds of the Kimmeridgian Alcobaça Formation. They support the erection of a new genus and species, characterized by a unique combination of four synapomorphies: a bulbous/flabellate outline of the internasal process of the frontal in dorsal or ventral view; no sculpture on postorbital wing of the parietals; the dorsal condyle of the axis with thickened edge; the long axis of the ilium strongly tilted posteriorly. This material is the oldest albanerpetontid species from the Iberian Peninsula and only the second

described from the Jurassic of Europe, at a time the Iberian Peninsula played a major paleobiogeographic role between Europe, northwestern Africa, and North America. Our results support the "Uña species" (Barremian, Spain) as closely related to *Wesserpeton evansae* (Barremian, England), and confirm the need to revise *Celtedens*. The material from the Lourinhã Formation suggest that other known multispecific microvertebrate bonebeds contain a greater variety of elements than is reported. We stress the need to review unpicked and unidentified material to look for other bones, instead of focusing on a couple of cranial bones, as they can help better characterizing this group.

Keywords: Albanerpetontidae; Upper Jurassic; Lusitanian Basin; Guimarota; Lourinhã Formation; systematics

3.2.1 Introduction

The albanerpetontids are usually recovered as isolated, disarticulated bones by sieving sediments, with only a handful of articulated specimens or three-dimensional skulls in association reported (McGowan & Evans, 1995; McGowan, 2002; Maddin *et al.*, 2013; Evans, 2016; Matsumoto & Evans, 2018; Daza *et al.*, 2020). Therefore, most of albanerpetontid taxonomy is based on isolated and highly diagnostic cranial bones, whereas the rest of the bones are considered much more conservative in the family (Gardner,

2000a, 2001; Gardner *et al.*, 2003; Gardner & Böhme, 2008; Sweetman & Gardner, 2013; Guillaume *et al.*, 2023b). Their fused frontals have, in particular, been long used to distinguish species (McGowan, 1998a; Gardner, 2000a). However, recent studies challenged this approach as albanerpetontid bones often exhibit intraspecific variation which conflict with available species diagnoses (Sweetman & Gardner, 2013; Guillaume *et al.*, 2023b).

The Portuguese albanerpetontid record in the Upper Jurassic is mainly known and represented by the Guimarota beds, from the Alcobaça Formation, Kimmeridgian in age (Schudack, 2000a), where thousands of specimens were recovered (Wiechmann, 2000, 2003). Nevertheless, some specimens were also reported in the coeval Lourinhã Formation (Wiechmann, 2003). Recent revision based on the frontal bone failed to discriminate material from both assemblages (Guillaume *et al.*, 2023b), highlighting its limitations as a diagnostic element to the species level, and should rather be used at the generic level with combination of other bones.

Here is presented the complete description of the new cranial and post-cranial albanerpetontid material from the Lourinhã Formation, found in association with the frontal bones previously mentioned, together with unpublished material from Guimarota. The observed intraspecific variation in the sample is also addressed, and we propose the erection of a new taxon.

3.2.2 Geological setting

Six vertebrate microfossil assemblages (later referred as VMA) localities were sampled in the outcrops at the top of cliffs in the municipality of Lourinhã (Portugal), namely from South to North: Valmitão VMA, red Valmitão VMA, Porto Dinheiro VMA, Zimbral VMA, Peralta VMA, and Porto das Barcas VMA (**Figure 3.2.1**). They are located within the Lourinhã Formation of the Lusitanian Basin, the largest sedimentary basin in Portugal (Wilson *et al.*, 1989; Alves *et al.*, 2003). The Lusitanian Basin is a rift basin situated along both the mainland and the adjacent continental shelf off the west and central coasts of Portugal. Its formation began with the opening of the North Atlantic Ocean, during the Late Triassic, and develops through four rift phases until the Cretaceous (Rasmussen *et al.*, 1998; Alves *et al.*, 2002; Kullberg *et al.*, 2006; Calvín *et al.*, 2023).

The Lourinhã Formation, deposited during the third rift phase, ranges from late Kimmeridgian to late Tithonian ages and lies between the Consolação unit and the Porto da Calada Formation (Taylor *et al.*, 2014; Mateus *et al.*, 2017). Its dominant continental deposits consist in sandy channel-fills and muddy floodplain deposits (Martinius & Gowland, 2011; Taylor *et al.*, 2014; Gowland *et al.*, 2017), and it is comprised of three members (**Figure 3.2.1D**): (1) the Porto Novo/Praia da Amoreira unit, Kimmeridgian; (2) the Praia Azul member, late Kimmeridgian – early Tithonian; and (3) the Santa Rita member, early Tithonian (Mateus *et al.*, 2017).

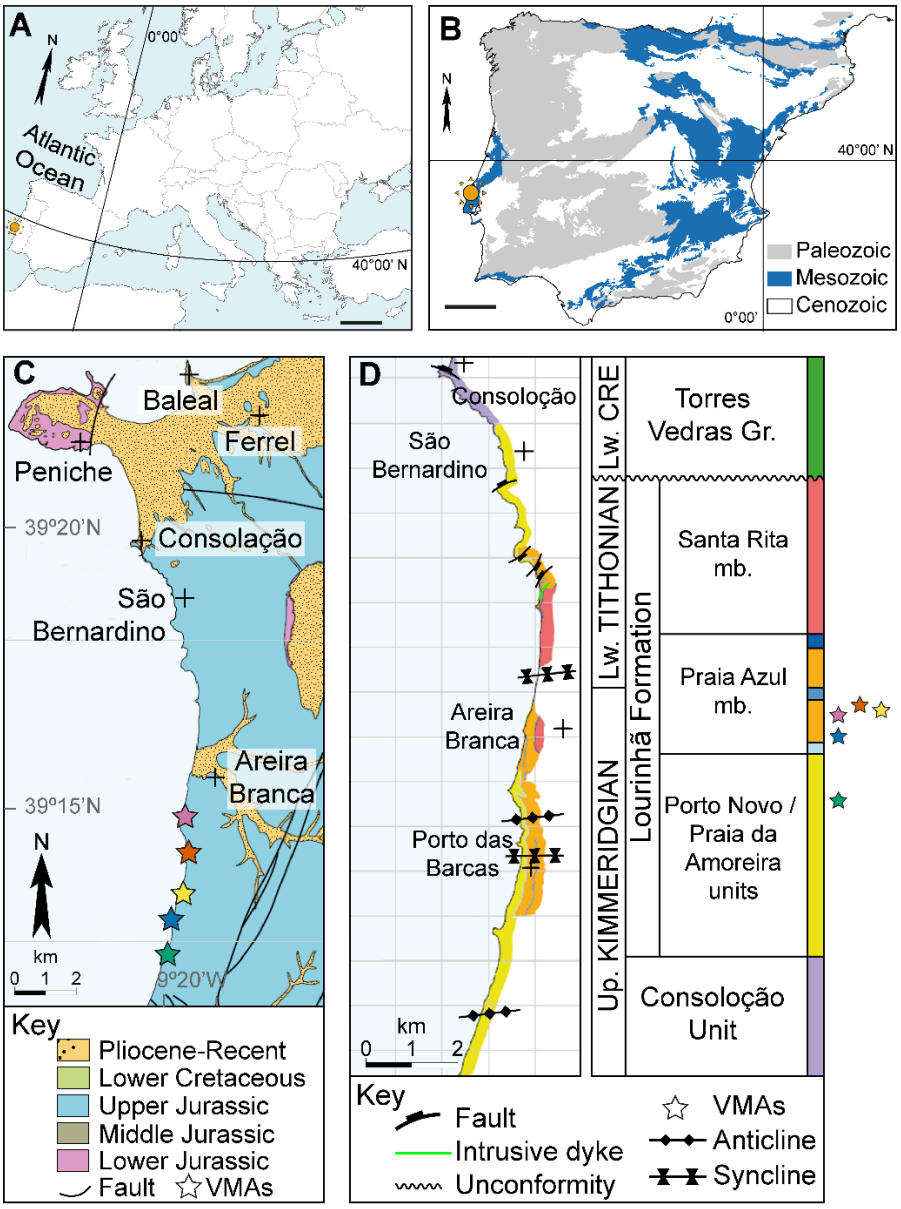

Figure 3.2.1: Geographical and geological context of the vertebrate microfossil assemblages (VMAs) localities from the Lourinhã Formation. **A**, Europe map modified from Erin Dill, scale represents 400 km. **B**, geological sketch of the Iberian Peninsula, showing the location of the study area (orange sun). **C**, map of the onshore part of the Consolação subbasin south of Peniche (modified from Taylor *et al.* 2014). The green star indicates the location of the Valmitão and red Valmitão VMAs, blue star is Porto Dinheiro VMA, yellow star corresponds to Zimbral VMA, vermillion star is Porto das Barcas VMA, and reddish-purple star indicates the location of Peralta VMA. **D**, north–south mapping of the main units in the area of study, and their corresponding chronostratigraphic framework and location of the sites indicated by stars (modified from Taylor *et al.* 2014, based on Mateus *et al.* 2017).

The Valmitão and red Valmitão VMAs are located in the upper half of the Porto Novo/Praia da Amoreira unit. The former lies on top of the latter and is distributed within a three meters thick mudstone layer with occasional intercalations of sandstones, while the latter constitutes a reddish mudstone layer. Porto Dinheiro, Zimbral, and Porto das Barcas VMAs are, from oldest to youngest, successive levels of the Praia Azul member.

These outcrops are respectively distributed within a metric greyish mudstone layer, between the first and second sandy bioclastic limestones characterizing the member (represented by blue levels in **Figure 3.2.1D**). Peralta VMA is the youngest, and it is located in the Praia Azul member, between the second and the third sandy bioclastic limestones.

Regarding the Guimarota fossil assemblage, these beds have consistently been considered as part of the Kimmeridgian Alcobaça Formation, based on ammonites, charophytes, ostracods, pollens, lithostratigraphic correlation, and isotopic analyses (Ribeiro *et al.*, 1979; Leinfelder & Wilson, 1989; Schudack *et al.*, 1998; Schudack, 2000a; Mateus *et al.*, 2017; Fürsich *et al.*, 2022).

The outcrop consists of two coal seams of similar structure, with intercalation of lignitic marls, occasionally rich in bivalve shells, separated by a single layer of around 5 meters thick limestone (Schudack, 2000b). However, the exact stratigraphic position of the studied specimens is

uncertain, and only the date of excavation is known (Gloy, 2000; Krebs, 2000a). Based on its similarity to other brown coal deposits and its geological setting, Guimarota has been regarded as a terrestrial to lagoonal environment similar to modern mangroves, with occasional freshwater influx and saltwater flooding (Gloy, 2000; Martin, 2000a).

3.2.3 Material and Methods

This study is based on 56 sample bags of sediments collected within the Lourinhã Fm in six different localities from the cliffs of Valmitão, Zimbral, Porto Dinheiro, Porto das Barcas, and Peralta (Lourinhã municipality, Portugal) during field campaigns between 2016 and 2022, representing a total rock sample of 1363 kg. They were dried, then disaggregated in water with hydrogen peroxide (H_2O_2, final solution at 0.5%), as cycles of physical and chemical processes are more efficient to break the rock (Eberth *et al.*, 2007a). The samples were screen-washed through a sieving table comprising of three levels of mesh (2 mm, 1 mm and 0.5 mm), then picked under stereomicroscopes.

In total, around 20,000 microfossils have been recovered, and identification and cataloguing of the material is ongoing. Most of them consist of charophytes and invertebrate remains, such as ostracods, gastropods, and incomplete bivalve shells fragments. However, the vertebrate microfossils include ray-finned fish scales and teeth; chondrichthyan teeth; disarticulated elements from lepidosaurs,

amphibians and unidentified archosauriforms; crocodylomorph teeth and osteoderms; dinosaurs and pterosaur teeth; tetrapod vertebral neural arches and long bone fragments; and dinosaur and crocodylomorph eggshells fragments (Guillaume *et al.*, 2023a).

To date, the five VMAs (Valmitão, red Valmitão, Zimbra, Porto das Barcas, and Peralta) have produced 468 bones attributed to Albanerpetontidae (**Figure 3.2.2A**). The specimens were recovered only from 1 mm and 0.5 mm fractions. Valmitão VMA is by far the most productive site, seconded by Zimbral and Porto das Barcas VMAs, while Peralta and red Valmitão VMAs have been only exploratory sampled, hence their low productivity. Cranial bones are usually the most frequent finds and appendicular bones are much less abundant; except in Zimbral, where cranial bones are found in similar quantities to axial bones, and red Valmitão, where appendicular bones are the most abundant elements.

Overall, vertebrae are the most common element, followed by dentaries, frontals, humeri, and premaxillae (**Figure 3.2.2B**). These are the element considered most diagnostic and, therefore, most well studied and most often described in the literature (Gardner, 1999c, 2000a,b; Gardner *et al.*, 2003; Gardner & Böhme, 2008; Sweetman & Gardner, 2013; Carrano *et al.*, 2022), as well as most often used to report indeterminate records (Grigorescu *et al.*, 1999; Rees & Evans, 2002; Folie & Codrea, 2005;

Skutschas, 2007; Blain *et al.*, 2010; Canudo *et al.*, 2010; Szentesi *et al.*, 2013).

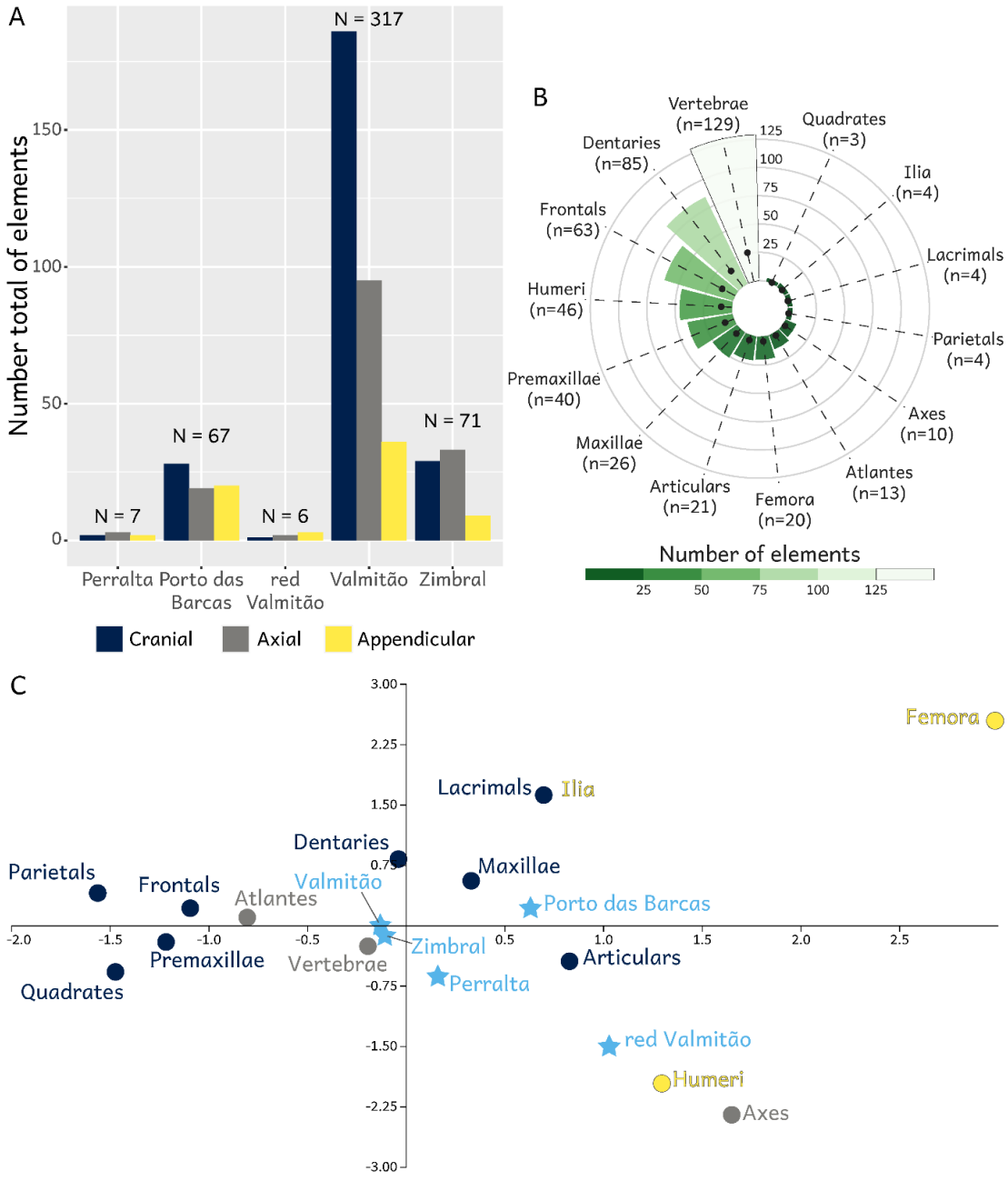

Figure 3.2.2: Count fossil remains referred to Albanerpetontidae collected from the Lourinhã Formation. **A**, count of elements by anatomical region for each five VMAs, with the number total of elements indicated on top of the bars. **B**, count by element, all VMAs combined together: the black dot *indicates* the mean between each VMAs. **C**, correspondence analysis scaling 1 (two first axes explained 76.484% of variation related to association).

However, Valmitão, Zimbral, and Peralta VMAs are strongly associated (**Figure 3.2.2C**), conveying relatively similar bone relative frequencies between them. Porto das Barcas VMA is slightly less similar, mostly influenced by its higher relative frequency in femora, more abundant there than in any other VMA. Red Valmitão VMA is apart from the rest, due to the high contribution of humeri and axes, but this pattern most likely results from an under-sampling bias, as these bones are usually much rarer and only 17 kg of sediments have been sampled, processed, and picked so far.

Additionally, historical specimens from the Alcobaça Fm have been included. They all come from the excavations of the Guimarota beds by Institut für Paläontologie, Freie Universität Berlin (IPFUB), and were previously studied (Wiechmann 2000), but never formally published with the exception of the frontals (Wiechmann, 2003; Guillaume *et al.*, 2023b). Therefore, these specimens are here formally published for the first time with their final accession numbers from Museu Geológico of Lisbon, representing 348 items. It is here noted that curation of the Guimarota material is still an ongoing process.

Thus, the exact number of elements remains unknown, as the accession numbers from MG refer to one sample box, which may contain several fragments (sometimes hundreds, or even mixed elements); but previous reports estimated to 9,000 the total number (Wiechmann, 2000).

Some specimens were already coated in gold (MG28502, MG28532, MG28677, and MG28694), and some are still embedded in coal (MG28396 to MG28402; MG28543).

On an important note, the specimen MG28568, an albanerpetontid premaxilla, is completely different in morphology, preservation, and colour to any other specimens, and thus does not belong to the Guimarota assemblage (see Appendix F.1 for more details). Comparison with images in the literature (SMNS 57819/1 and SMNS 57769/3; pl. 7, figs. 4, 5; Wiechmann 2003) has allowed to identify it as one of the SMNS specimens from Staatlichen Museum für Naturkunde Stuttgart (SMNS) assigned to *Albanerpeton inexpectatum* Estes & Hoffstetter 1976 from the Randecker Maar locality, early Miocene in age (Wiechmann, 2003). The specimen was probably mixed in the collections and inadvertently returned to Portugal with the rest of the material.

No lacrimals, quadrates, or ilia were reported from the Alcobaça Fm material. Because those three elements were poorly known when the material was processed, they were most likely not identified during the picking. However, it is uncertain if they were discarded with the sediments or put with other unidentified bones from the Guimarota beds, for which current housing and whereabouts are unknown. If they were misidentified at the time, they have not been found yet in the collections housed in the Museu Geológico in Lisbon. Similarly, no atlas is known from the Alcobaça

Fm, despite the bone being well known in albanerpetontid at the time as one of their key features (Gardner, 2001); therefore, it is unsure if they were misidentified, miscatalogued, or are truly absent of the assemblage.

Over 500 additional albanerpetontid remains were previously reported in the Lourinhã Formation (Wiechmann, 2003), but it is our understanding that they have been indistinctly stored with the specimens from the Guimarota beds since then and cannot be located among the thousands of specimens in that collection. Therefore, these specimens could not be set apart and were reviewed as part of the Guimarota assemblage. A selection of specimens from the Lourinhã Formation were µCT-scanned with a Nikon XT H 225 associated with CT Pro 3D file software at University College London in June 2022. More information on the parameters of the CT-scan is provided in Appendix F.2. The data were processed with Avizo Lite 2020.3.1 (Thermo Fisher Scientific) to create three-dimensional virtual models. As the specimens consists in isolated bones, the algorithm was not able to distinguish the bone from the remaining sediment in some of them (e. g. ML3012). The models were rendered with Blender 2.92.0, using the options "Smooth" (factor = 1; repeat = 10) and "Remesh" (voxel size = 0.008 m; adaptivity = 0 m).

Other relevant specimens were photographed with a Leica M165C stereomicroscope equipped with a Leica DFC295 camera and Leica Application Suite software v.4.10.0, developed by Leica Microsystems CMS

GmbH; and/or with a Jeol JSM 6400 Scanning Electron Microscope equipped with a digital computer for imaging acquisition (Universidad de Zaragoza facilities, Spain) and a SEM Hitachi SU3800 (NOVA School of Science and Technology, Portugal). The most representative specimens from Guimarota were photographed using a DinoLite AM7013MZT, using Dino software. Measurements were performed with ImageJ (Rasband, 2003). Specimens from the Lourinhã Fm are housed in the Museu da Lourinhã. All specimens from Guimarota are housed at Museu Geológico of Lisbon.

Institutional abbreviations

FCT-UNL, Faculdade de Ciências e Tecnologia – Universidade Nova de Lisboa; **IPFUB**, Institut für Paläontologie, Freie Universität Berlin; **IWCMS**, Isle of Wight County Museums Service, Sandown; **M**, Museo di Paleontologia, Napoli; **MCCM**, Museo de las Ciencias de Castilla La Mancha, Cuenca; **MG**, Museu Geológico, Lisbon; **ML**, Museu da Lourinhã; **NHMUK**, Natural History Museum, London; **OMNH**, Oklahoma Museum of Natural History, Norman, Oklahoma; **SMNS**, Staatlichen Museum für Naturkunde Stuttgart; **UALVP**, University of Alberta Laboratory for Vertebrate Palaeontology, Edmonton; **USNM**, National Museum of Natural History, Smithsonian Institution, Washington, DC; **TMM**, Vertebrate Paleontology Laboratory at the Jackson School Museum of Earth History, University of Texas, Austin, Texas; **YPMVP**, Yale Peabody Museum – Vertebrate Paleontology, New Haven, Connecticut.

3.2.4 Systematic palaeontology

Amphibia Linnaeus, 1758

Lissamphibia Haeckel, 1866

Albanerpetontidae Fox & Naylor, 1982

Albanerpetontidae gen. et sp. nov (New unnamed taxon 2)

Figure 3.2.3 to **Figure 3.2.17**, and **Figure F.2** to **Figure F.11** (in the appendices)

2003 *Celtedens guimarotae* Wiechmann, p24; pl. 1-2; pl. 5, fig. 4-5; pl. 6, fig. 3, 4, 6; pl. 7, fig. 1-3; pl. 8, fig. 2, 4, 5; pl. 9, fig. 1-8, 11-14; pl. 10, fig. 1, 2. 13-16; pl. 11, fig. 1-4, 19-22; pl. 12, fig. 1, 2, 6-10 ("Wiechmann's thesis is freely available online; however, the new species proposal has never been published otherwise, and thus, according to the ICZN, it does not meet the criteria for a valid nomenclatural published work (Arts. 8 & 9). [...] Thus, the name remains unavailable." (Martín *et al.*, 2012)).

Figured specimens from the Lourinhã Formation (**Figure 3.2.3** to **Figure 3.2.17**)—ML2743, one fused frontal (putative holotype; **Figure 3.2.5D**); premaxillae (n=4): ML2912-ML2915; maxillae (n= 2): ML2937-ML2938; frontals (n=3): ML2738–ML2739, ML2741; lacrimal (n=1): ML2947; parietals (n=2): ML2949-ML2950; dentaries (n=5): ML2951-ML2955; articular (n=3): ML2999-ML3001; quadrates (n=3): ML3009-ML3011; atlantes (n=2): ML3012-ML3013; axes (n=2): ML3018-ML3019; trunk &

caudal vertebrae (n=2): ML3023-ML3024; humeri (n=6): ML3103, ML3108-ML3112; ilium (n=1): ML3128; femora (n=2): ML3130-ML3131.

Figured specimens from the Alcobaça Formation (**Figure F.2** to **Figure F.11**, specimen numbers with asterisk refer to multiple elements sharing same number)—premaxillae (n=14): MG28583, MG28585, MG28600*, MG28611–MG28612, MG28624–MG28626, MG28630*, MG28645, MG28650–MG28651, MG28678, MG28682; maxillae (n=5): MG28432, MG28487, MG28675, MG28683, MG28724; frontals (n=16): MG28426–MG28427, MG28473, MG28502, MG28520–MG28521, MG28532, MG28539, MG2851, MG28543, MG28562*, MG28570, MG28572, MG28692, MG28694, MG28733; parietals (n=5): MG28595, MG28627, MG28646, MG28658, MG28672*; dentaries (n=24): MG28400, MG28407, MG28409, MG28412, MG28423, MG28428–MG28429, MG28431, MG28456, MG28474, MG28481, MG28534–MG28536, MG28551, MG28636*, MG28652, MG28657, MG28659*, MG28662, MG28670, MG28677*, MG28681, MG28685; articular (n=2): MG28208*, MG28677*; axes (n=7): MG28545, MG28666, MG28698, MG28705, MG28722, MG28730–MG28731; trunk & caudal vertebrae (n=9): MG28425, MG28450, MG28499, MG28555, MG28574–MG28575, MG28716 ,MG28729, MG28736; humeri (n=5): MG28443, MG28506, MG28690, MG28703, MG28720.

Putative diagnosis

New unnamed taxon 2 is an Albanerpetontidae with bell-shaped fused frontals differentiated from other members of this family by the following unique combination of four synapomorphies: bulbous/flabellate outline of the internasal process of the frontal in dorsal or ventral view (1*); no sculpture on postorbital wing of the parietals (2*); dorsal condyle of the axis with thickened edge (3*); long axis of the ilium strongly tilted posteriorly (4*). The number with an asterisk refers to said characters indicated and highlighted in the **Figure 3.2.5**, **Figure 3.2.7**, **Figure 3.2.13**, and **Figure 3.2.16**.

Putative differential diagnosis

New unnamed taxon 2 differs from *Anoualerpeton* by a flabellate (fan-shaped) internasal process of the frontal bones with bulbous and broad shape. It differs from *An. unicum* and *Celtedens megacephalus* by a parietal with a unique ventral anteromedial-posterolateral transverse crest and frontal bones with convex, beveled ventrolateral crests, instead of V-shaped; and further from *C. megacephalus* by a much less pronounced saddle-shaped cotylar facet of the glenoid fossa in the articular. It differs from all albanerpetontid for which the articular is known, but the "Purbeck species", by a falcate (sickle-shaped) ventral facet posterior apex on the medial surface. New unnamed taxon 2 differs from the "Purbeck species", *W. evansae*, *Y. perettii*, an *A. ektopistikon* by having a long axis of iliac shaft strongly tilted posteriorly. It differs from *Celtedens ibericus* by more curved

orbital margins of the frontal bones and an acetabulum with a more convex dorsal margin. New unnamed taxon 2 differs from *Wesserpeton*, *Yaksha*, *Shirerpeton*, *Albanerpeton*, and all more deeply nested albanerpetontid unformal species by frontal bones with a bell-shaped outline and a suprapalatal pit facing laterolingually. It further differs from *Shirerpeton isajii* by a parietal with short dorsally sculptured postorbital wing, a straight lateral margin, and without a secondary ventral transverse crest; and from *Yaksha perettii* and *Wesserpeton evansae* by a nasal process of the maxillae round to blunt, and a less pronounced saddle-shaped cotylar facet of the glenoid fossa in the articular. New unnamed taxon 2 further differ from *Albanerpeton* by frontal bones with convex, beveled ventrolateral crests, instead of V-shaped; and all *Albanerpeton* species but *A. arthridion* and *A. ektopistikon* by a small, oval, and relatively high suprapalatal pit. It differs from *Y. perettii* and the unformal "robust snouted clade" *sensu* Gardner 2002 by sutured and gracile premaxillae. New unnamed taxon 2 differs from *A. ektopistikon*, the "Blasi 2B species", and *A. pannonicum* by reniform anterior cotyles of the atlantes; and from the "Blasi 2B species", *A. inexpectatum*, and *A. pannonicum* by mediolaterally straight, shallow groove directly posterior to the anterior cotyle margins and anterior to the neural arch attachments in the atlantes. To complement the diagnosis, an extended comparison is provided in Appendix F.3.

Referred material

Lourinhã Fm—premaxillae (n=36): ML2916–ML2936, ML3139–ML3153; maxillae (n=24): ML2939–ML2946, ML3154–ML3169; frontals (n=57): ML2740, ML2742, ML2744–ML2749, ML2751–ML2772, ML2901–2911, ML3170–ML3187; lacrimals (n=3): ML2948, ML3188–ML3189; parietals (n=2): ML3190–ML3191; dentaries (n=80): ML2956–2998, ML3192–3228; articular (n=18): ML3002–ML3008, ML3229–ML3239; quadrate (n=1): ML3011; atlantes (n=11): ML3014–ML3017, ML3240–ML3246; axes (n=8): ML3020–ML3022, ML3240–ML3246; trunk & caudal vertebrae (n=127): ML3025–ML3101, ML3252–ML3301; humeri (n=40): ML3102, ML3104–ML3107, ML3113–ML3127, ML3302–ML3321; ilia (n=3): ML3129, ML3322–ML3323; femora (n=18): ML3132–ML3138, ML3324–ML3334.

Alcobaça Fm (specimen numbers with asterisk refer to multiple elements sharing same number)—premaxillae (n=18): MG28448, MG28562*, MG28568, MG28581, MG28582, MG28584, MG28596–MG28560*–*, MG28613–MG28615, MG28630*, MG28641, MG28661, MG28718*; maxillae (n=38): MG28430, MG28439, MG28442, MG28445, MG28447, MG28454–MG28455, MG28457, MG28461, MG28464, MG28466, MG28476–MG28478, MG28482, MG28488–MG28489, MG28482, MG28501, MG28504, MG28519*, MG28522*, MG28576, MG28578–MG28579, MG28608, MG28610, MG2649, MG28674, MG28680, MG28686–MG28689, MG28702, MG28725–MG28727; frontals (n=28): MG28436, MG28444, MG28451, MG28459, MG28491, MG28500, MG28516, MG28524, MG28527, MG28531, MG28533, MG28542, MG28559, MG28562*, MG28564, MG28569,

MG28571, MG28639, MG28648, MG28667, MG28691, MG28707, MG28710, MG28713–MG28714, MG28717, MG28721, MG28732; parietals (n=3): MG28580, MG28643, MG28708; dentaries (n=156): MG28278, MG28280, MG28294–MG28296, MG28298–MG28334, MG28336–MG28355, MG28357–MG28359, MG28361–MG28365, MG28367–MG28384, MG28386–MG28398, MG28401–MG28406, MG28408, MG28410–MG28411, MG28413–MG28415, MG28418–MG28420, MG28446, MG28453, MG28458, MG28503, MG28518, MG28528, MG28544, MG28548–MG28550, MG28560–MG28561, MG28609, MG28623, MG28636–MG28638*-*, MG28640*, MG28642; MG28644*, MG28653–MG28656, MG28659–MG28660*-*; MG28663–MG28665, MG28668–MG28669, MG28676, MG28679, MG28693*, MG28695*, MG28697*, MG28699*, MG28701*, MG28704*, MG28712, MG28723, MG28746; axes (n=2): MG28706, MG28719; trunk & caudal vertebrae (n=6): MG28422, MG28554, MG8576, MG28728, MG28737, MG28744; humeri (n=10): MG28399, MG28671, MG28696, MG28700, MG28709, MG28715, MG28735, MG28738–MG28739, MG28745; boxes of mixed content (n=5): MG28277, MG28536, MG28562 MG28672, MG28673.

Stratigraphic and geologic range—Known from the Kimmeridgian and the Tithonian of the Lourinhã Formation, where it has been recorded in five different horizons (Lourinhã municipality, district of Lisbon); and from the Kimmeridgian of the Alcobaça Formation, where it has been recorded only in the Guimarota lignite beds (District of Leiria).

Description

Premaxilla (**Figure 3.2.3**; **Figure F.2** and **Figure F.3**)

The premaxillae are gracile, although bigger specimens tend to be slightly more robust (e.g. ML2912, **Figure 3.2.3A**; MG28611, **Figure F.2B** MG28645, **Figure F.3A**). The teeth are non-pedicellate, tricuspid, pleurodont, and mesio-distally compressed, and numbered up to 11 based on the most complete specimens from the Alcobaça Fm (e.g. MG28650, **Figure F.3C**). None of the paired premaxillae found are fused, they rather display a medial groove extending from the dorsal boss to the *pars dentalis*, suggesting they were rather sutured during the life of the animal (**Figure 3.2.3Cc**). One of the MG28645 specimens (**Figure F.3A)** is the only one to display a small peg, at the level of the *pars dentalis*, while in MG28600 (**Figure F.2A**), MG28612 (**Figure F.2C**), and MG28625, there is a lateral invagination at the level of the *pars dentalis*. The *pars dentalis* exhibits a broad, spatulate, smooth labial emargination on its posterolabial surface, making the articular facet for the maxilla (**Figure 3.2.3Da**).

The *pars dorsalis* is straight. The facet of the dorsal edge is absent in MG28624 (**Figure F.2D**) and in the specimens from the Lourinhã Formation (**Figure 3.2.3**). However, the edge can protrude in MG28650 (**Figure F.3C**)**,** and MG28678. The facet can either be faint, with an occasional a small peg (MG28682), or indented as in other specimens from the Alcobaça Fm. The laterodorsal contact displays a small laterodorsal notch with articular facet (**Figure 3.2.3Ad** and **Bd**).

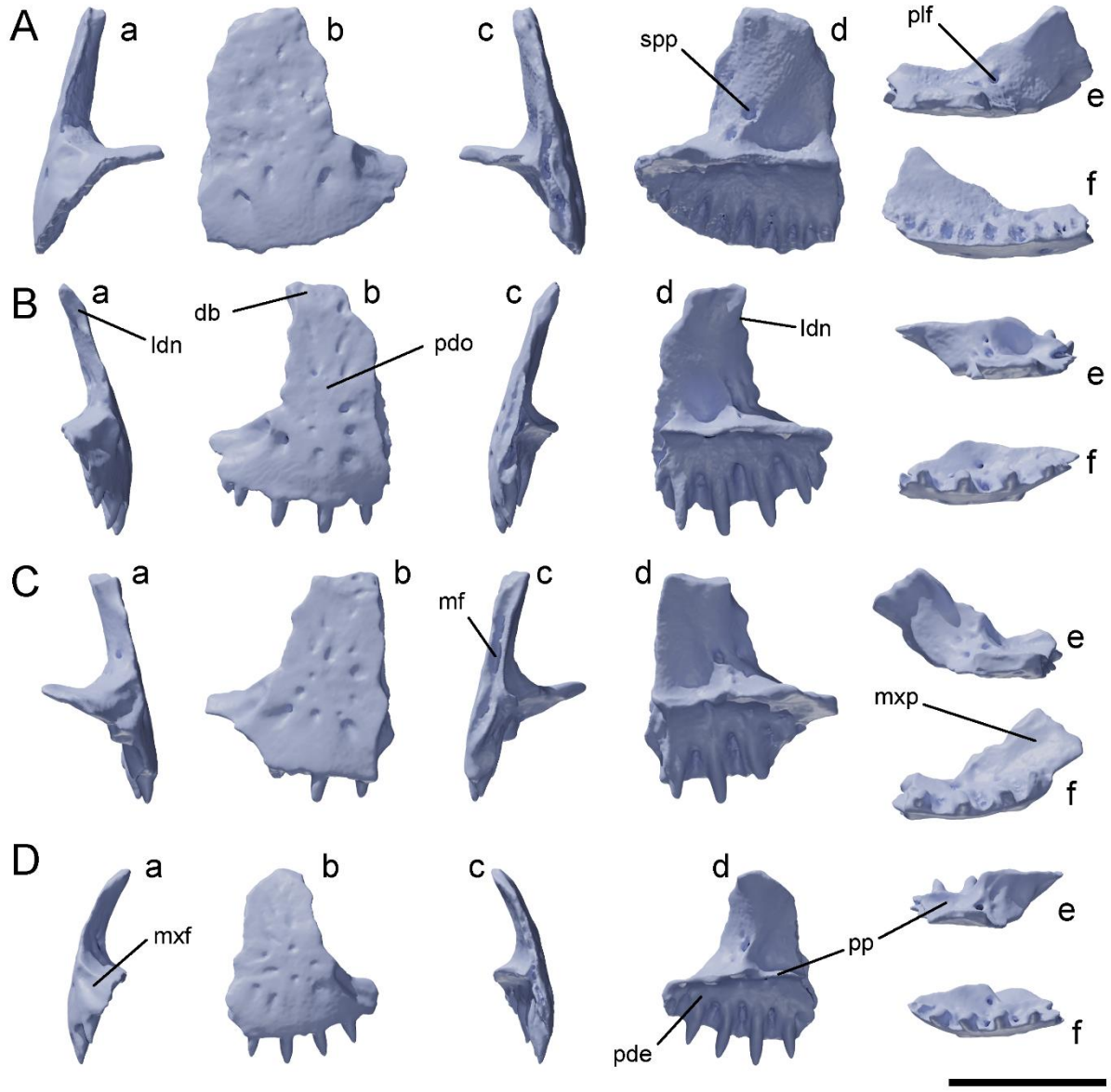

Figure 3.2.3: New unnamed taxon 2 images of three-dimensional models of premaxillary bones. **A**; left premaxilla ML2912 in lateral (a), labial (b), medial (c), lingual (d), dorsal (e), and ventral (f) views. **B**; right premaxilla ML2913 in lateral (a), labial (b), medial (c), lingual (d), dorsal (e), and ventral (f) views. **C**; right premaxilla ML2914 in lateral (a), labial (b), medial (c), lingual (d), dorsal (e), and ventral (f) views. **D**; left premaxilla ML2915 in lateral (a), labial (b), medial (c), lingual (d), dorsal (e), and ventral (f) views. Abbreviations: **db**, dorsal boss; **ldn**, laterodorsal notch; **mf**, medial flange; **mxf**, maxillary facet; **mxp**, maxillary process; **pdo**, *pars dorsalis*; **pde**, *pars dentalis*; **plf**, palatal foramen; **pp**, *pars palatinum*; **spp**, suprapalatal pit. Scale bar is 1 mm.

The labial surface of the *pars dorsalis* is ornamented by irregular pits of different size (e. g. **Figure 3.2.3Bb**). They cover around ¾ of the *pars dorsalis* lower part, between the *pars dentalis* and the dorsal boss, and can become rugous on the upper half.

The dorsal boss can be indistinct (**Figure 3.2.3Bb**) or prominent (**Figure F.2B** and **Figure F.3A**), being in both cases either smooth with small foramens or ornamented similarly than the frontal bones. A small suprapalatal pit is visible on the labial surface of the *pars dorsalis* (e. g. **Figure 3.2.3Ad**). It is facing laterally to laterolingually and can be single or divided. Furthermore, the lateral internal strut is perforated by 2 to 3 foramina.

The *pars palatinum* can be perforated by up to two foramina, however the palatal foramen can be absent or clogged in some specimens. When present, its ventral and dorsal openings are medial to the suprapalatal pit (e.g. **Figure 3.2.3Ae**), making the canal between them strictly dorsoventral to subvertical. The diameter of the palatal foramen varies from minute to being similar to the cross-section of adjacent premaxillary teeth (MG28583, MG28585, MG28626, and MG28645 **Figure F.3A**). The vomerine process is not sutured and displays a shallow lingual facet (**Figure F.2B**); while the lingual facet of the maxillary process displays a facet with a drumlin-shaped knob (**Figure 3.2.3Cf**).

Remarks—Premaxillae in albanerpetontids have always been distinguished between gracile and robust morphotypes (Fox & Naylor, 1982; Gardner, 2000*a*, 2002). However, some more discrete variations may occur: New unnamed taxon 2 displays gracile premaxillae, but they seem more robust than the specimens from Angeac-Charente from the Berriasian of France, while *Albanerpeton galaktion* Fox & Naylor 1982 and *Albanerpeton gracile* Gardner 2000*b* from the latest Upper Cretaceous of North America, and the "Blasi 2B species" look slightly more robust (ARDG, pers. obs., 2023, see Section 3.3). Furthermore, the "Sânpetru species" was originally described with a robust premaxilla (Folie & Codrea, 2005); but figured specimens clearly belong to the gracile morphotype, as suggested in later studies (Carrano *et al.*, 2022).

As seen in some other species, New unnamed taxon 2 displays a prominent ornamented boss; but, as previously noticed in *Wesserpeton evansae*, the prominence of the boss can be variable among specimens, suggesting some level of intraspecific variation and, most likely, preservation bias (Sweetman & Gardner, 2013).

The suprapalatal pit of the *pars dentalis* is a distinctive element of the premaxillae, although its function remains unknown. It has been suggested that it would have housed some kind of gland (Fox & Naylor, 1982), whose function, most likely linked to feeding, olfaction, or both, is still unsure (Gardner, 2000*a*). Furthermore, the dorsal opening of the palatal foramen

being located nearby the suprapalatal pit—in some species, within the ventral edge of the pit itself—would also suggest it held a duct connected to this gland (Gardner, 2000a). The variation of size among species, as well as its orientation, associated with a variation of size of palatal foramen and the orientation canal between dorsal and ventral opening, would imply a different size of assumed gland, and most likely different prevalence and function in the ecology of each species (Gardner, 2000a).

Combined with a stronger ossification of the premaxillae, becoming more robust and more consistently fused (Gardner, 2000a, 2002; Gardner & Böhme, 2008), the anatomical variations in the suprapalatal pits and the palatal foramen could suggest an ecological shift may have occurred between older species and younger species. See discussion for more details on albanerpetontid ecology.

As observed in *W. evansae*, the suprapalatal pit in New unnamed taxon 2 can be either single or divided, but with less prevalence than 1/3 of the specimens in the latter (Venczel & Gardner, 2005). This variation might represent intraspecific variation in this character (Sweetman & Gardner, 2013), but preservation bias may also interfere with the interpretation. Indeed, it requires to have enough specimens preserved to evaluated the prevalence, while most of the species are known only be few, and some only by one premaxillary bone (Gardner, 1999b; Daza *et al.*, 2020).

The suprapalatal pit in *Celtedens ibericus* was reported small and oval, but facing lingually (Gardner *et al.*, 2003). In contrast, it faces laterolingually in the stratigraphically older New unnamed taxon 2, both *Anoualerpeton* species, the 'Purbeck specimens', and the Guelb el Ahmar specimens (ARDG, pers. obs., 2023). However, this feature was never mentioned in the osteological descriptions of *C. ibericus* (McGowan & Evans, 1995; McGowan, 2002); and it actually appears to be obscured by sediments and crushed bones in the holotype MCCM-LH 6020, and to be covered by the matrix in the referred specimen MCCM-LH 15710 (ARDG, pers. obs., 2023), the only two specimens that preserved the premaxilla. Therefore, until CT-scan allows to uncover the part hidden in the matrix, this character cannot be assessed in *C. ibericus*.

Maxilla (**Figure 3.2.4**; **Figure F.4**)

The maxillae of New unnamed taxon 2 are slender, elongated, and posteriorly tapered. The bone seems to become more robust with increasing size in the Alcobaça specimens (**Figure F.4**), notably the area of the lacrimal and jugal facets. The dorsal edge of the *pars facialis* is bevelled at the base of the nasal process, with a small shelf to articulate with the lacrimal and a tapering jugal process (**Figure 3.2.4**, **Figure F.4C** and **D**), which exhibits a faint scar on the internal edge. The labial surface is ornamented with two rows of five (ML2938, **Figure 3.2.4Bd**) to eight foramina (ML2937, **Figure 3.2.4Ad**). These are organized in arcs or circles, centred below the nasal process.

The tooth count ranges between 15 and 32. The tooth row extends anteriorly to the nasal process by more than two teeth, and displays heterodonty, with the tallest teeth posterior to the nasal process (**Figure 3.2.4Bb**, **Figure F.4A**, and **E**). The nasal process has a triangular, round to acute apex (**Figure 3.2.4Ad**), which can faintly project anteriorly (ML2938, **Figure 3.2.4Bd,** and **Figure F.4**). The *pars dentalis* narrows posteriorly, with a ventral margin shallowly convex in lingual and labial view (**Figure 3.2.4Bb**, **Figure F.4A**, and **E**). The premaxillary dorsal process is a labially projected shelf (**Figure 3.2.4Bb**), triangular in dorsal view (**Figure 3.2.4Bc** and **Figure F.4**). Its extremity is dorsally curved and exhibits an idented articular facet (**Figure F.4C**).

The premaxillary lateral process is an anteriorly projected spatulated to acute flange (**Figure 3.2.4Bd** and **Figure F.4E**), which displays a horizontal ridge midway. The *pars palatinum* is tapered posteriorly, forming the jugal process. Its saddle-shaped dorsal surface extends up to the surface of the nasal process, with up to three foramina on the dorsolingual surface (**Figure 3.2.4A**). The *pars palatinum* extends lingually into a shelf, forming the maxillary shelf, which displays a ventral shallow trough bordered by the internal narial margin (**Figure 3.2.4Ac** and **Bc**). The width of the shelf remains relatively constant between specimens but become broader in the big ones. The internal narial margin becomes dorsally and labially indented around the nasal process, forming the narial choana (**Figure 3.2.4Ab** and **Bb**).

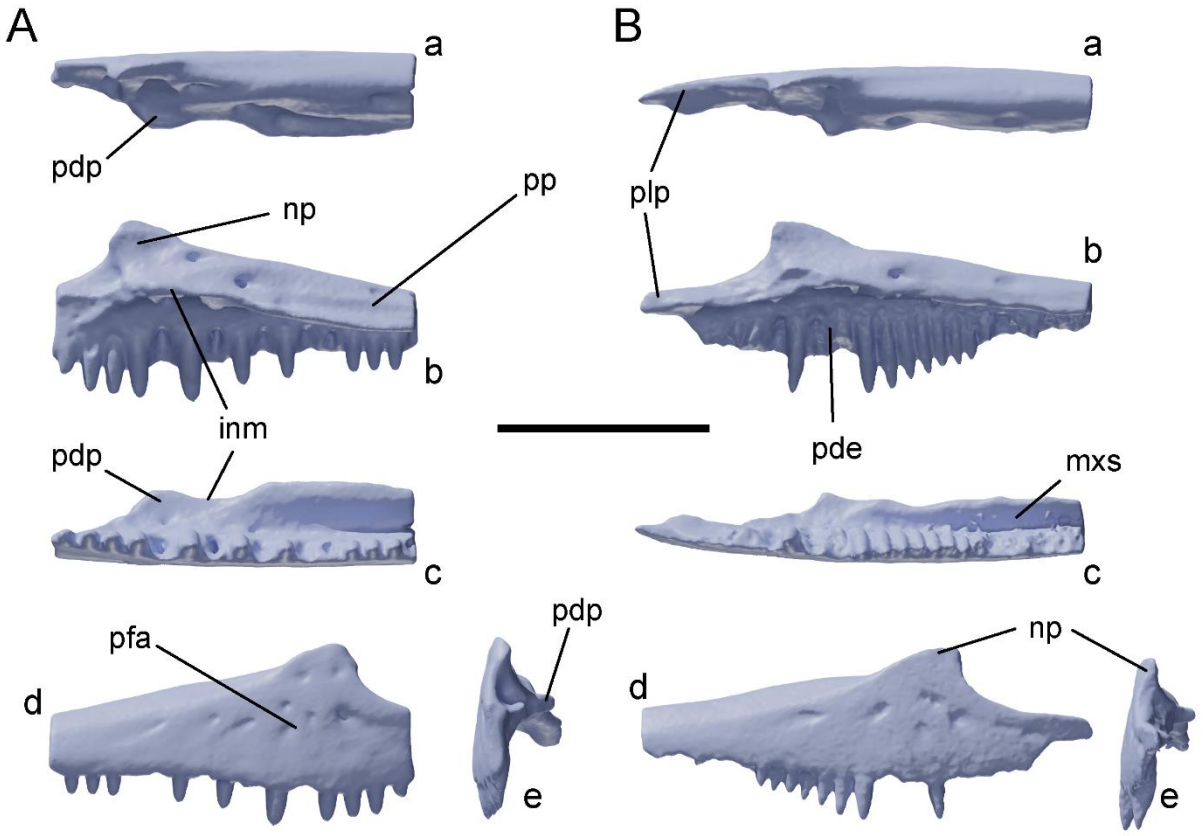

Figure 3.2.4: New unnamed taxon 2 images of three-dimensional models of maxillary bones. **A**; right maxilla ML2937 in dorsal (*a*), lingual (b), ventral (c), labial (d), and anterior (e) views. **B**; right maxilla ML2938 in dorsal (*a*), lingual (b), ventral (c), labial (d), and anterior (e) views. Abbreviations: **inm**, internal narial margin; **mxs**, maxillary shelf; **np**, nasal process; **pde**, *pars dentalis*; **pdp**, premaxillary dorsal process; **pfa**, *pars facialis*; **plp**, premaxillary lateral process; **pp**, *pars palatinum*. Scale bar is 1 mm.

Remarks—Although this feature has not been formally described in the literature, maxillae in New unnamed taxon 2 seem less robust than in *Albanerpeton arthridion*, *A. gracile*, *A. galaktion*, *A. nexuosum*, *A. inexpectatum*, *A. pannonicum*, *Shirerpeton isajii*, the "Sânpetru species", and the "Paskapoo species". The maxilla in *Celtedens megacephalus* is preserved but obscured by the dentary, thus cannot be compared (ARDG, pers. obs., 2022); as well as in *C. ibericus*, for which MCCM-LH 030B, MCCM-LH 17069, and MCCM-LH 6020B preserved the maxilla, but the bones are

either crushed or obscured to distinguish informative characters (ARDG, pers. obs., 2023).

The variation in the shape of the triangular nasal process, have been already reported in albanerpetontids (Matsumoto & Evans, 2018), as well as how much it projects anteriorly and how much its anterior edge is curved (Carrano *et al.*, 2022). The use of geomorphometrics could help to better characterize the discrete variations between species, but it may be limited by the fact that few maxillae are well-enough preserved, keeping the sample size small (Matsumoto & Evans, 2018). Similar conclusions can also be reached for the proportions and outlines of the lateral premaxillary process, which is also known to be variable in albanerpetontids (Gardner, 2000a, 2002; Wiechmann, 2003; Matsumoto & Evans, 2018); or with the dorsal curvature of the anterolingual extremity of the dorsal premaxillary process, that can be strongly marked in *Yaksha perettii*, *A. gracile*, and *A. galaktion*, making it look almost vertical (ARDG, pers. obs., 2023).

Albanerpeton gracile has been described with a tooth row not extending anteriorly to the maximum indentation on anterior leading edge of the nasal process (Gardner, 2000b); however, specimen OMNH 60325 displays at least two loci anterior to the leading edge of the nasal process (ARDG, pers. obs., 2023). The ventral margin in *A. ektopistikon* has been described as slightly sinuous, but with a weak heterodonty (Carrano *et al.*, 2022); although this feature seems less obvious on specimens observed in

USNM and pictured in the original work. However, as observed in *A. nexuosum*, it may be because of the preservation (Gardner, 2000b).

An internal narial margin, usually embayed, has been reported in the *pars palatinum* of the maxillae (Gardner, 2000b; Gardner *et al.*, 2003; Venczel & Gardner, 2005; Sweetman & Gardner, 2013; Carrano *et al.*, 2022), which has been interpreted as the lateral margin of the choana (Matsumoto & Evans, 2018). However, albanerpetontids seem to display various degrees of indentation, being more or less marked from one species to another. This variation could also be characterized with the help of geomorphometrics, especially since the indentation can either varies lingually, dorsally, or both. It is unclear how much the internal narial margin is indented *Shirerpeton isajii*, although described as "distinct" (Matsumoto & Evans, 2018); and the "Sânpetru species" seems to display a strong dorsal indentation in figured specimens (Folie & Codrea, 2005), but it is unsure if it is also indented labially.

Frontal (**Figure 3.2.5** and **Figure F.5**)

Frontal bones are characterized by a general bell-shaped outline and a flabellate, bulbous-shaped internasal process. The small anterolateral processes display an acute apex. The ventrolateral crests are convex ventrally and ridge-like in transverse profile, with the orbital margin bevelled and facing ventrolaterally. A weak ventromedian suture extend anteriorly towards the middle part of the bones. Although all specimens are

generally similar, some differences can be noted: (i) the dorsal ornamentation is more developed in adults, while it is more vermicular and shallower in younger specimens; (ii) the internasal process is relatively shorter in adult; (iii) the ventrolateral crest are wider and extend posteriorly after the parietal border in adults; and (iv) the ventromedian suture is less marked in adults. See Guillaume *et al.* (2023b) for a detailed description of the frontal bones and discussion on their intraspecific variation.

Remarks—Frontals have been used for years in Albanerpetontidae to differentiate species (McGowan, 1998a; Gardner, 2000a), but previous works on the Portuguese material show their limitations (Guillaume *et al.*, 2023b). At that time, the Portuguese frontals were attributed to aff. *Celtedens* sp., based on the bell-shaped outline of the frontal bone, with a curved orbital margin and a broad, and blunt internasal process (Guillaume *et al.*, 2023b); diagnostic features for the genus as currently defined (McGowan & Evans, 1995; McGowan, 1998a).

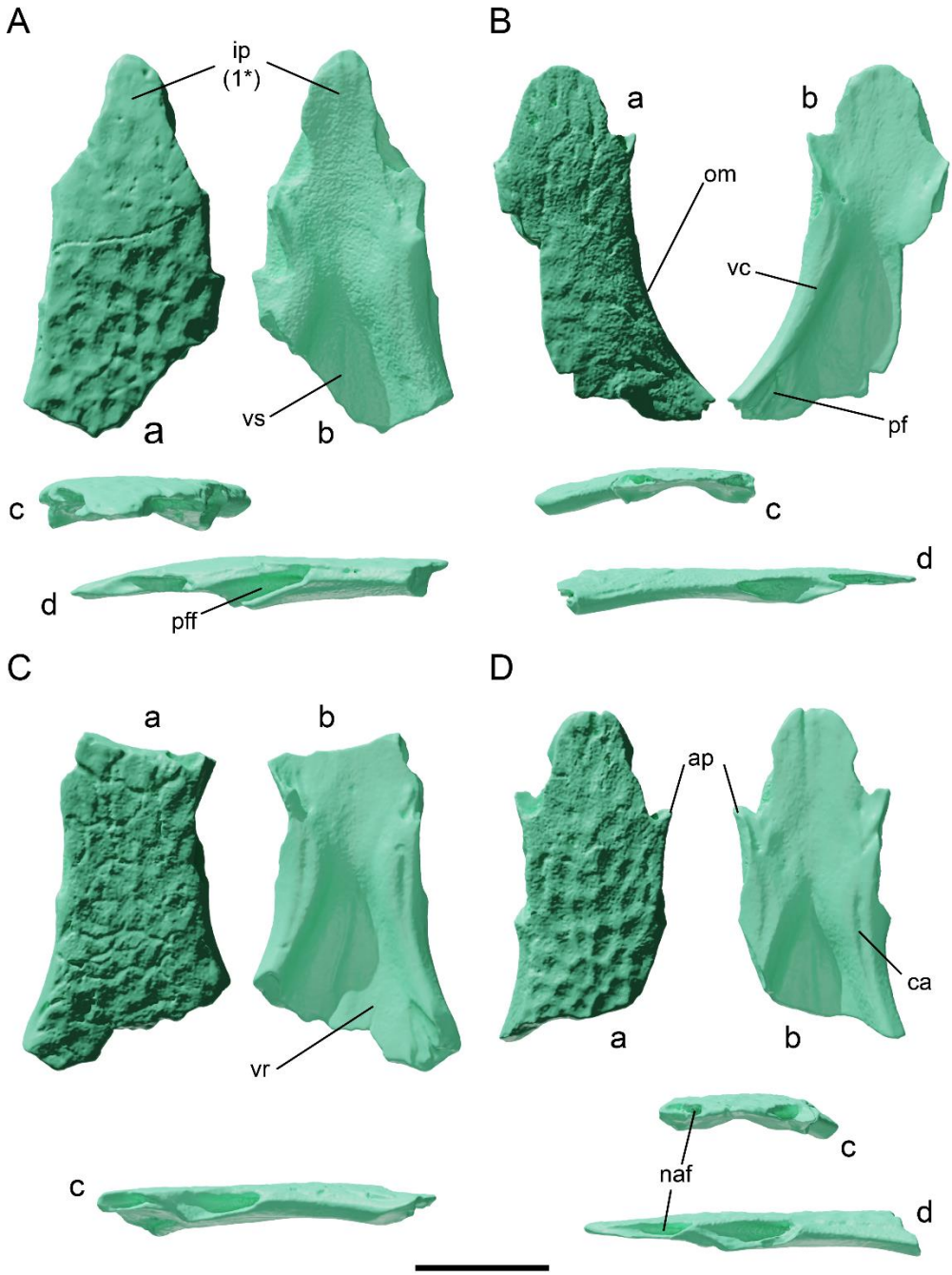

Figure 3.2.5: New unnamed taxon 2 images of three-dimensional models of fused frontal bones. **A**; frontal ML2741 in dorsal (*a*), ventral (b), anterior (c), and lateral (d) views. **B**; frontal ML2738 in dorsal (*a*), ventral (b), anterior (c), and lateral (d) views. **C**; frontal ML2739 in dorsal (*a*), ventral (b), and lateral (c) views. **D**; frontal ML2743 (putative holotype) in dorsal (*a*), ventral (b), anterior (c), and lateral (d) views. Abbreviations: **ap**, anterolateral process; **ca**, canal; **ip**, internasal process; **naf**, nasal facet; **om**, orbital margin; **pf**, parietal facet; **pff**, prefrontal facet; **vc**, ventrolateral crest; **vr**, ventral roof; **vrd**, ventral ridge of the anterolateral process; **vs**, ventromedian suture. Scale bar is 1 mm.

However, revision of the Spanish and Italian material casts doubts on the validity of these characters to define *Celtedens*. Indeed, the internasal process is not preserved—or at the very least, obscured—in the holotype and only specimen of *C. megacephalus*, while it is poorly preserved in the holotype MCCM-LH6020 of *C. ibericus* (ARDG, pers. obs., 2023). Only the referred specimen MCCM-LH15710 of *C. ibericus* preserved the internasal process, which looks broad but tapered (Carrano *et al.* 2022; S. Sweetman, pers. comm., 2022; see Fig. 18B in Matsumoto & Evans 2018). This morphology clearly differs from the original diagnosis, and from New unnamed taxon 2.

Furthermore, *Celtedens ibericus* and *C. megacephalus* differ in the overall shape of their frontals: the latter has more curved orbital margins (McGowan, 1998a), as observed in New unnamed taxon 2, than the former. Therefore, the frontal in *C. megacephalus* can be described as bell-shaped; while it can be described as hourglass-shaped in *C. ibericus*. Both morphologies are now considered strictly different (Carrano *et al.*, 2022), and cannot be used to diagnose the genus, as previously thought (Gardner, 2000a); especially since they are shared with *Anoualerpeton*.

Lacrimal (**Figure 3.2.6**)

Although being the most complete lacrimal specimen of the assemblage, ML2947 is missing the posterodorsal-most part of the dorsal process (dorsal arm *sensu* Venczel & Gardner (2005)) that would articulate

with the frontal and prefrontal. No ornamentation, neither labial nor lingual, could be observed. It exhibits a broad U-shaped overall outline but does not exhibit trough between dorsal and ventral process (ventral arm *sensu* Venczel & Gardner (2005)). This surface of the bone is smooth, only perforated by a large foramen, with a pandurate opening on the labial surface.

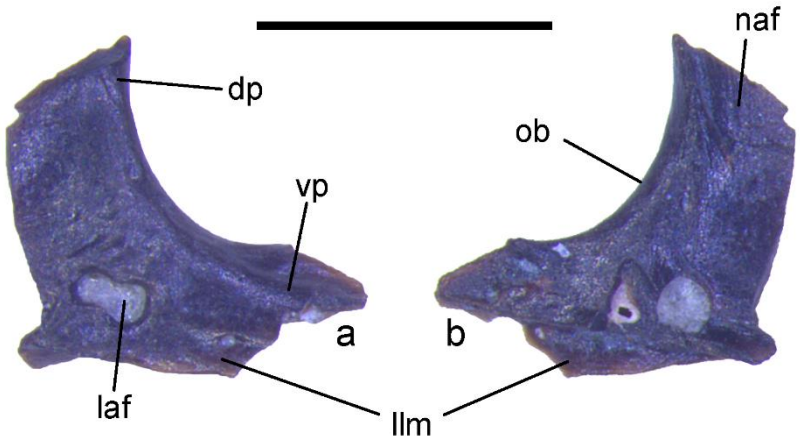

Figure 3.2.6: New unnamed taxon 2 lacrimal bone ML2947 in labial (a) and lingual (b) views. Abbreviations: **dp**, dorsal process; **laf**, lacrimal foramen; **llm**, lateral lamina; **naf**, nasal facet; **ob**, orbital border; **vp**, ventral proces. Scale bar is 1 mm.

The ventral process extends posteroventrally, to encapsulates the *pars palatinum* and the *pars facialis* of the maxilla. The dorsal process extends and flattens dorsoposteriorly, forming a large crest, and exhibits a concavity on the labial surface, the nasal facet. The anterior end is broken but seems to have been blunt; it displays a small process forming a shelf projecting anterolingually. A thick rim flanks the posterior margin, forming the orbital border. It oversteps on the lingual surface and participates into a small lingual facet at the posterior extremity of the ventral process.

Remarks—The lacrimal bones are extremely brittle in albanerpetontids and have been reported only in most recent material or in articulated specimens (Gardner, 1999c; McGowan, 2002; Venczel & Gardner, 2005; Matsumoto & Evans, 2018). The Lourinhã Fm material is unique both in the age and the kind of preservation of the element. Lacrimals in albanerpetontids are similar in shape, but can have minor morphological differences (Matsumoto & Evans, 2018); which could be better characterize also with geomorphometrics. The absence of ornamentation and posterodorsal-anteroventral trough observed in *Celtedens megacephalus*, features shared by New unnamed taxon 2 and *Shirerpeton isajii*, may be due to the preservation state of the holotype M542 of *C. megacephalus*; and although no ornamentation was observed in *C. ibericus*, the presence of the trough could not be confirmed (ARDG, pers. obs., 2023). No lacrimal bones are housed at MG, probably due to misidentification and collection bias (see Materials & methods).

Parietal (**Figure 3.2.7**; **Figure F.6**)

None of the parietal specimens of New unnamed taxon 2 are complete. Nevertheless, overlapping material between specimens would suggest sutured parietals would form an irregular hexagon (see reconstruction in **Figure 3.2.7**). MG28658 presents small interdigitation on what is interpreted as the interparietal suture, suggesting paired parietals during the life of the animal. The frontoparietal suture displays small interdigitations for the articular facet, with a socket on the ventral surface

(ML2949, **Figure 3.2.7Ab**). The socket is deeper in MG28595 (**Figure F.6A**) but absent in MG28672 (**Figure F.6D**).

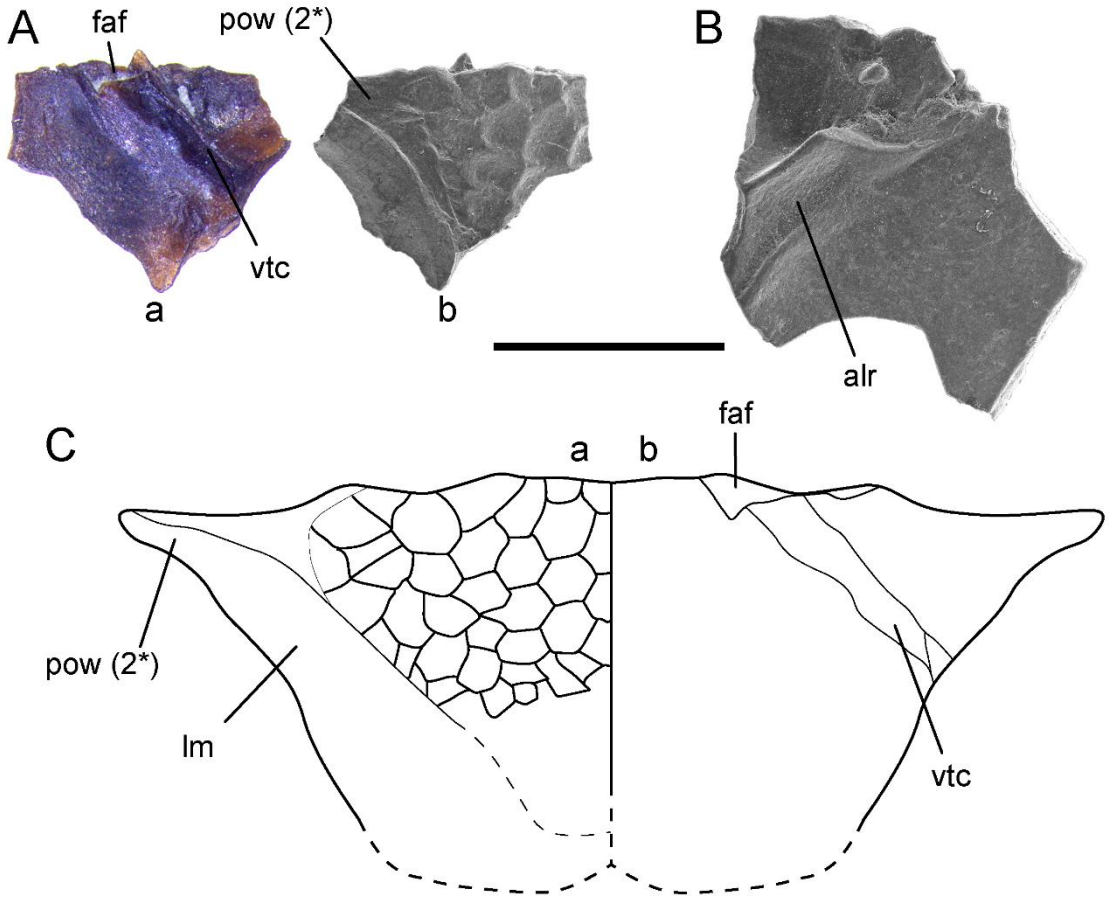

Figure 3.2.7 : New unnamed taxon 2 Parietal bones. **A**, parietal ML2949 in dorsal (*a*, SEM picture) and ventral (b) views. **B**, parietal ML2950 in ventral views (SEM picture). **C**, reconstruction of *a* parietal bone in dorsal (*a*) and ventral (b) views, not to scale. Abbreviations: **faf**, frontoparietal articular facet; **lm**, lateral margin; **pow**, postorbital wing; **vtc**, ventral transverse crest. Scale bar is 1 mm.

The dorsal surface is sculptured on its anteromedial part, displaying the same deep, polygonal pits with irregular honeycomb ornamentation observed in the frontal bones (**Figure 3.2.7A*a***). The ornamentation extends on the lateral postorbital wing, except for its tip and the anterior margin of the process (**Figure 3.2.7A*a*** and **Figure F.6C**). The size and elongation of

the postorbital wing varies from is usually short, but it can be reduced (MG28672, **Figure F.6D**) or more protruding (MG28646, **Figure F.6C**). The postorbital wing displays a smooth anterior margin and a concavity.

The occipital shelf is not preserved, however MG28658 seems to have preserved the posterior-most part of the bone (compared to other specimens), and it does not display any sign of posteroanterior emargination. Therefore, based on the overlapping material, the lateral margin of the parietal is straight from the tip of the postorbital wing to the occipital shelf. The ventral surface of the parietal possesses an anteromedial, posterolateral transverse crest, dividing the postorbital wing from the rest of the bone (**Figure 3.2.7Ab**). It runs along with a putative anterolateral recess (broken in MG28595, **Figure F.6A**; absent in MG28672, **Figure F.6D**); but there is no secondary anterior crest. An acute posterolateral process is ventrally projected in MG28672, but it is unclear if this difference is due to breakage or ontogeny.

Remarks—Due to the preservation of the specimens (presenting only ventral surface), the nature of the dorsal ornamentation in *Celtedens megacephalus*, contrary to what has been stated in previous phylogenetic analyses for the former (Matsumoto & Evans, 2018; Daza *et al.*, 2020; Carrano *et al.*, 2022), but both exhibit a short postorbital wing (ARDG, pers. obs., 2022, 2023).

Although parietals have been long known in albanerpetontids (Estes & Hoffstetter, 1976; Gardner, 1999c; Gardner *et al.*, 2003), the material from North America is more scattered (Fox & Naylor, 1982), and it is only recently that studies started focusing on them (Matsumoto & Evans, 2018; Daza *et al.*, 2020). These studies revealed the presence ventral anteromedial-posterolateral transverse crest with a sharp anterolateral recess, separating the short ornamented postorbital wing from the rest of the bone, and associated with a more smoothy secondary crest (Matsumoto & Evans, 2018).

However, these structures seems to not be as anchored as thought: *Celtedens megacephalus* and *Anoualerpeton unicum* Gardner *et al.* 2003 from the Berriasian of Morocco do not exhibit any transverse crest, while New unnamed taxon 2 does exhibit it, but not the secondary one. *Albanerpeton pannonicum* displays a ventral anteromedial-posterolateral transverse crest, but the presence of a secondary one could not be confirmed as this part is not preserved in the checked specimen (ARDG, pers. obs., 2023). The presence of anteromedial-posterolateral transverse crest is questioned in *C. ibericus*, as it is absent in the referred specimen MCCM-LH17069, but present in the holotype MCCM-LH6020, although weaker than the one in the Portuguese specimens (ARDG, pers. obs., 2023). The presence of the crest could not be confirmed in the "Paskapoo species", as the specimen is still embayed in the sediment matrix.

Dentary (**Figure 3.2.8** and **Figure 3.2.9**; **Figure F.7** and **Figure F.8**)

None of the dentaries from the Lourinhã Fm is complete and very few preserved teeth (**Figure 3.2.8** and **Figure 3.2.9**). Dentaries are the most common bone from the Alcobaça Fm. The description here is based on specimens assigned to in 62 sample boxes (MG28400 to MG28409 MG28423 to MG28536, and MG28636 to MG28685). They exhibit heterodonty, with non-pedicellate, pleurodont teeth with tricuspid crowns. The bones are overall gracile and elongated (especially MG28409), although larger ones are slightly more robust **Figure F.7** and **Figure F.8**). In dorsal or ventral views, the most complete specimens (MG28400, MG28409, and MG28412) display a lingually curved outline anteriorly.

The Meckelian canal is closed along its anteroposterior course (**Figure 3.2.8**, **Figure F.7** and **Figure F.8**), but it opens posteriorly with an acuminate to blunt opening (**Figure 3.2.9Aa, Figure F.7** and **Figure F.8**). In MG28429, MG28456, MG28657 (**Figure F.7G**), MG28659, and MG28681, the opening is located in the middle of the bone. However, in other specimens from the Alcobaça Fm this opening is more posteriorly placed. A second canal located dorsolabially to the Meckelian canal, and with a more posterior opening, can be observed and is interpreted as the inferior alveolar canal (**Figure 3.2.8Aa**). The symphysis presents a foramen in ML2951 (**Figure 3.2.8A**), ML2952 (**Figure 3.2.8B**), MG28407, and putatively in MG28551. However, other specimens from the Alcobaça Fm

exhibit *a* pit, which would suggest that the foramen might be clogged or obscured.

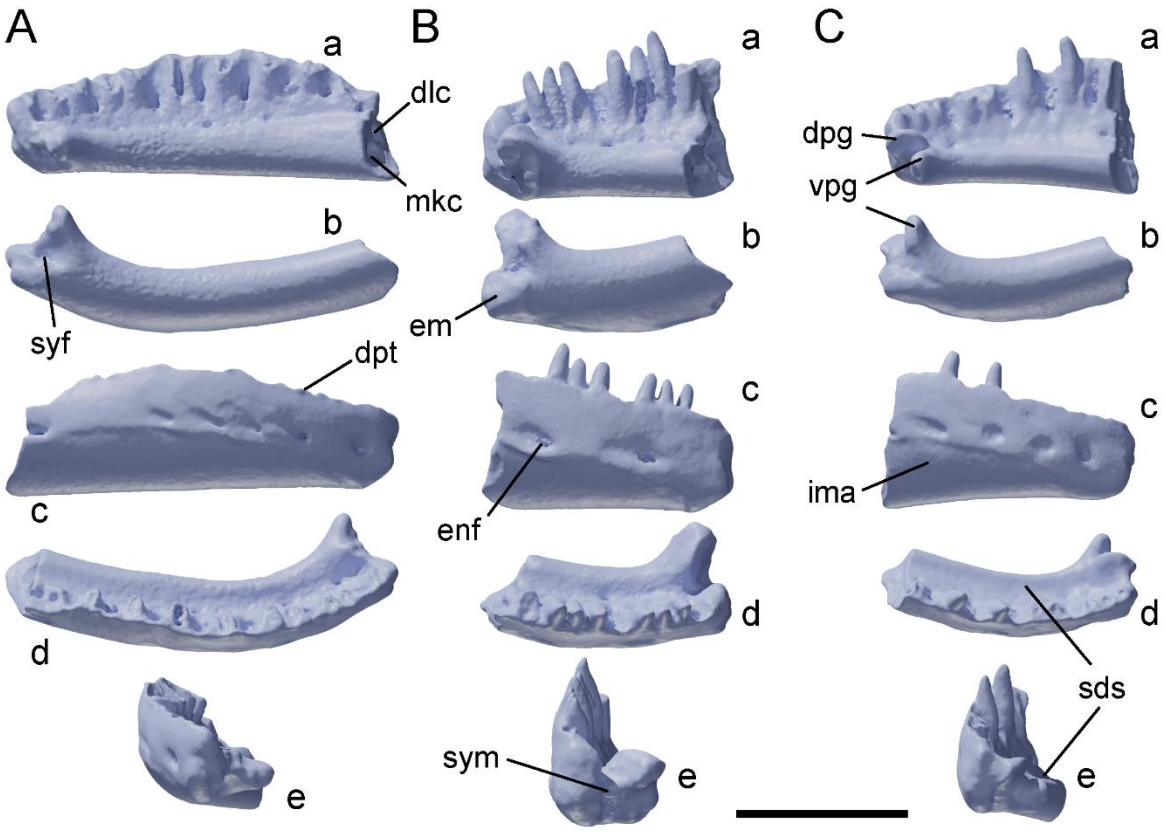

Figure 3.2.8: New unnamed taxon 2 images of three-dimensional models of dentary bones, anterior part. **A**; right dentary ML2951 in lingual (*a*), ventral (b), labial (c), dorsal (d), and anterior (e) views. **B**; right dentary ML2952 in lingual (*a*), ventral (b), labial (c), dorsal (d), and anterior (e) views. **C**; right dentary ML2954 in lingual (*a*), ventral (b), labial (c), dorsal (d), and anterior (e) views. Abbreviations: **dlc**, dorsolateral canal; **dpg**, dorsal prong; **dpt**, dental parapet; **enf**, external nutrient foramen; **em**, eminence; **ima**, *intermandibularis* musculature attachment; **mkc**, Meckelian canal; **sds**, subdental shelf; **syf**, symphiseal foramen; **sym**, symphysis; **vpg**, ventral prong. Scale bar is 1 mm.

The symphysis forms *a* subvertical anterior wall, and exhibits *a* round, blunt eminence, although it does not protrude much (e. g. ML2952, **Figure 3.2.8Bb**). Both left and right dentaries can exhibit one or two prongs (**Figure 3.2.8A*a*** and **C*a***), although the right ones seem to have one prong

more often than two. The robustness of the prongs differs between specimens, according to the size of the bones, but the dorsal one is always more massive. Most of the studied dentaries display a sinusoid, anteriorly convex dental parapet; although it can be straighter in some specimens from the Alcobaça Fm (MG28423, **Figure F.7A**; MG28429; MG28431, **Figure F.7B**; MG28474; and MG28535, **Figure F.7E**). The facet that articulates with the angular forms a small scar on a small parapet.

The most complete specimens have a lingually curved outline in dorsal view (**Figure F.7**). The labial surface is ornamented, with up to five nutritive foramina in line, and restricted to the anterior part of the bone (**Figure 3.2.8Bc**). Below them, there is a small ridge delimiting ventrally a smoother surface: the scar for the intermandibularis musculature (**Figure 3.2.8Cc**). Its extension may vary from one specimen to another (ML2952 seems lower than ML2954), and can be faint or absent. MG25428, MG28474, and MG28481 are the only ones to not display any ornamentation. The subdental shelf is gutter-like anteriorly (**Figure 3.2.8Cd**) and narrower posteriorly, becoming labiolingually compressed (**Figure 3.2.9Bd**). It is larger in bigger specimens. It also deepens dorsoventrally toward the posterior part of the bone.

No specimen displays a triangular process posterior to the tooth row. The pre-articular facet is located posterior to the subdental shelf and extends anterior to the tooth row with an acute apex (**Figure 3.2.9Aa**). It

is usually in line with the posterior Meckelian canal opening, but it can be posterior in some specimens (MG28409; MG28431, **Figure F.7B**; MG28456).

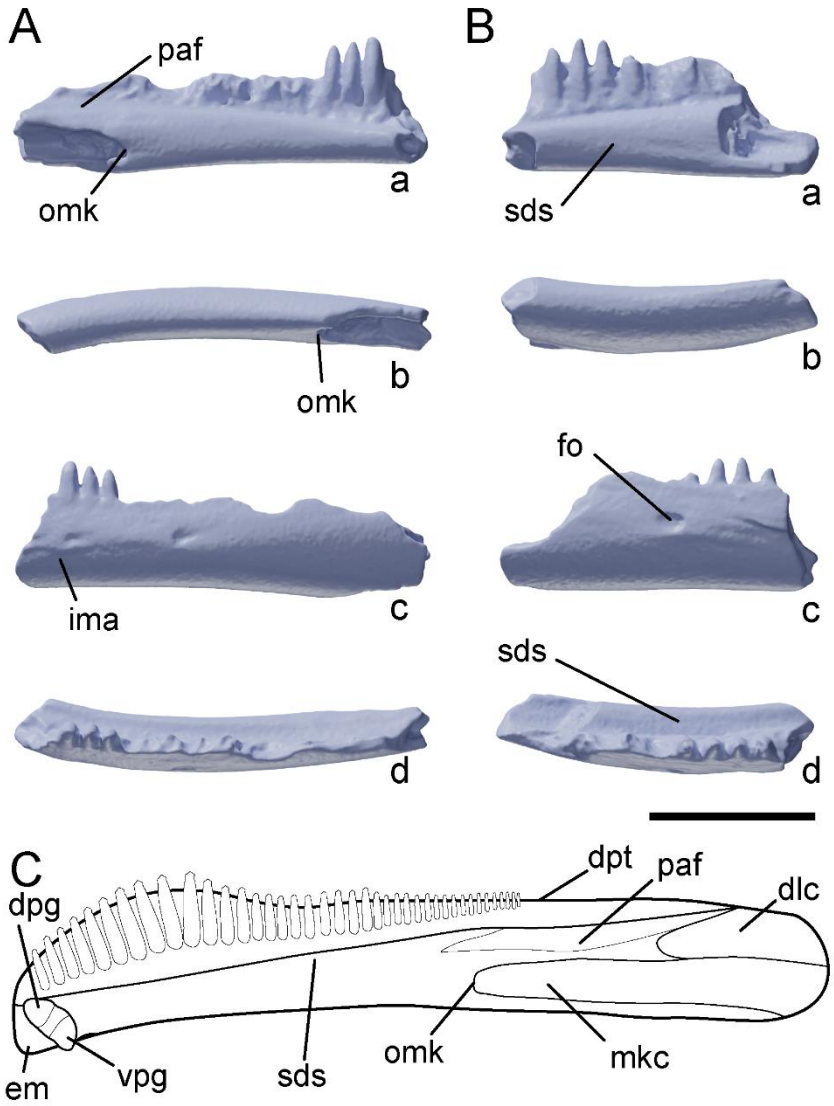

Figure 3.2.9: New unnamed taxon 2 images of three-dimensional models of dentary bones, posterior part. **A**; left dentary ML2953 in lingual (*a*), ventral (b), labial (c), and dorsal (d) views. **B**; right dentary ML2955 in lingual (*a*), ventral (b), labial (c), and dorsal (d) views. **C**, reconstruction of *a* right dentary in lingual view (not to scale). Abbreviations: **dlc**, dorsolateral canal; **dpg**, dorsal prong; **dpt**, dental parapet; **em**, eminence; **fo**, foramen; **ima**, *intermandibularis* musculature attachment; **mkc**, Meckelian canal; **omk**, opening of the Meckelian canal; **paf**, prearticular facet; **sds**, subdental shelf; **vpg**, ventral prong. Scale bar is 1 mm.

Remarks—The variation observed in the shape of the posterior opening of the Meckelian canal seems to be consistent through all species, suggesting it is highly influenced by preservation bias. As in all albanerpetontids, the symphysis consists of a subvertical anterior wall and two structures: the eminence and the prongs *sensu* Gardner & Averianov (1998). However, the symphysis is not preserved in any of the dentaries of *Albanerpeton gracile*, *Celtedens megacephalus* and *C. ibericus* (ARDG, pers. obs., 2022, 2023). The eminence can be more or less pronounced in albanerpetontids, from being weak or almost absent in some species, to strongly projecting anteriorly in others, almost pointy (ARDG, pers. obs., 2022, 2023).

As reported in all other species, New unnamed taxon 2 can display either one or two prongs on the right and left dentaries (Gardner & Averianov, 1998), suggesting some intraspecific variation. As it does not seem to be connected to the size of the specimens, ontogeny can be excluded. However, the proportions differ from one species to another, so it remains unclear if this variation could be connected to sexual dimorphism or else. Big dentaries tend to display larger prongs (Gardner & Averianov, 1998), and dorsal prongs can be relatively larger (Grigorescu *et al.* 1999; fig. 3.17) or smaller (Carrano *et al.* 2022, fig. 6A) than ventral prongs. Only *Shirerpeton isajii* display prongs similar in size.

New unnamed taxon exhibits a sinusoid, anteriorly convex dental parapet. However, this sinusoid pattern differs from that in *Shirerpeton*

isajii and *Yaksha perettii*, where the dental parapet displays two distinct concavities circumscribing one convexity (Matsumoto & Evans, 2018; Daza *et al.*, 2020), instead of having one big anterior convexity. It is unsure if the "Purbeck species" (McGowan & Ensom, 1997) displays a similar feature, as none of the dentaries are complete, but overlapping material would suggest that the dental parapet is only concave anteriorly with no heterodonty (ARDG, pers. obs., 2022).

The ventral scar for the intermandibularis muscle has been long reported in albanerpetontids, and is usually delimited by a rim on the ventrolabial surface of the dentary (Fox & Naylor, 1982; Gardner & Averianov, 1998). However, neither *Anoualerpeton priscum* and *Albanerpeton galaktion* seem to display such scar (although a faint ventral ridge can appear posteriorly in *A. galaktion*), and its presence could not be confirmed in any *Celtedens* species because of the preservation. Furthermore, the rim can become stronger in *Shirerpeton isajii*, *Yaksha perettii*, *A. arthridion*, *A. nexuosum*, *A. pannonicum*, and the "Sânpetru species", in which it forms a ridge; and the scar expands higher on the anterior section of the dental parapet in *An. unicum*, New unnamed taxon 2, and the "Paskapoo species", while it remains very low or strictly ventral in younger species. Nevertheless, the scar remains always more ventral than the nutritive foramina that ornamented the labial surface.

The dentaries are preserved in *Celtedens megacephalus*, but as only the ventral view is visible, only CT-scan would provide informative features, as well as most of *C. ibericus* specimens: only MCCM-LH030A was informative enough, as the dentaries are obscured in the holotype MCCM-LH6020.

Articular & angular (**Figure 3.2.10** and **Figure 3.2.11**; **Figure F.9**)

As previously reported in other albanerpetontids, the angular and the articular are fused with no visible suture (Estes & Hoffstetter, 1976; Estes, 1981; McGowan & Ensom, 1997; Gardner, 1999c; Venczel & Gardner, 2005; Sweetman & Gardner, 2013). Unfortunately, most of the specimens are anteriorly broken and did not preserve the angular well. The glenoid fossa of the articular presents a saddle-shaped cotylar articular facet to receive the quadrate, facing posteriorly (**Figure 3.2.10d** and **e**, **Figure 3.2.11Aa** and **Figure F.9A**). The lateral surface displays one large, seemingly oblong facet for the posterior process of the dentary (**Figure 3.2.11Ab** and **B**). One longitudinal groove runs ventrally, while a small tuberosity extends dorsally.

The medial surface displays one deep, falcate (sickle-shaped) ventral facet, whose apex curved downward (**Figure 3.2.10e**), especially well marked in ML2999 (**Figure 3.2.11Aa**). The deep dorsal groove participates to the abductor fossa (**Figure 3.2.10e** and **Figure 3.2.11Aa**). The glenoid fossa in MG28677 (**Figure F.9B**) from the Alcobaça Fm displays a rather

subvertical articular facet to receive the quadrate, facing posteriorly. It is unclear if the cotyle is unpreserved or if this facet is the actual articular facet, as the glenoid fossa is ventrally broken and asymmetrical (being more developed lingually), whereas it seems complete and looks symmetrical in MG28208 (**Figure F.9A**).

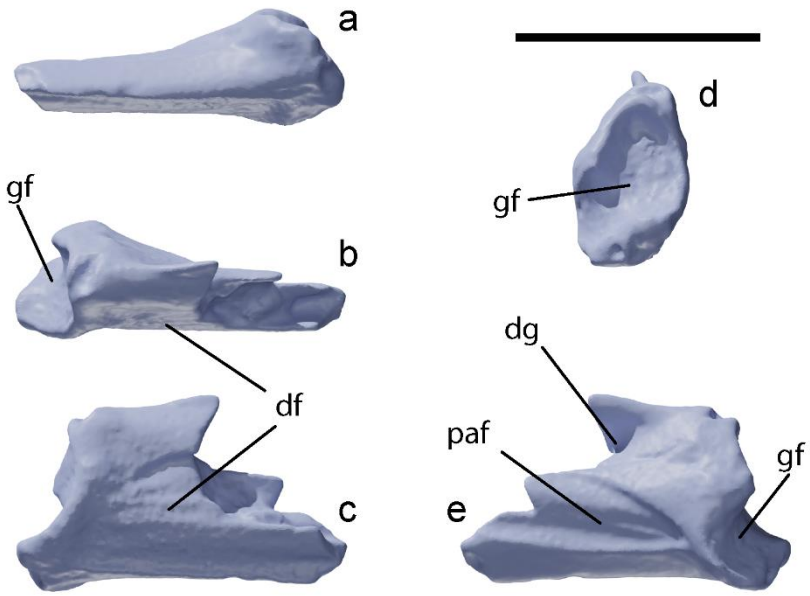

Figure 3.2.10 : New unnamed taxon 2 images of three-dimensional models of left articular ML3000 in ventral (a), dorsal (b), lateral (c), anterior (d), and medial (e) views. Abbreviations: **df**, dentary facet; **dg**, dorsal groove of the abductor fossa; **gf**, glenoid fossa; **paf**, prearticular facet. Scale bar is 1 mm.

Remarks—Articular and angular are fused in albanerpetontids (Estes, 1981; Gardner, 1999c; Venczel & Gardner, 2005; Sweetman & Gardner, 2013); although a line of fusion, which would distinguish albanerpetontids from caudates, was firstly reported (Estes & Hoffstetter, 1976), but later refuted (Gardner, 1999c; Sweetman & Gardner, 2013). A definitive statement on this peculiar aspect would however be complicated, as the articular and

angular are fragile bones and are often broken anteriorly, as seen with the Portuguese material, preserving only the posterior-most region that articulates with the quadrate (McGowan & Ensom, 1997; Sweetman & Gardner, 2013).

The vertically oriented glenoid fossa forming a concave saddle-shaped cotylar facet observed in New unnamed taxon 2, similar to what is observed in "Purbeck species" and TMM 45947-634 specimen from the Aguja Fm attributed to Albanerpeton sp. (McGowan & Ensom, 1997; Wick, 2021), is another diagnostic feature of albanerpetontids from other amphibians, notably caudates (Fox & Naylor, 1982; Gardner, 2000a; Evans *et al.*, 2004).

However, over the different albanerpetontid articular bones reported, the glenoid fossa can exhibit different shapes. The most striking is the one in *Celtedens megacephalus*, that displays a concavity much deeper than any other specimens (McGowan 2002, ARDG, pers. obs., 2022). Another striking morphology is the one displayed in the specimen MG28677 from the Alcobaça Fm, whose cotylar facet is faint, almost subvertical, and similar to the specimen IWCMS 2001.451 from the Barremian of the Isle of Wight (Evans *et al.*, 2004) and MCCM-LH6020A from Las Hoyas (ARDG, pers. obs., 2023). However, based on specimens from Blasi 2B (late Maastrichtian, Spain) with similar feature observed under SEM, these specimens may have rather been ventrally broken (see Section 3.3).

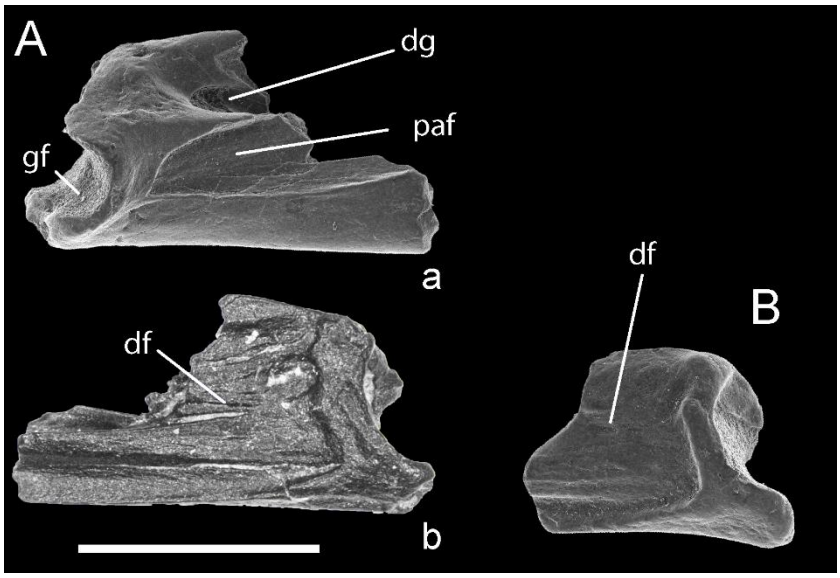

Figure 3.2.11: New unnamed taxon 2 left articular ML2999 in medial (a, SEM picture) and lateral views (b); and right articular ML3001 in lateral view (SEM picture). Abbreviations: **df**, dentary facet; dg, dorsal groove of the abductor fossa; **gf**, glenoid fossa; **paf**, prearticular facet. Scale bar is 1 mm.

Furthermore, lateral and medial surfaces of the articular display two different facets that articulate with the prearticular and the dentary (Gardner, 1999c; Venczel & Gardner, 2005), and appears to be variable among albanerpetontid: the posterior apex of the ventral facet on the medial surface displays at least two morphologies (falcate in New unnamed taxon 2 and the "Purbeck species" vs. acute in other albanerpetontids); while the facet on the lateral surface can either be flange-like, bilobate (Evans *et al.*, 2004), or with a ventral recess (Wick, 2021). The latter does not seem to be a preservation bias in the specimen TMM 45947-634 from the Aguja Fm. However, recovered or described angular bones in North America and Cretaceous albanerpetontids are scarce. Therefore, it remains unclear if this morphology is unique to the Aguja specimen and species, as

it is not reported in other known articular, or shared with other species, in which the articular is unknown still.

In conclusion, the cotylar shape of the glenoid fossa is complex but variable among other species, as well as other articular facets on the medial and lateral surfaces. Geomorphometrics can help to discriminate these issues, with implementation from CT-scans for specimens in which the bone is preserved but articulates with others, as observed in *Celtedens* species or *Albanerpeton inexpectatum*.

Quadrate (**Figure 3.2.12**)

The quadrate of New unnamed taxon 2 is a roughly trapezoidal to subrectangular bone, with a projecting hastate process. The anterior joint facet for the articular displays an asymmetric trochlear condyle, anteroposteriorly compressed and slightly concave ventrally (**Figure 3.2.12Ba**). The lateral lips, located right above the lateral concavity, are well pronounced, trickling dorsally (**Figure 3.2.12Bb**). The posteroventral surface displays a shallow, transversal fossa above the condyle. A thick, triangular, medial boss projects medioventrally, with a medial apex (**Figure 3.2.12A**). The preserved pterygoid facet is D-shaped. The posterodorsal surface exhibits a lateral pillar with a groove at the base, running longitudinally.

The lateroventral surface displays an elongated facet, with an acute anterior apex, running from the base of the trochlear condyle to the

extremity of the dorsal process (**Figure 3.2.12Bb**). The rugose surface suggests that it would be used as muscle attachment. The posterior projected section forms the long, straight, tapering dorsal process (**Figure 3.2.12A**). It is concave medially, or convex laterally, forming a long trough to wrap up the squamosal.

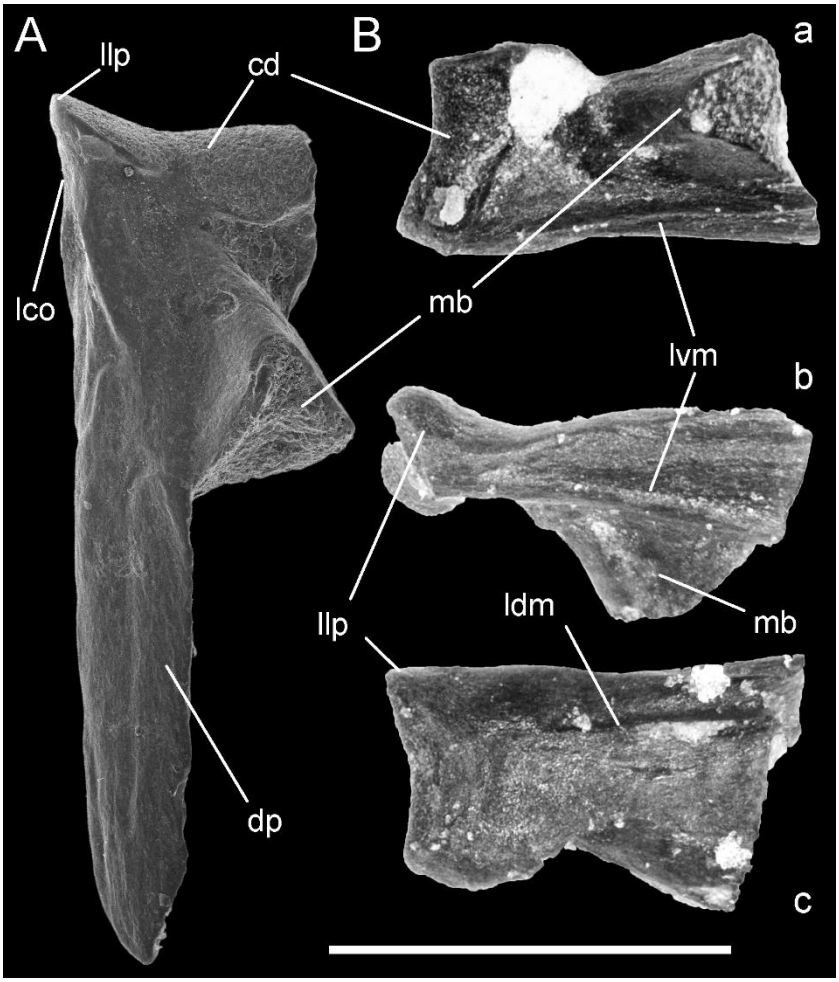

Figure 3.2.12: New unnamed taxon 2 quadrate bones. **A**, right quadrate ML3009 in ventral view (SEM picture). **B**, left quadrate ML3010 in ventral (a), lateral (b), and dorsal (c, SEM picture) view. Abbreviations: **cd**, condyle; **dp**, dorsal process; **lco**, lateral concavity; **ldm**, laterodorsal margin; **llp**, lateral lip; **lvm**, lateroventral margin; **mb**, medial boss. Scale bar is 1 mm.

Remarks—As for the articular, the trochlear convex anterior joint in the quadrate is a diagnostic feature of albanerpetontids differentiating them from caudates, in which the quadrate is rather concave (Fox & Naylor, 1982; Gardner, 2000a). However, quadrates are rare in the albanerpetontid record, even more from screen-washed material. Therefore, their osteology was poorly known (Estes & Hoffstetter, 1976; McGowan & Ensom, 1997; Gardner, 1999c; McGowan, 2002) until recently (Matsumoto & Evans, 2018). The quadrates from the Lourinhã Fm are the first ones to be reported from Late Jurassic screen-washing, and ML3010 (**Figure 3.2.12A**) is the first complete specimen from Mesozoic screen-washing to be reported.

The presence of a hastate dorsal process could not be confirmed in *Celtedens megacephalus*, as the bone is intricately articulated with the squamosal (ARDG, pers. obs., 2022), as well as the presence of a medial boss, as it was either not preserved or obscured in the holotype (ARDG, pers. obs., 2022). The lateroventral surface in *Albanerpeton pannonicum* and the "Blasi 2B species" displays a strong rim projecting laterally like an anterior shelf, contrary to *Shirerpeton isajii* and New unnamed taxon 2 (ARDG, pers. obs., 2023, see Section 3.3), which would suggest a stronger articulation between the quadrate and the squamosal to answer more stress applied on this part of the skull. No quadrate bones are housed at MG, probably due to misidentification and collection bias (see Materials & methods).

Atlas and axis (**Figure 3.2.13** and **Figure F.10**)

The atlas displays a short, ribless centrum, with a broad, blunt odontoid process (**Figure 3.2.13A** and **B**). The process is dorsally concave, making it gutter-like in anterior view (**Figure 3.2.13Ab**). A ridge between anterior and posterior cotyles edge creates a ventral notch, which separates the anterior cotyles and is pierced with one foramen. No foramen is visible on the ventral surface of the odontoid process, which is confluent with the two anterior concave cotyles (**Figure 3.2.13Ab** and **Bb**). They project laterally, perpendicular to anteroposterior axis of the atlas, facing anteriorly (**Figure 3.2.13Ae**). They are subcircular to reniform in anterior view (**Figure 3.2.13Ac**). The dorsal and ventral edges of the centrum are deeply excavated anteriorly, forming three subcircular, hemispherical posterior cotyles (**Figure 3.2.13B*a***). The unique dorsal cotyle is anteriorly concave, while the two ventral cotyles are laterodorsally inclined, making them slightly saddle-like (**Figure 3.2.13Bd**). There is no spinal foramen. However, faint, narrow transversal grooves for the spinal nerve can be observed between the neural arch attachment and immediately posterior to the dorsal margin of the anterior cotyles (**Figure 3.2.13B*a***).

As in other albanerpetontids, there is a specialized first post atlantal vertebra, conventionally named "axis", non-ossified with the first dorsal vertebra. It consists in an extremely short centrum, without ribs nor neural arch (**Figure 3.2.13C** and **D,** and **Figure F.10**). The deep, anteriorly tapered posterior notochordal pit is conical (**Figure 3.2.13Dd**). Its base is

dorsoventrally compressed, making it subcircular to oval, with a thicker ventral rim. The anterior condyles form a tri-partite articular facet. The dorsal condyle is horizontal, with a hemispherical convexity facing anteroventrally (**Figure 3.2.13Cb** and **Db**). Its ridges are dorsally thickened, except in MG28730 where they are not. The dorsal process can be more or less prominent, as in MG28545 and MG28698 (**Figure F.10B**), where it is so large that it almost covers the ventral condyles in dorsal view. The two ventral condyles form semilunar paired facet, facing dorsolaterally **Figure 3.2.13Cb** and **Db**). The curve is more or less pronounced, being more vertical in ML3018 (**Figure 3.2.13Cb**), MG28545, and MG28698 (**Figure F.10B**). The ventral projection of the condyle can form a ventral notch (**Figure F.10**), although this feature is absent in MG28666 (**Figure F.10A**), MG28705, and in specimens from the Lourinhã Fm (ML3018, **Figure 3.2.13Cb**). The edges of the ventral condyles form a ridge that is not thickened and is continuous with that of the dorsal condyle.

Remarks—The Albanerpetontidae differ from other amphibians by their unique two-joints neck, converging to the ones observed in mammals (Fox & Naylor, 1982). Their atlas display two lateral cotyles and a median tuberculum interglenoidium, also called odontoid process (Fox & Naylor, 1982; Gardner, 2001), forming an atlanto-occipital joint similar to caudates (McGowan, 1998b). However, the atlas differs from caudates and other Allocaudata, such as *Prosiren elinorae* Goin & Auffenberg 1958 from the Lower Cretaceous of Texas (USA), by being shorter and having a deep

posterior recess. It also articulates with a small centrum without neural arch, the 'axis', through three articular facets, forming the atlanto-axial joint specific to albanerpetontids (Fox & Naylor, 1982; McGowan, 1998b; Gardner, 2001).

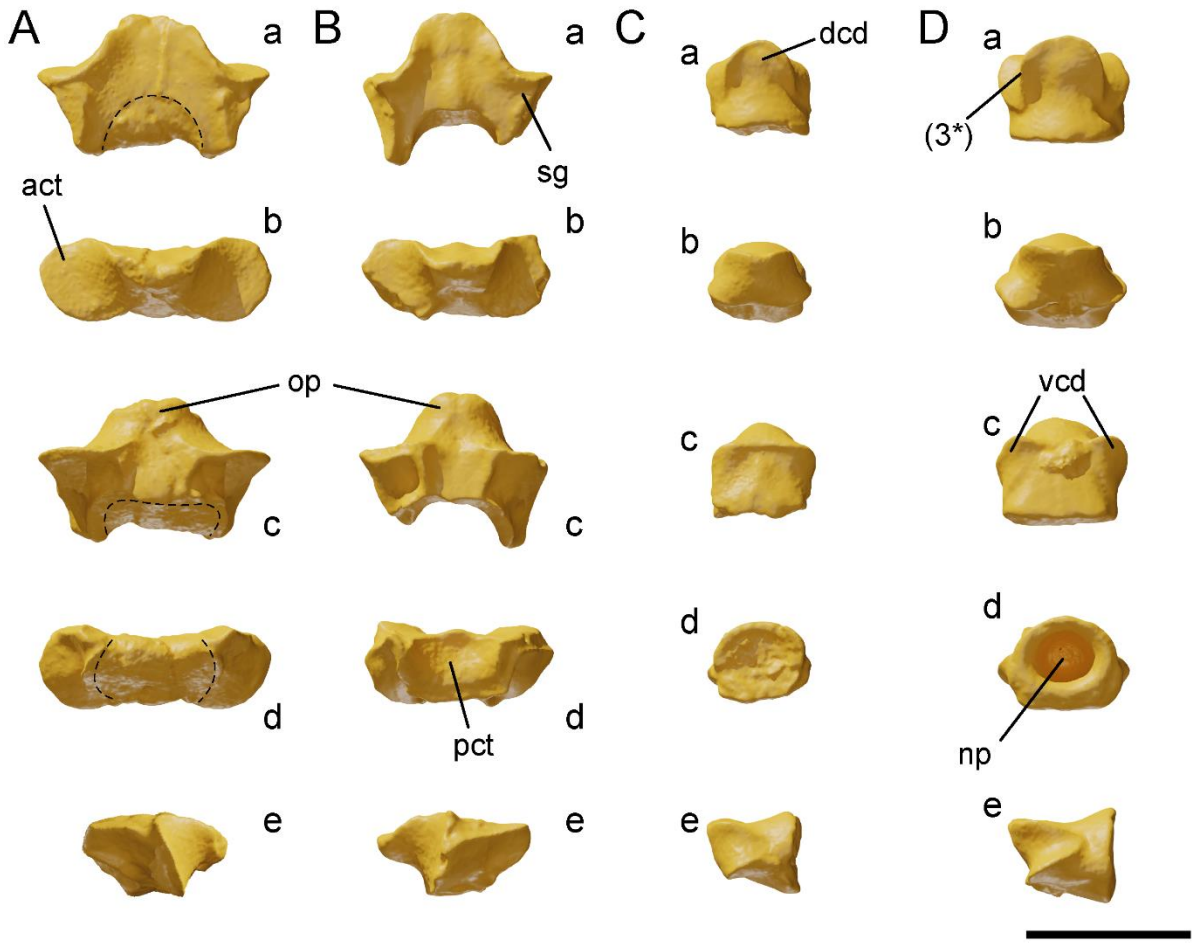

Figure 3.2.13: New unnamed taxon 2 images of three-dimensional models of cervical vertebral series. **A**, atlas ML3012 in dorsal (*a*), anterior (b), ventral (c), posterior (d), and lateral (e) views; the dash lines delimit the bone. **B**, atlas ML3013 in dorsal (*a*), anterior (b), ventral (c), posterior (d), and lateral (e) views. **C**, axis ML3018 in dorsal (*a*), anterior (b), ventral (c), posterior (d), and lateral (e) views. **D**, axis ML3019 in dorsal (*a*), anterior (b), ventral (c), posterior (d), and lateral (e) views. Abbreviations: **act**, anterior cotyle; **dcd**, dorsal condyle; **op**, odontoid process; **pct**, posterior cotyle; **sf**, spinal foramen; **sg**, spinal groove; **vcd**, ventral condyle. Scale bar is 1 mm.

The overall proportions of the odontoid process have never been quantified, but New unnamed taxon 2 seems closer to *Anoualerpeton unicum*, *Wesserpeton evansae*, *Celtedens ibericus*, the "Purbeck species", and the indetermined specimen from the Middle Jurassic of Gardies in France (Seiffert, 1969) than other albanerpetontids for which the atlas is known.

In *Albanerpeton inexpectatum*, *A. pannonicum*, and the UALVP specimens referred to *Albanerpeton* sp., the dorsal posterior edges are curved medially, making the recess wider and more invaginated than excavated, encapsulating the axis; and in *A. pannonicum*, the posterior extremities seem to bear articular facets similar to zygapophyses. Due to the preservation of MCCM-LH17069b, MCCM-LH 15710a, and MCCM-LH6020a, the shape of the anterior cotyles could not be assessed in *Celtedens ibericus* and would require CT-scan data of the specimens (ARDG, pers. Obs., 2023); and the atlas is poorly preserved in *C. megacephalus* holotype (M542) and could not be observed (ARDG, pers. Obs., 2022). The variability in the orientation of the ventral condyle facets of the axis and the prominence of the dorsal condyle compared to the ventral ones observed in the Portuguese material, would suggest that these features are influenced by intraspecific variation; although *C. ibericus* specimen MCCM-LH17069b displays large ventral condyles with anterolateral extremities curved backward (ARDG, pers. obs., 2023).

Dorsal & caudal vertebrae (**Figure 3.2.14**)

Dorsal vertebrae have amphicoelous centra, narrowly constricted in the middle, making them hourglass-shaped. The centrum can appear acoelous in some specimens from the Alcobaça Fm (MG28499, MG28425, MG28450, MG28575, MG28729, and MG28736), but it is unclear if this due to erosion or abrasion. Anterior and posterior cotyles are circular to subcircular, some being faintly compressed dorsoventrally, and display a thickened rim. Based on broken specimens, it can be assessed the notochordal canal is fully open.

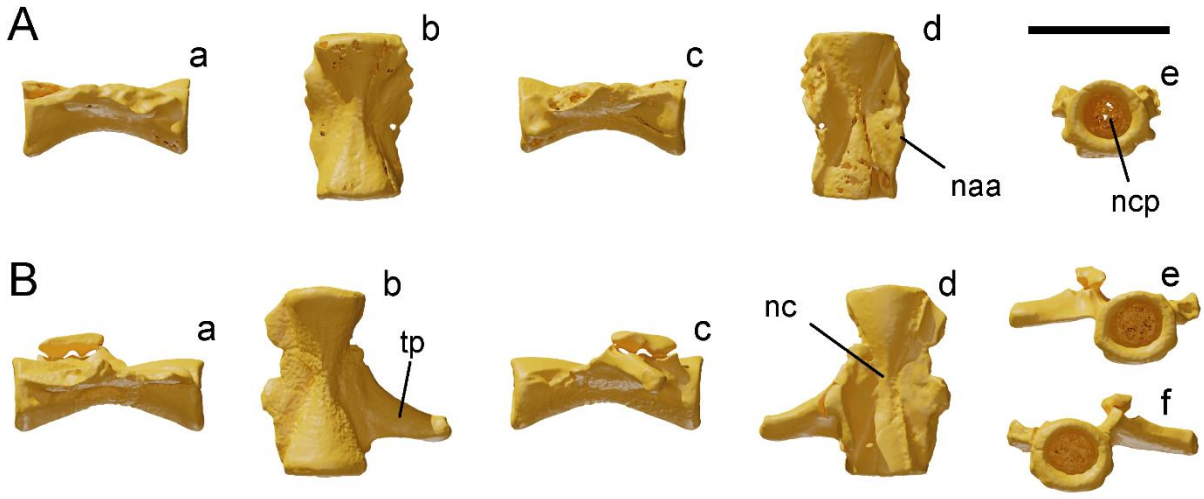

Figure 3.2.14 : New unnamed taxon 2 images of three-dimensional models of dorsal vertebral series. **A**, dorsal vertebra ML3023 in lateral (a), ventral (b), lateral (c), dorsal (d), and anteroposterior € views. **B**, dorsal vertebra ML3024 in lateral (a), ventral (b), lateral (c), dorsal (d), and anteroposterior (e, f) views. Abbreviations: **naa**, neural arch articulation; **nc**, neural canal; **np**, notochordal pit; **tp**, transverse process. Scale bar is 1 mm.

When preserved (e. g. ML3024, **Figure 3.2.14B**), the transverse processes are anteroposteriorly narrow and dorsoventrally deep, and are located around 1/3 of the total length of the bone. They can be associated

with a vertical crest. In the Alcobaça Fm specimens, the ventral foramen is preserved, but not present in all specimens, while it is absent in the specimens from Lourinhã. On the contrary, specimens from the Lourinhã Fm may display ventral paired pegs nearby one of the cotyles; while they are absent in specimens from the Alcobaça Fm. Due to the preservation of the specimens, it could not be inferred if these pegs were anterior or posterior, but they are on the same side than the transverse processes.

None of the specimens fully preserved the neural arch. Although isolated fragments have been picked, they could not be doubtlessly associated with the albanerpetontid material. Some specimens (MG28499, MG28425, MG28555, MG28574, and MG28716) are smoother, without any structure, suggesting they would be caudal vertebrae.

Humerus (**Figure 3.2.15**; **Figure F.11**)

The humeri are elongated, with a slender shaft in line with the proximodistal centre line of the radial condyle *sensu* Carrano *et al*. (2022) (**Figure 3.2.15Cc**; referred only as "condyle" by Estes and Hoffstetter (1976)), or humeral ball *sensu* Sweetman and Gardner (2013). As none of the humeri are complete, no within bone twisting could be evaluated. However, more complete specimens from Guimarota and Porto Dinheiro previously reported display a proximodistal axis rotated to almost 90° (Plate XII, Figs. 7, 9, and 10; Wiechmann 2003); but they could not be located in the Museu Geológico collection.

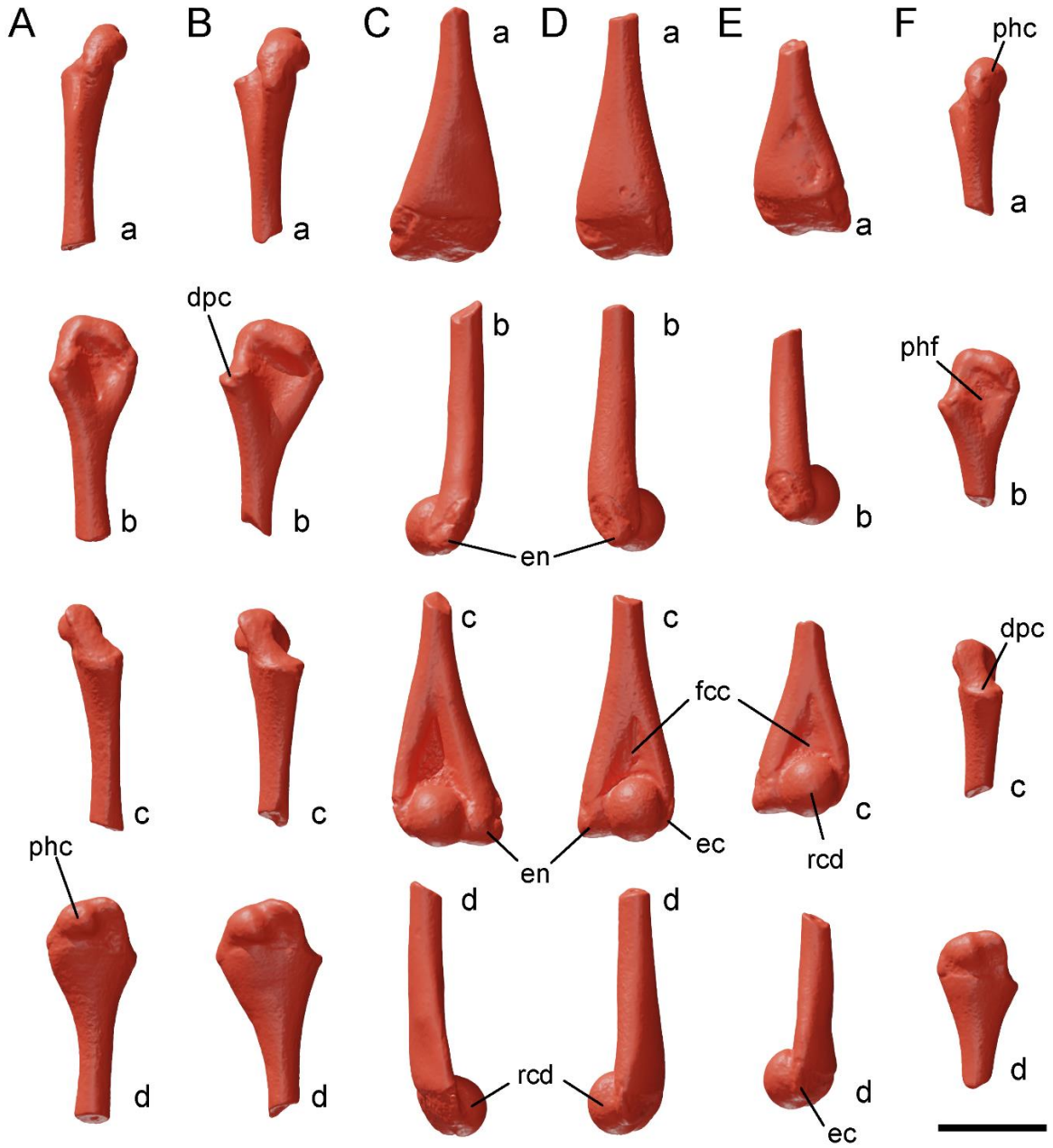

Figure 3.2.15: New unnamed taxon 2 images of three-dimensional models of hindlimbs. **A**, proximal right humerus ML3103 in dorsal (*a*), lateral (b), ventral (c), and medial (d) views. **B**, proximal right humerus ML3108 in dorsal (*a*), lateral (b), ventral (c), and medial (d) views. **C**, distal right humerus ML3109 in dorsal (*a*), lateral (b), ventral (c), and medial (d) views. **D**, distal left humerus ML3110 in dorsal (*a*), lateral (b), ventral (c), and medial (d) views. **E**, distal left humerus ML3111 in dorsal (*a*), lateral (b), ventral (c), and medial (d) views. **F**, proximal right humerus ML3112 in dorsal (*a*), lateral (b), ventral (c), and medial (d) views. Abbreviations: **dpc**, deltopectoral crest; **ec**, ectepicondyle; **en**, entepicondyle; **fcc**, *fossa cubitus cristalis*; **phc**, proximal humeral condyle; **phf**, proximal humeral fossa; **rcd**, Radial condyle. Scale bar is 1 mm.

The proximal condyle is hemispheric, smaller than the radial condyle (**Figure 3.2.15Fa**). The lateral edge can be posteriorly winded. The deltopectoral crest, or *crista ventralis sensu* McGowan (2002), is always present, and well developed in mature specimens (ML3108, **Figure 3.2.15Bb**). It projects laterally, forming the lateral edge of the deep proximal triangular fossa, which bears a small foramen on its distal vertex. There is no *crista dorsalis*. The triangular distal *fossa cubitus centralis* is well marked and bears up to two foramina on its proximal vertex (**Figure 3.2.15Dc**). It can be deeper and more distally extensive in some specimens (MG28443; MG28506; MG28690, (**Figure F.11B)**; MG28720, **Figure F.11C**; and ML3109, **Figure 3.2.15C**), with more conspicuous margins but no foramen, and a wider distal epiphysis.

The prominent, ossified radial condyle consists of a massive hemispherical ball in the centre of the distal epiphysis (**Figure 3.2.15Ec**), but can be absent in some specimen. Its size is similar between specimens, except in MG28703, which is significantly bigger than the other specimens. The ectepicondyle *sensu* Estes and Hoffstetter (1976), or ulnar condyle *sensu* Carrano *et al.,* (2022), is extremely reduced, with a subvertical, convex medial margin (**Figure 3.2.15Ed**). The entepicondyle *sensu* Estes and Hoffstetter (1976), or radial epicondyle *sensu* Sweetman and Gardner (2013), is more pronounced than the ectepicondyle, but remains smaller than the radial condyle (**Figure 3.2.15Cc**).

Remarks—In all albanerpetontid in which a complete humerus is known, the long axis is rotated to nearly 90° between the proximal and distal epiphyses, except in *Celtedens megacephalus* where there is no rotation (ARDG, pers. obs., 2022), but it is unclear if this is a preservation bias. When the fossa in the proximal epiphysis is known (New unnamed taxon 2, *C. ibericus*, *Wesserpeton evansae*, *Albanerpeton inexpectatum*, and *A. pannonicum*), it is usually shallower than the *fossa cubitus cristalis*. Furthermore, if the *fossa cubitus centralis* is present in all species, its proximodistal extension, as well as its depth, varies from one species to another; *W. evansae* being similar to New unnamed taxon 2 Marked *fossae cubitus centralis* are bordered by a deep, thick ridge; while they are smoother when the *fossa* is shallower. Both *Celtedens* and *A. inexpectatum* humeri seem more robust than those of New unnamed taxon 2.

Ilium (**Figure 3.2.16**)

The ilium does not possess a dorsal crest or tubercle. Although broken in all specimens, the thin iliac shaft seems to be straight, and does not bear dorsal nor lateral prominences. It is mediolaterally compressed, with an oval cross-section. The long axis is strongly titled posteriorly, forming an angle of 70° with the ventral margin.

The shallowly convex acetabulum covers most of the acetabular region, with an almost non-existent rim, and faces ventromedially (**Figure 3.2.16a**). It is dorsoventrally elongated, with a convex U-shaped dorsal

margin, making it lorate in overall shape. It is elevated on a ramped pedestal, being more prominent to subvertical on the posterodorsal margin. The smooth medial surface of the ilium is laterally concave and does not bear any foramen or ridge (**Figure 3.2.16b**). The pubic and ischial surfaces are connected by a sinuous ventral margin and flare broadly anteroposteriorly. The ischial surface presents a faint fossa and confirms the posterior end of the element.

Remarks—Ilia have been rarely reported in the albanerpetontid fossil record, especially from screen-washing. The ilium in *Celtedens megacephalus* is probably present, but it is obscured and/or crushed in M542 (ARDG, pers. obs., 2022). They differ from anurans by not having a dorsal crest, or tubercle, and from many urodeles by not having lateral prominence (Gardner *et al.*, 2010; Sweetman & Gardner, 2013). It was previously reported that the acetabulum shape, notably the convexity of the dorsal margin and its dorsoventrally extension, could vary among albanerpetontids (Carrano *et al.*, 2022). The variation of these two parameters would suggest at least three different morphologies (U, V, and D-shaped); however, only extensive sampling in other species would confirm this trend. Geomorphometrics could also allow to estimate if one parameter is more prevalent and significant than the other.

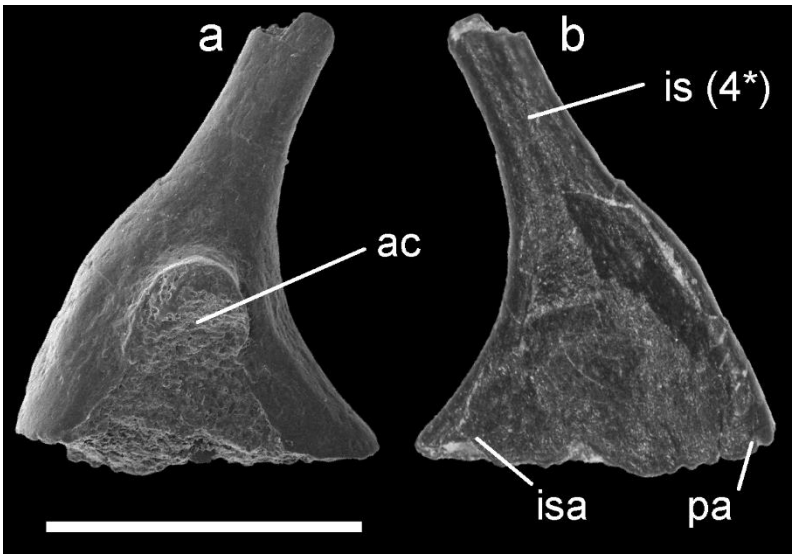

Figure 3.2.16: New unnamed taxon 2 left ilium ML3128 in lateral (*a*, SEM picture) and medial (b) views. Abbreviations: **ac**, acetabulum; **is**, iliac shaft; **isa**, ischial articulation; **pa**, pubic articulation. Scale bar is 1 mm.

New unnamed taxon 2 also shows that the long axis, or iliac shaft *sensu* Carrano *et al*. (2022), can vary according two parameters: its cross-section, being either tubular or more compressed mediolaterally, and its posterior tilt, that can be more or less pronounced. It remains unclear if both features are connected, as New unnamed taxon 2 is the only one to present a tubular iliac shaft strongly tilted posteriorly. A better sampling in other species will allow to better characterize these parameters.

It was also reported that the pubic and ischial articular surfaces were flaring anteroposteriorly (Sweetman & Gardner, 2013; Carrano *et al.*, 2022), but being more or less pronounced, which is confirmed with the Portuguese material. However, more sampling in other species and geomorphometrics could help to better characterize the differences. No ilia are housed at MG,

probably due to misidentification and collection bias (see Materials & methods).

Femur (**Figure 3.2.17**)

Bone with elongated, slender, straight shaft, and less robust than the humerus. A longitudinal furrow runs distally across the diaphysis, sometimes paired (**Figure 3.2.17Bd**). The distal epiphysis does not have ossified condyles but displays a convex surface instead. The convex proximal epiphysis is not complete but displays a femoral head and a small trochanter, the latter being associated with a small trochlear groove with a foramen at its end (**Figure 3.2.17Ac**). The ventral surface of the distal epiphysis displays a shallow triangular fossa.

Remarks—Femora have been rarely reported and described in the albanerpetontid fossil record and, therefore, are poorly known. Unfortunately, the femora reported from the Guimarota beds (Wiechmann, 2003) could not be located in the MG collection. Nevertheless, the morphology of the specimens from the Lourinhã Fm is congruent with the one described for Guimarota specimens and the figured specimens (pl.12, figs 1, 2; Wiechmann 2003). Furthermore, the global morphology of the Portuguese specimens is reminiscent of younger albanerpetontids *Celtedens ibericus* holotype MCCM-LH 6020 and referred specimen MCCM-LH 17069 (McGowan 2002; ARDG, pers. obs., 2023), *Albanerpeton inexpectatum* referred specimens MNHN.LGA 1954 and MNHN.LGA 1961 (Estes &

Hoffstetter, 1976; Gardner, 1999c; ARDG, pers. obs., 2023), and *Albanerpeton pannonicum* unnumbered specimens housed in the Royal Tyrrell Museum of Palaeontology (ARDG, pers. obs., 2023).

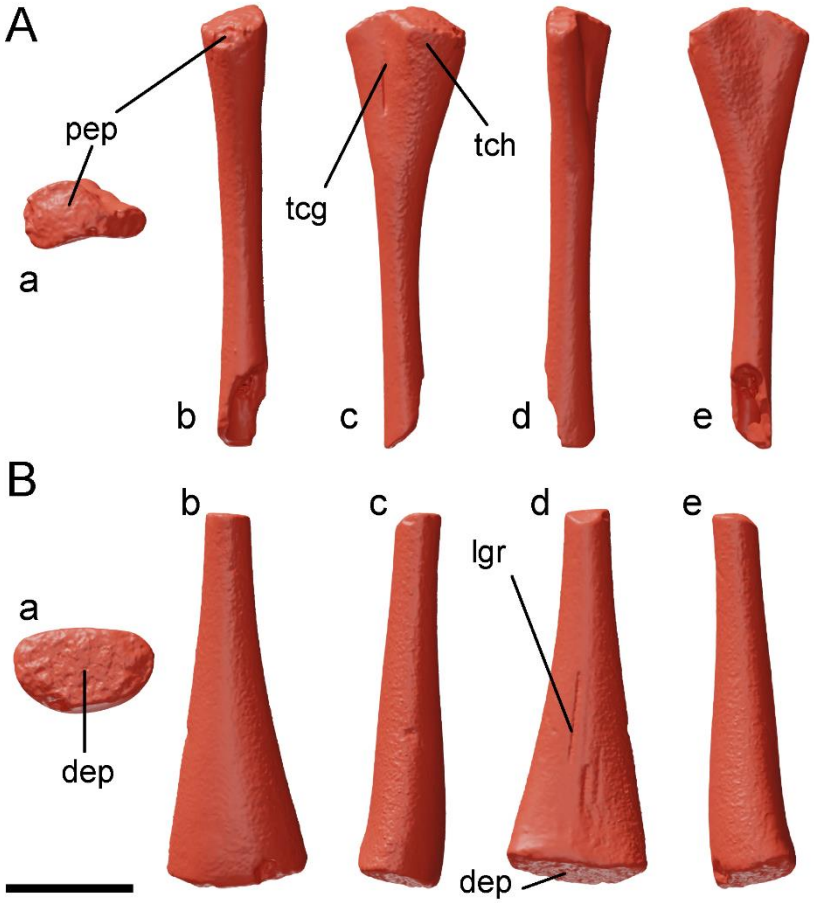

Figure 3.2.17 : New unnamed taxon 2 images of three-dimensional models of hindlimb. **A**, proximal left femur ML3131 in proximal (*a*), lateral (b), dorsal (c), medial (d), and ventral (e) views. **B**, distal femur ML3130 in distal (*a*), lateromedial left (b), anterior (c), lateromedial right (d), and posterior € views. Abbreviations: **dep**, distal epiphysis; **lgr**, longitudinal groove; **pep**, proximal epiphysis; **tcg**, trochlear groove; **tch**, trochanter. Scale bar is 1 mm.

3.2.5 Discussion

3.2.5.1 Relevance of the Portuguese material for albanerpetontid studies

Although all the material was collected from screen-washing, the preservation between both the Lourinhã Formation and the Alcobaça Formation allowed to extend the knowledge on the cranial and post cranial osteology of albanerpetontids. The Lourinhã Fm localities are multispecific microvertebrate assemblages no more different than others (Guillaume *et al.*, 2023a), and underneath the quality and quantity that can be found in Lagerstätten such as the Guimarota beds (Martin & Krebs, 2000).

Yet, it yields bones usually not reported elsewhere. More than any preservation bias, we infer this result is mostly due to a collection and identification bias during picking. With trained-eyes and anatomical expertise, most of the bones could be identified in the three main VMAs sampled in the Lourinhã Fm (Valmitão, Zimbral, and Porto das Barcas; see **Figure 3.2.18**), despite having different sedimentological settings, and so different environmental and preservation factors.

The Lourinhã Fm localities exemplifies that, most of the albanerpetontid bones should be present in microsites where they occur, whereas only few were usually reported or considered in detail (Gardner, 1999c, 2000a,b; Grigorescu *et al.*, 1999; Rees & Evans, 2002; Gardner *et al.*, 2003; Folie & Codrea, 2005; Skutschas, 2007; Gardner & Böhme, 2008; Blain

et al., 2010; Canudo *et al.*, 2010; Szentesi *et al.*, 2013). Even descriptions of most complete specimens suffer from this bias, often because of bad preservation, and are focused only on a few bones (McGowan & Evans, 1995; McGowan, 2002; Daza *et al.*, 2020). However, we show that these bones can provide meaningful information regarding the anatomy and systematics of the group, despite previous statements (Gardner, 2000a); hence the need to look for them.

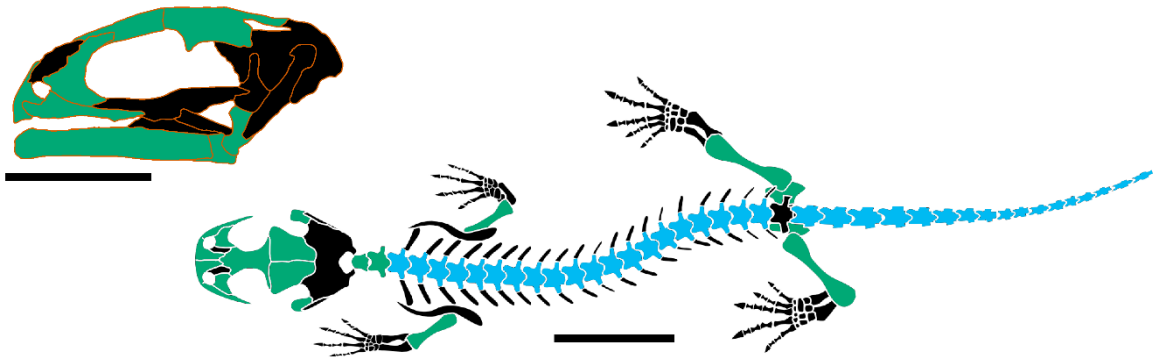

Figure 3.2.18: Albanerpetontidae skull (lateral view, scale 5mm) and skeleton (dorsal view, scale 10 mm) reconstructions, showing the bones found in the Lourinhã Formation. Dorsal and caudal vertebrae are in blue as their exact position cannot be assessed from isolated fragmented specimens. Skull reconstruction based on *Y. perettii* from Daza *et al.* (2020). Skeleton reconstruction from Schoch (2014), based on *C. ibericus* from McGowan (2002).

Localities where albanerpetontids have been already reported are as important as new ones, as they can provide new information on already existing species including the variabilities of the characters, old and new, presented in this study. Data from a variety of anatomical elements is particularly important, given that and characters are often homoplasic and

most species are diagnosed using a unique combination of characters showing plesiomorphic and derived states (Carrano *et al.*, 2022).

3.2.5.2 Palaeoecology of New unnamed taxon 2

Albanerpetontids were previously suggested to have terrestrial or even fossorial live-style, adapted to dry environments (Estes & Hoffstetter, 1976; Fox & Naylor, 1982; McGowan & Evans, 1995; Gardner, 1999c; Venczel & Gardner, 2005; Böhme, 2008, 2010). However, this is challenged by most of the Mesozoic albanerpetontid occurrences, as their remains are mostly found in more wet environments (Gardner & Böhme, 2008; Sweetman & Gardner, 2013; Carrano *et al.*, 2022), and even in coastal tropical rainforests (Daza *et al.*, 2020). This leads authors to suggest that, like extant lissamphibians, albanerpetontids were rather adapted for more stable, moist, and shaded conditions (Delfino & Sala, 2007; Gardner & Böhme, 2008) with humid soil available in the vicinity of freshwater ponds (Wiechmann, 2000; Blain *et al.*, 2010).

The distribution of New unnamed taxon 2 further support this interpretation. Indeed, the Guimarota beds have long been interpreted as a terrestrial to lagoonal environment similar to modern mangroves, with occasional freshwater influx and salt water flooding (Gloy, 2000; Martin, 2000a); while the Lourinhã Fm has been regarded as a fluvial environment with marked seasonality (Martinius & Gowland, 2011; Taylor *et al.*, 2014; Gowland *et al.*, 2017; Mateus *et al.*, 2017). More specifically in the Lourinhã

Fm, all the localities here studied provided albanerpetontid remains, but the Valmitão VMA has been the richer, both in quantity and diversity of the elements preserved. The variegated colours, lack of grading, coupled with more carbonate nodules and rhizocasts in the Valmitão locality, suggest an environment with low sediment supply and long periods of subaerial exposure. This can be interpreted as an oxbow lake, dominated by amphibious and facultative taxa (Guillaume *et al.*, 2023a).

On the opposite, Zimbral and Porto das Barcas localities imply more wet conditions, and even permanent sheet of water and anoxic environments in the latter, while having a less continental-influenced fauna (Guillaume *et al.*, 2023a). The faunal composition of each site compared to their interpreted environments indicates some degree of transport. However, considering the brittle nature of the elements, and that they are most likely broken in Porto das Barcas VMA while being rather well-preserved in Valmitão VMA, it can be argued that they have been moved on shorter distances in the latter and were living in the near vicinity (Carrano *et al.*, 2022).

Based on the preservation of the hyoid entoglossal process with soft-tissues, *Yaksha perettii* has been interpret as a sit-and-wait predator with a ballistic tongue, analogue to modern chameleons (Daza *et al.*, 2020). It is unsure yet in which extent ballistic-tongue strategies were widespread among albanerpetontids, as almost no hyoid entoglossal process has been

reported in other species. A hyobranchial apparatus with a long, rod-like process was reported in both *Celtedens megacephalus* and *Celtedens ibericus* (McGowan, 2002; Maddin *et al.*, 2013). Their morphology and structure match the hyoid entoglossal process observed in *Y. perettii* (ARDG, pers. obs., 2022, 2023), which would support that this anatomical structure was present in both *Celtedens* species and that they were also ballistic-tongue feeders. Unfortunately, no premaxilla is known from *C. megacephalus* and the morphology of the suprapalatal pit in *C. ibericus* remains dubious; therefore, no assumption can be made between its role in ballistic-tongue strategy. However, *Y. perettii* and *C. ibericus* premaxillae differ by the former being robust and the latter being gracile; the two main morphotypes in albanerpetontids (Fox & Naylor, 1982; Gardner, 2000a, 2002). If confirmed, this would suggest that the hyoid entoglossal process, and the ballistic tongue associated with it, is not related to the robustness of the premaxillae. Therefore, it could be more widespread among albanerpetontids.

Incidentally, a stronger ossification occurred gradually through the albanerpetontids evolution in both the premaxillae, becoming more robust and more consistently fused, and the fused frontals, becoming broader with stronger orbital margins (Gardner, 2000a, 2002; Gardner & Böhme, 2008). The new material from Blasi 2B suggests a similar pattern in the atlas (ARDG, pers. obs., 2023), implying more constrained head movements. These ossifications in cranial and cervical elements peaked with the

Cenozoic species *Albanerpeton inexpectatum* and *A. pannonicum*, and would be more suitable for burrowing (Estes & Hoffstetter, 1976; Fox & Naylor, 1982; Gardner, 1999c; Venczel & Gardner, 2005). Fossoriality and ballistic-tongue feeding are not mutually exclusive: some modern chameleons living in arid habitat are known for digging grooves or even burrowing completely into the substrate to cope with the variations in temperatures (Measey *et al.*, 2013), but there is no evidence if both traits occurred simultaneously in albanerpetontids. Anyhow, a major ecological shift in albanerpetontids took place through their evolution toward a more fossorial lifestyle, most likely as a result of niche partitioning due to competition with salamanders and small squamates, which were becoming more common and more diverse through the Cretaceous and the Cenozoic (Evans, 2003; Gardner & DeMar, 2013; Marjanović & Laurin, 2014; Simões *et al.*, 2018; Whiteside *et al.*, 2022).

3.2.6 Conclusions

A total of 468 albanerpetontid bones from the Lourinhã Formation and historical material from the Alcobaça Formation are described here as the single new species New unnamed taxon 2 from the Upper Jurassic (Kidmmerigian to Tithonian) of the Lusitanian Basin in Portugal. The referred material from the Lourinhã Fm, collected in different palaeoenvironments in fluvial and transitional settings, includes a relatively well sampled anatomy, suggesting other localities should yield as much diversity of elements, contrary to the previously reported overabundance of

cranial bones. Identification and collection errors is the most probable cause of this bias. Sedimentological and taphonomic data suggest that New unnamed taxon 2 was living in rather wet environments, with intermittent arid conditions and marine influences. New unnamed taxon 2 is the oldest albanerpetontid occurrence in the Iberian Peninsula, supporting its palaeobiogeographical importance for the group during the Jurassic/Cretaceous transition.

3.3 Chapter 6: Witnessing the last giants—a new Albanerpetontidae (Lissamphibia) from the latest Maastrichtian of Spain

Paper to be submitted in *Cretaceous research* (Journal impact factor for 2022: 2.1; CiteScore: 4.1; SJR: 0.792; H-index: 76)

Alexandre R. D. Guillaume, Hugues-Alexandre Blain, Eduardo Puértolas-Pascual & Miguel Moreno-Azanza. Witnessing the last giants: a new Albanerpetontidae (Lissamphibia) from the latest Maastrichtian of Europe and its paleobiogeographical implications

Abstract

The Cretaceous/Paleogene boundary records one of the key events in history of life, but not all clades were affected similarly. Albanerpetontidae are an extinct group of lissamphibians thought to have been little affected by the K/Pg mass extinction event. However, their patchy fossil record in the Late Cretaceous of Europe, concentrated in the uppermost stages (Santonian–Maastrichtian), complicates our understanding of this group during this interval. For the last 20 years, the Ibero-Armorican Island has been one of the key areas for studying the latest stages of the Upper Cretaceous; but despite several occurrences of albanerpetontids, none has been described in detail.

Here, we describe a new albanerpetontid species from the upper Maastrichtian Blasi 2B locality (Spain), based on disarticulated cranial and

postcranial bones; and the first species from the Late Cretaceous in Europe. This species is characterized by the anterior end of the orbital margin of the frontal located anterior to the anteroposterior midpoint of the frontal, and rectangular anterior cotyles of the atlas. It shares affinities with other Upper Cretaceous *Albanerpeton* species from North America, although their relationships cannot not be fully resolved, and with other material from the Ibero-Armorican Island. However, it differs from Upper Cretaceous albanerpetontid species from eastern Europe, notably in the shape of the suprapalatal pit and the size of the palatal foramen. Our results reinforce the monophyly of *Albanerpeton*, which was lately challenged, and suggest that two albanerpetontid lineages, with independent paleobiogeographic histories, were coeval in the Lates Cretaceous of Europe.

Keywords: Albanerpetontidae, Late Cretaceous, Lissamphibia, Tremp Formation, Phylogeny

3.3.1 Introduction

Albanerpetontids are mostly represented by isolated, fragmented bones recovered by sieving sediments from Laurasia and few northern Gondwanian localities (Gardner & Böhme, 2008; Carrano *et al.*, 2022), especially in North Africa (Gardner *et al.*, 2003; Haddoumi *et al.*, 2016; Lasseron *et al.*, 2020) and Iberia (e. g. Wiechmann, 2003; Blain *et al.*, 2010; Pérez-Pueyo *et al.*, 2021a). They are a characteristic component of non-

marine vertebrate assemblages (Gardner & Böhme, 2008; Carrano *et al.*, 2022). The European record is the most extensive, ranging from the early Bathonian (Seiffert, 1969; Evans & Milner, 1994) to the Early Pleistocene (Delfino & Sala, 2007; Villa *et al.*, 2018), demonstrating a temporal range of 165 million years history for the group. However, this record is patchy, with several lengthy temporal gaps, compared to the more continuous North American record ranging from the Aptian to the Paleocene (Gardner & Böhme, 2008; Carrano *et al.*, 2022).

In European, the Cretaceous albanerpetontid record is primarily confined to its early and latest stages, with a few scattered occurrences in between (see **Table 3.3.1** and references therein).

The latest stages of the Upper Cretaceous are key to an understanding of how faunas and floras were affected during the Cretaceous/Paleogene (K/Pg) mass extinction event (Rage, 2002; Schulte *et al.*, 2010; Witts *et al.*, 2016; Chiarenza *et al.*, 2020; Dzombak *et al.*, 2020). Before the 1990s, the European Upper Cretaceous record of continental vertebrates was generally poor scattered compared to that of North America (Buffetaut & Le Loeuff, 1991; Le Loeuff, 1991; Pereda-Suberbiola, 2009; Csiki-Sava *et al.*, 2015), especially regarding the lissamphibian record (Sanchíz, 1998; Blain *et al.*, 2010; Szentesi *et al.*, 2013).

However, this deficiency has been corrected by over two decades of extensive studies. These have involved the Haţeg Basin and the

Transylvanian Basin in Romania (Grigorescu *et al.*, 1999; Codrea *et al.*, 2002; Smith *et al.*, 2002; Csiki-Sava *et al.*, 2015, 2016; Venczel *et al.*, 2016); and the French and Spanish Pyrenees, which were part of the Ibero-Armorican Island at the westernmost edge of the southern European archipelago (le Loeuff, 2005; Blain *et al.*, 2010; Blanco *et al.*, 2016; Canudo *et al.*, 2016; Vila *et al.*, 2016; Pérez-Pueyo *et al.*, 2021a).

Europe was located at the crossover of three major paleobiogeographic realms during the Late Cretaceous: North America, Asia, and Gondwana; and by being intermittently connected to these provinces, would have been a potential corridor for continental vertebrate dispersal (Csiki-Sava *et al.*, 2015). This is reflected by the faunal composition of Europe during that interval, being a mixture of Gondwanan, Asiamerican, and local endemic taxa (Csiki-Sava *et al.*, 2015).

Although there could be some local faunal heterogeneity, European faunas are generally characterized by large-scale stasis, especially in eastern Europe where smaller insular habitats existed compared to the large continental areas provided by the Ibero-Armorican Island to the west (Csiki-Sava *et al.*, 2015, 2016). This results in a fauna shaped by both local vicariant evolution of an older Early Cretaceous fauna, and by several geo-dispersal immigration events through the Late Cretaceous (Le Loeuff, 1991; Lieberman & Eldredge, 1996; Lieberman, 2003; Pereda-Suberbiola, 2009; Weishampel *et al.*, 2010; Csiki-Sava *et al.*, 2015); and this despite the

presence of marine barriers hindering continental dispersion, especially for lissamphibians (Duellman & Trueb, 1994; Wells, 2007).

Table 3.3.1: Mesozoic Albanerpetontidae occurrences in Europe and North Africa, ordered from youngest to oldest. Age and correlation of Maastrichtian localities is based on the work of Pérez-Pueyo (2021a); age of the Pietraroja locality based on Bravi and Garassino (1998), Bartiromo (2013), and Graziano *et al.* (2024); and age of the Balve-Beckum locality based on Lanser and Heimhofer (2015). Information adapted and updated from Gardner and Böhme (2008), Sweetman and Gardner (2013), Szentesi *et al.* (2013), and Venczel *et al.* (2016).

Taxonomic identification	Locality	Age	References
Albanerpetontidae indet.	Cassagnau 1, Haute-Garonne, France	Late Maastrichtian	Laurent *et al.*, 2002
Albanerpetontidae indet.	Serrat del Pelleu, Tremp Basin, Lleida, Spain	Late Maastrichtian	Blanco *et al.*, 2016
Albanerpeton sp.	Crăguiş, Haţeg Basin, Hunedoara, Romania	Late Maastrichtian	Csiki-Sava *et al.*, 2016; Venczel *et al.*, 2016; Zaharia, 2011
New unnamed taxon 3	Blasi 2B, Tremp Basin, Huesca, Spain	Late Maastrichtian	Blain *et al.*, 2010; this article
Albanerpeton sp.	Livezi-General Berthelot, Haţeg Basin, Hunedoara, Romania	Late Maastrichtian	Csiki-Sava *et al.*, 2016
Albanerpetontidae indet.	Ausseing, Haute-Garonne, France	Late Maastrichtian	Laurent, 2003
Albanerpetontidae indet.	Toteşti-baraj, Haţeg Basin, Hunedoara, Romania	Late Maastrichtian	Codrea *et al.*, 2002
Albanerpetontidae indet.	La Solana, Iberian Basin, Valencia, Spain	Late Maastrichtian	Roček, 2000; Szentesi & Company, 2017
Albanerpetontidae indet.	Nălaţ-Vad, Haţeg Basin, Hunedoara, Romania	Late Maastrichtian	Smith *et al.*, 2002; Venczel *et al.*, 2016
Albanerpeton sp.	Tuştea-Oltoane nesting site, Haţeg Basin, Hunedoara, Romania	Late Maastrichtian	Grigorescu *et al.*, 1999; Venczel *et al.*, 2016

Albanerpeton spp.	Oarda de Jos, Transylvanian Basin, Alba, Romania	Late Maastrichtian	Codrea *et al.*, 2010a, 2010b; Jipa, 2012; Jipa *et al.*, 2010
Albanerpetontidae indet.	L'Espinau, Tremp Basin, Lleida, Spain	Late/early Maastrichtian boundary	Blanco *et al.*, 2016; Pérez-Pueyo *et al.*, 2021a
Albanerpetontidae indet.	Fărcădeana Brook, Rusca Montană Basin, Negoiu, central Romania	Late/early Maastrichtian boundary	Csiki-Sava *et al.*, 2016; Venczel *et al.*, 2016
Albanerpeton sp. "Sânpetru species" *sensu* Carrano *et al.* (2022)	Pui localities, Haţeg Basin, Hunedoara, Romania	Late/early Maastrichtian boundary	Carrano *et al.*, 2022; Codrea & Solomon, 2012; Duffaud, 2000; Folie & Codrea, 2005; Grigorescu *et al.*, 1999; Vasile & Panaitescu, 2012; Venczel *et al.*, 2016
Albanerpetontidae indet.	Serrat del Rostiar, Tremp Basin, Lleida, Spain	Early Maastrichtian	Blanco *et al.*, 2016; Pérez-Pueyo *et al.*, 2021a
Albanerpeton sp. / Albanerpetontidae indet.	Vălioara localities, Haţeg Basin, Hunedoara, Romania	Early Maastrichtian	Csiki *et al.*, 2008; Grigorescu *et al.*, 1999; Vasile, 2008; Venczel *et al.*, 2016
Albanerpetontidae indet.	Chera, Iberian Basin, Valencia, Spain	Late Campanian–early Maastrichtian	Company & Szentesi, 2012
Albanerpetontidae indet.	Massecaps locality, Cruzy, Hérault, France	Late Campanian–early Maastrichtian	Buffetaut, 2005; Buffetaut *et al.*, 1999
Albanerpetontidae indet.	Laño, Basque-Cantabric Basin, Burgos, Spain	Late Campanian–early Maastrichtian	Astibia *et al.*, 1990; Duffaud & Rage, 1999
Albanerpetontidae indet.	La Neuve, Bouches-du-Rhône, France	Middle Campanian–late Campanian	Duffaud, 2000; Garcia *et al.*, 2000
Albanerpetontidae indet.	Ollières, Var, France	Campanian	Dutour & Tortosa, 2010
Albanerpetontidae indet. "Csehbánya species" *sensu* Carrano *et al.* (2022)	Iharkút, Veszprém, Hungary	Santonian	Carrano *et al.*, 2022; Szentesi *et al.*, 2013
Celtedens megacephalus	"Le Cavere", Pietraroja, Benevento, Italy	Early Albian	Costa, 1864; Estes, 1981; McGowan, 2002
Albanerpetontidae indet.	Balve-Beckum locality, North Rhine-Westphalia, Märkischer Kreis, Germany	Late Barremian–early Aptian	Skutschas *et al.*, 2020

Wesserpeton evansae	Isle of Wight, England	Barremian	Sweetman & Gardner, 2013
cf. *Albanerpeton* / *Wesserpeton* sp.	Buenache de la Sierra locality, Iberian Basin, Cuenca, Spain	Late Barremian	Buscalioni *et al.*, 2008; Sweetman & Gardner, 2013
Celtedens ibericus	Las Hoyas locality, Iberian Basin, Cuenca, Spain	Late Barremian	McGowan & Evans, 1995; McGowan, 2002
Celtedens megacephalus *Albanerpeton* sp. nov. cf. *Wesserpeton* sp. "Uña species" *sensu* Sweetman and Gardner (2013)	Uña locality, Iberian Basin, Cuenca, Spain	Late Barremian	McGowan, 1998; Sweetman & Gardner, 2013; Wiechmann, 2003
Albanerpetontidae indet.	Vadillos-1 locality, Iberian Basin, Cuenca, Spain	Late Barremian	Barroso-Barcenilla *et al.*, 2017
Albanerpetontidae indet.	Pio Pajarón locality, Iberian Basin, Cuenca, Spain	Late Barremian	Hahn & Hahn, 2001; Wiechmann, 2003
Celtedens cf. *megacephalus* Albanerpetontidae indet.	Colladico Blanco, Galve localities, Iberian Basin, Teruel, Spain	Late Hauterivian–early Barremian	Estes, 1981; Estes & Sanchíz, 1982; McGowan, 1998; Sánchez-Hernández *et al.*, 2007
Albanerpetontidae indet.	La Cantalera locality, Iberian Basin, Teruel, Spain	Late Hauterivian–early Barremian	Canudo *et al.*, 2010
Albanerpetontidae indet.	Vitabäck Clays of Scania, Skåne, Sweden	Berriasian	Rees & Evans, 2002
Albanerpetontidae indet.	Unio Beds, Isle of Purbeck, Dorset, England	Berriasian	Evans & McGowan, 2002; Underwood & Rees, 2002
Celtedens sp. "Purbeck species" *sensu* Carrano *et al.* (2022)	Isle of Purbeck, Dorset, England	Berriasian	Evans & McGowan, 2002; Gardner, 2000b; McGowan & Ensom, 1997
Albanerpetontidae indet.	Angeac-Charente, Charente, France	Berriasian	Allain *et al.*, 2022
cf. *Celtedens* sp.	Cherve-de-Cognac, Charente, France	Berriasian	Mazin *et al.*, 2008, 2006; Pouech *et al.*, 2006
Anoualerpeton unicum	Ksar Metlili, Anoual syncline, Morocco	Tithonian-Berriasian	Gardner *et al.*, 2003; Lasseron *et al.*, 2020
Celtedens sp. nov. *sensu* Wiechmann (2003)	Lourinhã VMA localities, Lisboa district, Portugal	late Kimmeridgian–early Tithonian	Guillaume *et al.*, 2023b; Wiechmann, 2003; Section 3.2

aff. *Celtedens* sp. *sensu* Guillaume *et al.* (2023b) New unnamed taxon 2			
Celtedens sp. nov. *sensu* Wiechmann (2003) "Alcobaça species" *sensu* Carrano *et al.* (2022) aff. *Celtedens* sp. *sensu* Guillaume *et al.* (2023b) New unnamed taxon 2	Guimarota lignites beds, Leiria district, Portugal	Kidmmerigian	Guillaume *et al.*, 2023b; Wiechmann, 2003; Section 3.2
Anoualerpeton priscum	Kirtlington Mammal Bed, Oxfordshire, England	late Batonian	Gardner *et al.*, 2003
cf. *Anoualerpeton priscum*	Strathaird Peninsula, Isle of Skyle, Scotland	late Bathonian	Panciroli *et al.*, 2020
Albanerpetontidae indet.	GEA-2, Anoual syncline, Morocco	early Bathonian	Haddoumi *et al.*, 2016
Albanerpetontidae indet.	Hornsleasow Quarry, Gloustershire, England	early Bathonian	Evans & Milner, 1994; Evans & Waldman, 1996
Albanerpetontidae indet.	Gardies, Aveyron, France	early Bathonian	Seiffert, 1969

Despite having been reported in numerous localities in the Campanian and Maastrichtian (see **Table 3.3.1**), no Upper Cretaceous European albanerpetontid species have been described. In contrast, at least three species were coeval in North America (Gardner, 2000b; Gardner & Böhme, 2008); with apparent affinities to unnamed European material (Blain *et al.*, 2010). However, material from the Pui localities of the Haţeg Basin (Romania), informally referred to "Sânpetru species" (Carrano *et al.*, 2022), has been assigned to *Albanerpeton* sp. (Grigorescu *et al.*, 1999; Venczel *et al.*, 2016 and references therein). Albanerpetontids, as other

lissamphibians, seem to have been little affected by the catastrophic K/Pg event: they survived in the Paleocene of Alberta, Canada (Gardner, 2000a). However, they are not recorded in Europe post K/Pg until the Oligocene of Germany (Wiechmann, 2003; Böhme, 2008; Gardner *et al.*, 2021), despite the South-Pyrenean Basin in Spain providing numerous outcrops encompassing the K/Pg transition (Pérez-Pueyo *et al.*, 2021a).

The aim of our study is to review previously known albanerpetontid material from the uppermost Maastrichtian of Blasi 2B (Huesca Province, Spain), describe new cranial and post-cranial material from this locality, and use the new data to erect a new species representing the youngest European Mesozoic albanerpetontid.

3.3.2 Geological settings

The vertebrate-bearing localities of Arén and Blasi Hill in Ribagorza County (Huesca Province, Aragón Region, northeastern Spain) are exposed along the northwestern flank of the Tremp syncline (or Tremp-Graus Basin) in the South-Pyrenean Basin (*sensu* Seguret, 1972). The Blasi 2B fossils studied here come from the transitional levels of the "grey unit" (or "grey Garumnian unit", see **Figure 1.3.1**), directly overlying the top of the deltaic/barrier island deposits of the Arén Formation (López-Martínez *et al.*, 2001; Riera *et al.*, 2009; Moreno-Azanza *et al.*, 2014; Pérez-Pueyo *et al.*, 2021b), and dated to the late Maastrichtian (López-Martínez *et al.*,

2001) (Oms and Canudo, 2004; Pereda-Suberbiola *et al.*, 2009). See Section 1.3 for more details.

3.3.3 Material & methods

Our study relies on isolated albanerpetontid bones recovered from sediment samples collected at Blasi 2B during a field campaign in 1997. Over five tons of sediments were sampled, washed, and sieved using a 0.5 mm mesh-size (López-Martínez *et al.*, 2001; Blain *et al.*, 2010). The material was separated in three main collections: (1) the 40 specimens previously studied and described as *Albanerpeton* cf. *A. nexuosum* by Blain *et al.* (2010); (2) 25 additional specimens identified Albanerpetontidae indet. by Professor Nieves López Martínez among other vertebrate microfossils (still with their field number BLA2-AXXX), but not reported; and (3) 23 new specimens that we identified from the unchecked picked material.

Indeterminate partial jaws were not included, and dorsal vertebrae were not included in the description, as no new material was identified and the original description (Blain *et al.*, 2010) could not be improved. In the late 1990s early 2000s, some specimens were mounted with carbon tape onto metal stubs and gold coated. Pictures were taken using a Jeol JSM 6400 Scanning Electron Microscope equipped with an analog camera. These specimens were recoated and new material from the same sample were imaged again in 2022 using the same Jeol JSM 6400 SEM, now equipped with

a digital computer for image acquisition. Measurements were obtained with ImageJ (Rasband, 2003).

All specimens from Blasi 2B are stored in the paleontological collections of the Museo de Ciencias Naturales de la Universidad de Zaragoza, Spain (MPZ).

Abbreviations— **IPS**, Institut Català de Paleontologia Miquel Crusafont, Sabadell, Barcelona, Spain; **MCCM**, Museo de las Ciencias de Castilla La Mancha, Cuenca, Spain; **MNHN**, Muséum national d'Histoire naturelle, Paris, France; **MPZ**, Museo Paleontológico de Zaragoza (Museo de Ciencias Naturales de la Universidad de Zaragoza), Spain; **OMNH**, Oklahoma Museum of Natural History, Norman, Oklahoma, USA; **RTMP**, Royal Tyrrell Museum of Palaeontology, Drumheller, Alberta, Canada; **SEM**, Scanning electronic microscope; **TMM**, Vertebrate Paleontology Laboratory at the Jackson School Museum of Earth History (University of Texas), Austin, Texas; **UALVP**, University of Alberta Laboratory for Vertebrate Palaeontology, Edmonton, Alberta, Canada.

3.3.4 Systematic palaeontology

Class Amphibia Linnaeus, 1758

Subclass Lissamphibia Haeckel, 1866

Family Albanerpetontidae Fox & Naylor, 1982

Genus *Albanerpeton* Estes & Hoffstetter, 1976

Albanerpeton sp. nov. (New unnamed taxon 3)

(**Figure 3.3.1** to **Figure 3.3.7**)

2010 *Albanerpeton* cf. *A. nexuosum* Blain *et al*. p. 434; fig. 2

Figured specimens—MPZ 2009/219, fused frontals (putative holotype; **Figure 3.3.2A**); premaxillae (n=2), MPZ 2023/434, BLA2-A98; maxillae (n=3), MPZ 2009/184, MPZ 2023/433, MPZ 2023/445; fused frontals (n=3), MPZ 2023/430, MPZ 2023/431, MPZ 2023/442; parietals (n=1), MPZ 2023/432; dentaries (n=4), MPZ 2009/186, MPZ 2009/200; MPZ 2023/436, BLA2-A105; articulars (n=5), MPZ 2023/437–440, MPZ 2023/443; quadrate (n=1), MPZ 2023/441; atlas (n=1), BLA2-A43; axis + first dorsal centrum (n=1), BLA2-A110; humeri (n=6), MPZ 2009/221, MPZ 2023/427–429, MPZ 2023/444, MPZ 2023/445; femora (n=1), BLA2-A74.

Referred material—premaxillae (n=6), MPZ 2009/179–181, BLA2-A19, BLA2-A23, BLA2-A106; maxillae (n=7), MPZ 2009/182, MPZ 2009/183, MPZ 2009/185, MPZ 2023/448, BLA2-A14, BLA2-A28, BLA2-A108; fused frontals (n=3), BLA2-A61, BLA2-A78, BLA2-A120; parietals (n=3), BLA2-A97, unnumbered specimen; dentaries (n=34), MPZ 2009/187–199, MPZ

2009/201–10, MPZ 2023/447, BLA2-A22, BLA2-A25, BLA2-A56–A58, BLA2-A60, BLA2-A103, BLA2-A104, BLA2-A109, BLA2-A112; dorsal vertebrae (n=2), MPZ 2009/226, MPZ 2009/227; humeri (n=5), MPZ 2009/222–225, MPZ 2023/446.

Stratigraphic horizon—Blasi 2B, "grey unit" of the Tremp Formation, upper Maastrichtian (*Abathomphalus mayaroensis* biozone; polarity chron C30n; 67-66 Ma), Upper Cretaceous.

Geographic range— Ribagorza County, Huesca Province, NE Spain.

Putative diagnosis

New unnamed taxon 3 is distinguishable from the other members of Albanerpetontidae by the following unique combination of one autapomorphy and one synapomorphy (marked with an asterisk): anterior end of the orbital margin of the frontal anterior to the anteroposterior midpoint of the bone*; and rectangular anterior cotyles of the atlas.

Putative differential diagnosis

New unnamed taxon 3 differs from *Anoualerpeton priscum*, New unnamed taxon 2, and the "Purbeck species" by having a deeper spinal groove in the atlas. It differs from *Celtedens megacephalus* by having a less deep glenoid fossa in the articular. New unnamed taxon 3 further differs from all above mentioned albanerpetontid taxa by having triangular fused frontals. It differs from *Wesserpeton evansae* by by having the nasal process of the maxilla projecting faintly anteriorly, and a deeper spinal grove in the

atlas. New unnamed taxon 3 differs from *Yaksha perettii*, *Shirerpeton isajii*, and the "robust-snouted clade" (*Albanerpeton nexuosum*, *Albanerpeton inexpectatum*, and *Albanerpeton pannonicum*) by having a tapered/hasted internasal process of the fused frontals. New unnamed taxon 3 differs from all *Albanerpeton* species by having the nasal process projecting faintly anteriorly; and from all albanerpetontid species but *Albanerpeton galaktion* by having a large palatal foramen, although it is smaller than in *A. galaktion*. It furthers differs from *Albanerpeton arthridion* and *Albanerpeton ektopistikon* by having an anterior end of the tooth row of the maxilla not extending anteriorly to the maximum indentation along the leading edge of the nasal process. New unnamed taxon 3 further differs from *A. galaktion* by having a ventral scar for the mandibularis muscle, slightly curved orbital margins of the fused frontal, continuous anterior and posterior median fossae on the ventral surface of the fused frontals, and ventrolateral crests of the fused frontals separated by about half of their width. New unnamed taxon 3 differs from *Yaksha perettii*, the "robust-snouted clade", and the "Paskapoo species" by having a gracile premaxilla, and further from the "robust-snouted clade" by having orbital margins of the fused frontal with narrow and close to the lateral edge of the ventrolateral crests. It further differs from *A. nexuosum* differs by having a dentary with a straight occlusal margin and weak heterodonty, and an anterior end of the tooth row of the maxilla not extending anteriorly to the maximum indentation along the

leading edge of the nasal process; and from both *A. inexpectatum* and *A. pannonicum* by having the *pars dorsalis* of the premaxillae less inclined.

Description

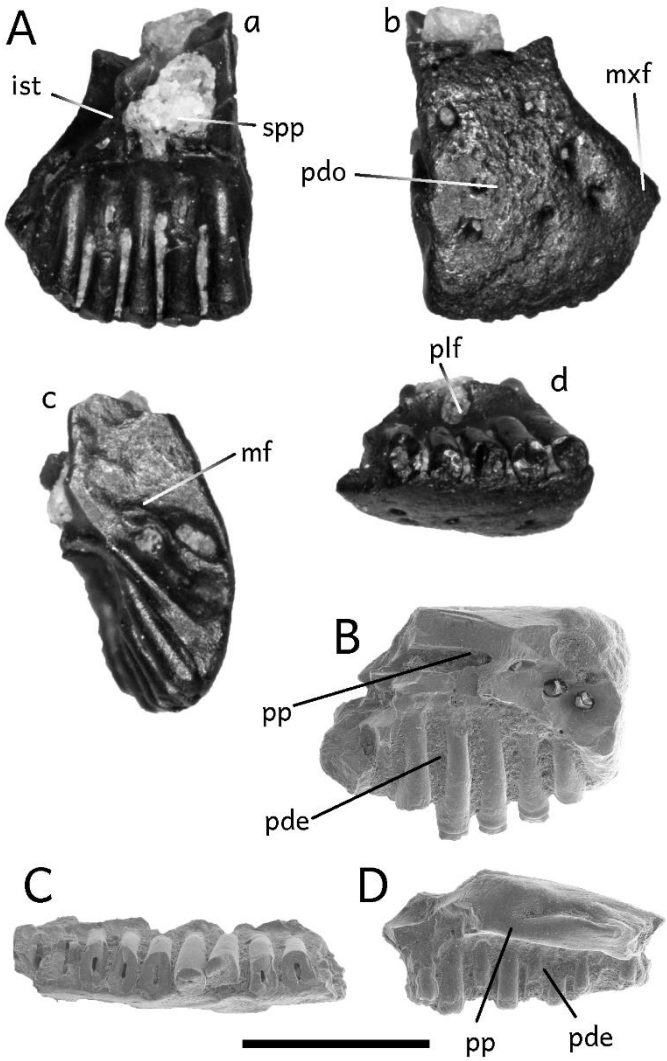

Figure 3.3.1: New unnamed taxon 3 upper jaw bones. **A**; left premaxilla BLA2-A98 in lingual (a), labial (b), medial (c), and ventral (d) views. **B**; left premaxilla MPZ 2023/434 in lingual view. **C**; left maxilla MPZ 2023/433 in ventral view. **D**; right maxilla MPZ 2023/435 in lingual view. A is photostacking photographs, B–D are SEM images. Abbreviations: **ist**, internal strut; **mf**, medial flange; **mxf**, maxillary facet; **pdo**, *pars dorsalis*; **pde**, *pars dentalis*; **plf**, palatal foramen; **pp**, *pars palatinum*; **spp**, suprapalatal pit. Scale bar represents 1 mm.

Premaxilla (**Figure 3.3.1A**, **B**)—The premaxillae belong to the gracile morphotype *sensu* Gardner (2002). There are between five and six tricuspid, pleurodont, non-pedicellate, mesiodistally compressed teeth. None of the premaxillae is fused, but they display a deep inter-premaxillary contact with a dorsoventral medial flange. Unfortunately, none of the elements preserve the dorsal-most part of the *pars dorsalis*. The preserved lower portions of the *pars dorsalis* are ornamented only by small labial foramina. The undivided suprapalatal pit is obscured internally by matrix in BLA2-A98 (**Figure 3.3.1A**), the only specimen that preserved it, but its borders can be seen. It is medial to the internal strut, which is not perforated.

The suprapalatal pit is triangular, faces lingually and appears moderate in size. Its ventral margin is low, continuous with the dorsal surface of the *pars palatinum*. The latter is not well preserved in any of the specimens. However, one palatal foramen can be observed in BLA2-A98, and its ventral and dorsal openings are medial to the suprapalatal pit, almost in contact with the internal strut, making the canal vertical. Although the foramen is not complete, it appears to be as big in diameter as the width of the largest teeth. The *pars dentalis* exhibits a marked slit oriented ventrolateral-dorsomedially on its laterodorsal corner, with a shallow groove rather than a true facet.

Maxilla (**Figure 3.3.1C**, **D**)—None of the maxillae is complete and all lack the posterior section of the bone. However, based on their preserved anatomy,

it can be safely assumed they had the usual slender, elongated morphology with a tapered posterior extremity. The *pars facialis* is ornamented by small foramina in line. The dorsal edge of the *pars facialis* is bevelled and dorsally merges to the labial surface of the nasal process. In BLA2-A28 (not figured), it protrudes, forming a strong ridge constricted by two shallow grooves at the base. MPZ 2009/184 (not figured) was the only specimen in which the nasal process was preserved, but it has been unfortunately broken during its examination. When intact, this nasal process was triangular, rather blunt in lingual view, and slightly projected anteriorly (see fig. 2 in Blain *et al.*, 2010). A faint labial recess with a shallow concavity and a lateral crest can be observed at its base. The teeth are tricuspid, pleurodont, non-pedicellate, and mesiodistally compressed.

Due to the lack of overlapping material, the length of the tooth row cannot be determined, although it was most likely over 10 teeth. Nevertheless, the tooth row does not extend more anteriorly than the maximum projection of the nasal process, as originally seen in MPZ 2009/184. The ventral margin of the *pars dentalis* is straight, with no significant heterodonty. Unfortunately, none of the premaxillary processes is preserved in our specimens. Also, the jugal process of the *pars palatinum* is not preserved in any of the specimens. The dorsal surface of the *pars palatinum* has the usual saddle-shaped morphology and extends up to the base of the nasal process dorsal rim. It can be ornamented with foramina that extend into longitudinal grooves. The *pars palatinum* extend lingually

into the maxillary shelf, which displays a shallow ventral trough. The internal narial margins are faintly indented labially, but not dorsally.

Frontals (**Figure 3.3.2A–D**)—None of the fused frontals are complete, however based on the fragments comprising the most-complete MPZ 2009/219 (**Figure 3.3.2A**), it can be determined that the general outline is strongly triangular and that the anterior end of the orbital margin is anterior to its anteroposterior midpoint of the bones (frontal length at the midline is 3.50 mm, orbital margin length is 2.04 mm, OML/FML ratio = 0.58). The dorsal surface exhibits the typical polygonal ornamentation; although some specimens display a smoother surface, indented with irregular grooves. The internasal process is tapered/hastate, with a flat ventral surface that does not extend ventrally. The anterolateral processes are acute, elongate, and project anteriorly. There is a ventral ridge extending from the anterolateral process to the ventrolateral crests, with a very faint triangular rugose surface placed anteriorly. It is unsure if this is an articular facet or a scar attachment for a muscle, orbital connective tissue, or fascia around the brain. Its posterior vertex is connected to a shallow groove that runs posteriorly up to the ventrolateral crests. There is one foramen, placed anteriorly on the ventral ridge.

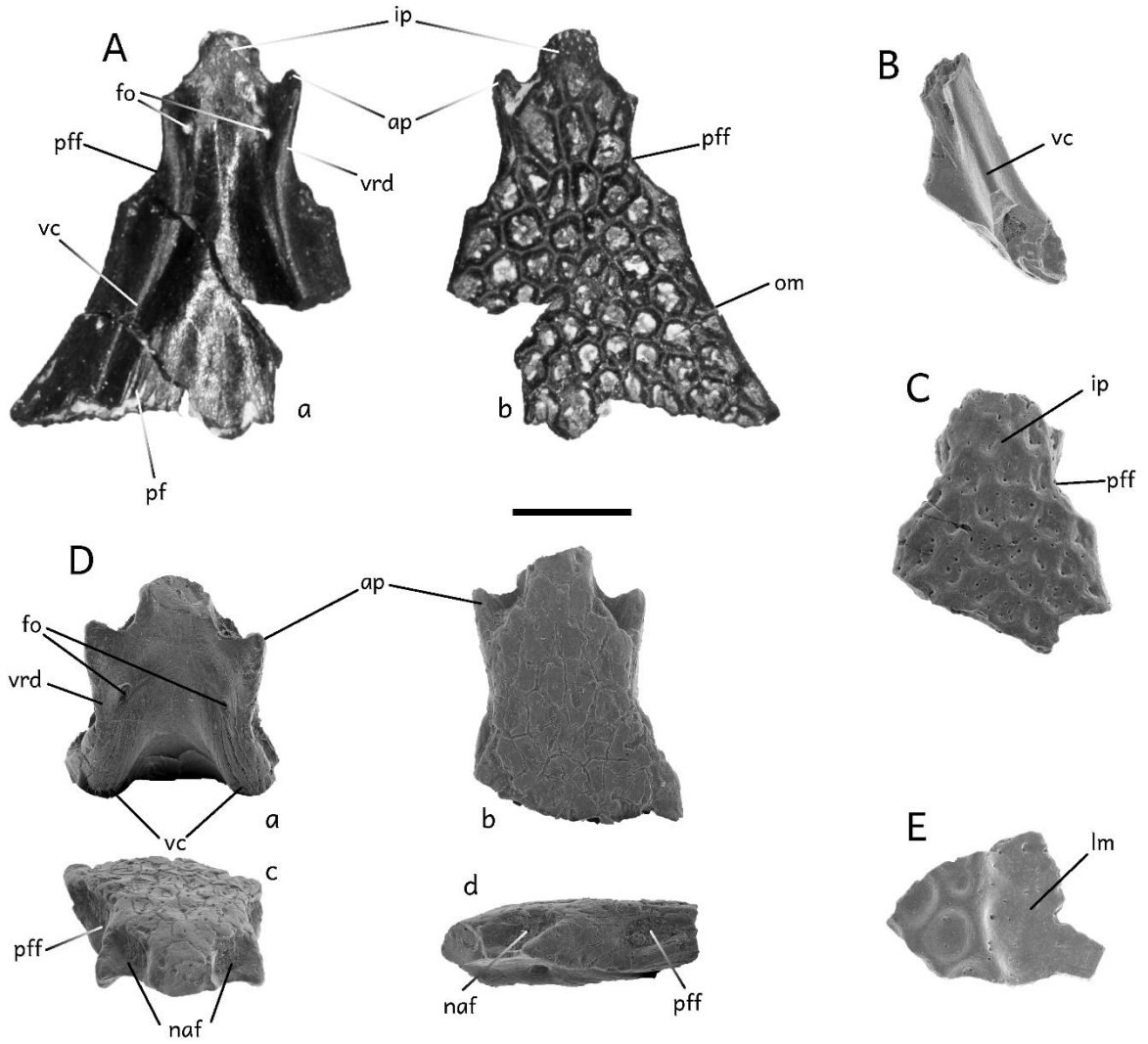

Figure 3.3.2: New unnamed taxon 3 skull roof bones. **A**; fused frontal bones MPZ 2009/219 (putative holotype) in ventral (*a*) and dorsal (b, reconstructed from fragments) views. **B**; frontal MPZ 2023/431 in ventral view. **C**; frontal MPZ 2023/430 in dorsal view. **D**; frontal MPZ 2023/442 in anteroventral (*a*), dorsal (b), anterodorsal (c), and lateral (d) views. **E**; parietal MPZ 2023/432 in dorsal view. Only the posterior part of MPZ 2009/219 was previously published (fig. 2; Blain *et al.*, 2010), but the anterior section was found with the same label and fits. A is photostacking photographs, B–D are SEM images. Abbreviations: **ap**, anterolateral process; **ip**, internasal process; **lm**, lateral margin; **naf**, nasal facet; **om**, orbital margin; **pf**, parietal facet; **pff**, prefrontal facet; **vc**, ventrolateral crest; **vrd**, ventral ridge of the anterolateral process. Scale bar represents 1 mm.

The narrow ventrolateral crests are triangular in dorsoventral profile, with a subconcave lateral margin, but they do not form a parapet. The anterior and posterior width of the ventrolateral crests are similar. Apart the groove connected anteriorly to the posterior vertex mentioned above, no clear canal could be observed posteriorly on the ventral rim of the ventrolateral crests. It is unclear as to whether the parietal facets are poorly preserved, or they lack indentation; as the skull roof and the right ventrolateral crest seem posteriorly complete and preserved in MPZ 2009/219. The lateroposterior margin of the ventral roof, however, is indented, but does not exhibit a recess. The orbital margins are faintly curved anteriorly, and almost straight posteriorly. They are bevelled, with a subconcave surface facing lateroventrally. No ventromedian suture or ventromedial keel are present in available specimens.

Parietal (**Figure 3.3.2E**)—Three bones in the new collection are identified as parietals. However, they are too fragmentary to be particularly informative. In MPZ 2023/432 (**Figure 3.3.2E**), only the anterodorsal section has been preserved with some part of the lateral margin, but no occipital shelf nor postorbital wing are preserved. Furthermore, no frontoparietal nor interparietal sutures can be seen. The ventral surface is completely smooth, without any facet, ridge, recess, or concavity; whereas the dorsal surface bears polygonal ornamentation similar to the frontals.

Dentary (**Figure 3.3.3**)—As for other jaw elements, none of the dentaries is complete, and most are small fragments of the bone. Therefore, the state of heterodonty could not be determined, although it seems to be weak. As seen in upper-jaw teeth, those of the dentary are tricuspid, pleurodont, non-pedicellate, and mesiodistally compressed, but there is not enough overlapping material to determine the length of the tooth row. The Meckelian canal is closed in all specimens, none preserves the posterior opening. A second canal is also present, located dorsolabially of the Meckelian canal.

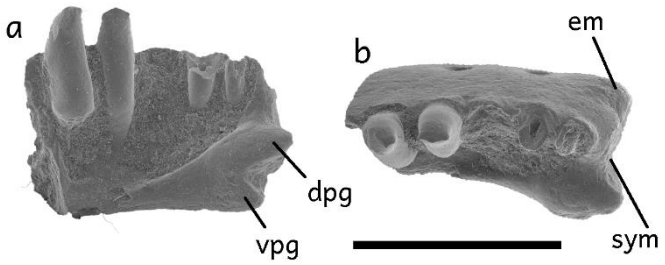

Figure 3.3.3: New unnamed taxon 3 left dentary MPZ 2023/436 in lingual (a) and dorsal (b) views (SEM images). Abbrevations: **em**, eminence; **dpg**, dorsal prong; **sym**, symphysis; **vpg**, ventral prong. Scale bar represents 1 mm.

The anteroventral surface of the symphysis is obscured by matrix but displays a deep fossa, suggesting the presence of an anterior foramen. The symphysis exhibits a subvertical wall, with a very faint and low eminence, almost not projecting, and prongs strongly projecting lingually. Right dentaries display one or two prongs, whereas the only left dentary preserving the symphyseal region has two (MPZ 2023/436; **Figure 3.3.3**). The dorsal prong is usually the most well-developed, except in MPZ 2009/200 (not figured) where the ventral one is larger. Despite the absence

of overlapping material, the dorsal edge of the dental parapet seems to be straight in lingual/labial outline in all specimens. The articular surface for the angular is not preserved. The labial surface is perforated with small foramina, but the fragmentary nature of the material prevents determination of the pattern. However, it appears that there are no more than four external foramina: they are relatively low, in line, and restricted to the anterior part of the dentary. The bone also exhibits a ventral ridge delimiting the scar for the intermandibularis muscle, the latter being restricted to the ventral margin. The delimitation comprises a longitudinal groove. The subdental shelf is relatively narrow, being slightly wider posteriorly than anteriorly. It displays a rather narrow but deep gutter-like trough. The subdental shelf becomes more lingually inclined posteriorly, with MPZ 2009/186 and BLA2-A105 (not figured) exhibiting a shallow facet with a long acuminate anterior apex. It is unclear if this corresponds to the prearticular facet. However, the facet occurs where this would be expected and extends much more anteriorly than the Meckelian opening and the end of the tooth row.

Articular (**Figure 3.3.4**)—None of the angular seems to have preserved their anterior section, MPZ 2023/443 (**Figure 3.3.4E**) being the better preserved on that regard. The angular is fused to the articular, but only its most posterior section is preserved. The posterior facing glenoid fossa of the articular is saddle-like and oriented vertically. It forms a broad but cotylar

articular facet. The facet is broken in MPZ 2023/437 (**Figure 3.3.4A**), making it appear subvertical.

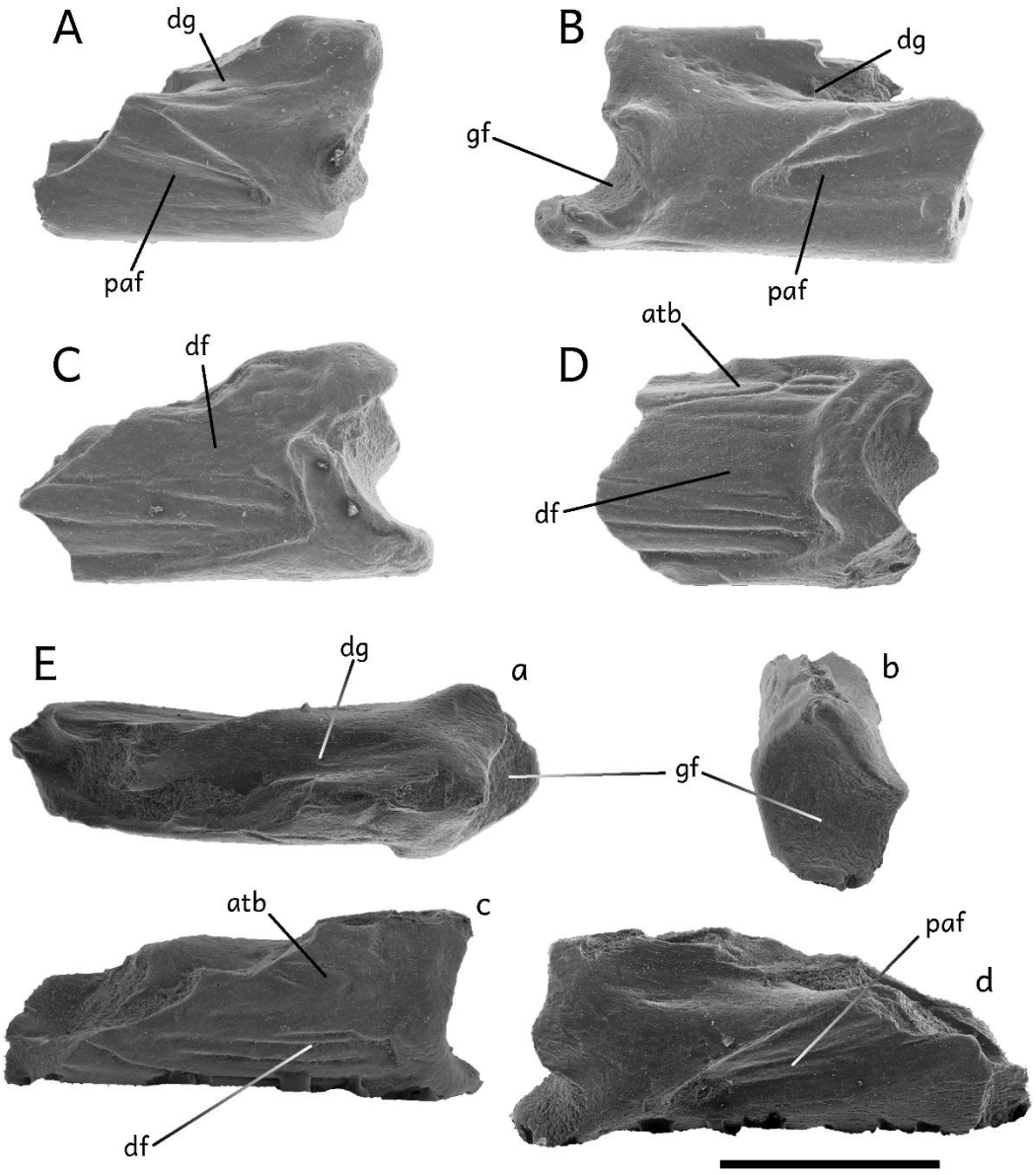

Figure 3.3.4: New unnamed taxon 3 articular. **A**; right articular MPZ 2023/437 in medial view. **B**; left articular MPZ 2023/439 in medial view. **C**; left articular MPZ 2023/438 in lateral view. **D**; left articular MPZ 2023/440 in lateral view. **E**; left articular MPZ 2023/443 in dorsal (a), posterior (b), dorsolateral (c), and dorsomedial (d) views. All are SEM images. Abbreviations: **atb**, anterior tuberosity; **df**, dentary facet; **dg**, dorsal groove of the abductor fossa; **gf**, glenoid fossa; **paf**, prearticular facet. Scale bar represents 1 mm.

The lateral surface of the articular displays a large, rectangular lateral facet, the posterior margin of which is curved. Anteriorly, this lateral facet exhibits dorsally an anterior tuberosity (**Figure 3.3.4D**), that is variably pronounced in individual specimens. In the most extreme cases (MPZ 2023/443; **Figure 3.3.4Ec**), the facet is limited to the ventral surface, while the tuberosity extends to the entire dorsal section. The medial surface of the articular displays an acute ventromedial facet. The facet is deep and displays a groove ventrally. Its ventral margin is straight and horizontal. The *adductor fossa* is marked by a deep dorsal groove.

Quadrate (**Figure 3.3.5**)—Just one quadrate has been identified. Only the anterior part is preserved, the dorsal process being broken. The anterior condyle is asymmetric, anteroposteriorly compressed, and ventrally concave, forming a trochlear articulation joint. The lateral lip is faintly pronounced, almost absent, whereas the lateral concavity is reduced to a faint groove. The lateroventral facet of the dorsal process is marked, with deep margins forming a slot with an acute anterior apex. More specifically, the laterodorsal margin strongly expands laterally, while its lateroventral margin forms a small shelf.

Medially, the posterodorsal surface displays a triangular ventral region with a groove running along the anterior condyle. The posterodorsal surface extends medially before becoming reduced more posteriorly. The bone displays a thickened medial boss, which is triangular with a medial

apex and a U-shaped posterodorsal surface to articulate with the pterygoid. The anterodorsal surface of the quadrate displays a strong lateral pillar but does not have a pit or posterior fossa.

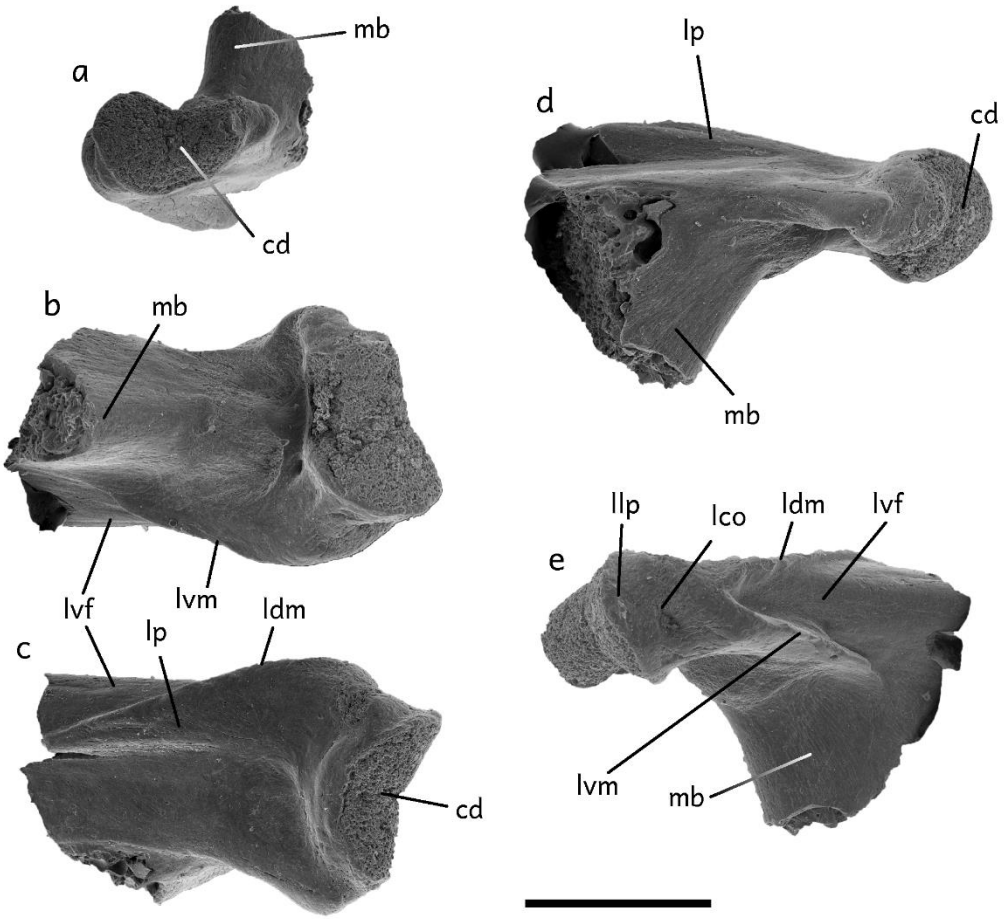

Figure 3.3.5: New unnamed taxon 3 left quadrate MPZ 2023/441 in anterior (a), ventral (b), dorsal (c), medial (d) and anterolateral (e) views. All are SEM pictures. Abbreviations: **cd**, anterior condyle; **lco**, lateral concavity; **ldm**, laterodorsal margin; **llp**, lateral lip; **lp**, lateral pillar; **lvf**, lateroventral facet; **lvm**, lateroventral margin; **mb**, medial boss. Scale bar is 1 mm.

Atlas (**Figure 3.3.6A**)—Only one specimen has been identified. It preserves the centrum and bases of the neural arch walls. The bone exhibits the characteristic short, ribless centrum of albanerpetontids. The odontoid

process is broad, blunt, and displays one ventral foramen. Its dorsal surface is flat, with the lateral margins dorsally curved and the anterior portion ventrally declined. A shallow groove on the dorsal surface follows the anterior outline of the odontoid process, delimiting the smooth anterior section and the more rugose posterior section. The paired anterior cotyles are not separated by a ventral groove; however, their dorsal margins are confluent with the thin lateral edge of the odontoid process. The articular surfaces of the anterior cotyles are mostly flat. Their surfaces are continuous across the ventral surface of the odontoid process.

The general outline of the anterior cotyles is subrectangular, with a faint lateral indentation in the middle of the anterior rim. The cotyles are subperpendicular to the main axis and faces anterodorsally. The dorsal and more pronounced ventral edges of the posterior cotyles are deeply excavated anteriorly, forming a large recess. It forms a tripartite articular facet, with one subhemispherical dorsal facet, and two semilunar ventral facets, the latter of which are indistinct. A spinal foramen is present on the left, between the posterior surface of the anterior cotyles and the base of the neural arch. On the right, the base of the neural arch wall is more broken and actually reveals a deep groove, connecting to the spinal foramen and receiving the spinal nerve. That groove is almost enclosed by the remaining ridges of the base of the neural arch wall.

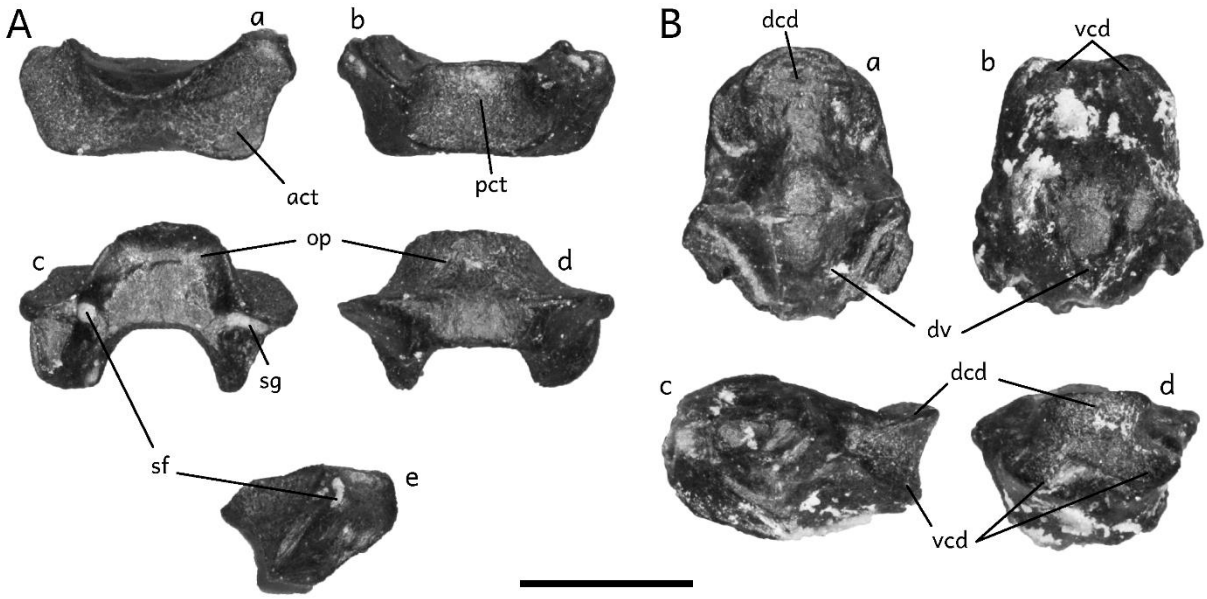

Figure 3.3.6: New unnamed taxon 3 cervical vertebral series. **A**, atlas centrum vertebra BLA2-A43 in anterior (a), posterior (b), dorsal (c), ventral (d), and left lateral (e) views. **B**, axis vertebra BLA2-A110 fused with anterior portion of centrum first dorsal vertebra in dorsal (a), ventral (b), right lateral (c), and anterior (d) views. A and B are photostacking photographs. Abbreviations: **act**, anterior cotyle; **dcd**, dorsal condyle; **dv**, 1st dorsal vertebra; **op**, odontoid process; **pct**, posterior cotyle; **sf**, spinal foramen; **sg**, spinal groove; **vcd**, ventral condyle. Scale bar represents 1 mm.

Axis (**Figure 3.3.6B**)—Only one axis has been identified, and it is fused with the first true dorsal vertebra, although the latter only preserves the anterior part of the centrum. The axis is short, ribless, without a neural arch, and appears very broad laterally. The posterior surface of the centrum is obscured by the first dorsal vertebra, preventing to see the notochordal pit, but its outline is subcircular. The ventral surface of the axis is strongly inflated posteriorly.

The anterior condyles form the characteristic tripartite facet. The hemispherical dorsal condyle exhibits a relative flat dorsal surface, with anterior ridges not thickened. However, the base is strongly constricted

posteriorly, joining the ventral condyle. Although the dorsal condyle is rather large, it does not obscure the ventral condyles in dorsal view. The two ventral condyles are semilunar and are face laterodorsally, with a curved anterior outline well-marked. On the ventral surface of the ventral condyle, a shallow indentation on the anterior margin separates two weak tips.

Humerus (**Figure 3.3.6**)—Although none is complete, judging by available specimens, the humerus has an elongated, slender shaft in line with the proximo-distal centreline of the radial condyle *sensu* Carrano *et al*. (2022) (referred only as "condyle" by Estes and Hoffstetter (1976)), or humeral ball *sensu* Sweetman and Gardner (2013). However, it cannot be determined if the axis of the bone is rotated and to what, if any, extent. The proximal humeral condyle is hemispherical and smaller than the radial condyle. Proximal to the former, the lateral surface of the humeral head displays a deep triangular proximal humeral fossa, flanked by strong medial and weak lateral ridges. There is no distal foramen, however this fossa extends into a short proximo-distal furrow at its distal extremity. The smooth deltopectoral crest is present but is relatively faint and does not project much lateroventrally. Its outline displays a convex inclination point with the humeral head. No *crista dorsalis*, or *crista ventralis*, *sensu* McGowan (2002) is observed, as observed in other albanerpetontids for which the humerus is known.

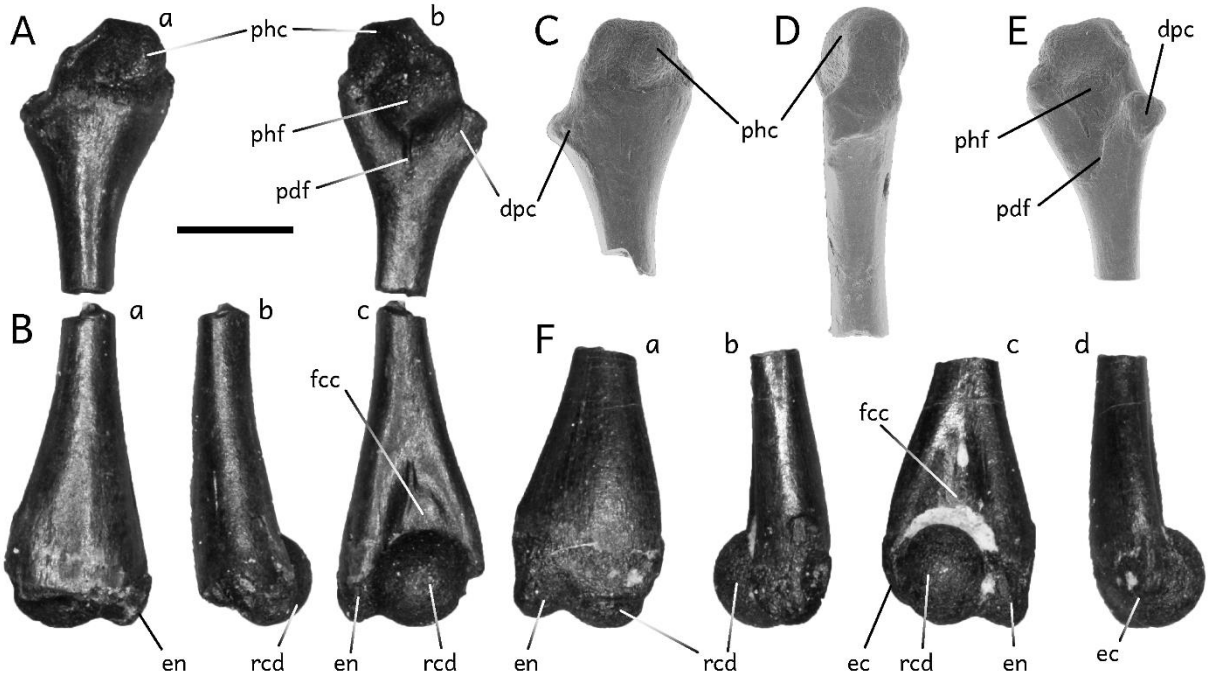

Figure 3.3.7: New unnamed taxon 3 forelimbs. **A**; proximal end of left humerus MPZ 2023/444 in medial (*a*) and lateral (b). **B**; distal end of left humerus MPZ 2023/445 in dorsal (*a*), lateral (b), and ventral (c) views. **C**; proximal end of left humerus MPZ 2023/428 in medial view. **D**; proximal end of left humerus MPZ 2023/427 in ventral view. **E**; proximal end of left humerus MPZ 2023/429 in lateral view. **F**; distal end of right humerus MPZ 2009/221 in dorsal (*a*), lateral (b), ventral (c), and medial (d) views. A, B, and F are photostacking photographs. C–E are SEM images. A and B are stored under the same label and were broken, but indeed seem to fit together. Abbreviations: **dpc**, Deltopectoral crest; **ec**, ectepicondyle; **en**, entepicondyle; **fcc**, *fossa cubitus centralis*; **pdf**, proximo-distal furrow; **phc**, proximal humeral condyle; **phf**, proximal humeral fossa; **rcd**, Radial condyle. Scale bar is 1 mm.

The radial condyle is a prominent, ossified, hemispherical ball, the width of which is between one-third and one-half of the total width of the distal end of the bones. The round entepicondyle *sensu* Estes and Hoffstetter (1976), or radial epicondyle *sensu* Sweetman and Gardner (2013), is separated from the radial condyle by a small groove. The round ectepicondyle *sensu* Estes and Hoffstetter (1976), or ulnar condyle *sensu*

Carrano *et al.* (2022), is present but reduced in comparison to the entepicondyle. The *fossa cubitus centralis* is well marked. It extends proximally, but always terminates as a small proximal foramen. It is bordered by robust margins on both sides.

Femur (not figured)—Only the distal part of one specimen (BLA2-A74) has been recovered and is relatively uninformative. As in other albanerpetontids, the epiphysis is not ossified, and the bone displays a concave distal surface. There are two mesiodistal furrows extending longitudinally, for attachment with the fibula.

Remarks

As it is used in microfossil vertebrate assemblages (Eberth *et al.*, 2007b), all bones identified in this study were disarticulated and highly fragmentary. Although broken into three pieces, the fused frontal MPZ 2009/219 appeared to be the best preserved. When multiple examples are available, homologous elements look similar and do not display major morphological variations. In consequence, all the specimens from Blasi 2B here described are considered to be monospecific.

Based on the parts that are preserved in the premaxillae, although the palatal foramen in New unnamed taxon 3 appears smaller than the one observed in *Albanerpeton galaktion* Fox and Naylor, 1982 from the Late Cretaceous of western North America (Gardner, 2000b; Sweetman & Gardner, 2013), it remains relatively bigger than the one observed in other

albanerpetontids. However, due to the low number of premaxillae from Blasi 2B preserving this character, it is difficult to evaluate it intraspecific variation in this character, which has been previously noted (Sweetman & Gardner, 2013). Nevertheless, we refute previous claim stating that the premaxilla in New unnamed taxon 3 does not share affinities with *A. galaktion* (Blain *et al.*, 2010), as both species are the only ones in Albanerpetontidae to display a palatal foramen that can be described as large. The maxillae seem more robust than the New unnamed taxon 2 (see Section 3.2) from the Late Jurassic of the Guimarota beds (Wiechmann, 2003) and the Lourinhã Formation in Portugal.

As previously reported in other species (Guillaume *et al.*, 2023b), the frontal ornamentation in New unnamed taxon 3 exhibits various ontogenetic stages. *Albanerpeton gracile* Gardner, 2000 from the Campanian of the western and southern North America was described with an acute internasal process (Gardner, 2000b; Carrano *et al.*, 2022), but illustrated specimens, as well as direct observations on referred specimens would suggest that both acute and hastate morphologies coexist, as they do not exhibit an internasal process as spike-like as observed in *A. inexpectatum* Estes and Hoffstetter, 1976 from the early Oligocene–late Miocene of western and central Europe (ARDG, pers. obs., 2023). The internasal process in MPZ 2009/219 may look a little bit more rounded than in other typical hastate/tapered internasal processes; but it is actually slightly worn.

The preservation of the dorsal ornamentation and the lateral margins suggest however this should have been limited and that the internasal process should have only expand little bit more forward. Most importantly, despite the internasal process missing its most-anterior part, this should not affect much the proportion in the fused frontals, a diagnostic feature compared to all others *Albanerpeton* species. Indeed, the ratio between the orbital margin length (OML) and the frontal length at the midline (FML) is 0.58. Then, it would require the internasal process to be at least twice longer than preserved for the anterior end of the orbital margin to be at the same level or posterior to the anteroposterior midpoint of the fused frontal. However, based on its current preservation and compared to referred specimens with internasal frontal preserved in *Albanerpeton arthridion* Fox and Naylor, 1982 from the Aptian-middle Albian of southern North America (e.g. OMNH32398), *A. gracile* (e. g. RTMP 86.60.110), and *A. galaktion* (e. g. UALVP39946), it does not seem that the internasal process is missing that much. Therefore, the measured proportion between OML and FML in MPZ 2009/219 is considered to be representative of the complete bone.

Previous work referred a subset of the Blasi 2B material reported here to *Albanerpeton* aff. *A. nexuosum*, based on some similarities in the frontal (Blain *et al.*, 2010). However, the frontal features used to propose this affinity (narrow triangular ventrolateral crest) turned out to have been mistaken. *Albanerpeton nexuosum* Estes, 1981 from the Upper Cretaceous of western and southern North America does display triangular

ventrolateral crests, but they are broad and their edge is medial to the orbital margin, creating a ventral step. These features are observed in other species of the "robust-snouted clade" *sensu* Venczel and Gardner, 2005, but not in the fused frontals MPZ 2009/219. In addition, although none of *A. galaktion* frontals is complete, the one in New unnamed taxon 3 is clearly more similar to them than it is to *A. nexuosum*. Therefore, here we refute the previous claim of affinity between the Blasi 2B material and *A. nexuosum* based on the frontals.

The articular in New unnamed taxon 3 displays the cotylar articular facet reported in other albanerpetontids (Daza *et al.*, 2020; Gardner, 1999a; McGowan and Ensom, 1997; Sweetman and Gardner, 2013; Venczel and Gardner, 2005; and see Section 3.2). However, it is not as deeply concave as observed in *Celtedens megacephalus* (Costa, 1864) from the Early Albian of Italy; and instead seems more similar to *Wesserpeton evansae* Sweetman and Gardner, 2013 from the Barremian of England. Geomorphometrics could help to better characterize the different cotylar shapes in albanerpetontids. Furthermore, the large, rectangular lateral facet of the articular can be restricted only to the ventral part of the lateral surface, the dorsal part becoming a tuberosity as observed in *W. evansae* (Sweetman & Gardner, 2013). It remains unsure how this character evolved in albanerpetontids, because isolated articular bones are rarely identified and figured, and unreported from other Upper Cretaceous localities.

Similarly, the quadrate is similar to other albanerpetontids in which the bone is known (Gardner *et al.*, 2003; Matsumoto and Evans, 2018; McGowan and Ensom, 1997; and see Section 3.2), and more specifically to *Albanerpeton pannonicum* Venczel and Gardner, 2005 from the late Miocene–Early Pleistocene of Hungary and Italy by displaying a pronounced lateroventral surface displaying a strong rim projecting laterally like an anterior shelf, as well as very faint lateral lip and lateral concavity (ARDG, pers. obs., 2023).

The atlas centrum seems bulkier than in other albanerpetontids species, as the gutter-like dorsal surface of the odontoid process appears much broader. The subrectangular shape of the cotyle does not seem to be the result of breakage or taphonomy or any pathology, as both are similar, and no sign of breakage can be observed. It could be the result of a genetic malformation or ontogeny. However, the centrum in BLA2-A43 seems to be fully ossified, suggesting the individual reach at least subadult size and, therefore, this is not due to ontogeny. Furthermore, such morphology has not been reported in other species presenting several specimens. Therefore, it is here considered that this peculiar shape is the true anatomy of the bone during the life of the individual.

The spinal foramen has been early reported in *Albanerpeton inexpectatum* (Estes & Hoffstetter, 1976); although authors challenged that description of *A. inexpectatum* and suggested that the atlas in

albanerpetontids was not pierced by a spinal foramina, based on their own observations of *Celtedens* and figured specimens of *A. galaktion* and *A. arthridion* (McGowan, 1998b). However, later studies confirmed the original description: the spinal foramen was reported in North American specimens (Gardner, 2000b) previously attributed to *A. galaktion* (Fox & Naylor, 1982), as well as other specimens of *A. inexpectatum* (Gardner, 1999c). Furthermore, a deep open groove was reported in the atlas of *A. arthridion*, (Gardner, 1999a), and a shallower groove was also reported in *Wesserpeton evansae*, *Albanerpeton ektopistikon* Carrano *et al.*, 2022 from the Albian of the Cloverly Formation (Wyoming, USA), *Anoualerpeton priscum* Gardner *et al.*, 2003 from the Bathonian of England, New unnamed taxon 2, and the "Purbeck species" (Carrano *et al.*, 2022; Gardner *et al.*, 2003; Sweetman and Gardner, 2013; and see Section 3.2).

Direct observations of the referred specimens confirmed the presence of either the spinal foramen or the groove carrying the spinal nerve in all previously named species for which atlantes are reliably known (ARDG, pers. obs., 2023). Direct observations of MNHN-LGA1270 *A. inexpectatum* atlas from the type locality (La Grive-Saint-Alban, southeastern France, Miocene), also confirms the original description of the spinal foramen in this species, confirming it is not a variable feature in the species (Gardner, 1999c). Furthermore, direct observation on referred specimens also confirmed for the first time the presence of a groove in *Anoualerpeton unicum* Gardner *et al.*, 2003 from the Lower Cretaceous of Anoual locality

(Talsinnt Province, Morocco) and of a spinal foramen in unpublished specimens of *A. pannonicum*.

However, the absence of a groove or foramen could not be confirmed in any of the *Celtedens* species, as the specimens preserving the atlas only display the ventral surface (ARDG, pers. obs., 2022, 2023); but CT-scans of these may help to answer the question. Illustrations of the specimen TMM 45947-632 from the Aguja Formation (Texas, USA, lower Campanian) are unconclusive on the presence of a spinal foramen or groove (Wick, 2021), as no dorsal view is provided and the lateral views do not clearly show the area. Finally, when the neural arch is preserved, the spinal foramen is indeed present in some indetermined UALVP specimens previously attributed to *A. galaktion*; but if the neural arch is not preserved, only a deep groove similar to the one observed in *A. arthridion* is visible (ARDG, pers. obs., 2023).

Consequently, the atlas in New unnamed taxon 3 stands as a major importance, as the arch is preserved in one side, displaying the spinal foramen, but broken on the other side, displaying the deep groove. This confirms an earlier theory suggesting that the deep groove would be closed as a foramen if the neural arch were fully preserved in *Albanerpeton arthridion* (Gardner, 1999a). More overall, the evolution of the feature encapsulating the spinal nerve would suggest a tendency toward a stronger ossification, as observed in the premaxillae becoming more robust and

consistently fused, and in the frontals becoming broader with stronger orbital margins (Gardner, 2000a, 2002; Gardner & Böhme, 2008).

Basal species display a shallower spinal groove, and none are known to have a fully preserved neural arch, which could be explained by two hypotheses: either the neural arch was not fully fused in adult specimens, or it was not encapsulating the spinal nerve. Then, more deeply nested species started to develop a deeper spinal groove, while the neural arch was becoming more strongly fused with the centrum and encapsulating the spinal nerve, as seen in New unnamed taxon 3; until reaching the level of ossification observed in *A. pannonicum* and *A. inexpectatum*, where the neural arch are better preserved and fully encapsulates the spinal nerves. This could translate into a change of the lifestyle, toward more constrained head movements, which is also reflected in the cranial bones.

The axis in New unnamed taxon 3 is more robust than in other species for which that element is known, but this could be linked to its fusion with the first trunk vertebra. Fused axes were reported in the holotype and some other specimens of *A. inexpectatum* (Estes & Hoffstetter, 1976; Estes, 1981; Gardner, 1999c), and were even suggested as a putative diagnostic feature of the species (McGowan, 1998b). It was suggested that it could be linked to ontogenetic development of the sclerotomes (McGowan, 1998b). This is also supported by the fact that the axes reported in other *Albanerpeton* species were found isolated and unfused. This could not be confirmed on the

holotype of *Celtedens megacephalus* because of the preservation of the specimen (ARDG, pers. obs., 2022), and this remains inconclusive in *Celtedens ibericus* McGowan & Evans, 1995 from the Barremian of Spain (Las Hoyas locality), as the axis is not ossified in the holotype MCCM-LH6020A but could not be confirmed in MCCM-LH17069B (ARDG, pers. obs., 2023).

Therefore, New unnamed taxon 3 is the second albanerpetontid species to be reported with an axis fused with the first dorsal vertebra, confirming that this feature is not unique to *A. inexpectatum*. However, it remains uncertain if this fusion takes place in all albanerpetontids or if it appears once or several times in the *Albanerpeton* lineage. Indeed, axes were previously reported only in two species: the more basal *A. ektopistikon* and the more deeply nested *A. inexpectatum* (Estes & Hoffstetter, 1976; Gardner, 1999c; Carrano *et al.*, 2022), so an important part of the morphological evolutionary history for that bone is missing.

The deltopectoral crest of the humerus appears less developed in New unnamed taxon 3 than in other species (Gardner, 1999a; Sweetman and Gardner, 2013; Guillaume *et al.*, in prep; ARDG, pers. obs., 2023). However, it remains unclear if this is due to preservation bias or some other factor. New unnamed taxon 3 shares with *Anoualerpeton unicum*, *Albanerpeton inexpectatum*, *A. pannonicum*, *Wesserpeton evansae*, New unnamed taxon 2, and the "Purbeck species" a marked *fossa cubitus centralis*, with strong and deep edges. However, the fossa extends proximally less than what can be

observed in *A. inexpectatum*, *A. pannonicum*, and *W. evansae*; and instead, it is closer to what is seen in *An. unicum* (Gardner, 1999a; Sweetman and Gardner, 2013; ARDG, pers. obs., 2023, and see Section 3.2).

3.3.5 Discussion

3.3.5.1 Differences and affinities with other Late Cretaceous albanerpetontids in Europe

Several albanerpetontid occurrences have been reported in the Upper Cretaceous of Europe (see **Table 3.3.1**) but were not included in this analysis. The Haţeg Basin yields most of these occurrences, but albanerpetontids remains are extremely fragmentary, precluding identification to genus or species level (Csiki-Sava *et al.*, 2016). Descriptions in the literature have noted morphological similarities between the different localities, and the remains have usually been regarded as belonging to the same taxon, as part of *Albanerpeton* sp. or closely affiliated to the "robust-snouted clade" *sensu* Venczel and Gardner, 2005 (Folie & Codrea, 2005; Venczel *et al.*, 2013; Csiki-Sava *et al.*, 2015, 2016). However, a recent study challenged this hypothesis (Carrano *et al.*, 2022).

Our analysis (see Section 3.4) supports the most recent hypothesis, suggesting that the Haţeg material even may belong to a different lineage than the "robust-snouted clade", and differs from New unnamed taxon 3 in many respects. However, the incomplete and fragmentary nature of the material leaves several character states unresolved. For now, we follow

previous work in considering the material from the Haţeg Basin as belonging to a single taxon, the so-called "Sânpetru species" *sensu* Carrano *et al.*, 2022. A complete revision of the Romanian material by locality would be required in future analyses to properly discuss it.

Outside of Blasi 2B and the Haţeg Basin, Late Cretaceous albanerpetontids in Europe have been reported from the Campanian to the latest Maastrichtian of France (Szentesi *et al.*, 2013; Pérez-Pueyo *et al.*, 2021a). The material from Cassagnau 2 (late Maastrichtian, Haute-Garonne) is reportedly the youngest Mesozoic occurrence (Pérez-Pueyo *et al.*, 2021a), but it is only represented by one poorly described dentary (Laurent *et al.*, 2002). It is highly fragmentary but seems to exhibit the usual straight occlusal margin observed in most deeply nested albanerpetontids, but it differs from Blasi 2B dentaries by having the dorsal symphysial prong more strongly developed than the ventral one (Laurent, 2003; pl. 5, fig. 16).

Similarly, the older material from Ausseing (late Maastrichtian, Haute-Garonne, southern France) consists of one fragmentary dentary with teeth preserved, but it lacks the symphysis (Laurent, 2003; pl. 16, fig.17). Another albanerpetontid dentary has been reported from the Massecaps (late Campanian–early Maastrichtian, Cruzy, Hérault, southern France) locality (Buffetaut *et al.*, 1999; Buffetaut, 2005), but that specimen has not been figured or described.

3.3 CHAPTER 6: NEW ALBANERPETONTIDAE FROM BLASI

More substantial albanerpetontid material from La Neuve (Campanian, Bouches-du-Rhône, southern France) has been figured and briefly described (Duffaud, 2000; Garcia *et al.*, 2000). Unfortunately, the jaw elements do not provide any relevant information, beside the general features allowing to refer the bones to Albanerpetontidae (Garcia *et al.*, 2000). However, the axis is similar to other albanerpetontids and less bulky than the Blasi 2B material. Furthermore, the posterior edge of the articular facet formed by the ventral and dorsal condyles is more acute than in New unnamed taxon 3, being closer to that observed in *Albanerpeton ektopistikon* and *A. inexpectatum*. Furthermore, the atlas from La Neuve exhibits reniform anterior cotyles, seen in most albanerpetontids (Carrano *et al.*, 2022), rather than subrectangular as seen in BLA2-A43.

Several Maastrichtian localities in Spain yield albanerpetontid remains (Blanco *et al.*, 2016; Pérez-Pueyo *et al.*, 2021a). Fragmentary dentaries are known from the Chera Basin (late Campanian–early Maastrichtian, Valencia province), and have been considered similar to the specimens from Blasi 2B (Company & Szentesi, 2012; Blanco *et al.*, 2016); but they are too fragmentary to be conclusive. Similarly, extremely fragmentary maxillae have been reported from La Solana (late Maastrichtian, Valencia province) (Szentesi & Company, 2017), but do not demonstrate anything other than generic albanerpetontid features.

One dentary and one humerus have been reported from Laño (late Campanian–early Maastrichtian, Burgos province) (Astibia *et al.*, 1990; Duffaud & Rage, 1999) and both are similar to the specimens from Blasi 2B (Blanco *et al.*, 2016). Notably, the humeri share a proximodistally short *fossa cubitus centralis*. Also, the humerus entepicondyle is described as "very large" (Duffaud and Rage, 1999; p. 112). However, based on the figured specimen, it does not appear to be more prominent than the radial condyle, and instead seems as developed as observed in other albanerpetontids. The dentary is described with a closed Meckelian canal (Duffaud & Rage, 1999), but only the anterior-most part of the bone is actually preserved.

In addition to Blasi 2B, Blanco *et al.* (2016) reported albanerpetontids from several localities in the Tremp Syncline (Maastrichtian, Huesca and Lleida provinces). Although the figured specimens look similar to New unnamed taxon 3, they are too fragmentary to permit positive attribution. Notably, the premaxilla IPS-85020 from L'Espinau (late Maastrichtian, Lleida province) has been described as similar to the premaxillae from Blasi 2B (Blanco *et al.*, 2016), but the specimen does not preserve either the suprapalatal pit or the palatal foramen, the latter being characteristic for the premaxilla of New unnamed taxon 3. More work and more complete material will be required in order to evaluate whether or not, ranging from the Campanian to the end of the Maastrichtian, they are conspecific.

3.3.5.2 Albanerpetontids in Europe at the dusk of dinosaurs

The albanerpetontid fossil record ranges through the Cretaceous in Europe, but, as seen in **Table 3.3.1**, it is mostly limited to its earliest and latest stages (Sweetman & Gardner, 2013; Blanco *et al.*, 2016; Csiki-Sava *et al.*, 2016; Venczel *et al.*, 2016; Pérez-Pueyo *et al.*, 2021a), creating a patchy record with long temporal gaps. This is not only true for Albanerpetontidae, but also for lissamphibians in general (Szentesi *et al.*, 2013) and in other taxonomic groups in Europe (Csiki-Sava *et al.*, 2015). It can be explained by three factors: (1) lissamphibians, like other small vertebrates represented by micro remains, are oftentimes undersampled in comparison to macrofossil taxa; (2) lissamphibian fossils are mostly represented by fragmentary and isolated bones, which are challenging to identify; and (3) European continental outcrops suitable for preserving lissamphibian remains are relatively scarce and are, in many cases, separated by large time intervals of the Cretaceous, this due to the paleobiogeographic and tectonic history of the European continent (Csiki-Sava *et al.*, 2015).

It is also worth noting that, in Europe during the Cretaceous, albanerpetontids are typically abundant in localities where anurans occur and are abundant; whereas urodeles are scarce or absent, while they were abundant in other major landmasses (Szentesi *et al.*, 2013; Venczel *et al.*, 2016). However, this diversity is mostly known from the later and better-known stages of the Late Cretaceous, from the Santonian to the Maastrichtian (Csiki-Sava *et al.*, 2015).

High sea-levels fragmented Europe, much more than other main landmasses, into an archipelago system with islands of various sizes at the beginning of the Late Cretaceous, substantially reducing the amount of emerged lands (Smith *et al.*, 2001; Golonka & Kiessling, 2002; Pereda-Suberbiola, 2009; Benson *et al.*, 2013; Csiki-Sava *et al.*, 2015). Progressive marine regressions, collisional events, and orogeneses lead to the emergence of widespread land areas during the Santonian; of which the most prominent was the Ibero-Armorican Island (le Loeuff, 2005; Blanco *et al.*, 2016; Pérez-Pueyo *et al.*, 2021a). This island was created during the Maastrichtian from the Pyrenees orogenesis and a westward marine regression, which merged previously isolated continental areas from the Iberian Meseta, the Ebro Massif, and the French Central Massif (Csiki-Sava *et al.*, 2015). Meanwhile, further to the east, marine regression and the rise of the orogenetic and volcanic Pontide mountains created the Rhodope-Maesian platform, in what is now Romania (Jianu & Boekschoten, 1999; Baraboshkin *et al.*, 2003; Szentesi *et al.*, 2013; Csiki-Sava *et al.*, 2015).

3.3.6 Conclusion

Revision of material from the well-known microvertebrate Blasi 2B locality (Huesca province, Spain), and augmented with previously undescribed specimens, finally provides sufficient material to describe the first albanerpetontid species of the Upper Cretaceous of Europe. New unnamed taxon 3 is currently the youngest Mesozoic European albanerpetontid species (late Maastrichtian, chron C30n). Taxonomic

revision of existing taxa and better sampling of known and new localities in the Late Cretaceous of Europe is needed to better characterize these faunal interchanges.

3.4 Chapter 7: New phylogeny of Albanerpetontidae and implications on their taxonomy and palaeobiogeography

Note: The following chapter is intended to be split in two parts and submitted independently, along with the two previous chapters, according to the relevance with the Lourinhã/Guimarota material and the Blasi 2B material.

Paper to in revision in *Journal of Systematic Palaeontology* (Journal impact factor for 2022: 2.2; CiteScore: 5.3; SJR: 0.836; H-index: 56)
Alexandre R. D. Guillaume, Marc E. H. Jones, Eduardo Puértolas-Pascual & Miguel Moreno-Azanza. New albanerpetontid species (Lissamphibia) from the Late Jurassic of Portugal

Paper to be submitted in *Cretaceous research* (Journal impact factor for 2022: 2.1; CiteScore: 4.1; SJR: 0.792; H-index: 76)
Alexandre R. D. Guillaume, Hugues-Alexandre Blain, Eduardo Puértolas-Pascual & Miguel Moreno-Azanza. Witnessing the last giants: a new Albanerpetontidae (Lissamphibia) from the latest Maastrichtian of Europe and its paleobiogeographical implications

3.4.1 Introduction

As for today, Albanerpetontidae comprises fifteen described species allocated into six genera: the type genus *Albanerpeton* Estes & Hoffstetter 1976 (Early Cretaceous – Pleistocene; Central Asia, Europe, and North America); *Anoualerpeton* Gardner *et al.* 2003 (Bathonian – Berriasian; England and Morocco); *Celtedens* McGowan & Evans 1995 (Kimmeridgian – Albian; Europe); *Shirerpeton* Matsumoto & Evans 2018 (Barremian; Japan);

Wesserpeton Sweetman & Gardner 2013 (Barremian; England); and *Yaksha* Daza *et al.* 2020 (Cenomanian, Myanmar).

However, the validity of the genus *Albanerpeton*, as currently defined, is debated. Some authors suggest it to be paraphyletic (Matsumoto and Evans 2018; Daza *et al*. 2020), and only Cenozoic species should be regarded as *Albanerpeton sensu stricto* (Daza *et al*. 2020); while other suggest to broaden its membership to other genera (Carrano *et al.*, 2022). Besides, more informally described and fragmentary material suggests a higher diversity (Estes & Sanchíz, 1982; McGowan & Ensom, 1997; Grigorescu *et al.*, 1999; Gardner, 2000a; Evans & McGowan, 2002; Wiechmann, 2003; Evans *et al.*, 2004; Folie & Codrea, 2005; Skutschas, 2007; Gardner & Böhme, 2008; Blain *et al.*, 2010; Szentesi *et al.*, 2013; Blanco *et al.*, 2016; Csiki-Sava *et al.*, 2016; Venczel *et al.*, 2016; Szentesi & Company, 2017; Lasseron *et al.*, 2020; Carrano *et al.*, 2022), as albanerpetontids are a common component of vertebrate microfossil assemblages, but frequently overlooked.

Here we follow the phylogenetic framework and taxonomical remarks proposed by Daza *et al*. (2020); and provide a new phylogenetic analysis including new taxa and new characters.

3.4.2 Material & methods

Phylogenetic analyses were performed using TNT 1.5 (Goloboff & Catalano, 2016). NEXUS files for the matrix were created with Mesquite

3.61 (Maddison & Maddison, 2019) and exported as a .tnt file that was modified in a text editor to add the necessary settings and commands (see Appendix G.1 for the TNT file). All character states of New unnamed taxon 2 from the Lourinhã Fm and the Alcobaça Fm and New unnamed taxon 3 from the Tremp Fm, as well as holotypes and referred material for most studied species, were based on direct observations by one of us (ARDG).

Nevertheless, the following taxa could not be observed in person and were coded and compared using bibliographic information and photographs: *Shirerpeton isajii* Matsumoto and Evans, 2018; *Yaksha perettii* Daza *et al.*, 2020; *Wesserpeton evansae* Sweetman and Gardner, 2013; and *Albanerpeton pannonicum* Venczel & Gardner 2005 (for A. *pannonicum* only unpublished and unnumbered specimens on loan at the Royal Tyrrell Museum of Palaeontology could be directly observed).

These observations were supplemented with re-examination of published figures of specimens, and descriptions from the literature when material was missing (e. g. parietals for *Anoualerpeton priscum* Gardner *et al.* 2003 from the Bathonian of England; or frontal from the Isle of Purbeck could not be located during the visit to NHMUK). Due to overall revision of the material, previous scores were edited when needed, and we further decided to order seven characters (see Appendix G.2).

The dataset used is based on the latest iteration of the Gardner (2002) dataset, updated in Carrano *et al.* (2022): Analysis 2. We agree on

the comments and new wording in Carrano *et al*. (2022) regarding the character list and follow it throughout this study. We have added to that dataset two characters published in our previous study (Guillaume *et al.*, 2023b), as well as three characters from Matsumoto & Evans (2018) and Daza *et al*. (2020).

The analyses in Carrano *et al*. (2022) did not include the scores from Daza *et al*. (2020), as "these do not match the character count in either matrix referenced by that work, and therefore [the authors] could not match these character states to their original characters" (Carrano *et al.*, 2022). However, after directly contacting the authors, we manage to recover the original scores (J. Daza & S. Evans, pers. comm., 2020). We reintroduced one character previously deleted: "premaxilla, pattern of labial ornament on labial *pars dorsalis*, in large specimens"; character 8 in previous studies (Gardner, 2002; Carrano *et al.*, 2022). The character allows representation of the diversity of ornament pattern among albanerpetontids; therefore, its states were redefined and rescored accordingly.

Finally, we present 23 new characters (see Appendix G.2 for the complete list of characters), both cranial and, for the first time in albanerpetontids, post-cranial. Among cranial elements, characters from the lacrimal, articular, and quadrate are for the first time implemented in the phylogeny. Furthermore, we highlight a mistake in the character lists and the matrix provided by Carrano *et al*. (2022) in their Supplementary

Files: character 1 “Body size (maximum size based on premaxilla height and width)” is described with two-character states, whereas it is scored with three. This issue appears to be an error in the original text (pers. comm. Carrano, 2023) and, in waiting to be fixed, we decided to remove this character from our analysis as we could not score it for our material and other of interest (see below).

The still uncertain position of Albanerpetontidae within Lissamphibia (Jones *et al.*, 2022; Kligman *et al.*, 2023) reflects the lack of a satisfactory outgroup. Previous studies have relied in an unsatisfying hypothetical –all 0– outgroup, assuming 0 was the ancestral condition for each character without further phylogenetic evidence (Gardner *et al.*, 2003). We followed Matsumoto & Evans (2018) and Daza *et al.* (2020), and disagreed with Carrano *et al.* (2022), in choosing *An. priscum* as our outgroup, because the genus *Anoualerpeton* has been consistently recovered as the phylogenetically least nested member of Albanerpetontidae (Gardner *et al.*, 2003; Venczel & Gardner, 2005; Sweetman & Gardner, 2013; Matsumoto & Evans, 2018; Daza *et al.*, 2020).

On top of all previous described species, we add two new taxa: (1) New unnamed taxon 2 based on the material from the Kimmeridgian-Tithonian of Portugal (Lourinhã Fm and Guimarota beds, see Section 3.2); and (2) New unnamed taxon 3 based on the material from the Maastrichtian

of Spain (Blasi 2B locality, Tremp Fm, see Section 3.3), that is here included into a phylogenetic analysis for the first time.

As in our previous study (Guillaume *et al.*, 2023b), we incorporated *Celtedens* with its two species, *Celtedens megacephalus* (Costa 1864) and *Celtedens ibericus* McGowan and Evans 1995, based on direct observations of one of us (ARDG) respectively on the holotype M542 from Pietraroja (lower Aptian, Italy) and the holotype and referred specimens from Las Hoyas (Barremian, Spain) (except MCCM- LH 15710, which was on loan at the time of the visit). We also include all albanerpetontid species published at the time of this study, using the species names following the emendation proposed by Marjanović and Laurin (2008), together with seven additional informal species-level taxa to which potentially meaningful character scores could be achieved:

- the "Paskapoo species" *Albanerpeton* sp. *sensu* Gardner 2002 (1) and "Uña species" cf. *Wesserpeton* sp. *sensu* Sweetman & Gardner 2013 (2), usually incorporated in previous analyses, and one of us (ARDG) having checked first hand referred material of the former;
- *Albanerpeton* sp., cf. *A. nexuosum* (3) from the Cedar Mountain Fm in US (Gardner, 1999b), the "Sânpetru species" *Albanerpeton* sp. *sensu* Carrano *et al.*, 2022 (4) from the Haţeg Basin in Romania (Grigorescu

et al., 1999; Folie & Codrea, 2005), and the "Csehbánya species" Albanerpetontidae indet. *sensu* Carrano *et al.*, 2022 (5) from the Csehbánya Fm in Hungary (Szentesi *et al.*, 2013); three of which were implemented in a previous study (Carrano *et al.*, 2022);

- the "Purbeck species" *Celtedens* sp. *sensu* Carrano *et al.*, 2022 (6) from the Lulworth Formation in England (McGowan & Ensom, 1997; Gardner, 2000a; Gardner *et al.*, 2003), of which material could be directly observed by one of us (ARDG).

The "Khodzhakul species" *sensu* Carrano *et al.*, 2022 was not included, despite having been in other studies (Skutschas, 2007; Carrano *et al.*, 2022), due to the lack of codable material; as well as specimens from the Lower Cretaceous of Galve in Spain (Estes & Sanchíz, 1982), from the Middle Jurassic of Gardies in France (Seiffert, 1969), and some specimens from the Lower Cretaceous of the Isle of Wight in England (Evans *et al.*, 2004).

The specimens from the Aguja Fm (West Texas, USA, Lower Campanian) were not included, as the new material referred to *Albanerpeton* sp., cf. *A. galaktion* was too fragmentary, and the rest was referred either to *Albanerpeton nexuosum* Estes 1981 from the Upper

Cretaceous of western and southern North America or Albanerpetontidae indet. (Wick, 2021).

Neither were included material from Guelb el Ahmar from the Bathonian Anoual Syncline (Morocco) (Haddoumi *et al.*, 2016) nor from the Berriasian Angeac-Charente Lagerstätte (France) (Allain *et al.*, 2022), as they are currently under study by another research team (R. Allain & M. Lasserron, pers. comm., 2023); although this material was checked for comparison.

With all the above modifications, the final dataset includes 23 terminal taxa and 61 characters, with multistate characters 3, 6, 14, 25, 26, 34, and 56 analysed as ordered.

The analyses were performed with a traditional search using 1000 replications of Wagner trees followed by tree bisection reconnection (TBR) saving 10 trees saved by replication; and an additional round of TBR was performed on the resulting most parsimonious trees (MPT) to further explore the tree space. A strict consensus tree was generated from all the MPTs recovered by each analysis. Branch support was calculated using bootstrap standard resampling with 1000 replicates. Consistency and retention indexes were calculated for each MPT and each individual character using the script "allstats.run" by Peterson Lopes (Universidade do Sau Paulo, Brazil).

3.4.3 Phylogenetic analysis

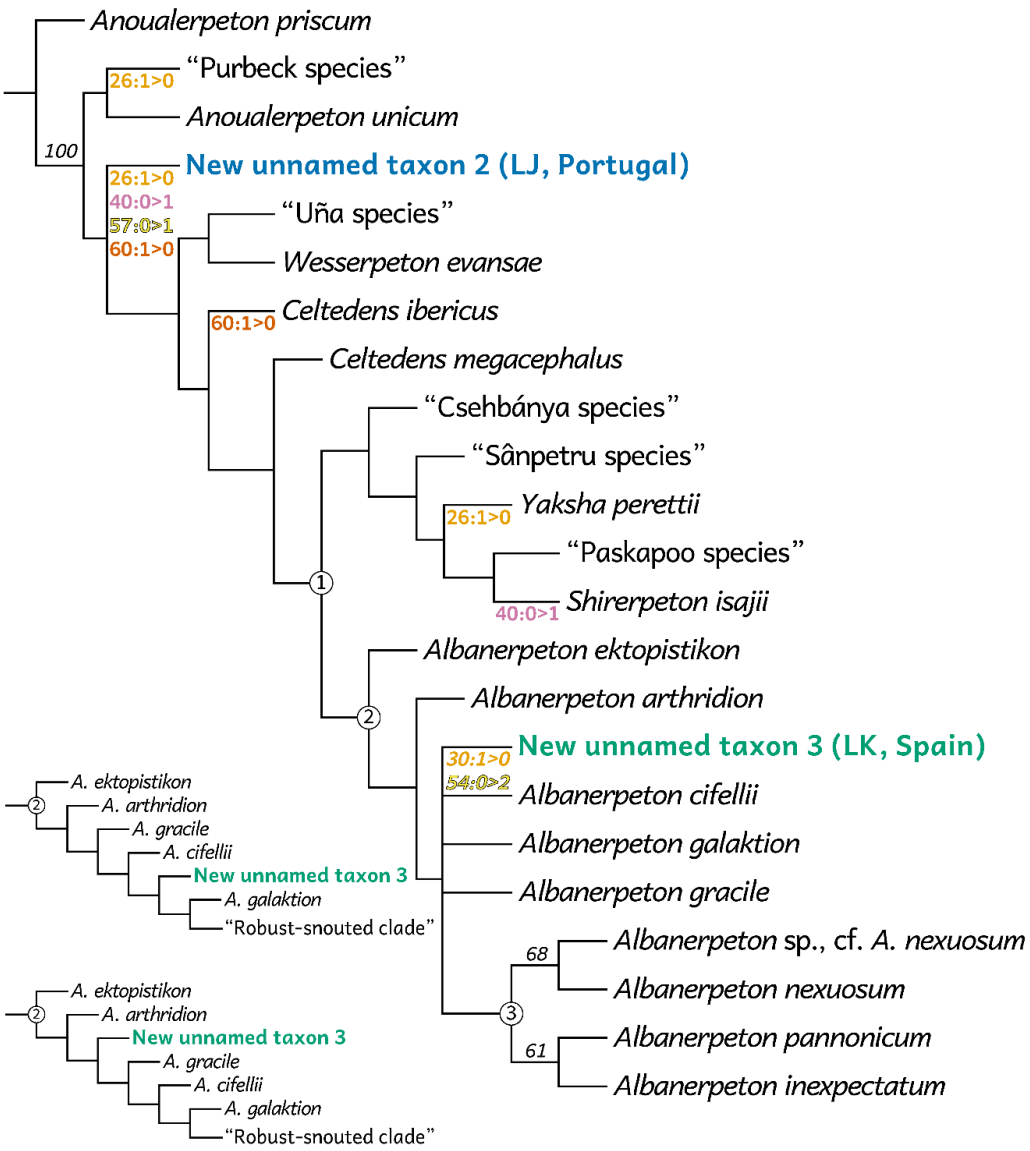

Figure 3.4.1: Strict consensus tree of the 2 MPTs recovered. Length = 163 steps; CI = 0.472; RI = 0.598. Black numbers above branches are bootstrap values over 50 for the corresponding nodes. Colour numbers are synapomorphies of New unnamed taxon 2 and New unnamed taxon 3 (orange are for frontal characters, reddish purple for parietal characters, yellow for cervical vertebrae characters, vermillion for ilium characters). Alternate branching from the two MPTs (lower left) are provided to illustrate the position of New unnamed taxon 3. **Node 1**, unnamed clade comprising species previously attributed to both *Albanerpeton* s.l. and *Albanerpeton* s.s. (Daza *et al.*, 2020; Carrano *et al.*, 2022); **Node 2**, Albanerpeton; **Node 3**, "robust-snouted clade" *sensu* Venczel & Gardner, 2005.

3.4 CHAPTER 7: NEW PHYLOGENY OF ALBANERPETONTIDAE

The phylogenetic analysis recovered 2 most parsimonious trees, MPTs, with 163 steps each (**Figure 3.4.1**). The consistency index (CI) is 0.472 and the retention index (RI) is 0.598, with a rescaled consistency index (RCI) of 0.282.

Anoualerpeton is found as the most basal group with *An. unicum* being now sister-taxa of the "Purbeck species", forming a clade characterized by three synapomorphies (char. 21:1; char. 25:0; char. 47:1), and suggesting that it may belong to the genus *Anoualerpeton*. It is noted that TNT requires the definition of a single outgroup, forcing the placement of A*n*. priscum as sister of all other albanerpetontids, but TNT did not allow to re-root the trees using a predefined taxonomic outgroup. Additional analysis designing other arbitrary outgroups withing the dataset always recovered the clade (*An. priscum* (Purbeck species + *An. unicum*), reinforcing the putative affinities among the three species.

New unnamed taxon 2 is recovered as sister-group of all 'non-*Anoualerpeton*' Albanerpetontidae, and is characterized by an unique combination of synapomorphies: (1) a bulbous/flabellate outline of the internasal process of the frontal in dorsal or ventral view (char. 26:0), shared with the "Purbeck species" and *Yaksha perettii*; (2) the absence of sculpture on postorbital wing of the parietals (char. 40:1), shared with *Shirerpeton isajii* and *Albanerpeton pannonicum*; (3) dorsal condyle of the axis with thickened edge (char. 57:1), shared with *A. inexpectatum*; and (4)

long axis of the ilium strongly tilted posteriorly (char. 60: 0), shared with *Celtedens ibericus*.

Then, the "Uña species" and *Wesserpeton evansae* are grouped together into a clade sister of more deeply-nested albanerpetontids and characterized by four synapomorphies (char. 11:0→1, suprapalatal pit of the premaxilla divided; char. 25:1→2, triangular outline of the fused frontals in dorsal and ventral view; char. 27:0→1, narrow internasal process of the frontal bones; char. 37:0→1, medial emargination of the prefrontal facet of the frontal bones, making a dorsal notch only).

The analysis found *Celtedens* as paraphyletic, as *C. ibericus* and *C. megacephalus* are found as successive sister taxa. *C. megacephalus* is actually sister taxa of a huge clade, characterized by three synapomorphies (char. 25:1→2, triangular outline of the fused frontals in dorsal and ventral view; char. 37:0→2, medial emargination of the prefrontal facet of the frontal bones, making a notch visible dorsally and ventrally; char. 38:0→1, overall shape of the lacrimal is V-shaped), and comprising of taxa previously referred to both *Albanerpeton sensu lato* and *Albanerpeton sensu stricto* according the definition given by Daza *et al*. (2020). Indeed, this unnamed clade bifurcates into two smaller sub-clades, one containing all *Albanerpeton* species described (plus New unnamed taxon 3); and one containing the remaining undescribed albanerpetontid species, including the Cenozoic "Paskapoo species", grouped with *Yaksha perettii* and

Shirerpeton isajii. The latter is characterized by two synapomorphies (char. 14:0→1, moderate size of the suprapalatal pit relative to the lingual surface area of the *pars dorsalis*; char. 15:0→1, low vertical position of the suprapalatal pit on the *pars dorsalis*). *Y. perettii* is sister-taxa of a clade formed by the "Paskapoo species" and *S. isajii*; while the "Csehbánya species" and "Sânpetru species" are more basal.

A more restricted *Albanerpeton* clade is characterized by two synapomorphies (char. 20:0→1, internal narial fossa present in the maxilla; char. 48:0→1, ventral prong of the symphysis in the dentary relatively bigger than the dorsal prong). It comprises the successive nesting taxa *Albanerpeton ektopistikon* and *A. arthridion*, and a polytomy formed by the American species *Albanerpeton cifellii* (Gardner, 1999b) from the Late Cretaceous of Utah (USA), *A. galaktion*, and *A. gracile*, the New unnamed taxon 3, and a clade comprised of *A. nexuosum*, *A. pannonicum*, and *A. inexpectatum*.

This latter clade is referrable to the informally named "robust-snouted clade" *sensu* Venczel & Gardner, 2005 (Gardner, 2002; Gardner & Böhme, 2008), although it does not include the "Paskapoo species", and is characterized by eight synapomorphies (char. 2:0→1, robust premaxilla; char. 5:0→1, inter-premaxillary contact fused; char.10:0→1, low height:width ratio of the *pars dorsalis* across the suprapalatal pit; char. 12:1→0, oval lingual outline of the suprapalatal pit; char. 26:1→2, spike-

like/acute outline of the internasal process of the frontal bones in dorsal or ventral view; char. 27:0→1, narrow proportion of the internasal process of the frontal bones (basal width:length); char.32:0→1, broad ventrolateral crest of the fused frontals; char. 33:0→1, edge of the ventrolateral crests medial to the orbital margin creating a ventral step, or parapet). The Late Cretaceous Americans *Albanerpeton* sp. cf. *A. nexuosum* and *A. nexuosum* are grouped together and as sister taxa of the Cenozoic European *A. pannonicum* and *A. inexpectatum*, grouped together. These two clades are the only ones to present a bootstrap value higher than 50.

3.4.3.1 Position of New unnamed taxon 3 with regard to other members of the genus *Albanerpeton*

The two MPTs suggest that the polytomy is the result of a floating position of New unnamed taxon 3 which can be either the basal-most taxa of this clade or nested deeper between *A. cifellii* and *A. galaktion*. This polytomy (albeit the Blasi material, not included) has been consistently recovered in other studies (Gardner, 2002; Venczel & Gardner, 2005; Gardner & Böhme, 2008; Sweetman & Gardner, 2013; Matsumoto & Evans, 2018; Daza *et al.*, 2020; Carrano *et al.*, 2022). When resolved, the three North American species were still closely related, with *A. galaktion* and *A. gracile* potentially more akin (Daza *et al.*, 2020; Guillaume *et al.*, 2023b), which is congruent with their respective spatiotemporal distribution (Gardner, 2000b).

The polytomy is supported by five synapomorphies: (1) char. 12:0→1, triangular to slit-shaped lingual outline of the suprapalatal pit of the premaxilla; (2) char. 14:0→1, moderate suprapalatal pit relative to lingual surface area of *pars dorsalis*; (3) char. 15:0→1, low vertical position of suprapalatal pit on *pars dorsalis*; (4) char. 18:0→1, anterior end of tooth row at same level or posterior than the maximum indentation on leading edge of the nasal process in the premaxilla; and (5) char. 36:2→1, ventrolateral crests of the fused frontals separated medially by about half of the width of one ventrolateral crest.

It is challenging to evaluate the similarity and potential relationship between New unnamed taxon 3 and *A. cifellii*, because the latter is known only by its holotype premaxilla. However, this single bone is quite different from the one observed in New unnamed taxon 3, notably by the relatively smaller size of the palatal foramen. The premaxillae and maxillae of New unnamed taxon 3 and *A. galaktion* are extremely similar. The only difference is the distribution of the scattered pits on the lower part of the labial surface of the *pars dorsalis* of the premaxilla. However, this feature is polymorphic in the American species, while only one specimen from Blasi 2B preserves a *pars dorsalis* complete enough to observe a global pattern. The overall morphology of the frontals is similar between the two species, but they display some differences on the orbital margins and the ventrolateral crest (see differential diagnosis above). Dentaries are also very similar but

differ by the prominence and the scar for the intermandibularis muscle. Therefore, both species share strong affinities, but remain distinct.

Similarly, New unnamed taxon 3 shares some affinities with *A. gracile*, but both differ by the size of the palatal foramen. Furthermore, *A. gracile* display some polymorphic characters that deviate from New unnamed taxon 3: (1) the anterior edge of the nasal process can be either weakly or strongly curved; (2) the outline of the internasal process in the fused frontals can be either tapered/hastate or spike-like/acute; (3) the fused frontal length can be either moderate or long; and (4) the anterior and posterior median fossae on the ventral surface of the fused frontals can be either continuous or separated by a step.

In conclusion, the Blasi 2B material is never found more closely related to a specific species than the others, which rejects any affinity or conformity with other species and supports its validity as a distinct species. This is further supported by the anterior position of the anterior end of the orbital margin relatively to the anteroposterior midpoint of the fused frontal, which is unique among all *Albanerpeton* species for which complete fused frontals are known.

3.4.4 Discussion

3.4.4.1 Phylogenetic results

As consistently found, *Anoualerpeton* is the least nested taxon (Gardner, 2002; Daza *et al.*, 2020; Guillaume *et al.*, 2023b), but as recently suggested, the genus might be paraphyletic (Carrano *et al.*, 2022), or include the "Purbeck species". Previous studies considered it as a basal albanerpetontid related to *Celtedens* (McGowan & Ensom, 1997; Gardner, 2000a; Evans & McGowan, 2002; Wiechmann, 2003; Sweetman & Gardner, 2013; Carrano *et al.*, 2022). Although some affinities were reported in its description between the "Purbeck species" and the material from the Bathonian Kirtlington Mammal Bed in England (McGowan & Ensom, 1997), later described as *An. priscum* (Gardner *et al.*, 2003); this was under comparison with other *Celtedens* material. Therefore, it is yet too soon to attribute the "Purbeck species" to *Anoualerpeton*, and a proper revision and description of the Purbeck material would be required.

3.4.4.1.1 The taxonomic status of New unnamed taxon 2

The phylogenetic position of New unnamed taxon 2 is congruent with previous analyses, which always considered the Portuguese material to belong to a relatively basal albanerpetontid clade (Wiechmann, 2003; Gardner & Böhme, 2008; Carrano *et al.*, 2022; Guillaume *et al.*, 2023b); and with its spatiotemporal range. However, New unnamed taxon 2 is here (**Figure 3.4.1**) found for the first time as a new genus and species,

characterized by a unique combination of characters, and not closely related to *Celtedens* (Gardner, 2000a; Wiechmann, 2003; Gardner & Böhme, 2008; Guillaume *et al.*, 2023b), nor to *Yaksha* and *Anoualerpeton* (Carrano *et al.*, 2022).

These intragroup relationships support the validity of New unnamed taxon 2 as a new genus, despite the absence of autapomorphies, something common in albanerpetontids described from isolated bones from screen-washed samples (Sweetman & Gardner, 2013; Carrano *et al.*, 2022). Furthermore, if the Portuguese material exhibits some degree of morphological disparity, the variability observed in both the Alcobaça Fm and the Lourinhã Fm encompassed the one observed in the other.

The articular MG28677 from the Alcobaça Fm displayed only a notable difference, the shape of its glenoid fossa, but this is most likely be due to a preservation bias. Indeed, the morphology presented by MG28208, another albanerpetontid articular bone from the Alcobaça Fm, fits the ones described in the specimens from the Lourinhã Fm. Therefore, there is no evidence suggesting that both geological units yield two different species, despite their disparity in time, space, and environment.

Thus, the albanerpetontid material from both assemblages probably corresponds to one common species, New unnamed taxon 2, with intraspecific variation, as has also been reported in other species (Gardner,

2000b; Venczel & Gardner, 2005; Sweetman & Gardner, 2013; Carrano *et al.*, 2022; Guillaume *et al.*, 2023b).

3.4.4.1.2 Taxonomic implications on *Wesserpeton* and *Celtedens*

Wesserpeton evansae and the "Uña species" have long been found closely related in previous analyses, usually as part of a polytomy with more deeply-nested albanerpetontids (Matsumoto & Evans, 2018; Carrano *et al.*, 2022; Guillaume *et al.*, 2023b) or as successive taxa (Daza *et al.*, 2020). In his PhD thesis, Wiechmann (2003) described the "Uña species" as a new species of *Albanerpeton*, but later work suggested affinities with *Wesserpeton* (Sweetman & Gardner, 2013). Our present analysis is the first one to support that the "Uña species" can indeed be referred as cf. *Wesserpeton* sp., and probably as a new species as it presents two autapomorphies different from *W. evansae*. This also confirms early statement of La Huérguina Fm being one of the only multispecific albanerpetontid assemblages known (Wiechmann, 2003; Buscalioni *et al.*, 2008), together with some geological units from Upper-most Cretaceous of North America (Gardner, 2000b).

As previously highlighted, the definitions of *Celtedens* and its two species may need revision, especially regarding frontal characters (Carrano *et al.* 2022; Guillaume *et al.* 2023; S. Sweetman, pers. comm., 2022). Our analysis (**Figure 3.4.1**) broke the genus, making it paraphyletic, reflecting

these statements. However, it is also important to notice than despite having the only articulated skeletons reported from Albanerpetontidae, both *C. ibericus* and *C. megacephalus* are the published species with the higher proportion of ambiguous characters (scored "?"; 75.19% and 46.77% respectively), with the exception of *A. cifellii* (75.8%), known only by one premaxilla (Gardner, 1999b).

On top of that, 14 and 12 characters respectively were updated out of 38 from previous analyses after direct observations on holotypes and referred specimens. In *Celtedens ibericus*, most of these updates are from characters becoming ambiguous, because of the preservation of the specimens and previous scores that could not be confirmed with direct observation, especially regarding the premaxilla. In *C. megacephalus*, most of the previous scored characters were restricted in the frontal and were indeed shared with *C. ibericus*. However, direct observations lead to update the characters linked to the internasal process or requiring a complete frontal as ambiguous (but in exchange, these observations allowed to score some characters of the parietal).

These results highlight the need for a proper revision of both species, with the help of CT-scan imagery, in order to access character information obscured by crushing bone or sediments. There is no reason to consider *Celtedens* invalid, as none of them are grouped with other species; but its

definition, diagnose, and composition would remain uncertain until further work.

Furthermore, contrary to all previous analyses (Daza *et al.*, 2020; Carrano *et al.*, 2022; Guillaume *et al.*, 2023b), both *Celtedens* are now more deeply-nested than *Wesserpeton* and the "Uña species" cf. *Wesserpeton* sp.

3.4.4.1.3 Taxonomic implications for *Albanerpeton*

Three recent analyses on albanerpetontid phylogeny recovered paraphyletic *Albanerpeton*, containing two Cretaceous Asian non-*Albanerpeton* species: *Shirerpeton isajii* Matsumoto and Evans, 2018 from the Kuwajima Formation (Barremian, Japan) and *Yaksha perettii* Daza *et al.*, 2020 from the Cenomanian amber deposits of Myanmar. That arrangement created a taxonomic conundrum without an obvious solution (Daza *et al.*, 2020; Carrano *et al.*, 2022; Guillaume *et al.*, 2023b).

The present analysis (**Figure 3.4.1**) seems to resolve this issue, as a more restricted *Albanerpeton* is found monophyletic and the sister to another clade of both Asian species and other informal species from the Late Cretaceous of eastern Europe and the Paleocene of North America; even though these informal species were previously referred to *Albanerpeton* sp. (Folie & Codrea, 2005; Gardner & Böhme, 2008; Szentesi *et al.*, 2013; Csiki-Sava *et al.*, 2016; Venczel *et al.*, 2016). Most striking is the now new position of the North-American "Paskapoo species" (late Paleocene, Alberta, Canada), which had been consistently found as deeply nested with other

European Cenozoic species *A. inexpectatum* and *A. pannonicum* in other analyses (Gardner, 2002; Venczel & Gardner, 2005; Sweetman & Gardner, 2013; Carrano *et al.*, 2022).

In our new analysis, it is closely related to the Cretaceous Asian species *Yaksha perettii* and *Shirerpeton isajii*, and other Cretaceous eastern European species. This is most likely a direct consequence of the new scores: the new characters increased the matrix by 61% compared to Guillaume *et al.* (2023b), 69% compared to Daza *et al.* (2020), and 85% compared to Carrano *et al.* (2022). However, most-recent analyses used scores provided in the earlier works of Gardner (2002) and Sweetman and Gardner (2013), instead of checking directly the material. One of us (ARDG) could observe the specimens attributed to the "Paskapoo species" first-hand, which resulted in updating 13 characters out of 38 (34%; in six of which the scores were changed, and in seven of which the scores were updated from "?" to another state).

Simultaneously, without considering details related to the paraphyletic issue, our analysis found a similar topology for *Albanerpeton* than in most recent studies (Daza *et al.*, 2020; Carrano *et al.*, 2022), with *A. ektopistikon* and *A. arthridion* being both the stratigraphically oldest and basal-most species, followed by a polytomy formed by the three Late Cretaceous species from North America *A. gracile*, *A. galaktion*, and *A. cifellii*, informally known as the "gracile-snouted clade" *sensu* Gardner,

2002, and then the more derived "robust-snouted clade" *sensu* Venczel and Gardner, 2005.

Although now found as monophyletic, the current composition and definition of *Albanerpeton* remains uncertain, as it would require a single genus to range over 100 My, from the Aptian–Albian (Gardner, 1999a; Carrano *et al.*, 2022) to the Early Pleistocene (Villa *et al.*, 2018), and two continents separated by seawaters, commonly considered barriers to dispersal for lissamphibians (Sumich & Morrissey, 2004). Previous studies suggested restricting the genus to a sub-set of species containing the type-species *A. inexpectatum*, either this sub-set being only Cenozoic taxa (Daza *et al.*, 2020) or the informally named "robust-snouted clade" *sensu* Venczel and Gardner, 2005 (Carrano *et al.*, 2022). However, based on our results, these would only provide a taxonomical solution, but not an evolutionary one, as the genus would still be spread between one or two continents well separated by that time, for a time-range between 30 and 100 My.

3.4.4.2 Insight on the palaeobiogeography of albanerpetontids

Europe has always been considered as a major area for the Albanerpetontidae evolution during the Early Cretaceous (Gardner & Böhme 2008). The Portuguese material highlight the albanerpetontid diversity in the Iberian Peninsula during the Jurassic/Cretaceous (J/K) transition by filling the gap separating the first Bathonian occurrences (Gardner *et al.*, 2003; Haddoumi *et al.*, 2016) and the Cretaceous occurrences in Spain,

Morrocco, England and France (McGowan & Ensom, 1997; Evans & McGowan, 2002; McGowan, 2002; Gardner *et al.*, 2003; Buscalioni *et al.*, 2008; Mazin *et al.*, 2008; Canudo *et al.*, 2010; Sweetman & Gardner, 2013; Lasseron *et al.*, 2020; Allain *et al.*, 2022). The occurrence of New unnamed taxon 2 supports the major paleobiogeographic role played by Portugal, and the Iberian Plate, between Europe and Africa during the J/K boundary (Brikiatis, 2016; Lasseron *et al.*, 2020; Allain *et al.*, 2022).

Furthermore, our results, combined with the absence of albanerpetontids in the Morrison Fm, even for most recognizable bones such as premaxillae or frontals (Carrano & Velez-Juarbe 2006; Gardner & DeMar 2013; Carrano 2022, pers. comm.), suggest that the group was indeed absent in North America during the Late Jurassic, and crossed the Atlantic Ocean only later during the Cretaceous (Gardner, 1999a; Wiechmann, 2003; Gardner & Böhme, 2008; Carrano *et al.*, 2022). This represents a different dispersal road than the one observed in the macrofauna for the Late Jurassic, especially dinosaurs (Mateus *et al.*, 2017), and that both ecosystems may have discrete ecological differences for their respective microfauna.

Albanerpetontids complex paleobiogeographical history remains to be fully understood (Gardner & Böhme, 2008; Carrano *et al.*, 2022), but it seems to reflect the tectonic events in the Late Cretaceous of Europe. Our results (**Figure 3.4.1**) suggest that during the Late Jurassic–Early

Cretaceous European albanerpetontid pool (*Anoualerpeton*, *Celtedens*, New unnamed taxon 2, and *Wesserpeton*) split into and was replaced by two independent albanerpetontid lineages: (1) non-*Albanerpeton* species, first occurring in Asia with *S. isajii*, but likely originating in Europe; and (2) *Albanerpeton*, first occurring and originating in North America, with *A. arthridion* and *A. ektopistikon*.

Both seem to have populate Europe during the Late Cretaceous, with the "Sânpetru species" and the "Csehbánya species" from the former clade, and New unnamed taxon 3 from the latter. Late Cretaceous biotic interchanges between the Asiamerican landmasses and the European archipelago have been documented for many taxa (Csiki-Sava *et al.*, 2015 and references therein). However, our analysis is the first one to suggest that albanerpetontids could have had independent dispersal events involving both North America and Asia (**Figure 3.4.2**).

The strong affinities shared between eastern European taxa and the potential similarities between New unnamed taxon 3 and other Spanish material suggest that the Rhodope-Maesian platform and the Ibero-Armorican Island did not share common albanerpetontid species. Therefore, their faunal compositions were the result of local small-scale heterogeneity as previously observed (Csiki-Sava *et al.*, 2015; Pérez-Pueyo *et al.*, 2021a).

The close relationship of New unnamed taxon 3 with other North American *Albanerpeton* species is congruent with that observed in other

clades. Taxa from North America (mostly Laramidia) were restricted to the Ibero-Armorican Island and used high latitude dispersal corridors, such as the De Geer corridor (Brikiatis, 2014). These corridors were accessible thanks to major sea-level falls during the early stages of the Late Cretaceous (Norris *et al.*, 2001; Miller *et al.*, 2003), although the exact timing is to evaluate without better material from those stages.

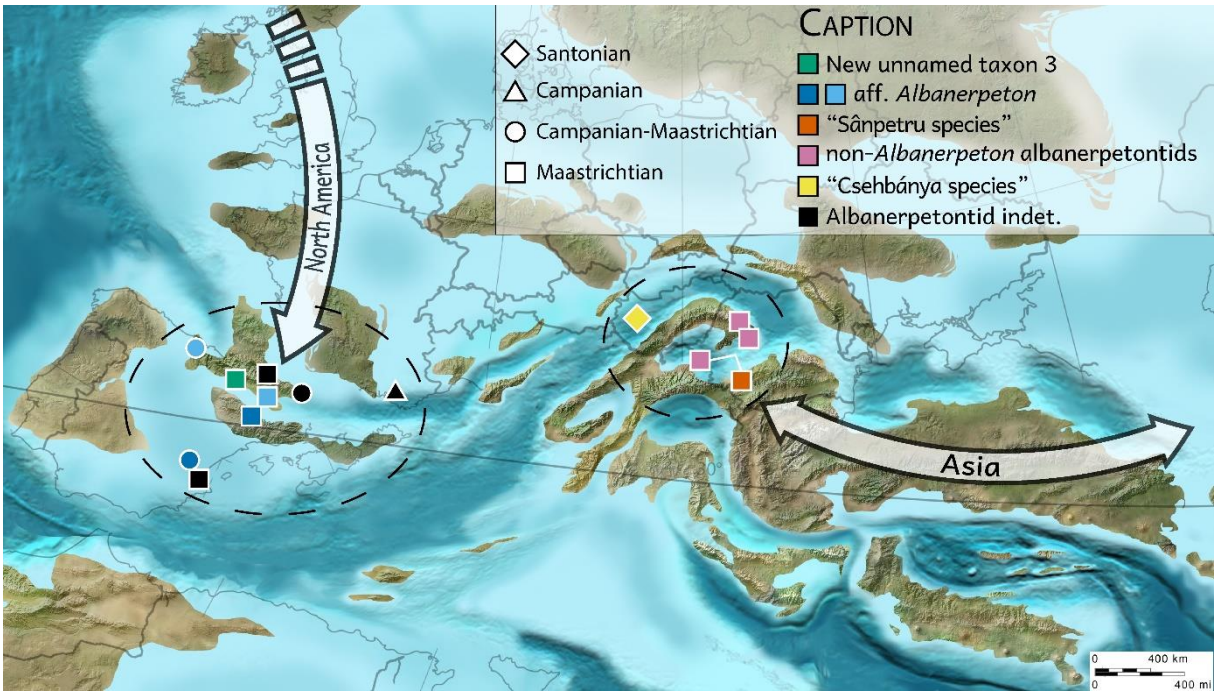

Figure 3.4.2: Palaeogeographic distribution of European albanerpetontid occurrences during the Late Cretaceous (Santonian–Maastrichtian), based on data from **Table 3.3.1**. Shapes refer to the age, colors to the taxonomic affinities. Dark blue occurrences share more affinities with New unnamed taxon 3 than light blue occurrences. Arrows illustrate the putative geographical influences of both European albanerpetontid faunas. Base map: Late Campanian ~75 Mya, Colorado Plateau Geosystems Inc., Deep Time Maps™.

Similarly, the close relationship between eastern-European species and Asian albanerpetontid species reflects what has also been observed in other taxa, as Asian influence seem to be more restricted to European

Tethyan landmasses and could have immigrated through different events (Csiki-Sava *et al.*, 2015), especially by island hopping along chains of volcanic archipelagos (Dalla Vecchia, 2009). However, the exact timing and dynamic of this dispersal remain unclear.

Our phylogeny suggest that the non-*Albanerpeton* clade made have originated in Europe in the early stages Early Cretaceous and later immigrated to Asia, while more unidentified more basal forms remain in Europe until the Late Cretaceous, creating a long Lazare lineage. On the other hand, *Shirerpeton isajii* from the Barremian of Japan is both the oldest fossil occurrence (Matsumoto & Evans, 2018; Daza *et al.*, 2020; Carrano *et al.*, 2022), but the deeper-nested taxon in our phylogeny. Based on this timing, an alternate hypothesis would be that the clade might have originated in Asia during the Early Cretaceous and more basal lineages might have immigrated to Europe in the Late Cretaceous. Nevertheless, a more sophisticated study including data from reported occurrences and better sampling of Upper Cretaceous outcrops is required in order to test either hypothesis.

The single European linage that survived the K/Pg boundary is the "robust-snouted clade" *sensu* Venczel and Gardner, 2005 (Gardner *et al.*, 2021). It is recorded from the Oligocene of Germany (Böhme, 2008) and Turkey (Georgalis *et al.*, 2021), but surprisingly not sampled during earlier stages of the Paleogene (Wiechmann, 2003; Venczel & Gardner, 2005;

Gardner & Böhme, 2008), despite the important sampling of European Eocene terrestrial outcrops presenting high diversity of other lissamphibians (Rage, 2012). Our results confirms that two Albanerpetontidae lineages were present in Europe at the end of the Maastrichtian. Furthermore, the material from Blasi 2B supports that a more restricted, monophyletic *Albanerpeton* lineage did cross the K/Pg boundary, rather than repopulating Europe from Cenozoic North American populations.

The absence of European occurrence for most of the Paleogene contrasts with the survival of the "Paskapoo species" in the Paleocene of North America (Gardner, 2000a; Gardner & Böhme, 2008), which share Asian origins in our phylogeny. However, it is unclear as to whether or not there were local Asian immigrants, from which the "Paskapoo species" later evolved, contemporaneous of North American *Albanerpeton* species, or if the dispersal event from Asia occurred shortly after the K/Pg extinction event.

3.4.5 Conclusion

The new material described in Sections 3.1, 3.2, and 3.3, with revision of previous published specimens in Europe, North Africa, and North America, allowed to create new characters to be included in phylogenetic analyses. New unnamed taxon 2 is found as a basal Albanerpetontidae recovered as a sister-taxon to all non-*Anoualerpeton* albanerpetontids. New

unnamed taxon 3 is found in a polytomy comprising of Late Cretaceous North American *Albanerpeton* species and the "robust-snouted clade".

The phylogenetic analysis recovered *Wesserpeton evansae* as sister of the "Uña species", as previously suggested, and forming a distinct clade; and it confirms the need for a revision of *Celtedens*, now recovered as paraphyletic. However, the analysis recovered a *Albanerpeton* as monophyletic, albeit with reduced membership, contrary to previous findings. It further supports that two distinct albanerpetontid lineages co-evolve during the Late Cretaceous: one with a Eurasian distribution, comprised of previously described Asian species and undescribed eastern-European species; and one with a Euramerican distribution, comprising all species assigned to a more restricted *Albanerpeton* that crossed the K/Pg boundary in Europe.

4 DISCUSSION & FUTURE WORKS

Besides works on albanerpetontids (Wiechmann, 2003), mammals (Antunes, 1998; Martin, 1999; Hahn & Hahn, 2001b), and dinosaur teeth (Hendrickx & Mateus, 2014b; Malafaia *et al.*, 2017; Mocho *et al.*, 2017) vertebrate microfossils have been largely overlooked in the Lourinhã Formation. During my master thesis (Guillaume, 2018), a preliminary study illustrated the potential for a high microvertebrate diversity in different localities, outcrops, and stages of the Lourinhã Formation. The present PhD dissertation reinforces the potential of the Upper Jurassic vertebrate microfossil assemblages from Portugal as a promising source of data to explore the paleoecology and the structure of ancient communities (Shotwell, 1955; Estes, 1964, 1976; Estes & Berberian, 1970; Sahni, 1972; Dodson, 1973, 1987; Eberth & Brinkman, 1997; Brinkman *et al.*, 2005).

A sneak peek on the VMAs from the Lourinhã Formation shows that some of our localities have been already properly sampled (Zimbral VMA), while other require more works (Porto das Barcas). However, they already provide enough data to exemplify the high diversity of the Lourinhã Formation, as almost all major vertebrate groups were represented in our

samples. Overall, the Lourinhã Fm is highly dominated by amphibious taxa when compared to other Mesozoic assemblages from around the Jurassic/Cretaceous transition, mostly due to the high number of crocodylomorph teeth and amphibians remains.

In contrary, squamates and mammals seems to be rarer than expected, despite numerous remains described from the nearby and coeval Guimarota assemblage. More work is required to better characterized the fauna present; but it can be assumed that the Lourinhã Fm was deposited in even wetter conditions that previously thought (Mateus *et al.*, 2017).

The crocodylomorph tooth assemblage displays a diverse ecology, with at least seven different taxa represented with four different feeding habits, illustrating a good example of niche partitioning in such environments. Small-sized shed teeth suggest a prevalence for either juvenile or dwarf individuals, which is congruent with some reported skeletal remains from the other localities (Puértolas-Pascual & Mateus, 2020). The dominance and large variety of crocodylomorphs in the Lourinhã Formation is also congruent with the one observed in the Guimarota beds (Krebs & Schwarz, 2000; Schwarz, 2002; Schwarz & Fechner, 2004, 2008; Schwarz & Salisbury, 2005), suggesting that they were a major component of the Late Jurassic freshwater to brackish water ecosystems in the western part of the Iberian Peninsula. Recent works further highlighted how diverse crocodylomoprhs were in Portugal during the Late Jurassic (López-Rojas *et al.*, 2024).

This high crocodylomorph diversity in amphibious settings is consistent with the scarcity and low diversity of other semi-aquatic reptiles sharing equivalent ecological niches, notably the choristoderes; as it has been observed in latter vertebrates assemblages through the Cretaceous and Paleogene (Matsumoto & Evans, 2010).

Choristoderes were early reported from the Guimarota beds (Seiffert, 1973), even though if not recognized as such by the time (Evans, 1990), with the basal form *Cteniogenys*. However, the assignment of the material remains taxomically dubious, and some specimens were later referred to another reptile, *Marmoretta* (Evans, 1991b). A review of the material of the Guimarota collection hold in the Museu Geológico in Lisbon, allows to identify and locate specimens that were mislabelled, thus increasing the material that could be assigned to *Cteniogenys*.

Further material could be also identified from the Lourinhã Formation. However, I was not able to confirm the taxonomic status, as the type species *Cteniogenys antiquus* Gilmore 1928 from the Late Jurassic of the Morisson Fm (USA) is only described based on dentaries, and no diagnostic features could be found, as previously reported (Estes, 1983; Evans, 1989). Other referred material from the US is only assigned to *Cteniogenys* sp.

However, more recent material was reported from the Middle Jurassic of England (Evans, 1989, 1990, 1991a), and display disparities with the Portuguese material. Therefore, it can be confirmed that early

choristoderes were present in the Late Jurassic of Portugal, sharing affinities with *Cteniogenys* occurrences in the US and the UK, but non-conspecific with the latter.

Revision from the Guimarota material also confirms the presence of a new stem-lepidosaur species, from a genus previously known only in the Middle Jurassic of UK (Evans, 1991b; Griffiths *et al.*, 2021). However, its absence so far from the Lourinhã Fm assemblages would support the final decline of this relic lineage, while true squamates were taking over the J/K ecosystems (Estes, 1983; Evans, 1993, 1998a, 2003; Conrad, 2008; Evans & Jones, 2010; Gauthier *et al.*, 2012; Caldwell *et al.*, 2015; Simões *et al.*, 2018; Herrera-Flores *et al.*, 2022a; Bolet *et al.*, 2022; Brownstein *et al.*, 2022).

Amphibians forms a major component in both the Guimarota beds and the Lourinhã Fm, and more particularly the Albanerpetontidae. Although being quite successful through the Mesozoic and being recovered frequently in microvertebrate assemblages, their anatomy was poorly known but for some diagnostic bones. Their monophyly is undisputed (Gardner, 2001; Kligman *et al.*, 2023), but their position within lissamphibians remains uncertain (Daza *et al.*, 2020). This complicates phylogenetic analyses, both in the selection of a satisfactory outgroup and the optimization of ancestral conditions of character states.

Furthermore, revision of the fused frontals from the Late Jurassic of Portugal highlighted their morphological plasticity through ontogeny,

depreciating their diagnostic use at species-level (McGowan, 1998a; Gardner, 2000a). It also suggested the genus *Celtedens* needs a revision, as it was found monophyletic but as part of a polytomy with more deeply nested albanerpetontid species. Thankfully, both the Lourinhã Fm and the Guimarota beds yield a massive amount of albanerpetontids remains. The former, especially, revealed to be extremely rich when compared with other Mesozoic sites of similar or larger sampling. More importantly, the material from the Lourinhã provided a unique insight on albanerpetontid anatomy.

Several cranial and post-cranial elements could be described and attributed to the new species New unnamed taxon 2, whereas they are usually overlooked or misidentified in other localities, as exemplified by the more abundant by the Guimarota beds and yet missing some of these elements. Another species from the Late Cretaceous of Spain, New unnamed taxon 3, provided further insights on the anatomical evolution of the group. Both constitute, so far, the oldest and youngest Mesozoic species described from the Iberian Peninsula, and in Europe outside the UK.

These works, combined with collection visits across European and North American collections, allowed to elaborate a new character matrix. With a total of 23 taxa, it is one of the most complete analyses with the one used by Carrano *et al*. (2022), although the terminal taxa are not the same (New unnamed taxon 3 was never implemented previously). In total, 61 characters were coded, including 23 new ones, and scoring for each were

rechecked for most of the formally described species with direct observation on holotypes and referred material. The only exception being *Shirerpeton isajii* Matsumoto and Evans, 2018 and *Yaksha perettii* Daza *et al.*, 2020, but both provided CT-data; *Wesserpeton evansae* Sweetman and Gardner, 2013, as the material could not be located on time during the visit in NHMUK; and *Albanerpeton pannonicum* Venczel & Gardner 2005, as the Geological Institute of Hungary was not visited (but unpublished referred material on loan could be reviewed in RTMP).

The new analysis found New unnamed taxon 2 as a basal Albanerpetontidae recovered as a sister-taxon to all non-*Anoualerpeton* albanerpetontids; while New unnamed taxon 3 is part of a polytomy formed by *Albanerpeton cifellii* Gardner, 1999b, *Albanerpeton galaktion* Fox & Naylor, 1982, *Albanerpeton gracile* Gardner, 2000b, and the "robust-snouted clade" *sensu* Gardner, 2002.

Most importantly, the analysis provided results highly divergent from most recent analyses (Matsumoto & Evans, 2018; Daza *et al.*, 2020; Carrano *et al.*, 2022). First, *Wesserpeton evansae* and the "Uña species" *sensu* Sweetman & Gardner, 2013 now form an independent clade more basal than *Celtedens megacephalus* (Costa, 1864); whereas *Celtedens* is actually recovered as paraphyletic. Furthermore, the analysis supports the monophyly of the genus *Albanerpeton*, albeit with reduced membership, notably by excluding the "Paskapoo species" *sensu* Gardner, 2002.

However, this does not resolve the extremely long temporal range of the genus (over 100 My through two continents), which would require further work to better characterize their relationship and their diversity in the Cenozoic (Daza *et al.*, 2020; Gardner *et al.*, 2021; Carrano *et al.*, 2022). The analysis suggests that two distinct lineages co-evolve during the Late Cretaceous: one with a Eurasian distribution, comprised of previously described Asian species and undescribed eastern-European species; and one with a Euramerican distribution, comprising all species assigned to a more restricted *Albanerpeton* that crossed the K/Pg boundary in Europe.

These works further reinforced the importance of the Iberian Peninsula for the albanerpetontid fossil record in Europe, they occur in the Late Jurassic, the Early Cretaceous (McGowan & Evans, 1995; Wiechmann, 2003; Buscalioni *et al.*, 2008; Canudo *et al.*, 2010; Barroso-Barcenilla *et al.*, 2017), and the Late Cretaceous. However, no occurrence has been reported for the Cenozoic, while the group was present in Europe (Gardner *et al.*, 2021). They also display a large diversity, with at least four different genera reported (new unnamed taxon 2 from the Late Jurassic of Portugal, *Celtedens* and the "Uña species" referred to *Wesserpeton* from the Early Cretaceous of Spain, and *Albanerpeton* from the Late Cretaceous of Spain)—more than any other geographical range of similar scale—, and five recognized species—second to only North America, with seven species through the Cretaceous and the Paleocene on a larger geographical scale (Gardner, 1999a,b, 2000b, 2002; Wick, 2021; Carrano *et al.*, 2022).

Although the work of this PhD is ended by the present thesis, much remains to be done. First and foremost, the three new unnamed taxa described here will be formally submitted in indexed peer-reviewed journal in the next couple of months, as well as the new albanerpetontid phylogeny. Thereafter, the preliminary palaeoecological study of the VMA localities from the Lourinhã Formation will be implemented with a complete description of the new material found and the last updated counting of the number of specimens, as well as more detailed analyses including a broader range of VMA localities.

Once the PhD works fully published, there will still lots of research to be carried out. The new microvertebrate collection of the Museu da Lourinhã opens new door to better understanding the vertebrate fauna of that area, notably the bony fishes and new lissamphibians taxa that could not be described in the time of the PhD. More work can also focus on the mammal and lizard diversity, to understand why they are fewer than expected or if this is due to a taphonomic bias. Finally, ostracods and charophytes could provide essential inputs on the palaeoenvironments.

Furthermore, a review of the North American *Cteniogenys* material, both from the type locality and other referred specimens, could help to solve the taxonomic issue with the European species. Likewise, the new Albanerpetontidae phylogeny stresses the need of taxonomic revision of the genus *Celtedens*, hopefully with the help of new CT-imagery. Additionally,

revision and formal description of known material from the Mesozoic of Europe and North America, together with better sampling of known and new localities, will help to confirm the results presented in this thesis. Eventually, they will provide stronger inputs to better characterize the albanerpetontid faunal interchanges during the Mesozoic, with palaeobiogeographical modelling.

5 CONCLUSIONS

This PhD aimed to characterize the herpetofauna (amphibian and small reptiles) from the Late Jurassic of Portugal, with the study of the fossil assemblage of Guimarota and the inputs of new localities from the Lourinhã Formation, as well as new insights from a Late Cretaceous locality in Spain, by evaluating the biodiversity and richness of the Lourinhã Formation, for illustrating its potential for palaeoecological and palaeoenvironmental analysis, and comparing it with the coeval, well known Guimarota bed palaeoecosystem; and reviewing the taxonomy and phylogeny of Albanerpetontidae, with focus on Iberian specimens.

Over two tons of sediments were sampled and screen-washed, yielding 20,000 fossil remains, including 5,100 vertebrate fossils. This considerably increase the microvertebrate paleontological collection of the Museu da Lourinhã. Based on a subsample of 3,971 vertebrate remains, a preliminary palaeoecological analysis showed that the Lourinhã Formation was dominated by amphibious taxa when compared to other equivalent microvertebrate localities from the J/K transition. Coupled with a detailed sedimentological analysis, this analysis supported that the degree of marine

influence in the Late Jurassic palaeoenvironments recorded by the Lourinhã Formation is much more marked than previously identified.

Description of crocodylomorph shed teeth from the Lourinhã Formation, with revision of material from the Guimarota beds, illustrated the high morphological (10 morphotypes and at least five clades represented) and ecological diversities (four different ecomorphotypes) of this group during the Late Jurassic in Portugal. This correlate with the scarcity of another group studied in reviewing the Guimarota collection, the Choristodera, often considered as eco-analogues of crocodile and were in direct competition with small aquatic crocodylomorphs.

Part of this thesis also focused on reviewing the Guimarota collection housed in Museu Geológico in Lisbon. Mislabelled, misidentified, and unpublished material helped describe a new stem-lepidosaur species, supporting the presence of this relic lineage in the Late Jurassic of Portugal. I could also confirm the assignment to a new choristodere taxon for specimens sharing strong affinities with *Cteniogenys*, but non-conspecific with other known material outside Portugal; and report the presence of choristoderes in the Lourinhã Formation.

Most of the thesis was dedicated in describing the albanerpetontid material from the Lourinhã Formation and reviewing the one from the Guimarota beds previously referred to *Celtedens*. A first work on the fused frontal failed to discriminate the species, due to their high plasticity

through ontogeny. However, a complete description of new cranial and post-cranial material from the Lourinhã Formation helped to draw a good picture of the anatomy of these small amphibians, which allowed to rise a new genus and new species not directly affiliated to *Celtedens*. It is the oldest albanerpetontid from the Iberian Peninsula so far. A side work emerged during collection visit to study comparative material of another locality from the Late Cretaceous of Spain, which further reinforced the knowledge on albanerpetontid anatomy and their morphological variation through the Mesozoic. This lead to rise a second species, the youngest albanerpetontid described from the Iberian Peninsula so far.

Both species encapsulate the Iberian albanerpetontid fossil record and provided valuable insights in the phylogeny and palaeobiogeography of the group. Although no satisfactory outgroup could be identified, the work accumulated during the thesis, both in describing new species and checking comparative material during collection visits in Europe and North America, helped to draw a new character matrix for phylogenetical analyses. The results depart from previous analyses: *Celtedens* is now recovered as paraphyletic and more deeply nested, whereas *Albanerpeton* is recovered as monophyletic, albeit with reduced membership. The results further suggest that two distinct lineages, with different geographic origins, co-evolve during the Late Cretaceous in Europe.

Eventually, this thesis succeeded in evaluating the diversity of the Lourinhã Formation, compared to the coeval Guimarota beds, and illustrating its potential for palaeoecological analyses and palaeoenvironmental reconstructions, notably by characterizing the crocodylomorph and lissamphibian diversity, and describing new herpetofauna material from the Guimarota beds. The thesis also succeeded in reviewing the taxonomy and phylogeny of Albanerpetontidae, notably challenging the presence of *Celtedens* in the Late Jurassic of Portugal and describing new material from the Late Cretaceous of Spain.

6 REFERENCES

Aberhan M, Bussert R, Heinrich WD, Schrank E, Schultka S, Sames B, Kriwet J, Kapilima S. 2002. Palaeoecology and depositional environments of the Tendaguru Beds (Late Jurassic to Early Cretaceous, Tanzania). *Fossil Record* 5: 19–44.

Aberhan M, Riedel F, Gloy U. 2000. The mollusk fauna of the Guimarota mine. In: Martin T,, In: Krebs B, eds. *Guimarota: a Jurassic ecosystem*. Munich: Verlag Dr. Friedrich Pfeil, 37–40.

Adams TL, Polcyn MJ, Mateus O, Winkler DA, Jacobs LL. 2011. First occurrence of the long-snouted crocodyliform *Terminonaris* (Pholidosauridae) from the Woodbine Formation (Cenomanian) of Texas. *Journal of Vertebrate Paleontology* 31: 712–716.

Allain R, Vullo R, Rozada L, Anquetin J, Bourgeais R, Goedert J, Martin J, de Fabrègues CP, Royo-Torres R, Augier D. 2022. Vertebrate paleobiodiversity of the Early Cretaceous (Berriasian) Angeac-Charente Lagerstätte (southwestern France): implications for continental faunal turnover at the J/K boundary. *Geodiversitas* 44: 683–752.

Alves TM, Gawthorpe RL, Hunt DW, Monteiro JH. 2002. Jurassic tectono-sedimentary evolution of the Northern Lusitanian Basin (offshore Portugal). *Marine and Petroleum Geology* 19: 727–754.

Alves T, Manuppella G, Gawthorpe R, Hunt D, Monteiro J. 2003. The depositional evolution of diapir- and fault-bounded rift basins: examples from the Lusitanian Basin of West Iberia. *Sedimentary Geology* 162: 273–303.

Anderson JS. **2008**. Focal review: The Origin(s) of Modern Amphibians. *Evolutionary Biology* 35: 231–247.

Andrade MD, Bertini RJ. **2008**. Morphology of the dental carinae in *Mariliasuchus amarali* (Crocodylomorpha, Notosuchia) and the pattern of tooth serration among basal Mesoeucrocodylia. *Arquivos do Museu Nacional* 66: 63–82.

Antunes MT. **1998**. A new Upper Jurassic Paulchoffatiid multituberculate (Mammalia) from Pai Mogo, Portugal. *Memórias da Academia de Ciências de Lisboa* 37: 125–153.

Antunes MT, Mateus O. **2003**. Dinosaurs of Portugal. *Comptes Rendus Palevol* 2: 77–95.

Araújo R, Castanhinha R, Martins RM, Mateus O, Hendrickx C, Beckmann F, Schell N, Alves LC. **2013**. Filling the gaps of dinosaur eggshell phylogeny: Late Jurassic Theropod clutch with embryos from Portugal. 3: 1924.

Ardèvol L, Klimowitz J, Malagón J, Nagtegaal PJ. **2000**. Depositional sequence response to foreland deformation in the Upper Cretaceous of the Southern Pyrenees, Spain. *AAPG bulletin* 84: 566–587.

Astibia H, Buffetaut E, Buscalioni AD, Cappetta H, Corral C, Estes R, Garcia-Garmilla F, Jaeger JJ, Jimenez-Fuentes E, Loeuff JL. **1990**. The fossil vertebrates from Laño (Basque Country, Spain); new evidence on the composition and affinities of the Late Cretaceous continental faunas of Europe. *Terra Nova* 2: 460–466.

Aurell I, Bádenas B, Canudo JI, Ruiz-Omeñaca JI. **2004**. Evolución tectosedimentaria de la Fm. Blesa (Cretácico Inferior) en el entorno del yacimiento de vertebrados de La Cantalera (Josa, Teruel). *Geogaceta* 35: 11–14.

Averianov AO. **2000**. *Sunosuchus* sp.(Crocodylomorpha, Goniopholididae) from the middle Jurassic of Kirghisia. *Journal of Vertebrate Paleontology* 20: 776–779.

Averianov AO, Martin T, Evans SE, Bakirov AA. **2006**. First Jurassic Choristodera from Asia. *Naturwissenschaften* 93: 46–50.

Avrahami HM, Gates TA, Heckert AB, Makovicky PJ, Zanno LE. **2018**. A new microvertebrate assemblage from the Mussentuchit Member, Cedar Mountain Formation: insights into the paleobiodiversity and paleobiogeography of early Late Cretaceous ecosystems in western North America. *PeerJ* 6: e5883.

Báez AM. **2013**. Anurans from the Early Cretaceous Lagerstätte of Las Hoyas, Spain: New evidence on the Mesozoic diversification of crown-clade Anura. *Cretaceous Research* 41: 90–106.

Baraboshkin EYu, Alekseev AS, Kopaevich LF. **2003**. Cretaceous palaeogeography of the North-Eastern Peri-Tethys. *Peri-Tethys Programme* 196: 177–208.

Barrett PM. **2000**. Prosauropod dinosaurs and iguanas: speculations on the diets of extinct reptiles. *Evolution of herbivory in terrestrial vertebrates: perspectives from the fossil record*. Cambridge: Cambridge University Press, 42–78.

Barrios F, Bona P, Paulina-Carabajal A, Leardi JM, Holliday CM, Lessner EJ. **2023**. An Overview on the Crocodylomorpha Cranial Neuroanatomy: Variability, Morphological Patterns and Paleobiological Implications. In: Dozo MT,, In: Paulina-Carabajal A,, In: Macrini TE,, In: Walsh S, eds. *Paleoneurology of Amniotes : New Directions in the Study of Fossil Endocasts*. Cham: Springer International Publishing, 213–266.

Barroso-Barcenilla F, Berrocal-Casero M, Blain HA, Callapez PM, Cambra-Moo O, Escaso F, Martín-Closas C, Ortega F, Pérez-García A, Prieto I, Rodríguez-Lázaro J, Ruiz-Galván A, Sanz JL, Segura M, Sevilla P. **2017**. Geological and Palaeontological context of three new Barremian (Lower Cretaceous) vertebrate sites in the Iberian Peninsula (Cuenca Province, Central Spain). *Proceedings of the Geologists' Association* 128: 256–270.

Bartiromo A. 2013. Plant remains from the Lower Cretaceous Fossil-Lagerstätte of Pietraroja, Benevento, southern Italy. *Cretaceous Research* 46: 65–79.

Baszio S. 2008. Information from microvertebrate localities: Potentials and limits. *Vertebrate Microfossil Assemblages: Their Role in Paleoecology and Paleobiogeography*. Bloomington & Indianapolis, IN: Indiana University Press, 3–8.

Benson RBJ, Mannion PD, Butler RJ, Upchurch P, Goswami A, Evans SE. 2013. Cretaceous tetrapod fossil record sampling and faunal turnover: Implications for biogeography and the rise of modern clades. *Vertebrate palaeobiodiversity patterns and the impact of sampling bias* 372: 88–107.

Benton MJ, Clark JM. 1988. Archosaur phylogeny and the relationships of the Crocodylia. *The phylogeny and classification of the tetrapods*. Oxford: Clarendon Press, 295–338.

Bertozzo F, Camilo Da Silva B, Martill D, Vorderwuelbecke E, Aureliano T, Schouten R, Aquino P. 2021. A large pterosaur femur from the Upper Jurassic (Lusitanian Basin) of Portugal. *Acta Palaeontologica Polonica* 66: 815–825.

Blain HA, Canudo JI, Cuenca-Bescós G, López-Martínez N. 2010. Amphibians and squamate reptiles from the latest Maastrichtian (Upper Cretaceous) of Blasi 2 (Huesca, Spain). *Cretaceous Research* 31: 433–446.

Blakey RC. 2008. Gondwana paleogeography from assembly to breakup—A 500 my odyssey (CR Fielding, TD Frank, and JL Isbell, Eds.). *Geological Society of America Special Papers* 441: 1–28.

Blanco A, Bolet A, Blain HA, Fondevilla V, Marmi J. 2016. Late Cretaceous (Maastrichtian) amphibians and squamates from northeastern Iberia. *Cretaceous Research* 57: 624–638.

Blanco A, Puértolas-Pascual E, Marmi J. 2018. Assessing the crocodylomorph diversity in the Maastrichtian (Late Cretaceous) of Ibero-

Armorica, based on tooth qualitative traits. In: Marzola M,, In: Mateus O,, In: Moreno-Azanza M, eds. Caparica, Portugal, 28.

Blanco A, Puértolas-Pascual E, Marmi J, Moncunill-Solé B, Llácer S, Rössner GE. 2020. Late Cretaceous (Maastrichtian) crocodyliforms from northeastern Iberia: A first attempt to explain the crocodylomorph diversity based on tooth qualitative traits. *Zoological Journal of the Linnean Society* 189: 584–617.

Blob RW, Badgley C. 2007. Numerical methods for bonebed analysis. In: Rogers RR,, In: Eberth DA,, In: Fiorillo AR, eds. *Bonebeds: Genesis, analysis, and paleobiological significance*. Chicago, IL: University of Chicago Press, 333–396.

Böhme M. 2008. Ectothermic vertebrates (Teleostei, Allocaudata, Urodela, Anura, Testudines, Choristodera, Crocodylia, Squamata) from the Upper Oligocene of Oberleichtersbach (Northern Bavaria, Germany). *Courier Forschungsinstitut Senckenberg* 260: 161–183.

Böhme M. 2010. Ectothermic vertebrates (Actinopterygii, Allocaudata, Urodela, Anura, Crocodylia, Squamata) from the Miocene of Sandelzhausen (Germany, Bavaria) and their implications for environment reconstruction and palaeoclimate. *Paläontologische Zeitschrift* 84: 3–41.

Bolet A, Stubbs TL, Herrera-Flores JA, Benton MJ. 2022. The Jurassic rise of squamates as supported by lepidosaur disparity and evolutionary rates (M Zhu, GH Perry, and M Zhu, Eds.). *eLife* 11: e66511.

Bolli H. 1951. The Genus *Globotruncana* in Trinidad, BWI: Notes on Occurrence, Nomenclature and Relationships between Species. *Journal of Paleontology*: 187–199.

Borcard D, Gillet F, Legendre P. 2018. *Numerical ecology with R*. New York City, NY: Springer.

Brauckmann C. 1978. Beitrag zur Flora der Grube Guimarota (Ober-Jura; Mittel-Portugal). *Geologica et Palaeontologica* 12: 213–222.

Bravi S, Garassino A. 1998. New biostratigraphic and palaeoecologic observations on the 'Plattenkalk' of the Lower Cretaceous (Albian) of Pietraroia (Benevento, S Italy), and its decapod crustaceans assemblage. *Atti della Società italiana di scienze naturali e del museo civico di storia naturale di Milano* 138: 119–171.

Brikiatis L. 2014. The De Geer, Thulean and Beringia routes: key concepts for understanding early Cenozoic biogeography. *Journal of Biogeography* 41: 1036–1054.

Brikiatis L. 2016. Late Mesozoic North Atlantic land bridges. *Earth-Science Reviews* 159: 47–57.

Brinkman DB, Russell AP, Peng JH. 2005. Vertebrate microfossil sites and their contribution to studies of paleoecology. *Dinosaur Provincial Park: a spectacular ancient ecosystem revealed*. Bloomington, IN: Indiana University Press, 88–98.

Brinkmann W. 1989. Vorläufige Mitteilung über die Krokodilier-Faunen aus dem Ober-Jura (Kimmeridgium) der Kohlegrube Guimarota, bei Leiria (Portugal) und der Unter-Kreide (Barremium) von Uña (Provinz Cuenca, Spanien). *Documenta naturae* 56: 1–28.

Brinkmann W. 1992. Die Krokodilier-Fauna aus der Unter-Kreide (Ober-Barremium) von Uña (Provinz Cuenca, Spanien). *Berliner Geowissenschaftliche Abhandlungen. Reihe E. Paläobiologie* 5.

Brochu CA. 2003. Phylogenetic Approaches Toward Crocodylian History. *Annual Review of Earth and Planetary Sciences* 31: 357–397.

de Broin F de L. 2002. *Elosuchus*, a new genus of crocodile from the Cretaceous of the North of Africa. *Comptes Rendus Palevol* 1: 275.

Bronzati M, Montefeltro FC, Langer MC. 2015. Diversification events and the effects of mass extinctions on Crocodyliformes evolutionary history. *Royal Society Open Science* 2: 140385.

Broschinski A. 2000. The lizards from the Guimarota mine. In: Martin T,, In: Krebs B, eds. *Guimarota: A Jurassic Ecosystem*. Munich: Verlag Dr. Friedrich Pfeil, 59–68.

Brownstein CD, Meyer DL, Fabbri M, Bhullar BAS, Gauthier JA. 2022. Evolutionary origins of the prolonged extant squamate radiation. *Nature Communications* 13: 7087.

Buckley GA, Brochu CA, Krause DW, Pol D. 2000. A pug-nosed crocodyliform from the Late Cretaceous of Madagascar. *Nature* 405: 941–944.

Buffetaut E. 1975. Sur l'anatomie et la position systématique de *Bernissartia fagesii* Dollo, L., 1883, crocodilien du Wealdien de Bernissart, Belgique. *Bulletin de l'Institut Royal des Sciences Naturelles de Belgique, Sciences de la Terre* 51: 1–20.

Buffetaut E. 2005. Late Cretaceous vertebrates from the Saint-Chinian area (southern France): a review of previous research and an update on recent finds. *Acta Palaeontologica Romaniae* 5: 39–48.

Buffetaut E, Ford RL. 1979. The crocodilian Bernissartia in the Wealden of the Isle of Wight. *Palaeontology* 22: 905–912.

Buffetaut E, Le Loeuff J. 1991. Late Cretaceous dinosaur faunas of Europe: some correlation problems. *Cretaceous Research* 12: 159–176.

Buffetaut É, Le Lœuff J, Tong H, Duffaud S, Cavin L, Garcia G, Ward D. 1999. Un nouveau gisement de vertébrés du Crétacé supérieur à Cruzy (Hérault, Sud de la France). *Comptes Rendus de l'Académie des Sciences-Series IIA-Earth and Planetary Science* 328: 203–208.

Buffetaut E, Taquet P. 1977. The giant crocodilian *Sarcosuchus* in the Early Cretaceous of Brazil and Niger. *Palaeontology* 20: 203–208.

Bunker G, Martill DM, Smith RE, Zouhri S, Longrich N. 2022. Plesiosaurs from the fluvial Kem Kem Group (mid-Cretaceous) of eastern Morocco and a review of non-marine plesiosaurs. *Cretaceous Research* 140: 105310.

Buscalioni AD, Fregenal MA, Bravo A, Poyato-Ariza FJ, Sanchíz B, Báez AM, Cambra Moo O, Martín Closas C, Evans SE, Marugán Lobón J. 2008. The vertebrate assemblage of Buenache de la Sierra (Upper Barremian of Serrania de Cuenca, Spain) with insights into its taphonomy and palaeoecology. *Cretaceous Research* 29: 687–710.

Buscalioni AD, Martín-Closas C, Delvene G, Munt MC, Barral A, Tinner-Grellet G, Gomez B, Daviero-Gomez V, Chamero B. 2018. Taphonomy and palaeoecology in the upper Barremian of the SW Iberian chain (Spain): A model to compare taxonomy and diversity of biotas from different coeval basins. *Palaeogeography, Palaeoclimatology, Palaeoecology* 490: 305–324.

Buscalioni AD, Ortega F, Pérez-Moreno BP, Evans SE. 1996. The Upper Jurassic maniraptoran theropod *Lisboasaurus estesi* (Guimarota, Portugal) reinterpreted as a crocodylomorph. *Journal of Vertebrate Paleontology* 16: 358–362.

Buscalioni AD, Ortega F, Vasse D. 1997. New crocodiles (Eusuchia: Alligatoroidea) from the Upper Cretaceous of southern Europe. *Comptes Rendus de l'Académie des Sciences-Series IIA-Earth and Planetary Science* 325: 525–530.

Buscalioni AD, Sanz-López J. 1988. Phylogenetic relationships of the Atoposauridae (Archosauria, Crocodylomorpha). *Historical Biology* 1: 233–250.

Caldwell MW. 2005. The squamates: origins, phylogeny, and paleoecology. In: Currie Philip J., Koppelhus EB, eds. *Dinosaur Provincial Park: A Spectacular Ancient Ecosystem Revealed*. Bloomington, IN: Indiana University Press, 235–248.

Caldwell M, Nydam R, Palci A, Apesteguia S. 2015. The oldest known snakes from the Middle Jurassic-Lower Cretaceous provide insights on snake evolution. *Nature Communication* 6.

Calvín P, Oliva-Urcia B, Kullberg JC, Torres-López S, Casas-Sainz A, Villalaín JJ, Soto R. 2023. Applying magnetic techniques to determine the

evolution of reactive diapirs: A case study of the Lusitanian basin. *Tectonophysics* 868: 230088.

Canudo JI, Gasca JM, Aurell M, Badiola A, Blain HA, Cruzado-Caballero P, Gómez-Fernández D, Moreno-Azanza M, Parrilla J, Rabal-Garcés R, Ruiz-Omeñaca JI. 2010. La Cantalera: an exceptional window onto the vertebrate biodiversity of the Hauterivian-Barremian transition in the Iberian Peninsula. *Journal of Iberian Geology* 36: 205–224.

Canudo JI, Oms O, Vila B, Galobart A, Fondevilla V, Puértolas-Pascual E, Sellés AG, Cruzado-Caballero P, Dinares-Turell J, Vicens E. 2016. The upper Maastrichtian dinosaur fossil record from the southern Pyrenees and its contribution to the topic of the Cretaceous–Palaeogene mass extinction event. *Cretaceous Research* 57: 540–551.

Carrano MT. 2006. Body-Size Evolution in the Dinosauria. In: Carrano MT, Gaudin T, Blob R, Wible JR, eds. *Amniote Paleobiology: Perspectives on the Evolution of Mammals, Birds, and Reptiles: a Volume Honoring James Allen Hopson*. London and Chicago: Chicago University Press, 225–268.

Carrano MT, Oreska MP, Lockwood R. 2016. Vertebrate paleontology of the Cloverly Formation (Lower Cretaceous), II: paleoecology. *Journal of Vertebrate Paleontology* 36: 2.

Carrano MT, Oreska MPJ, Murch A, Trujillo KC, Chamberlain KR. 2022. Vertebrate paleontology of the Cloverly Formation (Lower Cretaceous), III: a new species of *Albanerpeton*, with biogeographic and paleoecological implications. *Journal of Vertebrate Paleontology*: e2003372.

Carrano MT, Velez-Juarbe J. 2006. Paleoecology of the Quarry 9 vertebrate assemblage from Como Bluff, Wyoming (Morrison Formation, Late Jurassic). *Paleogeography, Paleoclimatology, Paleoecology* 237: 147–159.

Carvalho I de S, de Gasparini ZB, Salgado L, de Vasconcellos FM, Marinho T da S. 2010. Climate's role in the distribution of the Cretaceous

terrestrial Crocodyliformes throughout Gondwana. *Palaeogeography, Palaeoclimatology, Palaeoecology* 297: 252–262.

Chatterjee S, Scotese C. **2007**. Biogeography of the Mesozoic lepidosaurs on the wandering Indian plate. *Paleontologia: cenários de vida*. Rio de Janeiro: Interciência, 559–587.

Chiarenza AA, Farnsworth A, Mannion PD, Lunt DJ, Valdes PJ, Morgan JV, Allison PA. **2020**. Asteroid impact, not volcanism, caused the end-Cretaceous dinosaur extinction. *Proceedings of the National Academy of Sciences* 117: 17084–17093.

Chure DJ, Evans SE. **1998**. A new occurrence of *Cteniogenys*, with comments on its distribution and abundance. *Modern Geology* 23: 49.

Clark JM. **1986**. Phylogenetic relationships of the crocodylomorph archosaurs. Unpublished thesis, University of Chicago.

Clark JM, Norell M. **1992**. The Early Cretaceous crocodylomorph *Hylaeochampsa vectiana* from the wealden of the Isle of Wight. *American Museum novitates*; no. 3032. : 1–19.

Clark JM, Xu X, Forster CA, Wang Y. **2004**. A Middle Jurassic 'sphenosuchian' from China and the origin of the crocodylian skull. *Nature* 430: 1021–1024.

Codrea VA, Barbu O, Jipa-Murzea CC. **2010a**. Upper Cretaceous (maastrichtian) landvertebrate diversity in Alba district (Romania). *Bulletin of the Geological Society of Greece* 43: 594–601.

Codrea VA, Smith T, Dica P, Folie A, Garcia G, Godefroit P, Van Itterbeeck J. **2002**. Dinosaur egg nests, mammals and other vertebrates from a new Maastrichtian site of the Haţeg Basin (Romania). *Comptes Rendus Palevol* 1: 173–180.

Codrea VA, Solomon A. **2012**. Peculiar fossilization and taphonomy in Maastrichtian terrestrial deposits of Pui (Haţeg Basin, Romania). *Studii şi cercetări (Geologie-Geografie)* 17: 51–69.

Codrea VA, Vremir M, Jipa C, Godefroit P, Csiki Z, Smith T, Fărcaş C. 2010b. More than just Nopcsa's Transylvanian dinosaurs: A look outside the Haţeg Basin. *Palaeogeography, Palaeoclimatology, Palaeoecology* 293: 391–405.

Company J, Szentesi Z. 2012. Amphibians from the Late Cretaceous Sierra Perenchiza Formation of the Chera Basin, Valencia Province, Spain. *Cretaceous Research* 37: 240–245.

Conrad JL. 2008. Phylogeny and systematics of Squamata (Reptilia) based on morphology. *Bulletin of the American Museum of Natural History* 310: 1–182.

Cope ED. 1875. *Check-list of North American Batrachia and Reptilia: With a Systematic List of the Higher Groups, and an Essay on Geographical Distribution; Based on the Specimens Contained in the US National Museum*. Washington, DC: US Government Printing Office.

Cope ED. 1884. The Choristodera. *American Naturalist* 17: 815–817.

Costa OG. 1864. Paleontologia del Regno di Napoli. Part III. *Atti dell'Accademia Pontaniana* 8: 1–128.

Costa F, Mateus O. 2019. Dacentrurine stegosaurs (Dinosauria): A new specimen of *Miragaia longicollum* from the Late Jurassic of Portugal resolves taxonomical validity and shows the occurrence of the clade in North America. *PLOS ONE* 14: e0224263.

Cruzado-Caballero P, Canudo JI, Moreno-Azanza M, Ruiz-Omeñaca JI. 2013. New material and phylogenetic position of *Arenysaurus ardevoli*, a lambeosaurine dinosaur from the late Maastrichtian of Arén (northern Spain). *Journal of Vertebrate Paleontology* 33: 1367–1384.

Cruzado-Caballero P, Pereda-Suberbiola X, Ruiz-Omeñaca JI. 2010. *Blasisaurus canudoi* gen. et sp. nov., a new lambeosaurine dinosaur (Hadrosauridae) from the latest Cretaceous of Arén (Huesca, Spain). *Canadian Journal of Earth Sciences* 47: 1507–1517.

Csiki Z, Ionescu A, Grigorescu D. 2008. The Budurone microvertebrate site from the Maastrichtian of the Haţeg Basin-flora, fauna, taphonomy and paleoenvironment. *Acta Palaeontologica Romaniae* 6: 49–66.

Csiki-Sava Z, Buffetaut E, Ősi A, Pereda-Suberbiola X, Brusatte SL. 2015. Island life in the Cretaceous-faunal composition, biogeography, evolution, and extinction of land-living vertebrates on the Late Cretaceous European archipelago. *ZooKeys*: 1–161.

Csiki-Sava Z, Vremir M, Vasile Ş, Brusatte SL, Dyke G, Naish D, Norell MA, Totoianu R. 2016. The east side story–the Transylvanian latest Cretaceous continental vertebrate record and its implications for understanding Cretaceous–Paleogene boundary events. *Cretaceous Research* 57: 662–698.

Dalla Vecchia FM. 2009. *Tethyshadros insularis*, a new hadrosauroid dinosaur (Ornithischia) from the Upper Cretaceous of Italy. *Journal of Vertebrate Paleontology* 29: 1100–1116.

Daza JD, Stanley EL, Bolet A, Bauer AM, Arias JS, Čerňanský A, Bevitt JJ, Wagner P, Evans SE. 2020. Enigmatic amphibians in mid-Cretaceous amber were chameleon-like ballistic feeders. *Science* 370: 687–691.

Delfino M, Martin JE, Buffetaut E. 2008. A new species of *Acynodon* (Crocodylia) from the upper cretaceous (Santonian–Campanian) of Villaggio del Pescatore, Italy. *Palaeontology* 51: 1091–1106.

Delfino M, Sala B. 2007. Late Pliocene Albanerpetontidae (Lissamphibia) from Italy. *Journal of Vertebrate Paleontology* 27: 716–719.

DeMar Jr. DG, Jones MEH, Carrano MT. 2022. A nearly complete skeleton of a new eusphenodontian from the Upper Jurassic Morrison Formation, Wyoming, USA, provides insight into the evolution and diversity of Rhynchocephalia (Reptilia: Lepidosauria). *Journal of Systematic Palaeontology* 20: 1–64.

Dercourt J, Gaetani M, Vrielynck B, Barrier E, Biju-Duval B, Brunet MF, Cadet JP, Crasquin S, Sandulescu M. 2000. *Atlas Peri-Tethys*

Palaeogeographical Maps. Paris: Commission de la carte géologique du monde.

Dilkes DW. **1998**. The Early Triassic rhynchosaur *Mesosuchus browni* and the interrelationships of basal archosauromorph reptiles. *Philosophical Transactions of the Royal Society of London. Series B: Biological Sciences* 353: 501–541.

Dodson P. **1973**. The significance of small bones in paleoecological interpretation. *Rocky Mountain Geology* 12: 15–19.

Dodson P. **1987**. Microfaunal studies of dinosaur paleoecology, Judith River Formation of southern Alberta. In: Currie PJ, Koster E, eds. *Fourth Symposium on Mesozoic Terrestrial Ecosystems, Short Papers*. Occasional Papers of the Tyrrell Museum of Palaeontology, 71–75.

Dollo L. **1883**. Première note sur les crocodiliens de Bernissart. *Bulletin du Musée Royal des Sciences Naturelles de Belgique* 2: 309–338.

Dong L, Matsumoto R, Kusuhashi N, Wang Y, Wang Y, Evans SE. **2020**. A new choristodere (Reptilia: Choristodera) from an Aptian–Albian coal deposit in China. *Journal of Systematic Palaeontology* 18: 1223–1242.

Drescher E. **2000**. Preparation of vertebrate fossils from the Guimarota mine. In: Martin T, Krebs B, eds. *Guimarota: a Jurassic ecosystem*. Munich: Verlag Dr. Friedrich Pfeil, 137–142.

Dudgeon TW, Mallon JC, Evans DC. **2023**. The first report of *Champsosaurus lindoei* (Choristodera: Champsosauridae) from the Campanian of the United States: anatomical, phylogenetic, and palaeoecological significance. *Zoological Journal of the Linnean Society*: zlad087.

Duellman WE, Trueb L. **1994**. *Biology of amphibians*. Baltimore, MD: The John Hopkins University press.

Duffaud S. **2000**. Les faunes d'amphibiens du Crétacé supérieur à l'Oligocène inférieur en Europe: paléobiodiversité, évolution, mise en place. Unpublished thesis, Muséum national d'Histoire naturelle.

Duffaud S, Rage JC. **1999**. Amphibians from the Upper Cretaceous of Laño (Basque Country, Spain). *Estudios del Museo de Ciencias Naturales de Alava* 14: 111–120.

Dutour Y, Tortosa T. **2010**. Aix-en-Provence Basin - Between eggs and dinosaurs. *Abstract volume*.

Dzombak RM, Sheldon ND, Mohabey DM, Samant B. **2020**. Stable climate in India during Deccan volcanism suggests limited influence on K–Pg extinction. *Gondwana Research* 85: 19–31.

Eberth DA, Brinkman DB. **1997**. Paleoecology of an estuarine, incised-valley fill in the Dinosaur Park Formation (Judith River Group, Upper Cretaceous) of southern Alberta, Canada. *Palaios* 12: 43–58.

Eberth DA, Rogers RR, Fiorillo AR. **2007*a***. A practical approach to the study of bonebeds. In: Rogers RR, Eberth DA, Fiorillo AR, eds. *Bonebeds: Genesis, analysis, and paleobiological significance*. Chicago, IL: University of Chicago Press, 265–331.

Eberth DA, Rogers RR, Fiorillo AR. **2007b**. A Practical Approach to the Study of Bonebeds. In: Rogers RR, Eberth DA, Fiorillo AR, eds. *Bonebeds: Genesis, Analysis, and Paleobiological Significance*. Chicago, IL: University of Chicago Press, 265–331.

Eberth DA, Shannon M, Noland BG. **2007c**. A Bonebeds Database: Classification, Biases, and Patterns of Occurrence. In: Rogers RR, Eberth DA, Fiorillo AR, eds. *Bonebeds: Genesis, Analysis, and Paleobiological Significance*. Chicago, IL: University of Chicago Press, 103–219.

El Albani A, Fürsich FT, Colin JP, Meunier A, Hochuli P, Martín-Closas C, Mazin JM, Billon-Bruyat JP. **2004**. Palaeoenvironmental reconstruction of the basal Cretaceous vertebrate bearing beds in the Northern part of the

Aquitaine Basin (SW France): sedimentological and geochemical evidence. *Facies* 50: 195–215.

Erickson BR. 1987. *Simoedosaurus dakotensis*, new species, a diapsid reptile (Archosauromorpha; Choristodera) from the Paleocene of North America. *Journal of Vertebrate Paleontology* 7: 237–251.

Escaso F, Ortega F, Dantas P, Malafaia E, Pimentel N, Pereda-Suberbiola X, Sanz-López J, Kullberg JC, Kullberg MC, Barriga F. 2007. New evidence of shared dinosaur across Upper Jurassic Proto-North Atlantic: *Stegosaurus* from Portugal. *Naturwissenschaften* 94: 367–374.

Escaso F, Ortega F, Dantas P, Malafaia E, Silva B, Gasulla JM, Mocho P, Narváez I, Sanz JL. 2014. A new dryosaurid ornithopod (Dinosauria, Ornithischia) from the Late Jurassic of Portugal. *Journal of Vertebrate Paleontology* 34: 1102–1112.

Estes R. 1964. Fossil vertebrates from the late Cretaceous Lance Formation, eastern Wyoming. *University of California Publications in Geological Sciences* 49: 1–187.

Estes R. 1976. Middle Paleocene lower vertebrates from the Tongue River Formation, southeastern Montana. *Journal of Paleontology*: 500–520.

Estes R. 1981. Gymnophiona, Caudata. In: Wellnhofer P, ed. *Encyclopedia of Paleoherpetology*. Stuttgart, 1–115.

Estes R. 1983. *Sauria terrestria, Amphisbaenia* (P Wellnhofer, Ed.). Stuttgart: Gustav Fischer Verlag.

Estes R, Berberian P. 1970. Paleoecology of a Late Cretaceous vertebrate community from Montana. *Brevoria* 343: 1–35.

Estes R, Hoffstetter R. 1976. Les Urodèles du Miocène de La Grive-Saint-Alban (Isère, France). *Bulletin du Muséum national d'Histoire naturelle, 3e série* 398: 297–343.

Estes R, Sanchíz B. **1982**. Early cretaceous lower vertebrates from Galve (Teruel), Spain. *Journal of Vertebrate Paleontology* 2: 21–39.

Evans SE. **1988**. The early history and relationships of the Diapsida. In: Benton MJ, ed. *The phylogeny and classification of the tetrapods*. Oxford: Clarendon Press, 221–260.

Evans SE. **1989**. New material of *Cteniogenys* (Reptilia: Diapsida; Jurassic) and a reassessment of the phylogenetic position of the genus. *Neues Jahrbuch für Geologie und Paläontologie-Monatshefte* 181: 577–589.

Evans SE. **1990**. The skull of *Cteniogenys*, a choristodere (Reptilia: Archosauromorpha) from the Middle Jurassic of Oxfordshire. *Zoological Journal of the Linnean Society* 99: 205–237.

Evans SE. **1991a**. The postcranial skeleton of the choristodere *Cteniogenys* (Reptilia: Diapsida) from the Middle Jurassic of England. *Geobios* 24: 187–199.

Evans SE. **1991b**. A new lizard-like reptile (Diapsida: Lepidosauromorpha) from the Middle Jurassic of England. *Zoological Journal of the Linnean Society* 103: 391–412.

Evans SE. **1992**. Small reptiles and amphibians from the Forest Marble (Middle Jurassic) of Dorset. *Proceedings of the Dorset Natural History and Archaeological Society* 113: 201–202.

Evans SE. **1993**. Jurassic lizard assemblages. *Revue de Paléobiologie (Suisse)* 7: 55–65.

Evans SE. **1998a**. Lepidosaurian Faunas From The Early Cretaceous: A Clade In Transition. *Lower and Middle Cretaceous Continental Ecosystems*. Albuquerque, NM: New Mexico Museum of Natural History and Science, 195–200.

Evans SE. **1998b**. Crown group lizards from the Middle Jurassic. *Palaeontographica A* 250: 1–32.

Evans SE. **2003**. At the feet of the dinosaurs: the early history and radiation of lizards. *Biological Reviews* 78: 513–551.

Evans SE. **2009**. An early kuehneosaurid reptile from the Early Triassic of Poland. *Palaeontologia Polonica* 65: 145–178.

Evans SE. **2016**. Albanerpetontidae. In: Poyato-Ariza FJ, Buscalioni AD, eds. *Las Hoyas: a Cretaceous wetland*. Munich: Verlag Dr. Friedrich Pfeil, 133–137.

Evans SE, Barrett PM, Ward DJ. **2004**. The first record of lizards and amphibians from the Wessex Formation (Lower Cretaceous: Barremian) of the Isle of Wight, England. *Proceedings of the Geologists' Association* 115: 239–247.

Evans SE, Borsuk-Białynicka M. **2009**. The Early Triassic stemfrog *Czatkobatrachus* from Poland. *Palaeontologica Polonica* 65: 79–105.

Evans SE, Hecht MK. **1993**. A History of an Extinct Reptilian Clade, the Choristodera: Longevity, Lazarus-Taxa, and the Fossil Record. In: Hecht MK, MacIntyre RJ, Clegg MT, eds. *Evolutionary Biology*. Boston, MA: Springer US, 323–338.

Evans SE, Jones ME. **2010**. The origin, early history and diversification of lepidosauromorph reptiles. In: Bandyopadhyay S, ed. *Lecture Notes in Earth Sciences. New aspects of Mesozoic biodiversity*. Berlin: Springer, 27–44.

Evans SE, Klembara J. **2005**. A choristoderan reptile (Reptilia: Diapsida) from the lower Miocene of northwest Bohemia (Czech republic). *Journal of vertebrate Paleontology* 25: 171–184.

Evans SE, McGowan G. **2002**. An amphibian assemblage from the Purbeck Limestone Group. In: Milner AR, Batten DJ, eds. *Special Papers in Palaeontology. Life and Environments in Purbeck Times*.103–119.

Evans SE, Milner AR. **1993**. Frogs and salamanders from the Upper Jurassic Morrison Formation (Quarry Nine, Como Bluff) of North America. *Journal of Vertebrate Paleontology* 13: 24–30.

Evans SE, Milner AR. **1994**. Middle Jurassic microvertebrate assemblages from the British Isles. In: Fraser NC, Evans SE, eds. *In the shadow of the dinosaurs: Early Mesozoic Tetrapods*. Cambridge: Cambridge University Press, 303–321.

Evans SE, Milner AR. **1996**. A metamorphosed salamander from the Early Cretaceous of Las Hoyas, Spain. *Philosophical Transactions: Biological Sciences* 351: 627–646.

Evans SE, Milner AR, Mussett F. **1990**. A discoglossid frog from the Middle Jurassic of England. *Palaeontology* 33: 299–311.

Evans SE, Prasad G, Manhas B. **2002**. Fossil lizards from the Jurassic Kota Formation of India. *Journal of Vertebrate Paleontology* 22: 299–319.

Evans SE, Waldman M. **1996**. Reptiles and amphibians from the Middle Jurassic (Bathonian) of Skye, Scotland. (M Morales, Ed.). *The Continental Jurassic, Museum of Northern Arizona Bulletin* 60: 219–226.

Ezcurra MD. **2016**. The phylogenetic relationships of basal archosauromorphs, with an emphasis on the systematics of proterosuchian archosauriforms. *PeerJ* 4: e1778.

Ezcurra MD, Bandyopadhyay S, Sen K. **2021**. A new faunistic component of the Lower Triassic Panchet Formation of India increases the continental non-archosauromorph neodiapsid record in the aftermath of the end-Permian mass extinction. *Journal of Paleontology*: 1–11.

Fanti F, Miyashita T, Cantelli L, Mnasri F, Dridi J, Contessi M, Cau A. **2016**. The largest thalattosuchian (Crocodylomorpha) supports teleosaurid survival across the Jurassic-Cretaceous boundary. *Cretaceous Research* 61: 263–274.

Fara E. **2004**. Estimating minimum global species diversity for groups with a poor fossil record: a case study of Late Jurassic–Eocene lissamphibians. *Palaeogeography, Palaeoclimatology, Palaeoecology* 207: 59–82.

Fernandes AE, Beccari V, Kellner AWA, Mateus O. 2023. A new gnathosaurine (Pterosauria, Archaeopterodactyloidea) from the Late Jurassic of Portugal. *PeerJ* 11: e16048.

Fernandes AE, Mateus O, Bauluz B, Coimbra R, Ezquerro L, Núñez-Lahuerta C, Suteu C, Moreno-Azanza M. 2021. The Paimogo Dinosaur Egg Clutch Revisited: Using One of Portugal's Most Notable Fossils to Exhibit the Scientific Method. *Geoheritage* 13: 1–17.

Folie A, Codrea VA. 2005. New lissamphibians and squamates from the Maastrichtian of Haţeg Basin, Romania. *Acta Palaeontologica Polonica* 50: 57–71.

Fortier D, Perea D, Schultz C. 2011. Redescription and phylogenetic relationships of *Meridiosaurus vallisparadisi*, a pholidosaurid from the Late Jurassic of Uruguay. *Zoological Journal of the Linnean Society* 163: S257–S272.

Foster JR. 2001. Taphonomy and paleoecology of a microvertebrate assemblage from the Morrison Formation (Upper Jurassic) of the Black Hills, Crook County, Wyoming. *Brigham Young University Geology Studies* 46: 13–34.

Foster J. 2020. *Jurassic West: The Dinosaurs of the Morrison Formation and Their World*. Bloomington, IN: Indiana University Press.

Foster J, Heckert A. 2011. Ichthyoliths and other microvertebrate remains from the Morrison Formation (Upper Jurassic) of northeastern Wyoming A screen-washed sample indicates a significant aquatic component to the fauna. *Paleogeography, Paleoclimatology, Paleoecology* 305: 264–279.

Foster JR, Trujillo KC. 2000. New occurrences of *Cteniogenys* (Reptilia, Choristodera) in the Late Jurassic of Wyoming and South Dakota. *Brigham Young University Geology Studies* 45: 11–18.

Fox RC. 1968. Studies of Late Cretaceous Vertebrates I. The Braincase of *Champsosaurus* Cope (Reptilia: Eosuchia). *Copeia* 1968: 100–109.

Fox RC, Naylor BG. 1982. A reconsideration of the relationships of the fossil amphibian *Albanerpeton*. *Canadian Journal of Earth Sciences* 19: 118–128.

Freeman EF. 1976. Mammal Teeth from the Forest Marble (Middle Jurassic) of Oxfordshire, England. *Science* 194: 1053–1055.

Freeman EF. 1979. A Middle Jurassic mammal bed from Oxfordshire. *Palaeontology* 22: 135–166.

Fürsich FT, Schneider S, Werner W, Lopez-Mir B, Pierce CS. 2022. Life at the continental–marine interface: palaeoenvironments and biota of the Alcobaça Formation (Late Jurassic, Central Portugal), with a formal definition of the unit appended. *Palaeobiodiversity and Palaeoenvironments* 102: 265–329.

Gao K, Brinkman DB. 2005. Choristoderes from the Park and Its Vicinity. *Dinosaur Provincial Park: a spectacular ancient ecosystem revealed*. Bloomington, IN: Indiana University Press, 221–234.

Gao KQ, Chen J, Jia J. 2013. Taxonomic diversity, stratigraphic range, and exceptional preservation of Juro-Cretaceous salamanders from northern China. *Canadian Journal of Earth Sciences* 50: 255–267.

Gao K, Fox RC. 1998. New choristoderes (Reptilia: Diapsida) from the Upper Cretaceous and Palaeocene, Alberta and Saskatchewan, Canada, and phylogenetic relationships of Choristodera. *Zoological Journal of the Linnean Society* 124: 303–353.

Gao T, Li DQ, Li LF, Yang JT. 2019. The first record of freshwater plesiosaurian from the Middle Jurassic of Gansu, NW China, with its implications to the local palaeobiogeography. *Journal of Palaeogeography* 8: 27.

Gao KQ, Shubin NH. 2001. Late Jurassic salamanders from northern China. *Nature* 410: 574–577.

Gao KQ, Shubin NH. 2003. Earliest known crown-group salamanders. *Nature* 422: 424–428.

Gao KQ, Shubin NH. 2012. Late Jurassic salamandroid from western Liaoning, China. *Proceedings of the National Academy of Sciences* 109: 5767–5772.

Garcia G, Duffaud S, Feist M, Marandat B, Tambareau Y, Villatte J, Sigé B. 2000. La Neuve, gisement à plantes, invertébrés et vertébrés du Bégudien (Sénonien supérieur continental) du bassin d'Aix-en-Provence. *Geodiversitas* 22: 325–348.

Gardner JD. 1996. The North American fossil record of Albanerpeton (Lissamphibia, Albanerpetontidae). *Journal of Vertebrate Paleontology* 16: 36A.

Gardner JD. 1999a. The amphibian *Albanerpeton arthridion* and the Aptian–Albian biogeography of albanerpetontids. *Palaeontology* 42: 529–544.

Gardner JD. 1999b. New albanerpetontid amphibians from the Albian to Coniacian of Utah, USA—bridging the gap. *Journal of Vertebrate Paleontology* 19: 632–638.

Gardner JD. 1999c. Redescription of the geologically youngest albanerpetontid (? Lissamphibia): *Albanerpeton inexpectatum* Estes and Hoffstetter, 1976, from the Miocene of France. *Annales de Paléontologie* 85: 57–84.

Gardner JD. 2000a. Revised taxonomy of albanerpetontid amphibians. *Acta Palaeontologica Polonica* 45: 55–70.

Gardner JD. 2000b. Albanerpetontid amphibians from the Upper Cretaceous (Campanian and Maastrichtian) of North America. *Geodiversitas* 22: 349–388.

Gardner JD. 2001. Monophyly and affinities of albanerpetontid amphibians (Temnospondyli; Lissamphibia). *Zoological Journal of the Linnean Society* 131: 309–352.

Gardner JD. **2002**. Monophyly and intra-generic relationships of *Albanerpeton* (Lissamphibia; Albanerpetontidae). *Journal of Vertebrate Paleontology* 22: 12–22.

Gardner JD, Averianov AO. **1998**. Albanerpetontid amphibians from the Upper Cretaceous of Middle Asia. *Acta Palaeontologica Polonica* 43: 453–476.

Gardner JD, Böhme M. **2008**. Review of the Albanerpetontidae (Lissamphibia), with Comments on the Paleoecological Preferences of European Tertiary Albanerpetontids. In: Sankey JT, Bazio S, eds. *Vertebrate Microfossil Assemblages: Their Role in Paleoecology and Paleobiogeography*. Bloomington, IN: Indiana University Press, 178–218.

Gardner JD, DeMar DG. **2013**. Mesozoic and Palaeocene lissamphibian assemblages of North America: a comprehensive review. *Palaeobiodiversity and Palaeoenvironments* 93: 459–515.

Gardner JD, Evans SE, Sigogneau-Russel D. **2003**. New albanerpetontid amphibians from the Early Cretaceous of Morocco and Middle Jurassic of England. *Acta Paleontologica Polonica* 48: 301–319.

Gardner JD, Roček Z, Přikryl T, Eaton JG, Blob RW, Sankey JT. **2010**. Comparative morphology of the ilium of anurans and urodeles (Lissamphibia) and a re-assessment of the anuran affinities of *Nezpercius dodsoni* Blob et al., 2001. *Journal of Vertebrate Paleontology* 30: 1684–1696.

Gardner JD, Villa A, Colombero S, Venczel M, Delfino M. **2021**. A Messinian (latest Miocene) occurrence for *Albanerpeton* Estes & Hoffstetter, 1976 (Lissamphibia: Albanerpetontidae) at Moncucco Torinese, Piedmont Basin, northwestern Italy, and a review of the European Cenozoic record for albanerpetontids. *Geodiversitas* 43: 391–404.

Gasca JM, Badiola A, Canudo JI, Moreno-Azanza M, Puértolas-Pascual E. **2012**. La asociación de vertebrados fósiles del yacimiento Pochancalo 1 (Valanginiense–Hauteriviense, Villanueva de Huerva, Zaragoza, España).

Actas de V Jornadas Internacionales sobre Paleontología de Dinosaurios y su Entorno, Salas de los Infantes. Burgos, 159–172.

Gassner T. 2000. The turtles from the Guimarota mine. In: Martin T, Krebs B, eds. *Guimarota: a Jurassic ecosystem*. Munich: Verlag Dr. Friedrich Pfeil, 55–58.

Gauthier JA, Estes R, De Queiroz K. 1988a. A phylogenetic analysis of Lepidosauromorpha. In: Estes R, Pregill G, eds. *Phylogenetic Relationships of the Lizard Families: Essays Commemorating Charles L. Camp*. Standford, CA: Stanford University Press, 15–98.

Gauthier JA, Kearney M, Maisano JA, Rieppel O, Behlke AD. 2012. Assembling the squamate tree of life: perspectives from the phenotype and the fossil record. *Bulletin of the Peabody Museum of Natural History* 53: 3–308.

Gauthier J, Kluge AG, Rowe T. 1988b. Amniote phylogeny and the importance of fossils. *Cladistics* 4: 105–209.

Georgalis GL, Čerňanský A, Mayda S. 2021. Late Paleogene herpetofaunas from the crossroads between two continents – new amphibian and reptile remains from the Oligocene of southern Balkans and Anatolia. *Comptes Rendus Palevol*: 253–257.

Gervais FLP. 1871. Reptiles provenant des calcaires lithographiques de Cirin, dans le Bugey, qui sont conservés au Musée de Lyon. *Bulletin de la société géologique de France* 2: 171.

Gheerbrant E, Rage JC. 2006. Paleobiogeography of Africa: How distinct from Gondwana and Laurasia? *Palaeogeography, Palaeoclimatology, Palaeoecology* 241: 224–246.

Gilbert MM, Bamforth EL, Buatois LA, Renaut RW. 2018. Paleoecology and sedimentology of a vertebrate microfossil assemblage from the easternmost Dinosaur Park Formation (Late Cretaceous, Upper Campanian,) Saskatchewan, Canada: Reconstructing diversity in a coastal ecosystem. *Palaeogeography, Palaeoclimatology, Palaeoecology* 495: 227–244.

Gilmore CW. 1928. Fossil lizards of North America. *Memoirs of the National Academy of Sciences* 22: 1–201.

Gloy U. 2000. Taphonomy of the fossil lagerstatte Guimarota. In: Martin T, Krebs B, eds. *Guimarota: a Jurassic ecosystem*. Munich: Verlag Dr. Friedrich Pfeil, 129–136.

Goin CJ, Auffenberg W. 1958. New salamanders of the family Sirenidae from the Cretaceous of North America. *Fieldiana. Geology* 10: 449–459.

Goloboff PA, Catalano SA. 2016. TNT version 1.5, including a full implementation of phylogenetic morphometrics. *Cladistics* 32: 221–238.

Goloboff PA, Farris JS, Nixon KC. 2008. TNT, a free program for phylogenetic analysis. *Cladistics* 24: 774–786.

Golonka J, Kiessling W. 2002. Phanerozoic Time Scale and Definition of Time Slices (W Kiessling, E Flügel, and J Golonka, Eds.). *Phanerozoic Reef Patterns* 72: 11–20.

Gómez-Gras D, Roigé M, Fondevilla V, Oms O, Boya S, Remacha E. 2016. Provenance constraints on the Tremp Formation paleogeography (southern Pyrenees): Ebro Massif VS Pyrenees sources. *Cretaceous Research* 57: 414–427.

Gônet J, Rozada L, Bourgeais R, Allain R. 2019. Taphonomic study of a pleurosternid turtle shell from the Early Cretaceous of Angeac-Charente, southwest France. *Lethaia* 52: 232–243.

Goodwin MB, Clemens WA, Hutchison JH, Wood CB, Zavada MS, Kemp A, Duffin CJ, Schaff CR. 1999. Mesozoic continental vertebrates with associated palynostratigraphic dates from the northwestern Ethiopian Plateau. *Journal of Vertebrate Paleontology* 19: 728–741.

Gowland S, Taylor AM, Martinius AW. 2017. Integrated sedimentology and ichnology of Late Jurassic fluvial point bars–facies architecture and colonization styles (Lourinhã Formation, Lusitanian Basin, western Portugal). *Sedimentology*: 1–31.

Grambast L. 1962. Classification de l'embranchement des Charophytes. *Naturalia Monspeliensia, Série Botanique* 14: 63–86.

Grambast-Fessard N, Ramalho M. 1985. Charophytes du Jurassique supérieur du Portugal. *Revue de Micropaléontologie* 28: 58–66.

Graziano R, Raspini A, Bartiromo A. 2024. New insights into the palaeoenvironmental–palaeoclimatic significance and sedimentary dynamics of carbonate Lagerstätten: The lower Albian of Pietraroja (Southern Italy). *Sedimentology* 71: 619–686.

Griffiths EF, Ford DP, Benson RB, Evans SE. 2021. New information on the Jurassic lepidosauromorph *Marmoretta oxoniensis*. *Papers in Palaeontology* 7: 2255–2278.

Grigorescu D, Venczel M, Csiki Z, Limberea R. 1999. New latest Cretaceous microvertebrate fossil assemblages from the Haţeg Basin (Romania). *Geologie en Mijnbouw* 78: 301–314.

Guillaume ARD. 2018. Microvertebrates of the Lourinhã Formation (Late Jurassic, Portugal). Unpublished thesis, Faculdade de Ciências e Tecnologia - Universidade de Lisboa.

Guillaume ARD, Ezquerro L, Moreno-Azanza M, Mateus O. 2023*a*. Vertebrate microfossil assemblages from the Lourinhã Formation: a sneak peek on the paleoecology of the Late Jurassic in Portugal. In: Foster RK, Kirkland JI, Loewen MA, eds. *Special Issue: Special Issue:14th Symposium on Mesozoic Terrestrial Ecosystems and Biota*. Salt Lake City ,UT: The Anatomical Record, 118–121.

Guillaume ARD, Moreno-Azanza M, Mateus O. 2018. Microvertebrates from the Lourinhã Formation (Late Jurassic, Portugal). In: Crespo VD, Manzanares E, Marquina-Blasco R, Suñer M, Herráiz JL, Gamonal A, Arnal FAM, Ferrón HG, Gascó F, Martínez-Pérez C, eds. *Book of abstracts*.70.

Guillaume ARD, Moreno-Azanza M, Puértolas-Pascual E, Mateus O. 2020. Palaeobiodiversity of crocodylomorphs from the Lourinhã Formation based

on the tooth record: insights into the palaeoecology of the Late Jurassic of Portugal. *Zoological Journal of the Linnean Society* 189: 549–583.

Guillaume ARD, Natário C, Mateus O, Moreno-Azanza M. 2023b. Plasticity in the morphology of the fused frontals of Albanerpetontidae (Lissamphibia; Allocaudata). *Historical Biology* 35: 537–554.

Haddoumi H, Allain R, Meslouh S, Metais G, Monbaron M, Pons D, Rage JC, Vullo R, Zouhri S, Gheerbrant E. 2016. Guelb el Ahmar (Bathonian, Anoual Syncline, eastern Morocco): first continental flora and fauna including mammals from the Middle Jurassic of Africa. *Gondwana Research* 29: 290–319.

Haeckel E. 1866. *Generelle Morphologie der Organismen, Allgemeine Grundzuge der Organischen Formen-Wissenschaft, Mechanisch Begründet Durch die von Charles Darwin Reformirte Descendez-Theorie. Allgemeine entwickelungsgeschichte der organismen*. Berlin: Verlag von Georg Reimer.

Hahn G. 1969. Beiträge zur Fauna der Grube Guimarota Nr. 3. Die Multituberculata. *Palaeontographica Abteilung A*: 1–100.

Hahn G. 1971. The dentition of the Paulchoffatiidae (Multituberculata, upper Jurassic). Contribuição para o Conhecimento da Fauna do Kimeridgiano da Mina de Lignito Guimarota (Leiria, Portugal) II Parte: III. *Memórias dos Serviços geológicos de Portugal* 17: 7–39.

Hahn G. 1977. Neue Schädel-Reste von Multituberculaten (Mamm.) aus dem Malm Portugals. *Geologica et Palaeontologica* 11: 161–186.

Hahn G. 1978. Neue Unterkiefer von Multituberculaten aus dem Malm Portugals. *Geologica et Palaeontologica* 12: 177–212.

Hahn G. 1987. Neue beobachtungen zum schädel-und gebiss-bau der Paulchoffatiidae (Multituberculata, Ober-Jura). *Palaeovertebrata* 17: 155–196.

Hahn G. 1993. The systematic arrangement of the Paulchoffatiidae (Multituberculata) revisited. *Geologica et Palaeontologica* 27: 201–214.

Hahn G, Hahn R. **1998a**. Neue Beobachtungen an Plagiaulacoidea (Multituberculata) des Ober-Juras 3. Der Bau der Molaren bei den Paulchoffatiidae. *Berliner geowissenschaftliche Abhandlungen (E)* 28: 39–84.

Hahn G, Hahn R. **1998b**. Neue Beobachtungen an Plagiaulacoidea (Multituberculata) des Ober- Juras 4. Ein Vertreter der Albionbaataridae im Lusitanien Portugals. *Berliner geowissenschaftliche Abhandlungen (E)* 28: 85–89.

Hahn G, Hahn R. **1999a**. Pinheirodontidae n. fam.(Multituberculata)(Mammalia) aus der tiefen Unter-Kreide Portugals. *Palaeontographica Abteilung A*: 77–222.

Hahn G, Hahn R. **1999b**. Nomenklatorische Notiz: Namens- Änderung bei Multituberculata (Mammalia). *Geologica et Palaeontologica* 33: 156.

Hahn G, Hahn R. **2000**. Multituberculates from the Guimarota mine. In: Martin T, Krebs B, eds. *Guimarota: a Jurassic ecosystem*. Munich: Verlag Dr. Friedrich Pfeil, 97–108.

Hahn G, Hahn R. **2001a**. Multituberculaten-Zähne aus der Unter-Kreide (Barremium) von Pié Pajarón (Prov. Cuenca, Spanien). *Paläontologische Zeitschrift* 74: 587–589.

Hahn G, Hahn R. **2001b**. Multituberculaten-Zähne aus dem Ober-Jura von Porto das Barcas (Portugal). *Paläontologische Zeitschrift* 74: 583–586.

Hallam A. **2001**. A review of the broad pattern of Jurassic sea-level changes and their possible causes in the light of current knowledge. *Palaeogeography, Palaeoclimatology, Palaeoecology* 167: 23–37.

Hammer Ø, Harper DA, Ryan PD. **2001**. PAST: Paleontological statistics software package for education and data analysis. *Palaeontologia electronica* 4: 9.

Hay OP. **1929**. *Second bibliography and catalogue of the fossil Vertebrata of North America*. Washington, DC: Carnegie institution of Washington.

Helmdach FF. **1968**. Oberjurassische Süß- und Brackwasserostracoden der Kohlengrube Guimarota bei Leiria (Mittelportugal). Unpublished thesis, Freie Universität Berlin.

Helmdach FF. **1971**. Stratigraphy and ostracod-fauna from the coalmine Guimarota (Upper Jurassic). Contribuição para o Conhecimento da Fauna do Kimeridgiano da Mina de Lignito Guimarota (Leiria, Portugal) II Parte: IV. *Memórias dos Serviços geológicos de Portugal* 17: 41–88.

Hendrickx C, Mateus O. **2014a**. *Torvosaurus gurneyi* n. sp., the largest terrestrial predator from Europe, and a proposed terminology of the maxilla anatomy in nonavian theropods. *PLoS One* 9: e88905.

Hendrickx C, Mateus O. **2014b**. Abelisauridae (Dinosauria: Theropoda) from the Late Jurassic of Portugal and dentition-based phylogeny as a contribution for the identification of isolated theropod teeth. *Zootaxa* 3759: 1–74.

Henkel S. **1966**. Methoden zur Prospektion und Gewinnung kleiner Wirbeltierfossilien. *Neues Jahrbuch für Geologie und Paläontologie, Monatshefte* 1966: 178–184.

Herrera-Flores JA, Elsler A, Stubbs TL, Benton MJ. **2022a**. Slow and fast evolutionary rates in the history of lepidosaurs. *Palaeontology* 65: e12579.

Herrera-Flores J, Stubbs T, Sour-Tovar F. **2022b**. Redescription of the type specimens for the Late Jurassic rhynchocephalian *Opisthias rarus* and a new specimen of *Theretairus antiquus* from Quarry 9, Morrison Formation, Wyoming, USA. *Acta Palaeontologica Polonica* 67: 623–630.

Hill G. **1988**. The sedimentology and lithostratigraphy of the Upper Jurassic Lourinhã Formation, Lusitanian Basin, Portugal. Unpublished thesis, Open University.

Hill G. **1989**. Distal alluvial fan sediments from the Upper Jurassic of Portugal: controls on their cyclicity and channel formation. *Journal of the Geological Society* 146: 539–555.

Hua S, Buffetaut E, Legall C, Rogron P. 2007. *Oceanosuchus boecensis* n. gen, n. sp., a marine pholidosaurid (Crocodylia, Mesosuchia) from the Lower Cenomanian of Normandy (western France). *Bulletin de la Société géologique de France* 178: 503–513.

Jackson DA. 1993. Stopping rules in principal components analysis: a comparison of heuristical and statistical approaches. *Ecology* 74: 2204–2214.

Jäger KRK, Luo ZX, Martin T. 2020. Postcranial Skeleton of *Henkelotherium guimarotae* (Cladotheria, Mammalia) and Locomotor Adaptation. *Journal of Mammalian Evolution* 27: 349–372.

Jésus VJ, Mateus O, Milan J, Clemmensen LB. 2022. First occurrence of a frog-like batrachian (Amphibia) in the Late Triassic Fleming Fjord Group, central. *Bulletin of the Geological Society of Denamark* 70: 117–130.

Jia J, Gao KQ. 2016. A new hynobiid-like salamander (Amphibia, Urodela) from Inner Mongolia, China, provides a rare case study of developmental features in an Early Cretaceous fossil urodele. *PeerJ* 4: e2499.

Jianu CM, Boekschoten GJ. 1999. The Hateg-island or outpost? *Deinsea* 7: 195–198.

Jipa CC. 2012. Asociaţii de vertebrate continentale Cretacic terminale din aria de sedimentare Metaliferi: sistematică, paleoecologie şi paleobiogeografie. Unpublished thesis, Universitatea Babeş-Bolyai.

Jipa CC, Solomon A, Feigi Ş, Miclea A. 2010. Microvertebrate continentale maastrichtiene de la Oarda de Jos (Jud. Alba)–date preliminare. *Lucrările celui de-al X-lea Simpozion Naţional Studenţesc" Geoecologia*: 41–44.

Johnson MM, Foffa D, Young MT, Brusatte SL. 2022. The ecological diversification and evolution of Teleosauroidea (Crocodylomorpha, Thalattosuchia), with insights into their mandibular biomechanics. *Ecology and Evolution* 12: e9484.

Jones ME, Anderson CL, Hipsley CA, Müller J, Evans SE, Schoch RR. 2013. Integration of molecules and new fossils supports a Triassic origin for Lepidosauria (lizards, snakes, and tuatara). *BMC evolutionary biology* 13: 208.

Jones ME, Benson RB, Skutschas P, Hill L, Panciroli E, Schmitt AD, Walsh SA, Evans SE. 2022. Middle Jurassic fossils document an early stage in salamander evolution. *Proceedings of the National Academy of Sciences* 119: e2114100119.

Jouve S, Sarıgül V, Steyer JS, Sen S. 2019. The first crocodylomorph from the Mesozoic of Turkey (Barremian of Zonguldak) and the dispersal of the eusuchians during the Cretaceous. *Journal of Systematic Palaeontology* 17: 111–128.

Kieser JA, Klapsidis C, Law L, Marion M. 1993. Heterodonty and patterns of tooth replacement in Crocodylus niloticus. *Journal of Morphology* 218: 195–201.

King GM. 1996. *Reptiles and Herbivory*. London: Chapman & Hall.

Kirkland J, Carpenter K, Hirsch KF, Horner JR. 1994. Predation of dinosaur nests by terrestrial crocodilians. *Dinosaur eggs and babies*. Cambridge, MA: Cambridge University Press, 124–133.

Kligman BT, Gee BM, Marsh AD, Nesbitt SJ, Smith ME, Parker WG, Stocker MR. 2023. Triassic stem caecilian supports dissorophoid origin of living amphibians. *Nature*: 1–6.

Krebs B. 1967. Der Jura-Krokodilier Machimosaurus H. v. Meyer. *Paläontologische Zeitschrift* 41: 46–59.

Krebs B. 1968. Le Crocodilien *Machimosaurus*. Contribuição para a fauna do Kimeridgiano da Mina de Lignito Guimarota (Leiria, Portugal) I Parte: II. *Memórias dos Serviços geológicos de Portugal* 41: 21–53.

Krebs B. **1991**. *Das Skelett von* Henkelotherium guimarotae *gen. et sp. nov.(Eupantotheria, Mammalia) aus dem Oberen Jura von Portugal*. Selbstverlag Fachbereich Geowissenschaften, FU Berlin.

Krebs B. **1998**. *Drescheratherium acutum* gen. et sp. nov., ein neuer Eupantotherier (Mammalia) aus dem Oberen Jura von Portugal. *Berliner geowissenschaftliche Abhandlungen (E)* 28: 91–111.

Krebs B. **2000a**. The excavations in the Guimarota mine. In: Martin T, Krebs B, eds. *Guimarota: a Jurassic ecosystem*. Munich: Verlag Dr. Friedrich Pfeil, 9–20.

Krebs B. **2000b**. The henkelotheriids from the Guimarota mine. In: Martin T, Krebs B, eds. *Guimarota: a Jurassic ecosystem*. Munich: Verlag Dr. Friedrich Pfeil, 121–128.

Krebs B, Schwarz D. **2000**. The crocodiles from the Guimarota mine. In: Martin T, Krebs B, eds. *Guimarota: a Jurassic ecosystem*. Munich: Verlag Dr. Friedrich Pfeil, 69–75.

Kriwet J. **2000**. The fish fauna from the Guimarota mine. In: Martin T, Krebs B, eds. *Guimarota: a Jurassic ecosystem*. Munich: Verlag Dr. Friedrich Pfeil, 41–50.

Kriwet J. **2002**. Pycnodont fish remains (Neopterygii: Pycnodontiformes) from the Kimmeridgian (Upper Jurassic) of the Lusitanian Basin (Central Portugal). *Neues Jahrbuch für Geologie und Paläontologie - Monatshefte*: 577–587.

Kriwet J. **2004**. Late Jurassic selachians (Chondrichthyes: Hybodontiformes, Neoselachii) from Central Portugal. *Neues Jahrbuch fur Geologie und Palaontologie-Monatshefte* 4: 233–256.

Kriwet J. **2005**. An amioid fish (Neopterygii, Amiiformes) from the Late Jurassic of the Iberian Peninsula. *Geobios* 38: 99–106.

Krusat G. **1969**. Ein Pantotheria-Molar mit dreispitzigem Talonid aus dem Kimmeridge von Portugal. *Paläontologische Zeitschrift* 43: 52–56.

Krusat G. **1980**. *Haldanodon exspectatus* Kühne & Krusat 1972 (Mammalia, Docodonta). Contribuição para o Conhecimento da Fauna do Kimeridgiano da Mina de Lignito Guimarota (Leiria, Portugal) IV Parte. *Memórias dos Serviços geológicos de Portugal* 27: 1–79.

Kühne WG. **1961**. A mammalian fauna from the Kimmeridgian of Portugal. *Nature* 192: 274–275.

Kühne WG. **1968**. History of discovery, report on the work performed, procedure, technique and generalities. Contribuição para a fauna do Kimeridgiano da Mina de Lignito Guimarota (Leiria, Portugal) I Parte: I. *Memórias dos Serviços geológicos de Portugal* 14: 7–20.

Kühne WG, Krusat G. **1972**. Legalisierung des Taxon *Haldanodon* (Mammalia, Docodonta). *Neues Jahrbuch für Geologie und Paläontologie, Monatshefte* 1972: 300–302.

Kullberg JC, Rocha RB, Soares AF, Rey J, Terrinha P, Callapez P, Martins L. **2006**. A Bacia Lusitaniana: estratigrafia, paleogeografia e tectónica. *Geologia de Portugal no contexto da Ibéria*. Évora: Universidade de Évora, 317–368.

Kuzmin IT, Skutschas PP, Grigorieva OI, Krasnolutskii SA. **2013**. Goniopholidid crocodylomorph from the Middle Jurassic Berezovsk Quarry locality (Western Siberia, Russia). *Труды Зоологического института РАН* 317: 452–458.

Lanser KP, Heimhofer U. **2015**. Evidence of theropod dinosaurs from a Lower Cretaceous karst filling in the northern Sauerland (Rhenish Massif, Germany). *Paläontologische Zeitschrift* 89: 79–94.

de Lapparent de Broin F. **2001**. The European turtle fauna from the Triassic to the Present. *Dumerilia* 4: 155–217.

Lasseron M, Allain R, Gheerbrant E, Haddoumi H, Jalil NE, Métais G, Rage JC, Vullo R, Zouhri S. **2020**. New data on the microvertebrate fauna from the Upper Jurassic or lowest Cretaceous of Ksar Metlili (Anoual Syncline, eastern Morocco). *Geological Magazine* 157: 367–392.

Lauprasert K, Laojumpon C, Saenphala W, Cuny G, Thirakhupt K, Suteethorn V. 2011. Atoposaurid crocodyliforms from the Khorat Group of Thailand: first record of Theriosuchus from Southeast Asia. *Paläontologische Zeitschrift* 85: 37–47.

Laurent Y. 2003. Les faunes de vertébrés continentaux du Maastrichtien supérieur d'Europe : systématique et biodiversité. Unpublished thesis, Université Paul Sabatier - Toulouse III.

Laurent Y, Bilotte M, Le Loeuff J. 2002. Late Maastrichtian continental vertebrates from southwestern France: correlation with marine fauna. *Palaeogeography, Palaeoclimatology, Palaeoecology* 187: 121–135.

Le Loeuff J. 1991. The Campano-Maastrichtian vertebrate faunas from southern Europe and their relationships with other faunas in the world; palaeobiogeographical implications. *Cretaceous Research* 12: 93–114.

Leinfelder R. 1993. A sequence stratigraphic approach to the Upper Jurassic mixed carbonate-siliciclastic succession of the central Lusitanian Basin, Portugal. *Profil* 5: 119–140.

Leinfelder RR, Wilson RC. 1989. Seismic and sedimentologic features of Oxfordian-Kimmeridgian syn-rift sediments on the eastern margin of the Lusitanian Basin. *Geologische Rundschau* 78: 81–104.

Li Y, Chang SC, Zhang H, Wang J, Pei R, Zheng D, Fang Y, Hemming SR. 2023. A chronostratigraphic and biostratigraphic framework for the Yanliao Biota of northeastern China: Implications for Jurassic terrestrial ecosystems and evolution. *Palaeogeography, Palaeoclimatology, Palaeoecology* 630: 111818.

Li ZX, Powell CMcA. 2001. An outline of the palaeogeographic evolution of the Australasian region since the beginning of the Neoproterozoic. *Earth-Science Reviews* 53: 237–277.

Lieberman BS. 2003. Paleobiogeography: the relevance of fossils to biogeography. *Annual Review of Ecology, Evolution, and Systematics* 34: 51–69.

Lieberman BS, Eldredge N. 1996. Trilobite biogeography in the Middle Devonian: geological processes and analytical methods. *Paleobiology* 22: 66–79.

Lillegraven JA, Krusat G. 1991. Cranio-mandibular anatomy of *Haldanodon exspectatus* (Docodonta; Mammalia) from the Late Jurassic of Portugal and its implications to the evolution of mammalian characters. *Rocky Mountain Geology* 28: 39–138.

Linnaeus C. 1758. *Systema naturae, sive regna tria naturae systematice proposita per classes, ordines, genera, & species*. Leiden: Haak.

Lockley M, Garcia-Ramos JC, Pinuela L, Avanzini M. 2008. A review of vertebrates track assemblages from the Late Jurassic of Asturias, Spain with comparatives notes on coeval ichnofaunas from the western USA: implications for faunal diversity in siliciclastic facies assemblages. *Oryctos* 8: 53–70.

le Loeuff J. 2005. Romanian Late Cretaceous dinosaurs: big dwarfs or small giants? *Historical Biology* 17: 15–17.

López-Martínez N, Canudo JI, Ardévol L, Pereda-Suberbiola X, Orue-Etxebarría X, Cuenca-Bescós G, Ruiz-Omeñaca JI, Murelaga X, Feist M. 2001. New dinosaur localities near the Cretaceous/Tertiary boundary (Arén south central Pyrenees, Spain). *Cretaceous Research* 22: 41–61.

López-Martínez N, Vicens E. 2012. A new peculiar dinosaur egg, *Sankofa pyrenaica* oogen. nov. oosp. nov. from the Upper Cretaceous coastal deposits of the Aren Formation, south-central Pyrenees, Lleida, Catalonia, Spain. *Palaeontology* 55: 325–339.

López-Rojas V, Mateus S, Marinheiro J, Mateus O, Puértolas-Pascual E. 2024. A new goniopholidid crocodylomorph from the Late Jurassic of Portugal. *Palaeontologia Electronica* 27: 1–33.

Luo ZX, Martin T. 2023. Mandibular and dental characteristics of the Late Jurassic mammal *Henkelotherium guimarotae* (Paurodontidae, Dryolestida). *PalZ* 97: 569–619.

Luo ZX, Ruf I, Martin T. 2012. The petrosal and inner ear of the Late Jurassic cladotherian mammal *Dryolestes leiriensis* and implications for ear evolution in therian mammals. *Zoological Journal of the Linnean Society* 166: 433–463.

Maddin HC, Venczel M, Gardner JD, Rage JC. 2013. Micro-computed tomography study of a three-dimensionally preserved neurocranium of *Albanerpeton* (Lissamphibia, Albanerpetontidae) from the Pliocene of Hungary. *Journal of Vertebrate Paleontology* 33: 568–587.

Maddison WP, Maddison DR. 2019. Mesquite: a modular system for evolutionary analysis.

Mädler K. 1952. Charophyten aus dem nordwestdeutschen Kimmeridge. *Geologisches Jahrbuch* 67: 1–46.

Malafaia E, Escaso F, Mocho P, Serrano-Martínez A, Torices A, Cachão M, Ortega F. 2017. Analysis of diversity, stratigraphic and geographical distribution of isolated theropod teeth from the Upper Jurassic of the Lusitanian Basin, Portugal. *Journal of Iberian Geology* 43: 257–291.

Malafaia E, Mocho P, Escaso F, Dantas P, Ortega F. 2018. Carcharodontosaurian remains (Dinosauria, Theropoda) from the Upper Jurassic of Portugal. *Journal of Paleontology*: 1–16.

Malafaia E, Mocho P, Escaso F, Ortega F. 2020. A new carcharodontosaurian theropod from the Lusitanian Basin: evidence of allosauroid sympatry in the European Late Jurassic. *Journal of Vertebrate Paleontology* 40: e1768106.

Malafaia E, Ortega F, Escaso F, Dantas P, Pimentel N, Gasulla JM, Ribeiro B, Barriga F, Sanz-López J. 2010. Vertebrate fauna at the *Allosaurus* fossil-site of Andres (Upper Jurassic), Pombal, Portugal. *Journal of Iberian Geology* 36: 193–203.

Mannion PD, Upchurch P, Barnes RN, Mateus O. 2013. Osteology of the Late Jurassic Portuguese sauropod dinosaur Lusotitan atalaiensis

(Macronaria) and the evolutionary history of basal titanosauriforms. *Zoological Journal of the Linnean Society* 168: 98–206.

Mannion PD, Upchurch P, Mateus O, Barnes RN, Jones MEH. 2012. New information on the anatomy and systematic position of *Dinheirosaurus lourinhanensis* (Sauropoda: Diplodocoidea) from the Late Jurassic of Portugal, with a review of European diplodocoids. *Journal of Systematic Palaeontology* 10: 521–551.

Mannion PD, Upchurch P, Schwarz D, Wings O. 2019. Taxonomic affinities of the putative titanosaurs from the Late Jurassic Tendaguru Formation of Tanzania: phylogenetic and biogeographic implications for eusauropod dinosaur evolution. *Zoological Journal of the Linnean Society* 185: 784–909.

Marjanović D, Laurin M. 2008. A reevaluation of the evidence supporting an unorthodox hypothesis on the origin of extant amphibians. *Contributions to Zoology* 77: 149–199.

Marjanović D, Laurin M. 2014. An updated paleontological timetree of lissamphibians, with comments on the anatomy of Jurassic crown-group salamanders (Urodela). *Historical Biology* 26: 535–550.

Marjanović D, Laurin M. 2019. Phylogeny of Paleozoic limbed vertebrates reassessed through revision and expansion of the largest published relevant data matrix. *PeerJ* 6: e5565.

Marmi J, Blanco A, Fondevilla V, Dalla Vecchia FM, Sellés AG, Vicente A, Martín-Closas C, Oms O, Galobart A. 2016. The Molí del Baró-1 site, a diverse fossil assemblage from the uppermost Maastrichtian of the southern Pyrenees (north-eastern Iberia). *Cretaceous Research* 57: 519–539.

Marsh OC. 1880. Notice of Jurassic Mammals representing two New Orders. *American Journal of Science* 20: 235–239.

Marsh OC. 1887. American Jurassic Mammals. *Geological Magazine* 4: 289–299.

Martin T. 1997. Tooth replacement in Late Jurassic Dryolestidae (Eupantotheria, Mammalia). *Journal of Mammalian Evolution* 4: 1–18.

Martin T. 1999. Dryolestidae (Dryolestoidea, Mammalia) aus dem Oberen Jura-von Portugal. *Abhandlungen der Senckenbergischen Naturforschenden Gesellschart*: 1–119.

Martin T. 2000a. Overview over the Guimarota ecosystem. In: Martin T,, In: Krebs B, eds. *Guimarota. A jurassic ecosystem*. Munich: Verlag Dr. Friedrich Pfeil, 143–146.

Martin T. 2000b. The dryolestids and the primitive "peramurid" from the Guimarota mine. In: Martin T, Krebs B, eds. *Guimarota: a Jurassic ecosystem*. Munich: Verlag Dr. Friedrich Pfeil, 109–120.

Martin T. 2001. Mammalian fauna of the Late Jurassic Guimarota ecosystem. *Publicación Electrónica de la Asociación Paleontológica Argentina* 7: 123–126.

Martin T. 2002. New stem-lineage representatives of Zatheria (Mammalia) from the Late Jurassic of Portugal. *Journal of Vertebrate Paleontology* 22: 332–348.

Martin T. 2005. Postcranial anatomy of *Haldanodon exspectatus* (Mammalia, Docodonta) from the Late Jurassic (Kimmeridgian) of Portugal and its bearing for mammalian evolution. *Zoological Journal of the Linnean Society* 145: 219–248.

Martin JE. 2007. New material of the Late Cretaceous globidontan *Acynodon iberoccitanus* (Crocodylia) from southern France. *Journal of Vertebrate Paleontology* 27: 362–372.

Martin T. 2013. Mammalian postcranial bones from the Late Jurassic of Portugal and their implications for forelimb evolution. *Journal of Vertebrate Paleontology* 33: 1432–1441.

Martín C, Alonso-Zarazaga MA, Sanchiz B. 2012. Nomenclatural notes on living and fossil amphibians. *Graellsia* 68: 159–180.

Martin JE, Delfino M, Smith T. 2016a. Osteology and affinities of Dollo's goniopholidid (Mesoeucrocodylia) from the Early Cretaceous of Bernissart, Belgium. *Journal of Vertebrate Paleontology* 36: e1222534.

Martin T, Krebs B. 2000. *Guimarota: a Jurassic ecosystem*. Munich: Verlag Dr. Friedrich Pfeil.

Martin JE, Lauprasert K, Buffetaut E, Liard R, Suteethorn V. 2014a. A large pholidosaurid in the Phu Kradung Formation of north-eastern Thailand. *Palaeontology* 57: 757–769.

Martin T, Nowotny M. 2000. The docodont *Haldanodon* from the Guimarota mine. In: Martin T,, In: Krebs B, eds. *Guimarota: a Jurassic ecosystem*. Munich: Verlag Dr. Friedrich Pfeil, 91–96.

Martin JE, Rabi M, Csiki-Sava Z, Vasile Ş. 2014b. Cranial morphology of *Theriosuchus sympiestodon* (Mesoeucrocodylia, Atoposauridae) and the widespread occurrence of *Theriosuchus* in the Late Cretaceous of Europe. *Journal of Paleontology* 88: 444–456.

Martin JE, Raslan-Loubatié J, Mazin JM. 2016b. Cranial anatomy of *Pholidosaurus purbeckensis* from the Lower Cretaceous of France and its bearing on pholidosaurid affinities. *Cretaceous Research* 66: 43–59.

Martin JE, Smith T, Salaviale C, Adrien J, Delfino M. 2020. Virtual reconstruction of the skull of *Bernissartia fagesii* and current understanding of the neosuchian–eusuchian transition. *Journal of Systematic Palaeontology* 18: 1079–1101.

Martinius AW, Gowland S. 2011. Tide-influenced fluvial bedforms and tidal bore deposits (late Jurassic Lourinhã Formation, Lusitanian Basin, Western Portugal). *Sedimentology* 58: 285–324.

Mateus O. 2006. Late Jurassic Dinosaurs from the Morrison Formation (USA), the Lourinhã and Alcobaça Formations (Portugal), and the Tendaguru beds (Tanzania): A comparison. *Paleontology and Geology of the Upper Jurassic Morrison Formation. New Mexico Museum of Natural History and Science Bulletin* 36: 223–231.

Mateus O, Dinis J, Cunha P. 2017. The Lourinhã Formation: the Upper Jurassic to lowermost Cretaceous of the Lusitanian Basin, Portugal – landscapes where dinosaurs walked. *Ciências da Terra* 19: 75–97.

Mateus O, Maidment SC, Christiansen NA. 2009. A new long-necked 'sauropod-mimic'stegosaur and the evolution of the plated dinosaurs. *Proceedings of the Royal Society of London B: Biological Sciences* 279: 1815–1821.

Mateus O, Milàn J. 2010. A diverse Upper Jurassic dinosaur ichnofauna from central-west Portugal. *Lethaia* 43: 245–257.

Mateus O, Puértolas-Pascual E, Callapez PM. 2019. A new eusuchian crocodylomorph from the Cenomanian (Late Cretaceous) of Portugal reveals novel implications on the origin of Crocodylia. *Zoological Journal of the Linnean Society* 186: 501–528.

Mateus O, Walen A, Antunes MT. 2006. The Large Theropod fauna of the Lourinhã Formation and its similarity to that of the Morrison Formation, with a description of a new species of Allosaurus. *Paleontology and Geology of the Upper Jurassic Morrison Formation. New Mexico Museum of Natural History and Science Bulletin*. Albuquerque, NM: New Mexico Museum of Natural History and Science, 123–130.

Matsumoto R, Buffetaut E, Escuillie F, Hervet S, Evans SE. 2013. New material of the choristodere *Lazarussuchus* (Diapsida, Choristodera) from the Paleocene of France. *Journal of Vertebrate Paleontology* 33: 319–339.

Matsumoto R, Dong L, Wang Y, Evans SE. 2019. The first record of a nearly complete choristodere (Reptilia: Diapsida) from the Upper Jurassic of Hebei Province, People's Republic of China. *Journal of Systematic Palaeontology* 17: 1031–1048.

Matsumoto R, Evans SE. 2010. Choristoderes and the freshwater assemblages of Laurasia/Coristoderos y las asociaciones de agua dulce de Laurasia. *Journal of Iberian Geology* 36: 253–274.

Matsumoto R, Evans SE. 2018. The first record of albanerpetontid amphibians (Amphibia: Albanerpetontidae) from East Asia. *PloS one* 13: e0189767.

Matsumoto R, Fujiwara S ichi, Evans SE. 2022a. Feeding behaviour and functional morphology of the neck in the long-snouted aquatic fossil reptile *Champsosaurus* (Reptilia: Diapsida) in comparison with the modern crocodilian Gavialis gangeticus. *Journal of Anatomy* 240: 893–913.

Matsumoto R, Hirayama R, Miyata S, Yoshida M, Mitsuzuka S, Takisawa T, Evans SE. 2022b. The first choristoderan record from the Upper Cretaceous of Asia, Tamagawa Formation, Kuji Group, Japan. *Cretaceous Research* 129: 104999.

Matsumoto R, Suzuki S, Tsogtbaatar K, Evans SE. 2009. New material of the enigmatic reptile *Khurendukhosaurus* (Diapsida: Choristodera) from Mongolia. *Naturwissenschaften* 96: 233–242.

Mazin JM, Billon-Bruyat JP, Pouech J, Hantzpergue P. 2006. The Purbeckian site of Cherves-de-Cognac (Berriasian, Early Cretaceous, southwest France): a continental ecosystem accumulated in an evaporitic littoral depositional environment. *Ninth International Symposium on Mesozoic Terrestrial Ecosystems and Biota, Abstracts and Proceedings*. University of Manchester Manchester, 84–88.

Mazin JM, Pouech J, Hantzpergue P, Lenglet T. 2008. The Purbeckian site of Cherves-de-Cognac (Berriasian, Early Cretaceous, SW France): a first synthesis. *Travaux et Documents des Laboratoires de Géologie de Lyon* 164: 68–71.

McGowan GJ. 1998a. Frontals as diagnostic indicators in fossil albanerpetontid amphibians. *Bulletin of the National Science Museum, Series C (Geology and Paleontology)* 24: 185–194.

McGowan GJ. 1998b. The development and function of the atlanto-axial joint in albanerpetontid amphibians. *Journal of Herpetology* 32: 116–122.

McGowan GJ. **2002**. Albanerpetontid amphibians from the Lower Cretaceous of Spain and Italy: a description and reconsideration of their systematics. *Zoological Journal of the Linnean Society* 135: 1–32.

McGowan GJ, Ensom PC. **1997**. Albanerpetontid amphibians from the Lower Cretaceous of the Isle of Purbeck, Dorset. *Proceedings of the Dorset Natural History and Archaeological Society*.113–117.

McGowan GJ, Evans S. **1995**. Albanerpetontid amphibians from the Cretaceous of Spain. *Nature* 373: 143–145.

McKerrow WS, Johnson RT, Jakobson ME. **1969**. Palaeoecological studies in the Great Oolite at Kirtlington, Oxfordshire. *Palaeontology* 12: 56–83.

Measey JG, Raselimanana A, Herrel A. **2013**. 5. Ecology and Life History of Chameleons. In: Tolley KA, Herrel A, eds. *The Biology of Chameleons*. Berkeley, CA: University of California Press, 85–114.

Melstrom KM, Irmis RB. **2019**. Repeated Evolution of Herbivorous Crocodyliforms during the Age of Dinosaurs. *Current Biology*.

Mey PHW, Nagtegaal PJC, Roberti KJ, Hartevelt JJA. **1968**. Lithostratigraphic subdivision of post-Hercynian deposits in the south-central Pyrenees, Spain. *Leidse geologische mededelingen* 41: 221–228.

von Meyer CEH. **1837**. Mittheilungen, an Professor Bronn gerichtet. *Neues Jahrbuch für Mineralogie, Geognosie, Geologie und Petrefaktenkunde*: 557–562.

Micklich N. **2007**. Crocodiles in Messel—Treasures of the Eocene. *Book to the exhibition 'Messel on Tour'*. Darmstadt: Hessisches Landesmuseum, 72–76.

Miller CV, Pittman M, Wang X, Zheng X, Bright JA. **2023**. Quantitative investigation of pengornithid enantiornithine diet reveals macrocarnivorous ecology evolved in birds by Early Cretaceous. *iScience* 26: 106211.

Miller KG, Sugarman PJ, Browning JV, Kominz MA, Hernández JC, Olsson RK, Wright JD, Feigenson MD, Van Sickel W. 2003. Late Cretaceous chronology of large, rapid sea-level changes: Glacioeustasy during the greenhouse world. *Geology* 31: 585–588.

Milner AR. 2000. Mesozoic and tertiary Caudata and Albanerpetontidae. *Amphibian Biology, Volume 4, Palaeontology: The Evolutionary History of Amphibians*. Chipping Norton: Surrey Beatty & Sons, 1412–1444.

Milner AR, Evans SE. 1991. The Upper Jurassic diapsid *Lisboasaurus estesi*: a maniraptoran theropod. *Palaeontology* 34: 503–513.

Mocho P, Royo-Torres R, Malafaia E, Escaso F, Ortega F. 2016. Systematic review of Late Jurassic sauropods from the Museu Geológico collections (Lisboa, Portugal). *Journal of Iberian Geology* 42: 2.

Mocho P, Royo-Torres R, Malafaia E, Escaso F, Ortega F. 2017. Sauropod tooth morphotypes from the Upper Jurassic of the Lusitanian Basin (Portugal). *Papers in Palaeontology* 3: 259–295.

Mocho P, Royo-Torres R, Ortega F. 2019. A new macronarian sauropod from the Upper Jurassic of Portugal. *Journal of Vertebrate Paleontology*: e1578782.

Mohr B, Schudack ME. 2000. The flora of the Guimarota mine. In: Martin T, Krebs B, eds. *Guimarota: a Jurassic ecosystem*. Munich: Verlag Dr. Friedrich Pfeil, 27–32.

Moore GT, Hayashida DN, Ross CA, Jacobson SR. 1992. Paleoclimate of the Kimmeridgian/Tithonian (Late Jurassic) world: I. Results using a general circulation model. *Palaeogeography, Palaeoclimatology, Palaeoecology* 93: 113–150.

Moreno-Azanza M, Bauluz B, Canudo JI, Puértolas-Pascual E, Sellés AG. 2014. A re-evaluation of aff. Megaloolithidae eggshell fragments from the uppermost Cretaceous of the Pyrenees and implications for crocodylomorph eggshell structure. *Historical Biology* 26: 195–205.

Moreno-Azanza M, Perez-Pueyo M, Puertolas-Pascual E, Nunez-Lahuerta C, Mateus O, Bauluz B, Badenas B, Canudo JI. 2023. A new crocodylomorph related ootaxon from the late Maastrichtian of the Southern Pyrenees (Huesca, Spain). *Historical Biology* 35: 1460–1469.

Müller J. 2004. The relationships among diapsid reptiles and the influence of taxon selection. *Recent advances in the origin and early radiation of vertebrates*: 379–408.

Muñoz JA. 1992. Evolution of a continental collision belt: ECORS-Pyrenees crustal balanced cross-section. In: McClay KR, ed. *Thrust tectonics*. Springer Dordrecht, 235–246.

Murelaga X, Canudo JI. 2005. Descripción de los restos de quelonios del Maastrichtiense superior de Arén y Serraduy (Huesca). *Geogaceta* 38: 51–54.

Myers TS, Tabor NJ, Jacobs LL, Mateus O. 2012. Palaeoclimate of the Late Jurassic of Portugal: comparison with the western United States. *Sedimentology* 59: 1695–1717.

Néraudeau D, Allain R, Ballèvre M, Batten DJ, Buffetaut E, Colin JP, Dabard MP, Daviero-Gomez V, El Albani A, Gomez B. 2012. The Hauterivian–Barremian lignitic bone bed of Angeac (Charente, south-west France): stratigraphical, palaeobiological and palaeogeographical implications. *Cretaceous Research* 37: 1–14.

Nesbitt SJ. 2011. The Early Evolution of Archosaurs: Relationships and the Origin of Major Clades. *Bulletin of the American Museum of Natural History* 2011: 1–292.

Nobre PH, de Souza Carvalho I, de Vasconcellos MF, Souto PR. 2008. Feeding behavior of the gondwanic Crocodylomorpha *Mariliasuchus amarali* from the upper cretaceous Bauru Basin, Brazil. *Gondwana Research* 13: 139–145.

Norell MA, Clark JM. 1990. A reanalysis of *Bernissartia fagesii*, with comments on its phylogenetic position and its bearing on the origin and

diagnosis of the Eusuchia. *Bulletin de l'Institut Royal des Sciences Naturelles de Belgique* 60: 115–128.

Norris RD, Kroon D, Huber BT, Erbacher J. **2001**. Cretaceous-Palaeogene ocean and climate change in the subtropical North Atlantic. *Geological Society, London, Special Publications* 183: 1–22.

Novas FE, Agnolin FL, Lio GL, Rozadilla S, Suárez M, de la Cruz R, de Souza Carvalho I, Rubilar-Rogers D, Isasi MP. **2021**. New transitional fossil from late Jurassic of Chile sheds light on the origin of modern crocodiles. *Scientific Reports* 11: 14960.

Nydam RL. **2013**. Squamates from the Jurassic and Cretaceous of North America. *Palaeobiodiversity and Palaeoenvironments* 93: 535–565.

Oksanen J, Blancher FG, Friendly M, Kindt R, Legendre P, McGlinn D, Minchin PR, O'Hara RB, Simpson GL, Solymos P, Stevens MHH, Szoecs E, Wagner H. **2020**. vegan: Community Ecology Package.

Oms O, Canudo JI. **2004**. Datación magnetoestratigráfica de los dinosaurios del Cretácico terminal (Maastrichtiense superior) de Arén (Huesca, Unidad Surpirenaica Central). *Geo-Temas* 6: 51–54.

Oms O, Fondevilla V, Riera V, Marmi J, Vicens E, Estrada R, Anadón P, Vila B, Galobart À. **2016**. Transitional environments of the lower Maastrichtian South-Pyrenean Basin (Catalonia, Spain): The Fumanya Member tidal flat. *Cretaceous Research* 57: 428–442.

Oreska MP, Carrano MT, Dzikiewicz KM. **2013**. Vertebrate paleontology of the Cloverly Formation (Lower Cretaceous), I: faunal composition, biogeographic relationships, and sampling. *Journal of Vertebrate Paleontology* 33: 264–292.

Ortega F. **2009**. Faunas de répteis do Jurássico Superior de Portugal. *Paleolusitana* 1: 43–56.

Osborn HF. **1903**. The reptilian subclasses Diapsida and Synapsida and the early history of the Diaptosauria. *Memoirs of the American Museum of Natural History* 1: 449–507.

Ősi A, Clark JM, Weishampel DB. **2007**. First report on a new basal eusuchian crocodyliform with multicusped teeth from the Upper Cretaceous (Santonian) of Hungary. *Neues Jahrbuch für Geologie und Paläontologie-Abhandlungen* 243: 169–177.

Owen R. **1879**. Monograph on the fossil Reptilia of the Wealden and Purbeck formations. Supplement No. IX. *Crocodilia (Goniopholis, Brachydectes, Nannosuchus, Theriosuchus and Nuthetes). Monograph of the Palaeontographical Society* 33: 1–15.

Palmer TJ. **1979**. The Hampen Marly and White Limestone formations: Florida-type carbonate lagoons in the Jurassic of central England. *Palaeontology* 22.

Panciroli E, Benson RB, Walsh S, Butler RJ, Castro TA, Jones ME, Evans SE. **2020**. Diverse vertebrate assemblage of the Kilmaluag Formation (Bathonian, Middle Jurassic) of Skye, Scotland. *Earth and Environmental Science Transactions of the Royal Society of Edinburgh* 111: 135–156.

Pardo JD, Small BJ, Huttenlocker AK. **2017**. Stem caecilian from the Triassic of Colorado sheds light on the origins of Lissamphibia. *Proceedings of the National Academy of Sciences* 114: E5389–E5395.

Parrilla-Bel J, Young MT, Moreno-Azanza M, Canudo JI. **2013**. The First Metriorhynchid Crocodylomorph from the Middle Jurassic of Spain, with Implications for Evolution of the Subclade Rhacheosaurini. *PLOS ONE* 8: e54275.

Pereda-Suberbiola X. **2009**. Biogeographical affinities of Late Cretaceous continental tetrapods of Europe: a review. *Bulletin de la Société géologique de France* 180: 57–71.

Pereda-Suberbiola X, Canudo JI, Cruzado-Caballero P, Barco JL, López-Martínez N, Oms O, Ruiz-Omenaca JI. **2009**. The last hadrosaurid

dinosaurs of Europe: a new lambeosaurine from the uppermost Cretaceous of Arén (Huesca, Spain). *Comptes Rendus Palevol* 8: 559–572.

Pérez-García A. **2017**. The Iberian fossil record of turtles: an update. *Journal of Iberian Geology* 43: 155–191.

Pérez-García A, Ortega F. **2011**. *Selenemys lusitanica*, gen. et sp. nov., a new pleurosternid turtle (Testudines: Paracryptodira) from the Upper Jurassic of Portugal. *Journal of Vertebrate Paleontology* 31: 60–69.

Pérez-García A, Ortega F. **2014**. A new species of the turtle *Hylaeochelys* (Eucryptodira) outside its known geographic and stratigraphic ranges of distribution. *Comptes Rendus Palevol* 13: 183–188.

Pérez-García A, Ortega F. **2022**. New finds of the turtle *Plesiochelys* in the Upper Jurassic of Portugal and evaluation of its diversity in the Iberian Peninsula. *Historical Biology* 34: 121–129.

Pérez-Pueyo M. **2023**. Contributions of the Tremp Fm (upper Maastrichtian) in Ribagorza (Aragonese Pyrenees, Huesca) to the knowledge of the finicretaceous vertebrate communities of the Ibero-Armorican island. Unpublished thesis, Universidad de Zaragoza.

Pérez-Pueyo M, Cruzado-Caballero P, Moreno-Azanza M, Vila B, Castanera D, Gasca JM, Puértolas-Pascual E, Bádenas B, Canudo JI. **2021a**. The tetrapod fossil record from the uppermost Maastrichtian of the Ibero-Armorican Island: An integrative review based on the outcrops of the western Tremp Syncline (Aragón, Huesca Province, NE Spain). *Geosciences* 11: 162.

Pérez-Pueyo M, Moreno-Azanza M, Núñez-Lahuerta C, Puértolas-Pascual E, Bádenas B, Canudo JI. **2021b**. Eggshell association of the Late Maastrichtian (Late Cretaceous) at Blasi 2B fossil site: A scrambled of vertebrate diversity. *Ciências da Terra-Procedia* 1: 58–61.

Pintore R, Cornette R, Houssaye A, Allain R. **2023**. Femora from an exceptionally large population of coeval ornithomimosaurs yield evidence of

sexual dimorphism in extinct theropod dinosaurs (N Ibrahim, C Rutz, and M Benton, Eds.). *eLife* 12: e83413.

Piveteau J. **1936**. Origine et évolution morphologique des amphibiens anoures. *Comptes rendus de l'Académie de Sciences* 103: 1084–1086.

Pol D, Rauhut OWM, Lecuona A, Leardi JM, Xu X, Clark JM. **2013**. A new fossil from the Jurassic of Patagonia reveals the early basicranial evolution and the origins of Crocodyliformes. *Biological Reviews* 88: 862–872.

Pouech J, Mazin JM, Billon-Bruyat JP. **2006**. Microvertebrate biodiversity from Cherves-de-Cognac (Lower Cretaceous, Berriasian: Charente, France). *9th [Ninth] Symposium on Mesozoic Terrestrial Ecosystems: short papers*.96–100.

Prasad GV, de Lapparent de Broin F. **2002**. Late Cretaceous crocodile remains from Naskal (India): comparisons and biogeographic affinities. *Annales de Paléontologie* 88: 19–71.

Pritchard AC, Gauthier JA, Hanson M, Bever GS, Bhullar BAS. **2018**. A tiny Triassic saurian from Connecticut and the early evolution of the diapsid feeding apparatus. *Nature Communications* 9: 1213.

Puértolas E, Canudo JI, Cruzado-Caballero P. **2011**. A new crocodylian from the Late Maastrichtian of Spain: implications for the initial radiation of crocodyloids. *PLoS One* 6: e20011.

Puértolas-Pascual E, Aurell M, Bermúdez-Rochas DD, Canudo JI, Fernandes AE, Galobart A, Moreno-Azanza M, Pérez-García A, Castanera D. **2023**. A new vertebrate assemblage from the matute formation of the Cameros Basin (Ágreda, Spain): implications for the diversity during the jurassic/cretaceous boundary. *Journal of Iberian Geology*: 1–21.

Puértolas-Pascual E, Blanco A, Brochu CA, Canudo JI. **2016**. Review of the Late Cretaceous-early Paleogene crocodylomorphs of Europe: Extinction patterns across the K-PG boundary. *Cretaceous Research* 57: 565–590.

Puértolas-Pascual E, Canudo J, Sender L. 2015a. New material from a huge specimen of *Anteophthalmosuchus* cf. *escuchae* (Goniopholididae) from the Albian of Andorra (Teruel, Spain): Phylogenetic implications. *Journal of Iberian Geology* 41: 41–56.

Puértolas-Pascual E, Mateus O. 2020. A three-dimensional skeleton of Goniopholididae from the Late Jurassic of Portugal: implications for the Crocodylomorpha bracing system. *Zoological Journal of the Linnean Society* 189: 521–548.

Puértolas-Pascual E, Rabal-Garcés R, Canudo JI. 2015b. Exceptional crocodylomorph biodiversity of" La Cantalera" site (lower Barremian; Lower Cretaceous) in Teruel, Spain. *Palaeontologia Electronica* 18: 1–16.

Puigdefàbregas C, Muñoz JA, Marzo M. 1986. Thrust belt development in the eastern Pyrenees and related depositional sequences in the southern foreland basin. *Foreland basins*: 229–246.

Rage JC. 2002. The continental Late Cretaceous of Europe: toward a better understanding. *Comptes Rendus Palevol* 1: 257–258.

Rage JC. 2012. Amphibians and squamates in the Eocene of Europe: what do they tell us? *Palaeobiodiversity and Palaeoenvironments* 92: 445–457.

Rage JC. 2013. Mesozoic and Cenozoic squamates of Europe. *Palaeobiodiversity and Palaeoenvironments* 93: 517–534.

Rage JC, Roček Z. 1989. Redescription of *Triadobatrachus massinoti* (Piveteau, 1936) an anuran amphibian from the Early Triasic. *Palaeontographica A* 206: 789–796.

Rasband WS. 2003. Image J. *National Institutes of Health, Bethesda, Maryland, USA*.

Rasmussen ES, Lomholt S, Andersen C, Vejbæk OV. 1998. Aspects of the structural evolution of the Lusitanian Basin in Portugal and the shelf and slope area offshore Portugal. *Tectonophysics* 300: 199–225.

Rauhut OW. **2000**. The dinosaur fauna from the Guimarota mine. In: Martin T, Krebs B, eds. *Guimarota: a Jurassic ecosystem*. Munich: Verlag Dr. Friedrich Pfeil, 75–82.

Rauhut OW. **2001**. Herbivorous dinosaurs from the Late Jurassic (Kimmeridgian) of Guimarota, Portugal. *Proceedings of the Geologists' Association* 112: 273–283.

Rauhut OW. **2003**. A tyrannosauroid dinosaur from the Upper Jurassic of Portugal. *Palaeontology* 46: 903–910.

Rauhut OWM, Fechner R. **2005**. Early development of the facial region in a non-avian theropod dinosaur. *Proceedings of the Royal Society B: Biological Sciences* 272: 1179–1183.

Rauhut OWM, Heyng AM, López-Arbarello A, Hecker A. **2012**. A New Rhynchocephalian from the Late Jurassic of Germany with a Dentition That Is Unique amongst Tetrapods. *PLOS ONE* 7: e46839.

Rees J, Evans SE. **2002**. Amphibian remains from the Lower Cretaceous of Sweden: the first Scandinavian record of the enigmatic group Albanerpetontidae. *GFF* 124: 87–91.

Ribeiro A, Antunes MT, Ferreira MP, Rocha RB, Soares AF, Zbyszewski G, De Almeida FM, De Carvalho D, Monteiro JH. **1979**. *Introduction à la géologie générale du Portugal*. Lisboa: Serviços geológicos de Portugal.

Riera V, Oms O, Gaete R, Galobart À. **2009**. The end-Cretaceous dinosaur succession in Europe: the Tremp Basin record (Spain). *Palaeogeography, Palaeoclimatology, Palaeoecology* 283: 160–171.

Roček Z. **2000**. Mesozoic anurans. *Amphibian Biology. Volume 4. Palaeontology*. Chipping Norton: Surrey Beatty, 1295–1331.

Rogers R, Brady M. **2010**. Origin of microfossil bonebeds: insights from the Upper Cretaceous Judith River Formation of north-central Montana. *Paleobiology* 36: 80–112.

Rogers RR, Carrano MT, Rogers KA, Perez M, Regan AK. 2017. Isotaphonomy in concept and practice: an exploration of vertebrate microfossil bonebeds in the Upper Cretaceous (Campanian) Judith River Formation, north-central Montana. *Paleobiology* 43: 248–273.

Rogers RR, Kidwell SM. 2007. A conceptual framework for the genesis and analysis of vertebrate skeletal concentrations. In: Rogers RR, Eberth DA, Fiorillo AR, eds. *Bonebeds: Genesis, analysis, and paleobiological significance*. Chicago, IL: University of Chicago Press, 1–63.

Rosell J, Linares R, Llompart C. 2001. El "garumniense" prepirenaico. *Revista de la Sociedad Geológica de España* 14: 47–56.

Rotatori FM, Ferrari L, Sequero C, Camilo B, Mateus O, Moreno-Azanza M. 2024. An unexpected early diverging iguanodontian dinosaur (Ornithischia, Ornithopoda) from the Upper Jurassic of Portugal. *Journal of Vertebrate Paleontology*.

Rotatori FM, Moreno-Azanza M, Mateus O. 2020. New information on ornithopod dinosaurs from the Late Jurassic of Portugal. *Acta Palaeontologica Polonica* 65: 35–57.

Rotatori FM, Moreno-Azanza M, Mateus O. 2022. Reappraisal and new material of the holotype of *Draconyx loureiroi* (Ornithischia: Iguanodontia) provide insights on the tempo and modo of evolution of thumb-spiked dinosaurs. *Zoological Journal of the Linnean Society* 195: 125–156.

Ruf I, Luo ZX, Wible JR, Martin T. 2009. Petrosal anatomy and inner ear structures of the Late Jurassic *Henkelotherium* (Mammalia, Cladotheria, Dryolestoidea): insight into the early evolution of the ear region in cladotherian mammals. *Journal of Anatomy* 214: 679–693.

Ruget-Perrot C. 1961. Études stratigraphiques sur le Dogger et le Malm Inférieur de Portugal au Nord du Tage: Bajocien, Bathonien, Callonien, Lusitanien. *Memórias dos Serviços geológicos de Portugal* 7: 1–197.

Russo J, Mateus O. 2021. History of the discovery of the ankylosaur *Dracopelta zbyszewskii* (Upper Jurassic), with new data about the type specimen and its locality. *Comunicações Geológicas* 108: 27–34.

Russo J, Mateus O, Marzola M, Balbino AC. 2017. Two new ootaxa from the late Jurassic: The oldest record of crocodylomorph eggs, from the Lourinhã Formation. *PloS one* 12: 3.

Sahni A. 1972. The vertebrate fauna of the Judith River Formation, Montana. *Bulletin of the American Museum of Natural History*: 321–412.

Salisbury SW. 2002. Crocodilians from the Lower Cretaceous (Berriasian) Purbeck Limestone Group of Dorset, southern England. *Special Papers in Palaeontology* 68: 121–144.

Salisbury SW, Naish D. 2011. Crocodilians. In: Batten DJ, ed. *Palaeontological Association Field Guide to Fossils. English Wealden Fossils*. London: The Palaeontological Association, 305–369.

Salisbury SW, Willis PMA, Peitz S, Sander PM. 1999. The crocodilian Goniopholis simus from the Lower Cretaceous of north-western Germany. *Special Papers in Palaeontology* 60: 121–148.

Sánchez-Hernández B, Benton MJ, Naish D. 2007. Dinosaurs and other fossil vertebrates from the Late Jurassic and Early Cretaceous of the Galve area, NE Spain. *Palaeogeography, Palaeoclimatology, Palaeoecology* 249: 180–215.

Sanchíz B. 1998. Salientia. *Handbuch der Paläontologie*. Munich: Verlag Dr. Friedrich Pfeil, 275.

Sanz-López J, Buscalioni A, Casanovas ML, Santafé JV. 1984. The archosaur fauna from the Upper Jurassic/Lower Cretaceous of Galve (Teruel, Spain). In: Reif DWE, Westphal F, eds. Tübingen: Attempo Verlag, 207–210.

Scheyer TM, Aguilera OA, Delfino M, Fortier DC, Carlini AA, Sánchez R, Carrillo-Briceño JD, Quiroz L, Sánchez-Villagra MR. 2013. Crocodylian

diversity peak and extinction in the late Cenozoic of the northern Neotropics. *Nature communications* 4: 1907.

Scheyer TM, Delfino M. **2016**. The late Miocene caimanine fauna (Crocodylia: alligatoroidea) of the Urumaco Formation, Venezuela. *Palaeontologia Electronica* 19: 1–57.

Schoch RR. **2014**. *Amphibian evolution: the life of early land vertebrates*. Oxford: John Wiley & Sons.

Schoch RR, Sues HD. **2018**. A new lepidosauromorph reptile from the Middle Triassic (Ladinian) of Germany and its phylogenetic relationships. *Journal of Vertebrate Paleontology* 38: e1444619.

Schoch RR, Werneburg R, Voigt S. **2020**. A Triassic stem-salamander from Kyrgyzstan and the origin of salamanders. *Proceedings of the National Academy of Sciences* 117: 11584–11588.

Schudack ME. **1993**. Charophyten aus dem Kimmeridgium der Kohlengrube Guimarota (Portugal). *Mit einer eingehenden Diskussion zur Datierung der Fundstelle. Berliner Geowissenschaftliche Abhandlungen, E* 9: 211–231.

Schudack ME. **2000a**. Geological setting and dating of the Guimarota beds. In: Martin T, Krebs B, eds. *Guimarota: a Jurassic ecosystem*. Munich: Verlag Dr. Friedrich Pfeil, 21–26.

Schudack ME. **2000b**. Ostracodes and charophytes from the Guimarota beds. In: Martin T, Krebs B, eds. *Guimarota: a Jurassic ecosystem*. Munich: Verlag Dr. Friedrich Pfeil, 33–36.

Schudack ME, Turner CE, Peterson F. **1998**. Biostratigraphy, paleoecology and biogeography of charophytes and ostracodes from the Upper Jurassic Morrison Formation, Western Interior, USA. *Modern Geology* 22: 379–414.

Schulte P, Alegret L, Arenillas I, Arz JA, Barton PJ, Bown PR, Bralower TJ, Christeson GL, Claeys P, Cockell CS. **2010**. The Chicxulub asteroid impact and mass extinction at the Cretaceous-Paleogene boundary. *Science* 327: 1214–1218.

Schwarz D. **2002**. A new species of Goniopholis from the Upper Jurassic of Portugal. *Paleontology* 45: 185–208.

Schwarz D, Fechner R. **2004**. *Lusitanisuchus*, *a* new generic name for *Lisboasaurus mitracostatus* (Crocodylomorpha: Mesoeucrocodylia), with *a* description of new remains from the Upper Jurassic (Kimmeridgian) and Lower Cretaceous (Berriasian) of Portugal. *Canadian Journal of Earth Sciences* 41: 1259–1271.

Schwarz D, Fechner R. **2008**. The first dentary of *Lisboasaurus* (Crocodylomorpha, ?Mesoeucrocodylia) from the Lower Cretaceous (Barremian) of Uña, Cuenca Province, Spain. *Journal of Vertebrate Paleontology* 28: 264–268.

Schwarz D, Raddatz M, Wings O. **2017**. *Knoetschkesuchus langenbergensis* gen. nov. sp. nov., *a* new atoposaurid crocodyliform from the Upper Jurassic Langenberg Quarry (Lower Saxony, northwestern Germany), and its relationships to Theriosuchus. *PloS one* 12: 2.

Schwarz D, Salisbury SW. **2005**. A new species of *Theriosuchus* (Atoposauridae, Crocodylomorpha) from the late Jurassic (Kimmeridgian) of Guimarota, Portugal. *Geobios* 38: 779–802.

Schwarz-Wings D, Rees J, Lindgren J. **2009**. Lower cretaceous mesoeucrocodylians from Scandinavia (Denmark and Sweden). *Cretaceous Research* 30: 1345–1355.

Scotese CR. **2014**. The Jurassic and Triassic, Maps 32 - 42, Mollweide Projection.

Seguret M. **1972**. *Étude tectonique des nappes et séries décollées de la partie centrale du versant sud des Pyrénées : caractère synsédimentaire, rôle de la compression et de la gravité*. Montpellier: Publications de l'Université des sciences et techniques du Languedoc (USTELA).

Seiffert J. **1969**. Urodelen-atlas aus dem obersten Bajocien von SE-Aveyron (Südfrankreich). *Paläontologische Zeitschrift* 43: 32–36.

Seiffert J. 1970. Oberjurassische Lazertilier aus der Kohlengrube Guimarota bei Leiria:(Mittelportugal). Unpublished thesis, Freie Universität.

Seiffert J. 1973. Upper Jurassic lizards from Central Portugal. Contribução para o Conhecimento da Fauna do Kimeridgiano da Mina de Lignito Guimarota (Leiria, Portugal) III Parte: V. *Memórias dos Serviços geológicos de Portugal* 22: 7–85.

Seilacher A. 1970. Begriff und Bedeutung der Fossil-Lagerstätten. *Neues Jahrbuch für Geologie und Paläontologie, Monatshefte* 1970: 34–39.

Sellwood BW. 1978. Jurassic. In: McKerrow WS, ed. *The Ecology of Fossils: An Illustrated Guide*. London: Duckworth, 204.

Sereno PC, Larsson HC, Sidor CA, Gado B. 2001. The giant crocodyliform Sarcosuchus from the Cretaceous of Africa. *Science* 294: 1516–1519.

Shotwell JA. 1955. An approach to the paleoecology of mammals. *Ecology* 36: 327–337.

Simoes TR, Caldwell MW, Tałanda M, Bernardi M, Palci A, Vernygora O, Bernardini F, Mancini L, Nydam RL. 2018. The origin of squamates revealed by a Middle Triassic lizard from the Italian Alps. *Nature* 557: 706–709.

Simões TR, Caldwell MW, Tałanda M, Bernardi M, Palci A, Vernygora O, Bernardini F, Mancini L, Nydam RL. 2018. The origin of squamates revealed by a Middle Triassic lizard from the Italian Alps. *Nature* 557: 706–709.

Simões TR, Caldwell MW, Weinschütz LC, Wilner E, Kellner AW. 2017. Mesozoic Lizards from Brazil and Their Role in Early Squamate Evolution in South America. *Journal of Herpetology* 51: 307–315.

Simões TR, Vernygora O, Caldwell MW, Pierce SE. 2020. Megaevolutionary dynamics and the timing of evolutionary innovation in reptiles. *Nature communications* 11: 1–14.

Simões TR, Wilner E, Caldwell MW, Weinschütz LC, Kellner AW. 2015. A stem acrodontan lizard in the Cretaceous of Brazil revises early lizard evolution in Gondwana. *Nature communications* 6.

Skutschas PP. 2007. New specimens of albanerpetontid amphibians from the Upper Cretaceous of Uzbekistan. *Acta Palaeontologica Polonica* 52: 819–821.

Skutschas PP. 2013. Mesozoic salamanders and albanerpetontids of Middle Asia, Kazakhstan, and Siberia. *Palaeobiodiversity and Palaeoenvironments* 93: 441–457.

Skutschas PP. 2014. A relict stem salamander: Evidence from the Early Cretaceous of Siberia. *Acta Palaeontologica Polonica* 61: 119–123.

Skutschas PP, Kolchanov VV, Schwermann AH. 2020. First salamander from the Lower Cretaceous of Germany. *Cretaceous Research* 116: 104606.

Smith T, Codrea VA, Sasaran E, Van Itterbeeck J, Bultynck P, Csiki Z, Dica P, Fărcaş C, Folie A, Garcia G, Godefroit P. 2002. A new exceptional vertebrate site from the Late Cretaceous of the Hateg Basin (Romania). *Studia Universitatis Babes-Bolyai, Geologia*: 321–330.

Smith AB, Gale AS, Monks NEA. 2001. Sea-level change and rock-record bias in the Cretaceous: a problem for extinction and biodiversity studies. *Paleobiology* 27: 241–253.

Smith AG, Smith DG, Funnell BM. 2004. *Atlas of Mesozoic and Cenozoic coastlines*. Cambridge: Cambridge University Press.

Sobral G, Simões TR, Schoch RR. 2020. A tiny new Middle Triassic stem-lepidosauromorph from Germany: implications for the early evolution of lepidosauromorphs and the Vellberg fauna. *Scientific Reports* 10: 2273.

Stampfli GM, Borel GD. 2002. A plate tectonic model for the Paleozoic and Mesozoic constrained by dynamic plate boundaries and restored synthetic oceanic isochrons. *Earth and Planetary Science Letters* 196: 17–33.

Stewart DJ. **1981**. A meander-belt sandstone of the Lower Cretaceous of Southern England. *Sedimentology* 28: 1–20.

Stewart DJ. **1983**. Possible suspended-load channel deposits from the Wealden Group (Lower Cretaceous) of Southern England. In: Collinson JD, Lewin J, eds. *International Association of Sedimentologists*. *Modern and ancient fluvial systems*. Oxford: Blackwell, 369–384.

Sumich JL, Morrissey JF. **2004**. *Introduction to the biology of marine life*. Missisauga, ON: Jones & Bartlett Learning.

Sweetman SC. **2011a**. Vertebrate microfossils. In: Batten DJ, ed. *Palaeontological Association Field Guide to Fossils*. *English Wealden Fossils*. London: The Palaeontological Association, 192–204.

Sweetman SC. **2011b**. The Wealden of the Isle of Wight. *Palaeontological Association Field Guide to Fossils*. *English Wealden Fossils*. London: The Palaeontological Association, 52–78.

Sweetman SC. **2016**. A comparison of Barremian–early Aptian vertebrate assemblages from the Jehol Group, north-east China and the Wealden Group, southern Britain: the value of microvertebrate studies in adverse preservational settings. *Palaeobiodiversity and Palaeoenvironments* 96: 149–167.

Sweetman SC, Gardner JD. **2013**. A new albanerpetontid amphibian from the Barremian (Early Cretaceous) Wessex Formation of the Isle of Wight, southern England. *Acta Palaeontologica Polonica* 58: 295–324.

Sweetman SC, Pedreira-Segade U, Vidovic SU. **2015**. A new bernissartiid crocodyliform from the Lower Cretaceous Wessex Formation (Wealden Group, Barremian) of the Isle of Wight, southern England. *Acta Palaeontologica Polonica* 60: 257–268.

Szentesi Z, Company J. **2017**. Late Maastrichtian small-sized herpetofauna from Valencia province, eastern Spain. *Historical Biology* 29: 43–52.

Szentesi Z, Gardner JD, Venczel M. 2013. Albanerpetontid amphibians from the Late Cretaceous (Santonian) of Iharkút, Hungary, with remarks on regional differences in Late Cretaceous Laurasian amphibian assemblages. *Canadian Journal of Earth Sciences* 50: 268–281.

Taylor AM, Gowland S, Leary S, Keogh KJ, Martinius AW. 2014. Stratigraphical correlation of the Late Jurassic Lourinhã Formation in the Consolação Sub-basin (Lusitanian Basin), Portugal. *Geological Journal* 49: 143–162.

Teixeira C, Camarate França J, Zbyszewski G, Veiga Ferreira O, Manuppella G. 1966. Folha 23-C - Leiria.

Teixell A. 1998. Crustal structure and orogenic material budget in the west central Pyrenees. *Tectonics* 17: 395–406.

Tennant JP, Mannion PD. 2014. Revision of the Late Jurassic crocodyliform *Alligatorellus*, and evidence for allopatric speciation driving high diversity in western European atoposaurids. *PeerJ* 2.

Tennant JP, Mannion PD, Upchurch P. 2016a. Sea level regulated tetrapod diversity dynamics through the Jurassic/Cretaceous interval. *Nature Communications* 7: 12737.

Tennant JP, Mannion PD, Upchurch P. 2016b. Evolutionary relationships and systematics of Atoposauridae (Crocodylomorpha: Neosuchia): implications for the rise of Eusuchia. *Zoological Journal of the Linnean Society* 177: 854–936.

Tennant JP, Mannion PD, Upchurch P, Sutton MD, Price GD. 2017. Biotic and environmental dynamics through the Late Jurassic–Early Cretaceous transition: evidence for protracted faunal and ecological turnover. *Biological Reviews* 92: 776–814.

Thies D, Broschinski A. 2001. Teeth of a small durophagous crocodile from the Late Jurassic (Kimmeridgian) of North Germany. *Geologische Beiträge Hannover* 2: 65–70.

Thies D, Windolf R, Mudroch A. 1997. First record of Atoposauridae (Crocdylia: Metamesosuchia) in the Upper Jurassic (Kimmeridgian) of Northwest Germany. *Neues Jahrbuch fur Geologie und Palaontologie Abhandlungen* 205: 393–411.

Thulborn RA. 1973. Teeth of ornithischian dinosaurs from the Upper Jurassic of Portugal, with description of a hypsilophodontid (Phyllodon henkeli gen. et sp. nov.) from the Guimarota lignite. Contribução para o Conhecimento da Fauna do Kimeridgiano da Mina de Lignito Guimarota (Leiria, Portugal) III Parte: VI. *Memórias dos Serviços geológicos de Portugal* 22: 89–134.

Toljagić O, Butler RJ. 2013. Triassic–Jurassic mass extinction as trigger for the Mesozoic radiation of crocodylomorphs. *Biology Letters* 9: 20130095.

Torices A, Currie PJ, Canudo JI, Pereda-Suberbiola X. 2013. Theropod dinosaurs from the Upper Cretaceous of the South Pyrenees Basin of Spain. *Acta Palaeontologica Polonica* 60: 611–626.

Torices Hernández A, Ruiz Omeñaca JI, Canudo JI, López Martínez N. 2004. Nuevos datos sobre los dinosaurios terópodos (Saurischia: Theropoda) del Cretácico superior de los Pirineos Sur-Centrales (Huesca y Lleida). *Geotemas (Madrid)* 6: 71–74.

Tschopp E, Mateus O, Benson RBJ. 2015. A specimen-level phylogenetic analysis and taxonomic revision of Diplodocidae (Dinosauria, Sauropoda). *PeerJ* 3: e857.

Tucholke BE, Sawyer DS, Sibuet JC. 2007. Breakup of the Newfoundland–Iberia rift. *Imaging, mapping and modelling continental lithosphere extension and breakup*. London: Geological Society of London, 9–46.

Turner AH. 2006. Osteology and phylogeny of a new species of *Araripesuchus* (Crocodyliformes: Mesoeucrocodylia) from the Late Cretaceous of Madagascar. *Historical Biology* 18: 255–369.

Ullmann PV, Varricchio D, Knell MJ. 2012. Taphonomy and taxonomy of a vertebrate microsite in the mid-Cretaceous (Albian-Cenomanian) Blackleaf Formation, southwest Montana. *Historical Biology* 24: 311–328.

Underwood CJ, Rees J. 2002. Selachian faunas from the earliest Cretaceous Purbeck Group of Dorset, southern England. *Special Papers in Palaeontology* 68: 107–19.

Van Erve A, Mohr B. 1988. Palynological investigations of the Late Jurassic microflora from the vertebrate locality Guimarota coal mine (Leiria, Central Portugal). *Neues Jahrbuch für Geologie und Paläontologie-Monatshefte* 1988: 246–262.

Vasile Ş. 2008. A new microvertebrate site from the Upper Cretaceous (Maastrichtian) deposits of the Haţeg Basin. *Sargetia* 21: 5–15.

Vasile Ş, Panaitescu D. 2012. Primele resturi de vertebrate din "mlaştina" Cretacicului terminal de la Pui (Bazinul Haţeg, România). *Lucr. XI Simp. Naţ. Stud. "Geoecologia*: 59–62.

Venczel M, Gardner JD. 2005. The geologically youngest albanerpetontid amphibian, from the lower Pliocene of Hungary. *Palaeontology* 48: 1273–1300.

Venczel M, Gardner JD, Codrea VA, Csiki-Sava Z, Vasile Ş, Solomon AA. 2016. New insights into Europe's most diverse Late Cretaceous anuran assemblage from the Maastrichtian of western Romania. *Palaeobiodiversity and Palaeoenvironments* 96: 61–95.

Venczel M, Vasile Ş, Alexandru A, Csiki-Sava Z. 2013. Additional albanerpetontid remains from the Maastrichtian of Haţeg Basin (Romania). In: Ţabără D, ed. *Ninth Romanian Symposium on Paleontology, Abstract Book. Iaşi, Romania*.92–93.

Vila B, Sellés AG, Brusatte SL. 2016. Diversity and faunal changes in the latest Cretaceous dinosaur communities of southwestern Europe. *Cretaceous Research* 57: 552–564.

Villa A, Blain HA, Delfino M. 2018. The Early Pleistocene herpetofauna of Rivoli Veronese (Northern Italy) as evidence for humid and forested glacial phases in the Gelasian of Southern Alps. *Palaeogeography, Palaeoclimatology, Palaeoecology* 490: 393–403.

Villa A, Montie R, Röper M, Rothgaenger M, Rauhut OWM. 2021. *Sphenofontis velserae* gen. et sp. nov., a new rhynchocephalian from the Late Jurassic of Brunn (Solnhofen Archipelago, southern Germany). *PeerJ* 9: e11363.

Vrielynck B, Dercourt J, Cottereau N. 1996. The Tethys: an Ocean Broken by Seuils Lithospheriques. In: Nairn AEM, Ricou LE, Vrielynck B, Dercourt J, eds. *The Tethys Ocean*. Boston, MA: Springer US, 495–511.

Vullo R, Abit D, Ballevre M, Billon-Bruyat JP, Bourgeais R, Buffetaut E, Daviero-Gomez V, Garcia G, Gomez B, Mazin JM, Morel S, Néraudeau D, Pouech J, Rage JC, Schnyder J, Tong H. 2014. Palaeontology of the Purbeck-type (Tithonian, Late Jurassic) bonebeds of Chassiron (Oléron Island, western France). *Comptes Rendus Palevol* 13: 421–441.

Waldman M, Evans SE. 1994. Lepidosauromorph reptiles from the Middle Jurassic of Skye. *Zoological Journal of the Linnean Society* 112: 135–150.

Wang M, Xing L, Niu K, Liang Q, Evans SE. 2023. A new specimen of the Early Cretaceous long-necked choristodere *Hyphalosaurus* from Liaoning, China with exceptionally-preserved integument. *Cretaceous Research* 144: 105451.

Weishampel DB, Csiki Z, Benton MJ, Grigorescu D, Codrea VA. 2010. Palaeobiogeographic relationships of the Haţeg biota—Between isolation and innovation. *Palaeogeography, Palaeoclimatology, Palaeoecology* 293: 419–437.

Wellnhofer P. 1971. Die Atoposauridae (Crocodylia, Mesosuchia) der Oberjura-Plattenkalke Bayerns. *Palaeontographica Abteilung A*: 133–165.

Wells KD. 2007. *The ecology and behavior of amphibians*. Chicago, IL: University of Chicago press.

Weryński Ł, Błażejowski B. 2023. Late Jurassic teeth of plesiosauroid origin from the Owadów-Brzezinki Lägerstatte, Central Poland. *PeerJ* 11: e15628.

Whetstone KN, Whybrow PJ. 1983. A cursorial crocodilian from the Triassic of Lesotho (Basutoland), South Africa. *Occasional papers of the Museum of Natural History, the University of Kansas* 106: 1–37.

Whiteside DI, Chambi-Trowell SAV, Benton MJ. 2022. A Triassic crown squamate. *Science Advances* 8: eabq8274.

Wick SL. 2021. Albanerpetontids (Lissamphibia, Albanerpetontidae) from the Aguja Formation (lower Campanian) of West Texas, USA. *Canadian Journal of Earth Sciences* 58: 141–149.

Wickham H, Chang W, Henry L, Pedersen TL, Takahashi K, Wilke C, Woo K, Yutani H, Dunnington D. 2021. ggplot2: Create Elegant Data Visualisations Using the Grammar of Graphics.

Wiechman MF, Gloy U. 2000. Pterosaurs and urvogels from the Guimarota mine. In: Martin T, Krebs B, eds. *Guimarota: a Jurassic ecosystem*. Munich: Verlag Dr. Friedrich Pfeil, 83–86.

Wiechmann MF. 2000. The albanerpetontids from the Guimarota mine. In: Martin T, Krebs B, eds. *Guimarota: a Jurassic ecosystem*. Munich: Verlag Dr. Friedrich Pfeil, 51–54.

Wiechmann MF. 2003. Albanerpetontidae (Lissamphibia) aus dem Mesozoikum der Iberischen Halbinsel und dem Neogen von Süddeutschland. Unpublished thesis, Freie Universität Berlin.

Wilberg EW, Turner AH, Brochu CA. 2019. Evolutionary structure and timing of major habitat shifts in Crocodylomorpha. *Scientific reports* 9: 514.

Wilson RC, Hiscott RN, Willis MG, Gradstein FM. 1989. The Lusitanian Basin of West-Central Portugal: Mesozoic and Tertiary Tectonic, Stratigraphic, and Subsidence History. In: Tankard AJ, Balkwill HR, eds. *Extensional tectonics and stratigraphy of the North Atlantic margins. AAPG*

Memoir 46: American Association of Petroleum Geologists. Calgary, AB: Canadian Geological Foundation, 341–361.

Wings O, Schwarz-Wings D, Pfretzschner HU, Martin T. 2010. Overview of Mesozoic crocodylomorphs from the Junggar Basin, Xinjiang, Northwest China, and description of isolated crocodyliform teeth from the Late Jurassic Liuhuanggou locality. *Palaeobiodiversity and Palaeoenvironments* 90: 283–294.

Witts JD, Whittle RJ, Wignall PB, Crame JA, Francis JE, Newton RJ, Bowman VC. 2016. Macrofossil evidence for a rapid and severe Cretaceous–Paleogene mass extinction in Antarctica. *Nature communications* 7: 11738.

Wu XC, Russell AP, Cumbaa SL. 2001. *Terminonaris* (Archosauria: Crocodyliformes): new material from Saskatchewan, Canada, and comments on its phylogenetic relationships. *Journal of Vertebrate Paleontology* 21: 492–514.

Young MT, de Andrade MB. 2009. What is *Geosaurus*? Redescription of *Geosaurus giganteus* (Thalattosuchia: Metriorhynchidae) from the Upper Jurassic of Bayern, Germany. *Zoological Journal of the Linnean Society* 157: 551–585.

Young MT, Bell MA, de Andrade MB, Brusatte SL. 2011. Body size estimation and evolution in metriorhynchid crocodylomorphs: implications for species diversification and niche partitioning. *Zoological Journal of the Linnean Society* 163: 1199–1216.

Young MT, Brusatte SL, Ruta M, de Andrade MB. 2010. The evolution of Metriorhynchoidea (mesoeucrocodylia, thalattosuchia): an integrated approach using geometric morphometrics, analysis of disparity, and biomechanics. *Zoological Journal of the Linnean Society* 158: 801–859.

Young MT, Hua S, Steel L, Foffa D, Brusatte SL, Thüring S, Mateus O, Ruiz-Omeñaca JI, Havlik P, Lepage Y, de Andrade MB. 2014a. Revision of the Late Jurassic teleosaurid genus Machimosaurus (Crocodylomorpha, Thalattosuchia). *Royal Society Open Science* 1: 140222.

Young MT, Hua S, Steel L, Foffa D, Brusatte SL, Thüring S, Mateus O, Ruiz-Omeñaca JI, Havlik P, Lepage Y, De Andrade MB. 2014b. Revision of the Late Jurassic teleosaurid genus *Machimosaurus* (Crocodylomorpha, Thalattosuchia). *Royal Society Open Science* 1: 140222.

Young MT, Tennant JP, Brusatte SL, Challands TJ, Fraser NC, Clark ND, Ross DA. 2016a. The first definitive Middle Jurassic atoposaurid (Crocodylomorpha, Neosuchia), and a discussion on the genus Theriosuchus. *Zoological Journal of the Linnean Society* 176: 443–462.

Young MT, Tennant JP, Brusatte SL, Challands TJ, Fraser NC, Clark NDL, Ross DA. 2016b. The first definitive Middle Jurassic atoposaurid (Crocodylomorpha, Neosuchia), and a discussion on the genus Theriosuchus. *Zoological Journal of the Linnean Society* 176: 443–462.

Zaharia AM. 2011. Reconsiderarea poziţiei stratigrafice a depozitelor din zona General Berthelot–Crăguiş, Bazinul Haţeg. Unpublished thesis, University of Bucharest.

Žák K, Košťák M, Man O, Zakharov VA, Rogov MA, Pruner P, Rohovec J, Dzyuba OS, Mazuch M. 2011. Comparison of carbonate C and O stable isotope records across the Jurassic/Cretaceous boundary in the Tethyan and Boreal Realms. *Palaeogeography, Palaeoclimatology, Palaeoecology* 299: 83–96.

Zinke J. 1998. Small theropod teeth from the Upper Jurassic coal mine of Guimarota (Portugal). *Paläontologische Zeitschrift* 72: 179–189.

Zinke J, Rauhut OW. 1994. Small theropods (Dinosauria, Saurischia) from the Upper Jurassic and Lower Cretaceous of the Iberian Peninsula. *Berliner geowissenschaftliche Abhandlungen (E)* 13: 163–77.

Appendices

A INTRODUCTION

A.1 Specimen list from the Lourinhã Formation

Table A.1: List of the new specimens described from the Lourinhã Formation and now housed in Museu da Lourinhã (ML), at the time of the delivery of the thesis (note that some identifications and descriptions may change later). For more information and possible updates, please contact directly the curators of the museum. Abbreviation: **PB**, Porto das Barcas; **PD**, Porto Dinheiro; **PER**, Peralta; **VAL**, Valmitão; **VALRED**, red layer of Valmitão; **ZIM**, Zimbral.

Specimen number	High taxonomy	Low taxonomy	Genus	Bulk number	Fraction	Item
ML3335	Chondrichthyes	Batoidea		PB-03-19-01	0.5mm	Isolated tooth
ML3336	Chondrichthyes	Batoidea		PB-03-19-01	0.5mm	Isolated tooth
ML3337	Chondrichthyes	Batoidea		PB-03-19-01	1mm	Isolated tooth
ML3338	Chondrichthyes	Batoidea		VAL-06-16-01	0.5mm	Isolated tooth
ML3339	Chondrichthyes	Hybodontiformes	*Hybodus lusitanicus*	PB-10-17-02	0.5mm	Isolated tooth
ML3340	Chondrichthyes	Hybodontiformes	*Hybodus lusitanicus*	PB-06-17-03	0.5mm	Isolated tooth
ML3341	Chondrichthyes	Hybodontiformes	*Hybodus lusitanicus*	PB-06-17-05	0.5mm	Isolated tooth
ML3342	Chondrichthyes	Hybodontiformes		PB-03-19-01	0.5mm	Isolated tooth
ML3343	Chondrichthyes	Hybodontiformes		PB-03-19-01	0.5mm	Isolated tooth

ML3344	Chondrichthyes	Hybodontiformes	*Hybodus lusitanicus*	PB-06-17-03	1mm	Isolated tooth
ML3345	Chondrichthyes	Hybodontiformes	*Hybodus lusitanicus*	PB-06-17-03	1mm	Isolated tooth
ML3346	Chondrichthyes	Hybodontiformes		PD-05-18-01	0.5mm	Isolated tooth
ML3347	Chondrichthyes	Hybodontiformes		PD-05-18-01	0.5mm	Isolated tooth
ML3348	Chondrichthyes	Hybodontiformes		PB-03-19-01	0.5mm	Isolated tooth
ML3349	Chondrichthyes	Hybodontiformes		PB-03-19-01	0.5mm	Isolated tooth
ML3350	Chondrichthyes	Hybodontiformes		PB-03-19-01	0.5mm	Isolated tooth
ML3351	Chondrichthyes	Hybodontiformes		PB-10-17-02	0.5mm	Isolated tooth
ML3352	Chondrichthyes	Hybodontiformes		PB-10-17-02	0.5mm	Isolated tooth
ML3353	Chondrichthyes	Hybodontiformes		PB-10-17-02	0.5mm	Isolated tooth
ML3354	Chondrichthyes	Hybodontiformes		PB-10-17-02	0.5mm	Isolated tooth
ML3355	Chondrichthyes	Hybodontiformes	*Hybodus lusitanicus*	PB-10-17-02	0.5mm	Isolated tooth
ML3356	Chondrichthyes	Hybodontiformes	*Hybodus lusitanicus*	PB-10-17-02	0.5mm	Isolated tooth
ML3357	Chondrichthyes	Hybodontiformes		PB-06-17-01	0.5mm	Isolated tooth
ML3358	Chondrichthyes	Chondrichthyes indet.		ZIM-06-17-04	0.5mm	Scale
ML3359	Chondrichthyes	Chondrichthyes indet.		PB-10-17-02	0.5mm	Scale
ML3360	Chondrichthyes	Chondrichthyes indet.		PB-03-19-01	0.5mm	Scale
ML3361	Actinopterygii	Amiiformes	*Caturus*	PB-03-19-01	0.5mm	Isolated tooth
ML3362	Actinopterygii	Amiiformes	*Caturus*	PB-03-19-01	0.5mm	Isolated tooth
ML3363	Actinopterygii	Amiiformes	*Caturus*	PB-06-17-03	0.5mm	Isolated tooth
ML3364	Actinopterygii	Amiiformes	*Caturus*	VAL-06-16-01	0.5mm	Isolated tooth
ML3365	Actinopterygii	Amiiformes	*Caturus*	VAL-06-16-01	0.5mm	Isolated tooth
ML3366	Actinopterygii	Amiiformes	*Caturus*	ZIM-06-17-01	0.5mm	Isolated tooth
ML3367	Actinopterygii	Amiiformes	*Caturus*	ZIM-06-17-01	0.5mm	Isolated tooth
ML3368	Actinopterygii	Amiiformes	*Caturus*	ZIM-06-17-05	0.5mm	Isolated tooth
ML3369	Actinopterygii	Amiiformes	*Caturus*	ZIM-11-16-01	0.5mm	Isolated tooth
ML3370	Actinopterygii	Amiiformes	*Caturus*	ZIM-11-16-01	0.5mm	Isolated tooth
ML3371	Actinopterygii	Indet. (Macrosemiidae?)		PB-03-19-01	0.5mm	Isolated tooth
ML3372	Actinopterygii	Indet. (Macrosemiidae?)		PB-03-19-01	0.5mm	Isolated tooth
ML3373	Actinopterygii	Indet. (Macrosemiidae?)		PB-06-17-03	0.5mm	Isolated tooth
ML3374	Actinopterygii	Indet. (Macrosemiidae?)		PB-06-17-03	0.5mm	Isolated tooth
ML3375	Actinopterygii	Indet. (Macrosemiidae?)		PB-06-17-03	0.5mm	Isolated tooth

ML3376	Actinopterygii	Indet. (Macrosemiidae?)		ZIM-06-17-04	0.5mm	Isolated tooth
ML3377	Actinopterygii	Indet. (Macrosemiidae?)		ZIM-06-17-06	0.5mm	Isolated tooth
ML3378	Actinopterygii	Indet. (Macrosemiidae?)		PB-10-17-02	0.5mm	Isolated tooth
ML3379	Actinopterygii	Lepisosteiformes	*Lepidotes*	PB-10-17-02	1mm	Isolated tooth
ML3380	Actinopterygii	Lepisosteiformes	*Lepidotes*	PB-03-19-01	1mm	Isolated tooth
ML3381	Actinopterygii	Lepisosteiformes	*Lepidotes*	PB-03-19-01	1mm	Isolated tooth
ML3382	Actinopterygii	Lepisosteiformes	*Lepidotes*	PB-03-19-01	1mm	Isolated tooth
ML3383	Actinopterygii	Lepisosteiformes	*Lepidotes*	PB-03-19-01	1mm	Isolated tooth
ML3384	Actinopterygii	Lepisosteiformes	*Lepidotes*	PB-03-19-01	1mm	Isolated tooth
ML3385	Actinopterygii	Lepisosteiformes	*Lepidotes*	PB-03-19-01	0.5mm	Isolated tooth
ML3386	Actinopterygii	Lepisosteiformes	*Lepidotes*	PB-03-19-01	0.5mm	Isolated tooth
ML3387	Actinopterygii	Lepisosteiformes	*Lepidotes*	PB-03-19-01	0.5mm	Isolated tooth
ML3388	Actinopterygii	Lepisosteiformes	*Lepidotes*	PB-03-19-01	0.5mm	Isolated tooth
ML3389	Actinopterygii	Lepisosteiformes	*Lepidotes*	PB-03-19-01	0.5mm	Isolated tooth
ML3390	Actinopterygii	Lepisosteiformes	*Lepidotes*	PB-03-19-01	0.5mm	Isolated tooth
ML3391	Actinopterygii	Lepisosteiformes	*Lepidotes*	PB-03-19-01	0.5mm	Isolated tooth
ML3392	Actinopterygii	Lepisosteiformes	*Lepidotes*	PB-03-19-01	0.5mm	Isolated tooth
ML3393	Actinopterygii	Lepisosteiformes	*Lepidotes*	PB-03-19-01	0.5mm	Isolated tooth
ML3394	Actinopterygii	Lepisosteiformes	*Lepidotes*	PB-03-19-01	0.5mm	Isolated tooth
ML3395	Actinopterygii	Lepisosteiformes	*Lepidotes*	PB-03-19-01	0.5mm	Isolated tooth
ML3396	Actinopterygii	Lepisosteiformes	*Lepidotes*	PB-03-19-01	0.5mm	Isolated tooth
ML3397	Actinopterygii	Lepisosteiformes	*Lepidotes*	PB-03-19-01	0.5mm	Isolated tooth
ML3398	Actinopterygii	Lepisosteiformes	*Lepidotes*	PB-03-19-01	0.5mm	Isolated tooth
ML3399	Actinopterygii	Lepisosteiformes	*Lepidotes*	PB-03-19-01	0.5mm	Isolated tooth
ML3400	Actinopterygii	Lepisosteiformes	*Lepidotes*	PB-03-19-01	0.5mm	Isolated tooth
ML3401	Actinopterygii	Lepisosteiformes	*Lepidotes*	PB-03-19-01	0.5mm	Isolated tooth
ML3402	Actinopterygii	Lepisosteiformes	*Lepidotes*	PB-06-17-03	0.5mm	Isolated tooth
ML3403	Actinopterygii	Lepisosteiformes	*Lepidotes*	PB-06-17-03	0.5mm	Isolated tooth
ML3404	Actinopterygii	Lepisosteiformes	*Lepidotes*	PB-06-17-03	0.5mm	Isolated tooth
ML3405	Actinopterygii	Lepisosteiformes	*Lepidotes*	PB-06-17-03	0.5mm	Isolated tooth
ML3406	Actinopterygii	Lepisosteiformes	*Lepidotes*	PB-06-17-03	1mm	Isolated tooth
ML3407	Actinopterygii	Lepisosteiformes	*Lepidotes*	PB-06-17-03	1mm	Isolated tooth
ML3408	Actinopterygii	Lepisosteiformes	*Lepidotes*	PB-06-17-05	0.5mm	Isolated tooth

ML3409	Actinopterygii	Lepisosteiformes	*Lepidotes*	PB-10-17-02	0.5mm	Isolated tooth
ML3410	Actinopterygii	Lepisosteiformes	*Lepidotes*	VAL-06-16-01	0.5mm	Isolated tooth
ML3411	Actinopterygii	Lepisosteiformes	*Lepidotes*	ZIM-06-17-01	0.5mm	Isolated tooth
ML3412	Actinopterygii	Lepisosteiformes	*Lepidotes*	ZIM-06-17-01	0.5mm	Isolated tooth
ML3413	Actinopterygii	Lepisosteiformes	*Lepidotes*	ZIM-06-17-01	0.5mm	Isolated tooth
ML3414	Actinopterygii	Lepisosteiformes	*Lepidotes*	ZIM-06-17-01	0.5mm	Isolated tooth
ML3415	Actinopterygii	Lepisosteiformes	*Lepidotes*	ZIM-06-17-01	0.5mm	Isolated tooth
ML3416	Actinopterygii	Lepisosteiformes	*Lepidotes*	ZIM-06-17-01	1mm	Isolated tooth
ML3417	Actinopterygii	Lepisosteiformes	*Lepidotes*	ZIM-06-17-01	2mm	Isolated tooth
ML3418	Actinopterygii	Lepisosteiformes	*Lepidotes*	ZIM-06-17-02	0.5mm	Isolated tooth
ML3419	Actinopterygii	Lepisosteiformes	*Lepidotes*	ZIM-06-17-02	0.5mm	Isolated tooth
ML3420	Actinopterygii	Lepisosteiformes	*Lepidotes*	ZIM-06-17-02	0.5mm	Isolated tooth
ML3421	Actinopterygii	Lepisosteiformes	*Lepidotes*	ZIM-06-17-02	0.5mm	Isolated tooth
ML3422	Actinopterygii	Lepisosteiformes	*Lepidotes*	ZIM-06-17-04	0.5mm	Isolated tooth
ML3423	Actinopterygii	Lepisosteiformes	*Lepidotes*	ZIM-06-17-04	0.5mm	Isolated tooth
ML3424	Actinopterygii	Lepisosteiformes	*Lepidotes*	ZIM-06-17-04	0.5mm	Isolated tooth
ML3425	Actinopterygii	Lepisosteiformes	*Lepidotes*	ZIM-06-17-04	0.5mm	Isolated tooth
ML3426	Actinopterygii	Lepisosteiformes	*Lepidotes*	ZIM-06-17-04	0.5mm	Isolated tooth
ML3427	Actinopterygii	Lepisosteiformes	*Lepidotes*	ZIM-06-17-04	0.5mm	Isolated tooth
ML3428	Actinopterygii	Lepisosteiformes	*Lepidotes*	ZIM-06-17-04	0.5mm	Isolated tooth
ML3429	Actinopterygii	Lepisosteiformes	*Lepidotes*	ZIM-06-17-04	0.5mm	Isolated tooth
ML3430	Actinopterygii	Lepisosteiformes	*Lepidotes*	ZIM-06-17-04	0.5mm	Isolated tooth
ML3431	Actinopterygii	Lepisosteiformes	*Lepidotes*	ZIM-06-17-04	0.5mm	Isolated tooth
ML3432	Actinopterygii	Lepisosteiformes	*Lepidotes*	ZIM-06-17-04	0.5mm	Isolated tooth
ML3433	Actinopterygii	Lepisosteiformes	*Lepidotes*	ZIM-06-17-04	0.5mm	Isolated tooth
ML3434	Actinopterygii	Lepisosteiformes	*Lepidotes*	ZIM-06-17-04	0.5mm	Isolated tooth
ML3435	Actinopterygii	Lepisosteiformes	*Lepidotes*	ZIM-06-17-04	0.5mm	Isolated tooth
ML3436	Actinopterygii	Lepisosteiformes	*Lepidotes*	ZIM-06-17-04	0.5mm	Isolated tooth
ML3437	Actinopterygii	Lepisosteiformes	*Lepidotes*	ZIM-06-17-04	0.5mm	Isolated tooth
ML3438	Actinopterygii	Lepisosteiformes	*Lepidotes*	ZIM-06-17-04	0.5mm	Isolated tooth
ML3439	Actinopterygii	Lepisosteiformes	*Lepidotes*	ZIM-06-17-04	0.5mm	Isolated tooth
ML3440	Actinopterygii	Lepisosteiformes	*Lepidotes*	ZIM-06-17-04	0.5mm	Isolated tooth
ML3441	Actinopterygii	Lepisosteiformes	*Lepidotes*	ZIM-06-17-04	0.5mm	Isolated tooth

ML3442	Actinopterygii	Lepisosteiformes	*Lepidotes*	ZIM-06-17-04	0.5mm	Isolated tooth
ML3443	Actinopterygii	Lepisosteiformes	*Lepidotes*	ZIM-06-17-04	0.5mm	Isolated tooth
ML3444	Actinopterygii	Lepisosteiformes	*Lepidotes*	ZIM-06-17-04	0.5mm	Isolated tooth
ML3445	Actinopterygii	Lepisosteiformes	*Lepidotes*	ZIM-06-17-04	0.5mm	Isolated tooth
ML3446	Actinopterygii	Lepisosteiformes	*Lepidotes*	ZIM-06-17-04	0.5mm	Isolated tooth
ML3447	Actinopterygii	Lepisosteiformes	*Lepidotes*	ZIM-06-17-04	0.5mm	Isolated tooth
ML3448	Actinopterygii	Lepisosteiformes	*Lepidotes*	ZIM-06-17-04	0.5mm	Isolated tooth
ML3449	Actinopterygii	Lepisosteiformes	*Lepidotes*	ZIM-06-17-04	1mm	Isolated tooth
ML3450	Actinopterygii	Lepisosteiformes	*Lepidotes*	ZIM-11-16-01	0.5mm	Isolated tooth
ML3451	Actinopterygii	Lepisosteiformes	*Lepidotes*	ZIM-11-16-01	0.5mm	Isolated tooth
ML3452	Actinopterygii	Lepisosteiformes	*Lepidotes*	ZIM-11-16-01	0.5mm	Isolated tooth
ML3453	Actinopterygii	Lepisosteiformes	*Lepidotes*	ZIM-11-16-01	0.5mm	Isolated tooth
ML3454	Actinopterygii	Lepisosteiformes	*Lepidotes*	ZIM-11-16-02	0.5mm	Isolated tooth
ML3455	Actinopterygii	Lepisosteiformes	*Lepidotes*	ZIM-11-16-02	0.5mm	Isolated tooth
ML3456	Actinopterygii	Lepisosteiformes	*Lepidotes*	ZIM-11-16-02	0.5mm	Isolated tooth
ML3457	Actinopterygii	Lepisosteiformes	*Lepidotes*	ZIM-11-16-02	0.5mm	Isolated tooth
ML3458	Actinopterygii	Lepisosteiformes	*Lepidotes*	ZIM-11-16-02	0.5mm	Isolated tooth
ML3459	Actinopterygii	Lepisosteiformes	*Lepidotes*	ZIM-11-16-02	0.5mm	Isolated tooth
ML3460	Actinopterygii	Lepisosteiformes	*Lepidotes*	ZIM-11-16-02	0.5mm	Isolated tooth
ML3461	Actinopterygii	Pycnodontiformes		PB-03-19-01	0.5mm	Isolated tooth
ML3462	Actinopterygii	Pycnodontiformes		PB-03-19-01	0.5mm	Isolated tooth
ML3463	Actinopterygii	Pycnodontiformes		PB-03-19-01	0.5mm	Isolated tooth
ML3464	Actinopterygii	Pycnodontiformes		PB-03-19-01	0.5mm	Isolated tooth
ML3465	Actinopterygii	Pycnodontiformes		PB-03-19-01	1mm	Isolated tooth
ML3466	Actinopterygii	Pycnodontiformes		PB-06-17-03	0.5mm	Isolated tooth
ML3467	Actinopterygii	Pycnodontiformes		PB-06-17-04	1mm	Isolated tooth
ML3468	Actinopterygii	Pycnodontiformes		ZIM-06-17-04	0.5mm	Isolated tooth
ML3469	Actinopterygii	Pycnodontiformes		ZIM-06-17-04	0.5mm	Isolated tooth
ML3470	Actinopterygii	Pycnodontiformes		ZIM-11-16-02	0.5mm	Isolated tooth
ML3471	Actinopterygii	Actinopterygii indet.		ZIM-11-16-02	1mm	Vertebra
ML3472	Actinopterygii	Actinopterygii indet.		ZIM-06-17-01	1mm	Vertebra
ML3473	Actinopterygii	Actinopterygii indet.		ZIM-06-17-01	1mm	Vertebra
ML3474	Actinopterygii	Actinopterygii indet.		ZIM-06-17-01	1mm	Vertebra

ML3475	Actinopterygii	Actinopterygii indet.		ZIM-06-17-01	0.5mm	Vertebra
ML3476	Actinopterygii	Actinopterygii indet.		ZIM-06-17-01	0.5mm	Vertebra
ML3477	Actinopterygii	Actinopterygii indet.		PB-10-17-02	1mm	Vertebra
ML3478	Actinopterygii	Actinopterygii indet.		PB-10-17-02	0.5mm	Vertebra
ML3479	Actinopterygii	Actinopterygii indet.		PB-10-17-02	0.5mm	Vertebra
ML3480	Actinopterygii	Actinopterygii indet.		PB-10-17-02	0.5mm	Vertebra
ML3481	Actinopterygii	Actinopterygii indet.		PB-06-17-01	0.5mm	Vertebra
ML3482	Actinopterygii	Actinopterygii indet.		VAL-10-17-01	0.5mm	Vertebra
ML3483	Actinopterygii	Actinopterygii indet.		VAL-06-16-01	0.5mm	Vertebra
ML3484	Actinopterygii	Actinopterygii indet.		VAL-06-16-01	0.5mm	Vertebra
ML3485	Actinopterygii	Actinopterygii indet.		VAL-06-16-01	0.5mm	Vertebra
ML3486	Actinopterygii	Actinopterygii indet.		VAL-06-16-01	0.5mm	Vertebra
ML3487	Actinopterygii	Actinopterygii indet.		VAL-06-16-01	0.5mm	Vertebra
ML3488	Actinopterygii	Actinopterygii indet.		VAL-06-16-01	0.5mm	Vertebra
ML3489	Actinopterygii	Actinopterygii indet.		VAL-06-16-01	0.5mm	Vertebra
ML3490	Actinopterygii	Actinopterygii indet.		VAL-06-16-01	0.5mm	Vertebra
ML3491	Actinopterygii	Actinopterygii indet.		VAL-06-16-01	0.5mm	Vertebra
ML3492	Actinopterygii	Actinopterygii indet.		VAL-06-16-01	0.5mm	Vertebra
ML3493	Actinopterygii	Actinopterygii indet.		VAL-06-16-01	0.5mm	Vertebra
ML3494	Actinopterygii	Actinopterygii indet.		VAL-06-16-01	0.5mm	Vertebra
ML3495	Actinopterygii	Actinopterygii indet.		VAL-06-16-01	0.5mm	Vertebra
ML3496	Actinopterygii	Actinopterygii indet.		VAL-06-16-01	0.5mm	Vertebra
ML3497	Actinopterygii	Actinopterygii indet.		VAL-06-16-01	0.5mm	Vertebra
ML3498	Actinopterygii	Actinopterygii indet.		VAL-06-16-01	0.5mm	Vertebra
ML3499	Actinopterygii	Actinopterygii indet.		ZIM-06-17-02	1mm	Vertebra
ML3500	Actinopterygii	Actinopterygii indet.		ZIM-06-17-04	1mm	Vertebra
ML3501	Actinopterygii	Actinopterygii indet.		ZIM-06-17-04	1mm	Vertebra
ML3502	Actinopterygii	Actinopterygii indet.		ZIM-06-17-04	1mm	Vertebra
ML3503	Actinopterygii	Actinopterygii indet.		ZIM-06-17-04	1mm	Vertebra
ML3504	Actinopterygii	Actinopterygii indet.		ZIM-06-17-04	1mm	Vertebra
ML3505	Actinopterygii	Actinopterygii indet.		ZIM-06-17-04	1mm	Vertebra
ML3506	Actinopterygii	Actinopterygii indet.		ZIM-06-17-04	1mm	Vertebra
ML3507	Actinopterygii	Actinopterygii indet.		ZIM-06-17-04	1mm	Vertebra

ML3508	Actinopterygii	Actinopterygii indet.		ZIM-06-17-04	1mm	Vertebra
ML3509	Actinopterygii	Actinopterygii indet.		ZIM-06-17-04	1mm	Vertebra
ML3510	Actinopterygii	Actinopterygii indet.		ZIM-06-17-04	1mm	Vertebra
ML3511	Actinopterygii	Actinopterygii indet.		ZIM-06-17-04	1mm	Vertebra
ML3512	Actinopterygii	Actinopterygii indet.		ZIM-06-17-04	1mm	Vertebra
ML3513	Actinopterygii	Actinopterygii indet.		ZIM-06-17-04	1mm	Vertebra
ML3514	Actinopterygii	Actinopterygii indet.		ZIM-06-17-04	1mm	Vertebra
ML3515	Actinopterygii	Actinopterygii indet.		ZIM-06-17-04	1mm	Vertebra
ML3516	Actinopterygii	Actinopterygii indet.		ZIM-06-17-04	0.5mm	Vertebra
ML3517	Actinopterygii	Actinopterygii indet.		ZIM-06-17-04	0.5mm	Vertebra
ML3518	Actinopterygii	Actinopterygii indet.		ZIM-06-17-04	0.5mm	Vertebra
ML3519	Actinopterygii	Actinopterygii indet.		ZIM-06-17-04	0.5mm	Vertebra
ML3520	Actinopterygii	Actinopterygii indet.		ZIM-06-17-04	0.5mm	Vertebra
ML3521	Actinopterygii	Actinopterygii indet.		ZIM-06-17-04	0.5mm	Vertebra
ML3522	Actinopterygii	Actinopterygii indet.		ZIM-06-17-04	0.5mm	Vertebra
ML3523	Actinopterygii	Actinopterygii indet.		ZIM-06-17-04	0.5mm	Vertebra
ML3524	Actinopterygii	Actinopterygii indet.		ZIM-06-17-04	0.5mm	Vertebra
ML3525	Actinopterygii	Actinopterygii indet.		ZIM-06-17-04	0.5mm	Vertebra
ML3526	Actinopterygii	Actinopterygii indet.		ZIM-06-17-04	0.5mm	Vertebra
ML3527	Actinopterygii	Actinopterygii indet.		ZIM-06-17-04	0.5mm	Vertebra
ML3528	Actinopterygii	Actinopterygii indet.		ZIM-06-17-04	0.5mm	Vertebra
ML3529	Actinopterygii	Actinopterygii indet.		ZIM-11-16-01	0.5mm	Vertebra
ML3530	Actinopterygii	Actinopterygii indet.		ZIM-11-16-01	1mm	Vertebra
ML3531	Actinopterygii	Actinopterygii indet.		ZIM-11-16-01	1mm	Vertebra
ML3532	Actinopterygii	Actinopterygii indet.		ZIM-11-16-01	1mm	Vertebra
ML3533	Actinopterygii	Actinopterygii indet.		PB-06-17-03	1mm	Vertebra
ML3534	Actinopterygii	Actinopterygii indet.		PB-06-17-03	1mm	Vertebra
ML3535	Actinopterygii	Actinopterygii indet.		PB-06-17-03	1mm	Vertebra
ML3536	Actinopterygii	Actinopterygii indet.		PB-06-17-04	1mm	Vertebra
ML3537	Actinopterygii	Actinopterygii indet.		PB-03-19-01	0.5mm	Vertebra
ML3538	Actinopterygii	Actinopterygii indet.		PB-03-19-01	0.5mm	Vertebra
ML3539	Actinopterygii	Actinopterygii indet.		PB-03-19-01	0.5mm	Vertebra
ML3540	Actinopterygii	Actinopterygii indet.		PB-03-19-01	0.5mm	Vertebra

ML3541	Actinopterygii	Actinopterygii indet.		PB-03-19-01	0.5mm	Vertebra
ML3542	Actinopterygii	Actinopterygii indet.		PB-03-19-01	0.5mm	Vertebra
ML3543	Actinopterygii	Actinopterygii indet.		PB-03-19-01	1mm	Vertebra
ML3544	Actinopterygii	Actinopterygii indet.		PB-06-17-01	0.5mm	Jaw
ML3545	Actinopterygii	Actinopterygii indet.		PB-06-17-01	0.5mm	Jaw
ML3546	Actinopterygii	Actinopterygii indet.		PB-06-17-03	0.5mm	Jaw
ML3547	Actinopterygii	Actinopterygii indet.		PB-06-17-03	0.5mm	Jaw
ML3548	Actinopterygii	Actinopterygii indet.		PB-06-17-03	0.5mm	Jaw
ML3549	Actinopterygii	Actinopterygii indet.		PB-06-17-03	0.5mm	Jaw
ML3550	Actinopterygii	Actinopterygii indet.		PB-06-17-03	0.5mm	Jaw
ML3551	Actinopterygii	Actinopterygii indet.		PB-06-17-05	0.5mm	Jaw
ML3552	Actinopterygii	Actinopterygii indet.		VAL-06-16-01	0.5mm	Jaw
ML3553	Actinopterygii	Actinopterygii indet.		ZIM-06-17-01	0.5mm	Jaw
ML3554	Actinopterygii	Actinopterygii indet.		ZIM-06-17-02	0.5mm	Jaw
ML3555	Actinopterygii	Actinopterygii indet.		ZIM-06-17-02	0.5mm	Jaw
ML3556	Actinopterygii	Actinopterygii indet.		ZIM-06-17-02	0.5mm	Jaw
ML3557	Actinopterygii	Actinopterygii indet.		ZIM-06-17-04	0.5mm	Jaw
ML3558	Actinopterygii	Actinopterygii indet.		ZIM-06-17-04	0.5mm	Jaw
ML3559	Actinopterygii	Actinopterygii indet.		ZIM-06-17-04	0.5mm	Jaw
ML3560	Actinopterygii	Actinopterygii indet.		ZIM-06-17-04	0.5mm	Jaw
ML3561	Actinopterygii	Actinopterygii indet.		ZIM-06-17-04	0.5mm	Jaw
ML3562	Actinopterygii	Actinopterygii indet.		ZIM-11-16-01	0.5mm	Jaw
ML3563	Actinopterygii	Actinopterygii indet.		ZIM-11-16-01	0.5mm	Jaw
ML3564	Actinopterygii	Actinopterygii indet.		PB-06-17-03	0.5mm	Palatal bone
ML3565	Actinopterygii	Actinopterygii indet.		VAL-06-16-01	0.5mm	Palatal bone
ML3566	Actinopterygii	Actinopterygii indet.		VAL-06-16-01	0.5mm	Palatal bone
ML3567	Actinopterygii	Actinopterygii indet.		VAL-06-16-01	0.5mm	Palatal bone
ML3568	Actinopterygii	Actinopterygii indet.		ZIM-06-17-01	0.5mm	Palatal bone
ML3569	Actinopterygii	Actinopterygii indet.		ZIM-06-17-02	0.5mm	Palatal bone
ML3570	Actinopterygii	Actinopterygii indet.		ZIM-06-17-04	0.5mm	Palatal bone
ML3571	Actinopterygii	Actinopterygii indet.		ZIM-06-17-04	0.5mm	Palatal bone
ML3572	Actinopterygii	Actinopterygii indet.		ZIM-06-17-04	0.5mm	Palatal bone
ML3573	Actinopterygii	Actinopterygii indet.		ZIM-06-17-04	0.5mm	Palatal bone

ML3574	Actinopterygii	Actinopterygii indet.		ZIM-06-17-04	0.5mm	Palatal bone
ML3575	Actinopterygii	Actinopterygii indet.		ZIM-06-17-04	0.5mm	Palatal bone
ML3576	Actinopterygii	Actinopterygii indet.		ZIM-06-17-04	0.5mm	Palatal bone
ML3577	Actinopterygii	Actinopterygii indet.		ZIM-06-17-04	0.5mm	Palatal bone
ML3578	Actinopterygii	Actinopterygii indet.		ZIM-06-17-04	0.5mm	Palatal bone
ML3579	Actinopterygii	Actinopterygii indet.		ZIM-06-17-04	0.5mm	Palatal bone
ML3580	Actinopterygii	Actinopterygii indet.		ZIM-06-17-04	0.5mm	Palatal bone
ML3581	Actinopterygii	Actinopterygii indet.		ZIM-11-16-01	1mm	Palatal bone
ML3582	Actinopterygii	Actinopterygii indet.		ZIM-11-16-02	0.5mm	Palatal bone
ML3583	Actinopterygii	Actinopterygii indet.		PD-05-18-01	0.5mm	Fish scales
ML3584	Actinopterygii	Actinopterygii indet.		PB-06-17-04	1mm	Fish scales
ML3585	Actinopterygii	Actinopterygii indet.		PB-06-17-04	0.5mm	Fish scales
ML3586	Actinopterygii	Actinopterygii indet.		PB-06-17-03	1mm	Fish scales
ML3587	Actinopterygii	Actinopterygii indet.		PB-06-17-03	0.5mm	Fish scales
ML3588	Actinopterygii	Actinopterygii indet.		PB-06-17-01	0.5mm	Fish scales
ML3589	Actinopterygii	Actinopterygii indet.		PB-06-17-05	1mm	Fish scales
ML3590	Actinopterygii	Actinopterygii indet.		PB-06-17-05	0.5mm	Fish scales
ML3591	Actinopterygii	Actinopterygii indet.		PB-03-19-01	1mm	Fish scales
ML3592	Actinopterygii	Actinopterygii indet.		PB-03-19-01	0.5mm	Fish scales
ML3593	Actinopterygii	Actinopterygii indet.		PB-10-17-02	2mm	Fish scales
ML3594	Actinopterygii	Actinopterygii indet.		PB-10-17-02	1mm	Fish scales
ML3595	Actinopterygii	Actinopterygii indet.		PB-10-17-02	0.5mm	Fish scales
ML3596	Actinopterygii	Actinopterygii indet.		PB-10-17-02	0.5mm	Fish scales
ML3597	Actinopterygii	Actinopterygii indet.		ZIM-06-17-04	1mm	Fish scales
ML3598	Actinopterygii	Actinopterygii indet.		ZIM-06-17-04	0.5mm	Fish scales
ML3599	Actinopterygii	Actinopterygii indet.		ZIM-11-16-01	1mm	Fish scales
ML3600	Actinopterygii	Actinopterygii indet.		ZIM-11-16-01	0.5mm	Fish scales
ML3601	Actinopterygii	Actinopterygii indet.		ZIM-06-17-01	0.5mm	Fish scales
ML3602	Actinopterygii	Actinopterygii indet.		ZIM-06-17-01	0.5mm	Fish scales
ML3603	Actinopterygii	Actinopterygii indet.		ZIM-06-17-01	1mm	Fish scales
ML3604	Actinopterygii	Actinopterygii indet.		ZIM-06-17-02	0.5mm	Fish scales
ML3605	Actinopterygii	Actinopterygii indet.		ZIM-06-17-02	1mm	Fish scales
ML3606	Actinopterygii	Actinopterygii indet.		ZIM-11-16-02	0.5mm	Fish scales

ML3607	Actinopterygii	Actinopterygii indet.		VAL-03-19-04	0.5mm	Fish scales
ML3608	Actinopterygii	Actinopterygii indet.		VAL-03-19-04	1mm	Fish scales
ML3609	Actinopterygii	Actinopterygii indet.		VAL-03-19-10	0.5mm	Fish scales
ML3610	Actinopterygii	Actinopterygii indet.		VAL-03-19-03	1mm	Fish scales
ML3611	Actinopterygii	Actinopterygii indet.		VAL-03-19-07	0.5mm	Fish scales
ML3612	Actinopterygii	Actinopterygii indet.		VAL-10-17-01	2mm	Fish scales
ML3613	Actinopterygii	Actinopterygii indet.		VAL-10-17-01	1mm	Fish scales
ML3614	Actinopterygii	Actinopterygii indet.		VAL-10-17-01	0.5mm	Fish scales
ML3615	Actinopterygii	Actinopterygii indet.		VAL-06-16-01	1mm	Fish scales
ML3616	Actinopterygii	Actinopterygii indet.		VAL-06-16-01	0.5mm	Fish scales
ML2738	Lissamphibia	Albanerpetontidae	New unnamed taxon 2	VAL-06-16-01	0.5mm	Frontal
ML2739	Lissamphibia	Albanerpetontidae	New unnamed taxon 2	VAL-06-16-01	0.5mm	Frontal
ML2740	Lissamphibia	Albanerpetontidae	New unnamed taxon 2	VAL-06-16-01	0.5mm	Frontal
ML2741	Lissamphibia	Albanerpetontidae	New unnamed taxon 2	VAL-06-16-01	0.5mm	Frontal
ML2742	Lissamphibia	Albanerpetontidae	New unnamed taxon 2	PB-10-17-02	0.5mm	Frontal
ML2743	Lissamphibia	Albanerpetontidae	New unnamed taxon 2	VAL-03-19-05	0.5mm	Frontal
ML2744	Lissamphibia	Albanerpetontidae	New unnamed taxon 2	VAL-06-16-01	0.5mm	Frontal
ML2745	Lissamphibia	Albanerpetontidae	New unnamed taxon 2	VAL-06-16-01	0.5mm	Frontal
ML2746	Lissamphibia	Albanerpetontidae	New unnamed taxon 2	VAL-06-16-01	0.5mm	Frontal
ML2747	Lissamphibia	Albanerpetontidae	New unnamed taxon 2	VAL-06-16-01	0.5mm	Frontal
ML2748	Lissamphibia	Albanerpetontidae	New unnamed taxon 2	VAL-06-16-01	0.5mm	Frontal
ML2749	Lissamphibia	Albanerpetontidae	New unnamed taxon 2	VAL-06-16-01	0.5mm	Frontal
ML2751	Lissamphibia	Albanerpetontidae	New unnamed taxon 2	VAL-06-16-01	0.5mm	Frontal
ML2752	Lissamphibia	Albanerpetontidae	New unnamed taxon 2	VAL-06-16-01	0.5mm	Frontal
ML2753	Lissamphibia	Albanerpetontidae	New unnamed taxon 2	VAL-06-16-01	0.5mm	Frontal
ML2754	Lissamphibia	Albanerpetontidae	New unnamed taxon 2	VAL-06-16-01	0.5mm	Frontal
ML2755	Lissamphibia	Albanerpetontidae	New unnamed taxon 2	VAL-06-16-01	0.5mm	Frontal
ML2756	Lissamphibia	Albanerpetontidae	New unnamed taxon 2	VAL-06-16-01	0.5mm	Frontal
ML2757	Lissamphibia	Albanerpetontidae	New unnamed taxon 2	VAL-06-16-01	0.5mm	Frontal
ML2758	Lissamphibia	Albanerpetontidae	New unnamed taxon 2	ZIM-11-16-01	1mm	Frontal
ML2759	Lissamphibia	Albanerpetontidae	New unnamed taxon 2	ZIM-11-16-02	0.5mm	Frontal
ML2760	Lissamphibia	Albanerpetontidae	New unnamed taxon 2	ZIM-06-17-02	0.5mm	Frontal

ML2761	Lissamphibia	Albanerpetontidae	New unnamed taxon 2	ZIM-06-17-01	0.5mm	Frontal
ML2762	Lissamphibia	Albanerpetontidae	New unnamed taxon 2	ZIM-06-17-01	0.5mm	Frontal
ML2763	Lissamphibia	Albanerpetontidae	New unnamed taxon 2	ZIM-06-17-01	0.5mm	Frontal
ML2764	Lissamphibia	Albanerpetontidae	New unnamed taxon 2	ZIM-06-17-01	0.5mm	Frontal
ML2765	Lissamphibia	Albanerpetontidae	New unnamed taxon 2	ZIM-06-17-08	0.5mm	Frontal
ML2766	Lissamphibia	Albanerpetontidae	New unnamed taxon 2	ZIM-06-17-08	0.5mm	Frontal
ML2767	Lissamphibia	Albanerpetontidae	New unnamed taxon 2	VAL-06-16-01	0.5mm	Frontal
ML2768	Lissamphibia	Albanerpetontidae	New unnamed taxon 2	VAL-06-16-01	0.5mm	Frontal
ML2769	Lissamphibia	Albanerpetontidae	New unnamed taxon 2	VAL-06-16-01	0.5mm	Frontal
ML2770	Lissamphibia	Albanerpetontidae	New unnamed taxon 2	VAL-06-16-01	0.5mm	Frontal
ML2771	Lissamphibia	Albanerpetontidae	New unnamed taxon 2	VAL-06-16-01	0.5mm	Frontal
ML2772	Lissamphibia	Albanerpetontidae	New unnamed taxon 2	VAL-06-16-01	0.5mm	Frontal
ML2901	Lissamphibia	Albanerpetontidae	New unnamed taxon 2	VAL-06-16-01	0.5mm	Frontal
ML2902	Lissamphibia	Albanerpetontidae	New unnamed taxon 2	VAL-06-16-01	0.5mm	Frontal
ML2903	Lissamphibia	Albanerpetontidae	New unnamed taxon 2	VAL-06-16-01	0.5mm	Frontal
ML2904	Lissamphibia	Albanerpetontidae	New unnamed taxon 2	VAL-06-16-01	0.5mm	Frontal
ML2905	Lissamphibia	Albanerpetontidae	New unnamed taxon 2	VAL-06-16-01	0.5mm	Frontal
ML2906	Lissamphibia	Albanerpetontidae	New unnamed taxon 2	VAL-06-16-01	0.5mm	Frontal
ML2907	Lissamphibia	Albanerpetontidae	New unnamed taxon 2	VAL-10-17-01	0.5mm	Frontal
ML2908	Lissamphibia	Albanerpetontidae	New unnamed taxon 2	VAL-10-17-01	0.5mm	Frontal
ML2909	Lissamphibia	Albanerpetontidae	New unnamed taxon 2	VAL-03-19-05	0.5mm	Frontal
ML2910	Lissamphibia	Albanerpetontidae	New unnamed taxon 2	VAL-10-17-01	0.5mm	Frontal
ML2911	Lissamphibia	Albanerpetontidae	New unnamed taxon 2	VAL-03-19-03	0.5mm	Frontal
ML2912	Lissamphibia	Albanerpetontidae	New unnamed taxon 2	VAL-06-16-01	0.5mm	Premaxilla
ML2913	Lissamphibia	Albanerpetontidae	New unnamed taxon 2	VAL-06-16-01	0.5mm	Premaxilla
ML2914	Lissamphibia	Albanerpetontidae	New unnamed taxon 2	VAL-06-16-01	0.5mm	Premaxilla
ML2915	Lissamphibia	Albanerpetontidae	New unnamed taxon 2	VAL-06-16-01	0.5mm	Premaxilla
ML2916	Lissamphibia	Albanerpetontidae	New unnamed taxon 2	VAL-06-16-01	0.5mm	Premaxilla
ML2917	Lissamphibia	Albanerpetontidae	New unnamed taxon 2	VAL-06-16-01	0.5mm	Premaxilla
ML2918	Lissamphibia	Albanerpetontidae	New unnamed taxon 2	VAL-06-16-01	0.5mm	Premaxilla
ML2919	Lissamphibia	Albanerpetontidae	New unnamed taxon 2	VAL-06-16-01	0.5mm	Premaxilla
ML2920	Lissamphibia	Albanerpetontidae	New unnamed taxon 2	VAL-06-16-01	0.5mm	Premaxilla
ML2921	Lissamphibia	Albanerpetontidae	New unnamed taxon 2	VAL-06-16-01	0.5mm	Premaxilla

ML2922	Lissamphibia	Albanerpetontidae	New unnamed taxon 2	VAL-06-16-01	0.5mm	Premaxilla
ML2923	Lissamphibia	Albanerpetontidae	New unnamed taxon 2	VAL-06-16-01	0.5mm	Premaxilla
ML2924	Lissamphibia	Albanerpetontidae	New unnamed taxon 2	VAL-06-16-01	0.5mm	Premaxilla
ML2925	Lissamphibia	Albanerpetontidae	New unnamed taxon 2	VAL-06-16-01	0.5mm	Premaxilla
ML2926	Lissamphibia	Albanerpetontidae	New unnamed taxon 2	VAL-06-16-01	0.5mm	Premaxilla
ML2927	Lissamphibia	Albanerpetontidae	New unnamed taxon 2	VAL-06-16-01	0.5mm	Premaxilla
ML2928	Lissamphibia	Albanerpetontidae	New unnamed taxon 2	VAL-06-16-01	0.5mm	Premaxilla
ML2929	Lissamphibia	Albanerpetontidae	New unnamed taxon 2	VAL-03-19-01	0.5mm	Premaxilla
ML2930	Lissamphibia	Albanerpetontidae	New unnamed taxon 2	VAL-03-19-01	0.5mm	Premaxilla
ML2931	Lissamphibia	Albanerpetontidae	New unnamed taxon 2	VAL-03-19-01	0.5mm	Premaxilla
ML2932	Lissamphibia	Albanerpetontidae	New unnamed taxon 2	ZIM-11-16-01	0.5mm	Premaxilla
ML2933	Lissamphibia	Albanerpetontidae	New unnamed taxon 2	ZIM-11-16-01	0.5mm	Premaxilla
ML2934	Lissamphibia	Albanerpetontidae	New unnamed taxon 2	VAL-03-19-07	0.5mm	Premaxilla
ML2935	Lissamphibia	Albanerpetontidae	New unnamed taxon 2	VAL-06-16-01	0.5mm	Premaxilla
ML2936	Lissamphibia	Albanerpetontidae	New unnamed taxon 2	VAL-06-16-01	0.5mm	Premaxilla
ML2937	Lissamphibia	Albanerpetontidae	New unnamed taxon 2	VAL-06-18-01	0.5mm	Maxilla
ML2938	Lissamphibia	Albanerpetontidae	New unnamed taxon 2	ZIM-06-17-02	0.5mm	Maxilla
ML2939	Lissamphibia	Albanerpetontidae	New unnamed taxon 2	VAL-06-16-01	0.5mm	Maxilla
ML2940	Lissamphibia	Albanerpetontidae	New unnamed taxon 2	VAL-06-16-01	0.5mm	Maxilla
ML2941	Lissamphibia	Albanerpetontidae	New unnamed taxon 2	ZIM-06-17-02	0.5mm	Maxilla
ML2942	Lissamphibia	Albanerpetontidae	New unnamed taxon 2	VAL-03-19-01	0.5mm	Maxilla
ML2943	Lissamphibia	Albanerpetontidae	New unnamed taxon 2	PB-06-17-05	0.5mm	Maxilla
ML2944	Lissamphibia	Albanerpetontidae	New unnamed taxon 2	VAL-06-16-01	0.5mm	Maxilla
ML2945	Lissamphibia	Albanerpetontidae	New unnamed taxon 2	VAL-06-16-01	0.5mm	Maxilla
ML2946	Lissamphibia	Albanerpetontidae	New unnamed taxon 2	VAL-06-16-01	0.5mm	Maxilla
ML2947	Lissamphibia	Albanerpetontidae	New unnamed taxon 2	VAL-10-17-01	0.5mm	Lacrymal
ML2948	Lissamphibia	Albanerpetontidae	New unnamed taxon 2	VAL-10-17-01	0.5mm	Lacrymal
ML2949	Lissamphibia	Albanerpetontidae	New unnamed taxon 2	VAL-06-16-01	0.5mm	Parietal
ML2950	Lissamphibia	Albanerpetontidae	New unnamed taxon 2	VAL-06-16-01	0.5mm	Parietal
ML2951	Lissamphibia	Albanerpetontidae	New unnamed taxon 2	ZIM-06-17-02	0.5mm	Dentary
ML2952	Lissamphibia	Albanerpetontidae	New unnamed taxon 2	VAL-06-16-01	0.5mm	Dentary
ML2953	Lissamphibia	Albanerpetontidae	New unnamed taxon 2	VAL-06-16-01	0.5mm	Dentary
ML2954	Lissamphibia	Albanerpetontidae	New unnamed taxon 2	VAL-06-16-01	0.5mm	Dentary

ML2955	Lissamphibia	Albanerpetontidae	New unnamed taxon 2	VAL-06-16-01	0.5mm	Dentary
ML2956	Lissamphibia	Albanerpetontidae	New unnamed taxon 2	VAL-06-16-01	0.5mm	Dentary
ML2957	Lissamphibia	Albanerpetontidae	New unnamed taxon 2	VAL-06-16-01	0.5mm	Dentary
ML2958	Lissamphibia	Albanerpetontidae	New unnamed taxon 2	VAL-06-16-01	0.5mm	Dentary
ML2959	Lissamphibia	Albanerpetontidae	New unnamed taxon 2	VAL-03-19-10	0.5mm	Dentary
ML2960	Lissamphibia	Albanerpetontidae	New unnamed taxon 2	VAL-06-16-01	0.5mm	Dentary
ML2961	Lissamphibia	Albanerpetontidae	New unnamed taxon 2	VAL-06-16-01	0.5mm	Dentary
ML2962	Lissamphibia	Albanerpetontidae	New unnamed taxon 2	VAL-06-16-01	0.5mm	Dentary
ML2963	Lissamphibia	Albanerpetontidae	New unnamed taxon 2	VAL-06-16-01	0.5mm	Dentary
ML2964	Lissamphibia	Albanerpetontidae	New unnamed taxon 2	VAL-06-16-01	0.5mm	Dentary
ML2965	Lissamphibia	Albanerpetontidae	New unnamed taxon 2	VAL-06-16-01	0.5mm	Dentary
ML2966	Lissamphibia	Albanerpetontidae	New unnamed taxon 2	VAL-06-16-01	0.5mm	Dentary
ML2967	Lissamphibia	Albanerpetontidae	New unnamed taxon 2	VAL-06-16-01	0.5mm	Dentary
ML2968	Lissamphibia	Albanerpetontidae	New unnamed taxon 2	VAL-06-16-01	0.5mm	Dentary
ML2969	Lissamphibia	Albanerpetontidae	New unnamed taxon 2	VAL-06-16-01	0.5mm	Dentary
ML2970	Lissamphibia	Albanerpetontidae	New unnamed taxon 2	VAL-06-16-01	0.5mm	Dentary
ML2971	Lissamphibia	Albanerpetontidae	New unnamed taxon 2	VAL-06-16-01	0.5mm	Dentary
ML2972	Lissamphibia	Albanerpetontidae	New unnamed taxon 2	VAL-06-16-01	0.5mm	Dentary
ML2973	Lissamphibia	Albanerpetontidae	New unnamed taxon 2	VAL-06-16-01	0.5mm	Dentary
ML2974	Lissamphibia	Albanerpetontidae	New unnamed taxon 2	VAL-06-16-01	0.5mm	Dentary
ML2975	Lissamphibia	Albanerpetontidae	New unnamed taxon 2	VAL-06-16-01	0.5mm	Dentary
ML2976	Lissamphibia	Albanerpetontidae	New unnamed taxon 2	VAL-06-16-01	0.5mm	Dentary
ML2977	Lissamphibia	Albanerpetontidae	New unnamed taxon 2	VAL-06-16-01	0.5mm	Dentary
ML2978	Lissamphibia	Albanerpetontidae	New unnamed taxon 2	VAL-06-16-01	0.5mm	Dentary
ML2979	Lissamphibia	Albanerpetontidae	New unnamed taxon 2	VAL-06-16-01	0.5mm	Dentary
ML2980	Lissamphibia	Albanerpetontidae	New unnamed taxon 2	VAL-06-16-01	0.5mm	Dentary
ML2981	Lissamphibia	Albanerpetontidae	New unnamed taxon 2	VAL-06-16-01	0.5mm	Dentary
ML2982	Lissamphibia	Albanerpetontidae	New unnamed taxon 2	VAL-06-16-01	0.5mm	Dentary
ML2983	Lissamphibia	Albanerpetontidae	New unnamed taxon 2	PB-10-17-02	0.5mm	Dentary
ML2984	Lissamphibia	Albanerpetontidae	New unnamed taxon 2	VAL-10-17-01	0.5mm	Dentary
ML2985	Lissamphibia	Albanerpetontidae	New unnamed taxon 2	VAL-03-19-01	0.5mm	Dentary
ML2986	Lissamphibia	Albanerpetontidae	New unnamed taxon 2	VAL-03-19-01	0.5mm	Dentary
ML2987	Lissamphibia	Albanerpetontidae	New unnamed taxon 2	VAL-03-19-01	0.5mm	Dentary

ML2988	Lissamphibia	Albanerpetontidae	New unnamed taxon 2	VAL-03-19-01	0.5mm	Dentary
ML2989	Lissamphibia	Albanerpetontidae	New unnamed taxon 2	ZIM-11-16-01	0.5mm	Dentary
ML2990	Lissamphibia	Albanerpetontidae	New unnamed taxon 2	ZIM-11-16-01	0.5mm	Dentary
ML2991	Lissamphibia	Albanerpetontidae	New unnamed taxon 2	ZIM-11-16-01	0.5mm	Dentary
ML2992	Lissamphibia	Albanerpetontidae	New unnamed taxon 2	ZIM-11-16-01	0.5mm	Dentary
ML2993	Lissamphibia	Albanerpetontidae	New unnamed taxon 2	ZIM-11-16-01	0.5mm	Dentary
ML2994	Lissamphibia	Albanerpetontidae	New unnamed taxon 2	ZIM-11-16-01	0.5mm	Dentary
ML2995	Lissamphibia	Albanerpetontidae	New unnamed taxon 2	ZIM-06-17-01	0.5mm	Dentary
ML2996	Lissamphibia	Albanerpetontidae	New unnamed taxon 2	ZIM-06-17-01	0.5mm	Dentary
ML2997	Lissamphibia	Albanerpetontidae	New unnamed taxon 2	ZIM-06-17-01	0.5mm	Dentary
ML2998	Lissamphibia	Albanerpetontidae	New unnamed taxon 2	ZIM-11-16-02	0.5mm	Dentary
ML2999	Lissamphibia	Albanerpetontidae	New unnamed taxon 2	VAL-06-16-01	0.5mm	Articular
ML3000	Lissamphibia	Albanerpetontidae	New unnamed taxon 2	ZIM-06-17-02	0.5mm	Articular
ML3001	Lissamphibia	Albanerpetontidae	New unnamed taxon 2	VAL-06-16-01	0.5mm	Articular
ML3002	Lissamphibia	Albanerpetontidae	New unnamed taxon 2	VAL-03-19-01	0.5mm	Articular
ML3003	Lissamphibia	Albanerpetontidae	New unnamed taxon 2	VAL-06-16-01	0.5mm	Articular
ML3004	Lissamphibia	Albanerpetontidae	New unnamed taxon 2	VAL-06-16-01	0.5mm	Articular
ML3005	Lissamphibia	Albanerpetontidae	New unnamed taxon 2	VAL-06-16-01	0.5mm	Articular
ML3006	Lissamphibia	Albanerpetontidae	New unnamed taxon 2	VAL-06-16-01	0.5mm	Articular
ML3007	Lissamphibia	Albanerpetontidae	New unnamed taxon 2	VAL-06-16-01	0.5mm	Articular
ML3008	Lissamphibia	Albanerpetontidae	New unnamed taxon 2	VAL-06-16-01	0.5mm	Articular
ML3009	Lissamphibia	Albanerpetontidae	New unnamed taxon 2	VAL-03-19-01	0.5mm	Quadrate
ML3010	Lissamphibia	Albanerpetontidae	New unnamed taxon 2	VAL-06-16-01	0.5mm	Quadrate
ML3011	Lissamphibia	Albanerpetontidae	New unnamed taxon 2	ZIM-11-16-01	0.5mm	Quadrate
ML3012	Lissamphibia	Albanerpetontidae	New unnamed taxon 2	VAL-06-16-01	0.5mm	Atlas
ML3013	Lissamphibia	Albanerpetontidae	New unnamed taxon 2	ZIM-06-17-02	0.5mm	Atlas
ML3014	Lissamphibia	Albanerpetontidae	New unnamed taxon 2	VAL-03-19-04	0.5mm	Atlas
ML3015	Lissamphibia	Albanerpetontidae	New unnamed taxon 2	ZIM-06-17-08	0.5mm	Atlas
ML3016	Lissamphibia	Albanerpetontidae	New unnamed taxon 2	VAL-06-16-01	0.5mm	Atlas
ML3017	Lissamphibia	Albanerpetontidae	New unnamed taxon 2	VAL-06-16-01	0.5mm	Atlas
ML3018	Lissamphibia	Albanerpetontidae	New unnamed taxon 2	VAL-06-16-01	0.5mm	Axis
ML3019	Lissamphibia	Albanerpetontidae	New unnamed taxon 2	ZIM-06-17-02	0.5mm	Axis
ML3020	Lissamphibia	Albanerpetontidae	New unnamed taxon 2	VAL-03-19-04	0.5mm	Axis

ML3021	Lissamphibia	Albanerpetontidae	New unnamed taxon 2	VAL-03-19-10	0.5mm	Axis
ML3022	Lissamphibia	Albanerpetontidae	New unnamed taxon 2	VAL-03-19-01	0.5mm	Axis
ML3023	Lissamphibia	Albanerpetontidae	New unnamed taxon 2	PB-06-16-02	0.5mm	Vertebra
ML3024	Lissamphibia	Albanerpetontidae	New unnamed taxon 2	PB-06-16-02	0.5mm	Vertebra
ML3025	Lissamphibia	Albanerpetontidae	New unnamed taxon 2	VAL-06-16-01	0.5mm	Vertebra
ML3026	Lissamphibia	Albanerpetontidae	New unnamed taxon 2	VAL-06-16-01	0.5mm	Vertebra
ML3027	Lissamphibia	Albanerpetontidae	New unnamed taxon 2	VAL-06-16-01	0.5mm	Vertebra
ML3028	Lissamphibia	Albanerpetontidae	New unnamed taxon 2	VAL-06-16-01	0.5mm	Vertebra
ML3029	Lissamphibia	Albanerpetontidae	New unnamed taxon 2	ZIM-06-17-01	0.5mm	Vertebra
ML3030	Lissamphibia	Albanerpetontidae	New unnamed taxon 2	ZIM-06-17-01	0.5mm	Vertebra
ML3031	Lissamphibia	Albanerpetontidae	New unnamed taxon 2	PB-10-17-02	0.5mm	Vertebra
ML3032	Lissamphibia	Albanerpetontidae	New unnamed taxon 2	PB-10-17-02	0.5mm	Vertebra
ML3033	Lissamphibia	Albanerpetontidae	New unnamed taxon 2	ZIM-06-17-02	0.5mm	Vertebra
ML3034	Lissamphibia	Albanerpetontidae	New unnamed taxon 2	ZIM-06-17-02	0.5mm	Vertebra
ML3035	Lissamphibia	Albanerpetontidae	New unnamed taxon 2	VAL-03-19-01	0.5mm	Vertebra
ML3036	Lissamphibia	Albanerpetontidae	New unnamed taxon 2	VAL-03-19-01	0.5mm	Vertebra
ML3037	Lissamphibia	Albanerpetontidae	New unnamed taxon 2	VAL-03-19-01	0.5mm	Vertebra
ML3038	Lissamphibia	Albanerpetontidae	New unnamed taxon 2	VAL-03-19-01	0.5mm	Vertebra
ML3039	Lissamphibia	Albanerpetontidae	New unnamed taxon 2	VAL-03-19-01	0.5mm	Vertebra
ML3040	Lissamphibia	Albanerpetontidae	New unnamed taxon 2	ZIM-11-16-02	0.5mm	Vertebra
ML3041	Lissamphibia	Albanerpetontidae	New unnamed taxon 2	ZIM-11-16-02	0.5mm	Vertebra
ML3042	Lissamphibia	Albanerpetontidae	New unnamed taxon 2	ZIM-11-16-02	0.5mm	Vertebra
ML3043	Lissamphibia	Albanerpetontidae	New unnamed taxon 2	ZIM-11-16-02	0.5mm	Vertebra
ML3044	Lissamphibia	Albanerpetontidae	New unnamed taxon 2	ZIM-11-16-01	0.5mm	Vertebra
ML3045	Lissamphibia	Albanerpetontidae	New unnamed taxon 2	ZIM-11-16-01	0.5mm	Vertebra
ML3046	Lissamphibia	Albanerpetontidae	New unnamed taxon 2	ZIM-11-16-01	0.5mm	Vertebra
ML3047	Lissamphibia	Albanerpetontidae	New unnamed taxon 2	ZIM-11-16-01	0.5mm	Vertebra
ML3048	Lissamphibia	Albanerpetontidae	New unnamed taxon 2	ZIM-11-16-01	0.5mm	Vertebra
ML3049	Lissamphibia	Albanerpetontidae	New unnamed taxon 2	ZIM-11-16-01	0.5mm	Vertebra
ML3050	Lissamphibia	Albanerpetontidae	New unnamed taxon 2	ZIM-11-16-01	0.5mm	Vertebra
ML3051	Lissamphibia	Albanerpetontidae	New unnamed taxon 2	ZIM-11-16-01	0.5mm	Vertebra
ML3052	Lissamphibia	Albanerpetontidae	New unnamed taxon 2	ZIM-11-16-02	0.5mm	Vertebra
ML3053	Lissamphibia	Albanerpetontidae	New unnamed taxon 2	ZIM-06-17-01	0.5mm	Vertebra

ML3054	Lissamphibia	Albanerpetontidae	New unnamed taxon 2	ZIM-06-17-01	0.5mm	Vertebra
ML3055	Lissamphibia	Albanerpetontidae	New unnamed taxon 2	ZIM-06-17-01	0.5mm	Vertebra
ML3056	Lissamphibia	Albanerpetontidae	New unnamed taxon 2	ZIM-06-17-01	0.5mm	Vertebra
ML3057	Lissamphibia	Albanerpetontidae	New unnamed taxon 2	ZIM-06-17-01	0.5mm	Vertebra
ML3058	Lissamphibia	Albanerpetontidae	New unnamed taxon 2	ZIM-06-17-01	0.5mm	Vertebra
ML3059	Lissamphibia	Albanerpetontidae	New unnamed taxon 2	ZIM-06-17-01	0.5mm	Vertebra
ML3060	Lissamphibia	Albanerpetontidae	New unnamed taxon 2	VAL-06-16-01	0.5mm	Vertebra
ML3061	Lissamphibia	Albanerpetontidae	New unnamed taxon 2	VAL-06-16-01	0.5mm	Vertebra
ML3062	Lissamphibia	Albanerpetontidae	New unnamed taxon 2	VAL-06-16-01	0.5mm	Vertebra
ML3063	Lissamphibia	Albanerpetontidae	New unnamed taxon 2	VAL-06-16-01	0.5mm	Vertebra
ML3064	Lissamphibia	Albanerpetontidae	New unnamed taxon 2	VAL-06-16-01	0.5mm	Vertebra
ML3065	Lissamphibia	Albanerpetontidae	New unnamed taxon 2	VAL-06-16-01	0.5mm	Vertebra
ML3066	Lissamphibia	Albanerpetontidae	New unnamed taxon 2	VAL-06-16-01	0.5mm	Vertebra
ML3067	Lissamphibia	Albanerpetontidae	New unnamed taxon 2	VAL-06-16-01	0.5mm	Vertebra
ML3068	Lissamphibia	Albanerpetontidae	New unnamed taxon 2	VAL-06-16-01	0.5mm	Vertebra
ML3069	Lissamphibia	Albanerpetontidae	New unnamed taxon 2	VAL-06-16-01	0.5mm	Vertebra
ML3070	Lissamphibia	Albanerpetontidae	New unnamed taxon 2	VAL-06-16-01	0.5mm	Vertebra
ML3071	Lissamphibia	Albanerpetontidae	New unnamed taxon 2	VAL-06-16-01	0.5mm	Vertebra
ML3072	Lissamphibia	Albanerpetontidae	New unnamed taxon 2	VAL-06-16-01	0.5mm	Vertebra
ML3073	Lissamphibia	Albanerpetontidae	New unnamed taxon 2	VAL-06-16-01	0.5mm	Vertebra
ML3074	Lissamphibia	Albanerpetontidae	New unnamed taxon 2	VAL-06-16-01	0.5mm	Vertebra
ML3075	Lissamphibia	Albanerpetontidae	New unnamed taxon 2	VAL-06-16-01	0.5mm	Vertebra
ML3076	Lissamphibia	Albanerpetontidae	New unnamed taxon 2	VAL-06-16-01	0.5mm	Vertebra
ML3077	Lissamphibia	Albanerpetontidae	New unnamed taxon 2	VAL-06-16-01	0.5mm	Vertebra
ML3078	Lissamphibia	Albanerpetontidae	New unnamed taxon 2	VAL-06-16-01	0.5mm	Vertebra
ML3079	Lissamphibia	Albanerpetontidae	New unnamed taxon 2	VAL-06-16-01	0.5mm	Vertebra
ML3080	Lissamphibia	Albanerpetontidae	New unnamed taxon 2	VAL-06-16-01	0.5mm	Vertebra
ML3081	Lissamphibia	Albanerpetontidae	New unnamed taxon 2	VAL-06-16-01	0.5mm	Vertebra
ML3082	Lissamphibia	Albanerpetontidae	New unnamed taxon 2	VAL-06-16-01	0.5mm	Vertebra
ML3083	Lissamphibia	Albanerpetontidae	New unnamed taxon 2	VAL-06-16-01	0.5mm	Vertebra
ML3084	Lissamphibia	Albanerpetontidae	New unnamed taxon 2	VAL-06-16-01	0.5mm	Vertebra
ML3085	Lissamphibia	Albanerpetontidae	New unnamed taxon 2	VAL-06-16-01	0.5mm	Vertebra
ML3086	Lissamphibia	Albanerpetontidae	New unnamed taxon 2	VAL-06-16-01	0.5mm	Vertebra

ML3087	Lissamphibia	Albanerpetontidae	New unnamed taxon 2	VAL-06-16-01	0.5mm	Vertebra
ML3088	Lissamphibia	Albanerpetontidae	New unnamed taxon 2	VAL-06-16-01	0.5mm	Vertebra
ML3089	Lissamphibia	Albanerpetontidae	New unnamed taxon 2	VAL-06-16-01	0.5mm	Vertebra
ML3090	Lissamphibia	Albanerpetontidae	New unnamed taxon 2	VAL-06-16-01	0.5mm	Vertebra
ML3091	Lissamphibia	Albanerpetontidae	New unnamed taxon 2	VAL-06-16-01	0.5mm	Vertebra
ML3092	Lissamphibia	Albanerpetontidae	New unnamed taxon 2	VAL-06-16-01	0.5mm	Vertebra
ML3093	Lissamphibia	Albanerpetontidae	New unnamed taxon 2	VAL-06-16-01	0.5mm	Vertebra
ML3094	Lissamphibia	Albanerpetontidae	New unnamed taxon 2	VAL-06-16-01	0.5mm	Vertebra
ML3095	Lissamphibia	Albanerpetontidae	New unnamed taxon 2	VAL-06-16-01	0.5mm	Vertebra
ML3096	Lissamphibia	Albanerpetontidae	New unnamed taxon 2	VAL-06-16-01	0.5mm	Vertebra
ML3097	Lissamphibia	Albanerpetontidae	New unnamed taxon 2	VAL-06-16-01	0.5mm	Vertebra
ML3098	Lissamphibia	Albanerpetontidae	New unnamed taxon 2	VAL-06-16-01	0.5mm	Vertebra
ML3099	Lissamphibia	Albanerpetontidae	New unnamed taxon 2	VAL-06-16-01	0.5mm	Vertebra
ML3100	Lissamphibia	Albanerpetontidae	New unnamed taxon 2	VAL-06-16-01	0.5mm	Vertebra
ML3101	Lissamphibia	Albanerpetontidae	New unnamed taxon 2	VAL-06-16-01	0.5mm	Vertebra
ML3102	Lissamphibia	Albanerpetontidae	New unnamed taxon 2	ZIM-06-17-01	0.5mm	Proximal humerus
ML3103	Lissamphibia	Albanerpetontidae	New unnamed taxon 2	ZIM-06-17-01	0.5mm	Proximal humerus
ML3104	Lissamphibia	Albanerpetontidae	New unnamed taxon 2	VAL-03-19-04	0.5mm	Distal humerus
ML3105	Lissamphibia	Albanerpetontidae	New unnamed taxon 2	VAL-06-16-01	0.5mm	Distal humerus
ML3106	Lissamphibia	Albanerpetontidae	New unnamed taxon 2	VAL-06-16-01	0.5mm	Proximal humerus
ML3107	Lissamphibia	Albanerpetontidae	New unnamed taxon 2	PB-03-19-01	0.5mm	Proximal humerus
ML3108	Lissamphibia	Albanerpetontidae	New unnamed taxon 2	VAL-06-16-01	0.5mm	Proximal humerus
ML3109	Lissamphibia	Albanerpetontidae	New unnamed taxon 2	VAL-06-16-01	0.5mm	Distal humerus
ML3110	Lissamphibia	Albanerpetontidae	New unnamed taxon 2	VAL-06-16-01	0.5mm	Distal humerus
ML3111	Lissamphibia	Albanerpetontidae	New unnamed taxon 2	VAL-06-16-01	0.5mm	Distal humerus
ML3112	Lissamphibia	Albanerpetontidae	New unnamed taxon 2	VAL-06-16-01	0.5mm	Proximal humerus
ML3113	Lissamphibia	Albanerpetontidae	New unnamed taxon 2	ZIM-06-17-02	0.5mm	Distal humerus
ML3114	Lissamphibia	Albanerpetontidae	New unnamed taxon 2	VAL-06-16-01	0.5mm	Proximal humerus
ML3115	Lissamphibia	Albanerpetontidae	New unnamed taxon 2	VAL-06-16-01	0.5mm	Proximal humerus
ML3116	Lissamphibia	Albanerpetontidae	New unnamed taxon 2	VAL-06-16-01	0.5mm	Distal humerus
ML3117	Lissamphibia	Albanerpetontidae	New unnamed taxon 2	VAL-06-16-01	0.5mm	Distal humerus
ML3118	Lissamphibia	Albanerpetontidae	New unnamed taxon 2	VAL-06-16-01	0.5mm	Distal humerus
ML3119	Lissamphibia	Albanerpetontidae	New unnamed taxon 2	VAL-06-16-01	0.5mm	Distal humerus

ML3120	Lissamphibia	Albanerpetontidae	New unnamed taxon 2	VAL-06-16-01	0.5mm	Distal humerus
ML3121	Lissamphibia	Albanerpetontidae	New unnamed taxon 2	VAL-06-16-01	0.5mm	Distal humerus
ML3122	Lissamphibia	Albanerpetontidae	New unnamed taxon 2	VAL-06-16-01	0.5mm	Distal humerus
ML3123	Lissamphibia	Albanerpetontidae	New unnamed taxon 2	VAL-06-16-01	0.5mm	Distal humerus
ML3124	Lissamphibia	Albanerpetontidae	New unnamed taxon 2	VAL-10-17-01	0.5mm	Proximal humerus
ML3125	Lissamphibia	Albanerpetontidae	New unnamed taxon 2	VAL-10-17-01	0.5mm	Distal humerus
ML3126	Lissamphibia	Albanerpetontidae	New unnamed taxon 2	ZIM-06-17-08	0.5mm	Proximal humerus
ML3127	Lissamphibia	Albanerpetontidae	New unnamed taxon 2	PER-06-18-01	0.5mm	Proximal humerus
ML3128	Lissamphibia	Albanerpetontidae	New unnamed taxon 2	VAL-06-16-01	0.5mm	Ilium
ML3129	Lissamphibia	Albanerpetontidae	New unnamed taxon 2	VAL-06-16-01	0.5mm	Ilium
ML3130	Lissamphibia	Albanerpetontidae	New unnamed taxon 2	VAL-06-16-01	0.5mm	Distal femur
ML3131	Lissamphibia	Albanerpetontidae	New unnamed taxon 2	VAL-06-16-01	0.5mm	Proximal femur
ML3132	Lissamphibia	Albanerpetontidae	New unnamed taxon 2	PB-06-17-03	0.5mm	
ML3133	Lissamphibia	Albanerpetontidae	New unnamed taxon 2	PB-06-17-03	0.5mm	
ML3134	Lissamphibia	Albanerpetontidae	New unnamed taxon 2	VAL-06-16-01	0.5mm	Proximal femur
ML3135	Lissamphibia	Albanerpetontidae	New unnamed taxon 2	VAL-06-16-01	0.5mm	Distal femur
ML3136	Lissamphibia	Albanerpetontidae	New unnamed taxon 2	VAL-06-16-01	0.5mm	Distal femur
ML3137	Lissamphibia	Albanerpetontidae	New unnamed taxon 2	ZIM-11-16-01	0.5mm	Distal femur
ML3138	Lissamphibia	Albanerpetontidae	New unnamed taxon 2	PB-10-17-02	0.5mm	Distal femur
ML3139	Lissamphibia	Albanerpetontidae	New unnamed taxon 2	PER-06-18-01	0.5mm	Premaxilla
ML3140	Lissamphibia	Albanerpetontidae	New unnamed taxon 2	ZIM-06-17-08	0.5mm	Premaxilla
ML3141	Lissamphibia	Albanerpetontidae	New unnamed taxon 2	VAL-03-19-07	0.5mm	Premaxilla
ML3142	Lissamphibia	Albanerpetontidae	New unnamed taxon 2	VAL-03-19-07	0.5mm	Premaxilla
ML3143	Lissamphibia	Albanerpetontidae	New unnamed taxon 2	VAL-03-19-07	0.5mm	Premaxilla
ML3144	Lissamphibia	Albanerpetontidae	New unnamed taxon 2	VAL-03-19-07	0.5mm	Premaxilla
ML3145	Lissamphibia	Albanerpetontidae	New unnamed taxon 2	ZIM-03-19-03	0.5mm	Premaxilla
ML3146	Lissamphibia	Albanerpetontidae	New unnamed taxon 2	ZIM-03-19-03	0.5mm	Premaxilla
ML3147	Lissamphibia	Albanerpetontidae	New unnamed taxon 2	PB-03-19-02	0.5mm	Premaxilla
ML3148	Lissamphibia	Albanerpetontidae	New unnamed taxon 2	VAL-06-16-01	0.5mm	Premaxilla
ML3149	Lissamphibia	Albanerpetontidae	New unnamed taxon 2	VAL-03-19-04	0.5mm	Premaxilla
ML3150	Lissamphibia	Albanerpetontidae	New unnamed taxon 2	VAL-03-19-09	0.5mm	Premaxilla
ML3151	Lissamphibia	Albanerpetontidae	New unnamed taxon 2	VAL-03-19-09	0.5mm	Premaxilla
ML3152	Lissamphibia	Albanerpetontidae	New unnamed taxon 2	VAL-03-19-01	0.5mm	Premaxilla

ML3153	Lissamphibia	Albanerpetontidae	New unnamed taxon 2	VAL-03-19-01	0.5mm	Premaxilla
ML3154	Lissamphibia	Albanerpetontidae	New unnamed taxon 2	PER-06-18-01	0.5mm	Maxilla
ML3155	Lissamphibia	Albanerpetontidae	New unnamed taxon 2	PB-06-17-03	0.5mm	Maxilla
ML3156	Lissamphibia	Albanerpetontidae	New unnamed taxon 2	PB-06-17-03	0.5mm	Maxilla
ML3157	Lissamphibia	Albanerpetontidae	New unnamed taxon 2	VAL-10-17-01	0.5mm	Maxilla
ML3158	Lissamphibia	Albanerpetontidae	New unnamed taxon 2	VAL-03-19-09	0.5mm	Maxilla
ML3159	Lissamphibia	Albanerpetontidae	New unnamed taxon 2	VAL-03-19-09	0.5mm	Maxilla
ML3160	Lissamphibia	Albanerpetontidae	New unnamed taxon 2	VAL-03-19-09	0.5mm	Maxilla
ML3161	Lissamphibia	Albanerpetontidae	New unnamed taxon 2	VAL-03-19-09	0.5mm	Maxilla
ML3162	Lissamphibia	Albanerpetontidae	New unnamed taxon 2	VAL-03-19-04	0.5mm	Maxilla
ML3163	Lissamphibia	Albanerpetontidae	New unnamed taxon 2	VAL-03-19-04	0.5mm	Maxilla
ML3164	Lissamphibia	Albanerpetontidae	New unnamed taxon 2	VAL-03-19-01	0.5mm	Maxilla
ML3165	Lissamphibia	Albanerpetontidae	New unnamed taxon 2	VAL-03-19-01	0.5mm	Maxilla
ML3166	Lissamphibia	Albanerpetontidae	New unnamed taxon 2	VAL-06-18-01	0.5mm	Maxilla
ML3167	Lissamphibia	Albanerpetontidae	New unnamed taxon 2	ZIM-06-17-08	0.5mm	Maxilla
ML3168	Lissamphibia	Albanerpetontidae	New unnamed taxon 2	PB-06-16-09	0.5mm	Maxilla
ML3169	Lissamphibia	Albanerpetontidae	New unnamed taxon 2	PB-06-16-06	0.5mm	Maxilla
ML3170	Lissamphibia	Albanerpetontidae	New unnamed taxon 2	VAL-10-17-01	0.5mm	Frontal
ML3171	Lissamphibia	Albanerpetontidae	New unnamed taxon 2	VAL-10-17-01	0.5mm	Frontal
ML3172	Lissamphibia	Albanerpetontidae	New unnamed taxon 2	VAL-10-17-01	0.5mm	Frontal
ML3173	Lissamphibia	Albanerpetontidae	New unnamed taxon 2	VAL-03-19-09	0.5mm	Frontal
ML3174	Lissamphibia	Albanerpetontidae	New unnamed taxon 2	VAL-03-19-09	0.5mm	Frontal
ML3175	Lissamphibia	Albanerpetontidae	New unnamed taxon 2	VAL-03-19-09	0.5mm	Frontal
ML3176	Lissamphibia	Albanerpetontidae	New unnamed taxon 2	VAL-03-19-09	0.5mm	Frontal
ML3177	Lissamphibia	Albanerpetontidae	New unnamed taxon 2	VAL-03-19-09	0.5mm	Frontal
ML3178	Lissamphibia	Albanerpetontidae	New unnamed taxon 2	VAL-03-19-09	0.5mm	Frontal
ML3179	Lissamphibia	Albanerpetontidae	New unnamed taxon 2	VAL-03-19-09	0.5mm	Frontal
ML3180	Lissamphibia	Albanerpetontidae	New unnamed taxon 2	VAL-03-19-07	0.5mm	Frontal
ML3181	Lissamphibia	Albanerpetontidae	New unnamed taxon 2	VAL-03-19-07	0.5mm	Frontal
ML3182	Lissamphibia	Albanerpetontidae	New unnamed taxon 2	VAL-03-19-07	0.5mm	Frontal
ML3183	Lissamphibia	Albanerpetontidae	New unnamed taxon 2	VAL-10-17-01	0.5mm	Frontal
ML3184	Lissamphibia	Albanerpetontidae	New unnamed taxon 2	PB-06-16-07	0.5mm	Frontal
ML3185	Lissamphibia	Albanerpetontidae	New unnamed taxon 2	PB-06-16-07	0.5mm	Frontal

ML3186	Lissamphibia	Albanerpetontidae	New unnamed taxon 2	VAL-03-19-01	0.5mm	Frontal
ML3187	Lissamphibia	Albanerpetontidae	New unnamed taxon 2	VAL-03-19-01	1mm	Frontal
ML3188	Lissamphibia	Albanerpetontidae	New unnamed taxon 2	PB-06-17-03	0.5mm	Lacrymal
ML3189	Lissamphibia	Albanerpetontidae	New unnamed taxon 2	VAL-06-18-01	0.5mm	Lacrymal
ML3190	Lissamphibia	Albanerpetontidae	New unnamed taxon 2	VAL-10-17-01	0.5mm	Parietal
ML3191	Lissamphibia	Albanerpetontidae	New unnamed taxon 2	VAL-03-19-07	0.5mm	Parietal
ML3192	Lissamphibia	Albanerpetontidae	New unnamed taxon 2	VAL-10-17-01	0.5mm	Dentary
ML3193	Lissamphibia	Albanerpetontidae	New unnamed taxon 2	VAL-10-17-01	0.5mm	Dentary
ML3194	Lissamphibia	Albanerpetontidae	New unnamed taxon 2	VAL-10-17-01	0.5mm	Dentary
ML3195	Lissamphibia	Albanerpetontidae	New unnamed taxon 2	VAL-10-17-01	0.5mm	Dentary
ML3196	Lissamphibia	Albanerpetontidae	New unnamed taxon 2	VAL-10-17-01	0.5mm	Dentary
ML3197	Lissamphibia	Albanerpetontidae	New unnamed taxon 2	PB-06-17-03	0.5mm	Dentary
ML3198	Lissamphibia	Albanerpetontidae	New unnamed taxon 2	PB-03-19-02	0.5mm	Dentary
ML3199	Lissamphibia	Albanerpetontidae	New unnamed taxon 2	PB-03-19-02	0.5mm	Dentary
ML3200	Lissamphibia	Albanerpetontidae	New unnamed taxon 2	VAL-06-16-01	0.5mm	Dentary
ML3201	Lissamphibia	Albanerpetontidae	New unnamed taxon 2	PB-06-16-06	0.5mm	Dentary
ML3202	Lissamphibia	Albanerpetontidae	New unnamed taxon 2	PB-06-16-06	0.5mm	Dentary
ML3203	Lissamphibia	Albanerpetontidae	New unnamed taxon 2	VAL-03-19-04	0.5mm	Dentary
ML3204	Lissamphibia	Albanerpetontidae	New unnamed taxon 2	VAL-03-19-04	0.5mm	Dentary
ML3205	Lissamphibia	Albanerpetontidae	New unnamed taxon 2	PB-10-17-01	0.5mm	Dentary
ML3206	Lissamphibia	Albanerpetontidae	New unnamed taxon 2	PB-10-17-01	0.5mm	Dentary
ML3207	Lissamphibia	Albanerpetontidae	New unnamed taxon 2	VAL-03-19-05	0.5mm	Dentary
ML3208	Lissamphibia	Albanerpetontidae	New unnamed taxon 2	VAL-03-19-05	0.5mm	Dentary
ML3209	Lissamphibia	Albanerpetontidae	New unnamed taxon 2	VAL-03-19-09	0.5mm	Dentary
ML3210	Lissamphibia	Albanerpetontidae	New unnamed taxon 2	VAL-03-19-09	0.5mm	Dentary
ML3211	Lissamphibia	Albanerpetontidae	New unnamed taxon 2	VAL-03-19-09	0.5mm	Dentary
ML3212	Lissamphibia	Albanerpetontidae	New unnamed taxon 2	VAL-03-19-09	0.5mm	Dentary
ML3213	Lissamphibia	Albanerpetontidae	New unnamed taxon 2	VAL-03-19-09	0.5mm	Dentary
ML3214	Lissamphibia	Albanerpetontidae	New unnamed taxon 2	VAL-03-19-09	0.5mm	Dentary
ML3215	Lissamphibia	Albanerpetontidae	New unnamed taxon 2	PB-06-16-02	0.5mm	Dentary
ML3216	Lissamphibia	Albanerpetontidae	New unnamed taxon 2	VAL-03-19-01	0.5mm	Dentary
ML3217	Lissamphibia	Albanerpetontidae	New unnamed taxon 2	VAL-03-19-07	0.5mm	Dentary
ML3218	Lissamphibia	Albanerpetontidae	New unnamed taxon 2	VAL-03-19-07	0.5mm	Dentary

ML3219	Lissamphibia	Albanerpetontidae	New unnamed taxon 2	VAL-03-19-07	0.5mm	Dentary
ML3220	Lissamphibia	Albanerpetontidae	New unnamed taxon 2	VAL-03-19-07	0.5mm	Dentary
ML3221	Lissamphibia	Albanerpetontidae	New unnamed taxon 2	PB-06-16-09	0.5mm	Dentary
ML3222	Lissamphibia	Albanerpetontidae	New unnamed taxon 2	PB-06-16-09	0.5mm	Dentary
ML3223	Lissamphibia	Albanerpetontidae	New unnamed taxon 2	PB-06-16-09	0.5mm	Dentary
ML3224	Lissamphibia	Albanerpetontidae	New unnamed taxon 2	PB-06-16-09	0.5mm	Dentary
ML3225	Lissamphibia	Albanerpetontidae	New unnamed taxon 2	PB-06-16-09	0.5mm	Dentary
ML3226	Lissamphibia	Albanerpetontidae	New unnamed taxon 2	VAL-06-18-01	0.5mm	Dentary
ML3227	Lissamphibia	Albanerpetontidae	New unnamed taxon 2	VAL-06-18-01	0.5mm	Dentary
ML3228	Lissamphibia	Albanerpetontidae	New unnamed taxon 2	VAL-06-18-01	0.5mm	Dentary
ML3229	Lissamphibia	Albanerpetontidae	New unnamed taxon 2	PB-06-17-03	0.5mm	Articular
ML3230	Lissamphibia	Albanerpetontidae	New unnamed taxon 2	VAL-10-17-01	0.5mm	Articular
ML3231	Lissamphibia	Albanerpetontidae	New unnamed taxon 2	PB-06-16-09	0.5mm	Articular
ML3232	Lissamphibia	Albanerpetontidae	New unnamed taxon 2	VAL-06-18-01	0.5mm	Articular
ML3233	Lissamphibia	Albanerpetontidae	New unnamed taxon 2	VAL-03-19-09	0.5mm	Articular
ML3234	Lissamphibia	Albanerpetontidae	New unnamed taxon 2	PB-06-16-07	0.5mm	Articular
ML3235	Lissamphibia	Albanerpetontidae	New unnamed taxon 2	PB-06-16-06	0.5mm	Articular
ML3236	Lissamphibia	Albanerpetontidae	New unnamed taxon 2	VAL-06-16-01	0.5mm	Articular
ML3237	Lissamphibia	Albanerpetontidae	New unnamed taxon 2	VAL-06-16-01	0.5mm	Articular
ML3238	Lissamphibia	Albanerpetontidae	New unnamed taxon 2	VAL-03-19-01	0.5mm	Articular
ML3239	Lissamphibia	Albanerpetontidae	New unnamed taxon 2	VALRED-06-22-02	0.5mm	Articular
ML3240	Lissamphibia	Albanerpetontidae	New unnamed taxon 2	VAL-10-17-01	0.5mm	Atlas
ML3241	Lissamphibia	Albanerpetontidae	New unnamed taxon 2	VAL-10-17-01	0.5mm	Atlas
ML3242	Lissamphibia	Albanerpetontidae	New unnamed taxon 2	VAL-10-17-01	0.5mm	Atlas
ML3243	Lissamphibia	Albanerpetontidae	New unnamed taxon 2	ZIM-06-17-02	0.5mm	Atlas
ML3244	Lissamphibia	Albanerpetontidae	New unnamed taxon 2	VAL-11-22-01	0.5mm	Atlas
ML3245	Lissamphibia	Albanerpetontidae	New unnamed taxon 2	PB-06-16-07	0.5mm	Atlas
ML3246	Lissamphibia	Albanerpetontidae	New unnamed taxon 2	VAL-03-19-09	0.5mm	Atlas
ML3247	Lissamphibia	Albanerpetontidae	New unnamed taxon 2	VAL-10-17-01	0.5mm	Axis
ML3248	Lissamphibia	Albanerpetontidae	New unnamed taxon 2	VAL-03-19-04	0.5mm	Axis
ML3249	Lissamphibia	Albanerpetontidae	New unnamed taxon 2	PB-06-16-03	0.5mm	Axis
ML3250	Lissamphibia	Albanerpetontidae	New unnamed taxon 2	VALRED-06-22-02	0.5mm	Axis
ML3251	Lissamphibia	Albanerpetontidae	New unnamed taxon 2	PB-10-17-01	0.5mm	Axis

ML3252	Lissamphibia	Albanerpetontidae	New unnamed taxon 2	VAL-10-17-01	0.5mm	Vertebra
ML3253	Lissamphibia	Albanerpetontidae	New unnamed taxon 2	VAL-10-17-01	0.5mm	Vertebra
ML3254	Lissamphibia	Albanerpetontidae	New unnamed taxon 2	VAL-10-17-01	0.5mm	Vertebra
ML3255	Lissamphibia	Albanerpetontidae	New unnamed taxon 2	VAL-10-17-01	0.5mm	Vertebra
ML3256	Lissamphibia	Albanerpetontidae	New unnamed taxon 2	VAL-10-17-01	0.5mm	Vertebra
ML3257	Lissamphibia	Albanerpetontidae	New unnamed taxon 2	VAL-10-17-01	0.5mm	Vertebra
ML3258	Lissamphibia	Albanerpetontidae	New unnamed taxon 2	VAL-10-17-01	0.5mm	Vertebra
ML3259	Lissamphibia	Albanerpetontidae	New unnamed taxon 2	PER-04-23-01	0.5mm	Vertebra
ML3260	Lissamphibia	Albanerpetontidae	New unnamed taxon 2	PER-06-18-01	0.5mm	Vertebra
ML3261	Lissamphibia	Albanerpetontidae	New unnamed taxon 2	PER-06-18-01	0.5mm	Vertebra
ML3262	Lissamphibia	Albanerpetontidae	New unnamed taxon 2	VALRED-06-22-02	0.5mm	Vertebra
ML3263	Lissamphibia	Albanerpetontidae	New unnamed taxon 2	VAL-03-19-09	0.5mm	Vertebra
ML3264	Lissamphibia	Albanerpetontidae	New unnamed taxon 2	VAL-03-19-09	0.5mm	Vertebra
ML3265	Lissamphibia	Albanerpetontidae	New unnamed taxon 2	VAL-03-19-09	0.5mm	Vertebra
ML3266	Lissamphibia	Albanerpetontidae	New unnamed taxon 2	VAL-03-19-09	0.5mm	Vertebra
ML3267	Lissamphibia	Albanerpetontidae	New unnamed taxon 2	VAL-03-19-09	0.5mm	Vertebra
ML3268	Lissamphibia	Albanerpetontidae	New unnamed taxon 2	VAL-03-19-09	0.5mm	Vertebra
ML3269	Lissamphibia	Albanerpetontidae	New unnamed taxon 2	VAL-03-19-09	0.5mm	Vertebra
ML3270	Lissamphibia	Albanerpetontidae	New unnamed taxon 2	VAL-03-19-09	0.5mm	Vertebra
ML3271	Lissamphibia	Albanerpetontidae	New unnamed taxon 2	VAL-03-19-09	0.5mm	Vertebra
ML3272	Lissamphibia	Albanerpetontidae	New unnamed taxon 2	VAL-03-19-09	0.5mm	Vertebra
ML3273	Lissamphibia	Albanerpetontidae	New unnamed taxon 2	VAL-03-19-09	0.5mm	Vertebra
ML3274	Lissamphibia	Albanerpetontidae	New unnamed taxon 2	VAL-03-19-01	0.5mm	Vertebra
ML3275	Lissamphibia	Albanerpetontidae	New unnamed taxon 2	VAL-03-19-01	0.5mm	Vertebra
ML3276	Lissamphibia	Albanerpetontidae	New unnamed taxon 2	PB-06-17-03	0.5mm	Vertebra
ML3277	Lissamphibia	Albanerpetontidae	New unnamed taxon 2	PB-06-16-09	0.5mm	Vertebra
ML3278	Lissamphibia	Albanerpetontidae	New unnamed taxon 2	PB-06-16-09	0.5mm	Vertebra
ML3279	Lissamphibia	Albanerpetontidae	New unnamed taxon 2	PB-06-16-09	0.5mm	Vertebra
ML3280	Lissamphibia	Albanerpetontidae	New unnamed taxon 2	PB-06-16-09	0.5mm	Vertebra
ML3281	Lissamphibia	Albanerpetontidae	New unnamed taxon 2	PB-06-16-09	0.5mm	Vertebra
ML3282	Lissamphibia	Albanerpetontidae	New unnamed taxon 2	VAL-11-22-01	0.5mm	Vertebra
ML3283	Lissamphibia	Albanerpetontidae	New unnamed taxon 2	VAL-03-19-04	0.5mm	Vertebra
ML3284	Lissamphibia	Albanerpetontidae	New unnamed taxon 2	VAL-03-19-04	0.5mm	Vertebra

ML3285	Lissamphibia	Albanerpetontidae	New unnamed taxon 2	VAL-03-19-04	0.5mm	Vertebra
ML3286	Lissamphibia	Albanerpetontidae	New unnamed taxon 2	VAL-03-19-04	0.5mm	Vertebra
ML3287	Lissamphibia	Albanerpetontidae	New unnamed taxon 2	PB-06-16-06	0.5mm	Vertebra
ML3288	Lissamphibia	Albanerpetontidae	New unnamed taxon 2	PB-06-16-06	0.5mm	Vertebra
ML3289	Lissamphibia	Albanerpetontidae	New unnamed taxon 2	VAL-06-18-01	0.5mm	Vertebra
ML3290	Lissamphibia	Albanerpetontidae	New unnamed taxon 2	PB-06-16-02	0.5mm	Vertebra
ML3291	Lissamphibia	Albanerpetontidae	New unnamed taxon 2	PB-06-16-02	0.5mm	Vertebra
ML3292	Lissamphibia	Albanerpetontidae	New unnamed taxon 2	PB-06-16-02	0.5mm	Vertebra
ML3293	Lissamphibia	Albanerpetontidae	New unnamed taxon 2	PB-06-16-02	0.5mm	Vertebra
ML3294	Lissamphibia	Albanerpetontidae	New unnamed taxon 2	VAL-03-19-05	0.5mm	Vertebra
ML3295	Lissamphibia	Albanerpetontidae	New unnamed taxon 2	ZIM-03-19-03	0.5mm	Vertebra
ML3296	Lissamphibia	Albanerpetontidae	New unnamed taxon 2	ZIM-03-19-03	0.5mm	Vertebra
ML3297	Lissamphibia	Albanerpetontidae	New unnamed taxon 2	ZIM-06-17-08	0.5mm	Vertebra
ML3298	Lissamphibia	Albanerpetontidae	New unnamed taxon 2	ZIM-06-17-08	0.5mm	Vertebra
ML3299	Lissamphibia	Albanerpetontidae	New unnamed taxon 2	ZIM-06-17-08	0.5mm	Vertebra
ML3300	Lissamphibia	Albanerpetontidae	New unnamed taxon 2	VAL-03-19-07	0.5mm	Vertebra
ML3301	Lissamphibia	Albanerpetontidae	New unnamed taxon 2	VAL-03-19-07	0.5mm	Vertebra
ML3302	Lissamphibia	Albanerpetontidae	New unnamed taxon 2	PER-05-21-01	0.5mm	Proximal humerus
ML3303	Lissamphibia	Albanerpetontidae	New unnamed taxon 2	ZIM-06-17-08	0.5mm	Distal humerus
ML3304	Lissamphibia	Albanerpetontidae	New unnamed taxon 2	VAL-06-18-01	0.5mm	Distal humerus
ML3305	Lissamphibia	Albanerpetontidae	New unnamed taxon 2	PB-06-16-09	0.5mm	Proximal humerus
ML3306	Lissamphibia	Albanerpetontidae	New unnamed taxon 2	PB-06-16-09	0.5mm	Distal humerus
ML3307	Lissamphibia	Albanerpetontidae	New unnamed taxon 2	PB-06-16-09	0.5mm	Distal humerus
ML3308	Lissamphibia	Albanerpetontidae	New unnamed taxon 2	VAL-10-17-01	0.5mm	Proximal humerus
ML3309	Lissamphibia	Albanerpetontidae	New unnamed taxon 2	VAL-03-19-04	0.5mm	Proximal humerus
ML3310	Lissamphibia	Albanerpetontidae	New unnamed taxon 2	PB-10-17-01	0.5mm	Distal humerus
ML3311	Lissamphibia	Albanerpetontidae	New unnamed taxon 2	VAL-03-19-01	0.5mm	Distal humerus
ML3312	Lissamphibia	Albanerpetontidae	New unnamed taxon 2	VAL-03-19-01	0.5mm	Distal humerus
ML3313	Lissamphibia	Albanerpetontidae	New unnamed taxon 2	PB-06-16-07	0.5mm	Distal humerus
ML3314	Lissamphibia	Albanerpetontidae	New unnamed taxon 2	PB-06-16-07	0.5mm	Distal humerus
ML3315	Lissamphibia	Albanerpetontidae	New unnamed taxon 2	PB-06-16-07	0.5mm	Distal humerus
ML3316	Lissamphibia	Albanerpetontidae	New unnamed taxon 2	PB-06-16-07	0.5mm	Proximal humerus
ML3317	Lissamphibia	Albanerpetontidae	New unnamed taxon 2	ZIM-11-16-01	0.5mm	Distal humerus

ML3318	Lissamphibia	Albanerpetontidae	New unnamed taxon 2	ZIM-11-16-01	0.5mm	Distal humerus
ML3319	Lissamphibia	Albanerpetontidae	New unnamed taxon 2	VALRED-06-22-02	0.5mm	Proximal humerus
ML3320	Lissamphibia	Albanerpetontidae	New unnamed taxon 2	VALRED-06-22-02	0.5mm	Proximal humerus
ML3321	Lissamphibia	Albanerpetontidae	New unnamed taxon 2	VALRED-06-22-02	0.5mm	Distal humerus
ML3322	Lissamphibia	Albanerpetontidae	New unnamed taxon 2	VAL-03-19-04	0.5mm	Ilium
ML3323	Lissamphibia	Albanerpetontidae	New unnamed taxon 2	PB-06-16-07	0.5mm	Ilium
ML3324	Lissamphibia	Albanerpetontidae	New unnamed taxon 2	VAL-06-16-01	0.5mm	Proximal femur
ML3325	Lissamphibia	Albanerpetontidae	New unnamed taxon 2	VAL-06-16-01	0.5mm	Proximal femur
ML3326	Lissamphibia	Albanerpetontidae	New unnamed taxon 2	ZIM-03-19-03	0.5mm	Distal femur
ML3327	Lissamphibia	Albanerpetontidae	New unnamed taxon 2	PB-06-16-09	0.5mm	Distal femur
ML3328	Lissamphibia	Albanerpetontidae	New unnamed taxon 2	PB-06-16-09	0.5mm	Distal femur
ML3329	Lissamphibia	Albanerpetontidae	New unnamed taxon 2	PB-06-16-09	0.5mm	Proximal femur
ML3330	Lissamphibia	Albanerpetontidae	New unnamed taxon 2	PB-06-16-03	0.5mm	Proximal femur
ML3331	Lissamphibia	Albanerpetontidae	New unnamed taxon 2	PB-10-17-01	0.5mm	Distal femur
ML3332	Lissamphibia	Albanerpetontidae	New unnamed taxon 2	PB-06-16-06	0.5mm	Proximal femur
ML3333	Lissamphibia	Albanerpetontidae	New unnamed taxon 2	VAL-11-22-01	0.5mm	Proximal femur
ML3334	Lissamphibia	Albanerpetontidae	New unnamed taxon 2	PB-06-16-02	0.5mm	Proximal femur
ML3617	Lissamphibia	Albanerpetontidae		VAL-06-16-01	0.5mm	Articular
ML3618	Lissamphibia	Albanerpetontidae		VAL-06-16-01	0.5mm	Articular
ML3619	Lissamphibia	Albanerpetontidae		ZIM-11-16-02	0.5mm	Articular
ML3620	Lissamphibia	Albanerpetontidae		VAL-06-16-01	0.5mm	Distal femur
ML3621	Lissamphibia	Albanerpetontidae		VAL-06-16-01	0.5mm	Distal femur
ML3622	Lissamphibia	Albanerpetontidae		VAL-06-16-01	0.5mm	Femur
ML3623	Lissamphibia	Albanerpetontidae		VAL-06-16-01	0.5mm	Femur
ML3624	Lissamphibia	Albanerpetontidae		VAL-06-16-01	0.5mm	Femur
ML3625	Lissamphibia	Albanerpetontidae		VAL-06-16-01	0.5mm	Femur
ML3626	Lissamphibia	Albanerpetontidae		VAL-06-16-01	0.5mm	Lacrymal
ML3627	Lissamphibia	Anura		VAL-03-19-03	0.5mm	Ilium
ML3628	Lissamphibia	Anura		VAL-03-19-03	0.5mm	Ilium
ML3629	Lissamphibia	Anura		VAL-06-16-01	0.5mm	Ilium
ML3630	Lissamphibia	Anura		VAL-06-16-01	0.5mm	Ilium
ML3631	Lissamphibia	Anura		VAL-06-16-01	0.5mm	Ilium
ML3632	Lissamphibia	Anura		VAL-06-16-01	0.5mm	Ilium

ML3633	Lissamphibia	Anura		VAL-06-16-01	0.5mm	Ilium
ML3634	Lissamphibia	Anura		VAL-06-16-01	0.5mm	Ilium
ML3635	Lissamphibia	Anura		VAL-06-16-01	0.5mm	Ilium
ML3636	Lissamphibia	Anura		VAL-06-16-01	0.5mm	Ilium
ML3637	Lissamphibia	Anura		VAL-10-17-01	0.5mm	Ilium
ML3638	Lissamphibia	Anura		ZIM-06-17-02	1mm	Ilium
ML3639	Lissamphibia	Anura		VAL-06-16-01	0.5mm	Maxilla
ML3640	Lissamphibia	Anura		VAL-06-16-01	0.5mm	Maxilla
ML3641	Lissamphibia	Anura		VAL-06-16-01	0.5mm	Maxilla
ML3642	Lissamphibia	Anura		VAL-06-16-01	0.5mm	Maxilla
ML3643	Lissamphibia	Anura		PB-06-17-03	0.5mm	Radioulna
ML3644	Lissamphibia	Anura		VAL-03-19-04	1mm	Radioulna
ML3645	Lissamphibia	Anura		VAL-06-16-01	0.5mm	Radioulna
ML3646	Lissamphibia	Anura		VAL-06-16-01	0.5mm	Radioulna
ML3647	Lissamphibia	Anura		VAL-06-16-01	0.5mm	Radioulna
ML3648	Lissamphibia	Anura		VAL-06-16-01	0.5mm	Radioulna
ML3649	Lissamphibia	Anura		VAL-06-16-01	0.5mm	Radioulna
ML3650	Lissamphibia	Anura		VAL-06-16-01	0.5mm	Radioulna
ML3651	Lissamphibia	Anura		VAL-06-16-01	0.5mm	Radioulna
ML3652	Lissamphibia	Anura		VAL-06-16-01	0.5mm	Radioulna
ML3653	Lissamphibia	Anura		ZIM-06-17-01	0.5mm	Radioulna
ML3654	Lissamphibia	Anura		VAL-06-16-01	0.5mm	Sphenoide
ML3655	Lissamphibia	Anura		VAL-06-16-01	0.5mm	Sphenoide
ML3656	Lissamphibia	Anura		VAL-06-16-01	0.5mm	Tibiofibula
ML3657	Lissamphibia	Anura		VAL-06-16-01	0.5mm	Tibiofibula
ML3658	Lissamphibia	Anura		VAL-06-16-01	0.5mm	Tibiofibula
ML3659	Lissamphibia	Anura		VAL-06-16-01	0.5mm	Tibiofibula
ML3660	Lissamphibia	Anura		VAL-06-16-01	0.5mm	Tibiofibula
ML3661	Lissamphibia	Anura		VAL-06-16-01	0.5mm	Tibiofibula
ML3662	Lissamphibia	Anura		VAL-06-16-01	0.5mm	Tibiofibula
ML3663	Lissamphibia	Anura		VAL-10-17-01	0.5mm	Tibiofibula
ML3664	Lissamphibia	Anura		VAL-10-17-01	0.5mm	Tibiofibula
ML3665	Lissamphibia	Anura		ZIM-06-17-01	1mm	Tibiofibula

ML3666	Lissamphibia	Anura		PB-10-17-02	0.5mm	Zeugopod
ML3667	Lissamphibia	Anura		PB-10-17-02	0.5mm	Zeugopod
ML3668	Lissamphibia	Caudata		VAL-03-19-03	0.5mm	Atlas
ML3669	Lissamphibia	Caudata		VAL-06-16-01	0.5mm	Atlas
ML3670	Lissamphibia	Caudata		VAL-06-16-01	0.5mm	Maxilla
ML3671	Lissamphibia	Caudata		VAL-06-16-01	0.5mm	Maxilla
ML3672	Lissamphibia	Caudata		VAL-06-16-01	1mm	Vertebra
ML3673	Lissamphibia	Caudata		VAL-06-16-01	1mm	Vertebra
ML3674	Lissamphibia	Caudata		VAL-06-16-01	1mm	Vertebra
ML3675	Lissamphibia	Anura		ZIM-06-17-01	1mm	Distal humerus
ML3676	Lissamphibia	Lissamphibia indet.		VAL-06-16-01	0.5mm	Femur
ML3677	Lissamphibia	Lissamphibia indet.		VAL-06-16-01	0.5mm	Femur
ML3678	Lissamphibia	Lissamphibia indet.		VAL-06-16-01	0.5mm	Femur
ML3679	Lissamphibia	Lissamphibia indet.		VAL-06-16-01	0.5mm	Femur
ML3680	Lissamphibia	Lissamphibia indet.		VAL-06-16-01	0.5mm	Femur
ML3681	Lissamphibia	Lissamphibia indet.		VAL-06-16-01	0.5mm	Femur
ML3682	Lissamphibia	Lissamphibia indet.		VAL-06-16-01	0.5mm	Femur
ML3683	Lissamphibia	Lissamphibia indet.		VAL-06-16-01	0.5mm	Femur
ML3684	Lissamphibia	Lissamphibia indet.		VAL-06-16-01	0.5mm	Femur
ML3685	Lissamphibia	Lissamphibia indet.		VAL-06-16-01	0.5mm	Femur
ML3686	Lissamphibia	Lissamphibia indet.		VAL-06-16-01	0.5mm	Femur
ML3687	Lissamphibia	Lissamphibia indet.		ZIM-11-16-02	0.5mm	Femur
ML3688	Lissamphibia	Lissamphibia indet.		ZIM-06-17-01	1mm	Femur?
ML3689	Lissamphibia	Lissamphibia indet.		ZIM-06-17-01	0.5mm	Scapula
ML3690	Lissamphibia	Lissamphibia indet.		ZIM-06-17-01	0.5mm	Unidentified
ML3691	Lissamphibia	Lissamphibia indet.		PB-10-17-02	1mm	Vertebra
ML3692	Lissamphibia	Lissamphibia indet.		PB-10-17-02	1mm	Vertebra
ML3693	Lissamphibia	Lissamphibia indet.		VAL-06-16-01	0.5mm	Vertebra
ML3694	Lissamphibia	Lissamphibia indet.		VAL-06-16-01	0.5mm	Vertebra
ML3695	Lissamphibia	Lissamphibia indet.		VAL-06-16-01	0.5mm	Vertebra
ML2845	Mammalia	Dryolestidae	Sp1	PER-05-21-01		m1
ML2823	Mammalia	Dryolestidae	Sp1	Surface collecting		m6-8

ML2811	Mammalia	Dryolestidae	Sp1	VAL-03-19-02		Tooth m3?
ML2812	Mammalia	Dryolestidae	Sp1	VAL-03-19-09		M5
ML1147	Mammalia	Dryolestidae	Sp1			Hemimandible
ML2827	Mammalia	Dryolestidae	Sp1			p4
ML2810	Mammalia	Dryolestidae	Sp2	VAL-06-18-01		Lower molar
ML2826	Mammalia	Dryolestidae	Sp3	PB-06-16-05		Lower molar
ML2822	Mammalia	Eutriconodont				Lower molar
ML2824	Mammalia	Multituberculate	Sp1	PB-06-16-09		m2
ML2809	Mammalia	Multituberculate	Sp1	VALRED-06-22-02	0.5mm	Tooth P5
ML2820	Mammalia	Multituberculate	Sp2	PB-06-16-03		M2
ML2844	Mammalia	Multituberculate	Sp3			M2
ML2825	Mammalia	Multituberculate		PER-05-21-01		M2
ML3696	Mammalia	Multituberculate				Incisive
ML3697	Mammalia	Multituberculate				Incisive
ML2821	Mammalia	Zatheria		VAL-03-19-09	0,5mm	DP3/DP5?
ML2843	Mammalia	Zatheria				Premolar
ML3698	Lepidosauria	Paramacellodidae		PB-10-17-02	0.5mm	Dentary
ML3699	Lepidosauria	Paramacellodidae		VAL-06-16-01	0.5mm	Dentary
ML3700	Lepidosauria	Paramacellodidae		VAL-06-16-01	0.5mm	Dentary
ML3701	Lepidosauria	Paramacellodidae		ZIM-06-17-04	0.5mm	Dentary
ML3702	Lepidosauria	Paramacellodidae		ZIM-06-17-04	0.5mm	Dentary
ML3703	Lepidosauria	Lepidosauria indet.		VAL-06-16-01	0.5mm	Femur
ML3704	Lepidosauria	Lepidosauria indet.		ZIM-06-17-02	0.5mm	Femur
ML3705	Lepidosauria	Lepidosauria indet.		VAL-Charo	0.5mm	Femur
ML3706	Lepidosauria	Lepidosauria indet.		ZIM-06-17-01	0.5mm	Jaw
ML3707	Lepidosauria	Paramacellodidae		VAL-03-19-04	1mm	Osteoderm
ML3708	Lepidosauria	Paramacellodidae		VAL-03-19-04	1mm	Osteoderm
ML3709	Lepidosauria	Paramacellodidae		VAL-03-19-04	1mm	Osteoderm
ML3710	Lepidosauria	Paramacellodidae		ZIM-06-17-02	1mm	Osteoderm
ML3711	Lepidosauria	Paramacellodidae		ZIM-06-17-02	1mm	Osteoderm
ML3712	Lepidosauria	Paramacellodidae		ZIM-11-16-01	1mm	Osteoderm
ML3713	Lepidosauria	Lepidosauria indet.		VAL-06-16-01	0.5mm	Osteoderm

ML3714	Lepidosauria	Lepidosauria indet.		VAL-06-16-01	0.5mm	Osteoderm
ML3715	Lepidosauria	Lepidosauria indet.		VAL-06-16-01	0.5mm	Osteoderm
ML3716	Lepidosauria	Lepidosauria indet.		ZIM-06-17-01	1mm	Osteoderm
ML3717	Lepidosauria	Lepidosauria indet.		ZIM-06-17-04	0.5mm	Osteoderm
ML3718	Lepidosauria	Lepidosauria indet.		ZIM-06-17-04	0.5mm	Osteoderm
ML3719	Lepidosauria	Lepidosauria indet.		ZIM-06-17-04	0.5mm	Osteoderm
ML3720	Lepidosauria	Lepidosauria indet.		ZIM-06-17-04	0.5mm	Osteoderm
ML3721	Lepidosauria	Lepidosauria indet.		ZIM-06-17-04	0.5mm	Osteoderm
ML3722	Lepidosauria	Paramacellodidae		VAL-06-16-01	2mm	Parietal
ML3723	Lepidosauria	Paramacellodidae		VAL-06-16-01	2mm	Parietal
ML3724	Lepidosauria	Paramacellodidae		VAL-06-16-01	2mm	Parietal
ML3725	Lepidosauria	Paramacellodidae		VAL-06-16-01	2mm	Parietal
ML3726	Lepidosauria	Paramacellodidae		VAL-06-16-01	2mm	Parietal
ML3727	Lepidosauria	Paramacellodidae		VAL-10-17-01	0.5mm	Parietal
ML3728	Lepidosauria	Paramacellodidae		ZIM-06-17-01	1mm	Parietal
ML3729	Lepidosauria	Paramacellodidae		ZIM-11-16-02	2mm	Parietal
ML3730	Lepidosauria	Paramacellodidae		ZIM-11-16-02	2mm	Parietal
ML3731	Lepidosauria	Lepidosauria indet.		PB-06-17-03	1mm	Parietal
ML3732	Lepidosauria	Lepidosauria indet.		PB-10-17-02	0.5mm	Parietal
ML3733	Lepidosauria	Lepidosauria indet.		VAL-03-19-10	0.5mm	Parietal
ML3734	Lepidosauria	Lepidosauria indet.		VAL-06-16-01	0.5mm	Parietal
ML3735	Lepidosauria	Lepidosauria indet.		VAL-06-16-01	0.5mm	Parietal
ML3736	Lepidosauria	Lepidosauria indet.		VAL-06-16-01	0.5mm	Parietal
ML3737	Lepidosauria	Lepidosauria indet.		VAL-06-16-01	0.5mm	Parietal
ML3738	Lepidosauria	Lepidosauria indet.		VAL-10-17-01	0.5mm	Parietal
ML3739	Lepidosauria	Lepidosauria indet.		VAL-10-17-01	0.5mm	Parietal
ML3740	Lepidosauria	Lepidosauria indet.		VAL-10-17-01	0.5mm	Parietal
ML3741	Lepidosauria	Lepidosauria indet.		VAL-10-17-01	0.5mm	Parietal
ML3742	Lepidosauria	Scincomorpha		PB-10-17-02	0.5mm	Premaxilla
ML3743	Lepidosauria	Lepidosauria indet.		PB-03-19-01	1mm	Vertebra
ML3744	Lepidosauria	Lepidosauria indet.		VAL-03-19-10	2mm	Vertebra
ML3745	Lepidosauria	Lepidosauria indet.		VAL-06-16-01	0.5mm	Vertebra
ML3746	Lepidosauria	Lepidosauria indet.		VAL-06-16-01	0.5mm	Vertebra

ML3747	Lepidosauria	Lepidosauria indet.		VAL-06-16-01	0.5mm	Vertebra
ML3748	Lepidosauria	Lepidosauria indet.		VAL-06-16-01	0.5mm	Vertebra
ML3749	Lepidosauria	Lepidosauria indet.		VAL-06-16-01	0.5mm	Vertebra
ML3750	Lepidosauria	Lepidosauria indet.		VAL-06-16-01	0.5mm	Vertebra
ML3751	Lepidosauria	Lepidosauria indet.		VAL-06-16-01	0.5mm	Vertebra
ML3752	Lepidosauria	Lepidosauria indet.		VAL-06-16-01	0.5mm	Vertebra
ML3753	Lepidosauria	Lepidosauria indet.		VAL-06-16-01	1mm	Vertebra
ML3754	Lepidosauria	Lepidosauria indet.		VAL-06-16-01	2mm	Vertebra
ML3755	Lepidosauria	Lepidosauria indet.		VAL-10-17-01	0.5mm	Vertebra
ML3756	Lepidosauria	Lepidosauria indet.		ZIM-06-17-01	0.5mm	Vertebra
ML3757	Lepidosauria	Lepidosauria indet.		ZIM-06-17-01	0.5mm	Vertebra
ML3758	Lepidosauria	Lepidosauria indet.		ZIM-06-17-01	0.5mm	Vertebra
ML3759	Lepidosauria	Lepidosauria indet.		ZIM-06-17-01	0.5mm	Vertebra
ML3760	Lepidosauria	Lepidosauria indet.		ZIM-06-17-02	1mm	Vertebra
ML2422	Crocodylomorpha	Goniopholididae		VAL-06-16-01		Isolated tooth
ML2423	Crocodylomorpha	Goniopholididae		VAL-06-16-01		Isolated tooth
ML2424	Crocodylomorpha	Goniopholididae		VAL-06-16-01		Isolated tooth
ML2425	Crocodylomorpha	Goniopholididae		VAL-06-16-01		Isolated tooth
ML2426	Crocodylomorpha	Goniopholididae		VAL-06-16-01		Isolated tooth
ML2427	Crocodylomorpha	Goniopholididae		VAL-06-16-01		Isolated tooth
ML2428	Crocodylomorpha	Goniopholididae		VAL-06-16-01		Isolated tooth
ML2429	Crocodylomorpha	Goniopholididae		VAL-06-16-01		Isolated tooth
ML2430	Crocodylomorpha	Goniopholididae		VAL-06-16-01		Isolated tooth
ML2431	Crocodylomorpha	Goniopholididae		VAL-06-16-01		Isolated tooth
ML2432	Crocodylomorpha	Goniopholididae		VAL-06-16-01		Isolated tooth
ML2433	Crocodylomorpha	Goniopholididae		VAL-06-16-01		Isolated tooth
ML2434	Crocodylomorpha	Goniopholididae		VAL-06-16-01		Isolated tooth
ML2435	Crocodylomorpha	Goniopholididae		VAL-06-16-01		Isolated tooth
ML2436	Crocodylomorpha	Goniopholididae		VAL-06-16-01		Isolated tooth
ML2437	Crocodylomorpha	Goniopholididae		VAL-06-16-01		Isolated tooth
ML2438	Crocodylomorpha	Goniopholididae		VAL-06-16-01		Isolated tooth
ML2439	Crocodylomorpha	Goniopholididae		VAL-06-16-01		Isolated tooth

ML2440	Crocodylomorpha	Goniopholididae		VAL-06-16-01		Isolated tooth
ML2441	Crocodylomorpha	Goniopholididae		VAL-06-16-01		Isolated tooth
ML2442	Crocodylomorpha	Goniopholididae		VAL-06-16-01		Isolated tooth
ML2443	Crocodylomorpha	Goniopholididae		VAL-06-16-01		Isolated tooth
ML2444	Crocodylomorpha	Goniopholididae		VAL-06-16-01		Isolated tooth
ML2445	Crocodylomorpha	Goniopholididae		VAL-06-16-01		Isolated tooth
ML2446	Crocodylomorpha	Goniopholididae		VAL-06-16-01		Isolated tooth
ML2447	Crocodylomorpha	Goniopholididae		VAL-06-16-01		Isolated tooth
ML2448	Crocodylomorpha	Goniopholididae		VAL-06-16-01		Isolated tooth
ML2449	Crocodylomorpha	Goniopholididae		VAL-06-16-01		Isolated tooth
ML2450	Crocodylomorpha	Goniopholididae		VAL-06-16-01		Isolated tooth
ML2451	Crocodylomorpha	Goniopholididae		VAL-06-16-01		Isolated tooth
ML2452	Crocodylomorpha	Goniopholididae		VAL-06-16-01		Isolated tooth
ML2453	Crocodylomorpha	Goniopholididae		VAL-06-16-01		Isolated tooth
ML2454	Crocodylomorpha	Goniopholididae		VAL-06-16-01		Isolated tooth
ML2455	Crocodylomorpha	Goniopholididae		VAL-06-16-01		Isolated tooth
ML2456	Crocodylomorpha	Goniopholididae		VAL-06-16-01		Isolated tooth
ML2457	Crocodylomorpha	Goniopholididae		VAL-06-16-01		Isolated tooth
ML2458	Crocodylomorpha	Goniopholididae		VAL-06-16-01		Isolated tooth
ML2459	Crocodylomorpha	Goniopholididae		VAL-06-16-01		Isolated tooth
ML2460	Crocodylomorpha	Goniopholididae		VAL-06-16-01		Isolated tooth
ML2461	Crocodylomorpha	Goniopholididae		VAL-06-16-01		Isolated tooth
ML2462	Crocodylomorpha	Goniopholididae		VAL-06-16-01		Isolated tooth
ML2463	Crocodylomorpha	Goniopholididae		VAL-06-16-01		Isolated tooth
ML2464	Crocodylomorpha	Goniopholididae		VAL-06-16-01		Isolated tooth
ML2465	Crocodylomorpha	Goniopholididae		VAL-06-16-01		Isolated tooth
ML2466	Crocodylomorpha	Goniopholididae		VAL-06-16-01		Isolated tooth
ML2467	Crocodylomorpha	Goniopholididae		VAL-06-16-01		Isolated tooth
ML2468	Crocodylomorpha	Goniopholididae		VAL-06-16-01		Isolated tooth
ML2469	Crocodylomorpha	Goniopholididae		VAL-06-16-01		Isolated tooth
ML2470	Crocodylomorpha	Goniopholididae		VAL-06-16-01		Isolated tooth
ML2471	Crocodylomorpha	Goniopholididae		VAL-06-16-01		Isolated tooth
ML2472	Crocodylomorpha	Goniopholididae		VAL-06-16-01		Isolated tooth

ML2473	Crocodylomorpha	Mesoeucrocodylia		VAL-06-16-01		Isolated tooth
ML2474	Crocodylomorpha	Mesoeucrocodylia		VAL-06-16-01		Isolated tooth
ML2475	Crocodylomorpha	Mesoeucrocodylia		VAL-06-16-01		Isolated tooth
ML2476	Crocodylomorpha	Mesoeucrocodylia		VAL-06-16-01		Isolated tooth
ML2477	Crocodylomorpha	Mesoeucrocodylia		VAL-06-16-01		Isolated tooth
ML2478	Crocodylomorpha	Bernissartiidae		VAL-06-16-01		Isolated tooth
ML2479	Crocodylomorpha	Bernissartiidae		VAL-06-16-01		Isolated tooth
ML2480	Crocodylomorpha	Bernissartiidae		VAL-06-16-01		Isolated tooth
ML2481	Crocodylomorpha	Bernissartiidae		VAL-06-16-01		Isolated tooth
ML2482	Crocodylomorpha	Bernissartiidae		VAL-06-16-01		Isolated tooth
ML2483	Crocodylomorpha	Bernissartiidae		VAL-06-16-01		Isolated tooth
ML2484	Crocodylomorpha	Bernissartiidae		VAL-06-16-01		Isolated tooth
ML2485	Crocodylomorpha	Bernissartiidae		VAL-06-16-01		Isolated tooth
ML2486	Crocodylomorpha	Bernissartiidae		VAL-06-16-01		Isolated tooth
ML2487	Crocodylomorpha	Bernissartiidae		VAL-06-16-01		Isolated tooth
ML2488	Crocodylomorpha	Bernissartiidae		VAL-06-16-01		Isolated tooth
ML2489	Crocodylomorpha	Bernissartiidae		VAL-06-16-01		Isolated tooth
ML2490	Crocodylomorpha	Bernissartiidae		VAL-06-16-01		Isolated tooth
ML2491	Crocodylomorpha	Bernissartiidae		VAL-06-16-01		Isolated tooth
ML2492	Crocodylomorpha	Bernissartiidae		VAL-06-16-01		Isolated tooth
ML2493	Crocodylomorpha	Bernissartiidae		VAL-06-16-01		Isolated tooth
ML2494	Crocodylomorpha	Bernissartiidae		VAL-06-16-01		Isolated tooth
ML2495	Crocodylomorpha	Bernissartiidae		VAL-06-16-01		Isolated tooth
ML2496	Crocodylomorpha	Bernissartiidae		VAL-06-16-01		Isolated tooth
ML2497	Crocodylomorpha	Atoposauridae		VAL-06-16-01		Isolated tooth
ML2498	Crocodylomorpha	Atoposauridae		VAL-06-16-01		Isolated tooth
ML2499	Crocodylomorpha	Atoposauridae		VAL-06-16-01		Isolated tooth
ML2500	Crocodylomorpha	Atoposauridae		VAL-06-16-01		Isolated tooth
ML2501	Crocodylomorpha	Atoposauridae		VAL-06-16-01		Isolated tooth
ML2502	Crocodylomorpha	Atoposauridae		VAL-06-16-01		Isolated tooth
ML2503	Crocodylomorpha	Atoposauridae		VAL-06-16-01		Isolated tooth
ML2504	Crocodylomorpha	Atoposauridae		VAL-06-16-01		Isolated tooth
ML2505	Crocodylomorpha	Atoposauridae		VAL-06-16-01		Isolated tooth

ML2506	Crocodylomorpha	Atoposauridae		VAL-06-16-01		Isolated tooth
ML2507	Crocodylomorpha	Atoposauridae		VAL-06-16-01		Isolated tooth
ML2508	Crocodylomorpha	Atoposauridae		VAL-06-16-01		Isolated tooth
ML2509	Crocodylomorpha	Atoposauridae		VAL-06-16-01		Isolated tooth
ML2510	Crocodylomorpha	Atoposauridae		VAL-06-16-01		Isolated tooth
ML2511	Crocodylomorpha	Atoposauridae		VAL-06-16-01		Isolated tooth
ML2512	Crocodylomorpha	Atoposauridae		VAL-06-16-01		Isolated tooth
ML2513	Crocodylomorpha	Atoposauridae		VAL-06-16-01		Isolated tooth
ML2514	Crocodylomorpha	Atoposauridae		VAL-06-16-01		Isolated tooth
ML2515	Crocodylomorpha	Atoposauridae		VAL-06-16-01		Isolated tooth
ML2516	Crocodylomorpha	Atoposauridae		VAL-06-16-01		Isolated tooth
ML2517	Crocodylomorpha	Atoposauridae		VAL-06-16-01		Isolated tooth
ML2518	Crocodylomorpha	Atoposauridae		VAL-06-16-01		Isolated tooth
ML2519	Crocodylomorpha	Atoposauridae		VAL-06-16-01		Isolated tooth
ML2520	Crocodylomorpha	Atoposauridae		VAL-06-16-01		Isolated tooth
ML2521	Crocodylomorpha	Atoposauridae		VAL-06-16-01		Isolated tooth
ML2522	Crocodylomorpha	Atoposauridae		VAL-06-16-01		Isolated tooth
ML2523	Crocodylomorpha	Atoposauridae		VAL-06-16-01		Isolated tooth
ML2524	Crocodylomorpha	Atoposauridae		VAL-06-16-01		Isolated tooth
ML2525	Crocodylomorpha	Atoposauridae		VAL-06-16-01		Isolated tooth
ML2526	Crocodylomorpha	Atoposauridae		VAL-06-16-01		Isolated tooth
ML2527	Crocodylomorpha	Atoposauridae		VAL-06-16-01		Isolated tooth
ML2528	Crocodylomorpha	Atoposauridae		VAL-06-16-01		Isolated tooth
ML2529	Crocodylomorpha	Atoposauridae		VAL-06-16-01		Isolated tooth
ML2530	Crocodylomorpha	Atoposauridae		VAL-06-16-01		Isolated tooth
ML2531	Crocodylomorpha	Atoposauridae		VAL-06-16-01		Isolated tooth
ML2532	Crocodylomorpha	Atoposauridae		VAL-06-16-01		Isolated tooth
ML2533	Crocodylomorpha	Atoposauridae		VAL-06-16-01		Isolated tooth
ML2534	Crocodylomorpha	Atoposauridae		VAL-06-16-01		Isolated tooth
ML2535	Crocodylomorpha	Atoposauridae		VAL-06-16-01		Isolated tooth
ML2536	Crocodylomorpha	Atoposauridae		VAL-06-16-01		Isolated tooth
ML2537	Crocodylomorpha	Atoposauridae		VAL-06-16-01		Isolated tooth
ML2538	Crocodylomorpha	Atoposauridae		VAL-06-16-01		Isolated tooth

ML2539	Crocodylomorpha	Atoposauridae		VAL-06-16-01		Isolated tooth
ML2540	Crocodylomorpha	Atoposauridae		VAL-06-16-01		Isolated tooth
ML2541	Crocodylomorpha	Atoposauridae		VAL-06-16-01		Isolated tooth
ML2542	Crocodylomorpha	Atoposauridae		VAL-06-16-01		Isolated tooth
ML2543	Crocodylomorpha	Atoposauridae		VAL-06-16-01		Isolated tooth
ML2544	Crocodylomorpha	Atoposauridae		VAL-06-16-01		Isolated tooth
ML2545	Crocodylomorpha	Atoposauridae		VAL-06-16-01		Isolated tooth
ML2546	Crocodylomorpha	Atoposauridae		VAL-06-16-01		Isolated tooth
ML3761	Crocodylomorpha	Crocodylomorpha indet.		ZIM-11-16-02	2mm	Osteoderm
ML3762	Crocodylomorpha	Crocodylomorpha indet.		ZIM-11-16-02	2mm	Osteoderm
ML3763	Crocodylomorpha	Crocodylomorpha indet.		ZIM-11-16-02	2mm	Osteoderm
ML3764	Crocodylomorpha	Crocodylomorpha indet.		ZIM-11-16-02	1mm	Osteoderm
ML3765	Crocodylomorpha	Crocodylomorpha indet.		ZIM-11-16-02	1mm	Osteoderm
ML3766	Crocodylomorpha	Crocodylomorpha indet.		ZIM-11-16-02	1mm	Osteoderm
ML3767	Crocodylomorpha	Crocodylomorpha indet.		ZIM-11-16-02	1mm	Osteoderm
ML3768	Crocodylomorpha	Crocodylomorpha indet.		ZIM-11-16-02	1mm	Osteoderm
ML3769	Crocodylomorpha	Crocodylomorpha indet.		ZIM-11-16-02	1mm	Osteoderm
ML3770	Crocodylomorpha	Crocodylomorpha indet.		ZIM-11-16-02	1mm	Osteoderm
ML3771	Crocodylomorpha	Crocodylomorpha indet.		ZIM-11-16-02	1mm	Osteoderm
ML3772	Crocodylomorpha	Crocodylomorpha indet.		ZIM-11-16-02	1mm	Osteoderm
ML3773	Crocodylomorpha	Crocodylomorpha indet.		ZIM-11-16-02	1mm	Osteoderm
ML3774	Crocodylomorpha	Crocodylomorpha indet.		ZIM-11-16-02	1mm	Osteoderm
ML3775	Crocodylomorpha	Crocodylomorpha indet.		ZIM-11-16-02	1mm	Osteoderm
ML3776	Crocodylomorpha	Crocodylomorpha indet.		ZIM-11-16-02	1mm	Osteoderm
ML3777	Crocodylomorpha	Crocodylomorpha indet.		ZIM-11-16-02	1mm	Osteoderm
ML3778	Crocodylomorpha	Crocodylomorpha indet.		ZIM-11-16-02	1mm	Osteoderm
ML3779	Crocodylomorpha	Crocodylomorpha indet.		ZIM-11-16-02	1mm	Osteoderm
ML3780	Crocodylomorpha	Crocodylomorpha indet.		ZIM-11-16-02	1mm	Osteoderm
ML3781	Crocodylomorpha	Crocodylomorpha indet.		ZIM-11-16-02	0.5mm	Osteoderm
ML3782	Crocodylomorpha	Crocodylomorpha indet.		ZIM-11-16-02	0.5mm	Osteoderm
ML3783	Crocodylomorpha	Crocodylomorpha indet.		ZIM-11-16-02	0.5mm	Osteoderm
ML3784	Crocodylomorpha	Crocodylomorpha indet.		ZIM-11-16-02	0.5mm	Osteoderm
ML3785	Crocodylomorpha	Crocodylomorpha indet.		ZIM-11-16-02	0.5mm	Osteoderm

ML3786	Crocodylomorpha	Crocodylomorpha indet.		ZIM-11-16-02	0.5mm	Osteoderm
ML3787	Crocodylomorpha	Crocodylomorpha indet.		ZIM-11-16-02	0.5mm	Osteoderm
ML3788	Crocodylomorpha	Crocodylomorpha indet.		ZIM-11-16-02	0.5mm	Osteoderm
ML3789	Crocodylomorpha	Crocodylomorpha indet.		ZIM-11-16-02	0.5mm	Osteoderm
ML3790	Crocodylomorpha	Crocodylomorpha indet.		ZIM-11-16-02	0.5mm	Osteoderm
ML3791	Crocodylomorpha	Crocodylomorpha indet.		PB-06-17-03	1mm	Osteoderm
ML3792	Crocodylomorpha	Crocodylomorpha indet.		VAL-06-16-01	2mm	Osteoderm
ML3793	Crocodylomorpha	Crocodylomorpha indet.		VAL-06-16-01	2mm	Osteoderm
ML3794	Crocodylomorpha	Crocodylomorpha indet.		VAL-06-16-01	2mm	Osteoderm
ML3795	Crocodylomorpha	Crocodylomorpha indet.		ZIM-06-17-01	2mm	Osteoderm
ML3796	Crocodylomorpha	Crocodylomorpha indet.		ZIM-06-17-01	1mm	Osteoderm
ML3797	Crocodylomorpha	Crocodylomorpha indet.		ZIM-06-17-01	1mm	Osteoderm
ML3798	Crocodylomorpha	Crocodylomorpha indet.		ZIM-06-17-01	0.5mm	Osteoderm
ML3799	Crocodylomorpha	Crocodylomorpha indet.		ZIM-06-17-01	0.5mm	Osteoderm
ML3800	Crocodylomorpha	Crocodylomorpha indet.		ZIM-06-17-01	0.5mm	Osteoderm
ML3801	Crocodylomorpha	Crocodylomorpha indet.		VAL-03-19-03	2mm	Osteoderm
ML3802	Crocodylomorpha	Crocodylomorpha indet.		ZIM-11-16-01	0.5mm	Osteoderm
ML3803	Crocodylomorpha	Crocodylomorpha indet.		ZIM-11-16-01	1mm	Osteoderm
ML3804	Crocodylomorpha	Crocodylomorpha indet.		ZIM-11-16-01	1mm	Osteoderm
ML3805	Crocodylomorpha	Crocodylomorpha indet.		ZIM-11-16-01	1mm	Osteoderm
ML3806	Crocodylomorpha	Crocodylomorpha indet.		ZIM-11-16-01	1mm	Osteoderm
ML3807	Crocodylomorpha	Crocodylomorpha indet.		ZIM-11-16-01	1mm	Osteoderm
ML3808	Crocodylomorpha	Crocodylomorpha indet.		ZIM-11-16-01	1mm	Osteoderm
ML3809	Crocodylomorpha	Crocodylomorpha indet.		VAL-06-16-01	0.5mm	Osteoderm
ML3810	Crocodylomorpha	Crocodylomorpha indet.		VAL-06-16-01	0.5mm	Osteoderm
ML3811	Crocodylomorpha	Crocodylomorpha indet.		VAL-06-16-01	0.5mm	Osteoderm
ML3812	Crocodylomorpha	Crocodylomorpha indet.		VAL-06-16-01	0.5mm	Osteoderm
ML3813	Crocodylomorpha	Crocodylomorpha indet.		VAL-06-16-01	0.5mm	Osteoderm
ML3814	Crocodylomorpha	Crocodylomorpha indet.		VAL-06-16-01	0.5mm	Osteoderm
ML3815	Crocodylomorpha	Crocodylomorpha indet.		VAL-06-16-01	0.5mm	Osteoderm
ML3816	Crocodylomorpha	Crocodylomorpha indet.		VAL-06-16-01	0.5mm	Osteoderm
ML3817	Crocodylomorpha	Crocodylomorpha indet.		VAL-06-16-01	0.5mm	Osteoderm
ML3818	Crocodylomorpha	Crocodylomorpha indet.		VAL-06-16-01	0.5mm	Osteoderm

ML3819	Crocodylomorpha	Crocodylomorpha indet.		VAL-06-16-01	0.5mm	Osteoderm
ML3820	Crocodylomorpha	Crocodylomorpha indet.		VAL-06-16-01	0.5mm	Osteoderm
ML3821	Crocodylomorpha	Crocodylomorpha indet.		VAL-06-16-01	0.5mm	Osteoderm
ML3822	Crocodylomorpha	Crocodylomorpha indet.		VAL-06-16-01	0.5mm	Osteoderm
ML3823	Crocodylomorpha	Crocodylomorpha indet.		VAL-06-16-01	0.5mm	Osteoderm
ML3824	Crocodylomorpha	Atoposauridae		PB-06-17-03	0.5mm	Isolated tooth
ML3825	Crocodylomorpha	Atoposauridae		PB-06-17-03	0.5mm	Isolated tooth
ML3826	Crocodylomorpha	Atoposauridae		PB-06-17-03	0.5mm	Isolated tooth
ML3827	Crocodylomorpha	Atoposauridae		PB-06-17-03	1mm	Isolated tooth
ML3828	Crocodylomorpha	Atoposauridae		PB-06-17-04	0.5mm	Isolated tooth
ML3829	Crocodylomorpha	Atoposauridae		PB-06-17-05	0.5mm	Isolated tooth
ML3830	Crocodylomorpha	Atoposauridae		PB-06-17-05	0.5mm	Isolated tooth
ML3831	Crocodylomorpha	Atoposauridae		PB-10-17-02	0.5mm	Isolated tooth
ML3832	Crocodylomorpha	Atoposauridae		PB-10-17-02	0.5mm	Isolated tooth
ML3833	Crocodylomorpha	Atoposauridae		PB-10-17-02	0.5mm	Isolated tooth
ML3834	Crocodylomorpha	Atoposauridae		PB-10-17-02	0.5mm	Isolated tooth
ML3835	Crocodylomorpha	Atoposauridae		PB-10-17-02	0.5mm	Isolated tooth
ML3836	Crocodylomorpha	Atoposauridae		PB-10-17-02	0.5mm	Isolated tooth
ML3837	Crocodylomorpha	Atoposauridae		PB-10-17-02	0.5mm	Isolated tooth
ML3838	Crocodylomorpha	Atoposauridae		PD-05-18-01	0.5mm	Isolated tooth
ML3839	Crocodylomorpha	Atoposauridae		VAL-03-19-04	1mm	Isolated tooth
ML3840	Crocodylomorpha	Atoposauridae		VAL-03-19-04	1mm	Isolated tooth
ML3841	Crocodylomorpha	Atoposauridae		VAL-03-19-04	0.5mm	Isolated tooth
ML3842	Crocodylomorpha	Atoposauridae		VAL-03-19-04	0.5mm	Isolated tooth
ML3843	Crocodylomorpha	Atoposauridae		VAL-03-19-04	0.5mm	Isolated tooth
ML3844	Crocodylomorpha	Atoposauridae		VAL-03-19-04	0.5mm	Isolated tooth
ML3845	Crocodylomorpha	Atoposauridae		VAL-03-19-04	0.5mm	Isolated tooth
ML3846	Crocodylomorpha	Atoposauridae		VAL-03-19-04	0.5mm	Isolated tooth
ML3847	Crocodylomorpha	Atoposauridae		VAL-03-19-04	0.5mm	Isolated tooth
ML3848	Crocodylomorpha	Atoposauridae		VAL-03-19-04	0.5mm	Isolated tooth
ML3849	Crocodylomorpha	Atoposauridae		VAL-03-19-04	0.5mm	Isolated tooth
ML3850	Crocodylomorpha	Atoposauridae		VAL-03-19-10	0.5mm	Isolated tooth
ML3851	Crocodylomorpha	Atoposauridae		VAL-03-19-10	0.5mm	Isolated tooth

ML3852	Crocodylomorpha	Atoposauridae		VAL-06-16-01	0.5mm	Isolated tooth
ML3853	Crocodylomorpha	Atoposauridae		VAL-06-16-01	0.5mm	Isolated tooth
ML3854	Crocodylomorpha	Atoposauridae		VAL-06-16-01	0.5mm	Isolated tooth
ML3855	Crocodylomorpha	Atoposauridae		VAL-06-16-01	0.5mm	Isolated tooth
ML3856	Crocodylomorpha	Atoposauridae		VAL-06-16-01	0.5mm	Isolated tooth
ML3857	Crocodylomorpha	Atoposauridae		VAL-06-16-01	0.5mm	Isolated tooth
ML3858	Crocodylomorpha	Atoposauridae		VAL-06-16-01	0.5mm	Isolated tooth
ML3859	Crocodylomorpha	Atoposauridae		VAL-06-16-01	0.5mm	Isolated tooth
ML3860	Crocodylomorpha	Atoposauridae		VAL-06-16-01	0.5mm	Isolated tooth
ML3861	Crocodylomorpha	Atoposauridae		VAL-06-16-01	0.5mm	Isolated tooth
ML3862	Crocodylomorpha	Atoposauridae		VAL-06-16-01	0.5mm	Isolated tooth
ML3863	Crocodylomorpha	Atoposauridae		VAL-06-16-01	0.5mm	Isolated tooth
ML3864	Crocodylomorpha	Atoposauridae		VAL-06-16-01	0.5mm	Isolated tooth
ML3865	Crocodylomorpha	Atoposauridae		VAL-06-16-01	0.5mm	Isolated tooth
ML3866	Crocodylomorpha	Atoposauridae		VAL-06-16-01	0.5mm	Isolated tooth
ML3867	Crocodylomorpha	Atoposauridae		VAL-06-16-01	0.5mm	Isolated tooth
ML3868	Crocodylomorpha	Atoposauridae		VAL-06-16-01	0.5mm	Isolated tooth
ML3869	Crocodylomorpha	Atoposauridae		VAL-06-16-01	0.5mm	Isolated tooth
ML3870	Crocodylomorpha	Atoposauridae		VAL-06-16-01	0.5mm	Isolated tooth
ML3871	Crocodylomorpha	Atoposauridae		VAL-06-16-01	0.5mm	Isolated tooth
ML3872	Crocodylomorpha	Atoposauridae		VAL-06-16-01	0.5mm	Isolated tooth
ML3873	Crocodylomorpha	Atoposauridae		VAL-06-16-01	0.5mm	Isolated tooth
ML3874	Crocodylomorpha	Atoposauridae		VAL-06-16-01	0.5mm	Isolated tooth
ML3875	Crocodylomorpha	Atoposauridae		VAL-06-16-01	0.5mm	Isolated tooth
ML3876	Crocodylomorpha	Atoposauridae		VAL-06-16-01	0.5mm	Isolated tooth
ML3877	Crocodylomorpha	Atoposauridae		VAL-06-16-01	0.5mm	Isolated tooth
ML3878	Crocodylomorpha	Atoposauridae		VAL-06-16-01	0.5mm	Isolated tooth
ML3879	Crocodylomorpha	Atoposauridae		VAL-06-16-01	0.5mm	Isolated tooth
ML3880	Crocodylomorpha	Atoposauridae		VAL-06-16-01	0.5mm	Isolated tooth
ML3881	Crocodylomorpha	Atoposauridae		VAL-06-16-01	0.5mm	Isolated tooth
ML3882	Crocodylomorpha	Atoposauridae		VAL-06-16-01	0.5mm	Isolated tooth
ML3883	Crocodylomorpha	Atoposauridae		VAL-06-16-01	0.5mm	Isolated tooth
ML3884	Crocodylomorpha	Atoposauridae		VAL-06-16-01	0.5mm	Isolated tooth

ML3885	Crocodylomorpha	Atoposauridae		VAL-06-16-01	0.5mm	Isolated tooth
ML3886	Crocodylomorpha	Atoposauridae		VAL-06-16-01	0.5mm	Isolated tooth
ML3887	Crocodylomorpha	Atoposauridae		VAL-06-16-01	0.5mm	Isolated tooth
ML3888	Crocodylomorpha	Atoposauridae		VAL-06-16-01	0.5mm	Isolated tooth
ML3889	Crocodylomorpha	Atoposauridae		VAL-06-16-01	0.5mm	Isolated tooth
ML3890	Crocodylomorpha	Atoposauridae		VAL-06-16-01	0.5mm	Isolated tooth
ML3891	Crocodylomorpha	Atoposauridae		VAL-06-16-01	0.5mm	Isolated tooth
ML3892	Crocodylomorpha	Atoposauridae		VAL-06-16-01	0.5mm	Isolated tooth
ML3893	Crocodylomorpha	Atoposauridae		VAL-06-16-01	0.5mm	Isolated tooth
ML3894	Crocodylomorpha	Atoposauridae		VAL-06-16-01	0.5mm	Isolated tooth
ML3895	Crocodylomorpha	Atoposauridae		VAL-06-16-01	0.5mm	Isolated tooth
ML3896	Crocodylomorpha	Atoposauridae		VAL-06-16-01	0.5mm	Isolated tooth
ML3897	Crocodylomorpha	Atoposauridae		VAL-06-16-01	0.5mm	Isolated tooth
ML3898	Crocodylomorpha	Atoposauridae		VAL-06-16-01	0.5mm	Isolated tooth
ML3899	Crocodylomorpha	Atoposauridae		VAL-06-16-01	0.5mm	Isolated tooth
ML3900	Crocodylomorpha	Atoposauridae		VAL-06-16-01	0.5mm	Isolated tooth
ML3901	Crocodylomorpha	Atoposauridae		VAL-06-16-01	0.5mm	Isolated tooth
ML3902	Crocodylomorpha	Atoposauridae		VAL-06-16-01	0.5mm	Isolated tooth
ML3903	Crocodylomorpha	Atoposauridae		VAL-06-16-01	0.5mm	Isolated tooth
ML3904	Crocodylomorpha	Atoposauridae		VAL-06-16-01	0.5mm	Isolated tooth
ML3905	Crocodylomorpha	Atoposauridae		VAL-06-16-01	0.5mm	Isolated tooth
ML3906	Crocodylomorpha	Atoposauridae		VAL-06-16-01	0.5mm	Isolated tooth
ML3907	Crocodylomorpha	Atoposauridae		VAL-06-16-01	0.5mm	Isolated tooth
ML3908	Crocodylomorpha	Atoposauridae		VAL-06-16-01	0.5mm	Isolated tooth
ML3909	Crocodylomorpha	Atoposauridae		VAL-06-16-01	0.5mm	Isolated tooth
ML3910	Crocodylomorpha	Atoposauridae		VAL-06-16-01	0.5mm	Isolated tooth
ML3911	Crocodylomorpha	Atoposauridae		VAL-06-16-01	0.5mm	Isolated tooth
ML3912	Crocodylomorpha	Atoposauridae		VAL-06-16-01	0.5mm	Isolated tooth
ML3913	Crocodylomorpha	Atoposauridae		VAL-06-16-01	0.5mm	Isolated tooth
ML3914	Crocodylomorpha	Atoposauridae		VAL-06-16-01	0.5mm	Isolated tooth
ML3915	Crocodylomorpha	Atoposauridae		VAL-06-16-01	0.5mm	Isolated tooth
ML3916	Crocodylomorpha	Atoposauridae		VAL-06-16-01	0.5mm	Isolated tooth
ML3917	Crocodylomorpha	Atoposauridae		VAL-06-16-01	0.5mm	Isolated tooth

ML3918	Crocodylomorpha	Atoposauridae		VAL-06-16-01	0.5mm	Isolated tooth
ML3919	Crocodylomorpha	Atoposauridae		VAL-06-16-01	0.5mm	Isolated tooth
ML3920	Crocodylomorpha	Atoposauridae		VAL-06-16-01	0.5mm	Isolated tooth
ML3921	Crocodylomorpha	Atoposauridae		VAL-06-16-01	0.5mm	Isolated tooth
ML3922	Crocodylomorpha	Atoposauridae		VAL-06-16-01	0.5mm	Isolated tooth
ML3923	Crocodylomorpha	Atoposauridae		VAL-06-16-01	0.5mm	Isolated tooth
ML3924	Crocodylomorpha	Atoposauridae		VAL-06-16-01	0.5mm	Isolated tooth
ML3925	Crocodylomorpha	Atoposauridae		VAL-06-16-01	0.5mm	Isolated tooth
ML3926	Crocodylomorpha	Atoposauridae		VAL-06-16-01	0.5mm	Isolated tooth
ML3927	Crocodylomorpha	Atoposauridae		VAL-06-16-01	0.5mm	Isolated tooth
ML3928	Crocodylomorpha	Atoposauridae		VAL-06-16-01	0.5mm	Isolated tooth
ML3929	Crocodylomorpha	Atoposauridae		VAL-06-16-01	0.5mm	Isolated tooth
ML3930	Crocodylomorpha	Atoposauridae		VAL-06-16-01	0.5mm	Isolated tooth
ML3931	Crocodylomorpha	Atoposauridae		VAL-06-16-01	0.5mm	Isolated tooth
ML3932	Crocodylomorpha	Atoposauridae		VAL-06-16-01	0.5mm	Isolated tooth
ML3933	Crocodylomorpha	Atoposauridae		VAL-06-16-01	0.5mm	Isolated tooth
ML3934	Crocodylomorpha	Atoposauridae		VAL-06-16-01	0.5mm	Isolated tooth
ML3935	Crocodylomorpha	Atoposauridae		VAL-06-16-01	0.5mm	Isolated tooth
ML3936	Crocodylomorpha	Atoposauridae		VAL-06-16-01	0.5mm	Isolated tooth
ML3937	Crocodylomorpha	Atoposauridae		VAL-06-16-01	0.5mm	Isolated tooth
ML3938	Crocodylomorpha	Atoposauridae		VAL-06-16-01	0.5mm	Isolated tooth
ML3939	Crocodylomorpha	Atoposauridae		VAL-06-16-01	0.5mm	Isolated tooth
ML3940	Crocodylomorpha	Atoposauridae		VAL-06-16-01	0.5mm	Isolated tooth
ML3941	Crocodylomorpha	Atoposauridae		VAL-06-16-01	0.5mm	Isolated tooth
ML3942	Crocodylomorpha	Atoposauridae		VAL-06-16-01	0.5mm	Isolated tooth
ML3943	Crocodylomorpha	Atoposauridae		VAL-06-16-01	0.5mm	Isolated tooth
ML3944	Crocodylomorpha	Atoposauridae		VAL-06-16-01	0.5mm	Isolated tooth
ML3945	Crocodylomorpha	Atoposauridae		VAL-10-17-01	0.5mm	Isolated tooth
ML3946	Crocodylomorpha	Atoposauridae		VAL-10-17-01	0.5mm	Isolated tooth
ML3947	Crocodylomorpha	Atoposauridae		VAL-10-17-01	0.5mm	Isolated tooth
ML3948	Crocodylomorpha	Atoposauridae		VAL-10-17-01	0.5mm	Isolated tooth
ML3949	Crocodylomorpha	Atoposauridae		VAL-10-17-01	0.5mm	Isolated tooth
ML3950	Crocodylomorpha	Atoposauridae		VAL-10-17-01	0.5mm	Isolated tooth

ML3951	Crocodylomorpha	Atoposauridae		VAL-10-17-01	0.5mm	Isolated tooth
ML3952	Crocodylomorpha	Atoposauridae		VAL-10-17-01	0.5mm	Isolated tooth
ML3953	Crocodylomorpha	Atoposauridae		VAL-10-17-01	0.5mm	Isolated tooth
ML3954	Crocodylomorpha	Atoposauridae		VAL-10-17-01	0.5mm	Isolated tooth
ML3955	Crocodylomorpha	Atoposauridae		VAL-10-17-01	0.5mm	Isolated tooth
ML3956	Crocodylomorpha	Atoposauridae		VAL-10-17-01	0.5mm	Isolated tooth
ML3957	Crocodylomorpha	Atoposauridae		VAL-10-17-01	0.5mm	Isolated tooth
ML3958	Crocodylomorpha	Atoposauridae		VAL-10-17-01	0.5mm	Isolated tooth
ML3959	Crocodylomorpha	Atoposauridae		VAL-10-17-01	0.5mm	Isolated tooth
ML3960	Crocodylomorpha	Atoposauridae		VAL-10-17-01	0.5mm	Isolated tooth
ML3961	Crocodylomorpha	Atoposauridae		VAL-10-17-01	0.5mm	Isolated tooth
ML3962	Crocodylomorpha	Atoposauridae		VAL-10-17-01	0.5mm	Isolated tooth
ML3963	Crocodylomorpha	Atoposauridae		VAL-10-17-01	0.5mm	Isolated tooth
ML3964	Crocodylomorpha	Atoposauridae		VAL-10-17-01	0.5mm	Isolated tooth
ML3965	Crocodylomorpha	Atoposauridae		VAL-10-17-01	0.5mm	Isolated tooth
ML3966	Crocodylomorpha	Atoposauridae		VAL-10-17-01	0.5mm	Isolated tooth
ML3967	Crocodylomorpha	Atoposauridae		VAL-10-17-01	0.5mm	Isolated tooth
ML3968	Crocodylomorpha	Atoposauridae		VAL-10-17-01	0.5mm	Isolated tooth
ML3969	Crocodylomorpha	Atoposauridae		VAL-10-17-01	0.5mm	Isolated tooth
ML3970	Crocodylomorpha	Atoposauridae		VAL-10-17-01	0.5mm	Isolated tooth
ML3971	Crocodylomorpha	Atoposauridae		VAL-10-17-01	0.5mm	Isolated tooth
ML3972	Crocodylomorpha	Atoposauridae		VAL-10-17-01	0.5mm	Isolated tooth
ML3973	Crocodylomorpha	Atoposauridae		VAL-10-17-01	0.5mm	Isolated tooth
ML3974	Crocodylomorpha	Atoposauridae		VAL-10-17-01	0.5mm	Isolated tooth
ML3975	Crocodylomorpha	Atoposauridae		VAL-10-17-01	0.5mm	Isolated tooth
ML3976	Crocodylomorpha	Atoposauridae		VAL-10-17-01	0.5mm	Isolated tooth
ML3977	Crocodylomorpha	Atoposauridae		VAL-10-17-01	0.5mm	Isolated tooth
ML3978	Crocodylomorpha	Atoposauridae		VAL-10-17-01	0.5mm	Isolated tooth
ML3979	Crocodylomorpha	Atoposauridae		ZIM-06-17-01	1mm	Isolated tooth
ML3980	Crocodylomorpha	Atoposauridae		ZIM-06-17-01	1mm	Isolated tooth
ML3981	Crocodylomorpha	Atoposauridae		ZIM-06-17-01	0.5mm	Isolated tooth
ML3982	Crocodylomorpha	Atoposauridae		ZIM-06-17-01	0.5mm	Isolated tooth
ML3983	Crocodylomorpha	Atoposauridae		ZIM-06-17-01	0.5mm	Isolated tooth

ML3984	Crocodylomorpha	Atoposauridae		ZIM-06-17-01	0.5mm	Isolated tooth
ML3985	Crocodylomorpha	Atoposauridae		ZIM-06-17-01	0.5mm	Isolated tooth
ML3986	Crocodylomorpha	Atoposauridae		ZIM-06-17-01	0.5mm	Isolated tooth
ML3987	Crocodylomorpha	Atoposauridae		ZIM-06-17-01	0.5mm	Isolated tooth
ML3988	Crocodylomorpha	Atoposauridae		ZIM-11-16-02	1mm	Isolated tooth
ML3989	Crocodylomorpha	Atoposauridae		ZIM-11-16-02	1mm	Isolated tooth
ML3990	Crocodylomorpha	Atoposauridae		ZIM-11-16-02	1mm	Isolated tooth
ML3991	Crocodylomorpha	Atoposauridae		ZIM-11-16-02	1mm	Isolated tooth
ML3992	Crocodylomorpha	Atoposauridae		ZIM-11-16-02	0.5mm	Isolated tooth
ML3993	Crocodylomorpha	Atoposauridae		ZIM-11-16-02	0.5mm	Isolated tooth
ML3994	Crocodylomorpha	Atoposauridae		ZIM-11-16-02	0.5mm	Isolated tooth
ML3995	Crocodylomorpha	Atoposauridae		ZIM-11-16-02	0.5mm	Isolated tooth
ML3996	Crocodylomorpha	Atoposauridae		ZIM-11-16-02	0.5mm	Isolated tooth
ML3997	Crocodylomorpha	Atoposauridae		ZIM-11-16-02	0.5mm	Isolated tooth
ML3998	Crocodylomorpha	Atoposauridae		ZIM-11-16-02	0.5mm	Isolated tooth
ML3999	Crocodylomorpha	Atoposauridae		ZIM-11-16-02	0.5mm	Isolated tooth
ML4000	Crocodylomorpha	Atoposauridae		ZIM-11-16-02	0.5mm	Isolated tooth
ML4001	Crocodylomorpha	Atoposauridae		ZIM-11-16-02	0.5mm	Isolated tooth
ML4002	Crocodylomorpha	Atoposauridae		ZIM-11-16-02	0.5mm	Isolated tooth
ML4003	Crocodylomorpha	Atoposauridae		ZIM-11-16-02	0.5mm	Isolated tooth
ML4004	Crocodylomorpha	Atoposauridae		ZIM-11-16-02	0.5mm	Isolated tooth
ML4005	Crocodylomorpha	Atoposauridae		ZIM-11-16-02	0.5mm	Isolated tooth
ML4006	Crocodylomorpha	Atoposauridae		ZIM-11-16-02	0.5mm	Isolated tooth
ML4007	Crocodylomorpha	Atoposauridae		ZIM-11-16-02	0.5mm	Isolated tooth
ML4008	Crocodylomorpha	Atoposauridae		ZIM-11-16-02	0.5mm	Isolated tooth
ML4009	Crocodylomorpha	Atoposauridae		ZIM-11-16-02	0.5mm	Isolated tooth
ML4010	Crocodylomorpha	Atoposauridae		ZIM-11-16-02	0.5mm	Isolated tooth
ML4011	Crocodylomorpha	Bernissartiidae		PB-06-17-03	1mm	Isolated tooth
ML4012	Crocodylomorpha	Bernissartiidae		PB-06-17-05	0.5mm	Isolated tooth
ML4013	Crocodylomorpha	Bernissartiidae		PB-10-17-02	0.5mm	Isolated tooth
ML4014	Crocodylomorpha	Bernissartiidae		VAL-03-19-04	1mm	Isolated tooth
ML4015	Crocodylomorpha	Bernissartiidae		VAL-03-19-04	1mm	Isolated tooth
ML4016	Crocodylomorpha	Bernissartiidae		VAL-03-19-04	0.5mm	Isolated tooth

ML4017	Crocodylomorpha	Bernissartiidae		VAL-03-19-04	0.5mm	Isolated tooth
ML4018	Crocodylomorpha	Bernissartiidae		VAL-03-19-04	0.5mm	Isolated tooth
ML4019	Crocodylomorpha	Bernissartiidae		VAL-03-19-04	0.5mm	Isolated tooth
ML4020	Crocodylomorpha	Bernissartiidae		VAL-03-19-04	0.5mm	Isolated tooth
ML4021	Crocodylomorpha	Bernissartiidae		VAL-03-19-04	0.5mm	Isolated tooth
ML4022	Crocodylomorpha	Bernissartiidae		VAL-03-19-04	0.5mm	Isolated tooth
ML4023	Crocodylomorpha	Bernissartiidae		VAL-03-19-10	0.5mm	Isolated tooth
ML4024	Crocodylomorpha	Bernissartiidae		VAL-03-19-10	0.5mm	Isolated tooth
ML4025	Crocodylomorpha	Bernissartiidae		VAL-06-16-01	0.5mm	Isolated tooth
ML4026	Crocodylomorpha	Bernissartiidae		VAL-06-16-01	0.5mm	Isolated tooth
ML4027	Crocodylomorpha	Bernissartiidae		VAL-06-16-01	0.5mm	Isolated tooth
ML4028	Crocodylomorpha	Bernissartiidae		VAL-06-16-01	0.5mm	Isolated tooth
ML4029	Crocodylomorpha	Bernissartiidae		VAL-06-16-01	0.5mm	Isolated tooth
ML4030	Crocodylomorpha	Bernissartiidae		VAL-06-16-01	0.5mm	Isolated tooth
ML4031	Crocodylomorpha	Bernissartiidae		VAL-06-16-01	0.5mm	Isolated tooth
ML4032	Crocodylomorpha	Bernissartiidae		VAL-06-16-01	0.5mm	Isolated tooth
ML4033	Crocodylomorpha	Bernissartiidae		VAL-06-16-01	0.5mm	Isolated tooth
ML4034	Crocodylomorpha	Bernissartiidae		VAL-06-16-01	0.5mm	Isolated tooth
ML4035	Crocodylomorpha	Bernissartiidae		VAL-06-16-01	0.5mm	Isolated tooth
ML4036	Crocodylomorpha	Bernissartiidae		VAL-06-16-01	0.5mm	Isolated tooth
ML4037	Crocodylomorpha	Bernissartiidae		VAL-06-16-01	0.5mm	Isolated tooth
ML4038	Crocodylomorpha	Bernissartiidae		VAL-06-16-01	0.5mm	Isolated tooth
ML4039	Crocodylomorpha	Bernissartiidae		VAL-06-16-01	0.5mm	Isolated tooth
ML4040	Crocodylomorpha	Bernissartiidae		VAL-06-16-01	0.5mm	Isolated tooth
ML4041	Crocodylomorpha	Bernissartiidae		VAL-06-16-01	0.5mm	Isolated tooth
ML4042	Crocodylomorpha	Bernissartiidae		VAL-06-16-01	0.5mm	Isolated tooth
ML4043	Crocodylomorpha	Bernissartiidae		VAL-06-16-01	0.5mm	Isolated tooth
ML4044	Crocodylomorpha	Bernissartiidae		VAL-06-16-01	0.5mm	Isolated tooth
ML4045	Crocodylomorpha	Bernissartiidae		VAL-06-16-01	0.5mm	Isolated tooth
ML4046	Crocodylomorpha	Bernissartiidae		VAL-06-16-01	0.5mm	Isolated tooth
ML4047	Crocodylomorpha	Bernissartiidae		VAL-06-16-01	0.5mm	Isolated tooth
ML4048	Crocodylomorpha	Bernissartiidae		VAL-06-16-01	0.5mm	Isolated tooth
ML4049	Crocodylomorpha	Bernissartiidae		VAL-06-16-01	0.5mm	Isolated tooth

ML4050	Crocodylomorpha	Bernissartiidae		VAL-06-16-01	0.5mm	Isolated tooth
ML4051	Crocodylomorpha	Bernissartiidae		VAL-06-16-01	0.5mm	Isolated tooth
ML4052	Crocodylomorpha	Bernissartiidae		VAL-06-16-01	0.5mm	Isolated tooth
ML4053	Crocodylomorpha	Bernissartiidae		VAL-06-16-01	0.5mm	Isolated tooth
ML4054	Crocodylomorpha	Bernissartiidae		VAL-06-16-01	0.5mm	Isolated tooth
ML4055	Crocodylomorpha	Bernissartiidae		VAL-06-16-01	0.5mm	Isolated tooth
ML4056	Crocodylomorpha	Bernissartiidae		VAL-06-16-01	0.5mm	Isolated tooth
ML4057	Crocodylomorpha	Bernissartiidae		VAL-06-16-01	0.5mm	Isolated tooth
ML4058	Crocodylomorpha	Bernissartiidae		VAL-06-16-01	0.5mm	Isolated tooth
ML4059	Crocodylomorpha	Bernissartiidae		VAL-06-16-01	0.5mm	Isolated tooth
ML4060	Crocodylomorpha	Bernissartiidae		VAL-06-16-01	0.5mm	Isolated tooth
ML4061	Crocodylomorpha	Bernissartiidae		VAL-06-16-01	0.5mm	Isolated tooth
ML4062	Crocodylomorpha	Bernissartiidae		VAL-06-16-01	0.5mm	Isolated tooth
ML4063	Crocodylomorpha	Bernissartiidae		VAL-06-16-01	0.5mm	Isolated tooth
ML4064	Crocodylomorpha	Bernissartiidae		VAL-06-16-01	0.5mm	Isolated tooth
ML4065	Crocodylomorpha	Bernissartiidae		VAL-06-16-01	0.5mm	Isolated tooth
ML4066	Crocodylomorpha	Bernissartiidae		VAL-06-16-01	0.5mm	Isolated tooth
ML4067	Crocodylomorpha	Bernissartiidae		VAL-06-16-01	0.5mm	Isolated tooth
ML4068	Crocodylomorpha	Bernissartiidae		VAL-06-16-01	0.5mm	Isolated tooth
ML4069	Crocodylomorpha	Bernissartiidae		VAL-06-16-01	0.5mm	Isolated tooth
ML4070	Crocodylomorpha	Bernissartiidae		VAL-06-16-01	0.5mm	Isolated tooth
ML4071	Crocodylomorpha	Bernissartiidae		VAL-06-16-01	0.5mm	Isolated tooth
ML4072	Crocodylomorpha	Bernissartiidae		VAL-06-16-01	0.5mm	Isolated tooth
ML4073	Crocodylomorpha	Bernissartiidae		VAL-06-16-01	0.5mm	Isolated tooth
ML4074	Crocodylomorpha	Bernissartiidae		VAL-06-16-01	0.5mm	Isolated tooth
ML4075	Crocodylomorpha	Bernissartiidae		VAL-06-16-01	0.5mm	Isolated tooth
ML4076	Crocodylomorpha	Bernissartiidae		VAL-06-16-01	0.5mm	Isolated tooth
ML4077	Crocodylomorpha	Bernissartiidae		VAL-06-16-01	0.5mm	Isolated tooth
ML4078	Crocodylomorpha	Bernissartiidae		VAL-06-16-01	0.5mm	Isolated tooth
ML4079	Crocodylomorpha	Bernissartiidae		VAL-06-16-01	0.5mm	Isolated tooth
ML4080	Crocodylomorpha	Bernissartiidae		VAL-06-16-01	0.5mm	Isolated tooth
ML4081	Crocodylomorpha	Bernissartiidae		VAL-10-17-01	0.5mm	Isolated tooth
ML4082	Crocodylomorpha	Bernissartiidae		VAL-10-17-01	0.5mm	Isolated tooth

ML4083	Crocodylomorpha	Bernissartiidae		VAL-10-17-01	0.5mm	Isolated tooth
ML4084	Crocodylomorpha	Bernissartiidae		VAL-10-17-01	0.5mm	Isolated tooth
ML4085	Crocodylomorpha	Bernissartiidae		VAL-10-17-01	0.5mm	Isolated tooth
ML4086	Crocodylomorpha	Bernissartiidae		VAL-10-17-01	0.5mm	Isolated tooth
ML4087	Crocodylomorpha	Bernissartiidae		VAL-10-17-01	0.5mm	Isolated tooth
ML4088	Crocodylomorpha	Bernissartiidae		VAL-10-17-01	0.5mm	Isolated tooth
ML4089	Crocodylomorpha	Bernissartiidae		VAL-10-17-01	0.5mm	Isolated tooth
ML4090	Crocodylomorpha	Bernissartiidae		VAL-10-17-01	0.5mm	Isolated tooth
ML4091	Crocodylomorpha	Bernissartiidae		VAL-10-17-01	0.5mm	Isolated tooth
ML4092	Crocodylomorpha	Bernissartiidae		VAL-10-17-01	0.5mm	Isolated tooth
ML4093	Crocodylomorpha	Bernissartiidae		VAL-10-17-01	0.5mm	Isolated tooth
ML4094	Crocodylomorpha	Bernissartiidae		VAL-10-17-01	0.5mm	Isolated tooth
ML4095	Crocodylomorpha	Bernissartiidae		VAL-10-17-01	0.5mm	Isolated tooth
ML4096	Crocodylomorpha	Bernissartiidae		VAL-10-17-01	0.5mm	Isolated tooth
ML4097	Crocodylomorpha	Bernissartiidae		VAL-10-17-01	0.5mm	Isolated tooth
ML4098	Crocodylomorpha	Bernissartiidae		VAL-10-17-01	0.5mm	Isolated tooth
ML4099	Crocodylomorpha	Bernissartiidae		VAL-10-17-01	0.5mm	Isolated tooth
ML4100	Crocodylomorpha	Bernissartiidae		VAL-10-17-01	0.5mm	Isolated tooth
ML4101	Crocodylomorpha	Bernissartiidae		VAL-10-17-01	0.5mm	Isolated tooth
ML4102	Crocodylomorpha	Bernissartiidae		VAL-10-17-01	0.5mm	Isolated tooth
ML4103	Crocodylomorpha	Bernissartiidae		VAL-10-17-01	0.5mm	Isolated tooth
ML4104	Crocodylomorpha	Bernissartiidae		VAL-10-17-01	0.5mm	Isolated tooth
ML4105	Crocodylomorpha	Bernissartiidae		VAL-10-17-01	0.5mm	Isolated tooth
ML4106	Crocodylomorpha	Bernissartiidae		VAL-10-17-01	0.5mm	Isolated tooth
ML4107	Crocodylomorpha	Bernissartiidae		VAL-10-17-01	0.5mm	Isolated tooth
ML4108	Crocodylomorpha	Bernissartiidae		VAL-10-17-01	0.5mm	Isolated tooth
ML4109	Crocodylomorpha	Bernissartiidae		VAL-10-17-01	0.5mm	Isolated tooth
ML4110	Crocodylomorpha	Bernissartiidae		VAL-10-17-01	0.5mm	Isolated tooth
ML4111	Crocodylomorpha	Bernissartiidae		VAL-10-17-01	0.5mm	Isolated tooth
ML4112	Crocodylomorpha	Bernissartiidae		VAL-10-17-01	0.5mm	Isolated tooth
ML4113	Crocodylomorpha	Bernissartiidae		VAL-10-17-01	0.5mm	Isolated tooth
ML4114	Crocodylomorpha	Bernissartiidae		VAL-10-17-01	0.5mm	Isolated tooth
ML4115	Crocodylomorpha	Bernissartiidae		VAL-10-17-01	0.5mm	Isolated tooth

ML4116	Crocodylomorpha	Bernissartiidae		VAL-10-17-01	0.5mm	Isolated tooth
ML4117	Crocodylomorpha	Bernissartiidae		ZIM-06-17-01	1mm	Isolated tooth
ML4118	Crocodylomorpha	Bernissartiidae		ZIM-06-17-01	1mm	Isolated tooth
ML4119	Crocodylomorpha	Bernissartiidae		ZIM-06-17-01	1mm	Isolated tooth
ML4120	Crocodylomorpha	Bernissartiidae		ZIM-06-17-01	1mm	Isolated tooth
ML4121	Crocodylomorpha	Bernissartiidae		ZIM-06-17-01	0.5mm	Isolated tooth
ML4122	Crocodylomorpha	Bernissartiidae		ZIM-06-17-01	0.5mm	Isolated tooth
ML4123	Crocodylomorpha	Bernissartiidae		ZIM-06-17-01	0.5mm	Isolated tooth
ML4124	Crocodylomorpha	Bernissartiidae		ZIM-06-17-01	0.5mm	Isolated tooth
ML4125	Crocodylomorpha	Bernissartiidae		ZIM-06-17-01	0.5mm	Isolated tooth
ML4126	Crocodylomorpha	Bernissartiidae		ZIM-06-17-01	0.5mm	Isolated tooth
ML4127	Crocodylomorpha	Bernissartiidae		ZIM-06-17-01	0.5mm	Isolated tooth
ML4128	Crocodylomorpha	Bernissartiidae		ZIM-06-17-01	0.5mm	Isolated tooth
ML4129	Crocodylomorpha	Bernissartiidae		ZIM-06-17-01	0.5mm	Isolated tooth
ML4130	Crocodylomorpha	Bernissartiidae		ZIM-06-17-01	0.5mm	Isolated tooth
ML4131	Crocodylomorpha	Bernissartiidae		ZIM-06-17-01	0.5mm	Isolated tooth
ML4132	Crocodylomorpha	Bernissartiidae		ZIM-06-17-01	0.5mm	Isolated tooth
ML4133	Crocodylomorpha	Bernissartiidae		ZIM-11-16-02	1mm	Isolated tooth
ML4134	Crocodylomorpha	Bernissartiidae		ZIM-11-16-02	1mm	Isolated tooth
ML4135	Crocodylomorpha	Bernissartiidae		ZIM-11-16-02	1mm	Isolated tooth
ML4136	Crocodylomorpha	Bernissartiidae		ZIM-11-16-02	0.5mm	Isolated tooth
ML4137	Crocodylomorpha	Bernissartiidae		ZIM-11-16-02	0.5mm	Isolated tooth
ML4138	Crocodylomorpha	Bernissartiidae		ZIM-11-16-02	0.5mm	Isolated tooth
ML4139	Crocodylomorpha	Bernissartiidae		ZIM-11-16-02	0.5mm	Isolated tooth
ML4140	Crocodylomorpha	Bernissartiidae		ZIM-11-16-02	0.5mm	Isolated tooth
ML4141	Crocodylomorpha	Bernissartiidae		ZIM-11-16-02	0.5mm	Isolated tooth
ML4142	Crocodylomorpha	Bernissartiidae		ZIM-11-16-02	0.5mm	Isolated tooth
ML4143	Crocodylomorpha	Bernissartiidae		ZIM-11-16-02	0.5mm	Isolated tooth
ML4144	Crocodylomorpha	Bernissartiidae		ZIM-11-16-02	0.5mm	Isolated tooth
ML4145	Crocodylomorpha	Bernissartiidae		ZIM-11-16-02	0.5mm	Isolated tooth
ML4146	Crocodylomorpha	Bernissartiidae		ZIM-11-16-02	0.5mm	Isolated tooth
ML4147	Crocodylomorpha	Bernissartiidae		ZIM-11-16-02	0.5mm	Isolated tooth
ML4148	Crocodylomorpha	Goniopholididae		PB-06-17-03	0.5mm	Isolated tooth

ML4149	Crocodylomorpha	Goniopholididae		PB-06-17-03	0.5mm	Isolated tooth
ML4150	Crocodylomorpha	Goniopholididae		PB-06-17-03	0.5mm	Isolated tooth
ML4151	Crocodylomorpha	Goniopholididae		PB-06-17-03	0.5mm	Isolated tooth
ML4152	Crocodylomorpha	Goniopholididae		PB-06-17-03	0.5mm	Isolated tooth
ML4153	Crocodylomorpha	Goniopholididae		PB-06-17-03	0.5mm	Isolated tooth
ML4154	Crocodylomorpha	Goniopholididae		PB-06-17-03	0.5mm	Isolated tooth
ML4155	Crocodylomorpha	Goniopholididae		PB-06-17-03	1mm	Isolated tooth
ML4156	Crocodylomorpha	Goniopholididae		PB-06-17-03	1mm	Isolated tooth
ML4157	Crocodylomorpha	Goniopholididae		PB-06-17-03	1mm	Isolated tooth
ML4158	Crocodylomorpha	Goniopholididae		PB-06-17-05	0.5mm	Isolated tooth
ML4159	Crocodylomorpha	Goniopholididae		PB-10-17-02	1mm	Isolated tooth
ML4160	Crocodylomorpha	Goniopholididae		PB-10-17-02	1mm	Isolated tooth
ML4161	Crocodylomorpha	Goniopholididae		PB-10-17-02	1mm	Isolated tooth
ML4162	Crocodylomorpha	Goniopholididae		PB-10-17-02	1mm	Isolated tooth
ML4163	Crocodylomorpha	Goniopholididae		PB-10-17-02	0.5mm	Isolated tooth
ML4164	Crocodylomorpha	Goniopholididae		PB-10-17-02	0.5mm	Isolated tooth
ML4165	Crocodylomorpha	Goniopholididae		PB-10-17-02	0.5mm	Isolated tooth
ML4166	Crocodylomorpha	Goniopholididae		PB-10-17-02	0.5mm	Isolated tooth
ML4167	Crocodylomorpha	Goniopholididae		PB-10-17-02	0.5mm	Isolated tooth
ML4168	Crocodylomorpha	Goniopholididae		VAL-03-19-03	2mm	Isolated tooth
ML4169	Crocodylomorpha	Goniopholididae		VAL-03-19-03	1mm	Isolated tooth
ML4170	Crocodylomorpha	Goniopholididae		VAL-03-19-04	1mm	Isolated tooth
ML4171	Crocodylomorpha	Goniopholididae		VAL-03-19-04	1mm	Isolated tooth
ML4172	Crocodylomorpha	Goniopholididae		VAL-03-19-04	1mm	Isolated tooth
ML4173	Crocodylomorpha	Goniopholididae		VAL-03-19-04	1mm	Isolated tooth
ML4174	Crocodylomorpha	Goniopholididae		VAL-03-19-04	0.5mm	Isolated tooth
ML4175	Crocodylomorpha	Goniopholididae		VAL-03-19-04	0.5mm	Isolated tooth
ML4176	Crocodylomorpha	Goniopholididae		VAL-03-19-04	0.5mm	Isolated tooth
ML4177	Crocodylomorpha	Goniopholididae		VAL-03-19-04	0.5mm	Isolated tooth
ML4178	Crocodylomorpha	Goniopholididae		VAL-03-19-04	0.5mm	Isolated tooth
ML4179	Crocodylomorpha	Goniopholididae		VAL-03-19-07	0.5mm	Isolated tooth
ML4180	Crocodylomorpha	Goniopholididae		VAL-03-19-10	0.5mm	Isolated tooth
ML4181	Crocodylomorpha	Goniopholididae		VAL-03-19-10	0.5mm	Isolated tooth

ML4182	Crocodylomorpha	Goniopholididae		VAL-06-16-01	0.5mm	Isolated tooth
ML4183	Crocodylomorpha	Goniopholididae		VAL-06-16-01	0.5mm	Isolated tooth
ML4184	Crocodylomorpha	Goniopholididae		VAL-06-16-01	0.5mm	Isolated tooth
ML4185	Crocodylomorpha	Goniopholididae		VAL-06-16-01	0.5mm	Isolated tooth
ML4186	Crocodylomorpha	Goniopholididae		VAL-06-16-01	0.5mm	Isolated tooth
ML4187	Crocodylomorpha	Goniopholididae		VAL-06-16-01	0.5mm	Isolated tooth
ML4188	Crocodylomorpha	Goniopholididae		VAL-06-16-01	0.5mm	Isolated tooth
ML4189	Crocodylomorpha	Goniopholididae		VAL-06-16-01	0.5mm	Isolated tooth
ML4190	Crocodylomorpha	Goniopholididae		VAL-06-16-01	0.5mm	Isolated tooth
ML4191	Crocodylomorpha	Goniopholididae		VAL-06-16-01	0.5mm	Isolated tooth
ML4192	Crocodylomorpha	Goniopholididae		VAL-06-16-01	0.5mm	Isolated tooth
ML4193	Crocodylomorpha	Goniopholididae		VAL-06-16-01	0.5mm	Isolated tooth
ML4194	Crocodylomorpha	Goniopholididae		VAL-06-16-01	0.5mm	Isolated tooth
ML4195	Crocodylomorpha	Goniopholididae		VAL-06-16-01	0.5mm	Isolated tooth
ML4196	Crocodylomorpha	Goniopholididae		VAL-06-16-01	0.5mm	Isolated tooth
ML4197	Crocodylomorpha	Goniopholididae		VAL-06-16-01	0.5mm	Isolated tooth
ML4198	Crocodylomorpha	Goniopholididae		VAL-06-16-01	0.5mm	Isolated tooth
ML4199	Crocodylomorpha	Goniopholididae		VAL-06-16-01	0.5mm	Isolated tooth
ML4200	Crocodylomorpha	Goniopholididae		VAL-06-16-01	0.5mm	Isolated tooth
ML4201	Crocodylomorpha	Goniopholididae		VAL-06-16-01	0.5mm	Isolated tooth
ML4202	Crocodylomorpha	Goniopholididae		VAL-06-16-01	0.5mm	Isolated tooth
ML4203	Crocodylomorpha	Goniopholididae		VAL-06-16-01	0.5mm	Isolated tooth
ML4204	Crocodylomorpha	Goniopholididae		VAL-06-16-01	0.5mm	Isolated tooth
ML4205	Crocodylomorpha	Goniopholididae		VAL-06-16-01	0.5mm	Isolated tooth
ML4206	Crocodylomorpha	Goniopholididae		VAL-06-16-01	0.5mm	Isolated tooth
ML4207	Crocodylomorpha	Goniopholididae		VAL-06-16-01	0.5mm	Isolated tooth
ML4208	Crocodylomorpha	Goniopholididae		VAL-06-16-01	0.5mm	Isolated tooth
ML4209	Crocodylomorpha	Goniopholididae		VAL-06-16-01	0.5mm	Isolated tooth
ML4210	Crocodylomorpha	Goniopholididae		VAL-06-16-01	0.5mm	Isolated tooth
ML4211	Crocodylomorpha	Goniopholididae		VAL-06-16-01	0.5mm	Isolated tooth
ML4212	Crocodylomorpha	Goniopholididae		VAL-06-16-01	0.5mm	Isolated tooth
ML4213	Crocodylomorpha	Goniopholididae		VAL-06-16-01	0.5mm	Isolated tooth
ML4214	Crocodylomorpha	Goniopholididae		VAL-06-16-01	0.5mm	Isolated tooth

ML4215	Crocodylomorpha	Goniopholididae		VAL-06-16-01	0.5mm	Isolated tooth
ML4216	Crocodylomorpha	Goniopholididae		VAL-06-16-01	0.5mm	Isolated tooth
ML4217	Crocodylomorpha	Goniopholididae		VAL-06-16-01	0.5mm	Isolated tooth
ML4218	Crocodylomorpha	Goniopholididae		VAL-06-16-01	0.5mm	Isolated tooth
ML4219	Crocodylomorpha	Goniopholididae		VAL-06-16-01	0.5mm	Isolated tooth
ML4220	Crocodylomorpha	Goniopholididae		VAL-06-16-01	0.5mm	Isolated tooth
ML4221	Crocodylomorpha	Goniopholididae		VAL-06-16-01	0.5mm	Isolated tooth
ML4222	Crocodylomorpha	Goniopholididae		VAL-06-16-01	0.5mm	Isolated tooth
ML4223	Crocodylomorpha	Goniopholididae		VAL-06-16-01	0.5mm	Isolated tooth
ML4224	Crocodylomorpha	Goniopholididae		VAL-06-16-01	0.5mm	Isolated tooth
ML4225	Crocodylomorpha	Goniopholididae		VAL-06-16-01	0.5mm	Isolated tooth
ML4226	Crocodylomorpha	Goniopholididae		VAL-06-16-01	0.5mm	Isolated tooth
ML4227	Crocodylomorpha	Goniopholididae		VAL-06-16-01	0.5mm	Isolated tooth
ML4228	Crocodylomorpha	Goniopholididae		VAL-06-16-01	0.5mm	Isolated tooth
ML4229	Crocodylomorpha	Goniopholididae		VAL-06-16-01	0.5mm	Isolated tooth
ML4230	Crocodylomorpha	Goniopholididae		VAL-06-16-01	0.5mm	Isolated tooth
ML4231	Crocodylomorpha	Goniopholididae		VAL-06-16-01	0.5mm	Isolated tooth
ML4232	Crocodylomorpha	Goniopholididae		VAL-06-16-01	0.5mm	Isolated tooth
ML4233	Crocodylomorpha	Goniopholididae		VAL-06-16-01	0.5mm	Isolated tooth
ML4234	Crocodylomorpha	Goniopholididae		VAL-06-16-01	0.5mm	Isolated tooth
ML4235	Crocodylomorpha	Goniopholididae		VAL-06-16-01	0.5mm	Isolated tooth
ML4236	Crocodylomorpha	Goniopholididae		VAL-06-16-01	0.5mm	Isolated tooth
ML4237	Crocodylomorpha	Goniopholididae		VAL-06-16-01	0.5mm	Isolated tooth
ML4238	Crocodylomorpha	Goniopholididae		VAL-06-16-01	0.5mm	Isolated tooth
ML4239	Crocodylomorpha	Goniopholididae		VAL-06-16-01	0.5mm	Isolated tooth
ML4240	Crocodylomorpha	Goniopholididae		VAL-06-16-01	0.5mm	Isolated tooth
ML4241	Crocodylomorpha	Goniopholididae		VAL-06-16-01	0.5mm	Isolated tooth
ML4242	Crocodylomorpha	Goniopholididae		VAL-06-16-01	0.5mm	Isolated tooth
ML4243	Crocodylomorpha	Goniopholididae		VAL-06-16-01	0.5mm	Isolated tooth
ML4244	Crocodylomorpha	Goniopholididae		VAL-06-16-01	0.5mm	Isolated tooth
ML4245	Crocodylomorpha	Goniopholididae		VAL-06-16-01	0.5mm	Isolated tooth
ML4246	Crocodylomorpha	Goniopholididae		VAL-06-16-01	0.5mm	Isolated tooth
ML4247	Crocodylomorpha	Goniopholididae		VAL-06-16-01	0.5mm	Isolated tooth

ML4248	Crocodylomorpha	Goniopholididae		VAL-06-16-01	0.5mm	Isolated tooth
ML4249	Crocodylomorpha	Goniopholididae		VAL-06-16-01	0.5mm	Isolated tooth
ML4250	Crocodylomorpha	Goniopholididae		VAL-06-16-01	0.5mm	Isolated tooth
ML4251	Crocodylomorpha	Goniopholididae		VAL-06-16-01	0.5mm	Isolated tooth
ML4252	Crocodylomorpha	Goniopholididae		VAL-06-16-01	0.5mm	Isolated tooth
ML4253	Crocodylomorpha	Goniopholididae		VAL-06-16-01	0.5mm	Isolated tooth
ML4254	Crocodylomorpha	Goniopholididae		VAL-06-16-01	0.5mm	Isolated tooth
ML4255	Crocodylomorpha	Goniopholididae		VAL-06-16-01	0.5mm	Isolated tooth
ML4256	Crocodylomorpha	Goniopholididae		VAL-06-16-01	0.5mm	Isolated tooth
ML4257	Crocodylomorpha	Goniopholididae		VAL-06-16-01	0.5mm	Isolated tooth
ML4258	Crocodylomorpha	Goniopholididae		VAL-06-16-01	0.5mm	Isolated tooth
ML4259	Crocodylomorpha	Goniopholididae		VAL-06-16-01	0.5mm	Isolated tooth
ML4260	Crocodylomorpha	Goniopholididae		VAL-06-16-01	0.5mm	Isolated tooth
ML4261	Crocodylomorpha	Goniopholididae		VAL-06-16-01	0.5mm	Isolated tooth
ML4262	Crocodylomorpha	Goniopholididae		VAL-06-16-01	0.5mm	Isolated tooth
ML4263	Crocodylomorpha	Goniopholididae		VAL-06-16-01	0.5mm	Isolated tooth
ML4264	Crocodylomorpha	Goniopholididae		VAL-06-16-01	0.5mm	Isolated tooth
ML4265	Crocodylomorpha	Goniopholididae		VAL-06-16-01	0.5mm	Isolated tooth
ML4266	Crocodylomorpha	Goniopholididae		VAL-06-16-01	0.5mm	Isolated tooth
ML4267	Crocodylomorpha	Goniopholididae		VAL-06-16-01	0.5mm	Isolated tooth
ML4268	Crocodylomorpha	Goniopholididae		VAL-06-16-01	0.5mm	Isolated tooth
ML4269	Crocodylomorpha	Goniopholididae		VAL-06-16-01	0.5mm	Isolated tooth
ML4270	Crocodylomorpha	Goniopholididae		VAL-06-16-01	0.5mm	Isolated tooth
ML4271	Crocodylomorpha	Goniopholididae		VAL-06-16-01	0.5mm	Isolated tooth
ML4272	Crocodylomorpha	Goniopholididae		VAL-06-16-01	0.5mm	Isolated tooth
ML4273	Crocodylomorpha	Goniopholididae		VAL-06-16-01	0.5mm	Isolated tooth
ML4274	Crocodylomorpha	Goniopholididae		VAL-06-16-01	0.5mm	Isolated tooth
ML4275	Crocodylomorpha	Goniopholididae		VAL-06-16-01	0.5mm	Isolated tooth
ML4276	Crocodylomorpha	Goniopholididae		VAL-06-16-01	0.5mm	Isolated tooth
ML4277	Crocodylomorpha	Goniopholididae		VAL-06-16-01	0.5mm	Isolated tooth
ML4278	Crocodylomorpha	Goniopholididae		VAL-06-16-01	0.5mm	Isolated tooth
ML4279	Crocodylomorpha	Goniopholididae		VAL-06-16-01	0.5mm	Isolated tooth
ML4280	Crocodylomorpha	Goniopholididae		VAL-06-16-01	0.5mm	Isolated tooth

ML4281	Crocodylomorpha	Goniopholididae		VAL-06-16-01	0.5mm	Isolated tooth
ML4282	Crocodylomorpha	Goniopholididae		VAL-06-16-01	0.5mm	Isolated tooth
ML4283	Crocodylomorpha	Goniopholididae		VAL-06-16-01	0.5mm	Isolated tooth
ML4284	Crocodylomorpha	Goniopholididae		VAL-06-16-01	0.5mm	Isolated tooth
ML4285	Crocodylomorpha	Goniopholididae		VAL-06-16-01	0.5mm	Isolated tooth
ML4286	Crocodylomorpha	Goniopholididae		VAL-06-16-01	0.5mm	Isolated tooth
ML4287	Crocodylomorpha	Goniopholididae		VAL-06-16-01	0.5mm	Isolated tooth
ML4288	Crocodylomorpha	Goniopholididae		VAL-06-16-01	0.5mm	Isolated tooth
ML4289	Crocodylomorpha	Goniopholididae		VAL-06-16-01	0.5mm	Isolated tooth
ML4290	Crocodylomorpha	Goniopholididae		VAL-06-16-01	0.5mm	Isolated tooth
ML4291	Crocodylomorpha	Goniopholididae		VAL-06-16-01	0.5mm	Isolated tooth
ML4292	Crocodylomorpha	Goniopholididae		VAL-06-16-01	0.5mm	Isolated tooth
ML4293	Crocodylomorpha	Goniopholididae		VAL-06-16-01	0.5mm	Isolated tooth
ML4294	Crocodylomorpha	Goniopholididae		VAL-06-16-01	0.5mm	Isolated tooth
ML4295	Crocodylomorpha	Goniopholididae		VAL-06-16-01	0.5mm	Isolated tooth
ML4296	Crocodylomorpha	Goniopholididae		VAL-06-16-01	0.5mm	Isolated tooth
ML4297	Crocodylomorpha	Goniopholididae		VAL-06-16-01	0.5mm	Isolated tooth
ML4298	Crocodylomorpha	Goniopholididae		VAL-06-16-01	0.5mm	Isolated tooth
ML4299	Crocodylomorpha	Goniopholididae		VAL-06-16-01	0.5mm	Isolated tooth
ML4300	Crocodylomorpha	Goniopholididae		VAL-06-16-01	0.5mm	Isolated tooth
ML4301	Crocodylomorpha	Goniopholididae		VAL-06-16-01	0.5mm	Isolated tooth
ML4302	Crocodylomorpha	Goniopholididae		VAL-06-16-01	0.5mm	Isolated tooth
ML4303	Crocodylomorpha	Goniopholididae		VAL-06-16-01	0.5mm	Isolated tooth
ML4304	Crocodylomorpha	Goniopholididae		VAL-06-16-01	0.5mm	Isolated tooth
ML4305	Crocodylomorpha	Goniopholididae		VAL-06-16-01	0.5mm	Isolated tooth
ML4306	Crocodylomorpha	Goniopholididae		VAL-06-16-01	0.5mm	Isolated tooth
ML4307	Crocodylomorpha	Goniopholididae		VAL-06-16-01	0.5mm	Isolated tooth
ML4308	Crocodylomorpha	Goniopholididae		VAL-06-16-01	0.5mm	Isolated tooth
ML4309	Crocodylomorpha	Goniopholididae		VAL-06-16-01	0.5mm	Isolated tooth
ML4310	Crocodylomorpha	Goniopholididae		VAL-06-16-01	0.5mm	Isolated tooth
ML4311	Crocodylomorpha	Goniopholididae		VAL-06-16-01	0.5mm	Isolated tooth
ML4312	Crocodylomorpha	Goniopholididae		VAL-06-16-01	0.5mm	Isolated tooth
ML4313	Crocodylomorpha	Goniopholididae		VAL-06-16-01	0.5mm	Isolated tooth

ML4314	Crocodylomorpha	Goniopholididae		VAL-06-16-01	0.5mm	Isolated tooth
ML4315	Crocodylomorpha	Goniopholididae		VAL-06-16-01	0.5mm	Isolated tooth
ML4316	Crocodylomorpha	Goniopholididae		VAL-06-16-01	0.5mm	Isolated tooth
ML4317	Crocodylomorpha	Goniopholididae		VAL-06-16-01	0.5mm	Isolated tooth
ML4318	Crocodylomorpha	Goniopholididae		VAL-06-16-01	0.5mm	Isolated tooth
ML4319	Crocodylomorpha	Goniopholididae		VAL-06-16-01	0.5mm	Isolated tooth
ML4320	Crocodylomorpha	Goniopholididae		VAL-06-16-01	0.5mm	Isolated tooth
ML4321	Crocodylomorpha	Goniopholididae		VAL-06-16-01	0.5mm	Isolated tooth
ML4322	Crocodylomorpha	Goniopholididae		VAL-06-16-01	0.5mm	Isolated tooth
ML4323	Crocodylomorpha	Goniopholididae		VAL-06-16-01	0.5mm	Isolated tooth
ML4324	Crocodylomorpha	Goniopholididae		VAL-06-16-01	0.5mm	Isolated tooth
ML4325	Crocodylomorpha	Goniopholididae		VAL-06-16-01	0.5mm	Isolated tooth
ML4326	Crocodylomorpha	Goniopholididae		VAL-06-16-01	0.5mm	Isolated tooth
ML4327	Crocodylomorpha	Goniopholididae		VAL-10-17-01	0.5mm	Isolated tooth
ML4328	Crocodylomorpha	Goniopholididae		VAL-10-17-01	0.5mm	Isolated tooth
ML4329	Crocodylomorpha	Goniopholididae		VAL-10-17-01	0.5mm	Isolated tooth
ML4330	Crocodylomorpha	Goniopholididae		VAL-10-17-01	0.5mm	Isolated tooth
ML4331	Crocodylomorpha	Goniopholididae		VAL-10-17-01	0.5mm	Isolated tooth
ML4332	Crocodylomorpha	Goniopholididae		VAL-10-17-01	0.5mm	Isolated tooth
ML4333	Crocodylomorpha	Goniopholididae		VAL-10-17-01	0.5mm	Isolated tooth
ML4334	Crocodylomorpha	Goniopholididae		VAL-10-17-01	0.5mm	Isolated tooth
ML4335	Crocodylomorpha	Goniopholididae		VAL-10-17-01	0.5mm	Isolated tooth
ML4336	Crocodylomorpha	Goniopholididae		VAL-10-17-01	0.5mm	Isolated tooth
ML4337	Crocodylomorpha	Goniopholididae		VAL-10-17-01	0.5mm	Isolated tooth
ML4338	Crocodylomorpha	Goniopholididae		VAL-10-17-01	0.5mm	Isolated tooth
ML4339	Crocodylomorpha	Goniopholididae		VAL-10-17-01	0.5mm	Isolated tooth
ML4340	Crocodylomorpha	Goniopholididae		VAL-10-17-01	0.5mm	Isolated tooth
ML4341	Crocodylomorpha	Goniopholididae		VAL-10-17-01	0.5mm	Isolated tooth
ML4342	Crocodylomorpha	Goniopholididae		VAL-10-17-01	0.5mm	Isolated tooth
ML4343	Crocodylomorpha	Goniopholididae		VAL-10-17-01	0.5mm	Isolated tooth
ML4344	Crocodylomorpha	Goniopholididae		VAL-10-17-01	0.5mm	Isolated tooth
ML4345	Crocodylomorpha	Goniopholididae		VAL-10-17-01	0.5mm	Isolated tooth
ML4346	Crocodylomorpha	Goniopholididae		VAL-10-17-01	0.5mm	Isolated tooth

ML4347	Crocodylomorpha	Goniopholididae		VAL-10-17-01	0.5mm	Isolated tooth
ML4348	Crocodylomorpha	Goniopholididae		VAL-10-17-01	0.5mm	Isolated tooth
ML4349	Crocodylomorpha	Goniopholididae		VAL-10-17-01	0.5mm	Isolated tooth
ML4350	Crocodylomorpha	Goniopholididae		VAL-10-17-01	0.5mm	Isolated tooth
ML4351	Crocodylomorpha	Goniopholididae		VAL-10-17-01	0.5mm	Isolated tooth
ML4352	Crocodylomorpha	Goniopholididae		VAL-10-17-01	0.5mm	Isolated tooth
ML4353	Crocodylomorpha	Goniopholididae		VAL-10-17-01	0.5mm	Isolated tooth
ML4354	Crocodylomorpha	Goniopholididae		VAL-10-17-01	0.5mm	Isolated tooth
ML4355	Crocodylomorpha	Goniopholididae		VAL-10-17-01	0.5mm	Isolated tooth
ML4356	Crocodylomorpha	Goniopholididae		VAL-10-17-01	0.5mm	Isolated tooth
ML4357	Crocodylomorpha	Goniopholididae		VAL-10-17-01	0.5mm	Isolated tooth
ML4358	Crocodylomorpha	Goniopholididae		VAL-10-17-01	0.5mm	Isolated tooth
ML4359	Crocodylomorpha	Goniopholididae		VAL-10-17-01	0.5mm	Isolated tooth
ML4360	Crocodylomorpha	Goniopholididae		VAL-10-17-01	0.5mm	Isolated tooth
ML4361	Crocodylomorpha	Goniopholididae		VAL-10-17-01	0.5mm	Isolated tooth
ML4362	Crocodylomorpha	Goniopholididae		VAL-10-17-01	0.5mm	Isolated tooth
ML4363	Crocodylomorpha	Goniopholididae		VAL-10-17-01	0.5mm	Isolated tooth
ML4364	Crocodylomorpha	Goniopholididae		VAL-10-17-01	0.5mm	Isolated tooth
ML4365	Crocodylomorpha	Goniopholididae		VAL-10-17-01	0.5mm	Isolated tooth
ML4366	Crocodylomorpha	Goniopholididae		VAL-10-17-01	0.5mm	Isolated tooth
ML4367	Crocodylomorpha	Goniopholididae		VAL-10-17-01	0.5mm	Isolated tooth
ML4368	Crocodylomorpha	Goniopholididae		VAL-10-17-01	0.5mm	Isolated tooth
ML4369	Crocodylomorpha	Goniopholididae		VAL-10-17-01	0.5mm	Isolated tooth
ML4370	Crocodylomorpha	Goniopholididae		VAL-10-17-01	0.5mm	Isolated tooth
ML4371	Crocodylomorpha	Goniopholididae		ZIM-06-17-01	1mm	Isolated tooth
ML4372	Crocodylomorpha	Goniopholididae		ZIM-06-17-01	1mm	Isolated tooth
ML4373	Crocodylomorpha	Goniopholididae		ZIM-06-17-01	0.5mm	Isolated tooth
ML4374	Crocodylomorpha	Goniopholididae		ZIM-06-17-01	0.5mm	Isolated tooth
ML4375	Crocodylomorpha	Goniopholididae		ZIM-06-17-01	0.5mm	Isolated tooth
ML4376	Crocodylomorpha	Goniopholididae		ZIM-06-17-01	0.5mm	Isolated tooth
ML4377	Crocodylomorpha	Goniopholididae		ZIM-06-17-01	0.5mm	Isolated tooth
ML4378	Crocodylomorpha	Goniopholididae		ZIM-06-17-01	0.5mm	Isolated tooth
ML4379	Crocodylomorpha	Goniopholididae		ZIM-06-17-01	0.5mm	Isolated tooth

ML4380	Crocodylomorpha	Goniopholididae		ZIM-06-17-01	0.5mm	Isolated tooth
ML4381	Crocodylomorpha	Goniopholididae		ZIM-06-17-01	0.5mm	Isolated tooth
ML4382	Crocodylomorpha	Goniopholididae		ZIM-06-17-01	0.5mm	Isolated tooth
ML4383	Crocodylomorpha	Goniopholididae		ZIM-06-17-01	0.5mm	Isolated tooth
ML4384	Crocodylomorpha	Goniopholididae		ZIM-06-17-01	0.5mm	Isolated tooth
ML4385	Crocodylomorpha	Goniopholididae		ZIM-06-17-01	0.5mm	Isolated tooth
ML4386	Crocodylomorpha	Goniopholididae		ZIM-06-17-01	0.5mm	Isolated tooth
ML4387	Crocodylomorpha	Goniopholididae		ZIM-06-17-01	0.5mm	Isolated tooth
ML4388	Crocodylomorpha	Goniopholididae		ZIM-06-17-01	0.5mm	Isolated tooth
ML4389	Crocodylomorpha	Goniopholididae		ZIM-06-17-01	0.5mm	Isolated tooth
ML4390	Crocodylomorpha	Goniopholididae		ZIM-06-17-01	0.5mm	Isolated tooth
ML4391	Crocodylomorpha	Goniopholididae		ZIM-06-17-01	0.5mm	Isolated tooth
ML4392	Crocodylomorpha	Goniopholididae		ZIM-06-17-01	0.5mm	Isolated tooth
ML4393	Crocodylomorpha	Goniopholididae		ZIM-06-17-01	0.5mm	Isolated tooth
ML4394	Crocodylomorpha	Goniopholididae		ZIM-06-17-01	0.5mm	Isolated tooth
ML4395	Crocodylomorpha	Goniopholididae		ZIM-06-17-01	0.5mm	Isolated tooth
ML4396	Crocodylomorpha	Goniopholididae		ZIM-06-17-01	0.5mm	Isolated tooth
ML4397	Crocodylomorpha	Goniopholididae		ZIM-06-17-01	0.5mm	Isolated tooth
ML4398	Crocodylomorpha	Goniopholididae		ZIM-11-16-02	1mm	Isolated tooth
ML4399	Crocodylomorpha	Goniopholididae		ZIM-11-16-02	1mm	Isolated tooth
ML4400	Crocodylomorpha	Goniopholididae		ZIM-11-16-02	1mm	Isolated tooth
ML4401	Crocodylomorpha	Goniopholididae		ZIM-11-16-02	1mm	Isolated tooth
ML4402	Crocodylomorpha	Goniopholididae		ZIM-11-16-02	0.5mm	Isolated tooth
ML4403	Crocodylomorpha	Goniopholididae		ZIM-11-16-02	0.5mm	Isolated tooth
ML4404	Crocodylomorpha	Goniopholididae		ZIM-11-16-02	0.5mm	Isolated tooth
ML4405	Crocodylomorpha	Goniopholididae		ZIM-11-16-02	0.5mm	Isolated tooth
ML4406	Crocodylomorpha	Goniopholididae		ZIM-11-16-02	0.5mm	Isolated tooth
ML4407	Crocodylomorpha	Goniopholididae		ZIM-11-16-02	0.5mm	Isolated tooth
ML4408	Crocodylomorpha	Goniopholididae		ZIM-11-16-02	0.5mm	Isolated tooth
ML4409	Crocodylomorpha	Goniopholididae		ZIM-11-16-02	0.5mm	Isolated tooth
ML4410	Crocodylomorpha	Goniopholididae		ZIM-11-16-02	0.5mm	Isolated tooth
ML4411	Crocodylomorpha	Goniopholididae		ZIM-11-16-02	0.5mm	Isolated tooth
ML4412	Crocodylomorpha	Goniopholididae		ZIM-11-16-02	0.5mm	Isolated tooth

ML4413	Crocodylomorpha	Goniopholididae		ZIM-11-16-02	0.5mm	Isolated tooth
ML4414	Crocodylomorpha	Goniopholididae		ZIM-11-16-02	0.5mm	Isolated tooth
ML4415	Crocodylomorpha	Goniopholididae		ZIM-11-16-02	0.5mm	Isolated tooth
ML4416	Crocodylomorpha	Goniopholididae		ZIM-11-16-02	0.5mm	Isolated tooth
ML4417	Crocodylomorpha	Goniopholididae		ZIM-11-16-02	0.5mm	Isolated tooth
ML4418	Crocodylomorpha	Goniopholididae		ZIM-11-16-02	0.5mm	Isolated tooth
ML4419	Crocodylomorpha	Goniopholididae		ZIM-11-16-02	0.5mm	Isolated tooth
ML4420	Crocodylomorpha	Goniopholididae		ZIM-11-16-02	0.5mm	Isolated tooth
ML4421	Crocodylomorpha	Goniopholididae		ZIM-11-16-02	0.5mm	Isolated tooth
ML4422	Crocodylomorpha	Goniopholididae		ZIM-11-16-02	0.5mm	Isolated tooth
ML4423	Crocodylomorpha	Goniopholididae		ZIM-11-16-02	0.5mm	Isolated tooth
ML4424	Crocodylomorpha	Goniopholididae		ZIM-11-16-02	0.5mm	Isolated tooth
ML4425	Crocodylomorpha	Goniopholididae		ZIM-11-16-02	0.5mm	Isolated tooth
ML4426	Crocodylomorpha	Goniopholididae		ZIM-11-16-02	0.5mm	Isolated tooth
ML4427	Crocodylomorpha	Goniopholididae		ZIM-11-16-02	0.5mm	Isolated tooth
ML4428	Crocodylomorpha	Goniopholididae		ZIM-11-16-02	0.5mm	Isolated tooth
ML4429	Crocodylomorpha	Goniopholididae		ZIM-11-16-02	0.5mm	Isolated tooth
ML4430	Crocodylomorpha	Goniopholididae		ZIM-11-16-02	0.5mm	Isolated tooth
ML4431	Crocodylomorpha	Goniopholididae		ZIM-11-16-02	0.5mm	Isolated tooth
ML4432	Crocodylomorpha	Goniopholididae		ZIM-11-16-02	0.5mm	Isolated tooth
ML4433	Crocodylomorpha	Crocodylomorpha indet.		PB-10-17-02	0.5mm	Isolated tooth
ML4434	Crocodylomorpha	Crocodylomorpha indet.		PB-10-17-02	0.5mm	Isolated tooth
ML4435	Crocodylomorpha	Crocodylomorpha indet.		VAL-03-19-04	0.5mm	Isolated tooth
ML4436	Crocodylomorpha	Crocodylomorpha indet.		VAL-03-19-04	0.5mm	Isolated tooth
ML4437	Crocodylomorpha	Crocodylomorpha indet.		VAL-03-19-04	0.5mm	Isolated tooth
ML4438	Crocodylomorpha	Crocodylomorpha indet.		VAL-03-19-04	0.5mm	Isolated tooth
ML4439	Crocodylomorpha	Crocodylomorpha indet.		VAL-03-19-04	0.5mm	Isolated tooth
ML4440	Crocodylomorpha	Crocodylomorpha indet.		VAL-03-19-04	0.5mm	Isolated tooth
ML4441	Crocodylomorpha	Crocodylomorpha indet.		VAL-03-19-04	0.5mm	Isolated tooth
ML4442	Crocodylomorpha	Crocodylomorpha indet.		VAL-06-16-01	0.5mm	Isolated tooth
ML4443	Crocodylomorpha	Crocodylomorpha indet.		VAL-06-16-01	0.5mm	Isolated tooth
ML4444	Crocodylomorpha	Crocodylomorpha indet.		VAL-06-16-01	0.5mm	Isolated tooth
ML4445	Crocodylomorpha	Crocodylomorpha indet.		VAL-06-16-01	0.5mm	Isolated tooth

ML4446	Crocodylomorpha	Crocodylomorpha indet.		VAL-06-16-01	0.5mm	Isolated tooth
ML4447	Crocodylomorpha	Crocodylomorpha indet.		VAL-06-16-01	0.5mm	Isolated tooth
ML4448	Crocodylomorpha	Crocodylomorpha indet.		VAL-06-16-01	0.5mm	Isolated tooth
ML4449	Crocodylomorpha	Crocodylomorpha indet.		VAL-06-16-01	0.5mm	Isolated tooth
ML4450	Crocodylomorpha	Crocodylomorpha indet.		VAL-06-16-01	0.5mm	Isolated tooth
ML4451	Crocodylomorpha	Crocodylomorpha indet.		VAL-06-16-01	0.5mm	Isolated tooth
ML4452	Crocodylomorpha	Crocodylomorpha indet.		VAL-06-16-01	0.5mm	Isolated tooth
ML4453	Crocodylomorpha	Crocodylomorpha indet.		VAL-06-16-01	0.5mm	Isolated tooth
ML4454	Crocodylomorpha	Crocodylomorpha indet.		VAL-06-16-01	0.5mm	Isolated tooth
ML4455	Crocodylomorpha	Crocodylomorpha indet.		VAL-06-16-01	0.5mm	Isolated tooth
ML4456	Crocodylomorpha	Crocodylomorpha indet.		VAL-06-16-01	0.5mm	Isolated tooth
ML4457	Crocodylomorpha	Crocodylomorpha indet.		VAL-06-16-01	0.5mm	Isolated tooth
ML4458	Crocodylomorpha	Crocodylomorpha indet.		VAL-06-16-01	0.5mm	Isolated tooth
ML4459	Crocodylomorpha	Crocodylomorpha indet.		VAL-06-16-01	0.5mm	Isolated tooth
ML4460	Crocodylomorpha	Crocodylomorpha indet.		VAL-06-16-01	0.5mm	Isolated tooth
ML4461	Crocodylomorpha	Crocodylomorpha indet.		VAL-06-16-01	0.5mm	Isolated tooth
ML4462	Crocodylomorpha	Crocodylomorpha indet.		VAL-06-16-01	0.5mm	Isolated tooth
ML4463	Crocodylomorpha	Crocodylomorpha indet.		VAL-06-16-01	0.5mm	Isolated tooth
ML4464	Crocodylomorpha	Crocodylomorpha indet.		VAL-06-16-01	0.5mm	Isolated tooth
ML4465	Crocodylomorpha	Crocodylomorpha indet.		VAL-06-16-01	0.5mm	Isolated tooth
ML4466	Crocodylomorpha	Crocodylomorpha indet.		VAL-06-16-01	0.5mm	Isolated tooth
ML4467	Crocodylomorpha	Crocodylomorpha indet.		VAL-06-16-01	0.5mm	Isolated tooth
ML4468	Crocodylomorpha	Crocodylomorpha indet.		VAL-06-16-01	0.5mm	Isolated tooth
ML4469	Crocodylomorpha	Crocodylomorpha indet.		ZIM-06-17-01	0.5mm	Isolated tooth
ML4470	Crocodylomorpha	Crocodylomorpha indet.		ZIM-06-17-01	0.5mm	Isolated tooth
ML4471	Crocodylomorpha	Crocodylomorpha indet.		ZIM-06-17-01	0.5mm	Isolated tooth
ML4472	Crocodylomorpha	Crocodylomorpha indet.		ZIM-06-17-01	0.5mm	Isolated tooth
ML4473	Crocodylomorpha	Crocodylomorpha indet.		ZIM-06-17-01	0.5mm	Isolated tooth
ML4474	Crocodylomorpha	Crocodylomorpha indet.		ZIM-06-17-01	0.5mm	Isolated tooth
ML4475	Crocodylomorpha	Crocodylomorpha indet.		ZIM-06-17-01	0.5mm	Isolated tooth
ML4476	Crocodylomorpha	Crocodylomorpha indet.		ZIM-06-17-01	0.5mm	Isolated tooth
ML4477	Crocodylomorpha	Crocodylomorpha indet.		ZIM-06-17-04	0.5mm	Isolated tooth
ML4478	Crocodylomorpha	Crocodylomorpha indet.		ZIM-11-16-02	0.5mm	Isolated tooth

ML4479	Crocodylomorpha	Crocodylomorpha indet.		ZIM-11-16-02	0.5mm	Isolated tooth
ML4480	Crocodylomorpha	Crocodylomorpha indet.		ZIM-11-16-02	0.5mm	Isolated tooth
ML4481	Crocodylomorpha	Crocodylomorpha indet.		ZIM-11-16-02	0.5mm	Isolated tooth
ML4482	Crocodylomorpha	Crocodylomorpha indet.		ZIM-11-16-02	0.5mm	Isolated tooth
ML4483	Crocodylomorpha	Crocodylomorpha indet.		ZIM-11-16-02	0.5mm	Isolated tooth
ML4484	Crocodylomorpha	Crocodylomorpha indet.		ZIM-11-16-02	0.5mm	Isolated tooth
ML4485	Crocodylomorpha	Crocodylomorpha indet.		ZIM-11-16-02	0.5mm	Isolated tooth
ML4486	Crocodylomorpha	Crocodylomorpha indet.		ZIM-11-16-02	0.5mm	Isolated tooth
ML4487	Crocodylomorpha	Crocodylomorpha indet.		ZIM-11-16-02	0.5mm	Isolated tooth
ML4488	Crocodylomorpha	Crocodylomorpha indet.		ZIM-11-16-02	0.5mm	Isolated tooth
ML4489	Crocodylomorpha	Crocodylomorpha indet.		ZIM-11-16-02	0.5mm	Isolated tooth
ML4490	Crocodylomorpha	Crocodylomorpha indet.		ZIM-11-16-02	0.5mm	Isolated tooth
ML4491	Crocodylomorpha	Crocodylomorpha indet.		ZIM-11-16-02	0.5mm	Isolated tooth
ML4492	Crocodylomorpha	Crocodylomorpha indet.		ZIM-11-16-02	0.5mm	Isolated tooth
ML4493	Crocodylomorpha		*Lusitanisuchus*	PB-06-17-03	0.5mm	Isolated tooth
ML4494	Crocodylomorpha		*Lusitanisuchus*	VAL-03-19-04	0.5mm	Isolated tooth
ML4495	Crocodylomorpha		*Lusitanisuchus*	VAL-03-19-04	0.5mm	Isolated tooth
ML4496	Crocodylomorpha		*Lusitanisuchus*	VAL-03-19-04	0.5mm	Isolated tooth
ML4497	Crocodylomorpha		*Lusitanisuchus*	VAL-06-16-01	0.5mm	Isolated tooth
ML4498	Crocodylomorpha		*Lusitanisuchus*	VAL-06-16-01	0.5mm	Isolated tooth
ML4499	Crocodylomorpha		*Lusitanisuchus*	VAL-06-16-01	0.5mm	Isolated tooth
ML4500	Crocodylomorpha		*Lusitanisuchus*	VAL-06-16-01	0.5mm	Isolated tooth
ML4501	Crocodylomorpha		*Lusitanisuchus*	VAL-06-16-01	0.5mm	Isolated tooth
ML4502	Crocodylomorpha		*Lusitanisuchus*	VAL-06-16-01	0.5mm	Isolated tooth
ML4503	Crocodylomorpha		*Lusitanisuchus*	VAL-06-16-01	0.5mm	Isolated tooth
ML4504	Crocodylomorpha		*Lusitanisuchus*	VAL-06-16-01	0.5mm	Isolated tooth
ML4505	Crocodylomorpha		*Lusitanisuchus*	VAL-06-16-01	0.5mm	Isolated tooth
ML4506	Crocodylomorpha		*Lusitanisuchus*	VAL-06-16-01	0.5mm	Isolated tooth
ML4507	Crocodylomorpha		*Lusitanisuchus*	VAL-06-16-01	0.5mm	Isolated tooth
ML4508	Crocodylomorpha		*Lusitanisuchus*	VAL-06-16-01	0.5mm	Isolated tooth
ML4509	Crocodylomorpha		*Lusitanisuchus*	VAL-06-16-01	0.5mm	Isolated tooth
ML4510	Crocodylomorpha		*Lusitanisuchus*	VAL-06-16-01	0.5mm	Isolated tooth
ML4511	Crocodylomorpha		*Lusitanisuchus*	VAL-06-16-01	0.5mm	Isolated tooth

ML4512	Crocodylomorpha		*Lusitanisuchus*	VAL-06-16-01	0.5mm	Isolated tooth
ML4513	Crocodylomorpha		*Lusitanisuchus*	VAL-06-16-01	0.5mm	Isolated tooth
ML4514	Crocodylomorpha		*Lusitanisuchus*	VAL-06-16-01	0.5mm	Isolated tooth
ML4515	Crocodylomorpha		*Lusitanisuchus*	VAL-06-16-01	0.5mm	Isolated tooth
ML4516	Crocodylomorpha		*Lusitanisuchus*	VAL-06-16-01	0.5mm	Isolated tooth
ML4517	Crocodylomorpha		*Lusitanisuchus*	VAL-06-16-01	0.5mm	Isolated tooth
ML4518	Crocodylomorpha		*Lusitanisuchus*	VAL-06-16-01	0.5mm	Isolated tooth
ML4519	Crocodylomorpha		*Lusitanisuchus*	VAL-06-16-01	0.5mm	Isolated tooth
ML4520	Crocodylomorpha		*Lusitanisuchus*	VAL-06-16-01	0.5mm	Isolated tooth
ML4521	Crocodylomorpha		*Lusitanisuchus*	VAL-06-16-01	0.5mm	Isolated tooth
ML4522	Crocodylomorpha		*Lusitanisuchus*	VAL-10-17-01	0.5mm	Isolated tooth
ML4523	Crocodylomorpha		*Lusitanisuchus*	VAL-10-17-01	0.5mm	Isolated tooth
ML4524	Crocodylomorpha		*Lusitanisuchus*	VAL-10-17-01	0.5mm	Isolated tooth
ML4525	Crocodylomorpha		*Lusitanisuchus*	VAL-10-17-01	0.5mm	Isolated tooth
ML4526	Crocodylomorpha		*Lusitanisuchus*	VAL-10-17-01	0.5mm	Isolated tooth
ML4527	Crocodylomorpha		*Lusitanisuchus*	VAL-10-17-01	0.5mm	Isolated tooth
ML4528	Crocodylomorpha		*Lusitanisuchus*	VAL-10-17-01	0.5mm	Isolated tooth
ML4529	Crocodylomorpha		*Lusitanisuchus*	VAL-10-17-01	0.5mm	Isolated tooth
ML4530	Crocodylomorpha		*Lusitanisuchus*	ZIM-06-17-01	0.5mm	Isolated tooth
ML4531	Crocodylomorpha		*Lusitanisuchus*	ZIM-11-16-02	0.5mm	Isolated tooth
ML4532	Crocodylomorpha		*Lusitanisuchus*	ZIM-11-16-02	0.5mm	Isolated tooth
ML4533	Crocodylomorpha	Thalattosuchia	*Machimosaurus*	PB-06-17-03	1mm	Isolated tooth
ML4534	Crocodylomorpha	Thalattosuchia	*Machimosaurus*	VAL-06-16-01	0.5mm	Isolated tooth
ML4535	Crocodylomorpha	Thalattosuchia	*Machimosaurus*	VAL-06-16-01	0.5mm	Isolated tooth
ML4536	Crocodylomorpha	Mesoeucrocodylia		VAL-03-19-10	0.5mm	Isolated tooth
ML4537	Crocodylomorpha	Mesoeucrocodylia		VAL-06-16-01	0.5mm	Isolated tooth
ML4538	Crocodylomorpha	Mesoeucrocodylia		VAL-06-16-01	0.5mm	Isolated tooth
ML4539	Crocodylomorpha	Mesoeucrocodylia		VAL-06-16-01	0.5mm	Isolated tooth
ML4540	Crocodylomorpha	Mesoeucrocodylia		VAL-06-16-01	0.5mm	Isolated tooth
ML4541	Crocodylomorpha	Mesoeucrocodylia		VAL-06-16-01	0.5mm	Isolated tooth
ML4542	Crocodylomorpha	Mesoeucrocodylia		VAL-06-16-01	0.5mm	Isolated tooth
ML4543	Crocodylomorpha	Mesoeucrocodylia		VAL-06-16-01	0.5mm	Isolated tooth
ML4544	Crocodylomorpha	Pholidosauridae		VAL-03-19-10	0.5mm	Isolated tooth

ML4545	Crocodylomorpha	Pholidosauridae		VAL-06-16-01	0.5mm	Isolated tooth
ML4546	Crocodylomorpha	Pholidosauridae		VAL-06-16-01	0.5mm	Isolated tooth
ML4547	Crocodylomorpha	Pholidosauridae		VAL-06-16-01	0.5mm	Isolated tooth
ML4548	Crocodylomorpha	Pholidosauridae		VAL-10-17-01	0.5mm	Isolated tooth
ML4549	Crocodylomorpha	Pholidosauridae		VAL-10-17-01	0.5mm	Isolated tooth
ML4550	Crocodylomorpha	Pholidosauridae		VAL-10-17-01	0.5mm	Isolated tooth
ML4551	Crocodylomorpha	Pholidosauridae		VAL-10-17-01	0.5mm	Isolated tooth
ML4552	Sauropterygia	Plesiosauroidea		VAL-06-16-01	0.5mm	Isolated tooth
ML4553	Sauropterygia	Plesiosauroidea		VAL-06-16-01	0.5mm	Isolated tooth
ML4554	Sauropterygia	Plesiosauroidea		ZIM-06-17-04	0.5mm	Isolated tooth
ML2846	Pterosauria	Gnathosaurinae		VAL-06-16-01		Isolated tooth
ML2831	Pterosauria	Rhamphorynchinae		Surface collecting		Isolated tooth
ML4555	Pterosauria	Pterosauria indet.		ZIM-06-17-04	0.5mm	Isolated tooth
ML4556	Pterosauria	Pterosauria indet.		VAL-06-16-01	0.5mm	Isolated tooth
ML4557	Dinosauria	Sauropoda		VAL-06-16-01	0.5mm	Isolated tooth
ML4558	Dinosauria	Ornitischia		VAL-06-16-01	0.5mm	Isolated tooth
ML4559	Dinosauria	Heterodontosauridae		PB-10-17-02	0.5mm	Isolated tooth
ML4560	Dinosauria	Neornithischia		ZIM-11-16-02		Isolated tooth
ML4561	Dinosauria	Thyreophora		ZIM-06-17-04	0.5mm	Isolated tooth
ML4562	Dinosauria	Megalosauridae		ZIM-11-16-02	2mm	Isolated tooth
ML4563	Dinosauria	Megalosauridae		VAL-06-16-01	0.5mm	Isolated tooth
ML4564	Dinosauria	Coelurosauria	aff. *Richardoestesia*	VAL-06-16-01	0.5mm	Isolated tooth
ML4565	Dinosauria	Coelurosauria	aff. *Richardoestesia*	ZIM-11-16-01	0.5mm	Isolated tooth
ML4566	Dinosauria	Coelurosauria	aff. *Richardoestesia*	VAL-10-17-01	1mm	Isolated tooth
ML4567	Dinosauria	Coelurosauria		VAL-10-17-01	0.5mm	Isolated tooth
ML4568	Dinosauria	Tyrannosauroidea		PB-06-17-01	0.5mm	Isolated tooth
ML4569	Dinosauria	Theropoda		ZIM-06-17-04	0.5mm	Isolated tooth
ML4570	Dinosauria	Theropoda		VAL-06-16-01	0.5mm	Isolated tooth
ML4571	Dinosauria	Theropoda		VAL-06-16-01	0.5mm	Isolated tooth
ML4572	Dinosauria	Theropoda		VAL-06-16-01	0.5mm	Isolated tooth
ML4573	Dinosauria	Theropoda		PB-06-17-02	0.5mm	Isolated tooth
ML4574	Dinosauria	Theropoda		VAL-10-17-01	1mm	Isolated tooth

ML4575	Dinosauria	Dinosauria indet.		ZIM-06-17-04	1mm	Isolated tooth
ML4576	Diapsida	Choristodera	aff. *Cteniogenys*	ZIM-06-17-01	0.5mm	Vertebra
ML4577	Diapsida	Choristodera	aff. *Cteniogenys*	VAL-10-17-01	0.5mm	Vertebra
ML4578	Diapsida	Choristodera	aff. *Cteniogenys*	VAL-06-16-01	1mm	Vertebra
ML4579	Diapsida	Choristodera	aff. *Cteniogenys*	VAL-10-17-01	1mm	Vertebra
ML4580	Diapsida	Choristodera	aff. *Cteniogenys*	VAL-06-16-01	0.5mm	Femur
ML4581	Diapsida	Choristodera	aff. *Cteniogenys*	VAL-06-16-01	0.5mm	Femur
ML4582	Diapsida	Choristodera	aff. *Cteniogenys*	VAL-06-16-01	0.5mm	Surangular
ML4583	Archosauria	Archosauria indet.		VAL-06-16-01	0.5mm	Ungual
ML4584	Archosauria	Archosauria indet.		VAL-06-16-01	0.5mm	Ungual
ML4585	Archosauria	Archosauria indet.		ZIM-11-16-02	0.5mm	Ungual
ML4586	Diapsida	Diapsida indet.		ZIM-06-17-04	0.5mm	Isolated tooth
ML4587	Diapsida	Diapsida indet.		VAL-06-16-01	0.5mm	Isolated tooth
ML4588	Diapsida	Diapsida indet.		VAL-06-16-01	0.5mm	Isolated tooth
ML4589	Testudines	Testudines indet.		VAL-03-19-03	1mm	Shell
ML4590	Testudines	Testudines indet.		VAL-03-19-03	2mm	Shell
ML4591	Testudines	Testudines indet.		VAL-03-19-03	2mm	Shell
ML4592	Testudines	Testudines indet.		VAL-03-19-03	2mm	Shell
ML4593	Testudines	Testudines indet.		VAL-03-19-10	2mm	Shell
ML4594	Testudines	Testudines indet.		VAL-06-16-01	2mm	Shell
ML4595	Testudines	Testudines indet.		VAL-06-16-01	2mm	Shell
ML4596	Testudines	Testudines indet.		VAL-06-16-01	2mm	Shell
ML4597	Testudines	Testudines indet.		VAL-06-16-01	2mm	Shell
ML4598	Testudines	Testudines indet.		VAL-06-16-01	2mm	Shell
ML4599	Testudines	Testudines indet.		VAL-06-16-01	2mm	Shell
ML4600	Testudines	Testudines indet.		VAL-06-16-01	2mm	Shell
ML4601	Testudines	Testudines indet.		VAL-06-16-01	2mm	Shell
ML4602	Testudines	Testudines indet.		VAL-06-16-01	2mm	Shell
ML4603	Testudines	Testudines indet.		VAL-10-17-01	2mm	Shell
ML4604	Testudines	Testudines indet.		VAL-10-17-01	2mm	Shell
ML4605	Testudines	Testudines indet.		VAL-10-17-01	2mm	Shell
ML4606	Testudines	Testudines indet.		VAL-10-17-01	2mm	Shell

ML4607	Testudines	Testudines indet.		VAL-10-17-01	2mm	Shell
ML4608	Testudines	Testudines indet.		VAL-10-17-01	2mm	Shell
ML4609	Testudines	Testudines indet.		VAL-10-17-01	2mm	Shell
ML4610	Testudines	Testudines indet.		VAL-10-17-01	2mm	Shell
ML4611	Testudines	Testudines indet.		VAL-10-17-01	2mm	Shell
ML4612	Testudines	Testudines indet.		VAL-10-17-01	2mm	Shell
ML4613	Testudines	Testudines indet.		VAL-10-17-01	2mm	Shell
ML4614	Testudines	Testudines indet.		VAL-10-17-01	2mm	Shell
ML4615	Testudines	Testudines indet.		VAL-10-17-01	2mm	Shell
ML4616	Testudines	Testudines indet.		VAL-10-17-01	2mm	Shell
ML4617	Indet			VAL-03-19-04	1mm	Atlas?
ML4618	Indet			PB-06-17-01	0.5mm	Bone of interest
ML4619	Indet			PB-06-17-03	1mm	Bone of interest
ML4620	Indet			PB-06-17-03	1mm	Bone of interest
ML4621	Indet			PB-06-17-03	1mm	Bone of interest
ML4622	Indet			PB-06-17-03	0.5mm	Bone of interest
ML4623	Indet			PB-06-17-03	0.5mm	Bone of interest
ML4624	Indet			PB-06-17-03	0.5mm	Bone of interest
ML4625	Indet			PB-06-17-04	0.5mm	Bone of interest
ML4626	Indet			PB-06-17-05	0.5mm	Bone of interest
ML4627	Indet			PB-06-17-05	0.5mm	Bone of interest
ML4628	Indet			PB-06-17-05	0.5mm	Bone of interest
ML4629	Indet			PB-10-17-02	1mm	Bone of interest
ML4630	Indet			PB-10-17-02	0.5mm	Bone of interest
ML4631	Indet			PB-10-17-02	0.5mm	Bone of interest
ML4632	Indet			PB-10-17-02	0.5mm	Bone of interest
ML4633	Indet			PB-10-17-02	0.5mm	Bone of interest
ML4634	Indet			PB-10-17-02	0.5mm	Bone of interest
ML4635	Indet			PB-10-17-02	0.5mm	Bone of interest
ML4636	Indet			PB-10-17-02	0.5mm	Bone of interest
ML4637	Indet			PB-10-17-02	0.5mm	Bone of interest
ML4638	Indet			PB-10-17-02	0.5mm	Bone of interest

ML4639	Indet			PB-10-17-02	0.5mm	Bone of interest
ML4640	Indet			PB-10-17-02	0.5mm	Bone of interest
ML4641	Indet			PB-10-17-02	0.5mm	Bone of interest
ML4642	Indet			PD-05-18-01	0.5mm	Bone of interest
ML4643	Indet			PD-05-18-01	0.5mm	Bone of interest
ML4644	Indet			PD-05-18-01	0.5mm	Bone of interest
ML4645	Indet			VAL-03-19-04	0.5mm	Bone of interest
ML4646	Indet			VAL-03-19-04	0.5mm	Bone of interest
ML4647	Indet			VAL-03-19-04	0.5mm	Bone of interest
ML4648	Indet			VAL-03-19-04	1mm	Bone of interest
ML4649	Indet			VAL-03-19-04	1mm	Bone of interest
ML4650	Indet			VAL-06-16-01	0.5mm	Bone of interest
ML4651	Indet			VAL-06-16-01	0.5mm	Bone of interest
ML4652	Indet			VAL-06-16-01	0.5mm	Bone of interest
ML4653	Indet			VAL-06-16-01	0.5mm	Bone of interest
ML4654	Indet			VAL-06-16-01	0.5mm	Bone of interest
ML4655	Indet			VAL-06-16-01	0.5mm	Bone of interest
ML4656	Indet			VAL-06-16-01	0.5mm	Bone of interest
ML4657	Indet			VAL-06-16-01	0.5mm	Bone of interest
ML4658	Indet			VAL-06-16-01	0.5mm	Bone of interest
ML4659	Indet			VAL-06-16-01	0.5mm	Bone of interest
ML4660	Indet			VAL-06-16-01	0.5mm	Bone of interest
ML4661	Indet			VAL-06-16-01	0.5mm	Bone of interest
ML4662	Indet			VAL-06-16-01	0.5mm	Bone of interest
ML4663	Indet			VAL-06-16-01	0.5mm	Bone of interest
ML4664	Indet			VAL-06-16-01	0.5mm	Bone of interest
ML4665	Indet			VAL-06-16-01	0.5mm	Bone of interest
ML4666	Indet			VAL-06-16-01	0.5mm	Bone of interest
ML4667	Indet			VAL-06-16-01	0.5mm	Bone of interest
ML4668	Indet			VAL-06-16-01	0.5mm	Bone of interest
ML4669	Indet			VAL-06-16-01	0.5mm	Bone of interest
ML4670	Indet			VAL-06-16-01	0.5mm	Bone of interest
ML4671	Indet			VAL-06-16-01	0.5mm	Bone of interest

ML4672	Indet			VAL-06-16-01	0.5mm	Bone of interest
ML4673	Indet			VAL-06-16-01	0.5mm	Bone of interest
ML4674	Indet			VAL-06-16-01	0.5mm	Bone of interest
ML4675	Indet			VAL-06-16-01	0.5mm	Bone of interest
ML4676	Indet			VAL-06-16-01	0.5mm	Bone of interest
ML4677	Indet			VAL-06-16-01	0.5mm	Bone of interest
ML4678	Indet			VAL-06-16-01	0.5mm	Bone of interest
ML4679	Indet			VAL-06-16-01	0.5mm	Bone of interest
ML4680	Indet			VAL-06-16-01	0.5mm	Bone of interest
ML4681	Indet			VAL-06-16-01	0.5mm	Bone of interest
ML4682	Indet			VAL-06-16-01	0.5mm	Bone of interest
ML4683	Indet			VAL-06-16-01	0.5mm	Bone of interest
ML4684	Indet			VAL-06-16-01	0.5mm	Bone of interest
ML4685	Indet			VAL-06-16-01	0.5mm	Bone of interest
ML4686	Indet			VAL-06-16-01	0.5mm	Bone of interest
ML4687	Indet			VAL-06-16-01	0.5mm	Bone of interest
ML4688	Indet			VAL-06-16-01	0.5mm	Bone of interest
ML4689	Indet			VAL-06-16-01	0.5mm	Bone of interest
ML4690	Indet			VAL-06-16-01	0.5mm	Bone of interest
ML4691	Indet			VAL-06-16-01	0.5mm	Bone of interest
ML4692	Indet			VAL-06-16-01	0.5mm	Bone of interest
ML4693	Indet			VAL-06-16-01	0.5mm	Bone of interest
ML4694	Indet			VAL-06-16-01	0.5mm	Bone of interest
ML4695	Indet			VAL-06-16-01	0.5mm	Bone of interest
ML4696	Indet			VAL-06-16-01	0.5mm	Bone of interest
ML4697	Indet			VAL-06-16-01	0.5mm	Bone of interest
ML4698	Indet			VAL-06-16-01	0.5mm	Bone of interest
ML4699	Indet			VAL-06-16-01	0.5mm	Bone of interest
ML4700	Indet			VAL-06-16-01	0.5mm	Bone of interest
ML4701	Indet			VAL-06-16-01	0.5mm	Bone of interest
ML4702	Indet			VAL-06-16-01	0.5mm	Bone of interest
ML4703	Indet			VAL-06-16-01	0.5mm	Bone of interest
ML4704	Indet			VAL-06-16-01	0.5mm	Bone of interest

ML4705	Indet			VAL-06-16-01	0.5mm	Bone of interest
ML4706	Indet			VAL-06-16-01	0.5mm	Bone of interest
ML4707	Indet			VAL-06-16-01	0.5mm	Bone of interest
ML4708	Indet			VAL-06-16-01	0.5mm	Bone of interest
ML4709	Indet			VAL-06-16-01	0.5mm	Bone of interest
ML4710	Indet			VAL-06-16-01	0.5mm	Bone of interest
ML4711	Indet			VAL-06-16-01	0.5mm	Bone of interest
ML4712	Indet			VAL-06-16-01	0.5mm	Bone of interest
ML4713	Indet			VAL-06-16-01	0.5mm	Bone of interest
ML4714	Indet			VAL-06-16-01	0.5mm	Bone of interest
ML4715	Indet			VAL-06-16-01	0.5mm	Bone of interest
ML4716	Indet			VAL-06-16-01	0.5mm	Bone of interest
ML4717	Indet			VAL-06-16-01	0.5mm	Bone of interest
ML4718	Indet			VAL-06-16-01	0.5mm	Bone of interest
ML4719	Indet			VAL-06-16-01	0.5mm	Bone of interest
ML4720	Indet			VAL-06-16-01	0.5mm	Bone of interest
ML4721	Indet			VAL-06-16-01	0.5mm	Bone of interest
ML4722	Indet			VAL-06-16-01	0.5mm	Bone of interest
ML4723	Indet			VAL-06-16-01	0.5mm	Bone of interest
ML4724	Indet			VAL-06-16-01	0.5mm	Bone of interest
ML4725	Indet			VAL-06-16-01	0.5mm	Bone of interest
ML4726	Indet			VAL-06-16-01	0.5mm	Bone of interest
ML4727	Indet			VAL-06-16-01	0.5mm	Bone of interest
ML4728	Indet			VAL-06-16-01	0.5mm	Bone of interest
ML4729	Indet			VAL-06-16-01	0.5mm	Bone of interest
ML4730	Indet			VAL-06-16-01	0.5mm	Bone of interest
ML4731	Indet			VAL-06-16-01	0.5mm	Bone of interest
ML4732	Indet			VAL-06-16-01	0.5mm	Bone of interest
ML4733	Indet			VAL-06-16-01	0.5mm	Bone of interest
ML4734	Indet			VAL-06-16-01	0.5mm	Bone of interest
ML4735	Indet			VAL-06-16-01	0.5mm	Bone of interest
ML4736	Indet			VAL-06-16-01	0.5mm	Bone of interest
ML4737	Indet			VAL-06-16-01	0.5mm	Bone of interest

ML4738	Indet			VAL-06-16-01	0.5mm	Bone of interest
ML4739	Indet			VAL-06-16-01	0.5mm	Bone of interest
ML4740	Indet			VAL-06-16-01	0.5mm	Bone of interest
ML4741	Indet			VAL-06-16-01	0.5mm	Bone of interest
ML4742	Indet			VAL-06-16-01	0.5mm	Bone of interest
ML4743	Indet			VAL-06-16-01	0.5mm	Bone of interest
ML4744	Indet			VAL-06-16-01	0.5mm	Bone of interest
ML4745	Indet			VAL-06-16-01	0.5mm	Bone of interest
ML4746	Indet			VAL-06-16-01	0.5mm	Bone of interest
ML4747	Indet			VAL-06-16-01	0.5mm	Bone of interest
ML4748	Indet			VAL-06-16-01	0.5mm	Bone of interest
ML4749	Indet			VAL-10-17-01	0.5mm	Bone of interest
ML4750	Indet			VAL-10-17-01	0.5mm	Bone of interest
ML4751	Indet			VAL-10-17-01	0.5mm	Bone of interest
ML4752	Indet			VAL-10-17-01	0.5mm	Bone of interest
ML4753	Indet			VAL-10-17-01	0.5mm	Bone of interest
ML4754	Indet			VAL-10-17-01	0.5mm	Bone of interest
ML4755	Indet			VAL-10-17-01	0.5mm	Bone of interest
ML4756	Indet			VAL-10-17-01	0.5mm	Bone of interest
ML4757	Indet			VAL-10-17-01	0.5mm	Bone of interest
ML4758	Indet			VAL-10-17-01	0.5mm	Bone of interest
ML4759	Indet			VAL-10-17-01	0.5mm	Bone of interest
ML4760	Indet			VAL-10-17-01	0.5mm	Bone of interest
ML4761	Indet			VAL-10-17-01	0.5mm	Bone of interest
ML4762	Indet			VAL-10-17-01	0.5mm	Bone of interest
ML4763	Indet			ZIM-06-17-01	0.5mm	Bone of interest
ML4764	Indet			ZIM-06-17-01	0.5mm	Bone of interest
ML4765	Indet			ZIM-06-17-01	0.5mm	Bone of interest
ML4766	Indet			ZIM-06-17-01	0.5mm	Bone of interest
ML4767	Indet			ZIM-06-17-01	0.5mm	Bone of interest
ML4768	Indet			ZIM-06-17-01	0.5mm	Bone of interest
ML4769	Indet			ZIM-06-17-01	0.5mm	Bone of interest
ML4770	Indet			ZIM-06-17-01	0.5mm	Bone of interest

ML4771	Indet			ZIM-06-17-01	0.5mm	Bone of interest
ML4772	Indet			ZIM-06-17-01	0.5mm	Bone of interest
ML4773	Indet			ZIM-06-17-01	0.5mm	Bone of interest
ML4774	Indet			ZIM-06-17-01	0.5mm	Bone of interest
ML4775	Indet			ZIM-06-17-01	0.5mm	Bone of interest
ML4776	Indet			ZIM-06-17-01	0.5mm	Bone of interest
ML4777	Indet			ZIM-06-17-01	0.5mm	Bone of interest
ML4778	Indet			ZIM-06-17-01	0.5mm	Bone of interest
ML4779	Indet			ZIM-06-17-01	0.5mm	Bone of interest
ML4780	Indet			ZIM-06-17-01	0.5mm	Bone of interest
ML4781	Indet			ZIM-06-17-01	0.5mm	Bone of interest
ML4782	Indet			ZIM-06-17-01	0.5mm	Bone of interest
ML4783	Indet			ZIM-06-17-01	0.5mm	Bone of interest
ML4784	Indet			ZIM-06-17-01	0.5mm	Bone of interest
ML4785	Indet			ZIM-06-17-01	0.5mm	Bone of interest
ML4786	Indet			ZIM-06-17-01	0.5mm	Bone of interest
ML4787	Indet			ZIM-06-17-02	0.5mm	Bone of interest
ML4788	Indet			ZIM-06-17-04	0.5mm	Bone of interest
ML4789	Indet			ZIM-06-17-04	0.5mm	Bone of interest
ML4790	Indet			ZIM-06-17-04	0.5mm	Bone of interest
ML4791	Indet			ZIM-06-17-04	0.5mm	Bone of interest
ML4792	Indet			ZIM-06-17-04	0.5mm	Bone of interest
ML4793	Indet			ZIM-06-17-04	0.5mm	Bone of interest
ML4794	Indet			ZIM-06-17-04	0.5mm	Bone of interest
ML4795	Indet			ZIM-06-17-04	0.5mm	Bone of interest
ML4796	Indet			ZIM-06-17-04	0.5mm	Bone of interest
ML4797	Indet			ZIM-06-17-04	1mm	Bone of interest
ML4798	Indet			ZIM-11-16-01	1mm	Bone of interest
ML4799	Indet			ZIM-11-16-01	1mm	Bone of interest
ML4800	Indet			ZIM-11-16-01	1mm	Bone of interest
ML4801	Indet			ZIM-11-16-01	1mm	Bone of interest
ML4802	Indet			ZIM-11-16-01	1mm	Bone of interest
ML4803	Indet			ZIM-11-16-02	2mm	Bone of interest

ML4804	Indet			ZIM-11-16-02	0.5mm	Bone of interest
ML4805	Indet			ZIM-11-16-02	0.5mm	Bone of interest
ML4806	Indet			ZIM-11-16-02	0.5mm	Bone of interest
ML4807	Indet			ZIM-11-16-02	0.5mm	Bone of interest
ML4808	Indet			ZIM-11-16-02	0.5mm	Bone of interest
ML4809	Indet			ZIM-11-16-02	0.5mm	Bone of interest
ML4810	Indet			VAL-06-16-01	0.5mm	Carpal/tarsal bone
ML4811	Indet			VAL-06-16-01	0.5mm	Embryonic bone?
ML4812	Indet			VAL-06-16-01	0.5mm	Embryonic bone?
ML4813	Indet			VAL-06-16-01	0.5mm	Embryonic bone?
ML4814	Indet			PB-06-17-03	1mm	Isolated teeth
ML4815	Indet			PB-06-17-03	0.5mm	Isolated teeth
ML4816	Indet			PB-06-17-03	0.5mm	Isolated teeth
ML4817	Indet			PB-06-17-03	0.5mm	Isolated teeth
ML4818	Indet			PB-06-17-03	0.5mm	Isolated teeth
ML4819	Indet			PB-06-17-03	0.5mm	Isolated teeth
ML4820	Indet			PB-06-17-03	0.5mm	Isolated teeth
ML4821	Indet			PB-06-17-03	0.5mm	Isolated teeth
ML4822	Indet			PB-06-17-03	0.5mm	Isolated teeth
ML4823	Indet			PB-06-17-04	1mm	Isolated teeth
ML4824	Indet			PB-06-17-04	0.5mm	Isolated teeth
ML4825	Indet			PD-05-18-01	0.5mm	Isolated teeth
ML4826	Indet			PD-05-18-01	0.5mm	Isolated teeth
ML4827	Indet			PD-05-18-01	1mm	Isolated teeth
ML4828	Indet			VAL-03-19-03	1mm	Isolated teeth
ML4829	Indet			VAL-03-19-03	1mm	Isolated teeth
ML4830	Indet			VAL-03-19-03	1mm	Isolated teeth
ML4831	Indet			VAL-03-19-03	1mm	Isolated teeth
ML4832	Indet			VAL-03-19-03	1mm	Isolated teeth
ML4833	Indet			VAL-03-19-04	0.5mm	Isolated teeth
ML4834	Indet			VAL-03-19-04	0.5mm	Isolated teeth
ML4835	Indet			VAL-03-19-04	1mm	Isolated teeth
ML4836	Indet			VAL-06-16-01	0.5mm	Isolated teeth

ML4837	Indet			VAL-06-16-01	0.5mm	Isolated teeth
ML4838	Indet			VAL-06-16-01	0.5mm	Isolated teeth
ML4839	Indet			VAL-06-16-01	0.5mm	Isolated teeth
ML4840	Indet			VAL-06-16-01	0.5mm	Isolated teeth
ML4841	Indet			VAL-06-16-01	0.5mm	Isolated teeth
ML4842	Indet			VAL-06-16-01	0.5mm	Isolated teeth
ML4843	Indet			VAL-06-16-01	0.5mm	Isolated teeth
ML4844	Indet			VAL-06-16-01	0.5mm	Isolated teeth
ML4845	Indet			VAL-06-16-01	0.5mm	Isolated teeth
ML4846	Indet			VAL-06-16-01	0.5mm	Isolated teeth
ML4847	Indet			VAL-06-16-01	0.5mm	Isolated teeth
ML4848	Indet			VAL-06-16-01	0.5mm	Isolated teeth
ML4849	Indet			VAL-06-16-01	0.5mm	Isolated teeth
ML4850	Indet			VAL-06-16-01	0.5mm	Isolated teeth
ML4851	Indet			VAL-06-16-01	0.5mm	Isolated teeth
ML4852	Indet			VAL-06-16-01	0.5mm	Isolated teeth
ML4853	Indet			VAL-06-16-01	0.5mm	Isolated teeth
ML4854	Indet			VAL-06-16-01	0.5mm	Isolated teeth
ML4855	Indet			VAL-06-16-01	0.5mm	Isolated teeth
ML4856	Indet			VAL-06-16-01	0.5mm	Isolated teeth
ML4857	Indet			VAL-06-16-01	0.5mm	Isolated teeth
ML4858	Indet			VAL-06-16-01	0.5mm	Isolated teeth
ML4859	Indet			VAL-06-16-01	0.5mm	Isolated teeth
ML4860	Indet			VAL-06-16-01	0.5mm	Isolated teeth
ML4861	Indet			VAL-06-16-01	0.5mm	Isolated teeth
ML4862	Indet			VAL-06-16-01	0.5mm	Isolated teeth
ML4863	Indet			VAL-06-16-01	0.5mm	Isolated teeth
ML4864	Indet			VAL-06-16-01	0.5mm	Isolated teeth
ML4865	Indet			VAL-06-16-01	0.5mm	Isolated teeth
ML4866	Indet			VAL-06-16-01	0.5mm	Isolated teeth
ML4867	Indet			VAL-06-16-01	0.5mm	Isolated teeth
ML4868	Indet			VAL-06-16-01	0.5mm	Isolated teeth
ML4869	Indet			VAL-06-16-01	0.5mm	Isolated teeth

ML4870	Indet			VAL-06-16-01	0.5mm	Isolated teeth
ML4871	Indet			VAL-06-16-01	0.5mm	Isolated teeth
ML4872	Indet			VAL-06-16-01	0.5mm	Isolated teeth
ML4873	Indet			VAL-06-16-01	0.5mm	Isolated teeth
ML4874	Indet			VAL-06-16-01	0.5mm	Isolated teeth
ML4875	Indet			VAL-06-16-01	0.5mm	Isolated teeth
ML4876	Indet			VAL-06-16-01	0.5mm	Isolated teeth
ML4877	Indet			VAL-06-16-01	0.5mm	Isolated teeth
ML4878	Indet			VAL-06-16-01	0.5mm	Isolated teeth
ML4879	Indet			VAL-06-16-01	0.5mm	Isolated teeth
ML4880	Indet			VAL-06-16-01	0.5mm	Isolated teeth
ML4881	Indet			VAL-10-17-01	0.5mm	Isolated teeth
ML4882	Indet			VAL-10-17-01	0.5mm	Isolated teeth
ML4883	Indet			VAL-10-17-01	0.5mm	Isolated teeth
ML4884	Indet			VAL-10-17-01	0.5mm	Isolated teeth
ML4885	Indet			VAL-10-17-01	0.5mm	Isolated teeth
ML4886	Indet			VAL-10-17-01	0.5mm	Isolated teeth
ML4887	Indet			VAL-10-17-01	0.5mm	Isolated teeth
ML4888	Indet			VAL-10-17-01	0.5mm	Isolated teeth
ML4889	Indet			VAL-10-17-01	0.5mm	Isolated teeth
ML4890	Indet			VAL-10-17-01	0.5mm	Isolated teeth
ML4891	Indet			VAL-10-17-01	0.5mm	Isolated teeth
ML4892	Indet			VAL-10-17-01	0.5mm	Isolated teeth
ML4893	Indet			VAL-10-17-01	0.5mm	Isolated teeth
ML4894	Indet			VAL-10-17-01	0.5mm	Isolated teeth
ML4895	Indet			VAL-10-17-01	0.5mm	Isolated teeth
ML4896	Indet			VAL-10-17-01	0.5mm	Isolated teeth
ML4897	Indet			VAL-10-17-01	0.5mm	Isolated teeth
ML4898	Indet			VAL-10-17-01	0.5mm	Isolated teeth
ML4899	Indet			VAL-10-17-01	0.5mm	Isolated teeth
ML4900	Indet			VAL-10-17-01	0.5mm	Isolated teeth
ML4901	Indet			VAL-10-17-01	0.5mm	Isolated teeth
ML4902	Indet			VAL-10-17-01	0.5mm	Isolated teeth

ML4903	Indet			VAL-10-17-01	0.5mm	Isolated teeth
ML4904	Indet			VAL-10-17-01	0.5mm	Isolated teeth
ML4905	Indet			VAL-10-17-01	0.5mm	Isolated teeth
ML4906	Indet			VAL-10-17-01	0.5mm	Isolated teeth
ML4907	Indet			VAL-10-17-01	0.5mm	Isolated teeth
ML4908	Indet			VAL-10-17-01	0.5mm	Isolated teeth
ML4909	Indet			ZIM-06-17-01	0.5mm	Isolated teeth
ML4910	Indet			ZIM-06-17-04	1mm	Isolated teeth
ML4911	Indet			ZIM-06-17-04	0.5mm	Isolated teeth
ML4912	Indet			ZIM-06-17-04	0.5mm	Isolated teeth
ML4913	Indet			ZIM-06-17-04	0.5mm	Isolated teeth
ML4914	Indet			ZIM-06-17-04	0.5mm	Isolated teeth
ML4915	Indet			ZIM-06-17-04	0.5mm	Isolated teeth
ML4916	Indet			ZIM-06-17-04	0.5mm	Isolated teeth
ML4917	Indet			ZIM-11-16-01	0.5mm	Isolated teeth
ML4918	Indet			ZIM-11-16-01	0.5mm	Isolated teeth
ML4919	Indet			ZIM-11-16-01	0.5mm	Isolated teeth
ML4920	Indet			ZIM-11-16-01	0.5mm	Isolated teeth
ML4921	Indet			ZIM-11-16-01	0.5mm	Isolated teeth
ML4922	Indet			ZIM-11-16-01	1mm	Isolated teeth
ML4923	Indet			PB-06-17-03	0.5mm	Jaw
ML4924	Indet			VAL-03-19-04	1mm	Jaw
ML4925	Indet			VAL-03-19-04	0.5mm	Jaw
ML4926	Indet			VAL-06-16-01	0.5mm	Jaw
ML4927	Indet			VAL-06-16-01	0.5mm	Jaw
ML4928	Indet			VAL-06-18-01	0.5mm	Jaw
ML4929	Indet			VAL-10-17-01	0.5mm	Jaw
ML4930	Indet			VAL-10-17-01	0.5mm	Jaw
ML4931	Indet			VAL-10-17-01	0.5mm	Jaw
ML4932	Indet			VALRED-06-22-02	0.5mm	Jaw
ML4933	Indet			ZIM-06-17-04	0.5mm	Jaw
ML4934	Indet			ZIM-06-17-04	1mm	Jaw
ML4935	Indet			VAL-03-19-10	0.5mm	Maxilla

ML4936	Indet			VAL-06-18-01	0.5mm	Maxilla
ML4937	Indet			ZIM-06-17-01	1mm	Maxilla
ML4938	Indet			PB-10-17-02	0.5mm	Neural arch
ML4939	Indet			VAL-03-19-04	1mm	Neural arch
ML4940	Indet			VAL-03-19-07	0.5mm	Neural arch
ML4941	Indet			VAL-06-16-01	0.5mm	Neural arch
ML4942	Indet			VAL-10-17-01	0.5mm	Neural arch
ML4943	Indet			ZIM-06-17-01	0.5mm	Neural arch
ML4944	Indet			ZIM-06-17-04	0.5mm	Neural arch
ML4945	Indet			ZIM-11-16-02	0.5mm	Neural arch
ML4946	Indet			VAL-03-19-04	0.5mm	Phallanx
ML4947	Indet			VAL-03-19-04	0.5mm	Quadrate
ML4948	Indet			VAL-06-16-01	1mm	Skull bone
ML4949	Indet			VAL-06-16-01	0.5mm	Skull bone
ML4950	Indet			VAL-06-16-01	0.5mm	Skull bone
ML4951	Indet			VAL-06-16-01	0.5mm	Skull bone
ML4952	Indet			VAL-06-16-01	0.5mm	Skull bone
ML4953	Indet			ZIM-06-17-01	0.5mm	Skull bone
ML4954	Indet			ZIM-06-17-01	0.5mm	Skull bone
ML4955	Indet			ZIM-06-17-01	0.5mm	Skull bone
ML4956	Indet			ZIM-06-17-01	0.5mm	Skull bone
ML4957	Indet			ZIM-06-17-01	0.5mm	Skull bone
ML4958	Indet			ZIM-06-17-01	0.5mm	Skull bone
ML4959	Indet			ZIM-06-17-01	0.5mm	Skull bone
ML4960	Indet			ZIM-06-17-04	0.5mm	Skull bone
ML4961	Indet			ZIM-06-17-04	0.5mm	Skull bone
ML4962	Indet			ZIM-06-17-04	0.5mm	Skull bone
ML4963	Indet			ZIM-11-16-02	1mm	Skull bone
ML4964	Indet			ZIM-11-16-02	1mm	Skull bone
ML4965	Indet			ZIM-11-16-02	1mm	Skull bone
ML4966	Indet			ZIM-11-16-02	1mm	Skull bone
ML4967	Indet			VAL-03-19-04	0.5mm	Ungual
ML4968	Indet			VAL-03-19-04	0.5mm	Ungual

ML4969	Indet			VAL-03-19-04	1mm	Vertebra
ML4970	Indet			VAL-03-19-10	0.5mm	Vertebra
ML4971	Indet			VAL-03-19-10	0.5mm	Vertebra
ML4972	Indet			VAL-03-19-10	0.5mm	Vertebra
ML4973	Indet			VAL-03-19-10	0.5mm	Vertebra
ML4974	Indet			VAL-06-16-01	0.5mm	Vertebra
ML4975	Indet			VAL-06-16-01	0.5mm	Vertebra
ML4976	Indet			VAL-06-16-01	0.5mm	Vertebra
ML4977	Indet			VAL-06-16-01	0.5mm	Vertebra
ML4978	Indet			VAL-06-16-01	0.5mm	Vertebra
ML4979	Indet			VAL-06-16-01	0.5mm	Vertebra
ML4980	Indet			VAL-06-16-01	0.5mm	Vertebra
ML4981	Indet			VAL-06-16-01	0.5mm	Vertebra
ML4982	Indet			VAL-06-16-01	0.5mm	Vertebra
ML4983	Indet			VAL-06-16-01	0.5mm	Vertebra
ML4984	Indet			VAL-06-16-01	0.5mm	Vertebra
ML4985	Indet			VAL-06-16-01	0.5mm	Vertebra
ML4986	Indet			VAL-06-16-01	0.5mm	Vertebra
ML4987	Indet			VAL-06-16-01	0.5mm	Vertebra
ML4988	Indet			VAL-06-16-01	0.5mm	Vertebra
ML4989	Indet			VAL-06-16-01	0.5mm	Vertebra
ML4990	Indet			VAL-06-16-01	0.5mm	Vertebra
ML4991	Indet			VAL-06-16-01	0.5mm	Vertebra
ML4992	Indet			VAL-06-16-01	0.5mm	Vertebra
ML4993	Indet			VAL-06-16-01	0.5mm	Vertebra
ML4994	Indet			VAL-06-16-01	0.5mm	Vertebra
ML4995	Indet			VAL-06-16-01	0.5mm	Vertebra
ML4996	Indet			VAL-06-16-01	1mm	Vertebra
ML4997	Indet			VAL-06-16-01	0.5mm	Vertebra
ML4998	Indet			VAL-10-17-01	0.5mm	Vertebra
ML4999	Indet			VAL-10-17-01	0.5mm	Vertebra
ML5000	Indet			VAL-10-17-01	0.5mm	Vertebra
ML5001	Indet			ZIM-06-17-02	0.5mm	Vertebra

ML5002	Indet			ZIM-06-17-04	0.5mm	Vertebra
ML5003	Indet			ZIM-06-17-04	0.5mm	Vertebra
ML5004	Indet			ZIM-06-17-04	0.5mm	Vertebra
ML5005	Indet			ZIM-06-17-04	0.5mm	Vertebra
ML5006	Indet			ZIM-06-17-04	0.5mm	Vertebra
ML5007	Indet			ZIM-11-16-01	0.5mm	Vertebra

A.2 Specimen list from the Guimarota beds

Table A.2: List of specimens from the Guimarota collection that have been checked during this PhD Thesis, with the original information provided by the catalogue of Museu Geológico. Refer to the manuscript for the revision of the relevant material. Please note that several specimen numbers can refer to sample boxes containing dozens or hundreds of fossils.

Specimen numbers	Original classification	German label	Reference	Identification	Observation
MG27416	*Cteniogenys reedi*	FA_{11}	Gui.L.50		
MG27417	*Cteniogenys reedi*	Max	Gui.L.59	Max	
MG27418	*Cteniogenys reedi*	Ctenio	Gui.L.162		
MG27419	*Cteniogenys reedi*	FA_{11} Maxillare	Gui.L.234	maxilar	Fig.Seiffat
MG27420	*Cteniogenys reedi*	Gui 21.12.73 - Cteniogenys right			
MG27421		Gui 76 10.7 2 Choristodera			
MG27422		Gui 79 5.1 Choristodera?			
MG27423	*Cteniogenys*	Gui 80 22.12 surangular		Sobreangular - osso da mandíbula	
MG27586	*Cteniogenys*	$FÃ_{11}$	Gui. Ã. 26		
MG27587	*Cteniogenys*	$FÃ_{11}$	Gui. Ã. 27		
MG27588	*Cteniogenys*	FÃ11 - Praemax	Gui. Ã. 46	Pré-maxila	
MG27589	*Cteniogenys*	$FÃ_{11}$	Gui. Ã. 47		
MG27590	*Cteniogenys*	$FÃ_{11}$	Gui. Ã. 48		
MG27591	*Cteniogenys*	$FÃ_{11}$	Gui. Ã. 52		
MG27592	*Cteniogenys*	$FÃ_{11}$	Gui. Ã. 69		
MG27593	*Cteniogenys*	FÃ11 - Praemax	Gui. Ã. 70	Pré-maxila	
MG27594	*Cteniogenys*	FÃ11 - Max	Gui. Ã. 74	Maxila	
MG27595	*Cteniogenys*	$FÃ_{11}$	Gui. Ã. 85		

MG27596	*Cteniogenys*	FÃ11 - Praemax (juvenil)	Gui. L. 11	Pré-maxila	
MG27597	*Cteniogenys*	FÃ$_{11}$	Gui. L. 12		
MG27598	*Cteniogenys*	FÃ$_{11}$	Gui. L. 55		
MG27599	*Cteniogenys*	FÃ$_{11}$ - GUIM. Reptil "X" - Cteniogenys	Gui. L. 64		
MG27600	*Cteniogenys*	FÃ$_{11}$	Gui. L. 121		
MG27601	*Cteniogenys*	FÃ$_{11}$	Gui. L. 155		
MG27602	*Cteniogenys*	FÃ$_{11}$	Gui. G.E. 5		
MG27603	*Cteniogenys*	FÃ$_{11}$ - Cteniogenys	Gui. G.E. 10		
MG27604	*Cteniogenys*	Gui. 80 24.6 - Choristodera	S/N		
MG27605	*Cteniogenys*	FÃ$_{11}$	Gui. 1		
MG27606	*Cteniogenys*	FÃ$_{11}$	Gui. 27		
MG27607	*Cteniogenys*	FÃ$_{11}$ - Li. Max	Gui. 58	Maxila esquerda	
MG27608	*Cteniogenys*	FÃ11 - Zart Cteniogenys - parietale 22.III.61	Gui. 82	Osso parietal	
MG27609	*Cteniogenys*	FÃ$_{11}$	Gui. 242		
MG27610	*Cteniogenys*	FÃ$_{11}$	Gui. 275		
MG27611	*Cteniogenys*	FÃ$_{11}$	Gui. 276		
MG27612	*Cteniogenys*	FÃ$_{11}$	Gui. 277		
MG27613	*Cteniogenys*	FÃ$_{11}$	Gui. 291		
MG27614	*Cteniogenys*	FÃ$_{11}$	Gui. 295		
MG27615	*Cteniogenys*	FÃ$_{11}$	Gui. 301		
MG27616	*Cteniogenys*	FÃ$_{11}$	Gui. 304		
MG27617	*Cteniogenys*	FÃ$_{11}$	Gui. 306		
MG27618	*Cteniogenys*	FÃ$_{11}$	Gui. 308		
MG27619	*Cteniogenys*	FÃ$_{11}$	Gui. 310		
MG27620	*Cteniogenys*	FÃ$_{11}$	Gui. 311		
MG27621	*Cteniogenys*	FÃ$_{11}$ - Max	Gui. 312		
MG27622	*Cteniogenys*	FÃ$_{11}$	Gui. 323		

MG27623	*Cteniogenys*	FÃ11	Gui. 324		
MG27624	*Cteniogenys*	FÃ11 - Max	Gui. 329		
MG27625	*Cteniogenys*	FÃ11	Gui. 330		
MG27626	*Cteniogenys*	FÃ11	Gui. 334		
MG27627	*Cteniogenys*	FÃ11	Gui. Ã. 21		
MG27628	*Cteniogenys reedi n.sp.SEIFFERT, 1973*	FÃ11	Gui. Ã 33		Holótipo
MG27629	*Cteniogenys*	FÃ11	Gui. 20		
MG27630	*Cteniogenys*	FÃ11	Gui. 27		
MG27631	*Cteniogenys*	FÃ11 - Maxillare aus de Guimarota	Gui. 134		
MG27632	*Cteniogenys*	FÃ11	Gui. 153		
MG27633	*Cteniogenys*	FÃ11	Gui. 244		
MG27634	*Cteniogenys*	FÃ11	Gui. 258		
MG27635	*Cteniogenys*	FÃ11	Gui. 259		
MG27636	*Cteniogenys*	FÃ11	Gui. 268		
MG27637	*Cteniogenys*	FÃ11	Gui. 270		
MG27638	*Cteniogenys*	FÃ11	Gui. 272		
MG27639	*Cteniogenys*	FÃ11	Gui. 274		
MG27640	*Cteniogenys*	FÃ11 - max	Gui. 286		
MG27641	*Cteniogenys*	FÃ11 - Cteniogenys - symph..?	Gui. 307		
MG27642	*Cteniogenys*	FÃ11 - li Max	Gui. 332	Maxilar esquerdo	
MG27643	*Cteniogenys*	FÃ11 - Cteniogenys - symph..??	Gui. 344		
MG27644	*Cteniogenys*	FÃ11 - Prämax - Cteniogenys	Gui. 345	Pré-maxila	
MG27645	*Cteniogenys*	FÃ11 - max (ulén)	Gui. 407	Maxilar	
MG27646	*Cteniogenys*	FÃ11	Gui. 411		
MG27647	*Cteniogenys*	FÃ11	Gui. 415		
MG27648	*Cteniogenys*	FÃ11	Gui. 418		

MG27649	*Cteniogenys*	FÃ11	Gui. 423		
MG27650	*Cteniogenys*	FÃ11	Gui. 424		
MG27651	*Cteniogenys*	FÃ11	Gui. 427		
MG27652	*Cteniogenys*	FÃ11 - Ctenio - NB: Zalmm??	Gui. 430		
MG27653	*Cteniogenys*	FÃ11	Gui. 343		
MG27654	*Cteniogenys*	FÃ11	Gui. 346		
MG27655	*Cteniogenys*	FÃ11	Gui. 348		
MG27656	*Cteniogenys*	FÃ11	Gui. 370		
MG27657	*Cteniogenys*	FÃ11	Gui. 372		
MG27658	*Cteniogenys*	FÃ11 - stereo - scan -Aufnahme	Gui. 380		
MG27659	*Cteniogenys*	FÃ11	Gui. 386		
MG27660	*Cteniogenys*	FÃ11 - max	Gui. 387	maxilar	
MG27661	*Cteniogenys*	FÃ11	Gui. 388		
MG27662	*Cteniogenys*	FÃ11	Gui. 389		
MG27663	*Cteniogenys*	FÃ11 - prämax	Gui. 391	Pré-maxila	
MG27664	*Cteniogenys*	FÃ11	Gui. 392		
MG27665	*Cteniogenys*	FÃ11 - Cteniogenys - prämax	Gui. 394	Pré-maxila	
MG27666	*Cteniogenys*	FÃ11	Gui. 395		
MG27667	*Cteniogenys*	FÃ11	Gui. 396		
MG27668	*Cteniogenys*	FÃ11 - max	Gui. 399	maxilar	
MG28091	Squamata / *Parviraptor ?*	Gui. 81 24.8	Gui Squ.17	Maxila	
MG28092		Gui. 81 24.8			
MG28093		Gui. 81 12.11 - Choristodera oder ? Amphib			
MG28094	Squamata / *Parviraptor*		Gui Squ.18		
MG28095	Squamata / *Dorsetisaurus*	Gui. 37 FÃ11	Gui Squ. 673		
MG28096	Squamata / *Dorsetisaurus*	Gui. 43	Gui Squ. 674		

MG28097	Squamata / *Dorsetisaurus*	Gui.NG 19.12.75 premaxilla	Gui Squ. 371	Pré-maxila	
MG28098	Squamata / *Dorsetisaurus*	Gui. L. 232 FÃ$_{11}$	Gui Squ. 675		
MG28099	Squamata / *Dorsetisaurus*	Gui.NG 30.12.76 Dorsetisaurus Z	Gui Squ. 15		
MG28100	Squamata / *Dorsetisaurus*	Dorsetisaurus	Gui Squ. 81		
MG28101	Squamata / *Introrsisaurus pollicedens n. g. n. sp.*	Gui. Ã. 73 FÃ$_{11}$			Holótipo
MG28102	Squamata / *Paramacellodus*	Gui. Lac 1/73 30.6.73	Gui Squ. 289		
MG28103	Squamata	Gui. 240 FÃ$_{11}$	Gui Squ. 656		
MG28104	Squamata / *Paramacellodus*	Gui. 253 FÃ$_{11}$	Gui Squ. 694		
MG28105	Squamata / *Paramacellodus*	Gui. 397 FÃ$_{11}$ - Sdöne zähne (Krohen!)	Gui Squ. 699	dente ?	
MG28106	Paramacellodidae sensu lato - Coll. Seiffert	Gui. Ã. 37 FÃ$_{11}$ - Max li	Gui Squ. 712	maxilar esquerdo	
MG28107	cf. Bnit. Mus. (c.p.=18.z) R. 808 i ? ?	Gui. Ã. 45 FÃ$_{11}$ - Schlöner kiefer	Gui Squ. 715		
MG28108	Paramacellodidae ind.	Gui. Ã. 71 FÃ$_{11}$ - E.i.C.p. = 18.Z. cf. Gui. Ã56	Gui Squ. 716		
MG28109	Squamata / *Paramacellodus*	Gui. GE.7 FÃ$_{11}$	Gui Squ. 718		
MG28110	Squamata / *Paramacellodus*	Gui. 73 18.10	Gui Squ. 290		
MG28111	Squamata / *Paramacellodus*	Gui. 73 3.10	Gui Squ. 291		
MG28112	Squamata / *Paramacellodus*	Gui. 73 22.10	Gui Squ. 293		
MG28113	Paramacellodidae sensu lato - Coll. Seiffert		Gui Squ. 656	preparação SEM	

MG28114	*Paramacellodus oweni*		Gui Squ. 699	preparação SEM	
MG28115	Paramacellodidae sensu lato - Coll. Seiffert		Gui Squ. 715	preparação SEM	
MG28116	Squamata / *Paramacellodus*	Gui. 22 FÃ$_{11}$	Gui Squ. 702		
MG28117	Squamata / *Paramacellodus*	Gui. 36 FÃ$_{11}$	Gui Squ. 703		
MG28118	Squamata / *Paramacellodus*	Gui. 73 15.10	Gui Squ. 487		
MG28119	Squamata	Gui.165 FÃ$_{11}$ - 20.5.61	Gui Squ. 944	Húmero?	
MG28120	Squamata	Gui. L. 47 FÃ$_{11}$ 20.5.61 - Humerus li	Gui Squ. 945	Húmero esquerdo	
MG28121	Squamata	Gui.L.129 FÃ$_{11}$ - Humerus	Gui Squ. 946	Húmero	
MG28122	Squamata	Gui.L.127 FÃ$_{11}$ - Humerus	Gui Squ. 947	Húmero	
MG28123	Squamata	Gui.L.128 FÃ$_{11}$ - Humerus re - distal tail	Gui Squ. 948	Húmero direito - parte distal	
MG28124	Squamata	Humerus	Gui Squ. 949	Húmero	
MG28125	Squamata / Lacertilia	Gui.L.181 FÃ$_{11}$ - Lazertilia distal humerus li	Gui Squ. 950	Húmero esquerdo - parte distal	
MG28126	Squamata	73.12.9	Gui Squ. 214		
MG28127	Squamata	Gui.L.201 FÃ$_{11}$ - Humerus	Gui Squ. 931	Húmero	
MG28128	Squamata	Gui.L.187 FÃ$_{11}$ - Humerus	Gui Squ. 932	Húmero	
MG28129	Squamata	Gui. L. 108 FÃ$_{11}$	Gui Squ. 933		

MG28130	Squamata	Gui. 190 FÃ11	Gui Squ. 934		
MG28131	Squamata	Gui.L.82 FÃ11 - Chelonia	Gui Squ. 935		
MG28132	Squamata	Gui.L.81 FÃ11	Gui Squ. 936		
MG28133	Squamata	Gui.L.86 FÃ11 - humerus	Gui Squ. 937		
MG28134	Squamata	Gui.L.145 FÃ11	Gui Squ. 938		
MG28135	Squamata	Gui.L.145 FÃ11	Gui Squ. 939		
MG28136	Squamata	Gui.L.146 FÃ11	Gui Squ. 940		
MG28137	Squamata	Gui.L.203 FÃ11	Gui Squ. 941		
MG28138	Squamata	Gui.L.214 FÃ11	Gui Squ. 942		
MG28139	Squamata	Gui. Humerus distal	Gui Squ. 943	Húmero direito - parte distal	
MG28140	Squamata	Gui. surangular	Gui Squ. 915	sub-angular	
MG28141	Squamata	Gui.L.131 FÃ11 - li. atlas bögen	Gui Squ. 916	Arcos do Atlas - esquerdo	
MG28142	Squamata	Gui.L.130 - Basiocc	Gui Squ. 917	Basioccipital	
MG28143	Squamata	Gui.L.130 - FÃ11- Basiocc?	Gui Squ. 918	Basioccipital	
MG28144	Squamata	Gui.L.130 - FÃ11- Crânio	Gui Squ. 919	schädel	
MG28145	Squamata	Gui.L.130 - FÃ11- Supraoccip.	Gui Squ. 920	Supraoccipital	

MG28146	Squamata	Gui.L.169 - FÃ11- C1 - Interz.	Gui Squ. 921	Supraoccipital	
MG28147	Squamata	Gui.L.168 FÃ$_{11}$ - li. atlas bögen	Gui Squ. 922	Arcos do Atlas - esquerdo	
MG28148	Squamata	Gui.L.165 FÃ$_{11}$ - re atlas bögen	Gui Squ. 923	Arcos do Atlas - direito	
MG28149	Squamata	Gui.L.143 FÃ$_{11}$ - Atlasbögen	Gui Squ. 924	Arco do Atlas	
MG28150	Squamata	Atlas bögen Lacerta lep.Gui - C1 (L.165)	Gui Squ. 925	C1	
MG28151	Squamata	Gui.L.168 FÃ$_{11}$ - re atlas bögen	Gui Squ. 926		
MG28152	Squamata	Gui. L.172 FÃ$_{11}$ - interzentren	Gui Squ. 927	intercentro	
MG28153	Squamata	Gui.L.45 FÃ$_{11}$ - halswirbel	Gui Squ. 928	Cervical	
MG28154	Squamata	Gui.L.45 FÃ$_{11}$ - halswirbel	Gui Squ. 929	Cervical	
MG28155	Squamata	Gui.L.123 FÃ$_{11}$ - C2 (Axis) eines scincom.	Gui Squ. 929	C2 (Axis)	
MG28156	Squamata	Gui. L.175 FÃ$_{11}$ wirbel	Gui Squ. 825	Vértebras	
MG28157	Squamata	Gui. (cf. 377)	Gui Squ. 826		
MG28158	Squamata	Gui. Lac. Wirbel 11.7	Gui Squ. 827	Vértebras	
MG28159	Squamata	Gui.L.18 FÃ$_{11}$ (cf. Gui. 377)	Gui Squ. 828		
MG28160	Squamata	Gui.L.66 FÃ$_{11}$ (cf. Gui. 377)	Gui Squ. 829		
MG28161	Squamata	Gui.L.377 FÃ$_{11}$ - Lac . Wirbel	Gui Squ. 830	Vértebra	

MG28162	Squamata	Gui. L.377 FÃ11 - Lac . Wirbel	Gui Squ. 831	Vértebra	
MG28163	Squamata	cf. Gui. 377	Gui Squ. 832		
MG28164	Squamata	Gui.L.133 FÃ11 - cf. L.161	Gui Squ. 833		
MG28165	Squamata	Gui.L.134 FÃ11 . - cf. Gui. L.162	Gui Squ. 834		
MG28166	Squamata	Gui.L.72 FÃ11	Gui Squ. 835	Vértebras	
MG28167	Squamata	Gui.L.377 FÃ11	Gui Squ. 836		
MG28168	Squamata	Gui.L.178 FÃ11 - Gui. . 11.7. wirbel	Gui Squ. 837		
MG28169	Squamata	Gui.L.142 FÃ11	Gui Squ. 838	Vértebras	
MG28170	Squamata	Gui.L.152 FÃ11 th wirbel	Gui Squ. 839	Vértebras toráxicas	
MG28171	Squamata	Gui.L.160 FÃ11	Gui Squ. 840		
MG28172	Squamata	Gui.L.186 FÃ11	Gui Squ. 841	Vértebra toráxica	
MG28173	Squamata	Gui.L.161 FÃ11	Gui Squ. 842		
MG28174	Squamata - *Ctenogenis*	Gui. L.162 FÃ11	Gui Squ. 843		
MG28175	Squamata	Gui. L.181 FÃ11 - Skaralw II	Gui Squ. 844	2ª vértebra sacral	
MG28176	Squamata	Gui. L.176 FÃ11	Gui Squ. 845		
MG28177	Squamata	Gui.L.179 FÃ11	Gui Squ. 846		

MG28178	Squamata	Gui.L.1973	Gui Squ. 847		
MG28179	Squamata	Guimarota Lacert. Wirbel - wirbel Guim. Konvex - Konvav	Gui Squ. 848		
MG28180	Squamata	?N.bojo?	Gui Squ. 849		
MG28181	Squamata	Lac?	Gui Squ. 850		
MG28182	Squamata	Gui.L.19 Bb - 13.7	Gui Squ. 851		
MG28183	Squamata	Guimarota Lacert. Wirbel -	Gui Squ. 852		
MG28184	Squamata	Gui.L.76 FÃ11 - Sacralwirbel - S3	Gui Squ. 853	3ª Vértebra sacral	
MG28185	Squamata	Gui.L.136 FÃ11 - caudalia	Gui Squ. 854	Vértebras caudais	
MG28186	Squamata	Gui.L.124 FÃ11 - sacrale 3 od. 4	Gui Squ. 855	3ª e/ ou ? 4ª Vértebra sacral	
MG28187	Squamata	Gui.L.124 FÃ11 - sacrale 3 od. 4	Gui Squ. 856		
MG28188	Squamata	Gui.L.168 FÃ11 - Sakralw.I	Gui Squ. 857	1ª vértebra sacral	
MG28189	Squamata	Gui.L.168 FÃ11 - präSakralw	Gui Squ. 858	vértebra pré-sacral	
MG28190	Squamata	Gui.L.170 FÃ11 - hämelbögen	Gui Squ. 859	Arco hemal	
MG28191	Squamata	Gui.L.182 FÃ11 - sacrale 4 ohne osso? Cond.2	Gui Squ. 860	4ª vértebra sacral	
MG28192	Squamata	caudal wirbel	Gui Squ. 861	vértebra caudal	
MG28193	Squamata	Gui.167 Klaue	Gui Squ. 742	Garra	

MG28194	Squamata	Gui. 173 - (S1) Endphalangen	Gui Squ. 750	falange (extremidade)	
MG28195	Squamata	Gui.L.226 Phal. dist.	Gui Squ. 997	falanges distais	
MG28196	Squamata	Gui.L.228 - Klaue	Gui Squ. 998	Garras	
MG28197	Squamata	Gui.L.227 - Klaue	Gui Squ. 999	Garras	
MG28198	Squamata	Gui.L.192 - Klaue	Gui Squ. 1003	Garras	
MG28199	Squamata	ungual phalange	Gui Squ. 1009	falanges ungueais	
MG28200	Squamata	Gui.336	Gui Squ. 681		
MG28201	Squamata	Gui	Gui Squ. 816		
MG28202	Squamata	Gui.L.135 - Pterygoid	Gui Squ. 817	Pterigóide	
MG28203	Squamata	Gui.L.89 li. - Pterygoid	Gui Squ. 818	Pterigóide (esquerda?)	
MG28204	Squamata	Gui.L.202	Gui Squ. 819		
MG28205	Squamata	Gui.L.150 - Pterygoid	Gui Squ. 820	Pterigóide(s)?	
MG28206	Squamata	Gui.L.135 - Pterygoid	Gui Squ. 821	Pterigóide	
MG28207	Squamata	Gui.L.166 - Pterygoid	Gui Squ. 823	Pterigóide(s)?	
MG28208	Squamata	GE2	Gui Squ. 824	Pterigóide(s)?	
MG28209	Squamata	Gui.L.10 - Ptery -pal.	Gui Squ. 823	Pterigóide+palato ?	

MG28210	Squamata	Gui.L.189 FÃ11 - Rippen	Gui Squ. 975	Costelas	
MG28211	Squamata	Gui.L.21 FÃ11	Gui Squ. 975		
MG28212	Squamata	Gui.L.195 FÃ11 - Rippen	Gui Squ. 976	Costelas	
MG28213	Squamata	Gui.L.196 FÃ11 - dist.Rippe	Gui Squ. 977	Costelas - parte distal	
MG28214	Squamata	Gui.177 FÃ11 - 9.8.61	Gui Squ. 978		
MG28215	Squamata	Gui.199 FÃ11 - Rippen (rund mit graz)	Gui Squ. 979	Costelas (redonda com bordo)?	
MG28216	Squamata	Gui.70 FÃ11	Gui Squ. 980		
MG28217	Squamata	Gui.79 FÃ11	Gui Squ. 981		
MG28218	Squamata	Gui.187 FÃ11 - 25-6-61	Gui Squ. 983		
MG28219	Squamata - Lacertilia	Gui.L.78 FÃ11 - lacertilia Rippe	Gui Squ. 984	Costela	
MG28220	Squamata	Gui.L.78 FÃ11	Gui Squ. 985		
MG28221	Squamata	Gui.L.163 FÃ11 - Rippe	Gui Squ. 986	Costela	
MG28222	Squamata	Gui.L.195 FÃ11 - Rippe	Gui Squ. 987		
MG28223	Squamata	Gui.L.111 - Parietale	Gui Squ. 862	Parietal	
MG28224	Squamata	Gui.L.93	Gui Squ. 863		
MG28225	Squamata	Gui.L.197 -Front.	Gui Squ. 864	Frontal	

MG28226	Squamata	Gui.193 - Parietale	Gui Squ. 865	Parietal	
MG28227	Squamata	Gui.GE 12 - Parietale	Gui Squ. 866	Parietal	
MG28228	Squamata	Gui.GE 9 L14 cf. ??	Gui Squ. 867	Parietal	
MG28229	Squamata	Gui.L.106 - Parietalia	Gui Squ. 868	Parietais	
MG28230	Squamata	Gui.L.154 - Frontalia	Gui Squ. 869	Frontais	
MG28231	Squamata	Gui.L.170 - Frontalia	Gui Squ. 870		
MG28232	Squamata	Gui.L.235 - Frontalia	Gui Squ. 871	Frontais	
MG28233	Squamata	Gui.L.38 - Frontalia	Gui Squ. 872	Frontais	
MG28234	Squamata	Gui.L.141 (Typ Gui.GE 12)	Gui Squ. 873		
MG28235	Squamata	Gui.L.153 - Parietalia	Gui Squ. 874	Parietais	
MG28236	Squamata	Gui.L.237	Gui Squ. 875		
MG28237	Squamata	Gui.L.140 (Typ Gui.82)	Gui Squ. 876		
MG28238	Squamata	Gui.L.43	Gui Squ. 877		
MG28239	Squamata	Gui.L.104	Gui Squ. 878		
MG28240	Squamata	GE 30	Gui Squ. 879		
MG28241	Squamata	GE 3 - guimarota - eidechsen - frontale ñ. - parietale	Gui Squ. 880	lagarto - frontal.e parietal	

MG28242	Squamata	Gui.L.28 - parietale	Gui Squ. 881	Parietal	
MG28243	Squamata	Gui.74 cf. 75 - Parietale 22 III 61	Gui Squ. 882	Parietal	
MG28244	Squamata	Gui.75 - (vgl. Gui.L.43)	Gui Squ. 883	Parietal	
MG28245	Squamata	Gui.171 - Frontale	Gui Squ. 884	Frontal	
MG28246	Squamata	Gui.170 - Parietalia	Gui Squ. 885	Parietais	
MG28247	Squamata	Gui.L36	Gui Squ. 886		
MG28248	Squamata	Gui.L44	Gui Squ. 887		
MG28249	Squamata	Gui.L40	Gui Squ. 888		
MG28250	Squamata	Gui.L.206 - Scapula	Gui Squ. 889	escápula ou omoplata	
MG28251	Squamata	Gui.L.198 FÃ$_{11}$ - Clavicula	Gui Squ. 890	Clavícula	
MG28252	Squamata	Coracoide oder ? Interclavicula - Guimarota	Gui Squ. 891	coracoíde ou ? Interclavícula	
MG28253	Squamata	Gui.191 FÃ$_{11}$	Gui Squ. 892	Clavícula	
MG28254	Squamata	Gui.L.215 Ulna ?	Gui Squ. 892	Ulna (cúbito)	
MG28255	Squamata	Gui.L.229 Li. Radius	Gui Squ. 893	Rádio - esquerdo	
MG28256	Squamata	Gui.L.229 Radius	Gui Squ. 894	Rádio - esquerdo	
MG28257	Squamata	Gui.55 - articulare eines squamata guimarota	Gui Squ. 751	Articular	

MG28258	Squamata	Gui. 331- Articulare	Gui Squ. 752	Articular	
MG28259	Squamata	Gui. 381	Gui Squ. 753		
MG28260	Squamata	Gui. 172	Gui Squ. 754		
MG28261	Squamata	Gui. 163 - nasale	Gui Squ. 755	Nasal	
MG28262	Squamata	Gui.L.113	Gui Squ. 757		
MG28263	Squamata	Gui.188 FÃ11 - scapula	Gui Squ. 757	Escápula ou omoplata	
MG28264	Squamata	Gui.L.206 - Sal?	Gui Squ. 759		
MG28265	Squamata	Gui.141- 4.7.1964 - Ang.+Supra Ang	Gui Squ. 760	Angular+supra-angular	
MG28266	Squamata	Gui.266	Gui Squ. 682		
MG28267	Squamata	Macellodus brodiei, OWEN, 1854 - Gui. I	Gui Squ. 683		
MG28268	Squamata	Macellodus brodiei, OWEN, 1854 - Gui.II	Gui Squ. 684		
MG28269	Squamata	Gui.L.138 FÃ11 - Macellodus cf. brodiei, OWEN, 1854 -	Gui Squ. 677		All Crocodylia Nydun - Mar 2008
MG28270	Squamata	Gui.L.139 FÃ11 - Macellodus cf. brodiei, brodiei, OWEN, 1854 -	Gui Squ.678		All Crocodylia Nydun - Mar 2008
MG28271	Squamata	Gui.verwandt mit Macellodus	Gui Squ.679		Relacionado com macello-dus
MG28272	Squamata	Gui.L.158 FÃ11 - Macellodus cf. brodiei	Gui Squ.680		All Crocodylia Nydun - Mar 2008
MG28273	Amphibia/Anura indt.	Gui 28.5.74 - Ilium Frosch	Gui-NA-11	Ilium de sapo	
MG28274	Amphibia/Anura indt.	23.1.75 N directo da Mina - ossos completos - Ilium links	Gui-NA-4	ilium esquerdo	

MG28275	Amphibia/Anura indt.	Gui 73 20.8 - ilium	Gui-AN-1	ilium	
MG28276	Amphibia/Anura indt.	3.6.75 - 10.6.75 - Wirbel+Est.?		Vértebras+?	
MG28277	Amphibia/Anura indt.	Guimarota "sardaniscas" - squaraven nachanglicor		?	
MG28278	Amphibia/Anura indt.	Guimarota			
MG28279	Amphibia/Anura indt.	Gui-o.C. 30.1.73 - Coracoid Anura?	Gui-AN-80	Coracoide	
MG28280	Amphibia/Anura indt.	30.10.74-31.7.74 W.D. U-Kieler?			
MG28281	Amphibia/Anura indt.	Guimarota "sardaniscas" - Einzelknocken +Wirbel		ossos soltos+vértebras	
MG28282	Anura? ou Cteniogenys?	3.2.75 N-N - Directo da Mina - ossos completos - Ilium		2 Ilium	
MG28283	Anura? ou Cteniogenys?	Gui 78 NG 20.9.78 - Tibio - Fibula - ossos completos - mamal?	Gui-AN-55		
MG28284	Reptilia /Choristodera/*Cteni-ogenys*	28.10.80 - Caudal W	Gui-80 W2 O.C.	Vértebra caudal	
MG28285	Anura? ou Cteniogenys?	23.1.78 - Gui-O.C. - Ilium	Gui-AN-6 CT	Ilium	
MG28286	Anura? ou Cteniogenys?	AMPHI? - ANURA? - 12.3.75 DAN GUI-DOSE - ILIUM?	Gui-AN- 9 CT	Ilium?	
MG28287	Anura? ou Cteniogenys?	W Cteniogenys caudal	Gui-O.C. 25.5.81	vértebra caudal	
MG28288	Anura? ou Cteniogenys?	I AUS e - Schädel ossos vairios I CT	Gui-Na-UAA	Ossos do cânio	
MG28289	Reptilia /Choristodera/*Cteni-ogenys*	Gui 79 31.5 - Cteniogenis ilium	Gui-AN-10	Ilium?	
MG28290	Reptilia /Choristodera/*Cteni-ogenys*	Gui-O.C. 24.4.78 - Anura il	Gui-AN-7 CT	Ilium?	
MG28291	Amphibia/Anura	2.2.77 Gui-O.C. Anura ilum?	Gui-AN-8 CT	Ilium?	
MG28292	Amphibia/Albanerpetontidae	Gui 78 26.12			
MG28293	Amphibia/Albanerpetontidae	Gui 73			
MG28294	Amphibia/Albanerpetontidae	Gui 78 9.1			
MG28295	Amphibia/Albanerpetontidae	Gui 12.6			

MG28296	Amphibia/Albanerpetontidae	Gui NG 23.2.77			
MG28297	Amphibia/Albanerpetontidae	Gui 81 17.11			
MG28298	Amphibia/Albanerpetontidae	ACBA GUI -			
MG28299	Amphibia/Albanerpetontidae	Gui 79 23.1			
MG28300	Amphibia/Albanerpetontidae	Gui.- O.C. ALBA D 2XC			
MG28301	Amphibia/Albanerpetontidae	? 12.4.80			
MG28302	Amphibia/Albanerpetontidae	Gui 78 20.7			
MG28303	Amphibia/Albanerpetontidae				sem etiqueta
MG28304	Amphibia/Albanerpetontidae	Gui 78 2.8			
MG28305	Amphibia/Albanerpetontidae				sem etiqueta
MG28306	Amphibia/Albanerpetontidae	Gui 74 31.5 - U-K Linker!			
MG28307	Amphibia/Albanerpetontidae	Gui 79 17.7 Links ??			
MG28308	Amphibia/Albanerpetontidae	Gui 81 3.7			
MG28309	Amphibia/Albanerpetontidae	Gui 79 6.6. Amphib. Rechts			
MG28310	Amphibia/Albanerpetontidae	Gui 81 16.7, Links ??			
MG28311	Amphibia/Albanerpetontidae	11.3.80 U-K			
MG28312	Amphibia/Albanerpetontidae	Gui 81 26.6			
MG28313	Amphibia/Albanerpetontidae	gui 75 24 U- links???			
MG28314	Amphibia/Albanerpetontidae	Gui 75 Ng 20.10.75 - Salamander - Dentale			Dentário
MG28315	Amphibia/Albanerpetontidae	Gui 78 26.12			
MG28316	Amphibia/Albanerpetontidae	Gui 75 16.6			
MG28317	Amphibia/Albanerpetontidae	Gui 80 13.12 - Alba ??			
MG28318	Amphibia/Albanerpetontidae	Gui 79 - Amphibi			
MG28319	Amphibia/Albanerpetontidae	Gui 79 29.1			
MG28320	Amphibia/Albanerpetontidae	Gui Ng 26.6.74 - BEZ ??			
MG28321	Amphibia/Albanerpetontidae				sem etiqueta
MG28322	Amphibia/Albanerpetontidae	Gui 78 18.7 D rechts ??		dentário direito ?	
MG28323	Amphibia/Albanerpetontidae	Gui 80 14.10 - dentale		dentário	

MG28324	Amphibia/Albanerpetontidae	Gui 79 19.7 - links D		dentário esquerdo?	
MG28325	Amphibia/Albanerpetontidae	Gui NG 10.7.74 BEZ - links D		dentário esquerdo?	
MG28326	Amphibia/Albanerpetontidae	Gui 78 25.7 - rechts ?? D		dentário direito ?	
MG28327	Amphibia/Albanerpetontidae	Gui NG 8.7.74 BEZ - links D		dentário esquerdo?	
MG28328	Amphibia/Albanerpetontidae	Gui 80 29.9 - rechts D		dentário direito ?	
MG28329	Amphibia/Albanerpetontidae	Gui NG 28.12.76 - rechts D		dentário direito ?	
MG28330	Amphibia/Albanerpetontidae	Gui 82 3.6 - D links		dentário esquerdo?	
MG28331	Amphibia/Albanerpetontidae	Gui 80 27.8 - Amphibia rechts dentale		dentário direito ?	
MG28332	Amphibia/Albanerpetontidae	Gui 82 29.4 - links D ?		dentário esquerdo?	
MG28333	Amphibia/Albanerpetontidae	Gui 79 16.1 - links D ?		dentário esquerdo?	
MG28334	Amphibia/Albanerpetontidae				sem etiqueta
MG28335	Amphibia/Albanerpetontidae				sem etiqueta
MG28336	Amphibia/Albanerpetontidae	Gui 80 9.10 -- ?? D ??			
MG28337	Amphibia/Albanerpetontidae	O.C. Gui 30.8.79 - Phalange		Falange	
MG28338	Amphibia/Albanerpetontidae	Gui 79 25.6. - ?? D??			
MG28339	Amphibia/Albanerpetontidae	Gui. 81 2.9. ??D??			
MG28340	Amphibia/Albanerpetontidae	Gui 82 28.4. ??D ??			
MG28341	Amphibia/Albanerpetontidae	Gui Ng 11.7.74 BEZ - rechts D		dentário direito ?	
MG28342	Amphibia/Albanerpetontidae	Gui 80 26.8. - Amphi. Albane - D dentale ??		Dentário	
MG28343	Amphibia/Albanerpetontidae				sem etiqueta
MG28344	Amphibia/Albanerpetontidae	Gui 80 13.8. - dental		Dentário	
MG28345	Amphibia/Albanerpetontidae				sem etiqueta
MG28346	Amphibia/Albanerpetontidae	Gui 82 24.3 ??D??			
MG28347	Amphibia/Albanerpetontidae	Gui81 29.9 ??D links??			
MG28348	Amphibia/Albanerpetontidae	Gui NG 27.1.77 ??links??D??			
MG28349	Amphibia/Albanerpetontidae	Gui 79 20.8 - Alban. UK			
MG28350	Amphibia/Albanerpetontidae	8.5.75 BEZ - D - N - lin??			
MG28351	Amphibia/Albanerpetontidae	Gui NG 77? - rechts D		dentário direito ?	

MG28352	Amphibia/Albanerpetontidae	Gui 81 3.6 D l??			
MG28353	Amphibia/Albanerpetontidae	Gui 81 3.1.- ??lul?? D			
MG28354	Amphibia/Albanerpetontidae	Gui 88 28.8 - rechts D			
MG28355	Amphibia/Albanerpetontidae	gui 79 3.1 - lin??			
MG28356	Amphibia/Albanerpetontidae	ACTE GR. RIPPE ? GUI		Costela	
MG28357	Amphibia/Albanerpetontidae	11.1.77 - Gui NG D L??			
MG28358	Amphibia/Albanerpetontidae	ACBA Gui 2x links??			
MG28359	Amphibia/Albanerpetontidae	Gui NG 27.1.77 - links?? D			
MG28360	Amphibia/Albanerpetontidae	14.6.77 - O.C. - Gui FI ? SCH			
MG28361	Amphibia/Albanerpetontidae	Gui 75 29.7 U-UDEK links??			
MG28362	Amphibia/Albanerpetontidae	Gui 78 3.6 - D liles??			
MG28363	Amphibia/Albanerpetontidae	Gui 78 15.7 Déntale - links??		Dentário	
MG28364	Amphibia/Albanerpetontidae	Gui 794.9 - Dentale D links??		Dentário	
MG28365	Amphibia/Albanerpetontidae	Gui 80 14.1 dentale rechts		Dentário direito	
MG28366	Amphibia/Albanerpetontidae	18.7.77 Gui - O.C. Rippe ?		Costela?	
MG28367	Amphibia/Albanerpetontidae	Gui 81 20.11- rechts D			
MG28368	Amphibia/Albanerpetontidae	Gui NG 26.6.74 BEZ - Linkes D		dentário esquerdo?	
MG28369	Amphibia/Albanerpetontidae	Gui 76 30.6 - links D		dentário esquerdo?	
MG28370	Amphibia/Albanerpetontidae	gui 78 12.7 - links D		dentário esquerdo?	
MG28371	Amphibia/Albanerpetontidae	Gui 81 12.11 D??			
MG28372	Amphibia/Albanerpetontidae	Gui NG 23.2.77 -lin?? D			
MG28373	Amphibia/Albanerpetontidae				sem etiqueta
MG28374	Amphibia/Albanerpetontidae				sem etiqueta
MG28375	Amphibia/Albanerpetontidae				sem etiqueta
MG28376	Amphibia/Albanerpetontidae	Gui 81 8.9. - Rechts D		dentario direito?	
MG28377	Amphibia/Albanerpetontidae	Gui 81 4.12 - D Rechts		dentario direito?	
MG28378	Amphibia/Albanerpetontidae	6.1.78 - links D		dentário esquerdo?	
MG28379	Amphibia/Albanerpetontidae	Gui 79 26.1. - Albi			

MG28380	Amphibia/Albanerpetontidae	22.3.80 - links D ?			
MG28381	Amphibia/Albanerpetontidae				sem etiqueta
MG28382	Amphibia/Albanerpetontidae	Gui 82 3.6 - rechts D		dentario direito?	
MG28383	Amphibia/Albanerpetontidae	6.9. Gui - 80 - D rechts		dentario direito?	
MG28384	Amphibia/Albanerpetontidae				sem etiqueta
MG28385	Amphibia/Albanerpetontidae	22.10.76 Gui-O.C. CHEUZ PON.			
MG28386	Amphibia/Albanerpetontidae				sem etiqueta
MG28387	Amphibia/Albanerpetontidae	Gui. 78 30.12. Rechts D		dentario direito?	
MG28388	Amphibia/Albanerpetontidae	Gui NG 15.12.76 Linkes D?		dentário esquerdo?	
MG28389	Amphibia/Albanerpetontidae	Gui 1.11.78 Linkes D?		dentário esquerdo?	
MG28390	Amphibia/Albanerpetontidae	Gui 77 29.1 U.K.			
MG28391	Amphibia/Albanerpetontidae	16.5.70BEZ links D		dentário esquerdo?	
MG28392	Amphibia/Albanerpetontidae	3.5.75 BEZ - D links		dentário esquerdo?	
MG28393	Amphibia/Albanerpetontidae	Gui 80 12.11- links D		dentário esquerdo?	
MG28394	Amphibia/Albanerpetontidae	Gui - O.C.. ALBA D 1x R		dentário esquerdo?	
MG28395	Amphibia/Albanerpetontidae	Gui 75 18.2. - U.K. ALBA			
MG28396	Amphibia/Albanerpetontidae	Gui. 9137 2.7.73 - rechts D		dentario direito?	
MG28397	Amphibia/Albanerpetontidae	Gui 73 7.89. D "frente"		dentario	
MG28398	Amphibia/Albanerpetontidae	Alte cor. R-Dentale - Gui 21a amph. - plebx. R-		dentario direito?	
MG28399	Amphibia/Albanerpetontidae	Humeus ALBA		Húmero	
MG28400	Amphibia/Albanerpetontidae	Gui. 73 20.11 - D Rechts		dentario direito?	
MG28401	Amphibia/Albanerpetontidae	Gui. 73 16.8 - D links		dentário esquerdo?	
MG28402	Amphibia/Albanerpetontidae	Gui 10173 2.7.73 - D rechts		dentario direito?	
MG28403	Amphibia/Albanerpetontidae	Guimarota urodela mandibeln Brunch - Alba Cor. dentalia - 3x rechts 1x links		mandibulas fragmentadas : 3 direitas 1 esquerda	
MG28404	Amphibia/Albanerpetontidae	Alba Cor. dentalia - 3x rechts 1x links		dentarios: 3 direitos 1 esquerdo	
MG28405	Amphibia/Albanerpetontidae	Gui. 62 Mand. Typ urod. - Alba Cor. dentalia - 9x rechts 19x links		dentario 9 direitos 13 esquerdod	

MG28406	Amphibia/Albanerpetontidae	Guimarota urodela mandibeln Symphysialregion - Alba Cor. dentalia - 3x links - 1x rechts		mandibulas: 3esquerda 7direitas - região sinfisial da mandíbula ("queixo")	
MG28407	Amphibia/Albanerpetontidae	Alba Cor. dentalia - 3x rechts 10x links		dentarios: 3 direitos 10 esquerdo	
MG28408	Amphibia/Albanerpetontidae	Guimarota urodela mandibeln - Alba Cor. dentalia 1x rechts		mandibula esquerda (fragmento)	
MG28409	Amphibia/Albanerpetontidae	Gui 73 16.10 - D links - Grüße+Fo?o??		dentario esquerdo	
MG28410	Amphibia/Albanerpetontidae	Gui 73 30.11 -Amphibin - D links		dentario esquerdo	
MG28411	Amphibia/Albanerpetontidae	Gui 73 14.12 - D links		dentario esquerdo	
MG28412	Amphibia/Albanerpetontidae	Gui 73 10.10 - D rechts		dentario direito	
MG28413	Amphibia/Albanerpetontidae	Gui Urodele 14			
MG28414	Amphibia/Albanerpetontidae	A81*			
MG28415	Amphibia/Albanerpetontidae	Gui 108 - 4* - 3.6.31 IV			
MG28416	Amphibia/Albanerpetontidae	Gui 112 - unbrandbal ?- 25.5.61			
MG28417	Amphibia/Albanerpetontidae	21a P Gui. Amph.			
MG28418	Amphibia/Albanerpetontidae	A64			
MG28419	Amphibia/Albanerpetontidae	A9			
MG28420	Amphibia/Albanerpetontidae	Unbrandbal A18			
MG28421	Amphibia/Albanerpetontidae	3.10.74 - 10.7.74 EX! W Dosen? SCHROTT !			
MG28422	Amphibia/Albanerpetontidae	3.3.75 - AMPHI W -Dosen DRN			
MG28423	Amphibia/Albanerpetontidae	Gui 80 29.12 Dent*		Dentário	
MG28424	Amphibia/Albanerpetontidae	Amphi W - DOSEN / DAN 13.3.75 Gui			
MG28425	Amphibia/Albanerpetontidae	Gui - 80 13.11.80 O.C. AMPH W			
MG28426	Amphibia/Albanerpetontidae				sem etiqueta
MG28427	Amphibia/Albanerpetontidae	Gui 74 23.3 - Frontale Albanerpeton		Frontal	
MG28428	Amphibia/Albanerpetontidae	rechts D		Dentário direito	
MG28429	Amphibia/Albanerpetontidae	Gui 78 7.12 D links?		Dentário esquerdo	
MG28430	Amphibia/Albanerpetontidae	Gui 9			
MG28431	Amphibia/Albanerpetontidae	Gui 79 alban.UK - +- homoplat?? 36 Zähne !		36 dentes???	

MG28432	Amphibia/Albanerpetontidae	Gui - Links gut +-??			
MG28433	Amphibia/Albanerpetontidae	Gui 8124.8.RIPPE !		Costela	
MG28434	Amphibia/Albanerpetontidae	17.7.76 GUI - O.C. ?			
MG28435	Amphibia/Albanerpetontidae	30.7.74 - W. Dosen ?			
MG28436	Amphibia/Albanerpetontidae	Zachvard ? 30.7.74 - 5.6.74			
MG28437	Amphibia/Albanerpetontidae	Gui 12.75 Gui - O.C. ?			
MG28438	Amphibia/Albanerpetontidae	18.12.75 Gui - O.C. ?			
MG28439	Amphibia/Albanerpetontidae	80 Gui			
MG28440	Amphibia/Albanerpetontidae	3.10.74 - 10.7.74 - Weifre?'??			
MG28441	Amphibia/Albanerpetontidae	30.7.74 - 5.6.74 -W. Dosen ?			
MG28442	Amphibia/Albanerpetontidae	Gui 5			
MG28443	Amphibia/Albanerpetontidae	30.74 -5.6.74 ALBA - H GORX Dose ?			
MG28444	Amphibia/Albanerpetontidae	3.10.74 - 31.7.74 Front. Z! - Gui - ALBA G9			
MG28445	Amphibia/Albanerpetontidae	GUI 9e			
MG28446	Amphibia/Albanerpetontidae	Gui 77 9.7 ALBA D links - 31 zähne		dentes	
MG28447	Amphibia/Albanerpetontidae	9N Gui			
MG28448	Amphibia/Albanerpetontidae	Gui 81 23.1 - albanerpeton premax - Prämaxillare *		pré-maxilar	
MG28449	Amphibia/Albanerpetontidae	GUI - O.L. 10.5.78 ?			
MG28450	Amphibia/Albanerpetontidae	GUI - 79 - 9.1.79 - AMPHI - W - O.C.			
MG28451	Amphibia/Albanerpetontidae	ALBA ?? - 30.7.74 - 5.6.74			
MG28452	Amphibia/Albanerpetontidae	3.5.78 GUI - O.C. ??			
MG28453	Amphibia/Albanerpetontidae	ALBA U-KIEFER		Mandíbula inf.	
MG28454	Amphibia/Albanerpetontidae	GUI 9M			
MG28455	Amphibia/Albanerpetontidae	Guimarota "sardaniscas" - Albanerpeton - Links max		Maxilar esquerdo	
MG28456	Amphibia/Albanerpetontidae	Gui 78 11.7. - links D - ???		Dentário esquerdo	
MG28457	Amphibia/Albanerpetontidae	Gui - Max rechts galetso!		Dentário direito	
MG28458	Amphibia/Albanerpetontidae				sem etiqueta

MG28459	Amphibia/Albanerpetontidae	3.10 - 31.7.74 GUI ALBA - F			
MG28460	Amphibia/Albanerpetontidae	GUI 9-9			
MG28461	Amphibia/Albanerpetontidae	GUI 9f			
MG28462	Amphibia/Albanerpetontidae	3.6.75 - 10.6.75 - Frontalia ?		Frontalia	
MG28463	Amphibia/Albanerpetontidae	Guimarota 14.3.75 Amphibia posan			
MG28464	Amphibia/Albanerpetontidae	GUI - 9-V			
MG28465	Amphibia/Albanerpetontidae	Guimarota 15.3.75 Amphibia Dosen			
MG28466	Amphibia/Albanerpetontidae	GUI - 9-V			
MG28467	Amphibia/Albanerpetontidae	?			
MG28468	Amphibia/Albanerpetontidae	GUI - 73 - 23.10.73 ?			
MG28469	Amphibia/Albanerpetontidae	DAN 21.2.75- Amphibian - Knüchen??			
MG28470	Amphibia/Albanerpetontidae	Gui - Dose 26.2.75 - ? ?			
MG28471	Amphibia/Albanerpetontidae	7.7.76 GUI - O.C. ?			
MG28472	Amphibia/Albanerpetontidae	30.7.74 - 5.6.74 ??			
MG28473	Amphibia/Albanerpetontidae	Gui 77 Albi 5.8.F - Gui ALBA - 666			
MG28474	Amphibia/Albanerpetontidae	GUI NG 24.2.77 ???- Links D			dentario esquerdo
MG28475	Amphibia/Albanerpetontidae	30.7.74 - 5.6.74 W. Dose			
MG28476	Amphibia/Albanerpetontidae	Gui 9a			
MG28477	Amphibia/Albanerpetontidae	Gui 3			
MG28478	Amphibia/Albanerpetontidae	Gui 9 - 4			
MG28479	Amphibia/Albanerpetontidae	28.9.77 GUI - O.C. ?			
MG28480	Amphibia/Albanerpetontidae	Gui 9 - f			
MG28481	Amphibia/Albanerpetontidae	Gui 75 10.9. ALBA - D - links NEU! Ellen			
MG28482	Amphibia/Albanerpetontidae	GUI - 9C			
MG28483	Amphibia/Albanerpetontidae	3.10.74 - 31.7.74 W dosen			
MG28484	Amphibia/Albanerpetontidae	GUI 80 13-10.80 OSSOS COMPL. - EX			
MG28485	Amphibia/Albanerpetontidae	30.7.74 - 5.6.74 - Zükenchen?????			

MG28486	Amphibia/Albanerpetontidae	3.10.74 - 31.7.74 - Uisch			
MG28487	Amphibia/Albanerpetontidae	Gui 4			
MG28488	Amphibia/Albanerpetontidae	3.10. -31.7.74 ALBA F - DOSE 3X GUI			
MG28489	Amphibia/Albanerpetontidae	GUI 17			
MG28490	Amphibia/Albanerpetontidae	8.1.79 - GUI - O.C. ?			
MG28491	Amphibia/Albanerpetontidae	27.6.75 - Frauhole - GUI - ALBA - 81 T.D.			
MG28492	Amphibia/Albanerpetontidae	GUI - 9k			
MG28493	Amphibia/Albanerpetontidae	20.8.76 GUI - O.C. ?			
MG28494	Amphibia/Albanerpetontidae	3.10.77 GUI - O.C. ? S W			
MG28495	Amphibia/Albanerpetontidae	21.8.80 - GUI - O.C. ?			
MG28496	Amphibia/Albanerpetontidae	ALBA - ATLA - GUI - O.C.S 14.6.77?			
MG28497	Amphibia/Albanerpetontidae	GUI - O.C. 27.10.77 RIPPE+ PT+EID			
MG28498	Amphibia/Albanerpetontidae	GUI - O.C. 26.1.77?			
MG28499	Amphibia/Albanerpetontidae	24.12.79 GUI - 73 W O.C. AMPHI ?			
MG28500	Amphibia/Albanerpetontidae	GUI - ALBA 74			
MG28501	Amphibia/Albanerpetontidae	GUI 81 31.8 Frontale		Frontal	
MG28502	Amphibia/Albanerpetontidae	GUI - ALBA - 99			
MG28503	Amphibia/Albanerpetontidae				ilegível
MG28504	Amphibia/Albanerpetontidae	GUI 99			
MG28505	Amphibia/Albanerpetontidae	22.2.75 - GUI - ALBA - F WEIRE DOSE			
MG28506	Amphibia/Albanerpetontidae	GUI - 80 - 3.11.80 - OSS. COMPL. ALBA			
MG28507	Amphibia/Albanerpetontidae	GUI - 80 - 18.11.80 - O.S.			
MG28508	Amphibia/Albanerpetontidae	27.7.7 - GUI - O.C. ?			
MG28509	Amphibia/Albanerpetontidae	GUI - 80 - 18.5.81 - O.C. AMPH.			
MG28510	Amphibia/Albanerpetontidae	AMPH - W - 6.12.79 - O.C.			
MG28511	Amphibia/Albanerpetontidae	28.10.77 - O.C. GUI ?			
MG28512	Amphibia/Albanerpetontidae	GUI - 79 11.1.79 W - AMPHI			

MG28513	Amphibia/Albanerpetontidae	23.6.76 - GUI - O.C. ?			
MG28514	Amphibia/Albanerpetontidae	AMPHIB - W - O.C. - 13.9.81			
MG28515	Amphibia/Albanerpetontidae	GUI - 79 - 22.10.79 - O.C. ?			
MG28516	Amphibia/Albanerpetontidae	GUI - ALBA - 70			
MG28517	Amphibia/Albanerpetontidae	GUI 94			
MG28518	Amphibia/Albanerpetontidae				ilegível
MG28519	Amphibia/Albanerpetontidae	Guimarota "sardaniscas" Albanerp. Rechts Max.		Maxilar direito (fragmentos?)	
MG28520	Amphibia/Albanerpetontidae	Gui. 81 13.8 - D - Albanerpeton - Frontale		Frontal	
MG28521	Amphibia/Albanerpetontidae				sem etiqueta
MG28522	Amphibia/Albanerpetontidae	GUI - MAX rechts - Crut! ?		maxilar direito ??	
MG28523	Amphibia/Albanerpetontidae	1.7.76 GUI - O.C. ?			
MG28524	Amphibia/Albanerpetontidae	GUI - O.C. ALBA - F			
MG28525	Amphibia/Albanerpetontidae	GUI - O.C. 10.9.77 ?			
MG28526	Amphibia/Albanerpetontidae	25.7.76 - GUI - O.C. ?			
MG28527	Amphibia/Albanerpetontidae	24.6.75 - v.D .GUI - ALBA 2x - F			
MG28528	Amphibia/Albanerpetontidae				ilegível
MG28529	Amphibia/Albanerpetontidae	Schädel Knochen - PIV. Pij. F - ossos varios - 1 GUI		Ossos do crânio	
MG28530	Amphibia/Albanerpetontidae	6.3.76 GUI - O.C. ?			
MG28531	Amphibia/Albanerpetontidae	GUI - ALBA - 72			
MG28532	Amphibia/Albanerpetontidae	GUI - ALBA G0LD - 1 (15)			
MG28533	Amphibia/Albanerpetontidae	4.3.75 Dose - GUI - ALBA 84			
MG28534	Amphibia/Albanerpetontidae	GUI 77 9.7 D rechts		Dentário direito	
MG28535	Amphibia/Albanerpetontidae	Amphibian - Albanerpeton - Dentale rechts		Dentário direito	
MG28536	Amphibia/Albanerpetontidae	30.7 - 5.6. 74 GUI - ALBA 3x - A			
MG28537	Amphibia/Albanerpetontidae	29.8.76 - GUI - O.C. ?			
MG28538	Amphibia/Albanerpetontidae	30.4.74 - GUI - O.C. ?			
MG28539	Amphibia/Albanerpetontidae	GUI - ALBA - 82 - 22.2.75 - Dose			
MG28540	Amphibia/Albanerpetontidae	3.10.74 - 31.7.74 W.D. GUI - ALBA			

MG28541	Amphibia/Albanerpetontidae	GUI - ALBA - 76			
MG28542	Amphibia/Albanerpetontidae	11.3.75 - Dose - GUI - ALBA - 85			
MG28543	Amphibia/Albanerpetontidae	GUI 73 - 18.7 - FRONTALE - GUI - ALABA		frontal	
MG28544	Amphibia/Albanerpetontidae				sem etiqueta
MG28545	Amphibia/Albanerpetontidae	ALBA DRN AXIS O:C: GUI - 74		AXIS - 2ª vértebra Cervical	
MG28546	Amphibia/Albanerpetontidae	21.3.77 GUI - O.C. ?			
MG28547	Amphibia/Albanerpetontidae	PU - ALBA - PM -65 NO !			
MG28548	Amphibia/Albanerpetontidae				ilegível
MG28549	Amphibia/Albanerpetontidae	GUI. - ALBA O.C. - 19.1.81 ?			
MG28550					ilegível
MG28551					ilegível
MG28552	*Amphibia*	AMPHIB - W - 16.12.80 - O.C. GUI			
MG28553		GUI - O.C. - 21.12.76 ?			
MG28554	*Amphibia*	GUI - 79 - W O.C. AMPHI - 24.1.73			
MG28555	*Amphibia*	GUI - 81 27.5.812 O.C. - W AMPHI			
MG28556	Amphibia/Albanerpetontidae	GUI - ALBA - 74			
MG28557		Chevron 18.12.76 GUI - O.C. ?			
MG28558		28.7.76 GUI - O.C. ?			
MG28559	Amphibia/Albanerpetontidae	GUI - ALBA - 78			
MG28560		GUI - 77 - 18.4.77 - O.C. RIPPE ?		Costela ?	
MG28561		GUI NG - rechts D - 15.12.76 - +/- 38 Zähne eina-palett Gübe		Dentário direito +/- 38 dentes	
MG28562	Amphibia/Albanerpetontidae	GUI - ALBA 67 + P.N. ?? 30.7.74 - 5.6.74			
MG28563		Gui 73 9.7 - Humeus		Húmero	
MG28564	Amphibia/Albanerpetontidae	3.6.75 - 10.6.75 - ALBA 4X - Weife Dose			
MG28565		GUI - 78 16.12.78 O.C.			
MG28566		2.11.76 GUI - O.C. ?			
MG28567		2.6.80 O.G. GUI ?			

MG28568					sem etiqueta
MG28569	Amphibia/Albanerpetontidae	17.6.75 ?? - GUI - ALBA - 80			
MG28570	Amphibia/Albanerpetontidae	GUI - ALBA 95 3.10.74 - 31.7.74			
MG28571		16.6.75 frauhole? K. Dose - A			
MG28572	Amphibia/Albanerpetontidae	FRONTALE - GUI - ALBA 64		frontal	
MG28573	*Amphibia*	3.12.7 - AMPH W O.C.			
MG28574	*Amphibia*	Wirbel - ?? - AMPHIS ??		Costela	
MG28575	*Amphibia*	AMPHI W - 4.15.75 O.C.			
MG28576		GUI 9d			
MG28577		2.12.80 GUI - O.C. ?			
MG28578		GUI - 9i			
MG28579					sem etiqueta
MG28580	Amphibia/Albanerpetontidae	30.6.75 - 10.6.75 GUI - ALBA PT 104			
MG28581		S			sem etiqueta
MG28582		R			sem etiqueta
MG28583		9			sem etiqueta
MG28584	Amphibia/Albanerpetontidae	"Guimarota" "Sardaniscas" - Albanerpetontid Rechts prāmax		pré-maxilar ??	
MG28585					sem etiqueta
MG28586	Amphibia / Anura	7.12.78 - O.C.R - U! - ANURA - GUI - NA 71			
MG28587	Amphibia / Anura	AMPHIB ? - O.C. ANU - 9.10.79 - 1207? F-T ? - GUI AN 52			
MG28588	Amphibia / Anura	GUI - 74 ANURA - Radio -Ulna - DAN O.C. ?? - GUI AN 74		Radio - cúbito (ulna)	
MG28589	Amphibia / Anura	GUI - 3.6.77 - O.C. u.u. ANURA IR - GUI - Na 79			
MG28590	Amphibia / Anura	GUI - O.C. 18.10.76 - ANURA ? - GUI - NA 86			
MG28591	Amphibia / Anura	O.C. RADIO - ULNA - GUI - 81 2.7.81 O.C. ANURA - GUI - AN 88		Radio - cúbito (ulna)	
MG28592	Amphibia / Anura	13.11.76 GUI - O.C. ANURA - GUI - AN 77			

MG28593					sem etiqueta
MG28594		9 P GUI -			
MG28595	Amphibia/Albanerpetontidae	GUI - ALBA PT - 10 - 30.7.74 - 5.6.74			
MG28596		GUI - (2) Links Prämax - 8 Zähne		Pré-maxilar esquerdo - 8 dentes	
MG28597		G			
MG28598		GUI - R - Präm - 12 Z		Pré-maxilar direito - 12 dentes	
MG28599		Guimarota - Links Prämax - 12 Zähne		Pré-maxilar esquerdo - 12 dentes	
MG28600		GUI - R - Präm - 10 Z		Pré-maxilar direito - 10 dentes	
MG28601	Amphibia / Anura	Gui 80 26.3 ANURA ? MBIOFIBULA - GUI - AN 49 - NO!		Fíbula (perónio)	
MG28602	Amphibia / Anura	GUI - O. C. 6.9.77 ANURA ? U-R - GUI - RN 73		cúbito (ulna) direita	
MG28603	Amphibia / Anura	ANURA ? T - F 18.4.78 - GUI - O.C. - GUI - AN 54 NO!			
MG28604	Amphibia / Anura	19.3.81- T-F.- GUI - O.C. ANURA? GUI - AN 51 NO!			
MG28605	Amphibia / Anura	16.8.79 U-R - GUI O.C. ANURA ? GUI - AN 87 NO!			
MG28606	Amphibia / Anura	11.10.80 O.C. - GUI ANURA ? T-F - GUI - AN 47			
MG28607	Amphibia / Anura	19.3.77 - GUI - O.C. ANURA R - U - GUI AN 78			
MG28608		GUI 2			
MG28609		? GUI - GROBE			
MG28610					Ilegível
MG28611		Z			
MG28612		Guimarota links PRÄMAX - 2 Zähne		Pré-maxilar esquerdo - 2 dentes	
MG28613		8			
MG28614		10			
MG28615		Guimarota links PRÄMAX - Zähne ??		Pré-maxilar esquerdo - Dentes ???	
MG28616	Amphibia / Anura	1.3.76 - GUI - O.C. ANURA - R.U. - GUI - AN 80		cúbito (ulna) direito	
MG28617	Amphibia / Anura	7.11.77 - ANURA - R.U. - O.C. - GUI - GUI - AN 88		cúbito (ulna) direito	

MG28618	Amphibia / Anura	Gui - O.C. 23.11.77 - ANURA ? ULNA - RAD - GUI - AN 75		Radio - cúbito (ulna)	
MG28619	Amphibia / Anura	2.9.76 Gui - O.C. - ANURA - R-U - GUI - AN 85		cúbito (ulna) direito	
MG28620	Amphibia / Anura	16.6.80 GUI - O.C. ANURA ? F-T? - GUI - AN 48			
MG28621	Amphibia / Anura	Gui - O.C. 28.5.77 - ANURA ? U - R - GUI - AN 76		cúbito (ulna) direito	
MG28622	Amphibia / Anura	31.7.78 - GUI - O.C. ANURA - F-F - GUI - AN 50			
MG28623	Amphibia/Albanerpetontidae	GUI 75 6.8 ALBA -D Rechts		dentario direito	
MG28624					sem etiqueta
MG28625		GUI - Links Prämax - 9 Zähne		Pré-maxilar esquerdo - 9 dentes	
MG28626		GUI - R Prämax - 11 Z		Pré-maxilar direito - 11 dentes	
MG28627	Amphibia/Albanerpetontidae	GUI - ALBA - PT - 100 - links - 26.6.75 - Rosa Dose - parietale		Parietal esquerdo	
MG28628		? - sardaniscas - links Prämax		Pré-maxilar esquerdo	
MG28629		GUI - R Prämax - 13 Z		Pré-maxilar direito - 13 dentes	
MG28630		Rechts Prämax		Pré-maxilar direito	
MG28631	Amphibia / Anura	4.9.78 O.C. ANURA RE - ULN ? - GUI - AN 81		cúbito (ulna) direito ?	
MG28632	Amphibia / Anura	Gui - O.C. 9.3.76 R.U. - ANURA - GUI - AN 80		cúbito (ulna) direito	
MG28633	Amphibia / Anura	19.12.77 GUI - O.C. ANURA - R.U. ? - GUI - AN 83		cúbito (ulna) direito	
MG28634	Amphibia / Anura	ANURA ! ULN _ RADIO O.C. 20.8.79 - GUI - AN 72		Radio - cúbito (ulna)	
MG28635	Amphibia / Anura	ANURA ! R-U 3.3.76 GUI O.C. - GUI - AN 82		Radio - cúbito (ulna)	
MG28636		GUI ?? Dentale ??		dentario direito	
MG28637		GUI 75 - U-K - 16.4 - Rechts D		dentario direito	
MG28638		GUI 81 28.10 , Rechts D		dentario direito	
MG28639	Amphibia/Albanerpetontidae	Frontale 30.7.74 - 5.6.74- 62 - GUI - ALBA		Frontal	
MG28640		GUI - SARD			
MG28641		Rechtes prämax nichs Zähne Sardaniscas		Pré-maxilar direito - sem dentes	
MG28642		??? GUI ??? links			
MG28643		ALBA - 30.8.74 - 5.6.74 PT - 107 NEU !			

MG28644		GUI - SAR ??? - 11-30-175			
MG28645		GUI - R- PRÄM - 8Z		Pré-maxilar direito - 8 dentes	
MG28646	Amphibia/Albanerpetontidae	ALBA - 30.8.74 - 5.6.74 PT - 106 NEU !			
MG28647		GUI - O.C. 21.1.78 - R-U - ANURA - GUI AN 84			
MG28648	Amphibia/Albanerpetontidae	GUI - ALBA - 75			
MG28649		GUI 6			
MG28650		GUI - LINKES - PRÄMAX - 7Zähne		Pré-maxilar esquerdo - 8 dentes	
MG28651		GUI - R- PRÄM - 8Z		Pré-maxilar direito - 8 dentes	
MG28652	Amphibia/Albanerpetontidae	GUI - SAR ALBA - UK - rechts?? - Zähne ???		Mandibula direita	
MG28653	Amphibia/Albanerpetontidae	GUI - SAR ALBA - UK - rechts?? - Zähne ???			
MG28654		+3+1+4+1+4+1-174+1??			
MG28655		?? Gui ??rechts			
MG28656		Gui - sard D links			
MG28657		Gui 80 28.6 - D links		dentário esquerdo	
MG28658	Amphibia/Albanerpetontidae	GUI - ALBA - PT - 102 - 30.7.74 - 5.6.74			
MG28659					sem etiqueta
MG28660		D-links - Gui - SARD			
MG28661		GUI - Links Prämax - 10 Zähne		Pré-maxilar esquerdo - 8 dentes	
MG28662		-1-1-16 -142 - Gui Sar			
MG28663		GUI - SAR ??			
MG28664		aus GUI ??			
MG28665	Amphibia/Albanerpetontidae	GUI - SAR - ALBA - UK (unter kiefer) - links - Zähne ??		Mandíbulas esquerdas	
MG28666	Amphibia/Albanerpetontidae	25.5.77 - GUI - O.C. ALBA - AX IS		AXIS (2ª cervical)	
MG28667	Amphibia/Albanerpetontidae	GUI - ALBA - 94 - 3.10.74 - 31.7.74			
MG28668		GUI 75 - GRÖBE! .- links D		Dentário esquerdo	
MG28669		GUI 79 - 21.7 - O .- links D - ?		Dentário esquerdo	
MG28670		GUI 75 - 18.2 - rechts D??		Dentário direito	

MG28671					sem etiqueta
MG28672	Amphibia/Albanerpetontidae	Gui - ALBA - PT - 103			
MG28673	Amphibia/Albanerpetontidae	3.6 - 10.6.75 - GUI ALBA - F + U.K		Mandíbula ??	
MG28674		GUI G-S			
MG28675	Amphibia/Albanerpetontidae	GUI 76 19.7 - ALBAN - OK - M - PM			
MG28676	Amphibia/Albanerpetontidae	??? ALBA - ??			
MG28677					sem etiqueta
MG28678		3			
MG28679					sem etiqueta
MG28680		GUI 1			
MG28681		GUI 75 -11.6 - Links - D		Dentário esquerdo	
MG28682		4			
MG28683		GUI 96			
MG28684		U7O - KKN 39 - M - 1X			
MG28685		GUI 79 7.11 - rechts D ??		Dentário direito	
MG28686		GUI 9C			
MG28687		GUI 9Z			
MG28688		GUI 9K			
MG28689		GUI 82 25.8 - Rechts maxillare		maxilar direito	
MG28690					sem etiqueta
MG28691	Amphibia/Albanerpetontidae	11.6.75 Frontal - GUI - ALBA 89 v.os.??		Frontal	
MG28692	Amphibia/Albanerpetontidae	GUI - ALBA 90 30-Z - -5.6.74			
MG28693					sem etiqueta
MG28694	Amphibia/Albanerpetontidae	GUI - ALBA - GOLD - 2 (14)			
MG28695					sem etiqueta
MG28696					sem etiqueta
MG28697	Amphibia/Albanerpetontidae	Guimarota "sardaniscas" Albanerpetontidae - uk links und symphyse		Mandíbula esquerda e sínfise	

MG28698	Amphibia/Albanerpetontidae	O.S 74 GUI - ALBA AXIS		Axis	
MG28699	Amphibia/Albanerpetontidae	Guimarota "sardaniscas" Albanerpetontidae - uk links und symphyse		Mandíbula esquerda e sínfise	riscado
MG28700					sem etiqueta
MG28701					sem etiqueta
MG28702		Gui gj			
MG28703					sem etiqueta
MG28704					sem etiqueta
MG28705	Amphibia/Albanerpetontidae	ALBA - AXIS - O.C. GUI - 24.11.77		Axis	
MG28706	Amphibia/Albanerpetontidae	21.2.75 - Dosen DAN ALBA - AXIS		Axis	
MG28707	Amphibia/Albanerpetontidae	4.3. zs Dose - GUI - ALBA 83			
MG28708		3.6.75 - 10.6.75 ??			
MG28709					sem etiqueta
MG28710	Amphibia/Albanerpetontidae	GUI - ALBA - 71			
MG28711	Amphibia/Albanerpetontidae	GUI - ALBA - 73			
MG28712		GUI NG Links D - eramplat?? 38 Zähne		Dentário esquerdo - 38 dentes	
MG28713		11.3.75 Dor - GUI - ALBA - 86			
MG28714	Amphibia/Albanerpetontidae	GUI - ALBA 93 - 3.10.74 -31.7.75			
MG28715					sem etiqueta
MG28716	Amphibia	DOSE - MARC - 24.2.75 GUI AMPHI WL			
MG28717	Amphibia/Albanerpetontidae	Frontalia 21.6.75 ? - Rosa dose - GUI - ALBA 87			
MG28718	Amphibia/Albanerpetontidae	Guimatota "sardaniscas" - Albanerpetontidae - Links Prāmax - ??Zü??		Pré-maxilar esquerdo - 8 dentes	
MG28719	Amphibia/Albanerpetontidae	AXIS AMPHIB O.C. DRW - ALBA 74 ?			
MG28720	Amphibia/Albanerpetontidae				sem etiqueta
MG28721	Amphibia/Albanerpetontidae	GUI - ALBA 79			
MG28722	Amphibia/Albanerpetontidae	ALBA - GUI AXIS O.C. - 5.8.78		Axis	
MG28723	Amphibia/Albanerpetontidae	GUI 75 19.8 - ALBA -D rechts		Dentário direito	
MG28724		GUI 81 2.10 MAXILLARE*		Maxilar	

MG28725		GUI 8			
MG28726		GUI 9-W			
MG28727		GUI 9-X			
MG28728	Amphibia	AMPHI - W - O.C.		Vértebra ?	
MG28729	Amphibia	GUI - 81 30.6.81 - W - O.C. AMPHI		Vértebra ?	
MG28730	Amphibia/Albanerpetontidae	12.3.75 GUI - AXIS - DOSE DRM - ALBA		Axis	
MG28731	Amphibia/Albanerpetontidae	19.5.77 - GUI - O.C.- ALBA - AXIS		Axis	
MG28732	Amphibia/Albanerpetontidae	GUI - ALBA - 77			
MG28733	Amphibia/Albanerpetontidae	GUI - ALBA - 66 - 30.6.74			
MG28734	Amphibia/Albanerpetontidae	GUI - O.C. ALBA H - 10X			
MG28735					sem etiqueta
MG28736	0	AMPHI 74 O.C. DAN - WIRBEL		Vértebra	
MG28737	0	3.10.74 - 31.7.74 W. Dose - AMPHI - WIRBEL			
MG28738	Amphibia/Albanerpetontidae	ALBA - H - OSS. COMP. - GUI - 79 - 20.12.79 - 20.12.79 - Ossos completos			
MG28739					sem etiqueta
MG28740	Amphibia / Anura	GU - AN 55 - 28.5.77 - GUI - O.C. u.a. ANURA - Präfrontal ?		Pré-frontal	Caixa com etiqueta - FRONTALIA - ALBANERPETONTIDA
MG28741	Amphibia / Anura	GU - AN 59 - GUI 78 18.10 - F-P- ?		Frontal	Caixa com etiqueta - FRONTALIA - ALBANERPETONTIDA
MG28742	Amphibia / Anura	GU - AN 60 - GUI 80 21.10. 80 - F-P- ?		Frontal	Caixa com etiqueta - FRONTALIA - ALBANERPETONTIDA
MG28743	Amphibia / Anura	GU - AN 61 - GUI 81 26.11 F-P- ?		Frontal	Caixa com etiqueta - FRONTALIA - ALBANERPETONTIDA
MG28744	0	AMPH - 2 - SACR- VERTEBRA		Vértebra sacral	
MG28745	Amphibia/Albanerpetontidae	GUI - ALBA - H - 200 - ALBA - rechtes - 1.4.75. gui 75 NG - ossos completos			

MG28746		A4 * - L - dentale - alta - A4 - GUI - GruBe?? + edo??			
MG28747		GUI 80 - 23.10.			
MG28748		GUI 75 - 17.6.			
MG28749		GUI 79 - 11.7.			
MG28750		GUI 76 - 30.6.			
MG28751		GUI 81 - 31.3			
MG28752		GUI 75 - 3.7.			
MG28753		GUI 77 - 18.7.			
MG28754		GUI 78 - 14.6.			
MG28755		GUI 79 - 30.11.			
MG28756		GUI 75 - 13.3.			
MG28757		GUI 81 - 1.4.			
MG28758		GUI 81 - 14.8.			
MG28759		GUI 80 - 25-8-80 - h - Osso comp		Húmero	
MG28760		Gui 75 - 17.3			
MG28761		GUI 81 - 3.1.			
MG28762	Reptilia/Squamata /	16.3.77 - GUI - O.C. EID W		Vértebras ?	
MG28763		GUI 81 - 1.10.			
MG28764		GUI 81 - 6.11.			
MG28765		GUI 75 - 26.3			
MG28766	Reptilia/Squamata /	28.3.77 - GUI O.C. - EID - Humerus		Húmero	
MG28767	Reptilia/Squamata /	30.7.74. - 5.6.74.- EID - GUI dose - H -		Húmero	
MG28768	Reptilia/Squamata /	13.3.75 - GUI - EID - 3 H		Húmero	
MG28769		GUI 75 - 16.6.			
MG28770		GUI 81 6.10			
MG28771		GUI 80 - 20.12.			
MG28772		GUI 80 - H - 3.11.80. Oss.compl.		Húmero	

MG28773	Reptilia/Squamata /	Pterygoid EID 3.6.75 - W. dose		Pterigoide	
MG28774		GUI 75 - 26.6			
MG28775		GUI 75 - 25.6.			
MG28776		EID GUI			
MG28777		GUI 75 8.4.			
MG28778		GUI 75 25.7			
MG28779		GUI 81 7.2			
MG28780		GUI NG 18.1.77			
MG28781		GUI 81 1.7			
MG28782	Reptilia /Choristodera	GUI 79 8.5 - Chorist. Zähn		dente	dente de Choristodera
MG28783		GUI 77 2.7			
MG28784		GUI 82 18.5			
MG28785		GUI NG 5.1.77			
MG28786	Reptilia/Squamata /	30.7.74 - 5.6.74 WiDosen ? - EID 2x proximum quadratum		Quadrado parte proximal	
MG28787		5.6.75.N BEZ			
MG28788	Reptilia/Squamata /	26.5.76 - GUI - O.C. EID - H			
MG28789		GUI 79 18.7			
MG28790		GUI 77 15.7			
MG28791		GUI 81 10.12			
MG28792	Reptilia /Choristodera/*Cteni-ogenys*	GUI 21.12.73			
MG28793		GUI 81 24.11			
MG28794		GUI 81 21.5			
MG28795		GUI 79 3.7			
MG28796		GUI 75 1.4			
MG28797		GUI 79 25.6			
MG28798		GUI 79 16.1			
MG28799		GUI 80 8.10			

MG28800		GUI 80 10.10			
MG28801		Gui 75 7.6			
MG28802		Gui 79 20.7			
MG28803		Gui 79 7.12			
MG28804		GUI 80 18.1			
MG28805	Reptilia/Squamata /	Gui 74 NG 24.7 Problematikum supraoccipitale ? - REPTI ? EID!		supra-occipital	
MG28806		**PARIETALE EIDECHSE GUI**		Parietal - Lagarto	
MG28807		GUI NG 22.5.76			
MG28808	Reptilia/Squamata /	GUI. LAC. 14/73 16.7.73			
MG28809	Reptilia/Squamata /	**Pterygoid rechts EID (EIDECHSE = LAGARTO) - W. Dose - 3.10 - 31.7.74**		Pterigoide direito	
MG28810	Reptilia/Squamata / ?	3.10.74 - 31.7.74 Frontale - EID ? DOSE		Frontal	
MG28811	Reptilia	Reptile GUI. 82 4.6			
MG28812		GUI 76 30.6 ?!			
MG28813	Reptilia/Squamata /	Gui - 79 - H - 1-6-79 ossos completos - Humerus EID		Húmero	
MG28814					Caixa vazia
MG28815		Gui 78 15.6			
MG28816		Gui 79 11.1			
MG28817	Reptilia/Squamata /	GUI 80 - EID - 16.9.80 - H -Oss.comp. H		húmero	
MG28818	Reptilia/Squamata /	24.2.75 GUI - DOSE - EID Jugale intercentrum - V. FFT - CRS - SUPRA - OCCIPITALE / DOSE MARC		Jugale "intercentro" - Supra - Occipital	
MG28819		Gui 75 22.9 ? Pterygoide !		Pterigoide	
MG28820		GUI 81 10.8			
MG28821		GUI 76 13.7			
MG28822	Reptilia/Squamata /	? GUI 14.3.75 ? - DOSEN / DAN - EID - 601 - QUADRATUM / PROC		Quadrado	
MG28823		GUI 75 18.6			

MG28824	Reptilia/Squamata /	GUI 75 27.3 HUMERUS? EID.			
MG28825		GUI 82 4.6.			
MG28826	Reptilia /Choristodera/*Cteni-ogenys*	GUI 78 29.6. - Cteniogenys			
MG28827	Reptilia/Squamata /	10.11.76 - GUI - O.C. EID - ULNA		ulna (cúbito)	
MG28828		GUI 81 5.5.			
MG28829		GUI 81 24.3			
MG28830		20.12.77			
MG28831	Reptilia /Choristodera/*Cteni-ogenys*	GUI 81 13.11 - Cteniogenys			
MG28832	Reptilia/Squamata /	EID - 2X Articulare - GUI - Ossos vários ans X - Schädel		Ossos do Crânio - Articular	
MG28833		Gui 79 9.11			
MG28834	Reptilia/Squamata /	Parietale - EID - GUI ans - 1		Parietal	
MG28835		GUI 75 1.4			
MG28836		Gui 76 3.7.			
MG28837	Crocodyliformes	Gui 81 13.1 - cf. *Lisboasaurus*			
MG28838	Reptilia/Squamata /	19.7.77 GUI - O.C. EID - W		Vértebra	
MG28839	Reptilia/Squamata /	GUI 82 15.6. Frontale ? EID.		Frontal	
MG28840	Reptilia /Choristodera/*Cteni-ogenys*	GUI 81 2.11 Cteniogenis Parietal		Parietal	
MG28841		Gui 82 31.12			
MG28842		GUI 81 30.6			
MG28843		GUI 76 1.7			
MG28844	Reptilia/Squamata /	EID O.C. GUI - (1 12.5.81 Axis		Axis	
MG28845	Reptilia/Squamata /	28.9.76 - GUI - O.C. EID - PT			
MG28846	Reptilia/Squamata /	Gui - 75 20.3 EID M-1			
MG28847		Gui 74 5.4			
MG28848		Gui 80 11.9			

MG28849	Reptilia/Squamata /	25.2.76 - EID 3 X - GUI O.C.			
MG28850	Reptilia/Squamata /	GUI - /5 24.3 EID PRÄMAX + NASALIA+PR¨FRON-TALIA !!!		Prémaxilar+nasal+ préfrontal	
MG28851		Gui 77 14.7			
MG28852		GUI NG 28.1.77			
MG28853	Reptilia/Squamata /	GUI - 80 2.7.80- EID H - OSS Comp		Húmero	
MG28854	"Tecodonte"	GUI 79 7.5 - Dentale thecodont		Dentário	
MG28855		Gui 76 29.7			
MG28856		Gui 75 25.3			
MG28857		Gui 80 24.11			
MG28858		Gui 75 9.6			
MG28859		Gui 79 21.2			
MG28860		Gui 8120.11			
MG28861	*Reptilia*	Gui NG 14.12.76 - Reptile			
MG28862	Reptilia/Squamata /	GUI EID H			
MG28863		Gui NG 22.1.77			
MG28864	Reptilia/Squamata /	EID - GUI - Quadratum ans		osso quadrado	
MG28865	Reptilia/Squamata /	EID - GUI - Ptery ans		pterigóide	
MG28866	Reptilia/Squamata /	DOSE? EID?- ? 30.7.74 -5.6.74			
MG28867	Reptilia/Squamata /	Pterygoide - EID - PTERY - Dosen GUI - ? 14.3.75 - DAN			
MG28868	Reptilia/Squamata /	12.12.77			
MG28869	Reptilia/Squamata /	GUI 81 28.12.Links jugale EIUD		Jugal	
MG28870	Reptilia/Squamata /	EID - GUI - Pterygoide - An S 1 Schädel - Dose os-sos varios			
MG28871	Reptilia/Squamata /	12.5.76 GUI - O.C. EID . -PT			
MG28872	Reptilia/Squamata /	13.3.75. Gui Dose - EID F			
MG28873	Reptilia/Squamata /	Gui 75 8.4. EID			
MG28874	Reptilia/Squamata /	GUI 81 7.4.			

MG28875	Reptilia/Squamata /	GUI - 82 31.3.2 - EID - PTERY		Pterigóide	
MG28876	Reptilia/Squamata /	3.10.74 - 31.7.74 DOSE EID?			
MG28877		Gui 82 26.3			
MG28878		19.12.77			
MG28879	Reptilia /Choristodera/*Cteni-ogenys*	Gui 21.12.73 - Humerus *cf . Cteniogenys*		Húmero	
MG28880		Gui 79 30.5			
MG28881	Reptilia/Squamata /	EID - Coronoide aus 1 - Schädel ossos varios GUI !		Coronoide	
MG28882	Reptilia /Choristodera/*Cteni-ogenys*	Gui 81 17.11 *Cteniogenys*			
MG28883		Gui 80 6.10 EID ? - Frontalia		Frontal	
MG28884	Reptilia/Squamata /	EID - GUI JUGALE - 2x ans 1		Jugal	
MG28885		GUI 75 9.7			
MG28886	Reptilia/Squamata /	GUI - O.C. 4.10.77 EID ? Ucn			
MG28887		Gui 80 7.10			
MG28888		GUI NG 13.7.74 BEZ			
MG28889		Gui 82 6.5.			
MG28890	Reptilia /Choristodera/*Cteni-ogenys*	Gui 21.12.73 - Humerus cf . Cteniogenys		Húmero	
MG28891	Reptilia/Squamata /	25.2.75 EID Dose Parietale		Parietal	
MG28892	Reptilia/Squamata /	26.4.79 - GUI 79 EID - Ossos Comp. H		Húmero	
MG28893	Reptilia/Squamata /	Gui 76 18.9 EID ?			
MG28894		Gui 82 17.5			
MG28895	Reptilia/Squamata /	Gui - 79 14-7-79 - ossos compl. - EX - EID			
MG28896	Reptilia/Squamata /	EID - GUI WIRBEL		Vértebra	
MG28897	Reptilia/Squamata /	3.6.75 - 10.6.75 H - EID - GUI - 4		Húmero	
MG28898	Reptilia/Squamata /	GUI - 81 5-8-81 Ossos compl. EID			
MG28899		GUI 75 17.7.			
MG28900		GUI - EID - 12xF - aus intersectes Unuchen??			

MG28901	*cf. Cteniogenys*	GUI 81 25.11			
MG28902	Reptilia /Choristodera/*Cteni-ogenys*	Gui 73 13.12			
MG28903		GuiI 82 10.5			
MG28904		Gui 82 1.4.			
MG28905		Gui 79 24.2			
MG28906	Reptilia/Squamata /	GUI 82 7.6 - F- EID.			
MG28907		Gui 79 23.1			
MG28908		Gui 77 16.7			
MG28909	Reptilia/Squamata /	Gui 77 29.10 H EID		Húmero	
MG28910		Gui 76 3.7			
MG28911	Mesoeucrocodylia incertae sedis /*Lisboasaurus ?*	Gui 75 6.9			
MG28912		Gui 80 12.8			
MG28913		Gui 75 16.4			
MG28914		Gui 80 27.8			
MG28915	Reptilia/Squamata /	Intercentrum EID ! GUI 74 ?indet.?Bau.		intercentro	
MG28916		Gui 82 4.6.			
MG28917		Gui 79 3.11			
MG28918	Reptilia/Squamata /	Gui - O.C. 4.3.76 EID - H		Húmero	
MG28919		22.4.76 - Gui - O.C. EID - JUGALE		Jugal	
MG28920		Gui 77 18.7			
MG28921		Gui 75 3.9			
MG28922		Gui 77 30.6			
MG28923		Gui 81 2.11			
MG28924	Reptilia/Squamata /	29.10.77 Gui O.C. EID ? R+U		rádio+cúbito (ulna)	
MG28925		Gui 81 23.11			
MG28926		Gui 81 26.10			
MG28927	Reptilia/Squamata /	Gui. Lac. 13/73 - 14.7.73			

MG28928	Reptilia/Squamata /	24.8.76 - Gui - O.C. EID ? - H			
MG28929		Gui 77 15.7			
MG28930	Reptilia/Squamata /	Gui - EID PTERYGOID		Pterigoide	
MG28931		Gui 81 18.8 - Schädel element- Dach!		elementos do crânio	
MG28932		3.10.74 - 31.7.74 Eoachale?? -DOSE E ?EID			
MG28933		8.2.76 GUI - O.C. EID. ! H		Húmero	
MG28934		Gui 10.10.73			
MG28935		Gui 79 21.6			
MG28936		Gui 79 26.12			
MG28937		Gui 75 7.6			
MG28938		Aus 1 Schädel ossos varios Schmauzwirbel		vertebras 2x	
MG28939		Gui 81 9.9			
MG28940		Gui 82 29.3			
MG28941	Reptilia /Choristodera/*Cteni-ogenys*	Gui 79 22.5 Choristodere? Tecodonte			
MG28942		Gui 79 13.1			
MG28943		Gui 82 29.3			
MG28944		Gui - EID PTERYGOID aus1 Schädel Oss. Vor		pterigoide	
MG28945		Gui 80 17.12			
MG28946		DOSE - GUI 22.2.75 intercentrum /FFTLOS ?		intercentro	
MG28947		Gui 81 3.7.			
MG28948		GUI 81 22.6			
MG28949		Gui NG 18.1.77			
MG28950		GUI - EID - H - húmero			
MG28951		Gui NG 27.1.77			

B SNEAK PEEK ON THE VERTEBRATE MICROFOSSIL ASSEMBLAGES FROM THE LOURINHÃ FORMATION

Table B.1: Simplified diversity and abundance data from the Lourinhã Formation.

	Porto das Barcas	Zimbral	Valmitão	Abundance	Diversity
Chondrichthyes	16	0	0	16	2
Osteichthyes	376	1014	1274	2664	4
Lissamphibia	20	39	231	290	4
Mammalia	3	0	6	9	2
Plesiosauroidea	0	2	1	3	1
Lepidosauria	8	27	53	88	1
Choristodera	2	3	3	8	1
Crocodylomorpha	104	288	477	869	7
Dinosauria	2	8	11	21	6
Pterosauria	0	1	2	3	1

Table B.2: Global counting of microfossil remains in each VMA from the Lourinhã Fm.

	Porto das Barcas	Zimbral	Valmitão	Total general
Hybodontidae	14	0	0	14
Batoidea?	2	0	0	2
Indet Actinopterygii	338	963	1271	2572
Semionotiformes	21	27	1	49
Pycnodontiformes	12	20	0	32
Caturidae	5	4	2	11
Indet Amphibia	0	6	15	21
Albanerpetontidae	19	31	190	240
Caudata	0	0	3	3
Anura	1	2	23	26
Dryolestidae	1	0	4	5
Multituberculata	2	0	2	4
Plesiosauroidea	0	2	1	3
Lepidosauria	8	27	53	88
Chrositodera	2	3	3	8
Crocodylomorpha indet	3	150	33	186
Goniopholidae	44	69	187	300
Atoposauridae	30	34	121	185
Bernissartiidae	23	32	95	150
Pholidosauridae	0	0	8	8
Machimosaurus	1	0	1	2
Lusitanisuchus	3	3	32	38
Thyreophora	0	0	1	1
Heterodontosauria	0	1	1	2
Sauropoda	0	3	2	5
Theropoda	0	2	5	7
Dromaeosauridae	2	1	1	4
Megalosauridae	0	1	1	2
Pterosauria	0	1	2	3
Total	531	1382	2058	3971

Table B.3: Raw data of counting from each sample bulk studied in the analysis.

	PB-10-17-02	PB-06-17-01	PB-06-17-03	PB-06-17-04	PB-06-17-05	PB-03-19-01	ZIM-11-16-01	ZIM-11-16-02	ZIM-06-17-01	ZIM-06-17-04	VAL-06-16-01	VAL-10-17-01	VAL-03-19-03	VAL-03-19-04	VAL-03-19-07	VAL-03-19-10
Hybodontidae	3	1	3	0	1	6	0	0	0	0	0	0	0	0	0	0
Batoidea?	0	0	0	0	0	2	0	0	0	0	0	0	0	0	0	0
Indet Actinopterygii	32	22	131	8	3	142	34	62	153	714	1040	218	3	2	4	4
Semionotiformes	1	0	2	0	1	17	2	4	4	17	1	0	0	0	0	0
Pycnodontiformes	0	0	1	1	0	10	2	2	2	14	0	0	0	0	0	0
Caturidae	2	0	1	0	0	2	1	1	1	1	2	0	0	0	0	0
Indet Amphibia	0	0	0	0	0	0	0	1	4	1	15	0	0	0	0	0
Albanerpetontidae	8	0	8	0	1	2	9	6	14	2	143	46	0	0	1	0
Caudata	0	0	0	0	0	0	0	0	0	0	2	0	1	0	0	0
Anura	0	0	1	0	0	0	0	0	1	1	18	3	2	0	0	0
Dryolestidae	0	0	0	0	1	0	0	0	0	0	1	0	2	0	0	1
Multituberculata	0	0	2	0	0	0	0	0	0	0	2	0	0	0	0	0
Plesiosauroidea	0	0	0	0	0	0	0	0	0	2	1	0	0	0	0	0
Lepidosauria	3	1	1	0	0	3	4	2	13	8	42	6	0	3	0	2
Choristodera	2	0	0	0	0	0	0	2	1	0	2	1	0	0	0	0
Crocodylomorpha indet	2	0	1	0	0	0	87	46	14	3	32	0	0	0	0	1
Goniopholidae	11	0	9	0	1	23	0	38	31	0	134	44	2	4	1	2
Atoposauridae	10	3	4	1	2	10	0	24	10	0	83	34	0	2	0	2
Bernissartiidae	2	1	0	0	1	19	0	15	17	0	55	36	0	2	0	2
Pholidosauridae	0	0	0	0	0	0	0	0	0	0	3	4	0	0	0	1
Machimosaurus	0	0	1	0	0	0	0	0	0	0	1	0	0	0	0	0
Lusitanisuchus	0	0	1	0	0	2	0	2	1	0	24	8	0	0	0	0
Thyreophora	0	0	0	0	0	0	0	0	0	0	1	0	0	0	0	0

Heterodontosauria	0	0	0	0	0	0	0	1	0	0	1	0	0	0	0	0
Sauropoda	0	0	0	0	0	0	0	0	0	3	2	0	0	0	0	0
Theropoda	0	0	0	0	0	0	0	0	0	2	4	1	0	0	0	0
Dromaeosauridae	0	1	0	1	0	0	1	0	0	0	1	0	0	0	0	0
Megalosauridae	0	0	0	0	0	0	0	1	0	0	1	0	0	0	0	0
Pterosauria	0	0	0	0	0	0	0	1	0	0	2	0	0	0	0	0
Total	76	29	166	11	11	238	140	208	266	768	1613	401	10	13	6	15

Table B.4: Palaeoecological diversity in different Mesozoic VMAs.

	Las Hoyas	Cloverly	Buenache	Angeac-Charente	Ksar Metlili	Cherves-de-Cognac	Porto das Barcas	Zimbral	Valmitão	Uña	Quarry 9
Obligate	15	11	9	9	8	7	6	5	4	3	2
Amphibious	12	12	8	9	7	5	9	9	12	8	10
Facultative	8	27	7	26	16	17	4	5	8	13	53

Table B.5: Palaeoecological abundance in different Mesozoic VMAs.

	Ecological preference	Porto das Barcas	Zimbral	Valmitão	Cloverly	Angeac-Charente	Ksar Metlili	Quarry 9
Chondrichthyes	Obligate	16	0	0	299	886	29	0
Osteichthyes	Obligate	376	1014	1274	3601	10656	17638	571
Lissamphibia	Amphibious	20	39	231	729	325	97	110
Mammalia	Facultative	3	0	6	68	21	63	282
Plesiosaura	Obligate	0	2	1	0	0	0	0
Lepidosauria	Facultative	8	27	53	40	40	31	857
Choristodera	Amphibious	2	3	3	0	2	14	0
Crocodylomorpha	Amphibious	104	288	477	2223	1262	5303	1016
Dinosauria	Facultative	2	8	11	1153	4973	99	494
Pterosauria	Facultative	0	1	2	0	33	605	15

C PALAEOBIODIVERSITY OF CROCODYLOMORPHS FROM THE LOURINHÃ FORMATION BASED ON THE TOOTH RECORD: INSIGHTS INTO THE PALAEOECOLOGY OF THE LATE JURASSIC OF PORTUGAL

Table C.1: List of remains picked from the sediments of the Valmitão VMA in 2019, according to the taxa they have been attributed.

Taxa	Remains found
Bivalvia	56 shell fragments
Gastropoda	65 shell fragments / molds / counter molds
Actinopterygii	6 teeth, 97 scales
Undetermined Tetrapoda	41 vertebral arches, 1 fragmentary acetabulum, 5 phalanxes
Lissamphibia	9 dentaries, 1 frontal, 13 vertebrae, 6 femurs
Undetermined Sauropsida	1 humerus, 3 femurs, 1 tibia
Lepidosauria	5 fragmentary frontals, 7 vertebrae, 6 osteoderms
Undetermined Archosauria	1 ungual falange
Crocodylomorpha	126 teeth, 4 osteoderms
Pterosauria	1 tooth
Dinosauria	5 teeth
Others	9 unidentified vertebrae, 22 unidentified teeth, 75 eggshells, 58 splint bones

Table C.2: Selected measurements (in mm for lengths, in degrees for angles) of the crocodylomorphs teeth morphotypes. **NLgS**, number of lingual striations; **NLbS**, number of labial striations; **DoM**, Denticles on mesial and distal margins.

	Morphotype	Height	Width	Ratio H/W	Labiolingual	Mesiodistal	Ratio Lb/Mb	Apex	Axis	NLgS	NLbS	DoM	Striations
ML2586	1	0,734	0,830	0,884	0,371	0,809	0,459	0,000	0,000	14	10	Absent	Flabelliform
ML2497	2	1,345	0,667	2,016	0,521	0,654	0,797	20,397	0,000	11	0	Absent	Subparallel
ML2498	2	1,223	0,773	1,582	1,159	1,440	0,805	16,403	0,000	14	10	Absent	Subparallel
ML2499	3	1,875	0,763	2,457	0,533	0,654	0,815	42,610	0,000	12	0	Absent	Flabelliform
ML2511	3	1,949	0,952	2,047	0,580	0,728	0,797	29,200	0,000	0	0	Absent	Flabelliform
ML2512	3	1,490	0,768	1,940	0,287	0,701	0,409	33,270	0,000	13	0	Absent	Flabelliform
ML2522	4	2,577	1,680	1,534	1,128	1,530	0,737	0,000	0,000	30	31	Absent	Flabelliform
ML2523	4	1,432	0,966	1,482	0,622	0,896	0,694	0,000	0,000	21	18	Absent	Flabelliform
ML2424	4	1,035	0,760	1,362	0,438	0,671	0,653	0,000	0,000	19	18	Absent	Flabelliform
ML2532	5	1,381	1,474	0,937	0,637	1,055	0,604	0,000	0,000	33	34	Absent	Flabelliform
ML2533	5	1,225	1,381	0,887	0,571	1,041	0,549	0,000	0,000	24	31	Absent	Flabelliform
ML2534	5	1,489	1,357	1,097	0,595	1,121	0,531	0,000	0,000	24	19	Absent	Flabelliform
ML2535	5	1,162	1,043	1,114	0,579	0,921	0,629	0,000	0,000	23	23	Absent	Flabelliform
ML2422	6	3,337	1,689	1,976	1,208	1,591	0,759	32,125	0,000	9	7	Absent	Subparallel
ML2423	6	2,861	0,972	2,943	0,867	0,880	0,985	13,206	0,000	6	9	Absent	Subparallel
ML2424	6		1,793		1,471	1,676	0,878		0,000	10	7	Absent	Subparallel
ML2425	6	2,889	1,034	2,794	0,905	1,028	0,880	41,148	0,000	8	8	Absent	Subparallel
ML2426	6	2,787	1,557	1,790	1,291	1,474	0,876	15,556	0,000	0	0	Absent	Absent
ML2427	6	1,931	0,964	2,003	0,686	0,954	0,719	18,054	0,000	0	0	Absent	Absent
ML2455	7	2,089	1,882	1,110	1,445	1,916	0,754		0,000	10	12	Absent	Subparallel
ML2456	7	4,079	2,237	1,823	2,165	2,252	0,961	23,486	0,000	11	11	Absent	Subparallel
ML2457	7	3,237	2,474	1,308	1,873	2,447	0,765		0,000	0	0	Absent	Unpreserved
ML2458	7	4,539	2,165	2,097	1,918	2,080	0,922	37,925	0,000	9	12	Absent	Subparallel
ML2478	8		1,279		0,992	1,115	0,890			19	14	Absent	Subparallel
ML2479	9	1,195	1,780	0,671	0,676	1,223	0,553	0,000	0,000	21	30	Absent	Subparallel
ML2480	9	0,758	1,071	0,708				0,000	0,000	21	23	Absent	Subparallel
ML2481	9	0,711	1,090	0,652	0,325	0,827	0,393	0,000	0,000	27	19	Absent	Subparallel
ML2482	9	0,776	0,976	0,795	0,338	0,689	0,491	0,000	0,000	17	19	Absent	Subparallel
ML2483	9	1,484	2,553	0,581	0,373	0,941	0,396	0,000	0,000	32	28	Absent	Subparallel
ML2473	10	3,653	1,830	1,996	1,215	1,616	0,752	14,299	12,531	0	0	Present	Absent
ML2474	10		1,759		1,253	1,605	0,781			0	0	Present	Absent
ML2475	10	3,595	1,527	2,354	1,010	1,474	0,685	15,152	7,600	0	0	Present	Absent

D THE ENIGMATIC DUO—REVISION OF *CTENIOGENYS* (CHORISTODERA) AND *MARMORETTA* (LEPIDOSAUROMORPHA) FROM THE GUIMAROTA BEDS (LUSITANIAN BASIN, PORTUGAL)

Table D.1: List of the specimens from the Guimarota collection examined to identify *Cteniogenys* and *Marmoretta* specimens.

MG specimen n°	Previous identification in MG catalogue		This work		
	Taxon assigned	Bone identified	Remarks	Taxon assigned	Bone identified
MG27417	Reptilia /Choristodera/*Cteniogenys*	Maxilla		Diapsida / Choristodera / *Cteniogenys* aff. *C. antiquus*	Maxilla
MG27419	Reptilia /Choristodera/*Cteniogenys*	Maxilla		Diapsida / Choristodera / *Cteniogenys* aff. *C. antiquus*	Maxilla
MG27420	Reptilia /Choristodera/*Cteniogenys*			Diapsida / Choristodera / *Cteniogenys* aff. *C. antiquus*	Surangular
MG27586	Reptilia /Choristodera/*Cteniogenys*		Highly fragmented	Diapsida / Choristodera / *Cteniogenys* aff. *C. antiquus*	Dentary?
MG27588	Reptilia /Choristodera/*Cteniogenys*	Premaxilla		Diapsida / Lepidosauromorpha / New unnamed taxon 1	Premaxilla

MG27589	Reptilia /Choristodera/*Cteniogenys*		Highly fragmented	Diapsida / Choristodera / *Cteniogenys* aff. *C. antiquus*	Dentary?
MG27593	Reptilia /Choristodera/*Cteniogenys*	Premaxilla		Diapsida / Lepidosauromorpha / New unnamed taxon 1	Premaxilla
MG27594	Reptilia /Choristodera/*Cteniogenys*	Maxilla	Highly fragmented	Diapsida / Choristodera / *Cteniogenys* aff. *C. antiquus*	Maxilla?
MG27599	Reptilia /Choristodera/*Cteniogenys*		Highly fragmented	Diapsida / Choristodera / *Cteniogenys* aff. *C. antiquus*	Dentary?
MG27600	Reptilia /Choristodera/*Cteniogenys*			Diapsida / Choristodera / *Cteniogenys* aff. *C. antiquus*	Premaxilla
MG27601	Reptilia /Choristodera/*Cteniogenys*		Highly fragmented	Diapsida / Choristodera / *Cteniogenys* aff. *C. antiquus*	Dentary?
MG27602	Reptilia /Choristodera/*Cteniogenys*		Highly fragmented	Diapsida / Choristodera / *Cteniogenys* aff. *C. antiquus*	Dentary?
MG27603	Reptilia /Choristodera/*Cteniogenys*		Highly fragmented	Diapsida / Choristodera / *Cteniogenys* aff. *C. antiquus*	Dentary?
MG27605	Reptilia /Choristodera/*Cteniogenys*			Diapsida / Choristodera / *Cteniogenys* aff. *C. antiquus*	Dentary
MG27607	Reptilia /Choristodera/*Cteniogenys*	Maxilla	Highly fragmented	Diapsida / Choristodera / *Cteniogenys* aff. *C. antiquus*	Dentary?
MG27609	Reptilia /Choristodera/*Cteniogenys*			Diapsida / Choristodera / *Cteniogenys* aff. *C. antiquus*	Dentary
MG27610	Reptilia /Choristodera/*Cteniogenys*		Highly fragmented	Diapsida / Choristodera / *Cteniogenys* aff. *C. antiquus*	Dentary?
MG27611	Reptilia /Choristodera/*Cteniogenys*		Highly fragmented	Diapsida / Choristodera / *Cteniogenys* aff. *C. antiquus*	Dentary?
MG27612	Reptilia /Choristodera/*Cteniogenys*		Highly fragmented	Diapsida / Choristodera / *Cteniogenys* aff. *C. antiquus*	Dentary?
MG27613	Reptilia /Choristodera/*Cteniogenys*		Highly fragmented	Diapsida / Choristodera / *Cteniogenys* aff. *C. antiquus*	Dentary?
MG27614	Reptilia /Choristodera/*Cteniogenys*		Highly fragmented	Diapsida / Choristodera / *Cteniogenys* aff. *C. antiquus*	Dentary?

MG27615	Reptilia /Choristodera/*Cteniogenys*		Highly fragmented	Diapsida / Choristodera / *Cteniogenys* aff. *C. antiquus*	Dentary?
MG27616	Reptilia /Choristodera/*Cteniogenys*		Highly fragmented	Diapsida / Choristodera / *Cteniogenys* aff. *C. antiquus*	Dentary?
MG27619	Reptilia /Choristodera/*Cteniogenys*		Highly fragmented	Diapsida / Choristodera / *Cteniogenys* aff. *C. antiquus*	Dentary?
MG27620	Reptilia /Choristodera/*Cteniogenys*		Highly fragmented	Diapsida / Choristodera / *Cteniogenys* aff. *C. antiquus*	Dentary?
MG27621	Reptilia /Choristodera/*Cteniogenys*	Maxilla	Highly fragmented	Diapsida / Choristodera / *Cteniogenys* aff. *C. antiquus*	Maxilla?
MG27622	Reptilia /Choristodera/*Cteniogenys*		Highly fragmented	Diapsida / Choristodera / *Cteniogenys* aff. *C. antiquus*	Dentary?
MG27623	Reptilia /Choristodera/*Cteniogenys*		Highly fragmented	Diapsida / Choristodera / *Cteniogenys* aff. *C. antiquus*	Dentary?
MG27624	Reptilia /Choristodera/*Cteniogenys*	Maxilla	Highly fragmented	Diapsida / Choristodera / *Cteniogenys* aff. *C. antiquus*	Dentary?
MG27625	Reptilia /Choristodera/*Cteniogenys*		Highly fragmented	Diapsida / Choristodera / *Cteniogenys* aff. *C. antiquus*	Dentary?
MG27626	Reptilia /Choristodera/*Cteniogenys*			Diapsida / Lepidosauromorpha / New unnamed taxon 1	Dentary
MG27627	Reptilia /Choristodera/*Cteniogenys*			Diapsida / Choristodera / *Cteniogenys* aff. *C. antiquus*	Dentary
MG27628	*Reptilia /Choristodera/Cteniogenys reedi sp. nov.*		Seiffert, 1973 Holotype	Diapsida / Choristodera / *Cteniogenys* aff. *C. antiquus*	Dentary
MG27629	Reptilia /Choristodera/*Cteniogenys*		Highly fragmented	Diapsida / Choristodera / *Cteniogenys* aff. *C. antiquus*	Dentary?
MG27630	Reptilia /Choristodera/*Cteniogenys*		Highly fragmented	Diapsida / Choristodera / *Cteniogenys* aff. *C. antiquus*	Dentary?
MG27631	Reptilia /Choristodera/*Cteniogenys*	Maxilla	Highly fragmented	Diapsida / Choristodera / *Cteniogenys* aff. *C. antiquus*	Maxilla?
MG27633	Reptilia /Choristodera/*Cteniogenys*			Diapsida / Lepidosauromorpha / New unnamed taxon 1	Dentary

MG27635	Reptilia /Choristodera/*Cteniogenys*		Highly fragmented	Diapsida / Choristodera / *Cteniogenys* aff. *C. antiquus*	Dentary?
MG27636	Reptilia /Choristodera/*Cteniogenys*		Highly fragmented	Diapsida / Choristodera / *Cteniogenys* aff. *C. antiquus*	Dentary?
MG27637	Reptilia /Choristodera/*Cteniogenys*		Highly fragmented	Diapsida / Choristodera / *Cteniogenys* aff. *C. antiquus*	Dentary?
MG27638	Reptilia /Choristodera/*Cteniogenys*			Diapsida / Choristodera / *Cteniogenys* aff. *C. antiquus*	Dentary
MG27641	Reptilia /Choristodera/*Cteniogenys*			Diapsida / Lepidosauromorpha / New unnamed taxon 1	Dentary
MG27642	Reptilia /Choristodera/*Cteniogenys*	Maxilla	Highly fragmented	Diapsida / Choristodera / *Cteniogenys* aff. *C. antiquus*	Maxilla?
MG27643	Reptilia /Choristodera/*Cteniogenys*			Diapsida / Lepidosauromorpha / New unnamed taxon 1	Dentary
MG27644	Reptilia /Choristodera/*Cteniogenys*	Premaxilla		Diapsida / Lepidosauromorpha / New unnamed taxon 1	Premaxilla
MG27645	Reptilia /Choristodera/*Cteniogenys*	Maxilla	Highly fragmented	Diapsida / Choristodera / *Cteniogenys* aff. *C. antiquus*	Maxilla?
MG27646	Reptilia /Choristodera/*Cteniogenys*			Diapsida / Choristodera / *Cteniogenys* aff. *C. antiquus*	Dentary
MG27649	Reptilia /Choristodera/*Cteniogenys*		Highly fragmented	Diapsida / Choristodera / *Cteniogenys* aff. *C. antiquus*	Maxilla?
MG27650	Reptilia /Choristodera/*Cteniogenys*		Highly fragmented	Diapsida / Choristodera / *Cteniogenys* aff. *C. antiquus*	Dentary?
MG27651	Reptilia /Choristodera/*Cteniogenys*		Highly fragmented	Diapsida / Choristodera / *Cteniogenys* aff. *C. antiquus*	Maxilla?
MG27652	Reptilia /Choristodera/*Cteniogenys*			Diapsida / Choristodera / *Cteniogenys* aff. *C. antiquus*	Dentary
MG27652	Reptilia /Choristodera/*Cteniogenys*		Highly fragmented	Diapsida / Choristodera / *Cteniogenys* aff. *C. antiquus*	Dentary?
MG27653	Reptilia /Choristodera/*Cteniogenys*			Diapsida / Choristodera / *Cteniogenys* aff. *C. antiquus*	Dentary

MG27654	Reptilia /Choristodera/*Cteniogenys*		Highly fragmented	Diapsida / Choristodera / *Cteniogenys* aff. *C. antiquus*	Dentary?
MG27655	Reptilia /Choristodera/*Cteniogenys*		Highly fragmented	Diapsida / Choristodera / *Cteniogenys* aff. *C. antiquus*	Dentary?
MG27656	Reptilia /Choristodera/*Cteniogenys*		Highly fragmented	Diapsida / Choristodera / *Cteniogenys* aff. *C. antiquus*	Dentary?
MG27658	Reptilia /Choristodera/*Cteniogenys*		Highly fragmented	Diapsida / Choristodera / *Cteniogenys* aff. *C. antiquus*	Dentary?
MG27659	Reptilia /Choristodera/*Cteniogenys*			Diapsida / Lepidosauromorpha / New unnamed taxon 1	Dentary
MG27660	Reptilia /Choristodera/*Cteniogenys*	Maxilla	Highly fragmented	Diapsida / Choristodera / *Cteniogenys* aff. *C. antiquus*	Dentary?
MG27661	Reptilia /Choristodera/*Cteniogenys*		Highly fragmented	Diapsida / Choristodera / *Cteniogenys* aff. *C. antiquus*	Dentary?
MG27662	Reptilia /Choristodera/*Cteniogenys*			Diapsida / Choristodera / *Cteniogenys* aff. *C. antiquus*	Dentary
MG27664	Reptilia /Choristodera/*Cteniogenys*			Diapsida / Choristodera / *Cteniogenys* aff. *C. antiquus*	Dentary
MG27665	Reptilia /Choristodera/*Cteniogenys*	Premaxilla		Diapsida / Lepidosauromorpha / New unnamed taxon 1	Dentary
MG27666	Reptilia /Choristodera/*Cteniogenys*			Diapsida / Choristodera / *Cteniogenys* aff. *C. antiquus*	Dentary
MG27667	Reptilia /Choristodera/*Cteniogenys*			Diapsida / Lepidosauromorpha / New unnamed taxon 1	Dentary
MG27940	Reptilia /Choristodera/*Cteniogenys*		Highly fragmented	Diapsida / Choristodera / *Cteniogenys* aff. *C. antiquus*	Maxilla?
MG28282	Anura? ou *Cteniogenys*?	Ilium		Diapsida / Choristodera / *Cteniogenys* aff. *C. antiquus*	Ilium
MG28284	Reptilia /Choristodera/*Cteniogenys*	Caudal vertebra		Diapsida / Choristodera / *Cteniogenys* aff. *C. antiquus*	Caudal vertebra
MG28287	Anura? ou *Cteniogenys*?	Caudal vertebra		Diapsida / Choristodera / *Cteniogenys* aff. *C. antiquus*	Caudal vertebra

MG28288	Anura? ou *Cteniogenys*?	Cranial bone		Diapsida / Choristodera / *Cteniogenys* aff. *C. antiquus*	Ilium
MG28289	Reptilia /Choristodera/*Cteniogenys*	Ilium		Diapsida / Choristodera / *Cteniogenys* aff. *C. antiquus*	Ilium
MG28290	Reptilia /Choristodera/*Cteniogenys*	Ilium	German label identified as Anura ilium	Diapsida / Choristodera / *Cteniogenys* aff. *C. antiquus*	Ilium
MG28291	Amphibia/Anura	Ilium?		Diapsida / Choristodera / *Cteniogenys* aff. *C. antiquus*	Ilium
MG28423	Amphibia/Albanerpetontidae	Dentary		Diapsida / Choristodera / *Cteniogenys* aff. *C. antiquus*	Surangular
MG28512	Amphibia/Albanerpetontidae			Diapsida / Choristodera / *Cteniogenys* aff. *C. antiquus*	Dorsal vertebra
MG28514	Amphibia/Albanerpetontidae			Diapsida / Choristodera / *Cteniogenys* aff. *C. antiquus*	Anterior caudal vertebra
MG28552	Amphibia			Diapsida / Choristodera / *Cteniogenys* aff. *C. antiquus*	Dorsal/sacral vertebra
MG28740	Amphibia / Anura	Prefrontal	Box labelled "FRONTAL-ALBANERPETONTIDAE"	Diapsida / Lepidosauromorpha / New unnamed taxon 1	Frontal
MG28741	Amphibia / Anura	Frontal	Box labelled "FRONTAL-ALBANERPETONTIDAE"	Diapsida / Lepidosauromorpha / New unnamed taxon 1	Frontal
MG28742	Amphibia / Anura	Frontal	Box labelled "FRONTAL-ALBANERPETONTIDAE"	Diapsida / Lepidosauromorpha / New unnamed taxon 1	Frontal
MG28743	Amphibia / Anura	Frontal	Box labelled "FRONTAL-ALBANERPETONTIDAE"	Diapsida / Lepidosauromorpha / New unnamed taxon 1	Frontal
MG28751	Amphibia/Albanerpetontidae			Diapsida / Lepidosauromorpha / New unnamed taxon 1	Maxilla
MG28757	Amphibia/Albanerpetontidae			Diapsida / Lepidosauromorpha / New unnamed taxon 1	Maxilla
MG28761	Amphibia/Albanerpetontidae			Diapsida / Choristodera / *Cteniogenys* aff. *C. antiquus*	Dentary
MG28763	Reptilia/Squamata/			Diapsida / Lepidosauromorpha / New unnamed taxon 1	Dentary

MG28764	Reptilia/Squamata/		Highly fragmented	Diapsida / Lepidosauromorpha / New unnamed taxon 1	Dentary
MG28770	Reptilia/Squamata/		Highly fragmented	Diapsida / Lepidosauromorpha / New unnamed taxon 1	Dentary
MG28771	Reptilia/Squamata/			Diapsida / Lepidosauromorpha / New unnamed taxon 1	Maxilla
MG28778	Reptilia/Squamata/			Diapsida / Lepidosauromorpha / New unnamed taxon 1	Dentary
MG28779	Reptilia/Squamata/			Diapsida / Lepidosauromorpha / New unnamed taxon 1	Dentary
MG28784	Reptilia /Choristodera			Diapsida / Lepidosauromorpha / New unnamed taxon 1	Dentary
MG28785	Reptilia /Choristodera			Diapsida / Lepidosauromorpha / New unnamed taxon 1	Dentary
MG28791	Reptilia/Squamata/			Diapsida / Lepidosauromorpha / New unnamed taxon 1	Dentary
MG28792	Reptilia /Choristodera/*Cteniogenys*			Diapsida / Choristodera / *Cteniogenys* aff. *C. antiquus*	Associated bones
MG28793	Reptilia /Choristodera/*Cteniogenys*		Highly fragmented	Diapsida / Lepidosauromorpha / New unnamed taxon 1	Dentary
MG28794	Reptilia /Choristodera/*Cteniogenys*			Diapsida / Lepidosauromorpha / New unnamed taxon 1	Dentary
MG28795	Reptilia /Choristodera/*Cteniogenys*		Highly fragmented	Diapsida / Lepidosauromorpha / New unnamed taxon 1	Dentary
MG28797	Reptilia /Choristodera/*Cteniogenys*			Diapsida / Lepidosauromorpha / New unnamed taxon 1	Dentary
MG28798	Reptilia /Choristodera/*Cteniogenys*			Diapsida / Lepidosauromorpha / New unnamed taxon 1	Maxilla
MG28802	Reptilia /Choristodera/*Cteniogenys*		Highly fragmented	Diapsida / Lepidosauromorpha / New unnamed taxon 1	Dentary
MG28803	Reptilia /Choristodera/*Cteniogenys*			Diapsida / Lepidosauromorpha / New unnamed taxon 1	Dentary

MG28804	Reptilia /Choristodera/*Cteniogenys*		Highly fragmented	Diapsida / Lepidosauromorpha / New unnamed taxon 1	Dentary
MG28811	Reptilia		Highly fragmented	Diapsida / Lepidosauromorpha / New unnamed taxon 1	Dentary
MG28812	Reptilia		Highly fragmented	Diapsida / Lepidosauromorpha / New unnamed taxon 1	Dentary
MG28815	Reptilia/Squamata/			Diapsida / Lepidosauromorpha / New unnamed taxon 1	Maxilla
MG28816	Reptilia/Squamata/			Diapsida / Lepidosauromorpha / New unnamed taxon 1	Maxilla
MG28825	Reptilia/Squamata/		Highly fragmented	Diapsida / Lepidosauromorpha / New unnamed taxon 1	Dentary
MG28826	Reptilia /Choristodera/*Cteniogenys*			Diapsida / Choristodera / *Cteniogenys* aff. *C. antiquus*	Dentary
MG28828	Reptilia/Squamata/			Diapsida / Lepidosauromorpha / New unnamed taxon 1	Dentary
MG28829	Reptilia/Squamata/		Highly fragmented	Diapsida / Lepidosauromorpha / New unnamed taxon 1	Dentary
MG28831	Reptilia /Choristodera/*Cteniogenys*			Diapsida / Choristodera / *Cteniogenys* aff. *C. antiquus*	Dentary
MG28833	Reptilia/Squamata/			Diapsida / Lepidosauromorpha / New unnamed taxon 1	Dentary
MG28841	Reptilia /Choristodera/*Cteniogenys*			Diapsida / Lepidosauromorpha / New unnamed taxon 1	Maxilla
MG28842	Reptilia /Choristodera/*Cteniogenys*			Diapsida / Lepidosauromorpha / New unnamed taxon 1	Maxilla
MG28843	Reptilia /Choristodera/*Cteniogenys*			Diapsida / Choristodera / *Cteniogenys* aff. *C. antiquus*	Dentary
MG28852	Reptilia/Squamata/		Highly fragmented	Diapsida / Lepidosauromorpha / New unnamed taxon 1	Dentary
MG28854	"Thecodont"	Dentary	Highly fragmented	Diapsida / Lepidosauromorpha / New unnamed taxon 1	Dentary

MG28857	Reptilia/Squamata/			Diapsida / Lepidosauromorpha / New unnamed taxon 1	Dentary
MG28859	Reptilia/Squamata/		Highly fragmented	Diapsida / Lepidosauromorpha / New unnamed taxon 1	Dentary
MG28860	Reptilia/Squamata/		Highly fragmented	Diapsida / Lepidosauromorpha / New unnamed taxon 1	Dentary
MG28861	Reptilia		Highly fragmented	Diapsida / Lepidosauromorpha / New unnamed taxon 1	Dentary
MG28868	Reptilia/Squamata /		Highly fragmented	Diapsida / Lepidosauromorpha / New unnamed taxon 1	Dentary
MG28874	Reptilia/Squamata /			Diapsida / Lepidosauromorpha / New unnamed taxon 1	Dentary
MG28877	Reptilia/Squamata/		Highly fragmented	Diapsida / Lepidosauromorpha / New unnamed taxon 1	Dentary
MG28878	Reptilia/Squamata/		Highly fragmented	Diapsida / Lepidosauromorpha / New unnamed taxon 1	Dentary
MG28882	Reptilia /Choristodera/*Cteniogenys*			Diapsida / Choristodera / *Cteniogenys* aff. *C. antiquus*	Dentary
MG28887	Reptilia/Squamata/			Diapsida / Lepidosauromorpha / New unnamed taxon 1	Maxilla
MG28888	Reptilia/Squamata/			Diapsida / Lepidosauromorpha / New unnamed taxon 1	Maxilla
MG28889	Reptilia/Squamata/		Highly fragmented	Diapsida / Lepidosauromorpha / New unnamed taxon 1	Dentary
MG28890	Reptilia /Choristodera/*Cteniogenys*	Humerus		Diapsida / Choristodera / *Cteniogenys* aff. *C. antiquus*	Humerus
MG28901	cf. *Cteniogenys*			Diapsida / Choristodera / *Cteniogenys* aff. *C. antiquus*	Dentary
MG28905	Reptilia /Choristodera/*Cteniogenys*			Diapsida / Lepidosauromorpha / New unnamed taxon 1	Dentary
MG28907	Reptilia/Squamata/			Diapsida / Lepidosauromorpha / New unnamed taxon 1	Maxilla

MG28908	Reptilia/Squamata/			Diapsida / Lepidosauromorpha / New unnamed taxon 1	Maxilla
MG28910	Reptilia/Squamata/			Diapsida / Lepidosauromorpha / New unnamed taxon 1	Dentary
MG28914	Mesoeucrocodylia incertae sedis /*Lisboasaurus*?			Diapsida / Choristodera / *Cteniogenys* aff. *C. antiquus*	Dentary
MG28916	Reptilia/Squamata/		Highly fragmented	Diapsida / Lepidosauromorpha / New unnamed taxon 1	Dentary
MG28925	Reptilia/Squamata/			Diapsida / Lepidosauromorpha / New unnamed taxon 1	Maxilla
MG28926	Reptilia/Squamata/		Highly fragmented	Diapsida / Lepidosauromorpha / New unnamed taxon 1	Dentary
MG28927	Reptilia/Squamata /		Highly fragmented	Diapsida / Lepidosauromorpha / New unnamed taxon 1	Dentary
MG28928	Reptilia/Squamata/			Diapsida / Choristodera / *Cteniogenys* aff. *C. antiquus*	Humerus
MG28936	Reptilia/Squamata/		Highly fragmented	Diapsida / Lepidosauromorpha / New unnamed taxon 1	Dentary
MG28939	Reptilia/Squamata/		Highly fragmented	Diapsida / Lepidosauromorpha / New unnamed taxon 1	Dentary
MG28940	Reptilia/Squamata/		Highly fragmented	Diapsida / Lepidosauromorpha / New unnamed taxon 1	Dentary
MG28941	Reptilia /Choristodera/*Cteniogenys*		Highly fragmented	Diapsida / Lepidosauromorpha / New unnamed taxon 1	Dentary
MG28942	Reptilia /Choristodera/*Cteniogenys*			Diapsida / Lepidosauromorpha / New unnamed taxon 1	Dentary
MG28943	Reptilia /Choristodera/*Cteniogenys*		Highly fragmented	Diapsida / Lepidosauromorpha / New unnamed taxon 1	Dentary
MG28947	Reptilia /Choristodera/*Cteniogenys*		Highly fragmented	Diapsida / Lepidosauromorpha / New unnamed taxon 1	Dentary
MG28948	Reptilia /Choristodera/*Cteniogenys*		Highly fragmented	Diapsida / Lepidosauromorpha / New unnamed taxon 1	Dentary

MG28951	Reptilia /Choristodera/*Cteniogenys*		Highly fragmented	Diapsida / Lepidosauromorpha / New unnamed taxon 1	Dentary

E PLASTICITY IN THE MORPHOLOGY OF THE FUSED FRONTALS OF ALBANERPETONTIDAE (LISSAMPHIBIA; ALLOCAUDATA)

E.1 Morphometric analysis - R Markdown script

This is an R Markdown document. Markdown is a simple formatting syntax for authoring HTML, PDF, and MS Word documents. For more details on using R Markdown see http://rmarkdown.rstudio.com.

Uploading packages

Here are the packages required to load for the function needed in the analysis

```
library(vegan)
library(tidyverse)
library(readr)
library(GGally)
library(ggfortify)
library(readxl)
```

E.1.1 Linear regression

Creating the data base

Here are created the objects containing the data used for the linear regression. We recommend the user to create a dedicated R project folder and a new R project, to work with the script shared here. The project folder should also contain subfolders for

INPUT and OUTPUT, the former with another subfolder DATA, in which the excel supplementary file could be copy-paste.

VLCrest is for the allometry in the ventrolateral crests ; Nasal is for the allometry in the internasal process ; Width is for the allometry in the slot width, between the posterior slots for the prefrontal (also referred as anterior inter-lacrimal width in the litterature). As the original data are in an excel file, we use the function read_excel (from readxl package), specifying which sheet we are using and asking R to consider the name of the column.

```
VLCrest <- read_excel("INPUT/DATA/Supplementary file 2 - Frontal morphometr
ic data.xlsx", sheet = 1, col_names = TRUE)
Nasal <- read_excel("INPUT/DATA/Supplementary file 2 - Frontal morphometric
data.xlsx", sheet = 2, col_names = TRUE)
Width <- read_excel("INPUT/DATA/Supplementary file 2 - Frontal morphometric
data.xlsx", sheet = 3, col_names = TRUE)
VLCrest
```

```
## # A tibble: 11 x 4
##    Specimen Locality     FIW     VCAW
##    <chr>    <chr>      <dbl>    <dbl>
##  1 “Xana”   Lourinha  0.137  -0.469
##  2 “Micael” Lourinha  0.286  -0.194
##  3 MG28426  Guimarota 0.182  -0.0506
##  4 MG28427  Guimarota 0.369   0.0969
##  5 MG28473  Guimarota 0.0934 -0.222
##  6 MG28502  Guimarota 0.140   0.00860
##  7 MG28520  Guimarota 0.137  -0.0969
##  8 MG28543  Guimarota 0.0969 -0.276
##  9 MG28733  Guimarota 0.0414 -0.357
## 10 MG28539  Guimarota 0.0128 -0.387
## 11 MG28692  Guimarota 0.182  -0.252
```

```
Nasal
```

```
## # A tibble: 7 x 4
##   Specimen Locality    FML     INL
##   <chr>    <chr>     <dbl>   <dbl>
## 1 “Xana”   Lourinha  0.415 -0.328
## 2 MG28426  Guimarota 0.767 -0.119
## 3 MG28502  Guimarota 0.755  0.0934
## 4 MG28520  Guimarota 0.678  0.0755
## 5 MG28521  Guimarota 0.760 -0.0706
## 6 MG28532  Guimarota 0.589 -0.0655
## 7 MG28543  Guimarota 0.515 -0.187
```

```
Width
```

```
## # A tibble: 10 x 4
##    Specimen Locality     FW      SW
##    <chr>    <chr>     <dbl>   <dbl>
```

```
##  1 “Xana”   Lourinhã  0.303 -0.102
##  2 “Micael” Lourinhã  0.422  0.121
##  3 MG28426  Guimarota 0.638  0.334
##  4 MG28427  Guimarota 0.682  0.367
##  5 MG28473  Guimarota 0.364  0.0934
##  6 MG28502  Guimarota 0.569  0.283
##  7 MG28520  Guimarota 0.542  0.127
##  8 MG28543  Guimarota 0.305  0.0899
##  9 MG28733  Guimarota 0.204  0.0212
## 10 MG28539  Guimarota 0.336  0.0294
```

Liner regression of the ventrolateral crests

We first used ggplot function in order to visualize our data. The argument geom_point is to show the data (as request by the grammar of the function). The argument geom_smooth is to represent the statistics of the data, in this case the linear model with the argument method = “lm” and the characteristic formula of a simple linear regression. Note that, as the data have been log-transformed in a previous step, the labels for the axis specifies that they represent the log of these measurements.

To create the linear model, we use the function lm, and then the function autoplot (from the package ggfortify) to validate the model by checking how the residuals behave. The argument which = c(1,2,3,4) allows to call the specific graphs needed to check for normality, homosecdasticity, and outliers in the residuals.

Following here is the analysis for the allometry in the ventrolateral crests.

```
ggplot(data = VLCrest, aes(x = FIW, y = VCAW)) +
  geom_point(color = "black") +
  geom_smooth(method = "lm", colour = "blue", formula = y ~ x, se = TRUE) +
  labs(x = "Log of the frontal inner width (FIW)", y = "Log of the ventrola
teral crest anterior width (VCAW)") +
  theme_classic()
```

```
Linearreg1 <- lm (VCAW ~ FIW, data = VLCrest)
summary(Linearreg1)
```

```
##
## Call:
## lm(formula = VCAW ~ FIW, data = VLCrest)
##
## Residuals:
##       Min        1Q    Median        3Q       Max
## -0.25135 -0.05916 -0.01438  0.08628  0.22226
```

```
##
## Coefficients:
##             Estimate Std. Error t value Pr(>|t|)
## (Intercept) -0.36888    0.07785  -4.739  0.00106 **
## FIW          1.10968    0.42974   2.582  0.02959 *
## ---
## Signif. codes:  0 '***' 0.001 '**' 0.01 '*' 0.05 '.' 0.1 ' ' 1
##
## Residual standard error: 0.1396 on 9 degrees of freedom
## Multiple R-squared:  0.4256, Adjusted R-squared:  0.3617
## F-statistic: 6.668 on 1 and 9 DF,  p-value: 0.02959
```

```
autoplot(Linearreg1, which = c(1,2,3,4), ncol = 2, label.size = 3)
```

```
## Warning: `arrange_()` was deprecated in dplyr 0.7.0.
## Please use `arrange()` instead.
## See vignette('programming') for more help
```

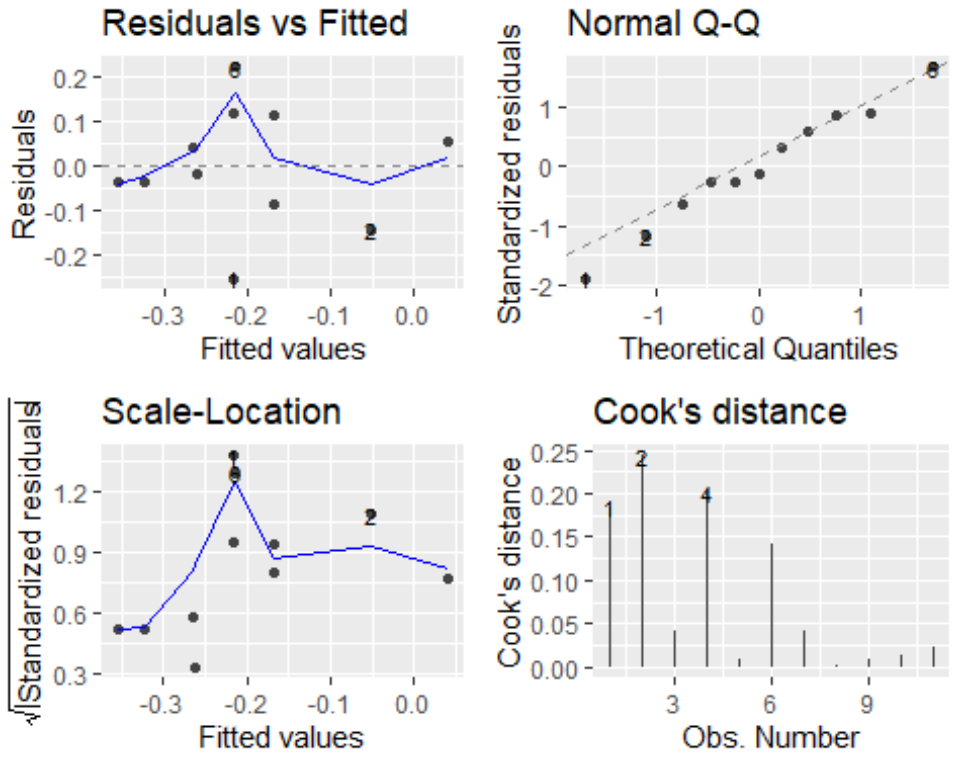

Liner regression of the internasal process

Following here is the analysis for the allometry in the internasal process.

```
ggplot(data = Nasal, aes(x = FML, y = INL)) +
  geom_point(color = "black") +
  geom_smooth(method = "lm", colour = "blue", formula = y ~ x, se = TRUE) +
  labs(x = "Log of the frontal medial length (FML)", y = "Log of the intern
asal process length (INL)") +
  theme_classic()
```

```
Linearreg2 <- lm (INL ~ FML, data = Nasal)
summary(Linearreg2)

##
## Call:
## lm(formula = INL ~ FML, data = Nasal)
##
## Residuals:
##         1         2         3         4         5         6         7
## -0.064162 -0.134020  0.088115  0.131546 -0.080089  0.060718 -0.002109
##
## Coefficients:
##             Estimate Std. Error t value Pr(>|t|)
## (Intercept)  -0.5920     0.2065  -2.867   0.0351 *
## FML           0.7910     0.3165   2.499   0.0545 .
## ---
## Signif. codes:  0 '***' 0.001 '**' 0.01 '*' 0.05 '.' 0.1 ' ' 1
##
## Residual standard error: 0.107 on 5 degrees of freedom
## Multiple R-squared:  0.5554, Adjusted R-squared:  0.4665
## F-statistic: 6.247 on 1 and 5 DF,  p-value: 0.05453

autoplot(Linearreg2, which = c(1,2,3,4), ncol = 2, label.size = 3)
```

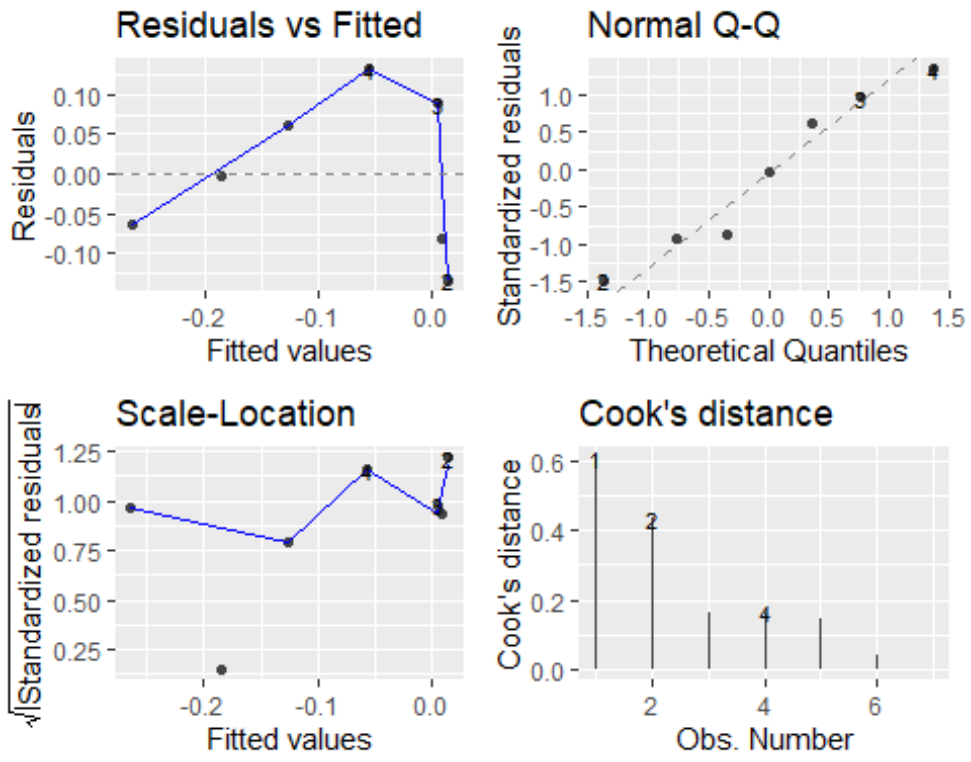

Liner regression of the slot width

Following here is the analysis for the allometry in the slot width, between the posterior slots for the prefrontal.

```
ggplot(data = Width, aes(x = FW, y = SW)) +
  geom_point(color = "black") +
  geom_smooth(method = "lm", colour = "blue", formula = y ~ x, se = TRUE) +
  labs(x = "Log of frontal width across caudal edges (FW)", y = "Log of slo
t width, between the posterior slots for the prefrontal (SW)") +
  theme_classic()
```

```
Linearreg3 <- lm (SW ~ FW, data = Width)
summary(Linearreg3)

##
## Call:
## lm(formula = SW ~ FW, data = Width)
##
## Residuals:
##      Min       1Q   Median       3Q      Max
## -0.12834 -0.01896  0.02251  0.03540  0.07726
##
## Coefficients:
##             Estimate Std. Error t value Pr(>|t|)
## (Intercept) -0.22509    0.06719  -3.350 0.010081 *
## FW           0.82805    0.14523   5.702 0.000454 ***
## ---
## Signif. codes:  0 '***' 0.001 '**' 0.01 '*' 0.05 '.' 0.1 ' ' 1
##
## Residual standard error: 0.07031 on 8 degrees of freedom
## Multiple R-squared:  0.8025, Adjusted R-squared:  0.7778
## F-statistic: 32.51 on 1 and 8 DF,  p-value: 0.0004535

autoplot(Linearreg3, which = c(1,2,3,4), ncol = 2, label.size = 3)
```

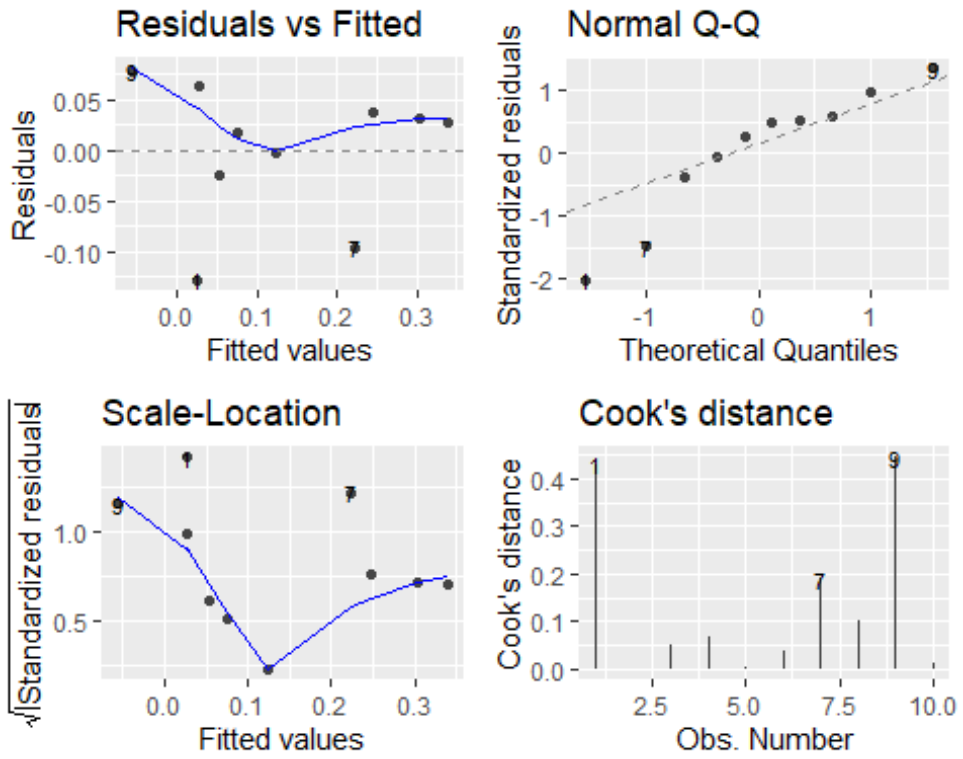

E.1.2 Morphometrics analysis; k-means

PCA and LDA will be performed using PAST; however, here will be perform the analysis for the k-mean group partitioning. First, we load the data by creating a new object using the PCA scores obtained from the previous steps in PAST.

```
PCA <- read_excel("INPUT/DATA/Supplementary file 2 - Frontal morphometric d
ata.xlsx", sheet = 4, col_names = TRUE)
```

K-mean partitioning

To calculate the most optimal group partitioning using K-mean, we are using the function cascadeKM, that will estimate for each combination how well they group the sample.inf.gr and sup.gr arguments set the interval in which the analysis will be performed, knowing that it requires a minimum of two groups. The upper limit is set at 5 due to the number of specimens. The criterion argument indicate which index will be used; here ssi has been selected as it is well suited for this kind of analysis.

```
PCA.KM.cascade <- cascadeKM(PCA, inf.gr = 2, sup.gr = 5, iter = 100, criter
ion = "ssi")
```

We called them the values results and partition in order to obtain the values of the ssi for the best partition, and the table of partitions for each combination of group. Then, we call the plot function to visualize the results.

```
PCA.KM.cascade$results
```

```
##       2 groups   3 groups   4 groups   5 groups
## SSE 51.8538346 40.0186631 30.8549265 21.7253723
## ssi  0.3027288  0.5899812  0.5027588  0.4615604
```

```
PCA.KM.cascade$partition
```

```
##    2 groups 3 groups 4 groups 5 groups
## 1         1        1        3        4
## 2         1        1        3        4
## 3         1        2        4        5
## 4         1        1        3        4
## 5         1        1        3        4
## 6         2        3        2        3
## 7         2        3        2        3
## 8         1        1        4        5
## 9         2        3        2        3
## 10        2        2        1        2
## 11        2        3        2        1
## 12        1        2        4        5
## 13        1        1        3        4
## 14        2        3        2        3
## 15        1        1        3        4
## 16        1        2        4        5
## 17        1        1        3        4
```

```
plot(PCA.KM.cascade, sortg = TRUE)
```

Exploring further

However, due to the data and as suggested by the authors of the function cascadeKM, we will explore other value of maximum combination in order to see if a most optimal partition exists. We will perform the analysis with 16 groups (the maximum due to the sample size).

```
PCA.KM.cascade3 <- cascadeKM(PCA, inf.gr = 2, sup.gr = 16, iter = 100, crit
erion = "ssi")

PCA.KM.cascade3$results
```

```
##       2 groups   3 groups   4 groups   5 groups   6 groups   7 groups  8
groups
## SSE 51.8538346 40.0186631 30.8549265 21.7253723 14.5082745 10.2109564 6.
8696956
## ssi  0.3027288  0.5899812  0.5027588  0.4615604  0.6914326  0.5521866 0.
8668583
##      9 groups 10 groups 11 groups 12 groups 13 groups 14 groups 15 group
s
## SSE 5.2042912  3.817051  2.774039  1.850313  1.064931 0.5987805 0.262366
8
## ssi 0.6942013  1.348851  1.401871  1.461133  1.410260 1.4828596 1.467612
7
##      16 groups
## SSE 0.08216178
## ssi 2.80497345

PCA.KM.cascade3$partition

##    2 groups 3 groups 4 groups 5 groups 6 groups 7 groups 8 groups 9 grou
ps
## 1         2        2        1        1        1        6        2
1
## 2         2        2        1        1        3        4        4
7
## 3         2        1        2        2        2        5        7
8
## 4         2        2        1        1        1        6        2
1
## 5         2        2        1        1        1        6        2
1
## 6         1        3        3        5        6        3        1
4
## 7         1        3        3        5        6        3        1
6
## 8         2        2        2        2        2        5        8
3
## 9         1        3        3        5        6        1        5
2
## 10        1        1        4        3        4        2        3
5
## 11        1        3        3        4        5        7        6
9
## 12        2        1        2        2        2        5        7
8
## 13        2        2        1        1        1        6        8
3
## 14        1        3        3        5        6        1        5
2
## 15        2        2        1        1        1        6        2
1
## 16        2        1        2        2        2        5        7
8
## 17        2        2        1        1        1        6        8
3
##    10 groups 11 groups 12 groups 13 groups 14 groups 15 groups 16 groups
## 1          5         1         5         6         8         2        12
## 2          9         9         4        12         9        14        14
## 3          8         2        12        10         4        15         5
## 4          3         7         7         4         2        13        10
```

```
## 5           3          7          7          4          2         13          8
## 6           4          3         11         11          6          4         13
## 7           7         10          9          9         14         10         11
## 8           6          2          6          7         10          7          9
## 9           1         11          8          2          3          3          3
## 10         10          4          3          1          7          6          7
## 11          2          8          1          5         11          1         16
## 12          8          5          2          3          5          8          2
## 13          6          6         10         13         13          9         15
## 14          1         11          8          8         12         11          4
## 15          6          6         10         13          1         12          6
## 16          8          5          2          3          5          5          1
## 17          6          6         10         13         13          9         15
```

```
plot(PCA.KM.cascade3, sortg = TRUE)
```

E.2 Frontal morphometric data

Table E.1: Log-transformed measurements for internasal process linear regression. **FML**, frontal length at the midline; **INL**, internasal length at the midline.

Specimen	Locality	logFML	logINL
ML2738	Lourinhã	0,414973	-0,3279
MG28426	Guimarota	0,767156	-0,11919
MG28502	Guimarota	0,755112	0,09342
MG28520	Guimarota	0,677607	0,07555
MG28521	Guimarota	0,760422	-0,07058
MG28532	Guimarota	0,588832	-0,0655
MG28543	Guimarota	0,514548	-0,18709

Table E.2: Log-transformed measurements for ventrolateral crest linear regression. **FIW**, frontal inner width between ventrolateral crests, across posterior edges of the frontal ventral roof; **VCAW**, ventrolateral crest anterior width, behind prefrontal facets.

Specimen	Locality	logFIW	logVCAW
ML2738	Lourinhã	0,1367206	-0,468521
ML2739	Lourinhã	0,2855573	-0,19382
MG28426	Guimarota	0,1818436	-0,05061
MG28427	Guimarota	0,3692159	0,09691
MG28473	Guimarota	0,0934217	-0,221849
MG28502	Guimarota	0,1398791	0,0086002
MG28520	Guimarota	0,1367206	-0,09691
MG28543	Guimarota	0,09691	-0,275724
MG28733	Guimarota	0,0413927	-0,356547
MG28539	Guimarota	0,0128372	-0,387216
MG28692	Guimarota	0,1818436	-0,251812

Table E.3: Log-transformed measurements for slot width linear regression. **FW**, frontal width across posterior edges; **SW**, slot width, between the posterior slots for the prefrontal.

Specimen	Locality	logFW	logSW
ML2738	Lourinhã	0,3032	-0,1024
ML2739	Lourinhã	0,4216	0,1206
MG28426	Guimarota	0,6385	0,3345
MG28427	Guimarota	0,6821	0,3674
MG28473	Guimarota	0,3636	0,0934
MG28502	Guimarota	0,5694	0,2833
MG28520	Guimarota	0,5416	0,1271
MG28543	Guimarota	0,3054	0,0899
MG28733	Guimarota	0,2041	0,0212
MG28539	Guimarota	0,3365	0,0294

Table E.4: PCA scores from the frontal bone measurements.

Specimen	PC 1	PC 2	PC 3	PC 4	PC 5	PC 6	PC 7
ML2738	-2,515400	0,781650	-0,196610	-0,255600	-0,510840	0,052269	0,131930
ML2739	-1,421900	2,823000	0,467080	0,081600	-0,033305	0,279520	0,103310
ML2741	-0,612020	-0,875010	-0,194580	0,120330	-0,356710	-0,135670	-0,310510
FCT/UNL-CN00016	-2,868200	-0,476000	-0,693770	-0,030803	0,149640	0,022854	-0,042589
FCT/UNL-CN00018	-2,369400	-0,484460	-0,399970	0,108710	0,074495	0,032487	-0,038705
MG28426	2,148600	1,439700	-0,951710	-0,568830	-0,160690	-0,513080	0,167780
MG28427	3,552600	0,953950	-1,378800	-0,481950	0,288090	0,283660	-0,144450
MG28473	-0,584300	-0,124620	0,347980	0,370740	0,297990	0,031763	0,374950
MG28502	2,844900	0,122720	-0,394640	1,271900	-0,203370	-0,041099	-0,011438
MG28520	2,339600	-2,724100	0,009507	-0,419490	-0,308210	0,389740	0,150410
MG28521	2,132000	1,050500	2,572400	-0,282880	-0,043541	-0,020724	-0,140630
MG28532	-0,218600	-1,671700	0,514730	-0,300160	0,344240	-0,237950	0,028086
MG28543	-1,276000	0,441540	0,004804	0,048110	0,203330	0,040253	-0,212910
MG28694	2,245400	-0,190050	-0,044952	0,350430	0,170890	-0,075458	0,018542
MG28733	-1,697000	-0,065451	-0,360280	-0,035706	0,026243	-0,060768	-0,056336
MG28539	-0,741580	-1,316700	0,706160	0,018540	-0,008399	-0,134630	0,035144
MG28692	-0,958630	0,315100	-0,007378	0,005074	0,070147	0,086838	-0,052584

Table E.5: PCA coefficient loadings.

	PC 1	PC 2	PC 3	PC 4	PC 5	PC 6	PC 7
INL	0.38526	-0.40624	-0.0081866	0.65651	-0.25981	-0.049777	-0.43069
INW	0.45131	-0.09494	0.064088	-0.69154	-0.39474	0.17515	-0.34421
SW	0.44247	0.26345	-0.046288	-0.091207	0.54738	-0.6012	-0.25157
IVCW	0.079134	0.58294	0.75058	0.20762	-0.17434	0.10053	-0.083306
VCAW	0.44633	0.19574	-0.23075	0.14295	0.39438	0.72102	0.11567
VCPW	0.46442	0.11944	-0.14371	0.083077	-0.40624	-0.27388	0.70884
VCC	0.17596	-0.60345	0.597	-0.10961	0.35509	0.020271	0.33161

Table E.6: PCA correlation loadings.

	PC 1	PC 2	PC 3	PC 4	PC 5	PC 6	PC 7
INL	0.80192	-0.51992	-0.0069503	0.27868	-0.063235	-0.010359	-0.069245
INW	0.93941	-0.12151	0.05441	-0.29355	-0.096077	0.036448	-0.05534
SW	0.92099	0.33718	-0.039298	-0.038716	0.13323	-0.12511	-0.040446
IVCW	0.16472	0.74607	0.63723	0.088131	-0.042432	0.020921	-0.013394
VCAW	0.92904	0.25052	-0.19591	0.06068	0.09599	0.15004	0.018596
VCPW	0.96669	0.15287	-0.122	0.035265	-0.098875	-0.056994	0.11396
VCC	0.36626	-0.77232	0.50684	-0.046528	0.086426	0.0042183	0.053315

E.3 Analysis R1, using the hypothesis of two Portuguese species

```
piwe=12;
taxonomy=;
nstates 8 ;
taxname + 200;
taxname [!;
xread
38 18
&[num]
Celtedens_Guimarota_____@Albanerpetontidae_Celtedens
010?010000000?0?0000000001?0101?00?000
Celtedens_Lourinha_____@Albanerpetontidae_Celtedens
0100000000000000000000000?0?01?1?0??000
Anoualerpeton_priscus_____@Albanerpetontidae_Anoualerpeton
        0?0???0?000000000110001100?001?0??000
Anoualerpeton_unicus_____@Albanerpetontidae_Anoualerpeton
010000000000?00??1100000000001?????00
Celtedens_ibericus_____@Albanerpetontidae_Celtedens
000???0?000????0000?000001?01000000000
Albanerpeton_arthridion_____@Albanerpetontidae
00000000000000?000001100111100[01]?????00
Albanerpeton_gracilis_____@Albanerpetontidae
000000001110000000011100011100?????10
Albanerpeton_galaktion_____@Albanerpetontidae
000000001210010?0000110101110000?????00
Albanerpeton_cifellii_____@Albanerpetontidae
00020000111000???????????11?0?????????
Albanerpeton_nexuosus_____@Albanerpetontidae
11110101110100100110111101110000?????21
Albanerpeton_inexpectatum_____@Albanerpetontidae
11111?12110000111001121201110 1[01]1100121
Albanerpeton_pannonicus_____@Albanerpetontidae
11110000110000100001121211110 11??0??21
Paskapoo_species_____@Albanerpetontidae
11111?10110010100001 1?101111010??????0
```

```
Wesserpeton_evansae_____@Albanerpetontidae
0[01]010000[01][01]00?0[01]0000[01]100011[01]001110??010
Uña_albanerpetontid_____@Albanerpetontidae
000?000?000?????????100001?00?0??????0
Shirerpeton_isaji_____@Albanerpetontidae
        ????????????????00?1101[01]111??10?10111100
Yaksha_perettii_____@Albanerpetontidae
11020001111000000 1101[01]0010110011011100
Celtedens_megacephalus_____@Albanerpetontidae_Celtedens
        ????????????????????0??0000???01???????00
;
Outgroup 2;
Outgroup[Anoualerpeton;
Hold 50000;
mult 1000;bb;reroot[;ne;
proc/;
```

E.4 Analysis R2, using the hypothesis of one Portuguese species

```
piwe=12;
taxonomy=;
nstates 8 ;
taxname + 200;
taxname [!;
xread
38 17
&[num]
Celtedens_Portugal_____@Albanerpetontidae_Celtedens
01000[01]00000000000000000000[01]?0101?00?000
Anoualerpeton_priscus_____@Albanerpetontidae_Anoualerpeton
        0?0???0?000000000110001100 0?001?0??000
Anoualerpeton_unicus_____@Albanerpetontidae_Anoualerpeton
010000000000?00??1100000000000 1?????00
Celtedens_ibericus_____@Albanerpetontidae_Celtedens
000???0?000????0000?000001?01000000000
```

```
Albanerpeton_arthridion_____@Albanerpetontidae
000000000000000?000001100111100[01]?????00
Albanerpeton_gracilis_____@Albanerpetontidae
00000000111000000001110001110000?????10
Albanerpeton_galaktion_____@Albanerpetontidae
000000001210010?000011010111000?????00
Albanerpeton_cifellii_____@Albanerpetontidae
00020000111000???????????11?0?????????
Albanerpeton_nexuosus_____@Albanerpetontidae
11110101110100100110111110111000?????21
Albanerpeton_inexpectatum_____@Albanerpetontidae
11111?12110000111001121201110 1[01]1100121
Albanerpeton_pannonicus_____@Albanerpetontidae
11110000110000100001121211110 11??0??21
Paskapoo_species_____@Albanerpetontidae
11111?10110010100001 1?101111010??????0
Wesserpeton_evansae_____@Albanerpetontidae
0[01]010000[01][01]00?0[01]0000[01]100011[01]001110??010
Uña_albanerpetontid_____@Albanerpetontidae
000?000?000??????????100001?00?0??????0
Shirerpeton_isaji_____@Albanerpetontidae
        ??????????????00?1101[01]111??10?10111100
Yaksha_perettii_____@Albanerpetontidae
11020001111000000 1101[01]0010110011011100
Celtedens_megacephalus_____@Albanerpetontidae_Celtedens
        ????????????????????0??0000???01???????00
;
Outgroup 1;
Outgroup[Anoualerpeton;
Hold 50000;
mult 1000;bb;reroot[;ne;
proc/;
```

E.5 List of characters

Characters 1-31 are taken from Sweetman and Gardner (2013); characters 32-34 from Matsumoto & Evans (2018); characters 35-36 from Daza et al. (2020); red characters are related to the frontals; green character are new from this analysis.

1. Build of premaxilla: **0**, gracile; **1**, robust.

2. Ratio of height of premaxillary pars dorsalis versus width across suprapalatal pit: **0**, "high", ratio greater than about 1.55: **1**, "low", ratio less than about 1.55.

3. Inter-premaxillary contact: **0**, sutured medially (i.e., paired); **1**, fused medially in some individuals.

4. Premaxillary-nasal contact: **0**, premaxillary pars dorsalis minimally overlaps and abuts against or weakly sutured with anterior end of nasal; **1**, premaxillary pars dorsalis minimally overlaps and strongly sutured with anterior end of nasal; **2**, anterior end of nasal fits into lingual facet on premaxillary pars dorsalis and braced ventrolaterally by expanded dorsal end of lateral internal strut.

5. Boss on premaxilla: **0**, present; **1**, absent.

6. Relative size of premaxillary boss, if present: **0**, covers about dorsal one-quarter to one-third of pars dorsalis; **1**, covers about dorsal one-half of pars dorsalis.

7. Distribution of labial ornament on large premaxillae: **0**, restricted to dorsal part of pars dorsalis; **1**, covers entire face of pars dorsalis.

8. Pattern of premaxillary labial ornament: **0**, discontinuous, anastomosing ridges and irregular pits; **1**, continuous ridges defining polygonal pits; **2**, pustulate.

9. Vertical position of suprapalatal pit on pars dorsalis: **0**, "high", with ventral edge of pit well above dorsal face of pars palatinum; **1**, "low", with ventral edge of pit just above or, more typically, continuous with dorsal face of pars palatinum

10. Size of suprapalatal pit relative to lingual surface area of pars dorsalis: **0**, "small", about 1%; **1**, "moderate", about 4–15%; **2**, "large", about 20–25%.

11. Outline of suprapalatal pit: **0**, oval; **1**, triangular or slit-like.

12. Form of dorsal process on lingual edge of maxillary process: **0**, low, isolated ridge; **1**, high flange, continuous labially with base of lateral internal strut.

13. Form of vomerine process on premaxilla: **0**, prominent; **1**, weak.

14. Diameter of palatal foramen in premaxilla relative to diameter of base of medial teeth on bone: **0**, "small", foramen diameter ≤ tooth diameter; **1**, "large", foramen diameter > about one and one-third tooth diameter.

15. Length of premaxillary lateral process on maxilla relative to height of process at base: **0**, "long", length > height; **1**, "short", length ≤ height.

16. Dorsally projecting process on dentary immediately behind tooth row: **0**, absent; **1**, present.

17. Labial ornament on large maxilla and dentary: **0**, absent; **1**, present.

18. Labial or lingual profile of occlusal margin of maxilla and dentary: **0**, essentially straight; **1**, strongly convex or angular, with apex adjacent to tallest teeth.

19. Size heterodonty of teeth on maxilla and dentary: **0**, weakly heterodont anteriorly; **1**, strongly heterodont anteriorly.

20. Position of anterior end of maxillary tooth row relative to point of maximum indentation along leading edge of nasal process: **0**, anterior to; **1**, approximately in line.

21. Dorsal or ventral outline of fused frontals: **0**, approximately rectangular or bell-shaped; **1**, approximately triangular.

22. Ratio of midline length of fused frontals versus width across posterior edge of bone, between lateral edges of ventrolateral crests, in large specimens: **0**, "long", ratio more

than about 1.2; **1**, “moderate”, ratio between about 1.2 and 1.1; **2**, “short”, ratio equal to or less than about 1.0.

23. Proportions of internasal process on fused frontals: **0**, “short”, length ≈ width; **1**, “long”, length > width.

24. Form of ventrolateral crest on large, fused frontals: **0**, narrow and convex ventrally to bevelled ventrolaterally in transverse view; **1**, narrow and triangular in transverse view, with ventral face flat to shallowly concave; **2**, wide and triangular in transverse view, with ventral face deeply concave.

25. Estimated maximum snout-pelvic length: **0**, “large”, > about 50 mm; **1**, “small”, < about 45 mm.

26. Direction faced by suprapalatal pit in pars dorsalis of premaxilla: **0**, laterolingually; **1**, lingually.

27. Path followed by canal through pars palatinum in premaxilla, between dorsal and ventral openings of palatal foramen: **0**, dorso-laterally-ventromedially; **1**, vertically.

28. Position in frontals of anterior end of orbital margin relative to anteroposterior midpoint of frontals: **0**, in front of; **1**, in line with or behind.

29. Dorsal or ventral outline of internasal process on frontals: **0**, tapered anteriorly; **1**, bulbous.

30. Suprapalatal pit variably divided: **0**, undivided; **1**, divided in about one-third or more of specimens.

31. Flattened ventromedian keel extending along posterior two thirds of fused frontals: **0**, absent; **1**, present.

32. Postorbital wing of parietal length: **0**, equal or longer than width of frontoparietal suture; **1**, shorter than width of frontoparietal suture.

33. Sculpture extent on postorbital wing of parietal: **0**, sculpture extends on to wing; **1**, wing unsculptured.

34. Posterior process of parietal: **0**, single; **1**, double.

35. Posterodorsal fenestrae on skull roof: **0**, absent; **1**, present.

36. Postorbital process of parietal, sculptured vs unsculptured parts ratio: **0**, sculptured longest; **1**, unsculptured longest.

37. Frontal-lacrimal contact: **0**, slot (not visible dorsal or ventrally); **1**, medial emargination of the prefrontal facet making a dorsal notch only, not visible ventrally (the lacrimal sits dorsal to the frontal); **2**, medial emargination of the prefrontal facet making a notch visible dorsally and ventrally (the lacrimal sits lateral to the frontal).

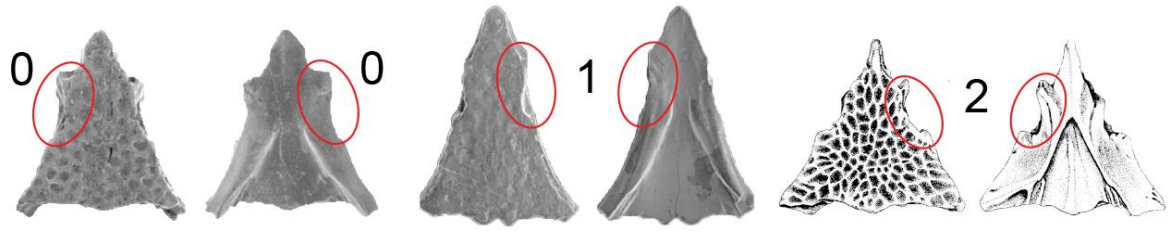

Figure E.1: Character states in *Albanerpeton arthridion* (0), *Wesserpeton evansae* (1), and *Albanerpeton pannonicum* (2) in character 37.

38. Edge of ventrolateral crests, position along the orbital margin: **0**, close/contiguous to the orbital margin; **1**, medial to the orbital margin creating a ventral step, or parapet.

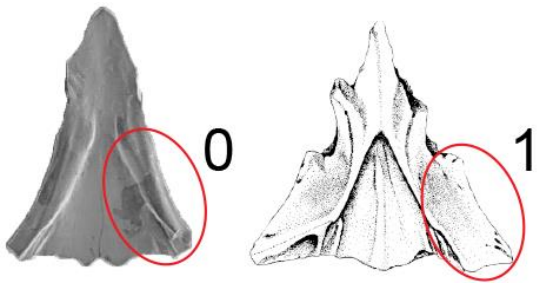

Figure E.2: Character states in *Wesserpeton evansae* (0) and *Albanerpeton pannonicum* (1) in character 38.

References

Daza JD, Stanley EL, Bolet A, Bauer AM, Arias JS, Čerňanský A, Bevitt JJ, Wagner P, Evans SE. 2020. Enigmatic amphibians in mid-Cretaceous amber were chameleon-like ballistic feeders. Science. 370(6517):687–691.

Matsumoto R, Evans SE. 2018. The first record of albanerpetontid amphibians (Amphibia: Albanerpetontidae) from East Asia. PloS one. 13(1):e0189767.

Sweetman SC, Gardner JD. 2013. A new albanerpetontid amphibian from the Barremian (Early Cretaceous) Wessex Formation of the Isle of Wight, southern England. Acta Palaeontologica Polonica. 58(2):295–324.

E.6 Supplementary text

E.6.1 Observations on the preservation status

Preservation status of best preserved Lourinhã specimens

ML2738, ML2739, ML2741 (see **Figure 3.1.4**A, B, and D), ML2743, and ML2744 (not figured) are the best-preserved specimens. ML2738 (**Figure 3.1.4**A) preserves the internasal process and the ventromedian suture, and its right edge is complete with the

parietal facet preserved. However, the left anterolateral process is broken, and the left orbital margin is missing. ML2739 (**Figure 3.1.4**B) preserves the ventromedian suture but its internasal process is broken away. Its roof is translucent, permitting observation of the dorsal ornamentation in ventral view. ML2740 (**Figure 3.1.4**C) and ML2742 (not figured) preserve a full anterolateral process. The latter preserves only the middle part of the frontal and displays an eroded dorsal surface. ML2741 (**Figure 3.1.4**D) preserves the internasal process and anterior part of its edges. However, no posterior part could be associated and none of the anterolateral processes are preserved. The left edge is better preserved, with the anterolateral process only missing the posterior-most part of the parietal facet. The right anterolateral process is preserved, but the orbital margin is broken just before the parietal facet. FCT/UNL-CN00016 (**Figure 3.1.4**E) only preserves the anterior-most part of the frontal and is broken from the right anterolateral process to at least two thirds of the left ventrolateral crest (the canal is still visible, see **Figure 3.1.4**E). FCT/UNL-CN00018 (**Figure 3.1.4**F) also preserves the anterior-most part of the frontal, being transversally broken between a half and two thirds of the length of the ventrolateral crests, and both anterolateral processes are poorly preserved.

Preservation status of best preserved Guimarota specimens

MG28426, MG28427, MG28502, MG28520, and MG28521 (**Figure 3.1.5**A, B, D, E, and F) are the most complete specimens. MG28473 and MG28543 (**Figure 3.1.5**C and J) are observable only in ventral view because they are still in their coal matrix. MG28502, MG28532, and MG28694 (**Figure 3.1.5**D, G, and O) were coated in gold for SEM in a previous study of the material (Wiechmann 2003). MG28426 and MG28427 (**Figure 3.1.5**A and B) are fragmented specimens whose pieces were assembled for the images presented here. MG28520 (**Figure 3.1.5**E) is fragmented and was curated adhering to Bostik Blu Tack before this study.

E.6.2 Morphometrics analysis

For the PC1-PC2 graph in scaling 1 (**Figure 3.1.6**; A), MG28426, MG25521, MG28427, MG28502, and MG28694 are associated with higher values of variables SW, VCAW, VCPW, and INW. MG28520 is associated with higher value of variables INL and VCC. ML2739 is associated with high value of IVCW, but lower value of VCC and INL. ML2741), MG28539, and MG28532 are associated with high value of VCC, but low value of IVCW. The other specimens are associated with lower values of SW, VCAW, VCPW, and INW.

For the PC3-PC2 graph in scaling 1, MG28473, MG28539 and MG28532 are associated with high values of VCC and INW. MG28520 is associated with high values of INL, while ML2739 is rather associated with low value. ML2738 is associated with a high value of SW, and low value of INW and VCC. MG28502, MG28733, MG28426 and MG28427 are associated with high value of VCAW and VCPW, but low values of INW and VCC. FCT/UNL-CN00016 and FCT/UNL-CN00018 are associated with low value of IVCW. MG28694 is in the centre of the graph and therefore does not seem to be associated with any peculiar variable.

For the PC1-PC2 graph in scaling 2 (**Figure 3.1.6**; B), SV, VCAW and VCPW are highly and positively correlated between them, and INW is to a lesser extent positively correlated to those three. IVCW is positively correlated with this group of four variables. INL is equally positively correlated to INW and VCC, but negatively correlated to IVCW. VCC and IVCW are highly and negatively correlated. Finally, VCC seems uncorrelated (or at least weakly correlated) to SW, VCAM, and VCOW, and same can be said between IVCW and INW, due to their quasi-orthogonal vectors.

For the PC3-PC2 graph in scaling 2, SW, VCAW, and VCPW are once again highly positively correlated, VCAW and VCPW being the strongest correlation. They are highly

negatively correlated with INW and VCC, which are both highly and positively correlated. To a lesser extent, they are positively correlated with IVCW and INL. The former is negatively correlated to VCPW and VCAW, but uncorrelated to SW. The latter is highly negatively correlated to SW, and to a much lesser extent to VCAW, VCPW, and IVCW.

All PCA scores and loadings can be found in Appendix E.2.

E.6.3 Phylogenetic analysis

Synapomorphies found in previous studies

Our analyses recovered the following synapomorphies from previous studies (Gardner 2002; Gardner et al. 2003; Venczel and Gardner 2005; Sweetman and Gardner 2013; Matsumoto and Evans 2018; Daza et al. 2020):

(1) *Anoualerpeton priscum*

A long internasal process on fused frontals (char. 23: 1); and narrow and triangular ventrolateral crest on large, fused frontals in transverse view, with ventral face flat to shallowly concave (char. 24: 1);

(2) *Celtedens*

A bulbous dorsal or ventral outline of internasal process on frontals (char. 29: 1);

(3) Clade (*Wesserpeton* + Uña specimen + *Yaksha* + *Shirerpeton* + *Albanerpeton* s.l.)

An approximately triangular dorsal or ventral outline of the fused frontal (char. 21: 1);

(4) *Albanerpeton pannonicum*

Presence of a flattened ventromedial keel extending along posterior two thirds of fused frontals (char. 31: 1);

(5) *Albanerpeton* s.s.

A short ratio of midline length of fused frontals vs. width across posterior edge of bone, between lateral edges of ventrolateral crests, in large specimens as synapomorphy of (char. 22: 2).

Synapomorphies recovered in the new analysis

Compared to previous phylogenies, the analyses presented here propose amendments to character changes:

(1) Clade formed by the common ancestor of *A. galaktion* and *A. inexpectatum*, and all its descendants

Narrow and triangular ventrolateral crest on large, fused frontals in transverse view, with ventral face flat to shallowly (char. 24: 1).

(2) Clade (*Yaksha perettii* + *Shirerpeton isajii*)

Presence of a flattened ventromedial keel extending along posterior two thirds of fused frontals is now regarded a synapomorphy of the (char. 31: 1).

(3) *Albanerpeton* s.s.

Wide and triangular ventrolateral crest on large, fused frontals in transverse view, with ventral face deeply concave (char. 24: 2).

Our analysis also proposes new synapomorphies that were not previously discussed or reported:

(1) Independently acquired in *Celtedens ibericus* and the clade formed by the common ancestor of the Uña specimen and *A. inexpectatum*, and all its descendants

Absence of a flattened ventromedial keel extending along posterior two thirds of fused frontals (char. 31: 0).

(2) Independently acquired in *Wesserpeton evansae* and *Albanerpeton gracile*

Presence medial emargination of the prefrontal facet making a dorsal notch only, not visible ventrally (the lacrimal sits dorsal to the frontal) (char. 37: 1).

(3) *Albanerpeton* s.l.

Moderate ratio of midline length of fused frontals versus width across posterior edge of bone, between lateral edges of ventrolateral crests, in large specimens (char. 22: 1); and anterior end of orbital margin in line with or behind the anteroposterior midpoint of frontals (char. 28: 1).

(4) 'Robust-snouted' clade

Medial emargination making a notch visible dorsally and ventrally (the lacrimal sits lateral to the frontal) (char. 37: 2); and edge of ventrolateral crests medial to the orbital margin creating a ventral step, or parapet (char. 38: 1).

(5) *Yaksha perettii*

Narrow and convex ventrally to beveled ventrolaterally ventrolateral crest on large, fused frontals in transverse view is here considered as an autapomorphy of (char. 24: 0).

(6) Paskapoo species

Narrow and convex ventrally to beveled ventrolaterally ventrolateral crest on large, fused frontals in transverse view (char. 24: 0); and edge of ventrolateral crests, position along the orbital margin medial close/contiguous to the orbital margin (char. 38: 0).

E.7 Bibliography

Daza JD, Stanley EL, Bolet A, Bauer AM, Arias JS, Čerňanský A, Bevitt JJ, Wagner P, Evans SE. 2020. Enigmatic amphibians in mid-Cretaceous amber were chameleon-like ballistic feeders. Science. 370(6517):687–691. doi:10.1126/science.abb6005.

Gardner JD. 2002. Monophyly and intra-generic relationships of *Albanerpeton* (Lissamphibia; Albanerpetontidae). Journal of Vertebrate Paleontology. 22(1):12–22. doi:10.1671/0272-4634(2002)022[0012:MAIGRO]2.0.CO;2.

Gardner JD, Evans SE, Sigogneau-Russel D. 2003. New albanerpetontid amphibians from the Early Cretaceous of Morocco and Middle Jurassic of England. Acta Paleontologica Polonica. 48(2):301–319.

Matsumoto R, Evans SE. 2018. The first record of albanerpetontid amphibians (Amphibia: Albanerpetontidae) from East Asia. PloS one. 13(1):e0189767. doi:https://doi.org/10.1371/journal.pone.0189767.

Sweetman SC, Gardner JD. 2013. A new albanerpetontid amphibian from the Barremian (Early Cretaceous) Wessex Formation of the Isle of Wight, southern England. Acta Palaeontologica Polonica. 58(2):295–324.

Venczel M, Gardner JD. 2005. The geologically youngest albanerpetontid amphibian, from the lower Pliocene of Hungary. Palaeontology. 48(6):1273–1300. doi:https://doi.org/10.1111/j.1475-4983.2005.00512.x.

Wiechmann MF. 2003. Albanerpetontidae (Lissamphibia) aus dem Mesozoikum der Iberischen Halbinsel und dem Neogen von Süddeutschland [PhD dissertation]. [Berlin]: Freie Universität Berlin.

F New albanerpetontid species (Lissamphibia) from the Late Jurassic of Portugal

F.1 Mislabelling of SMNS specimen

While checking the collection from the Guimarota beds, specimen MG28568 stood out from the other specimens (**Figure F.1A**). No further label was attached to the sample bow, although this is not uncommon in the MG collection. It could clearly be identified as a single and unfused albanerpetontid premaxilla. However, its morphology is clearly different from all other specimens studied, by being rather short, robust, with a moderate suprapalatal pit facing strictly lingually, as well as a thicker medial flange; and therefore, shares affinities with *Albanerpeton pannonicum* (it differs from *Albanerpeton inexpectatum* by the presence of a small boss, a less pustulate labial ornamentation, and undivided suprapalatal pit). This specimen can in no circumstance be attributed to New unnamed taxon 2 and constitute a completely different taxa from all other Guimarota bed material. However, considering the quantity of the material, it would be considered offbeat that only one premaxilla (while being a common bone other way), or even one single bone, from a different coeval taxon would have been preserved. Furthermore, while all other specimens from Guimarota are either black/dark grey or brownish, MG28568 is white, suggesting a completely different deposit.

However, in his work on albanerpetontids, Wiechmann not only extensively studied the Guimarota assemblage, but also focused on specimens from the Randecker Maar locality in Germany, early Miocene in age, which were assigned to *A. inexpectatum* and are housed in the Staatlichen Museum für Naturkunde Stuttgart (Wiechmann, 2003). When compared with figured specimens SMNS 57819/1 and SMNS 57769/3, MG28568 is extremely similar and shared with them characters mentioned above.

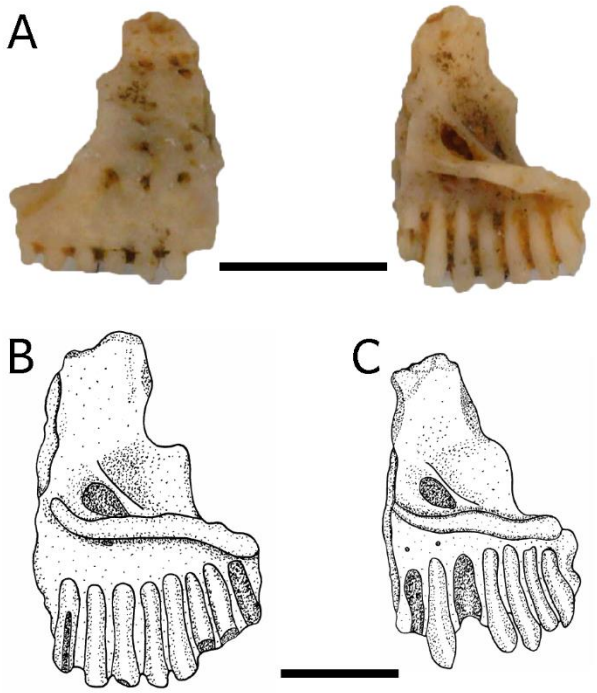

Figure F.1: **A**; MG28568 in labial (right) and lingual view (left). **B**; SMNS 57819/1 in lingual view. **C**; SMNS 57769/3 in lingual view. B and C are from Wiechmann Phd thesis (2003; pl. VII, fig.4-6). Scales are 1 mm.

Consequently, it assumed that MG28568 belongs to the same taxa than the SMNS specimens. It is unclear yet which Cenozoic *Albanerpeton* species they belong, as the material may need to be reviewed to include other bones. However, MG28568 is definitively an example of mislabeling, and the specimen does not belong to the Guimarota bed assemblage, although it is unclear to what is his SMNS specimen number, as it differs from both that was figured. We assume that it was misplaced and mixed with the Portuguese specimens when they were shipped back from Germany in the 2000s.

F.2 Parameters of the µCT-scan.

A total of 30 specimens were µCT-scanned. The complete list is provided below, with the different parameters used from each.

Table F.1: List of specimens that went under µCT-scan and the parameters associated for each.

Specimens	Bone	Voltage (kV)	Intensity (µA)	Nb images	Voxel size (mm)	Resolution (px)
ML2743	Frontal	60	42	601	0.00490578	1425x1425
ML2912	Premaxilla	60	42	601	0.00490578	1425x1425
ML2913	Premaxilla	60	42	601	0.00490578	1425x1425
ML2914	Premaxilla	60	42	601	0.00490578	1425x1425
ML2915	Premaxilla	60	42	601	0.00490578	1425x1425
ML2938	Maxilla	60	42	601	0.00490578	1425x1425
ML3000	Articular	60	42	601	0.00490578	1425x1425
ML2937	Maxilla	60	42	601	0.00498625	1425x1425
ML2952	Dentary	60	42	601	0.00499917	1425x1425
ML2953	Dentary	60	42	601	0.00499917	1425x1425
ML2954	Dentary	60	42	601	0.00499917	1425x1425
ML2955	Dentary	60	42	601	0.00516079	1425x1425
ML3103	Humerus	60	42	601	0.00516079	1425x1425
ML3108	Humerus	60	42	601	0.00516079	1425x1425
ML3109	Humerus	60	42	601	0.00516079	1425x1425
ML3110	Humerus	60	42	601	0.00516079	1425x1425
ML3111	Humerus	60	42	601	0.00516079	1425x1425
ML3112	Humerus	60	42	601	0.00516079	1425x1425
ML3023	Vertebra	60	42	601	0.00527485	1425x1425
ML3024	Vertebra	60	42	601	0.00527485	1425x1425
ML3031	Femur	60	42	601	0.00527485	1425x1425
ML3131	Femur	60	42	601	0.00527485	1425x1425
ML2951	Dentary	60	42	601	0.00544397	1425x1425
ML2738	Frontal	65	38	601	0.00491359	1425x1425
ML2739	Frontal	65	38	601	0.00491359	1425x1425
ML2741	Frontal	65	38	601	0.00491359	1425x1425
ML3012	Atlas	65	38	601	0.00491359	1425x1425
ML3013	Atlas	65	38	601	0.00491359	1425x1425
ML3018	Axis	65	38	601	0.00491359	1425x1425
ML3019	Axis	65	38	601	0.00491359	1425x1425

F.3 Extended comparison of New unnamed taxon 2

New unnamed taxon 2 shared with all albanerpetontids (1) the premaxillary, maxillary, and dentary dentition comprised of pleurodont, non-pedicellate, tricuspid, and mesio-distally compressed teeth; (2) elongated maxillae with a tapered posterior end, forming the jugal process, a labial surface ornamented by small foramina, a triangular nasal process projecting dorsally, a *pars facialis* with a bevelled dorsal margin and a *pars palatinum* with a saddle-shaped dorsal surface to articulate with the lachrymal and the jugal, and a lingually extended maxillary shelf with a longitudinal ventral trough; (3) fused frontal bones; (4) lacrimals with a gutter-like ventral process projecting ventroposteriorly and a flat dorsal process projecting dorsoposteriorly; (5) dentaries with "mortise and tenon" interdentary joint and an anteriorly closed Meckelian canal opening more posteriorly with an acuminate to blunt aperture and connected to a minute anterior foramen in the symphysis; (6) quadrates roughly trapezoidal to subrectangular, with a projecting hastate dorsal process, a medial triangular boss and asymmetric trochlear condyle; (7) an atlas mediolaterally wider than anteroposteriorly long on the midline, with a wide, dorsally arcuate odontoid process, a ventral notch separating anterior cotyles surfaces, and deep posterior recess with three articular facets; (8) an axis with a very short centrum, a deep, conical notochordal pit, anterior condyles forming a tripartite articular facet, and a small ventral notch separating both ventral condyles; (9) dorsal vertebrae with an amphicoelous centrum, narrowly constricted in the middle making them hourglass-shaped, an opened notochordal canal, and subcircular anterior and posterior cotyles, with thick rim; (10) humeri with an elongated, slender shaft in line with the proximo-distal centreline of the radial condyle, which is a prominent ossified hemispherical ball, an extremely reduced ectepicondyle and a more pronounced entepicondyle smaller than the radial condyle, a subtriangular *fossa cubitus centralis*, and a developed deltopectoral crest, but without a *crista dorsalis*; (11) an ilium without dorsal

crest, or tubercle, nor lateral prominence; and (12) a femur less robust than the humerus, and displaying a large triangular proximal head with a small trochanter and trochlear groove.

New unnamed taxon 2 differs from *Anoualerpeton* by (1) a spatulate, short dorsal emargination in the premaxillae, instead of a faint maxillary facet; (2) a dorsal premaxillary process of the maxillae with an indented ventral surface and missing the transverse ridge delimiting the posterior edge; (3) a flabellate internasal process of the frontal bones with bulbous and broad shape; and (4) a prearticular facet of the dentaries anterior to the end of the tooth row and in line with the posterior opening of the Meckelian canal. It further differs from *An. unicum* by (1) a lingually extended maxillary shelf with a longitudinal ventral trough less prominent and with a less deep ventral trough; (2) an indentation forming the internal narial margin more marked, being dorsally concave in labial view and laterally concave in dorsal view; (3) the frontal bones with convex, beveled ventrolateral crests, instead of V-shaped; (4) a parietal with a unique ventral anteromedial-posterolateral transverse crest with an anterolateral recess, separating the short ornamented postorbital wing from the rest of the bone; (5) a more pronounced but less opened laterally saddle-shaped cotylar facet of the glenoid fossa in the articular; (6) missing a deep ventral groove on the medial surface; (7) a single large articular facet on the lateral surface of the articular, instead of being bilobate; and (8) a more proximodistally extended marked *fossa cubitus cristalis* in the humeri.

New unnamed taxon 2 differs the "Purbeck species" by (1) an indentation forming the internal narial margin more marked, being dorsally concave in labial view and laterally concave in dorsal view; (2) dentaries with a secondary canal, located dorsolabially of the Meckelian canal; (3) a labial scar relatively high on the anterior section of the dentaries (1/3 to half of the height); and (4) a long axis of iliac shaft strongly tilted posteriorly.

New unnamed taxon 2 differs from *Celtedens megacephalus* by (1) frontal bones with convex, beveled ventrolateral crests, instead of V-shaped; (2) a parietal a unique ventral anteromedial-posterolateral transverse crest with an anterolateral recess, separating the short ornamented postorbital wing from the rest of the bone; (3) a less pronounced saddle-shaped cotylar facet of the glenoid fossa in the articular; and (4) a marked fossa cubitus cristalis. It differs from Galve specimen assigned to *Celtedens* cf. *megacephalus* (Estes & Sanchíz, 1982) by reniform anterior cotyles of the atlantes. It differs from *Celtedens ibericus* by (1) the frontal bones having more curved orbital margins; (2) dentaries with a secondary canal, located dorsolabially of the Meckelian canal; (3) a prearticular facet in the dentaries anterior to the end of the tooth row and in line with the posterior opening of the Meckelian canal; (4) dorsal vertebrae with foramen or peg on their ventral surface; (5) a marked *fossa cubitus cristalis* in the humeri; (6) an acetabulum in the ilia with a more convex dorsal margin, making it rather U-shape rather than V-shaped; and (7) a long axis of iliac shaft tubular rather than blade-like.

New unnamed taxon 2 differs from all other more deeply nested albanerpetontid species by having a suprapalatal pit of the premaxillae facing laterolingually. It further differs from *Wesserpeton* by (1) the frontal bones with a bell-shaped outline and a bulbous flabellate internasal process; and (2) a slot for the frontal-lacrimal/prefrontal contact. It further differs from *Wesserpeton evansae* by (1) a nasal process of the maxillae round to blunt, instead of acute (except NHMUK PV R36528); (2) a nasal process of the maxillae projecting slightly anteriorly, instead of strongly; (3) a labial scar relatively high on the anterior section of the dentaries (1/3 to half of the height); (4) a prearticular facet of the dentaries anterior to the end of the tooth row and in line with the posterior opening of the Meckelian canal less marked; (5) a less pronounced saddle-shaped cotylar facet of the glenoid fossa in the articular; (6) a long axis of iliac shaft strongly tilted posteriorly; and (7) the pubic and ischial articular surfaces of the ilia flaring more broadly

anteroposteriorly. It further differs from the "Uña species" cf. *Wesserpeton* sp. by (1) the frontal bones lacking an anterior contact between the ventrolateral crests.

New unnamed taxon 2 differs from *Yaksha perettii* by (1) sutured and gracile premaxillae, instead of robust and fused; (2) premaxillae not as much lingually inclined; (3) a small, oval, and relatively high suprapalatal pit; (4) a nasal process of the maxillae round to blunt, instead of acute; (5) a dorsal premaxillary process lingual extremity less dorsally curved; (6) the frontal bones with a bell-shaped outline and a bulbous flabellate internasal process; (7) the frontal bones lacking an anterior contact between the ventrolateral crests; (8) the frontal bones being rather more elongated than wide; (9) the frontal bones with convex, beveled ventrolateral crests, instead of V-shaped; (10) a slot for the frontal-lacrimal/prefrontal contact; (11) lacrimals less broad; (12) the absence of ornamentation on the lingual surface of the lacrimal and the posterodorsal-anteroventral trough between the ventral and dorsal processes; (13) a pandurate foramen above ventral process being instead of subcircular; (14) a sculptured surface of the parietal extending more laterally; (15) a non-bifurcate occipital shelf of the parietal; (16) a straight lateral margins of the parietal; (17) parietal without secondary ventral transverse crest; (18) a labial scar relatively high on the anterior section of the dentaries (1/3 to half of the height); (19) a less pronounced saddle-shaped cotylar facet of the glenoid fossa in the articular; (20) an ilium with a dorsoventrally elongated acetabulum; and (21) a long axis of iliac shaft strongly tilted posteriorly.

New unnamed taxon 2 differs from *Shirerpeton isajii* by (1) a dorsal premaxillary process lingual extremity in the maxillae dorsally curved; (2) the frontal bones with a bell-shaped outline and a bulbous flabellate internasal process; (3) the frontal bones lacking an anterior contact between the ventrolateral crests; (4) short anterolateral processes of the frontal bones rather than long; (5) the frontal bones with convex, beveled ventrolateral crests, instead of V-shaped; (6) lacrimals less broad; (7) a pandurate

foramen above ventral process being instead of subcircular; (8) a short dorsally sculptured postorbital wing in the parietal; (9) a non-bifurcate occipital shelf of the parietal; (10) straight lateral margins of the parietal; (11) parietal without secondary ventral transverse crest; (12) a labial scar relatively high on the anterior section of the dentaries (1/3 to half of the height); (13) a prearticular facet of the dentaries anterior to the end of the tooth row and in line with the posterior opening of the Meckelian canal; and (14) a less laterally expanded posteroventral surface of the quadrates.

New unnamed taxon 2 differs from the "Paskapoo species" by (1) sutured and gracile premaxillae, instead of robust and fused; (2) small peg or indentations in the dorsal margin of the premaxillae weakly marked, suggesting only a minimal overlap and a weak suture with the nasal; (3) premaxillae not as much lingually inclined; (4) a small, oval, and relatively high suprapalatal pit; (5) a spatulate, short dorsal emargination for the maxillary facet in the premaxillae, instead of notch or deep indentation that extends into a wide shelf; (6) a dorsal premaxillary process of the maxillae with an indented ventral surface and missing the transverse ridge delimiting the posterior edge; (7) the frontal bones with a bell-shaped outline and a bulbous flabellate internasal process; (8) short anterolateral processes of the frontal bones rather than long; (9) the frontal bones being rather more elongated than wide; (10) the frontal bones with convex, beveled ventrolateral crests, instead of V-shaped; and (11) a horizontal subdental shelf instead of inclined, at the level of the Meckelian canal opening.

New unnamed taxon 2 differs from the "Csehbánya species" and the "Sânpetru species" by a nasal process of the maxillae round to blunt, instead of acute. It further differs from the "Sânpetru species" by (1) the frontal bones with a bell-shaped outline; (2) the frontal bones with convex, beveled ventrolateral crests, instead of V-shaped; (3) a slot for the frontal-lacrimal/prefrontal contact; (4) a less pronounced ventral notch separating the anterior cotyles of the atlantes; (5) a less pronounced small ventral notch separating both

ventral condyles of the axes; (6) a dorsal cotyle of the axes dorsally inclined and with articular facet ending posteriorly less acute; and (7) a marked *fossa cubitus cristalis* in the humeri.

New unnamed taxon 2 differs from *Albanerpeton* by (1) the frontal bones with a bell-shaped outline and a bulbous flabellate internasal process; (2) short anterolateral processes of the frontal bones rather than long; (3) the frontal bones being rather more elongated than wide; (4) the frontal bones with convex, beveled ventrolateral crests, instead of V-shaped; and (5) a labial scar relatively high on the anterior section of the dentaries (1/3 to half of the height; except in *A. cifellii* which did not preserved the dentary). It further differs from *Albanerpeton ektopistikon* by (1) a premaxilla medial flange less carved; (2) a nasal process of the maxillae round to blunt, instead of acute; (3) a nasal process of the maxillae missing the internal narial fossa *sensu* Carrano et al. (2022) at the base; (4) a nasal process of the maxillae projecting slightly anteriorly, instead of strongly; (5) a slot for the frontal-lacrimal/prefrontal contact; (6) a prearticular facet of the dentaries anterior to the end of the tooth row and in line with the posterior opening of the Meckelian canal; (7) reniform anterior cotyles of the atlantes; (8) a less pronounced small ventral notch separating both ventral condyles of the axes; (9) a dorsal cotyle dorsally inclined and with articular facet ending posteriorly less acute; (10) a marked *fossa cubitus cristalis* in the humeri; (11) an ilium with a dorsoventrally elongated acetabulum; (12) a long axis of iliac shaft strongly tilted posteriorly; and (13) the pubic and ischial articular surfaces of the ilia flaring more broadly anteroposteriorly. It further differs from *Albanerpeton arthridion* by (1) a premaxilla medial flange less carved; (2) a nasal process of the maxillae round to blunt, instead of acute; (3) a nasal process of the maxillae missing the internal narial fossa *sensu* Carrano et al. (2022) at the base; (4) a lingually extended maxillary shelf with a longitudinal ventral trough less prominent and with a less deep ventral trough; (5) an indentation forming the internal narial margin more marked, being dorsally concave in labial view and laterally concave in

dorsal view; (6) atlantes with a shallow spinal groove, instead of deep with encapsulating margins; and (7) a marked *fossa cubitus cristalis* in the humeri.

New unnamed taxon 2 differs from *Albanerpeton cifellii*, *A. galaktion*, *A. gracile*, *Albanerpeton* sp., cf. *A. nexuosum*, *A. nexuosum*, *A. inexpectatum*, *A. pannonicum*, and the "Blasi 2B species" by (1) a small, oval, and relatively high suprapalatal pit. It further differs from the "Blasi 2B species" by (1) a smaller palatal foramen; (2) a slot for the frontal-lacrimal/prefrontal contact; (3) a less marked and pronounced lateroventral surface of the quadrate; (4) shallower lateral pillar and the ventral fossa posterior to the condyle of the quadrate; (5) reniform anterior cotyles of the atlantes; (6) atlantes with a mediolaterally straight groove, instead of a spinal foramen, for the first spinal nerve directly posterior to the anterior cotyle margins and anterior to the neural arch attachments; (7) atlantes with a shallow spinal groove, instead of deep with encapsulating margins; and (8) none of the axes is fused with the first dorsal vertebra. It further differs from *Albanerpeton cifellii* by (1) a premaxilla medial flange less carved; and (2) premaxilla outline inclined but not sinusoid in medial view. It further differs from *A. galaktion* and *A. gracile* by (1) a nasal process of the maxillae missing the internal narial fossa *sensu* Carrano et al. (2022) at the base; (2) a dorsal premaxillary process lingual extremity less dorsally curved; (3) an indentation forming the internal narial margin more marked, being dorsally concave in labial view and laterally concave in dorsal view. It further differs from *A. galaktion* by (1) premaxillae not as much lingually inclined; (2) a smaller palatal foramen; (3) a spatulate, short dorsal emargination for the maxillary facet in the premaxillae, instead of notch or deep indentation that extends into a wide shelf; (4) a nasal process of the maxillae round to blunt, instead of acute; (5) a nasal process of the maxillae projecting slightly anteriorly, instead of strongly; and (6) relatively shorter long-projected vertical flange for the lateral premaxillary process in the maxillae. It further differs from *A. gracile* by (1) a dorsal premaxillary process of the maxillae with an indented ventral surface and missing the transverse ridge delimiting the

posterior edge; (2) a slot for the frontal-lacrimal/prefrontal contact; and (3) a less marked prearticular facet of the dentaries anterior to the end of the tooth row and in line with the posterior opening of the Meckelian canal.

New unnamed taxon 2 further differs from *Albanerpeton* sp., cf. *A. nexuosum*, *A. nexuosum*, *A. inexpectatum*, *A. pannonicum* (unformal "robust-snouted clade" *sensu* Gardner 2002) by (1) sutured and gracile premaxillae, instead of robust and fused. *Albanerpeton* sp., cf. *A. nexuosum* having not preserved the maxilla nor the frontal, New unnamed taxon 2 further differs from *A. nexuosum*, *A. inexpectatum*, *A. pannonicum* by (1) premaxillae not as much lingually inclined; (2) a spatulate, short dorsal emargination for the maxillary facet in the premaxillae, instead of notch or deep indentation that extends into a wide shelf; (3) small peg or indentations in the dorsal margin of the premaxillae weakly marked, suggesting only a minimal overlap and a weak suture with the nasal; (4) a nasal process of the maxillae round to blunt, instead of acute; (5) a nasal process of the maxillae projecting slightly anteriorly, instead of strongly; (6) an indentation forming the internal narial margin more marked, being dorsally concave in labial view and laterally concave in dorsal view; (7) a lingually extended maxillary shelf with a longitudinal ventral trough less prominent and with a less deep ventral trough; and (8) a slot for the frontal-lacrimal/prefrontal contact. New unnamed taxon 2 further differs from *A. nexuosum* by (1) a premaxilla medial flange less carved; and (2) a nasal process of the maxillae missing the internal narial fossa *sensu* Carrano et al. (2022) at the base.

New unnamed taxon 2 further differs from *A. inexpectatum* and *A. pannonicum* by (1) a smaller palatal foramen; (2) a straight dorsal edge of the *pars dorsalis* in the premaxillae; (3) a dorsal premaxillary process of the maxillae with an indented ventral surface and missing the transverse ridge delimiting the posterior edge; (4) less broad lacrimal; (5) the absence of ornamentation on the lingual surface of the lacrimal and the posterodorsal-

anteroventral trough between the ventral and dorsal processes; (6) a pandurate foramen above ventral process being instead of subcircular; (7) a less constricted saddle-shaped cotylar facet of the glenoid fossa in the articular; (8) atlantes with a mediolaterally straight groove, instead of a spinal foramen, for the first spinal nerve directly posterior to the anterior cotyle margins and anterior to the neural arch attachments; (9) a less proximodistally extended marked *fossa cubitus cristalis* of the humeri; and (10) a less robust and developed deltopectoral crest. It further differs from *A. pannonicum* by (1) a prearticular facet of the dentaries anterior to the end of the tooth row and in line with the posterior opening of the Meckelian canal; (2) missing a deep ventral groove on the medial surface; (3) a less marked and pronounced lateroventral surface of the quadrate; (4) shallower lateral pillar and the ventral fossa posterior to the condyle of the quadrate; (5) a less pronounced ventral notch separating the anterior cotyles of the atlantes; and (6) reniform anterior cotyles of the atlantes. It further differs from *A. inexpectatum* by (1) a nasal process of the maxillae missing the internal narial fossa *sensu* Carrano et al. (2022) at the base; (2) a horizontal subdental shelf instead of inclined, at the level of the Meckelian canal opening; (3) a short dorsally sculptured postorbital wing in the parietal; (4) parietal without secondary ventral transverse crest; (5) a less pronounced ventral notch separating both ventral condyles of the axes; (6) a dorsal cotyle of the axes dorsally inclined and with articular facet ending posteriorly less acute; (7) none of the axes is fused with the first dorsal vertebra; (8) dorsal vertebrae with foramen or peg on their ventral surface; and (9) *fossa cubitus cristalis* of the humeri triangular rather than circular.

New unnamed taxon 2 differs from the specimens from Guelb el Ahmar (Haddoumi *et al.*, 2016; Lasseron *et al.*, 2020) by a spatulate, short dorsal emargination in the premaxillae, instead of a faint maxillary facet; and from Angeac (Allain *et al.*, 2022) by being less deep. It further differs from the specimens from Guelb el Ahmar by a marked *fossa cubitus cristalis* in the humeri. It differs from the Aguja Fm specimen TMM 45947 attributed to

Albanerpeton sp. (Wick, 2021) by a single large single articular facet with ventral recess on the lateral surface of the articular. It differs from the Isles of Wight specimen IWCMS 2001.451 (Evans *et al.*, 2004) by a single large single articular facet on the lateral surface, instead of being bilobate. It differs from the Yale specimen YPMVP059452 assigned to *Albanerpeton* sp. by ventral surface of dorsal vertebrae not being strongly dorsally concave and without longitudinal crests.

F.4 Specimens from the Guimarota beds

F.4.1 Premaxillae

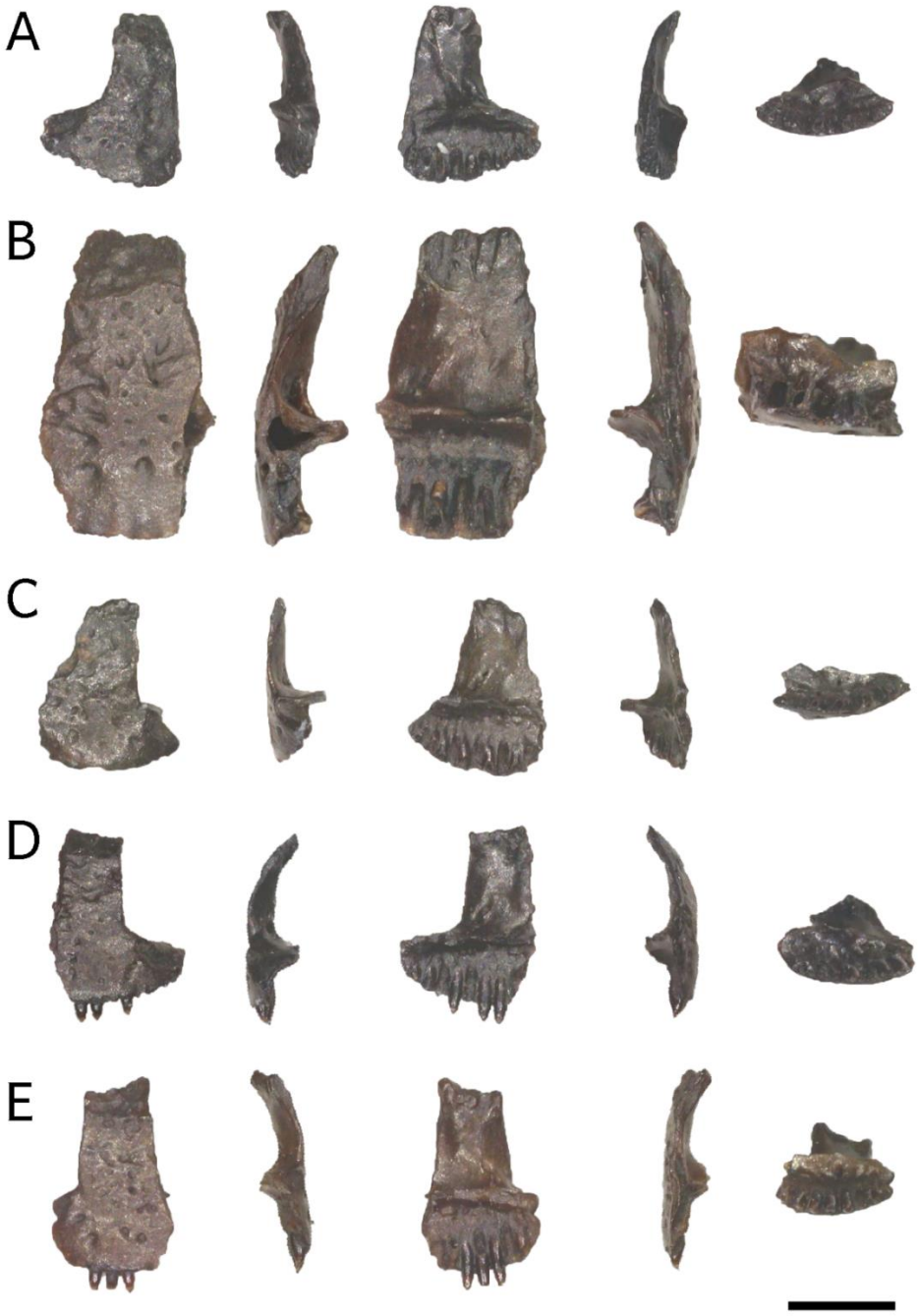

Figure F.2: Premaxillae from Guimarota beds. **A**, MG28600. **B**, MG28611. **C**, MG28612. **D**, MG28624. **E**, MG28630. Specimens are shown from left to right in labial, lateral, lingual, medial, and ventral views. Scale is 1 mm.

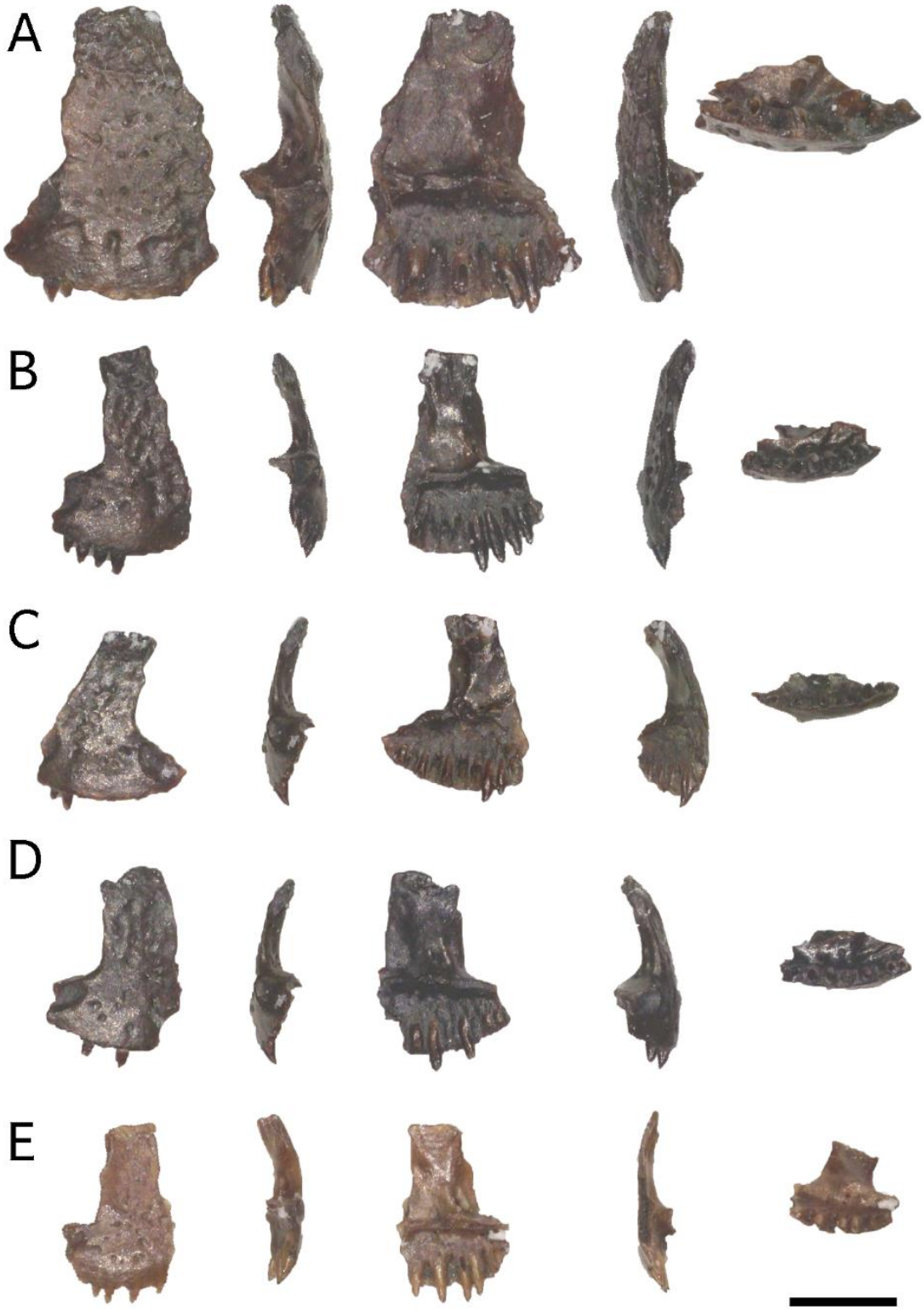

Figure F.3: Premaxillae from Guimarota beds. **A**, MG28645. **B**, MG28645. **C**, MG28650. **D**, MG28650. **E**, MG28651. Specimens are shown from left to right in labial, lateral, lingual, medial, and ventral views. B and C and D and E are respectively from the same labelled box, hence the same specimen number. Scale is 1 mm.

F.4.2 Maxillae

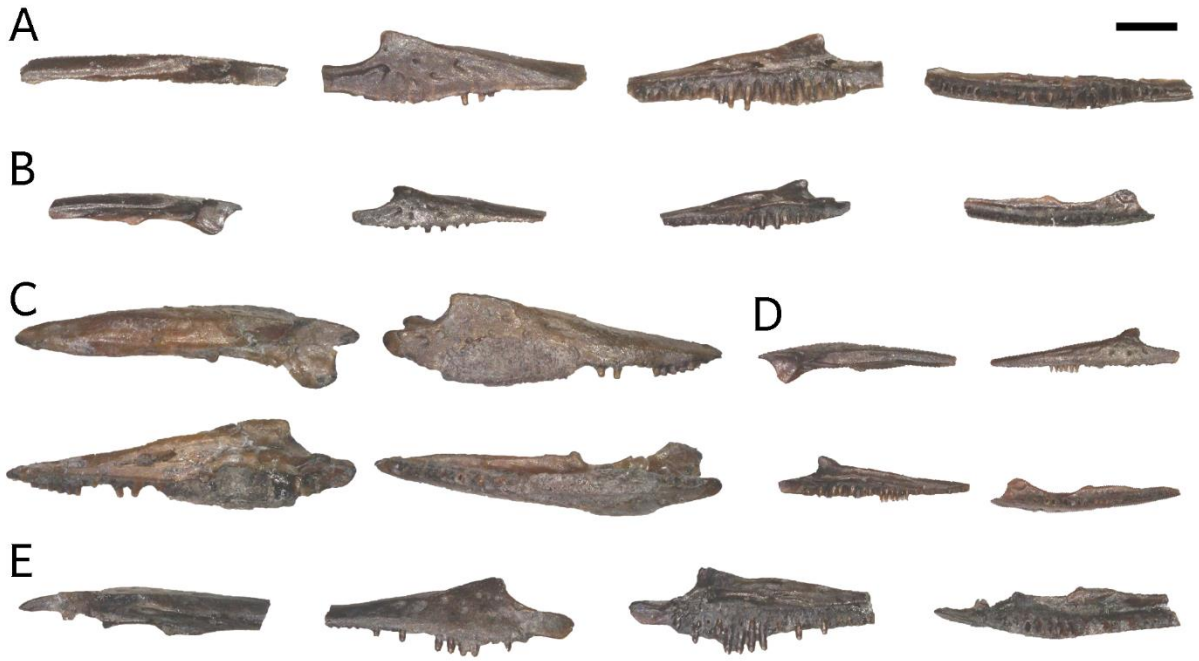

Figure F.4: Maxillae from Guimarota beds. **A**, MG28432. **B**, MG28487. **C**, MG28675. **D**, MG28683. **E**, MG28724. Specimens are shown from left to right in dorsal, labial, lingual, and ventral views. Scale is 1 mm.

F.4.3 Frontals

Figure F.5: Frontal bones from Guimarota beds in dorsal (left) and ventral view (right). **A**, MG28426. **B**, MG28427. **C**, MG28473. **D**, MG28502. **E**, MG28520. **F**, MG28521. **G**, MG28532. **H**, MG28539. **I**, MG28541. **J**, MG28543. **K**, MG28562. **L**, MG28570. **M**, MG28572. **N**, MG28692. **O**, MG28694. **P**, MG28733. Scale bars represent 1 mm.

F.4.4 Parietals

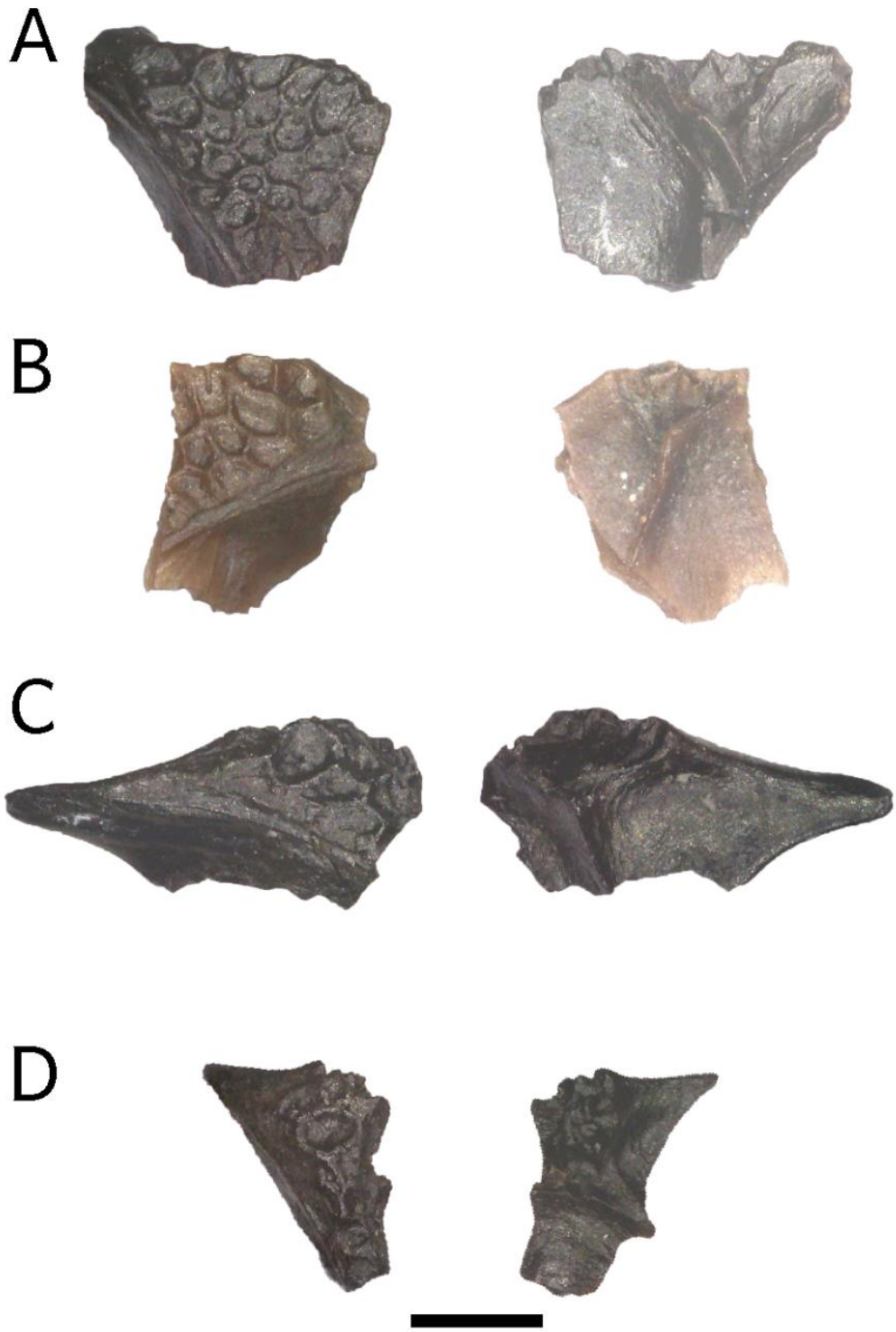

Figure F.6: Parietals from Guimarota beds. **A**, MG28595. **B**, MG28627. **C**, MG28646. **D**, MG28672. Specimens are shown from left to right in dorsal and ventral views. Scale is 1 mm.

F.4.5 Dentaries

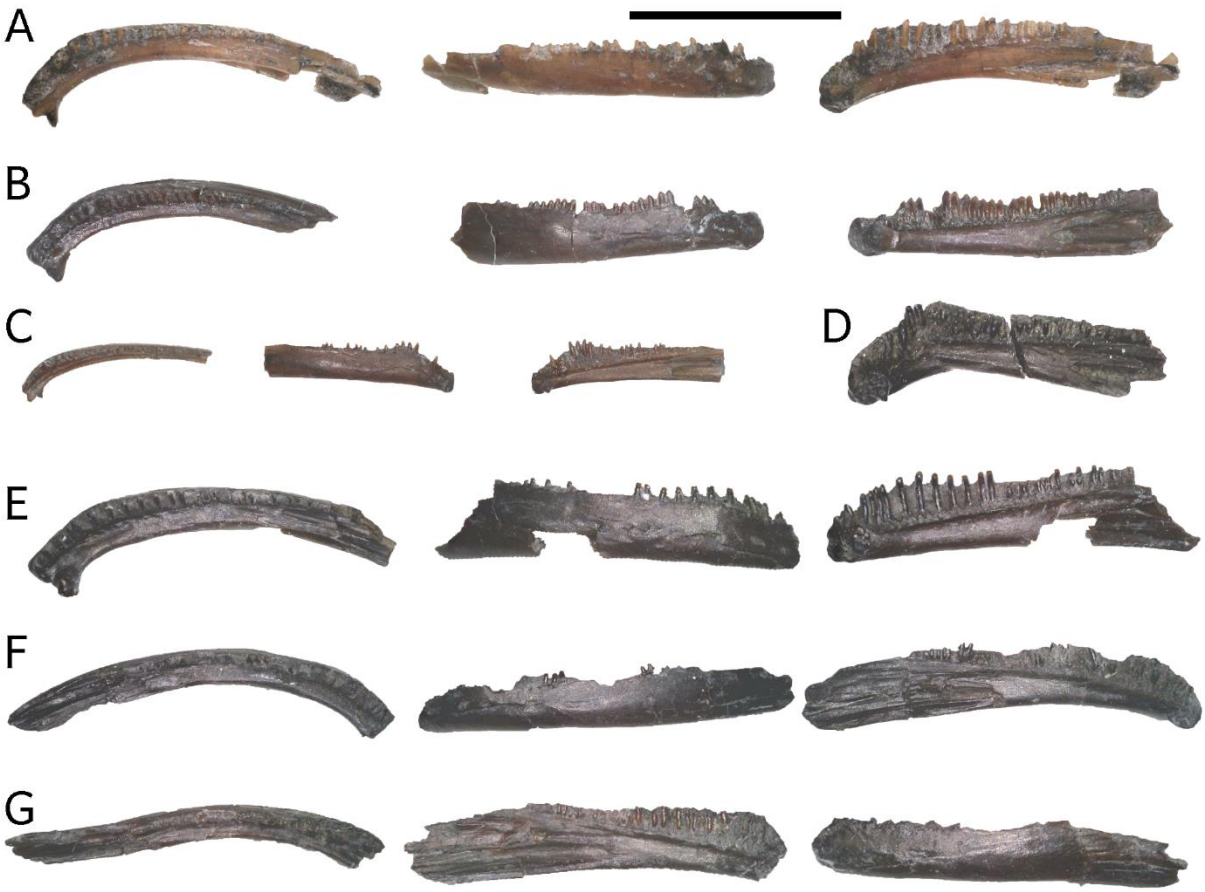

Figure F.7: Dentaries from Guimarota beds. **A**, MG28423. **B**, MG28431. **C**, MG28534. **D**, MG28670. **E**, MG28535. **F**, MG28668. **G**, MG28657. Specimens are shown from left to right in dorsal, labial, and lingual views. Scale is 5mm.

Figure F.8: Dentaries from Guimarota beds. **A**, MG28677. **B–D**, MG28652. **E–G**, MG28662. Specimens A–D are shown from left to right in dorsal, labial, and lingual views; specimens E–G are shown from left to right in dorsal, labial, lingual, and ventral views. B–D and E–G are respectively from the same labelled box, hence the same specimen number. Scale is 3 mm.

F.4.6 Articulars

Figure F.9: Articulars from Guimarota beds. **A**, MG28208. **B**, MG28677. Specimens are shown from left to right in medial, lateral, and dorsal views. Scale is 1 mm.

F.4.7 Axes

Figure F.10: Axes from Guimarota beds. **A**, MG28666. **B**, MG28698. **C**, MG28722. **D**, MG28731. Specimens are shown from left to right in anterior, posterior, lateral, dorsal, and ventral views. Scale is 1 mm.

F.4.8 Humeri

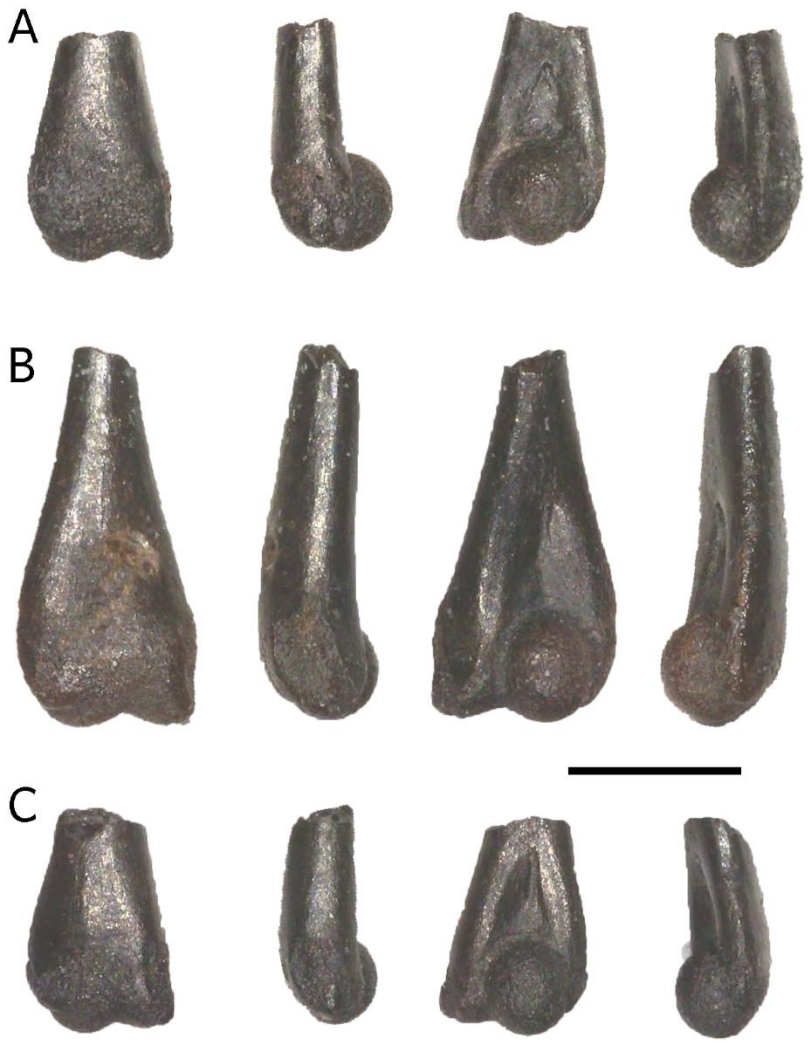

Figure F.11: Humeri from Guimarota beds. **A**, MG28506. **B**, MG28690. **C**, MG28720. Specimens are shown from left to right in dorsal, lateral, ventral, and medial views. Scale is 1 mm.

F.5 References

Allain R, Vullo R, Rozada L, Anquetin J, Bourgeais R, Goedert J, Martin J, de Fabrègues CP, Royo-Torres R, Augier D. 2022. Vertebrate paleobiodiversity of the Early Cretaceous (Berriasian) Angeac-Charente Lagerstätte (southwestern France): implications for continental faunal turnover at the J/K boundary. Geodiversitas 44: 683–752.

Carrano MT, Oreska MPJ, Murch A, Trujillo KC, Chamberlain KR. 2022. Vertebrate paleontology of the Cloverly Formation (Lower Cretaceous), III: a new species of *Albanerpeton*, with biogeographic and paleoecological implications. Journal of Vertebrate Paleontology: e2003372.

Estes R, Sanchíz B. 1982. Early cretaceous lower vertebrates from Galve (Teruel), Spain. Journal of Vertebrate Paleontology 2: 21–39.

Evans SE, Barrett PM, Ward DJ. 2004. The first record of lizards and amphibians from the Wessex Formation (Lower Cretaceous: Barremian) of the Isle of Wight, England. Proceedings of the Geologists' Association 115: 239–247.

Gardner JD. 2002. Monophyly and intra-generic relationships of *Albanerpeton* (Lissamphibia; Albanerpetontidae). Journal of Vertebrate Paleontology 22: 12–22.

Haddoumi H, Allain R, Meslouh S, Metais G, Monbaron M, Pons D, Rage JC, Vullo R, Zouhri S, Gheerbrant E. 2016. Guelb el Ahmar (Bathonian, Anoual Syncline, eastern Morocco): first continental flora and fauna including mammals from the Middle Jurassic of Africa. Gondwana Research 29: 290–319.

Lasseron M, Allain R, Gheerbrant E, Haddoumi H, Jalil NE, Métais G, Rage JC, Vullo R, Zouhri S. 2020. New data on the microvertebrate fauna from the Upper Jurassic or lowest Cretaceous of Ksar Metlili (Anoual Syncline, eastern Morocco). Geological Magazine 157: 367–392.

Wick SL. 2021. Albanerpetontids (Lissamphibia, Albanerpetontidae) from the Aguja Formation (lower Campanian) of West Texas, USA. Canadian Journal of Earth Sciences 58: 141–149.

Wiechmann MF. 2003. Albanerpetontidae (Lissamphibia) aus dem Mesozoikum der Iberischen Halbinsel und dem Neogen von Süddeutschland. Unpublished thesis, Freie Universität Berlin.

G NEW PHYLOGENY OF ALBANERPETONTIDAE AND IMPLICATIONS ON THEIR TAXONOMY AND PALAEOBIOGEOGRAPHY

G.1 Nexus file for the total phylogenetical analysis

```
taxname+ 100
xread
62 23
Anoualerpeton_priscum
        00000??00?000000000000101110??1100010??0??0??0000?????????????
Anoualerpeton_unicum      0000000001000000000001010010000010[0
1]010??010100010100??000?0????
Celtedens_ibericus   10000?0?????????????00001000000000000??[0
1]0?1???????0??0??11010
Celtedens_megacephalus
        ??????????????????????01?????1000?2000?00?01????1???????1????
Albanerpeton_arthridion    0000000010001000?00110002100211001[0
1]20????????11[0 1]2????011?1????
Albanerpeton_ektopistikon
        10000??01?101000?011?000210101100002 2????????1012????100012110
Albanerpeton_gracile       100000001001111001[0   1]111002[1   2]00[1   2]11002[0
1]11????????1??2?????????????
Albanerpeton_galaktion     201[0
1]0101100112100111110021 00??1002120????????1210?????????????
Albanerpeton_cifellii1010020010-
11110??????????????????????????????????????????????
Albanerpeton_nexuosum    211[0
1]11101100111000111010221011111211 2????????1002?????????????
Albanerpeton_inexpectatum
        21211121111011111111100122102111111021101012?10[0 1]20???00210????
```

```
Albanerpeton_pannonicum  111[0                    1]1101110011111111100022[0
1]12111111121117?1??12120011112?0????
Wesserpeton_evansae      10000100[0      1][0      1]1010[0      1]0[0      1][0
1]10000021100000000117?01????100200??000000101
Shirerpeton_isajii
      ??????????????????0000?0102210011000120101011211202??00?????????
Yaksha_perettii      1121020011-
11111000001102000011101002110111210002?????????2110
Paskapoo_species
      11111220110011111107?00002??0??000?010??00?1??1101?????????????
Una_species  00010000??1[0
1]1000????????211000?000121?????????????????????????
Albanerpeton_sp.,_cf._A._nexuosum      2110111011-
01110??????10??????????????????????????????????????
Sanpetru_species
      10210000110011101000??002??0??1?000?2??????????02????????1????
Csehbanya_species
      10?00??01?001110??0???00?????????????????????002????????????
Purbeck_species
      ?0000??????0000000001?1000000000000?0?????????1??011?000000111
Blasi_2B_species
      ?0?00??11??11210?1011?00210020100101 2????????112001120[1 2]00????
Portuguese_species  ?000000001000000000000101000000 1000[1
2]00011?11?10010100000100000
;
cc+ 2 5 13 24 25 33 55;
cc]0;
Hold 50000;

proc /;
comments 0
;
```

G.2 List of characters

Prior numbering for first publication, and potential later renumbering, are shown in brackets [] following the reference. It is here noted that Gardner *et al.* (2003); Venczel & Gardner (2005); Sweetman & Gardner (2013); Matsumoto & Evans (2018); Daza et *al.*

(2020); and Guillaume *et al*. (2023b) followed the numbering from Gardner (Gardner, 2002), adding subsequent characters.

The characters anatomical breakdown has been reorganized to match the anatomical description and sequence, starting with cranial characters, then axial, and finally appendicular, and for each following the sequence from anterior to posterior and dorsal from ventral. Then, characters were organized in order to facilitate the scoring on future specimens.

1. Body size (maximum size based on premaxilla height and width): 0 = large (> 2.75 mm/1.7 mm); 1 = small (< 2.7 mm/1.6 mm) (Gardner 2000*a*, 2002 [25]; Carrano *et al.* 2022 [1])

State changes: *C. megacephalus* 1 → ?;

S. isajii 1 → ?;

"Purbeck species" 1 → ?;

In their new definition of the character, Carrano *et al*. (2022) based their scores on the size of the premaxilla for the largest known individual of each species. However, such items are unknown in *C. megacephalus* and *S. isajii*, and none is enough complete to be scored in the "Purbeck species"; therefore, the character cannot be scored in these species, even though it could be with the previous definition (estimated snout-vent length based on frontal size).

G.2.1 Premaxilla

2. Premaxilla, overall build: 0 = gracile; 1 = robust (Gardner 2000*a*, 2002 [1]; Carrano *et al.* 2022 [8])

State changes: "Csehbánya species" ? → 0

Based on figured specimens (Szentesi *et al.*, 2013), the premaxillae in the "Csehbánya species" looks more of the gracile morphotype rather than robust.

3. Premaxilla, pattern of labial ornament, excluding nutritive foramina, on labial *pars dorsalis*, in large specimens: 0, discontinuous anastomosing ridges enclosing irregular to polygonal pits; 1, continuous anastomosing ridges enclosing irregular to polygonal pits; 2, vermiculate to pustulate sculpturing (Gardner 2002 [8])

{ORDERED}

In their analysis, Carrano *et al*. (2022) removed the pattern of the labial ornament, as they considered states 1 and 2 were probably autapomorphies of *A. nexuosum* and *A. inexpectatum*, respectively, in the way they were originally defined and scored Gardner, 2002. However, we reintroduced this character, as it avoids confusion in scoring the character, and reworded the states of character to better represent the variability among the species.

Indeed, *Y. perettii* display anastomosing ridges more developed than in *A. nexuosum*, and it is described with a "dorsal process bearing vermiculate sculpturing" (Daza *et al*. 2020); and the "Sânpetru species" is as well described with "the entire labial side of the pars dorsalis is slightly ornamented by pustules and anastomosed ridges and is perforated by a few foramina" (Folie & Codrea 2005); so both can be scored with state 2. Furthermore, after close examination of referred specimens, *A. galaktion* and the "Paskapoo species" display an ornament pattern closer to *A. nexuosum* than other albanerpetontid and can all be scored with state 1. Therefore, both state 1 and state 2 are no longer autapomorphies of *A. nexuosum* and *A. inexpectatum*, respectively; and the original issue highlight by Carrano et al. 2022 has been solved.

Character was ordered, because it is understood that passing from state 0 to state 2, or vice versa, would require to pass by state 1 during the development.

4. Premaxilla, distribution of ornament, excluding nutritive foramina, on labial *pars dorsalis*, in large specimens: 0 = restricted to dorsal part or the boss; 1 = covers entire face (Gardner 2000*a*, 2002 [7]; Wiechmann 2003 [24]; Carrano *et al.* 2022 [4])

State changes: *A. galaktion* 0 → 0&1;

A. nexuosum 0 → 0&1;

A. pannonicum 0 → 0&1;

Based on referred specimens, *A. galaktion* and *A. nexuosum* display some variation in the distribution of the ornament on labial *pars dorsalis*, extending as far as *A. inexpectatum* in some specimens. Similarly, the distribution extension observed in figured specimens in Gardner *et al.* (2021) from *A. pannonicum* and some uncatalogued specimens on loan at the Royal Tyrrell Museum of Palaeontology (RTMP; ARDG, pers. obs, 2023) assessed to *A. pannonicum* suggests some variation.

Furthermore, we have not changed the scoring of the "Uña species" done by Carrano *et al*. (2022), although we are not sure of the authors interpretation of the drawing of figured specimen Uña A7 in Wiechmann thesis (2003), especially based on the character description: "Character 24: premaxillary; Sculpting over the entire labial surface of the pars dorsalis (in large individuals), (1) present, (0) sculpting predominantly in the dorso-labial area"; the "Uña species" being scored 0 (Wiechmann 2003, 129-130). Direct observation of the material would help to assess the actual state of this character. (Original text in German "Merkmal 24: Prämaxillare; Skulptierung auf der gesamten labialen Fläche der Pars dorsalis (bei großen Individuen), (1) vorhanden, (0) Skulptierung überwiegend im dorso-labialen Bereich")

5. Premaxilla, pattern of inter-premaxillary contact: 0 = sutured medially (i.e. paired) ; 1 = fused medially (Gardner 2000*a*, 2002 [3]; Wiechmann 2003 [21]; Carrano *et al.* 2022 [10])

6. Premaxilla, pattern of pars dorsalis contact with nasal: 0 = minimally overlaps and abuts/weakly sutures with anterior nasal; 1 = minimally overlaps and strongly sutures with anterior nasal; 2 = has lingual facet for anterior nasal, braced ventrolaterally by expanded dorsal end of lateral internal strut (Gardner 2000*a*, 2002[4]; Carrano *et al.* 2022 [11])

{ORDERED}

State changes: "Paskapoo species" 1 → 2;

"Uña species" ? → 0;

Direction observation of specimens from the "Paskapoo species" in RTMP suggest a more pronounced facet as originally described, similar to the one observed in *A. cifellii*. The description of the "Uña species" "The dorsal ridge runs more or less in a straight line and may be faintly sculpted" (Wiechmann 2003; p50) suggests only weak suture, but only direct observations would confirm it. (Original text in German "Die dorsale Kante nimmt einen mehr oder weniger geradlinigen Verlauf und kann schwach skulptiert sein.")

Character was ordered, because it is understood that passing from state 0 to state 2, or vice versa, would require to pass by state 1 during the development.

7. Premaxilla, relative size of boss on pars dorsalis: 0 = covers dorsal 1/4 to 1/3; 1 = covers dorsal ½; 2 = absent (Gardner 2000*a*, 2002 [5,6]; Wiechmann 2003 [26,23]; Carrano *et al.* 2022 [12])

State changes: *C. ibericus* ? → 0;

A. ektopistikon 0&2 → ?;

Figured specimens MCCM-LH 15710B (Maddin *et al.*, 2013; Matsumoto & Evans, 2018) suggest that the boss is present in *C. ibericus*, although reduced. Nevertheless, microCT-scan of Las Hoyas specimens would help to clarify the state of character. Carrano *et al.* originally scored the boss in *A. ektopistikon* as simultaneously absent and reduced, but described "that it would not have housed a large boss with an associated ventral rim. Instead, the dorsalmost preserved portion seems to have borne a faint fossa." (Carrano *et al.*, 2022). Nevertheless, no specimen preserved this part; therefore, the actual state should be considered unknown.

8. Premaxilla, diameter of palatal foramen relative to diameter of base of any of more medial teeth: 0 = small; 1 = large (Gardner 2000*a*, 2002 [14]; Carrano *et al.* 2022 [2])

State changes: *A. inexpectatum* 0 → 1;

"Uña species" ? → 0;

"Purbeck species" 0 → ?;

Direct observation on referred specimens of *A. inexpectatum* revealed that the species also displays a large palatal foramen. The palatal foramen is most likely preserved in specimens from the "Purbeck species", but it is obscured by sediments; therefore its size could not be assessed. The palatal foramen in the Uña species was described as small and round (Wiechmann 2003; p50); although only direct observation of the specimen would

confirm it. (Original text in German “In einigen Exemplaren ist aufgrund der abgebrochenen Parspalatina der Kanal, der das kleine, rundliche palatale Foramen mit der suprapalatalen Grube verbindet, freigelegt.”)

9. Premaxilla, path of canal through pars palatinum: 0 = dorsolateral-ventromedial; 1 = dorsal-ventral (Sweetman & Gardner 2013 [27]; Carrano *et al.* 2022 [9])

10. Premaxilla, height/width proportion of pars dorsalis across suprapalatal pit: 0 = high (>1.55); 1 = low (<1.55) (Gardner 2000*a*, 2002 [2]; Wiechmann 2003 [22]; Carrano *et al.* 2022 [5])

State changes: *C. ibericus* 0 → ?;

“Uña species” 0 → ?;

Wiechmann originally choose the threshold for this character at 1.5 (2003), instead of 1.55 as proposed by Gardner (2002). He scored “Uña species” for 0, with the character being defined as “Character 22: premaxillary relatively short pars dorsalis, (1) HPDO:BPDO < 1.5, (0) HPDO:BPDO > 1.5”, where HPDO stand for the height of the *pars dentalis* and BPDO stands for the width of the *pars dentalis*. Therefore, the state is ambiguous, as the proportion could lie between 1.5 and 1.55. Measures on the figured specimen Uña A7 (Wiechmann 2003; pl VII, fig.8) suggest a proportion around 2; but were done on the labial surface, instead of the lingual surface across the suprapalatal pit, as recommended by Gardner (2002).

Similarly, the ration could not be done on referred specimens of *C. ibericus* during direct observation, and the only other figured specimens MCCM-LH 15710 B presents the labial surface. Measures suggest a proportion slightly above 1.55; but the same problem of

methodology occurs. So far, *Celtedens* have been scored as one species and only based on *C. ibericus*, as *C. megacephalus* did not preserved premaxillae. However, in his analysis, Wiechmann did separate both species, and both were scored with ? (Wiechmann, 2003).

Until better pictures are provided, we suggest to keep both species with a ?. The character may also need a global revision to take into account the intraspecific variation, as shown in *W. evansae* (Sweetman & Gardner, 2013); and a clear protocol to take the measurements, as the suprapalatal pit can be moderate to big in size, and therefore can give different measurement according to what "across" refers to.

11. Premaxilla, division of suprapalatal pit: 0 = undivided; 1 = divided (in 1/3+ of specimens) (Venczel & Gardner 2005 [30]; Carrano *et al.* 2022 [3])

State changes: *C. ibericus* 0 → ?;

Y. perettii 0 → -;

A. cifellii ? → -;

Albanerpeton sp., cf. A. nexuosum 0 → -;

As the suprapalatal pit is obscured in *C. ibericus*, the state of the character cannot be assessed. Furthermore, state 1 clearly specifies that the pit must be divided in at least 1/3 of the specimens. Therefore, as only one specimen is known in *A. cifellii*, *Y. perettii*, and *Albanerpeton sp., cf. A. nexuosum* from the Cedar Mountain Fm (Gardner, 1999b), the character is not applicable in these species.

It is here noted that only one specimens from the "Uña species" (Uña A8, Wiechmann, 2003; pl. VII, fig. 9) is figured with his lingual surface, showing a divided suprapalatal pit. However, the pit was originally described as it "can be divided into an upper and a lower rounded opening by a ridge of varying thickness" (Wiechmann 2003; p50).

Therefore, this feature is here interpreted as common enough in the "Uña species", and so we follow the Carrano *et al.* proposal (2022) to score it 1; although, only direct observation of the specimens can confirm it. (Original text in German "Die suprapalatale Grube ist nach lingual geöffnet und kann durch einen unterschiedlich stark ausgebildeten Grat in eine obere und eine untere rundliche Öffnung unterteilt sein")

12. Premaxilla, lingual outline of suprapalatal pit: 0 = oval; 1 = triangular to slit-shaped (Gardner 2000*a*, 2002 [11]; Carrano *et al.* 2022 [6])

State changes: *C. ibericus* 0 → ?;

"Uña species" 0 → 0&1;

As the suprapalatal pit is obscured in *C. ibericus*, the state of the character cannot be assessed. The only figured specimen on lingual view of the "Uña species", Uña A8, displays a suprapalatal pit closer to the oval morphotype (Wiechmann, 2003; pl. VII, fig. 9). However, Wiechmann described it as "oval to slit-like" in thesis (2003; p50), suggesting there is some intraspecific variation in this species. Only direct observation will confirm it.

13. Premaxilla, orientation of suprapalatal pit in pars dorsalis: 0 = laterolingual; 1 = lingual (Gardner *et al.* 2003 [26]; Wiechmann 2003 [18]; Carrano *et al.* 2022 [7])

State changes: *C. ibericus* 1 → ?;

Y. perettii 0 → 1;

As the suprapalatal pit is obscured in *C. ibericus*, the state of the character cannot be assessed. The figured specimen of *Y. perettii* (Daza *et al.*, 2020) displays a suprapalatal pit that is strictly facing lingually.

14. Premaxilla, size of suprapalatal pit relative to lingual surface area of pars dorsalis: 0 = small (1%); 1 = moderate (4–15%); 2 = large (20–25%) (Gardner 2000*a*, 2002 [10]; Wiechmann 2003 [20]; Carrano *et al.* 2022 [13])

{ORDERED}

State changes: *C. ibericus* 0 → ?;

As the suprapalatal pit is obscured in *C. ibericus*, the state of the character cannot be assessed.

Character was ordered, because it is understood that passing from state 0 to state 2, or vice versa, would require to pass by state 1 during the development. Furthermore, the size of the suprapalatal pit has important constraints on the structure of the premaxilla; therefore, passing from one state to another will affect it.

15. Premaxilla, vertical position of suprapalatal pit on pars dorsalis: 0 = high; 1 = low (Gardner 2000*a*, 2002 [9]; Wiechmann 2003 [25]; Carrano *et al.* 2022 [14])

State changes: *C. ibericus* 0 → ?;

As the suprapalatal pit is obscured in *C. ibericus*, the state of the character cannot be assessed.

16. Premaxilla, mediolateral position of lateral edge of suprapalatal pit: 0 = lateral half; 1 = medial half (Carrano *et al.* 2022 [15])

State changes: *Y. perettii* 0 → 1;

"Paskapoo species" ? → 1;

As the character was understood, it is a representation of the proportion between the distance from the medial border of the pars dorsalis to the lateral edge of the suprapalatal pit and the width of the pars dorsalis across the suprapalatal pit; scored 0 if the proportion is > 0.5, and 1 if the proportion <0.5. Yet, measures on figured specimen of *Y. perettii* (Daza *et al.*, 2020) and specimens from "Paskapoo species" gave a proportion <0.5.

Nevertheless, as for character 10, this character may need a global revision with a clear protocol to take the measurements, as the suprapalatal pit can have various shapes and sizes, and therefore can give different measurement according to what "the lateral edge" refers to.

G.2.2 Maxilla

17. Maxilla, length:basal height ratio of lateral premaxillary process: 0 = long, length > height; 1 = short, length ≤ height (Gardner 2000*a*, 2002 [15]; Wiechmann 2003 [27]; Carrano *et al.* 2022 [16])

State changes: *C. ibericus* 0 → ?;

A. nexuosum 1 → 0;

"Sânpetru species" 0 → 1;

None of the specimens directly observed or figured from *C. ibericus* preserved a maxilla with a lateral premaxillary process visible. Only MCCM-LH 030 B displays a process that could be interpreted as the lateral premaxillary process, however it is in dorsal view,

therefore the measurement cannot be done. MicroCT-scans of Las Hoyas specimens should allow to confirm the character state.

Direct observations and measurements giving on referred specimens of *A. nexuosum* confirmed that the lateral premaxillary process was long rather than short. Conversely, measurements on figured specimens of the "Sânpetru species" confirmed the process was instead short rather than long, as originally described (Folie & Codrea, 2005).

18. Maxilla, position of anterior end of tooth row relative to maximum indentation on leading edge of nasal process: 0 = anterior; 1 = same level or posterior (Gardner 2000*a*, 2002 [20]; Wiechmann 2003 [28]; Carrano *et al.* 2022 [17])

19. Maxilla, nasal process: 0 = anterior edge weakly curved, little or no overhang; 1 = strongly curved, marked overhang (Carrano *et al.* 2022 [18])

State changes: *C. ibericus* 0 → ?;

A. gracile 1 → 0&1;

"Paskapoo species" ? → 0;

Nasal process is either obscured, not preserved, or crushed in specimens of *C. ibericus*. Nasal processes in some referred specimens of *A. gracile* do not overhang, or only a little, and do not seem broken. Direct observations on specimens of the "Paskapoo species" shows the nasal process do not project anteriorly.

20. Maxilla, internal narial fossa: 0 = absent; 1 = present {NEW}

Some species display a small fossa at the anterior base of the nasal process lingual surface. It is labially bordered by the crest joining the nasal process to the lateral premaxillary process.

21. Maxilla, lingual and dorsal indentation of the internal narial margin: 0 = strong indentation; 1 = weak indentation or absent {NEW}

Most species display an indented internal narial margin. However, this indentation can be more or less pronounced lingually and/or dorsally from one species to another. Geomorphometrics should help to characterize all the variation among albanerpetontids.

22. Maxilla, dorsal curvature of the dorsal premaxillary process: 0 = uncurved or weakly dorsally curved; 1 = strongly dorsally curved {NEW}

The dorsal premaxillary process is always dorsally curved in most albanerpetontids. However, this can be more or less pronounced from one species to another.

23. Maxilla/dentary, labial or lingual profile of occlusal margins and associated heterodonty: 0 = essentially straight, with weak heterodonty; 1 = strongly convex or angular, with marked heterodonty about 1/3 from anterior end (Gardner 2000*a*, 2002 [18,19]; Carrano *et al.* 2022 [19])

State changes: “Sânpetru species” ? → 0;

Figured maxilla of the “Sânpetru species” display a straight occlusal margin and no heterodonty. Although no dentary is complete, it is assumed they would follow a similar

pattern, considering how the character is defined. Nevertheless, a revision of this character may be need, in order to better characterize the shape in both maxilla and dentary and to take into account preservation bias.

24. Maxilla/dentary: labial ornament on large individuals: 0 = absent, smooth with nutritive foramina; 1 = present, pustulate (Gardner 2000*a*, 2002 [17]; Carrano *et al.* 2022 [20])

State changes: "Uña species" 1 → ?;

Carrano *et al.* changed the score to 1 (2022), based on the description of the material from Uña (Wiechmann, 2003). However, in his work, Wiechmann could not assess the taxonomy of either the maxillae or the dentaries, and only referred premaxillae and frontals to the "Uña species" (Wiechmann 2003; p22). Considering that Wiechmann reported at least two different species from that locality, assessing the taxonomy of these bones without new direct observation of the material is dubious.

G.2.3 Frontal

25. Frontals, outline of fused bones in dorsal or ventral view: 0 = hourglass-shaped; 1 = bell-shaped; 2 = triangular (McGowan 1998, Gardner 2000*a* [1,8,9], 2002 [21]; Wiechmann 2003 [6,7]; Carrano *et al.* 2022 [22])

{ORDERED}

State changes (ancient score in parenthesis): *An. unicum* 1(2) → 0;

C. megacephalus 0 → 1(2);

Y. perettii 1(2) → 2(1);

Ancient scores (Carrano *et al.*, 2022): 0 = hourglass-shaped; 1 = triangular; 2 = bell-shaped

Carrano *et al.* split the two original character states into three. However, due to the constraints the shape of the frontals put on the overall structure of the skull and the contact with other bones, we decided to reorganize the character states and to order them, from the hourglass to the bell-shaped to the triangular morphology.

Direct observation on holotype of *C. megacephalus* revealed that the frontal outline is bell-shaped rather than hourglass, according to the new character states defined by Carrano *et al.* (2022): "state 2 is relatively clearly defined as the condition wherein the anterior section of the lateral edge of the frontals is nearly state, transitioning abruptly to a concave outline in the posterior one-third or one-quarter". Following this assessment, direct observation on referred specimens of *An. unicum* revealed a more hour-glass morphology, closer to what is observed in *C. ibericus*. Finally, figured specimens of *Y. perettii* suggests more a triangular outline. However, we agree with Carrano *et al.* on the difficulties to assess correctly the global outline, especially in species with incomplete and broken frontals. This could be solved by the use of geomorphometrics, which also could help to differentiate subtle changes into the triangular morphotype, currently described with "a gentle transition from straighter to more concave anteroposteriorly" (Carrano *et al.*, 2022); and would also take into consideration character 29.

26. Frontals, outline of internasal process in dorsal or ventral view: 0 = bulbous/flabellate, > 90°; 1 = tapered/hastate, 45° to 90°; 2 = spike-like/acute, < 45° (McGowan 1998, Gardner 2000*a* [3]; Gardner *et al.* 2003 [29]; Wiechmann 2003 [2,3,4,5]; Carrano *et al.* 2022 [23])

{ORDERED}

State changes (ancient score in parenthesis): *C. ibericus* 0(2) → 1;

C. megacephalus 0(2) → ?;

A. gracile 2(0) → 1&2;

"Paskapoo species" 2(0) → ?;

"Uña species" 2(0) → 1;

Ancient scores (Carrano *et al.*, 2022): 0 = spike-like/acute, < 45°; 1 = tapered/hastate, 45° to 90°; 2 = bulbous/flabellate, > 90°

Carrano *et al.* split the two original character states into three. However, due to the constraints the shape of the internasal process put on the overall structure of the skull and the contact with other bones, notably with the nasal and premaxillae, we decided to reorganize the character states and to order them, from the bulbous/flabellate to the tapered/hastate to the spike-like/acute morphology.

As previously reported (Carrano *et al.*, 2022) and confirmed by direct observations, the internasal process in *C. megacephalus* is not preserved—or at the very least, obscured—in the holotype and cannot be scored; as well as the holotype of *C. ibericus* MCCM-LH6020 (both part and counterpart). Only the figured specimen MCCM-LH 15710B (Maddin *et al.*, 2013; Matsumoto & Evans, 2018) displays a well-preserved nasal process for *C. ibericus*, where it appears broad but tapered (Carrano et al. 2022; S. Sweetman, pers. comm., 2022).

Direct observation of the only frontal attributed to the "Paskapoo species" would suggest a spike-like to tapered morphology; however, the internasal process is broken and deformed, which prevents to confirm which state between both. Direct observation on referred specimens of *A. gracile* revealed both spike-like and tapered morphologies, and it does not seem to be caused by a preservation bias.

The internasal process in the "Uña species" was previously scored 0 (Carrano *et al.*, 2022), and was originally described with a "broad tip" (Wiechmann, 2003). However, based on the figured specimen Uña A1 (Wiechmann 2003; pl.III, fig.1) that looks closer to *W. evansae* than *A. inexpectatum*, and the original scoring by Wiechmann ("Character 2: Frontal; short, pointed internasal process, (1) present, (0) absent"; scored as present); it is interpreted as that the internasal process in the "Uña species" belongs to the tapered morphotype.

As for the general outline, this character could be updated in order to better define the different morphotypes. A clearly defined protocol to measure the angle, as there can be several ways to do it: (1) the angle formed by the base of the process and the tip of the process; (2) the angle formed by the base of the process and the intersection of the tangent of the lateral edges of the process; and (3) the angle formed when the tangent of the lateral edges of the process would intersect at the tip of the process. Another solution could be the use of geomorphometrics, which would also allow to take into consideration character 27.

27. Frontals, proportions of internasal process (basal width:length): 0 = broad (> 1); 1 = narrow (≤ 1) (McGowan 1998, Gardner 2000*a* [4], 2002 [23]; Wiechmann 2003 [1,2,3,4,5]; Carrano *et al.* 2022 [28])

State changes: *C. megacephalus* 0 → ?;

A. gracile 1 → 0;

W. evansae 0 → 1

"Paskapoo species" 1 → ?;

As explained above, the states of preservation for the internasal process in *C. megacephalus* and the "Paskapoo species" prevent to assess any state for this character.

Measures on figured specimens of *W. evansae* (Sweetman & Gardner, 2013) gave a ration lower than 1. Measures on figured specimens (Gardner, 2000b) and direct observation on referred specimens of *A. gracile* gave ratio slightly above 1 (1.05 to 1.08).

28. Frontals, flattened ventromedian keel extending along posterior 2/3 of bones: 0 = absent; 1 = present (Venczel & Gardner 2005 [31]; Carrano *et al.* 2022 [24])

State changes: *S. isajii* 1 → 0;

Y. perettii 1 → 0;

New unnamed taxon 2 1 → 0;

"Sânpetru species" 1 → 0;

The flattened ventromedian keel was first described in *A. pannonicum* (Venczel & Gardner, 2005), and was clearly differentiated from any ventromedian crest or suture line (as observed in most of albanerpetontids, depending their ontogenetic stages) that could result from the fusion of the frontals. Direct observations on specimens attributed to *A. pannonicum* on loan at RTMP confirmed that said keel is more prominent than crests and suture lines observed in other species; and that its ventral edge is flat.

Therefore, based on these observations and figured specimens, *S. isajii*, *Y. perettii*, New unnamed taxon 2, and the "Sânpetru species" do not display such keel. Furthermore, both Asian species are described with "a weak ventromedian crest" (Matsumoto & Evans, 2018) or "a weak mid-ventral crest" (Daza *et al.*, 2020), contradicting therefore the way they were originally scored by the respective authors.

Doubts remains regarding *A. ektopistikon*, as figured specimen and description match the description of the ventromedian keel (Carrano *et al.*, 2022), but direct observations of the specimens were unconclusive on its presence or absence.

29. Frontals, midline length relative proportion to posterior width between lateral edges of ventrolateral crests, in large specimens: 0 = long (> 1.2); 1 = moderate (1.2–1.1); 2 = short (< 1.1) (McGowan 1998, Gardner 2000*a* [2], 2002 [22]; Wiechmann 2003 [15]; Carrano *et al.* 2022 [26])

State changes: *An. priscum* 0 → ?;

C. megacephalus 0 → ?;

A. arthridion 1 → 2;

A. ektopistikon 1 → 0;

A. gracile 0 → 1&2;

A. galaktion 1 → ?;

S. isajii 0&1 → 0

Y. perettii 0&1 → 0;

As the internasal process is not preserved in *C. megacephalus*, the midline length cannot be measured. Similarly, *An. priscum* and *A. galaktion* have the internasal process preserved in some specimens, but no frontal is complete enough to allow measuring the midline length. Direct measures on referred specimens of *A. arthridion* gave a proportion around 1.05. Direct measures on referred specimens of *A. ektopistikon* gave proportion of 1.28. Direct measured on referred and figured specimens of *A. gracile* gave proportion from 1.02 to 1.16. Measurement on referred specimen of *Y. perettii* gave a proportion of 1.44, while it was originally coded 0&1 (Daza *et al.*, 2020). Similarly, Matsumoto & Evans calculated a proportion of 1.21 and decided to score it 0&1 (2018), despite the state of character being define by "strictly superior to 1.2"; furthermore, new measurement on figured specimen gave a ratio of 1.27.

As stated above, this character could use geomorphometric for a better characterization of the proportion of the frontal, taking into consideration the intraspecific variation.

30. Frontals, position of anterior end of orbital margin to anteroposterior midpoint of bone: 0 = anterior; 1 = same level or posterior (McGowan 1998, Gardner 2000*a* [10]; Wiechmann 2003 [8]; Sweetman & Gardner 2013 [28]; Carrano *et al.* 2022 [27])

State changes: *An. unicum* 1 → 0;

C. megacephalus 0 → ?;

A. galaktion 1 → ?;

"Paskapoo species" 1 → ?;

As stated previously, the preservation in *C. megacephalus*, *A. galaktion*, and the "Paskapoo species" prevents to assess the length of the frontal, and therefore the position of its midpoint. Direct measurements on referred specimens of *An. unicum* revealed the anterior end of orbital margin was anterior to the anteroposterior midpoint of the frontal.

31. Frontals, transverse form of ventrolateral crest, in large specimens: 0 = convex; 1 = triangular (Gardner 2000*a* [12], 2002 [24, in part]; Carrano *et al.* 2022 [25])

State changes: *C. megacephalus* ? → 1;

A. arthridion 0 → 1;

A. gracile 0 → 1;

"Uña species" 0 → ?;

The “Uña species” was previously scored with convex ventrolateral crests (Carrano *et al.*, 2022); however, figured specimens and the original description would rather suggest they were triangular (Wiechmann, 2003). Therefore, until better pictures of the specimens or direct observations are made, the character is considered to be ambiguous.

Direct observations on the holotype of *C. megacephalus* and referred specimens to both *A. arthridion* and *A. gracile* revealed ventrolateral crests are triangular in all three species.

32. Frontals, width of ventrolateral crest relative proportion to frontal inner width between ventrolateral crests (FIW), across posterior edges of the frontal ventral roof: 0 = narrow (< 0.38); 1 = broad (≥ 0.38) (Gardner 2002 [24, in part]; Wiechmann 2003 [14]; Carrano *et al.* 2022 [29])

State changes: *An. priscum* 0 → 1;

An. unicum 0 → 1;

A. arthridion 1 → 0;

Y. perettii 0 → 1;

“Sânpetru species” 0 → ?;

Preservation of the frontals in figured specimens of the “Sânpetru species” does not allow to take the measures required for this character. Direct measures on referred specimens to *A. arthridion* gave proportion below 0.38. Direct measures on referred specimens of *An. priscum* and *An. unicum* gave proportion above 0.38. Measures on figured specimen of *Y. perettii* gave ratio above 0.38.

33. Frontals, edge of ventrolateral crests, position along the orbital margin: 0 = close/contiguous to the orbital margin; 1 = medial to the orbital margin creating a ventral step, or parapet (Guillaume *et al.* 2023 [38])

34. Frontals, indentation of the frontoparietal margin at the level of the parietal facets: 0 = absent or faint; 1 = marked; 2 = strong, forming a recess {NEW}

{ORDERED}

The skull roof of the frontal can bear an indentation where it connects between the frontoparietal margin and the ventrolateral crests, at the level of the parietal facets. The indentation can be so strong that it creates a recess of the margin.

Character was ordered, because it is understood that passing from state 0 to state 2, or vice versa, would require to pass by state 1 during the development. Furthermore, as it concerns the part of the bone in direct contact with the parietal, any change would affect the contact between both bones.

35. Frontals, anterior and posterior median fossae on ventral surface: 0 = continuous; 1 = separated by step or shelf (Carrano *et al.* 2022 [30])

State changes: *C. megacephalus* 0 → ?;

A. arthridion 0 → 0&1;

A. gracile 0 → 0&1;

“Paskapoo species” 1 → 0;

The state of preservation of the frontal in *C. megacephalus* prevent assessing this state of character. Direct observations on referred specimens of *A. arthridion* and *A. gracile*

revealed that both state can coexist. Direction observation of the specimen attributed to the "Paskapoo species" suggest the surface is continuous.

36. Frontals, anterior approximation of ventrolateral crests medially: 0 = closely appressed or contacting; 1 = separated by about half the width of one ventrolateral crest; 2 = separated by about the width of one ventrolateral crest (Carrano *et al.* 2022 [31])

State changes: *C. megacephalus* 0 → 2;

A. inexpectatum 1 → 0;

Y. perettii 1 → 0;

"Sânpetru species" 2 → ?;

"Purbeck species" 1 → ?;

Preservation in the "Sânpetru species" and "Purbeck species" prevent to properly assess this character. Direct observation on the holotype of *C. megacephalus* reveals the ventrolateral crest are medially well separated. Conversely, direct observation on referred specimen of *A. inexpectatum*, and the figured specimens of *Y. perettii* suggest the ventrolateral crest are medially closely appressed but not contacting; although they were described as meeting in *Y. perettii* (Daza *et al.*, 2020).

This character would require a better characterization, with defined thresholds, as some direct observation of *Albanerpeton s.l.* species could display ventrolateral crest not really separated by a full width, but neither by half a width. Furthermore, the measures done on the Portuguese material suggest this character can be subjected to intraspecific variation.

37. Frontals, frontal-lacrimal/prefrontal contact: 0 = slot (not visible dorsal or ventrally); 1 = medial emargination of the prefrontal facet making a dorsal notch only, not visible ventrally (the lacrimal sits dorsal to the frontal); 2 = medial emargination of the prefrontal facet making a notch visible dorsally and ventrally (the lacrimal sits lateral to the frontal) (McGowan 1998, Gardner 2000*a* [7]; Guillaume *et al.* 2023 [37])

State changes: "Paskapoo species" ? → 0;

"Uña species" ? → 1;

Direct observation on specimens attributed to the "Paskapoo species" revealed there was no medial emargination. Figured specimens Uña A4 of the "Uña species" (Wiechmann 2003; pl.III, fig.4) suggest a small dorsal medial emargination; and Wiechmann originally described the slot for the prefrontal as "incised medially" in "dorsal view" (Wiechmann 2003; p56). (Original text in German "In der Mitte hat der präfrontale Artikulationsschlitz seinen tiefsten Punkt. In dorso-ventraler Ansicht ist er nach medial eingeschnitten.")

G.2.4 Lacrimal

38. Lacrimal, overall shape of the lacrimal: 0 = U-shaped; 1 = V-shaped {NEW}

As previously reported (Matsumoto & Evans, 2018), although similar in shape, lacrimals among albanerpetontids display minor morphological differences. Here, we proposed to discriminate between those with V-shape, displaying a posteriorly broad lacrimal with an acute apex, to those with U-shape, displaying a less posteriorly broad lacrimal with a more blunt apex. However, because of preservation bias and the fact that lacrimal are not reported in many species, the plesiomorphic state of character remains unclear. The use of geomorphometrics could help to better characterize the different shapes, as well as capture the more subtle variations.

39. Lacrimal, deep trough separating ventral and dorsal processes on lateral surface: 0 = absent; 1 = present {NEW}

The lacrimal display one ventral process and one dorsal process, both extending posteriorly. In some species, both arms can be separated by a deep and wide anteroposterior trough on the lateral surface of the bone. However, considering how few complete lacrimals are known, it remains unclear how this character is affected by ontogeny, as well as its plesiomorphic state.

G.2.5 Parietals

40. Parietals, sculpture on postorbital wing: 0 = present; 1 = absent (Matsumoto & Evans 2018 [33]; Carrano *et al.* 2022 [32])

State changes: *An. unicum* ? → 0;

C. ibericus 0 → ?;

"Paskapoo species" ? → 0;

Direct observations on referred specimens of *An. unicum* and specimens attributed to the "Paskapoo species" could confirm the presence of sculptured postorbital wing. However, direct observation on holotype and referred specimens of *C. ibericus* could not confirm it, contrary to what was previously stated (Matsumoto & Evans, 2018).

41. Parietals, length of postorbital wing: 0 = equal or longer than width of frontoparietal suture; 1 = shorter than width of frontoparietal suture (Matsumoto & Evans 2018 [32]; Carrano *et al.* 2022 [33])

State changes: *An. unicum* ? → 1;

C. ibericus 0 → 0&1;

C. megacephalus ? → 0;

"Paskapoo species" ? → 0;

Direct measures on referred specimens of *An. unicum* could confirm the postorbital wing is shorter than the frontoparietal suture; while direct measures on the holotype of *C. megacephalus* and specimens attributed to the "Paskapoo species" confirmed it was longer. Measures on referred specimens and the holotype of *C. ibericus* suggested both state coexisted in the species.

42. Parietals, posterior process of parietal: 0 = single; 1 = double (Matsumoto & Evans 2018 [34])

State changes: *An. unicum* ? → 0;

C. megacephalus ? → 0;

Direct observations in referred specimens of *An. unicum* and holotype of *C. megacephalus* confirmed that the posterior process of the parietal is single.

43. Parietals, postorbital process sculptured vs unsculptured parts ratio: 0 = sculptured longest; 1 = unsculptured longest (Daza *et al.* 2020 [36])

State changes: *An. unicum* ? → 1;

C. ibericus 0 → ?;

"Paskapoo species" ? → 1;

Direct observations on referred specimens of *An. unicum* and specimens attributed to the "Paskapoo species" confirmed the unsculptured part of the postorbital process was the

longest. However, the state could not be confirmed in the holotype and referred specimens of *C. ibericus*.

44. Parietals, anteromedial-ventrolateral transverse crest on the ventral surface: 0 = absent; 1 = single; 2 = with a secondary crest {NEW}

Recent studies reported an anteromedial-ventrolateral transverse crest with an anterolateral recess, separating the short ornamented postorbital wing from the rest of the parietal, along with a secondary crest (Matsumoto & Evans, 2018; Daza *et al.*, 2020). Direct observations on other parietals revealed that the anteromedial-ventrolateral crest is not always present, neither always along with a secondary crest.

45. Posterodorsal fenestrae on skull roof: 0 = absent; 1 = present (Daza *et al.* 2020 [35])

State changes: *An. unicum* ? → 0;

C. ibericus 0 → ?;

C. megacephalus ? → 1;

Direct observations on referred specimens of *An. unicum* and the holotype of *C. megacephalus* could confirmed that the posterodorsal fenestrae on the skull roof was absent in the former and present in the later. However, the state could not be confirmed in the holotype and referred specimens of *C. ibericus*.

G.2.6 Dentary

46. Dentary, tooth count: 0 = ≥ 35; 1 = < 35 (Carrano *et al.* 2022 [21])

State changes: "Paskapoo species" ? → 1;

Direct observation on dentaries attributed to the "Paskapoo species" confirmed no more than 24 teeth in best preserved specimens.

47. Dentary, projection of the anterior extension, or eminence *sensu* Gardner & Averianov (1998): 0 = round, blunt projection; 1 = faint projection, almost absent; 2 = tapered, strong projection {NEW}

The eminence is present in almost all species, but the degree of projection varies from one to another.

48. Dentary, relative size of dorsal prong vs. ventral prong: 0 = dorsal prong ≥ ventral prong; 1 = ventral prong > dorsal prong {NEW}

The prongs are elements of the interdentary joint that characterized Albanerpetontidae. One dentary bears one prong; while the opposed one bears two to create the lock. However, the relative size between ventral and dorsal prongs is not the same from one species to another. It is still unsure how characters 47 and 48 are connected together, and how they are affected by preservation bias and ontogeny.

49. Dentary, scar for the intermandibularis muscle: 0 = absent; 1 = present, relatively high on the anterior section of the bone (1/3 to half of the dental parapet height); 2 = present, low or strictly ventral {NEW}

Almost all species display a scar delimited by a ridge for the intermandibularis muscle (Gardner & Averianov, 1998). However, this scar can extend more or less on the anterior section of the labial surface of the dental parapet. In all species where the character is present, the ridge delimiting the scar is always ventral to all nutritive foramina.

G.2.7 Articular-angular

50. Articular-angular, shape of the glenoid fossa: 0 = saddle-shaped cotylar; 1 = deep concavity {NEW}

As defined now, state 1 is autapomorphy of *C. megacephalus*. However, other albanerpetontids display subtle variation in the shape of the glenoid fossa that could be better characterized with the use of geomorphometrics.

51. Articular-angular, posterior shape of the prearticular facet apex on medial surface: 0 = acute; 1 = sickle-shaped/falcate {NEW}

The posterior apex of the ventral facet on the medial surface display different shape among albanerpetontids, from a pointed to more blunt morphology, or forming a sickle (being acute but also curved ventrally). This character could be better characterized with the use of geomorphometrics.

G.2.8 Quadrate

52. Quadrate, extended lateral lip and marked lateral concavity: 0 = present; 1 = reduced or absent {NEW]

The lateral lip and lateral concavity of the quadrate are present in most species in which the bone has been reported, but they can be extremely reduced to almost absent.

53. Quadrate, depth of the lateroventral surface: 0 = shallow, almost like a scar or small facet; 1 = deep with strong edges, like a slot {NEW}

The lateroventral surface depth varies among some species, from being relatively shallow and looking like a facet, to a deep slot with strong edges. The latter morphology is usually associated with an expanded posteroventral surface, where the strong edges form a shelf.

G.2.9 Atlas

54. Atlas, overall shape of the anterior cotyles: 0 = reniform; 1 = D-shaped; 2 = rectangular {NEW}

The anterior cotyles exhibit at least three different morphologies among albanerpetontid, although the rectangular morphology seems to be an autapomorphy of the "Blasi 2B species".

55. Atlas, orientation of the anterior cotyle surfaces: 0 = facing anteriorly; 1 = facing anteroventrally {NEW}

When observed in lateral view, the anterior cotyle surfaces can be either vertical (facing anteriorly) or more or less inclined ventrally (facing anteroventrally).

56. Atlas, receipt for the first spinal nerve: 0 = shallow mediolaterally straight groove; 1 = deep mediolaterally straight groove; 2 = closed spinal foramen {NEW}

{ORDERED}

All albanerpetontid species with the atlas reported display a receipt for the spinal nerve. It can be mediolaterally straight groove, either shallow or deep with encapsulating ridge; or through an actual spinal foramen. See Guillaume et al. in prep for more detail on this character.

Character was ordered, because it is understood that passing from state 0 to state 2, or vice versa, would require to pass by state 1 during the development.

G.2.10 Axis

57. Axis, development of the dorsal condyle edges: 0 = not thickened; 1 = thickened {NEW}

The dorsal condyle edges can be strongly thickened in some species.

G.2.11 Humerus

58. Humerus, state of the *fossa cubitus cristalis*: 0 = marked, with strong and deep edges; 1 = shallow {NEW}

The *fossa cubitus cristalis* can be more or less marked between the different species. When it is marked, it is bordered by deep and strong edge; while they are smoother when it is shallow.

G.2.12 Ilium

59. Ilium, shape of the acetabulum: 0 = U-shaped, dorsoventrally elongated acetabulum with convex dorsal margin; 1 = V-shaped, dorsoventrally elongated acetabulum with acute dorsal margin; 2 = D-shaped, shorter acetabulum with convex dorsal margin {NEW}

Among species in which ilium has been reported, three morphologies exist depending on how much it is dorsoventrally elongated and how convex the dorsal margin is. As ilia have been reported only in few species, the plesiomorphic state of the character, as well as its variability among species, remain currently unclear. The use of geomorphometrics could also help to better characterize the variation in morphologies.

60. Ilium, posterior tilt of the long axis: 0 = strongly tilted posteriorly; 1 = weakly to almost straight {NEW}

The long axis can be more or less posteriorly tilted between the species in which ilium has been reported. However, as this concerns only few species and that the long axis is most likely to be broken, the plesiomorphic state of the character, as well as its variability among species, remain currently unclear.

61. Ilium, shape of the long axis: 0 = tubular; 1 = blade-like {NEW}

The long axis displays two different morphologies: one tubular, in which it is subcircular in cross-section, and one blade-like, in which it is compressed mediolaterally. However, as this concerns only few species and that the long axis is most likely to be broken, the plesiomorphic state of the character, as well as its variability among species, remain currently unclear.

62. Ilium, pubic/ischial anteroposterior flaring: 0 = broad; 1 = constricted {NEW}

The pubic and ischial articular surfaces flare anteroposteriorly in all species in which this part of the ilium is preserved. However, this flaring seems to be more or less broad. This can be evaluated by the angle measured at the intersection of the edge tangents of the pubis and iliac shafts. However, as for previous ilium characters, the plesiomorphic state of the character, as well as its variability among species, remain currently unclear. The use of geomorphometrics could also help to better characterize the variation in morphologies.

G.2.13 References

Carrano MT, Oreska MPJ, Murch A, Trujillo KC, Chamberlain KR. 2022. Vertebrate paleontology of the Cloverly Formation (Lower Cretaceous), III: a new species of

Albanerpeton, with biogeographic and paleoecological implications. Journal of Vertebrate Paleontology: e2003372.

Daza JD, Stanley EL, Bolet A, Bauer AM, Arias JS, Čerňanský A, Bevitt JJ, Wagner P, Evans SE. 2020. Enigmatic amphibians in mid-Cretaceous amber were chameleon-like ballistic feeders. Science 370: 687–691.

Folie A, Codrea VA. 2005. New lissamphibians and squamates from the Maastrichtian of Haţeg Basin, Romania. Acta Palaeontologica Polonica 50: 57–71.

Gardner JD. 1999. New albanerpetontid amphibians from the Albian to Coniacian of Utah, USA—bridging the gap. Journal of Vertebrate Paleontology 19: 632–638.

Gardner JD. 2000a. Revised taxonomy of albanerpetontid amphibians. Acta Palaeontologica Polonica 45: 55–70.

Gardner JD. 2000b. Albanerpetontid amphibians from the Upper Cretaceous (Campanian and Maastrichtian) of North America. Geodiversitas 22: 349–388.

Gardner JD. 2002. Monophyly and intra-generic relationships of *Albanerpeton* (Lissamphibia; Albanerpetontidae). Journal of Vertebrate Paleontology 22: 12–22.

Gardner JD, Averianov AO. 1998. Albanerpetontid amphibians from the Upper Cretaceous of Middle Asia. Acta Palaeontologica Polonica 43: 453–476.

Gardner JD, Evans SE, Sigogneau-Russel D. 2003. New albanerpetontid amphibians from the Early Cretaceous of Morocco and Middle Jurassic of England. Acta Paleontologica Polonica 48: 301–319.

Gardner JD, Villa A, Colombero S, Venczel M, Delfino M. 2021. A Messinian (latest Miocene) occurrence for *Albanerpeton* Estes & Hoffstetter, 1976 (Lissamphibia: Albanerpetontidae) at Moncucco Torinese, Piedmont Basin, northwestern Italy, and a review of the European Cenozoic record for albanerpetontids. Geodiversitas 43: 391–404.

Guillaume AR, Natário C, Mateus O, Moreno-Azanza M. 2023. Plasticity in the morphology of the fused frontals of Albanerpetontidae (Lissamphibia; Allocaudata). Historical Biology 35: 537–554.

Maddin HC, Venczel M, Gardner JD, Rage JC. 2013. Micro-computed tomography study of a three-dimensionally preserved neurocranium of *Albanerpeton* (Lissamphibia, Albanerpetontidae) from the Pliocene of Hungary. Journal of Vertebrate Paleontology 33: 568–587.

Matsumoto R, Evans SE. 2018. The first record of albanerpetontid amphibians (Amphibia: Albanerpetontidae) from East Asia. PloS one 13: e0189767.

McGowan GJ. 1998. Frontals as diagnostic indicators in fossil albanerpetontid amphibians. Bulletin of the National Science Museum, Series C (Geology and Paleontology) 24: 185–194.

Sweetman SC, Gardner JD. 2013. A new albanerpetontid amphibian from the Barremian (Early Cretaceous) Wessex Formation of the Isle of Wight, southern England. Acta Palaeontologica Polonica 58: 295–324.

Szentesi Z, Gardner JD, Venczel M. 2013. Albanerpetontid amphibians from the Late Cretaceous (Santonian) of Iharkút, Hungary, with remarks on regional differences in Late Cretaceous Laurasian amphibian assemblages. Canadian Journal of Earth Sciences 50: 268–281.

Venczel M, Gardner JD. 2005. The geologically youngest albanerpetontid amphibian, from the lower Pliocene of Hungary. Palaeontology 48: 1273–1300.

Wiechmann MF. 2003. Albanerpetontidae (Lissamphibia) aus dem Mesozoikum der Iberischen Halbinsel und dem Neogen von Süddeutschland. Unpublished thesis, Freie Universität Berlin.

2024

ALEXANDRE RENAUD DANIEL GUILLAUME

THE MINUTE BEASTS AT THE FEET OF THE DINOSAURS: HERPETOFAUNA FROM THE LATE JURASSIC OF PORTUGAL

UNIVERSIDADE NOVA DE LISBOA